REPORT NO. DOT-TSC-NHTSA-79-62.II

DOT-HS-805 277

DATA BASE FOR LIGHT-WEIGHT AUTOMOTIVE DIESEL POWER PLANTS
Volume II: Discussion And Results

B. Wiedemann, R. Schmidt, et al.
Volkswagenwerk
Research Division
3180 Wolfsburg
Federal Republic of Germany

1979
FINAL REPORT

Prepared for

U.S. DEPARTMENT OF TRANSPORTATION
NATIONAL HIGHWAY TRAFFIC SAFETY ADMINISTRATION
Office of Passenger Vehicle Research
Washington DC 20590

REPORT NO. DOT-TSC-NHTSA-79-62.II DOT-HS-805 277

DATA BASE FOR LIGHT-WEIGHT AUTOMOTIVE DIESEL POWER PLANTS
Volume II: Discussion And Results

B. Wiedemann, R. Schmidt, et al.
Volkswagenwerk
Research Division
3180 Wolfsburg
Federal Republic of Germany

1979
FINAL REPORT

Prepared for

U.S. DEPARTMENT OF TRANSPORTATION
NATIONAL HIGHWAY TRAFFIC SAFETY ADMINISTRATION
Office of Passenger Vehicle Research
Washington DC 20590

NOTICE

This document is disseminated under the sponsorship of the Department of Transportation in the interest of information exchange. The United States Government assumes no liability for its contents or use thereof.

NOTICE

The United States Government does not endorse products or manufacturers. Trade or manufacturer's names appear herein solely because they are considered essential to the object of this report.

NOTICE

The views and conclusions contained in the document are those of the author(s) and should not be interpreted as necessarily representing the official policies or opinions, either expressed or implied, of the Department of Transportation.

Technical Report Documentation Page

1. Report No.	2. Government Accession No.	3. Recipient's Cotolog No.
DOT-HS-805 277		

4. Title and Subtitle	5. Report Date
TA BASE FOR LIGHT-WEIGHT AUTOMOTIVE DIESEL POWER ANTS, Volume II: Discussion and Results	December 1979
	6. Performing Orgonizotion Code
7. Author(s) Wiedemann, R. Schmidt, et al.	8. Performing Orgonizotion Report No. DOT-TSC-NHTSA-79-62.II
9. Performing Orgonizotion Nome and Address lkswagenwerk* search Division 80 Wolfsburg deral Republic of Germany	10. Work Unit No. (TRAIS) HS017/R0411
	11. Contract or Grant No. DOT/TSC-1193
12. Sponsoring Agency Nome and Address S. Department of Transportation tional Highway Traffic Safety Administration fice of Passenger Vehicle Research shington DC 20590	13. Type of Report and Period Covered Final Report June 30 '76-July 30 '77
	14. Sponsoring Agency Code

15. Supplementary Notes

nder contract to: U.S. Department of Transportation
Research and Special Programs Administration
Transportation Systems Center
Cambridge MA 02142

16. Abstract

The effects on fuel economy, emissions, passenger car safety and other variables e to the installation of light-weight Diesel powerplants were studied. Experimen- l data was obtained on naturally aspirated and turbocharged Diesel engines installed subcompact and compact passenger vehicles. The data includes fuel economy as a nction of engine type and horsepower, as a function of vehicle inertia weight and a function of regulated emission constraints. Unregulated emissions have been aracterized during the course of the work. The compatibility of the Diesel engine udied with passenger car structures incorporating advanced frontal crashworthiness pabilities was also verified.

The report consists of three volumes. Volume I, the Executive Summary, presents summary of the data obtained and a review of the important conclusions. Volume II, e main body of the report, provides a discussion of the fuel economy and emissions tained, a description of the engine/vehicle systems tested and the results of fac- ry driveability tests. Volume III, the appendixes, presents miscellaneous data used ring the program.

17. Key Words	18. Distribution Stotement
esels, CI-Engines, Passenger cars, el economy, Safety, Emissions, tomobiles	DOCUMENT IS AVAILABLE TO THE PUBLIC THROUGH THE NATIONAL TECHNICAL INFORMATION SERVICE, SPRINGFIELD, VIRGINIA 22161

19. Security Classif. (of this report)	20. Security Classif. (of this page)	21. No. of Pages	22. Price
Unclassified	Unclassified	503	

orm DOT F 1700.7 (8-72) Reproduction of completed page authorized

PREFACE

In support of the National Highway Traffic Safety Administration, Office of Passenger Vehicle Research, the Department of Transportation-Transportation Systems Center contracted with Volkswagenwerk AG, Federal Republic of Germany to develop a data base on light-weight Diesel engines suitable for passenger cars. Volkswagen research, pre-production and production Diesel engines were used for the test portion of the work and for the 'analytical extrapolation.'

A Volkswagen research vehicle with advanced crashworthiness characteristics was provided by Volkswagen to demonstrate and document compatibility with an advanced diesel engine design (Integrated Research Vehicle). Through the effort the Diesel engines were evaluated in the context of an integrated vehicle system with the aspects of fuel economy, environment, consumer requirements and cost in mind.

The authors wish to acknowledge the guidance provided by Mr. H.Gould and Dr.R.John of the Department of Transportation-Transportation Systems Center and Dr. K. Digges of the Department of Transportation-National Highway Traffic Safety Administration.

Our working team consisted of the following persons:
Miss C. Schwarz, Messrs. R. Graupmann, W. Lange, K.-J. Lemke, H. Leptien, Dr. G. W. Schweimer and M. Willmann.

They were supported by:
Miss J. Dommschack and Messrs. H.-D. Beckmann, P. M. Deja, P. Jirousek, W. Kiegeland, W. Kurpiers, Dr. K.-H. Lies, J. Nitz, E. Pommer, K.-H. Schneider and P. Seifert together with members of the staff from the VW prototype shop, the VW transmission development department and the VW measuring and testing department.

METRIC CONVERSION FACTORS

Approximate Conversions to Metric Measures

Symbol	When You Know	Multiply by	To Find	Symbol
	LENGTH			
in	inches	*2.5	centimeters	cm
ft	feet	30	centimeters	cm
yd	yards	0.9	meters	m
mi	miles	1.6	kilometers	km
	AREA			
in^2	square inches	6.5	square centimeters	cm^2
ft^2	square feet	0.09	square meters	m^2
yd^2	square yards	0.8	square meters	m^2
mi^2	square miles	2.6	square kilometers	km^2
	acres	0.4	hectares	ha
	MASS (weight)			
oz	ounces	28	grams	g
lb	pounds	0.45	kilograms	kg
	short tons (2000 lb)	0.9	tonnes	t
	VOLUME			
tsp	teaspoons	5	milliliters	ml
Tbsp	tablespoons	15	milliliters	ml
fl oz	fluid ounces	30	milliliters	ml
c	cups	0.24	liters	l
pt	pints	0.47	liters	l
qt	quarts	0.95	liters	l
gal	gallons	3.8	liters	l
ft^3	cubic feet	0.03	cubic meters	m^3
yd^3	cubic yards	0.76	cubic meters	m^3
	TEMPERATURE (exact)			
°F	Fahrenheit temperature	5/9 (after subtracting 32)	Celsius temperature	°C

*1 in = 2.54 (exactly). For other exact conversions and more detailed tables, see NBS Misc. Publ. 286, Units of Weights and Measures. Price $2.25. SD Catalog No. C13.10:286.

Approximate Conversions from Metric Measures

Symbol	When You Know	Multiply by	To Find	Symbol
	LENGTH			
mm	millimeters	0.04	inches	in
cm	centimeters	0.4	inches	in
m	meters	3.3	feet	ft
m	meters	1.1	yards	yd
km	kilometers	0.6	miles	mi
	AREA			
cm^2	square centimeters	0.16	square inches	in^2
m^2	square meters	1.2	square yards	yd^2
km^2	square kilometers	0.4	square miles	mi^2
ha	hectares (10,000 m^2)	2.5	acres	
	MASS (weight)			
g	grams	0.035	ounces	oz
kg	kilograms	2.2	pounds	lb
t	tonnes (1000 kg)	1.1	short tons	
	VOLUME			
ml	milliliters	0.03	fluid ounces	fl oz
l	liters	2.1	pints	pt
l	liters	1.06	quarts	qt
l	liters	0.26	gallons	gal
m^3	cubic meters	35	cubic feet	ft^3
m^3	cubic meters	1.3	cubic yards	yd^3
	TEMPERATURE (exact)			
°C	Celsius temperature	9/5 (then add 32)	Fahrenheit temperature	°F

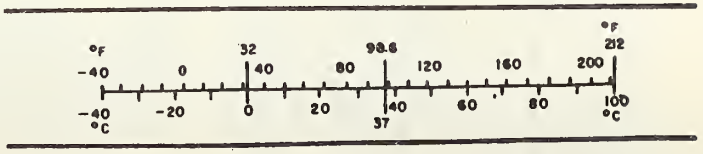

TABLE OF CONTENTS

LIST OF FIGURES AND TABLES

1. SUMMARY

1.1 OBJECTIVES

The objective of this program was to obtain a data base on light-weight automotive diesel power plants for passenger cars so that projections could be established of the potential effects of the large-scale introduction of diesel-powered passenger cars into the U.S. automobile population. The power range of the engines studied was from 50 to 100 horsepower, and the inertia-weight range of the investigated vehicles was from 2,000 to 3,000 pounds.

The characterization and trade-offs of fuel economy, regulated and unregulated exhaust emissions, performance, driveability, and other consumer-related attributes of these engine/vehicle systems constituted the major effort of this program.

1.2 SCOPE AND CONDITIONS OF THE PROGRAM.

The program included analytical and experimental efforts. It is subdivided into the following four main sections:

- Analysis and evaluation of passenger-car diesel engine concepts, layout and design. The setting up of possible engine families for the performance class of 50 to 100 HP.

- Evaluation of two Volkswagen diesel engine families using the technologies of displacement variation and turbocharging. Main emphasis was given to the following items:

  Fuel economy as a function of vehicle weight, emission level, performance, engine technology, and drivetrain. Feasible technologies by means of which the two emission levels of .41/3.4/2.0 and .41/3.4/1.0 grams per mile of HC/CO/NOx could be reasonably attained. Measurement of unregulated exhaust emissions.

- Analysis of typical engine/vehicle systems in order to determine the extent to which modifications are required for the concept and design of diesel-powered automobiles that satisfy safety requirements.

- The evaluation of the compatibility of diesel engines with advanced vehicle concepts. This was demonstrated by two typical engine/vehicle systems presented to the DOT.

1.3 CONCLUSIONS

1.3.1 Layout and Design of Diesel Engines

An analytical evaluation was performed in order to arrive at a definition of the test engines.

A comparison between the basic combustion processes, i.e. pre-chamber, swirl chamber, and direct injection, shows that the swirl-chamber design today is especially suitable for passenger-car operation.

This is mainly due to the efficient utilization of air and its wider range of engine speeds. The specific output of the swirl chamber engine is therefore, higher than that of the other two processes. Furthermore, the swirl-chamber engine has a higher potential of ensuring compliance with emission constraints.

Passenger-car engine design is characterized by the following basic parameters:

- Performance
- Engine weight
- Engine dimensions.

These characteristics are affected by displacement, engine speed, number and arrangement of cylinders, boosting and material. The investigation in the performance range studied (50 - 100 HP) was performed on the current 1.5 l, 4-cylinder VW production diesel engine (Figure 1.3-1).

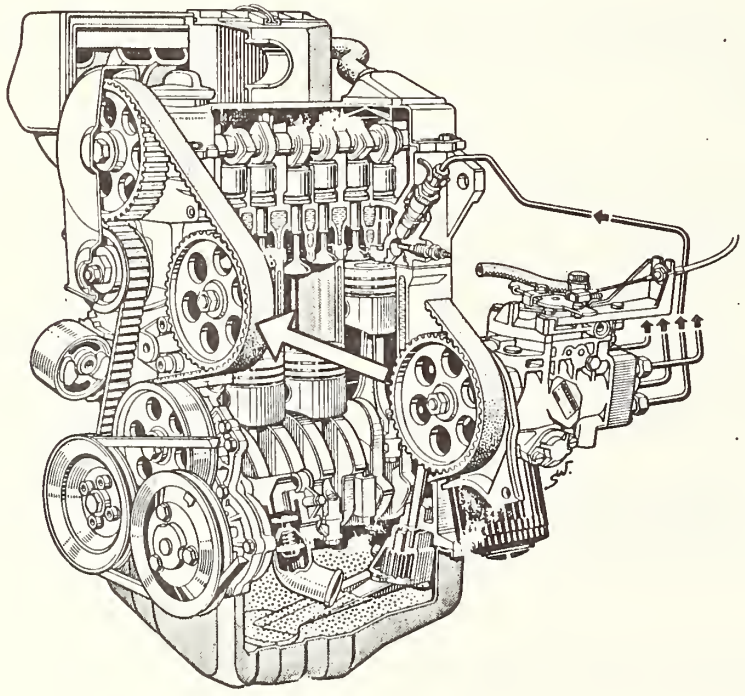

FIGURE 1.3-1: VOLKSWAGEN 1.5-LITER DIESEL ENGINE

Performance

Engine performance increases in direct proportion to the engine rpm to the point where the decrease in volumetric efficiency and the increasing friction losses become predominant.

The effectiveness of combustion decreases at high engine speeds since there is no longer sufficient time available for the mixture formation. For this reason the nominal rpm of swirl chamber engines should not exceed 5000.

Considering these restrictions, the possible nominal output of an engine, assuming constant brake mean effective pressure (bmep) is a function of the displacement, number of cylinders and, in some cases, their arrangement. This interrelation is illustrated in Figures 1.3-2 and 1.3-3. Engine output increases in direct proportion to the displacement, while the specific output in terms of kW/liter displacement decreases.

Trade-offs for different displacement volumes per cylinder unit indicate that cylinder units of 300 to 400 cm^3 produce the highest specific output in terms of kW/l (Figure 1.3-3).

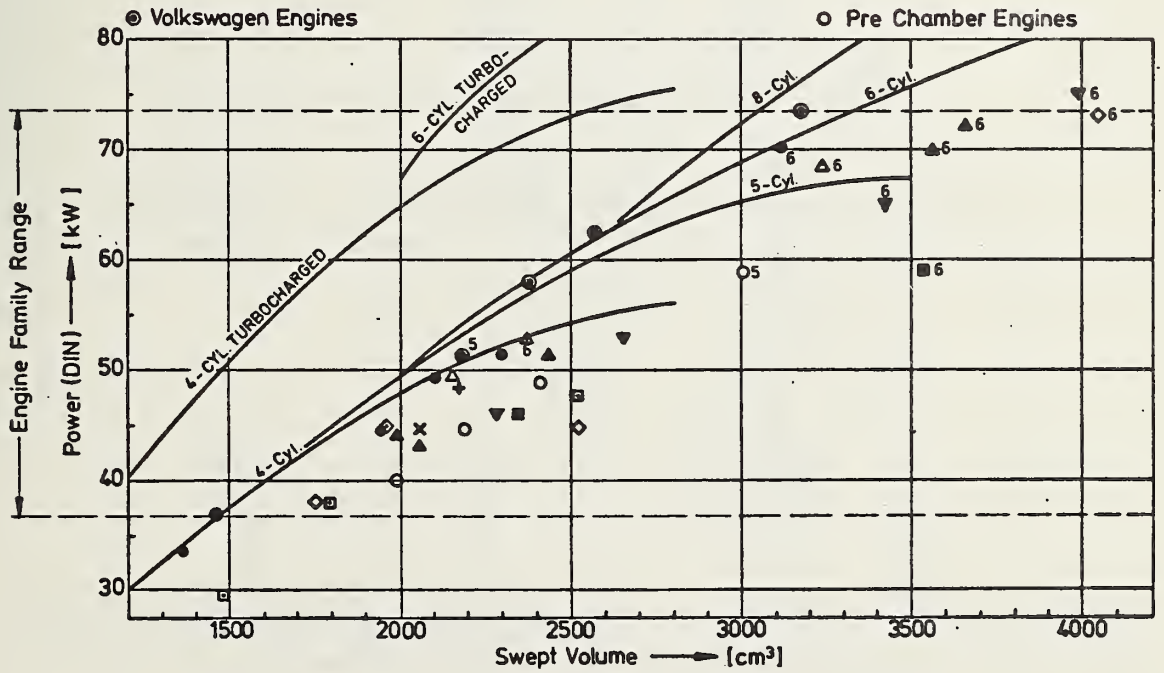

FIGURE 1.3-2: RELATIONSHIP BETWEEN MAXIMUM PERFORMANCE AND SWEPT VOLUME FOR AUTOMOTIVE SWIRL CHAMBER DIESEL ENGINE

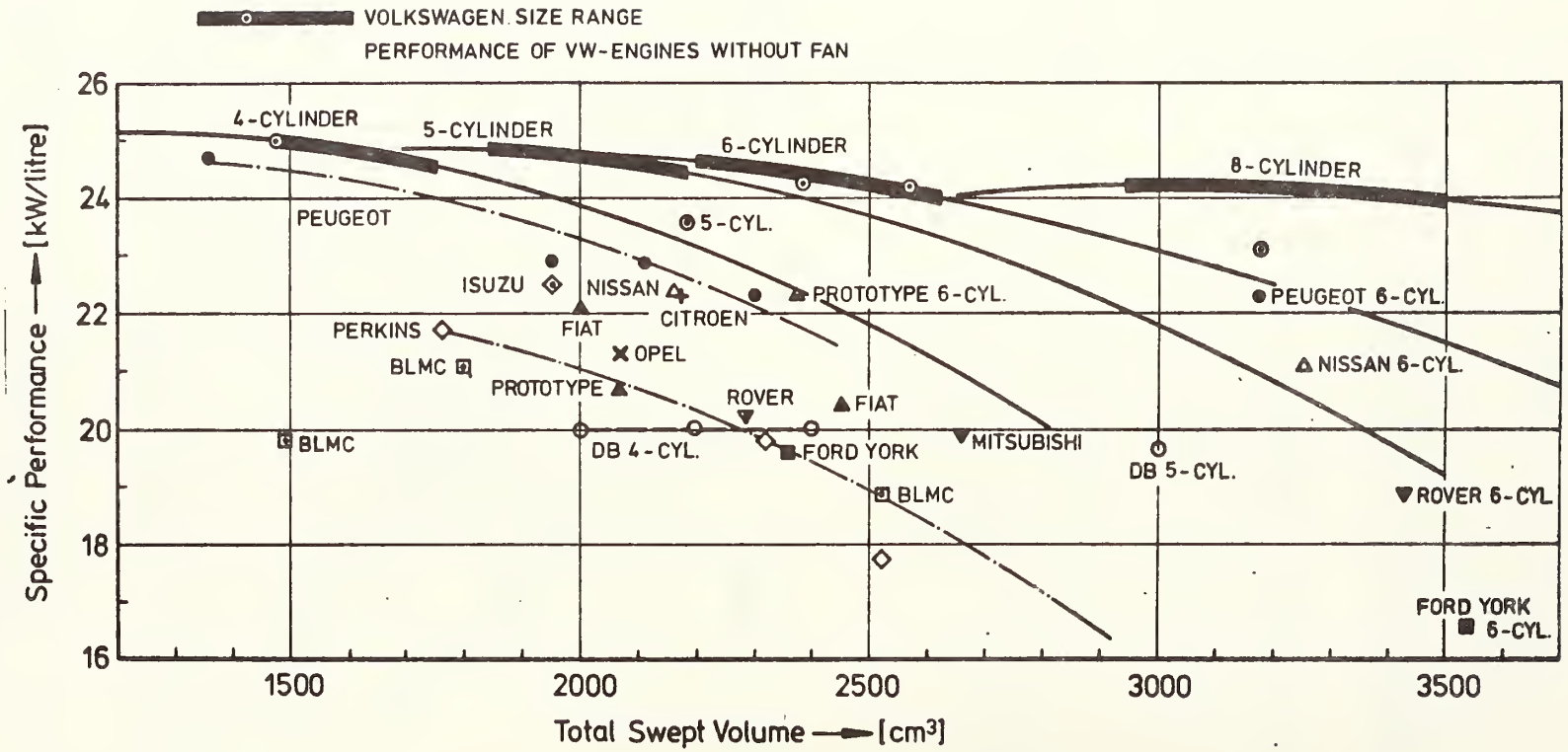

FIGURE 1.3-3: EFFECT OF CYLINDERS ON SPECIFIC PERFORMANCE LEVELS OF TWO-STAGE COMBUSTION DIESEL ENGINES

Table 1.3-1 shows the swept volumes per unit for optimized engine characteristics.

TABLE 1.3-1

SWEPT VOLUME PER UNIT FOR OPTIMIZED ENGINE CHARACTERISTICS

Engine Characteristics	Optimum	Optimum Swept Volume (cm^3)
Specific Output (kW/l)	24.3 ... 25.2	300 ... 400
Weight-to-Power Ratio (kg/kW)	2.5 ... 3	500 ... 600
Power-to-Volume Ratio (kW/m^3)	210 ... 270	375 ... 650

Table 1.3-2 shows the compromise suitable for passenger-car diesel engines considering the following three characteristics: specific output, power-to-weight ratio, and power-to-volume ratio. However, the individual characteristics may be weighed differently for a particular compromise in individual cases.

TABLE 1.3-2

CYLINDER UNIT FOR PASSENGER CAR DIESEL ENGINES

Number of Cylinders	Optimum Swept Volume per Cylinder Unit (cm^3)
4	350 ... 480 (1.4 ... 1.9 l)
5	400 ... 500 (2.0 ... 2.5 l)
6	420 ... 520 (2.4 ... 3.1 l)
8 (V)	450 ... 550 (3.6 ... 4.4 l)

Figure 1.3-4 shows the stroke/bore ratio of current production passenger-car diesel engines and Volkswagen engines. It is interesting to note that almost half of all engines have a stroke/bore ratio of between .9 and 1.0. These are the results of efforts made to provide for a maximum displacement in available cylinder blocks in order to compensate, at least in part, for the lower output of the diesel compared with the conventional gasoline engine. These efforts led to an unfavorable stroke/bore ratio for some diesel engines.

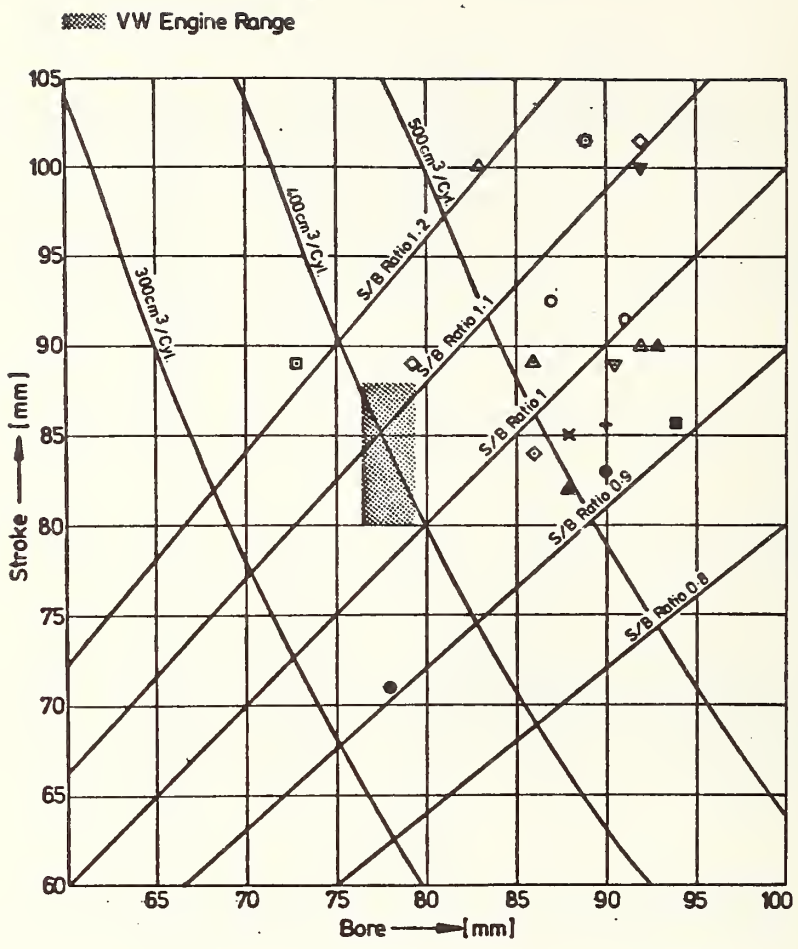

FIGURE 1.3-4: RELATIONSHIP BETWEEN BORE/STROKE FOR VARIOUS SWEPT VOLUMES AND STROKE/BORE RATIOS

The optimum bore/stroke ratio is between 1 and 1.2 for small, high-speed passenger-car diesel engines with cylinder unit displacements of between 300 and 500 cm^3.

Engine Weight

Engine weight generally increases in direct proportion to the increase in displacement (Figure 1.3-5), while there is a drop in the specific weight (kg/liter).

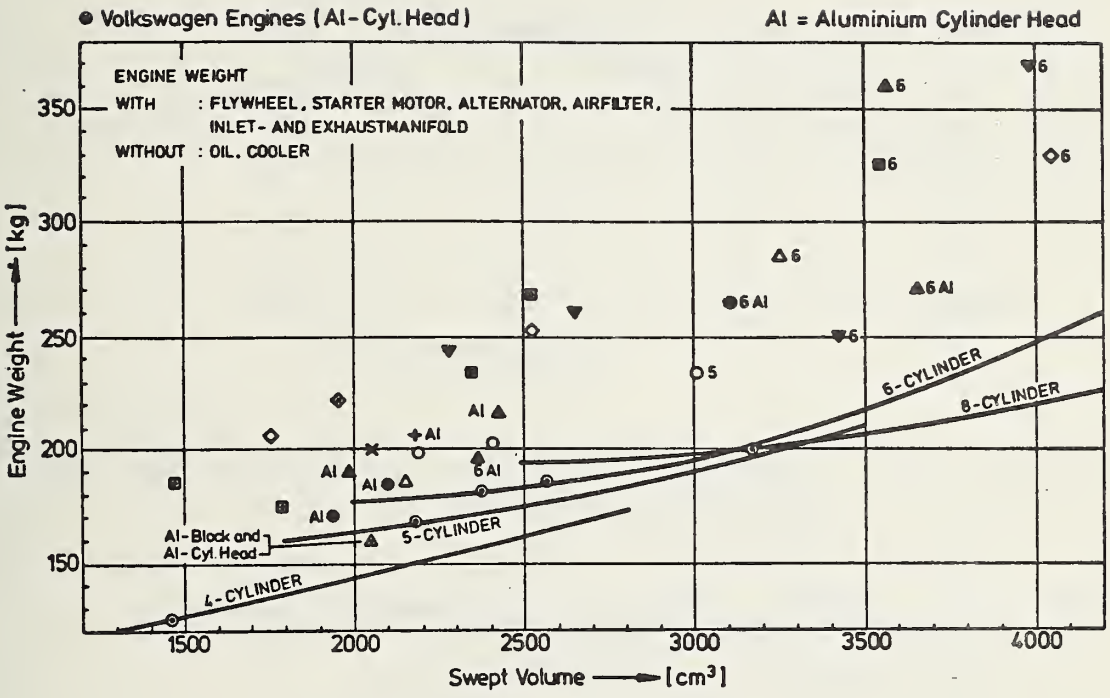

FIGURE 1.3-5: CORRELATION BETWEEN ENGINE WEIGHT, SWEPT VOLUME, AND NUMBER OF CYLINDERS FOR TWO-STAGE COMBUSTION DIESEL ENGINES.

Engine Dimensions

An evaluation of the base engine without accessories reduces the impact of the stroke/bore ratio on engine length, height, and width.

Figure 1.3-6 shows the resulting installed engine volume. Figure 1.3-7 also includes the volume of the cylinder block which is affected by the stroke/bore ratio to a higher degree.

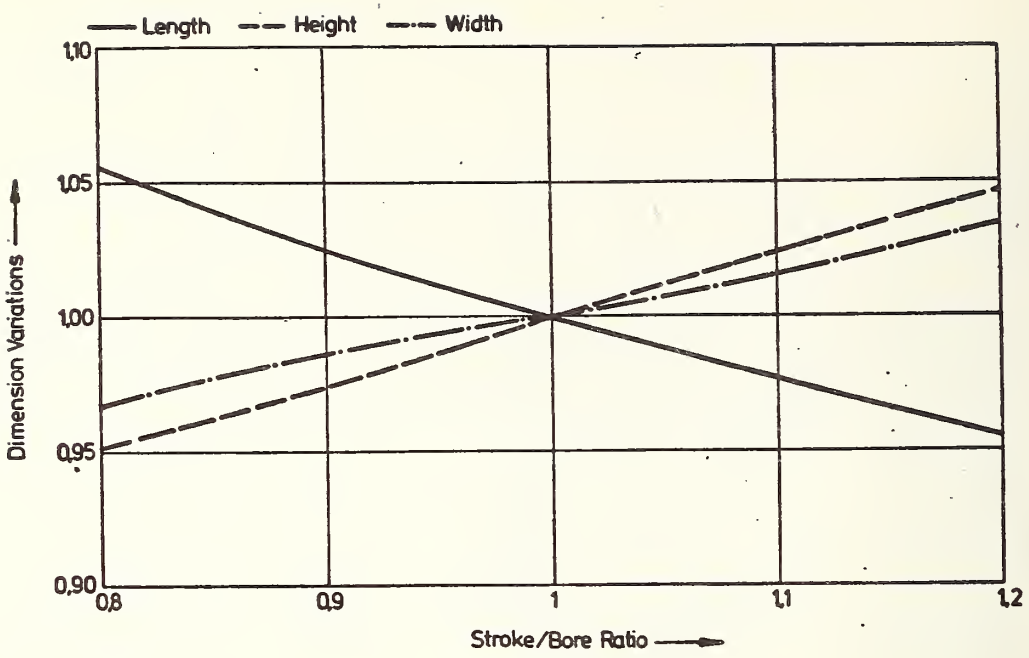

FIGURE 1.3-6: THEORETICAL RELATIONSHIP BETWEEN STROKE/BORE RATIO AND MAJOR DIMENSIONS.

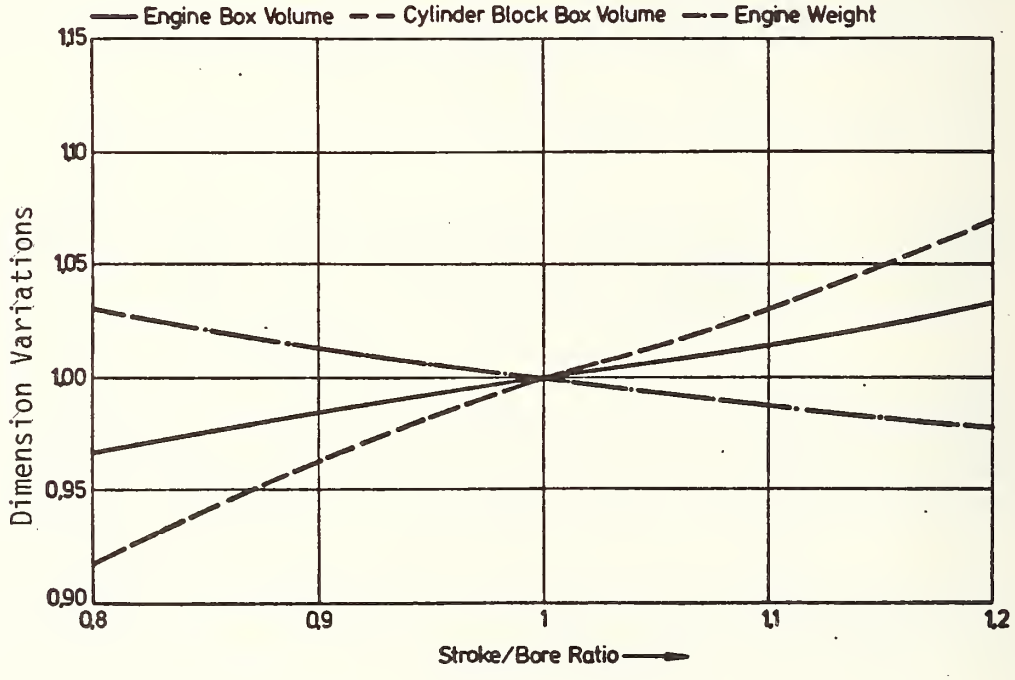

FIGURE 1.3-7: EFFECT OF STROKE/BORE RATIO ON WEIGHT AND BOX VOLUME.

There is an almost linear relationship between displacement and box dimensions (Figure 1.3-8). The most compact engines reach 0.09 m^3/l, less compact ones 0.14 m^3/l. Displacements up to approximately 2.6 l result in an advantage in the case of four-cylinder engines. An increase in the number of cylinders in units beyond this displacement range makes the engine more compact. The V-configuration offers increasing advantages with larger displacement.

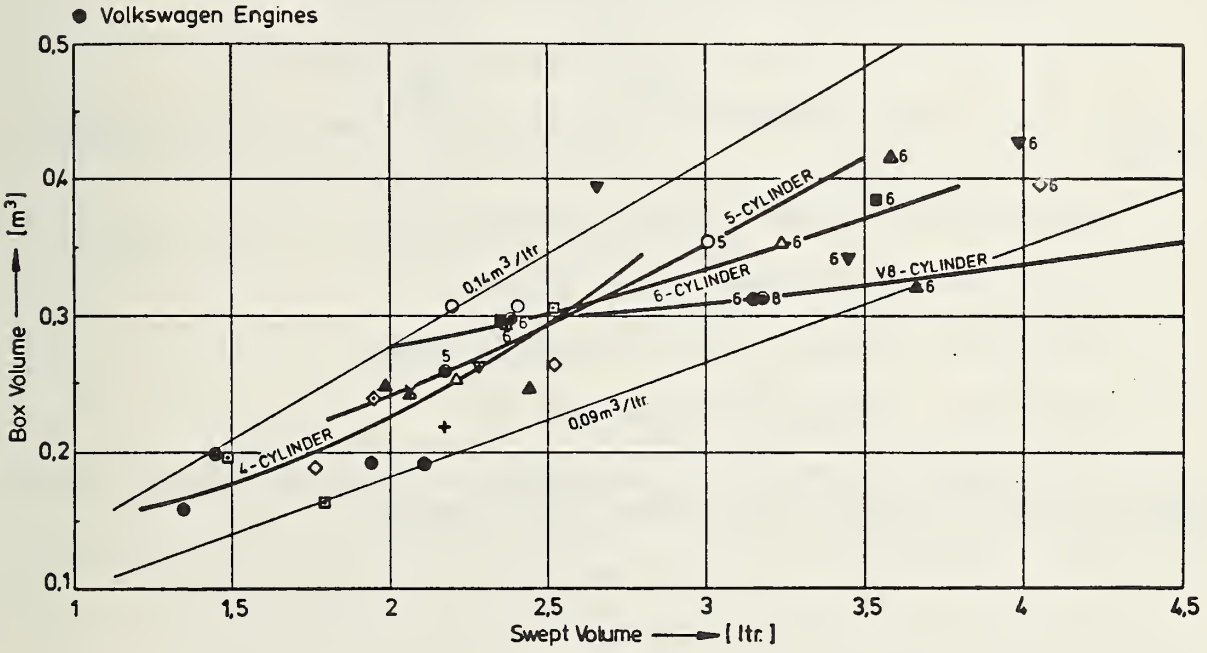

FIGURE 1.3-8: VARIATION OF BOX VOLUME WITH SWEPT VOLUME FOR AUTOMOTIVE DIESEL ENGINES

1.3.2 Engine Family

According to the contract, the engine family should cover an output range from 37 to 73.5 kW (50 to 100 HP). From a manufacturer's standpoint, such an engine concept should be based on a modular-unit system. The optimum cylinder unit size for small, high-speed passenger car diesel engines was assumed to be in the range of 350 to 450 cm^3.

Four engines are meant to cover the output range from 37 to 73.5 kW. Two engine families were selected alternatively to accomplish this purpose (Figure 1.3-9). Family A includes naturally-aspirated engines only. Family B includes two naturally-aspirated engines and their turbocharged variances. The turbocharged engines have been designed for a 30 to 40% increase in power. The first engine family is made up of four engines:

- 4-cylinder, naturally-aspirated engine, 50 HP
- 5-cylinder, naturally-aspirated engine, 68 HP
- 6-cylinder, naturally-aspirated engine, 80 HP
- 8-cylinder (V-8), naturally-aspirated engine, 100 HP

The second family consists of two basic engines and two turbocharged versions:

- 4-cylinder, naturally-aspirated engine, 50 HP
- 4-cylinder, turbocharged engine, 70 HP
- 6-cylinder, naturally, aspirated engine, 80 HP
- 6-cylinder, turbocharged engine, 100 HP

The turbocharged engines offer advantages in regard to weight, overall dimensions and, to some extent, improved fuel economy.

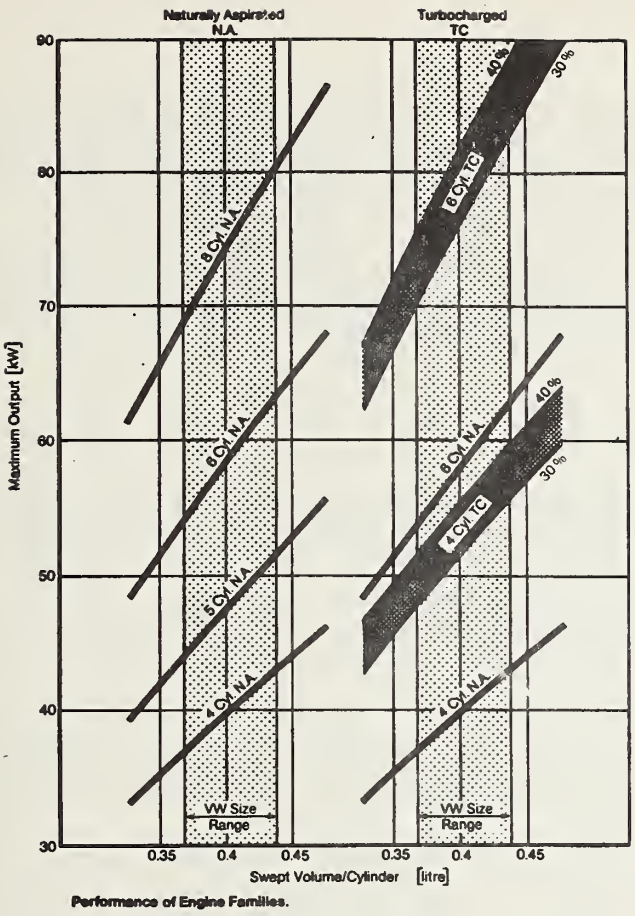

FIGURE 1.3-9: PERFORMANCE OF ENGINE FAMILIES

1.3.3 Typical Engine/Vehicle Systems Evaluated

The applicability of both diesel engine families for present and future vehicles in the inertia-weight range of 2,000 to 3,000 pounds was analyzed, and all reasonable engine/vehicle combinations were evaluated. Three typical engine/vehicle systems with differing horsepower-to-inertia-weight ratios (HP/IW: 0.022; 0.025; 0.030) were tested at engine as well as at vehicle level. The results showed that the modern design of automotive diesel power plants makes them well suited for application in vehicles of this weight class.

1.3.4 Results

The data concerning the evaluated vehicles and engines is listed in Table 1.3-3. In connection with the engine/vehicle systems mentioned in this table, 12 different manual transmissions, including four- and five-speed gearboxes, were analyzed, and a number of them was tested.

In addition, three typical vehicles were analyzed to investigate the compatibility between light-weight automotive diesel power plants and frontal impact crash-worthiness at three safety levels.

1.3.4.1 Fuel Economy

To determine the interdependence between fuel economy, vehicle weight, and performance as described by the horsepower-to-inertia-weight ratio, engine technology, and two emission levels (0.41/3.4/2.0 and .41/3.4/1.0 gram/mile HC/CO/NOx), the engine/vehicle systems were dynamically simulated at the engine level and actually tested at the vehicle level in the 1,750 to 3,000 lb. intertia-weight range using nominal EPA roadload settings.

The 50 HP naturally-aspirated 4-cylinder diesel was tested in the 1,750 to 2,500-lb. inertia-weight classes. Its fuel economy was found to range from 43 to 40 mpg in the Composite Driving Cycle (Figure 1.3-10).

The 68 HP naturally-aspirated 5-cylinder research diesel engine was tested in the 2,250 to 3,000-lb. inertia-weight classes; the resultant fuel economy ranged from 36 to 33 mpg. According to our experience with the 4-cylinder engine now in production, we project a potential improvement of two mpg for this engine.

The 70 HP turbocharged 4-cylinder research diesel engine was tested in the 2,250 to 3,000-lb. inertia-weight classes. Compared to the naturally-aspirated 5-cylinder engine, its fuel economy is better, ranging between 45 and 40 mpg (Figure 1.3-10).

Figure 1.3-11 shows the computed fuel economy values for several engines as installed in two vehicles. These sensitivity studies were mainly performed at the engine level in order to limit the number of uncontrolled parameters and statistical errors otherwise present in vehicle testing.

A difference of 10% in composite fuel economies is observed in the vehicle inertia-weight class of 2,250 lbs. between naturally-aspirated (NA) and turbocharged (TC) engines. This large difference is due to a variation at the vehicle level: different gear ratios can be used for the turbocharged engine. By using the same transmission for both engines, the improvement drops down to 1 mpg. A fuel economy decrease of 1 mpg (3%) in the 90 CID 4-cylinder engines, 50 HP (NA) and 70 HP (TC) is caused by exhaust gas recirculation (EGR). An improvement of 1 mpg is observed for water injection (H_2O).

Main Results of the Evaluated Engine/Vehicle Systems

No	Vehicle Size	No. of Passengers	Inertia Weight (IW)	Diesel Engine Type	No. of Cylinders	CID	HP	HP/IW	Accel. Time 0-60	Accel. Time 30-70	Comp-Fuel Econ.	Applicable Emission Standard HC/CO/NOx	Emissions Achieved in Lab. HC/CO/NOx	Particul. Emiss-ions	Odo-rants (TIA)	Noise Idle 0.5 m (19,7')	Noise Accel. 15 m (59,1')	Noise Const. 15 m (59,1')
1	SC	4	1750	N.A.	4	90	50	0.029	14.0	16.9	43	.41/3.4/2	.16/0.9/1.3					
2	SC	4	2000	N.A.	4	90	50	0.025	16.2	19.8	42		.15/1.4/1.3					
3	SC	4	2250	N.A.	4	90	50	0.022	18.3	22.9	41		.16/1.0/1.2	0.35	1.9	78	75	63
4	SC	4	2500	N.A.	4	90	50	0.020	20.6	26.3	40		.15/1.2/1.3					
5	SC	4	2250	N.A.	5	130	66	0.029	13.0	14.8	36		.35/1.7/1.5					
6	C	5	2750	N.A.	5	130	66	0.024	15.9	19.0	34		.40/1.7/1.7					
7	C	5	3000	N.A	5	130	66	0.022	17.6	20.5	33		.35/1.8/1.8			75	76	63
8	SC	4	2250	TC	4	90	70	0.031	12.7	14.5	45		.11/0.8/0.9	0.24	1.9	79	73	63
9	C	5	2750	TC	4	90	70	0.025	15.7	18.2	42		.15/0.7/1.1					
10	C	5	3000	TC	4	90	70	0.023	17.4	20.1	40		.14/0.8/1.2					
11	C	5	3000	N.A.*	6	146	75	0.025										
12	C	5	3000	TC*	6	146	100	0.033										
13	C	5	3000	N.A.*	8	180	100	0.033	11.1	12.0	30	.41/3.4/2	.43/2.0/1.3					
14	SC	4	1750	N.A. EGR	4	90	50	0.029	14.0	16.9	41	.41/3.4/1	.45/2.5/.40					
15	SC	4	2000	N.A. EGR	4	90	50	0.025	16.2	19.8	40		.45/2.5/.46					
16	SC	4	2250	N.A. EGR	4	90	50	0.022	18.3	22.9	39		.40/2.5/.47	0.34	2.9	73	71	61
17	SC	4	2250	TC EGR	4	90	70	0.031	12.7	14.5	43		.20/1.2/.40	0.45	2.9	76	69	61
18	C	5	2750	TC EGR	4	90	70	0.025	15.7	18.2	40		.17/1.5/.40					
19	C	5	3000	TC EGR	4	90	70	0.023	17.4	20.1	38	.41/3.4/1	.17/1.6/.50					

*Projected Engines

Abbreviations: SC: Subcompact, C: Compact
N.A.: Naturally Aspirated, TC: Turbocharged
EGR: Exhaust Gas Recirculation
TIA: Total Intensity of Aroma (ADL-Method)
CID: Engine Displacement in Cubic Inch
HP/IW: Horsepower to Inertia Weight Ratio, HP/lb

Units: Acceleration Time in sec.
Fuel Economy in mpg
Emissions in gram/mile
Weight in lb
Noise in dB (A)

TABLE 1.3-3: MAIN RESULTS OF THE EVALUATED ENGINE/VEHICLE SYSTEMS

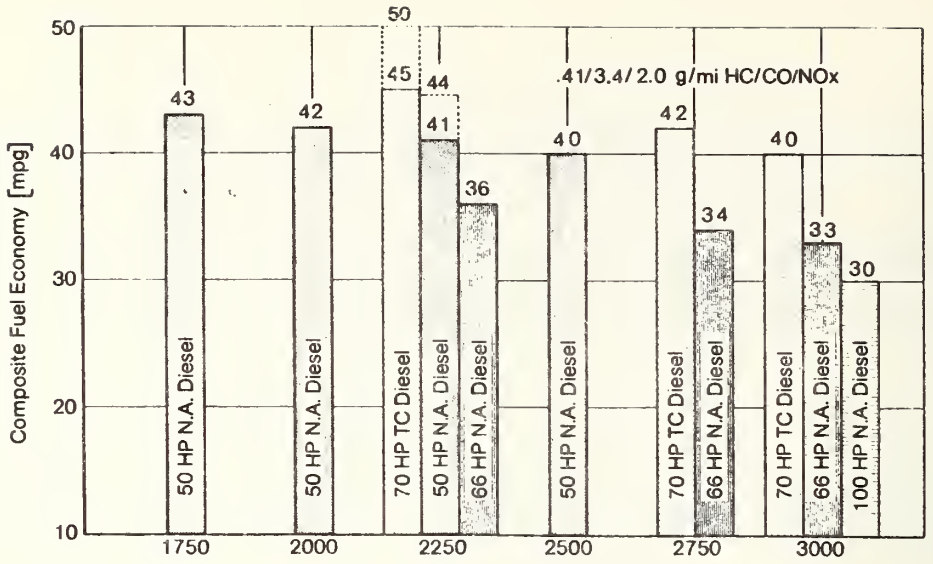

FIGURE 1.3-10: COMPOSITE FUEL ECONOMY OF VARIOUS DIESEL ENGINES AVERAGED OVER THE CITY AND HIGHWAY DRIVING CYCLES
The fuel economy is given in terms of No. 2 Diesel fuel based on nominal EPA road-load ± 2 mpg setting.

------recently obtained results by EPA at actual road-load setting.

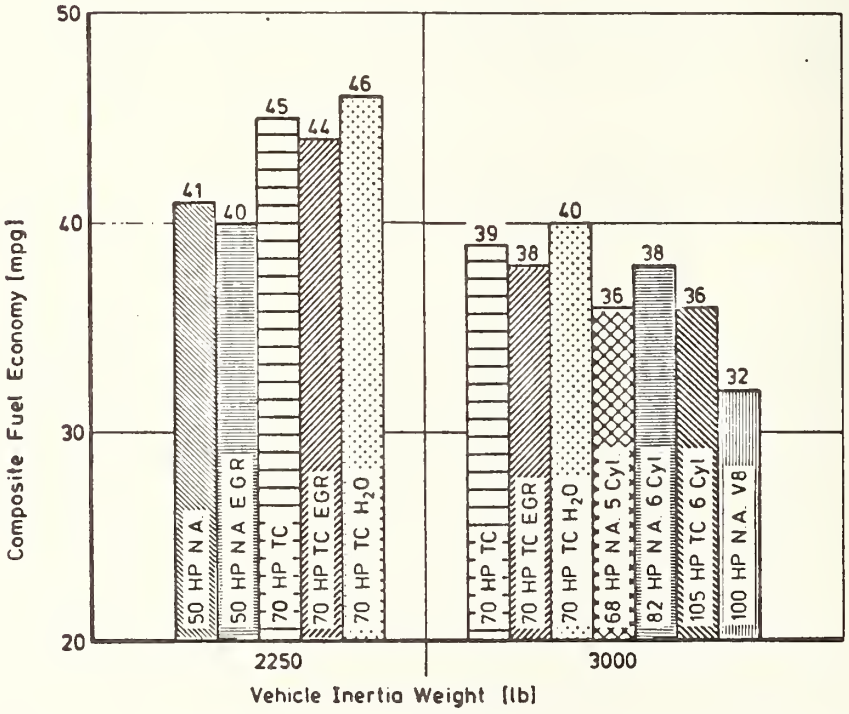

FIGURE 1.3-11: COMPUTED FUEL ECONOMY FROM STEADY-STATE ENGINE MAPS. COMPARISON OF VARIOUS ENGINE CONCEPTS.

With regard to the NA 68 and TC 70 HP engines in vehicles of the same weight and transmission (Figures 1.3-10 and 1.3-11), the naturally-aspirated engine consumes 10% more fuel than the turbocharged engine. The larger fuel consumption may be partly due to the larger swept volume and increased friction losses for the same power output.

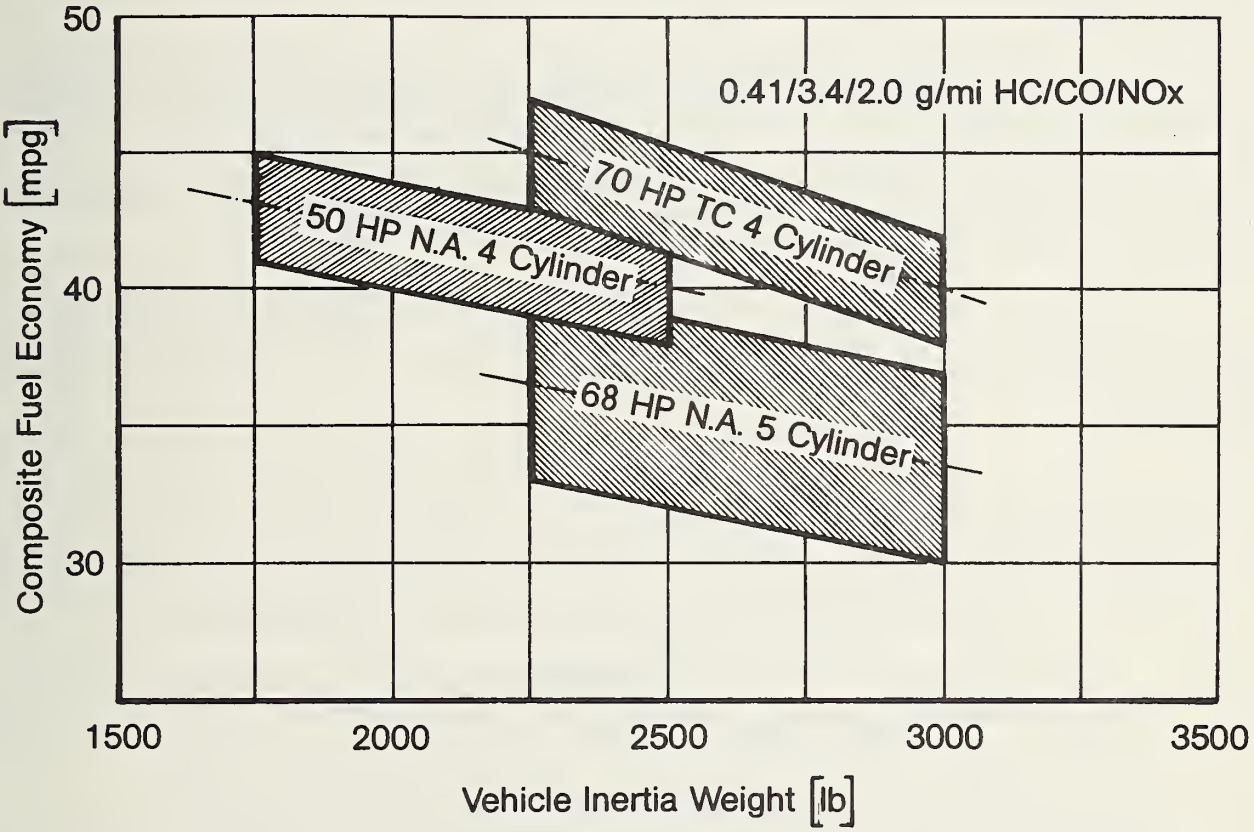

FIGURE 1.3-12: COMPARISON OF FUEL ECONOMY OF 3 DIFFERENT DIESEL ENGINES. The scatter band of the 68 HP engine is wider because of its state of development.

The resulting fuel economy may be plotted as a function of the vehicle inertia weight (Figure 1.3-12). This shows the fuel economy decreases with increasing vehicle weight while maintaining a constant horsepower-to-inertia-weight ratio HP/IW. The differing slopes between fuel economy drop, as shown by the shaded regions is the result of two opposite effects:

- increase of required mechanical energy (inertia weight),

- increase of the mean thermal energy efficiency for increased vehicle weight.

Increasing the HP/IW ratio from 0.022 to 0.030 leads to a deterioration in the fuel economy of the naturally-aspirated engine by approximately 8% in the 2,250-lb. inertia-weight class. This can be explained by the fact that in naturally-aspirated engines, any increase in the number of cylinders and in displacement results in an increase in internal friction losses. It should be noted, however, that this difference in fuel economy is covered by the scatter band.

In addition to engine parameters and vehicle inertia weight, particular importance was attributed to proper matching of transmission and axle ratios to the engine/vehicle system. Since a manual transmission has only a limited number of gears, the engine operating range cannot be restricted to the optimum fuel consumption line. Therefore, the effects of the various transmission ratios on fuel economy were evaluated at EPA roadload settings.

In Figure 1.3-13 the fuel economy values of 96 different projections are plotted versus the effective transmission radius (R). The effective transmission radius R (mm) is given by the test distance / (2π · engine revolutions per test).

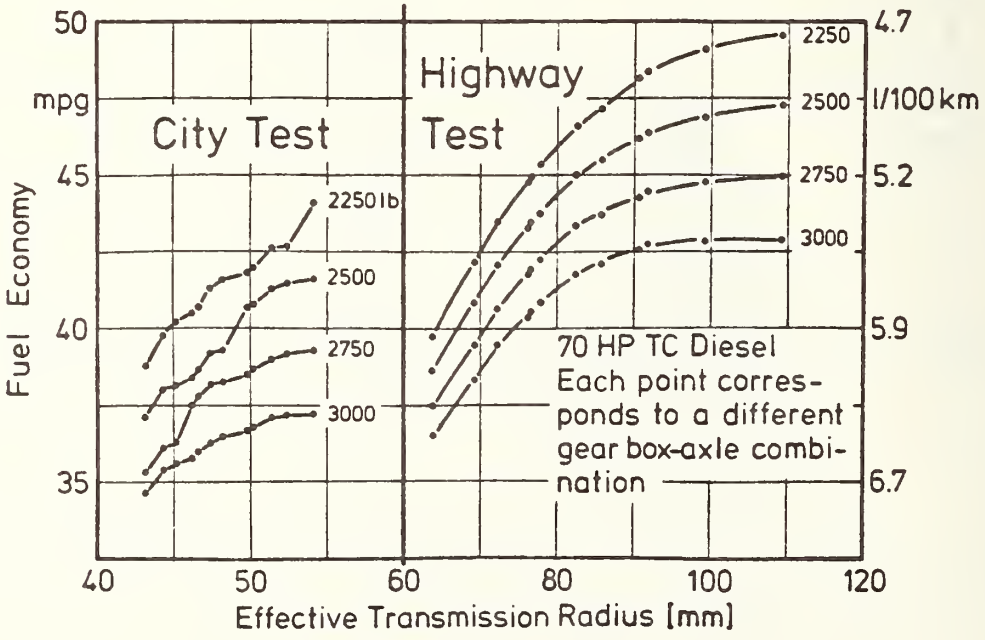

FIGURE 1.3-13: COMPUTED FUEL ECONOMY (EPA ROADLOAD SETTING) AS A FUNCTION OF THE EFFECTIVE TRANSMISSION RADIUS FOR VARIOUS VEHICLE WEIGHTS.

1.3.4.2 Regulated Exhaust Emissions

Figures 1.3-14 and 1.3-15 show the regulated exhaust emission results for both emission levels as far as the 4-cylinder naturally-aspirated engine and the turbocharged version are concerned. The results obtained from the 68 HP naturally-aspirated diesel engine and the projected 100 HP naturally-aspirated diesel engine are sufficient to meet an NOx emission level of 2.0 gram/mile.

As far as laboratory results are concerned, it was possible to just meet the emission level requirement of .41/3.4/1.0 gram/mile HC/CO/NOx for a 2,250-lb. inertia-weight vehicle.

Compliance with the stringent emission standards of .41/3.4/1.0 gram/mile of HC/CO/NOx requires some modifications. Production tolerances and deterioration factors necessitate a tolerance margin.

The following modifications were contemplated:

- Fuel injection timing

- Ceramic swirl chamber

- Water injection

- Exhaust-gas recirculation (EGR).

So far, none of these measures sufficed to lead to a technological breakthrough. Modulated exhaust gas recirculation, however, appears to be the most promising candidate. Using EGR entails some adverse effects, such as increased smoke and odor levels, poor driveability and less durability.

Exhaust gas recirculation is a well-known measure to reduce the NOx emissions of diesel engines. Up to 20% of exhaust gas can be recirculated (effective) at partial load before engine driveability is affected severely.

Research prototypes fitted with modulated EGR reached the required NOx level; but the HC emissions deteriorated much more significantly, increasing to twice the original amount, meaning that the naturally-aspirated engine went beyond the .41 gram/mile limit in some tests. The emission of CO also rose significantly. In order to overcome the most adverse effects of EGR, such as

- increased HC level

- increased smoke level

- increased particulate emissions

- increased odor level

- reduced durability

- increased maintenance requirements, and

- poor driveability

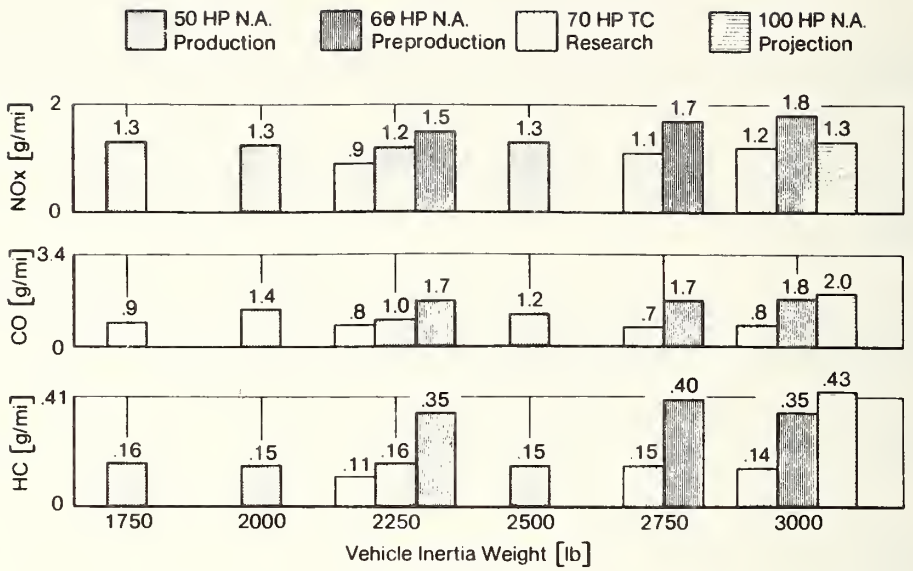

FIGURE 1.3-14: REGULATED EXHAUST EMISSIONS FROM VARIOUS DIESEL ENGINES
Deterioration factors and variances due to manufacturing (30% of the figures indicated) are not taken into account.

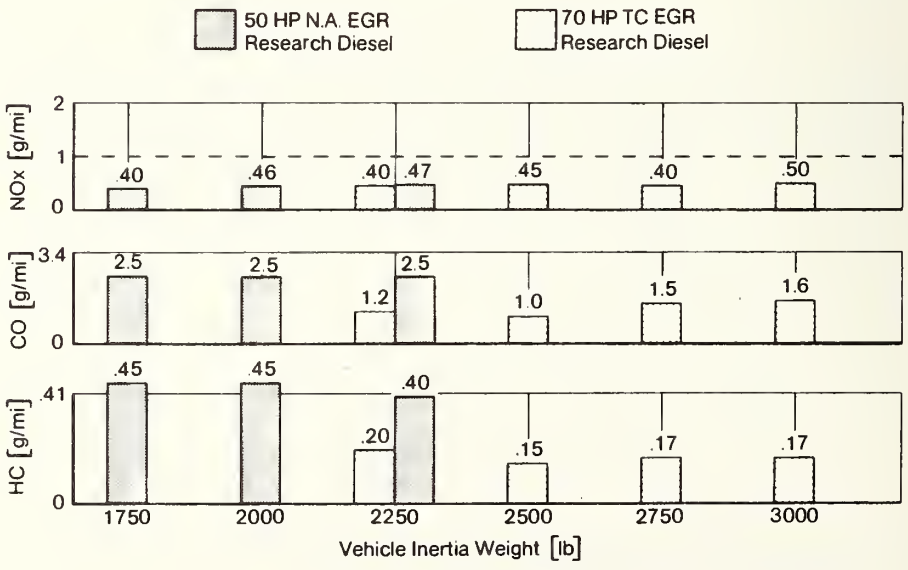

FIGURE 1.3-15: REGULATED EXHAUST EMISSIONS OF TWO DIESEL ENGINES WITH CONTROLLED EXHAUST GAS RECIRCULATION

it appears that major technological advancements are required to successfully implement EGR in production engines.

1.3.4.3 Unregulated Exhaust Emissions

For the two emission levels of .41/3.4/2.0 and .41/3.4/1.0 gram/mile HC/CO/NOx, unregulated emission data have been generated using the FTP-75 and the sulfate (SET) drive cycle for both the 50 HP naturally-aspirated and the 70 HP turbocharged engine.

While cruising, the smoke emissions of all engine/vehicle systems without EGR were found to be invisible (Bosch Number: less than 3.5). Introducing EGR caused smoke during transients, and especially when altitude tests were performed (Bosch Number: higher than 8.0).

Figure 1.3-16 shows the emission of particulates at the two emission levels. The emissions of the 50 HP naturally-aspirated engine (0.35 gram/mile) and of the 70 HP turbocharged engine (0.25 gram/mile) indicate low values within the range of current diesel engines. Due to the limited time available we could not investigate the reasons for the relatively high particulate emissions of the 70 HP turbocharged engine with EGR.

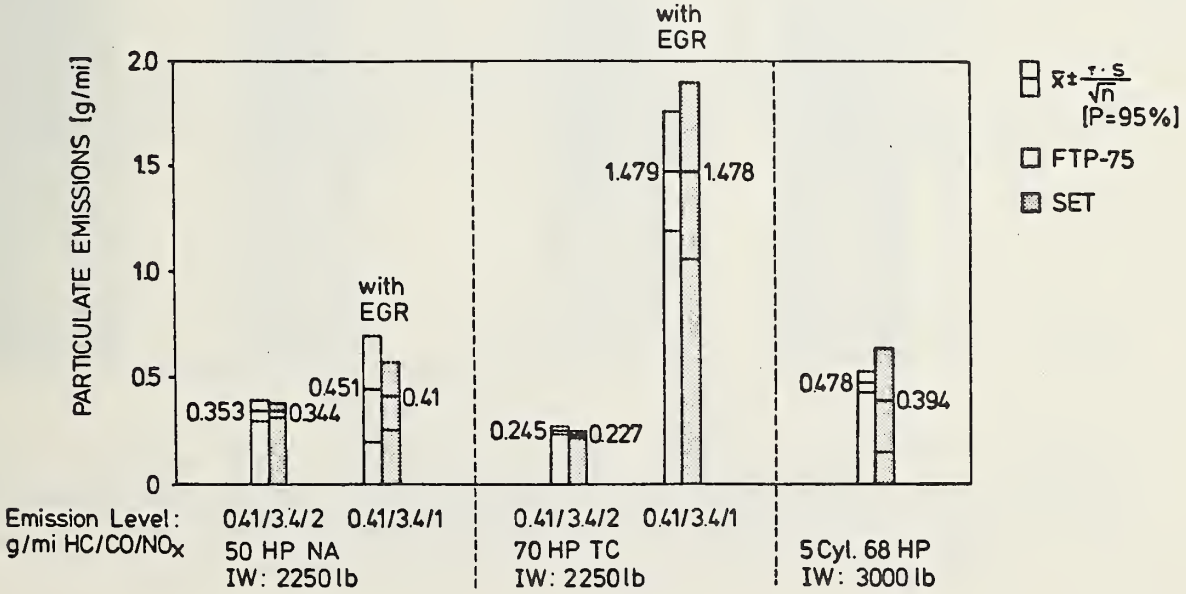

FIGURE 1.3-16: PARTICULATE EMISSIONS

The odor level was determined mainly from the mass emissions of two odorants, aromatic hydrocarbons and partially oxygenated hydrocarbons (A.D. Little Method). When combined on a logarithmic scale indicating the so-called total intensity of aroma (TIA), their indication seems to agree with the response of the average human nose. Figure 1.3-17 shows the influence of EGR and of fuel composition on odor. There is no difference between naturally-aspirated and turbocharged engines in this respect. If EGR is applied, the odor level rises by one unit. Fluctuations amounting to half a unit are caused by the differences in the composition of the two fuels used.

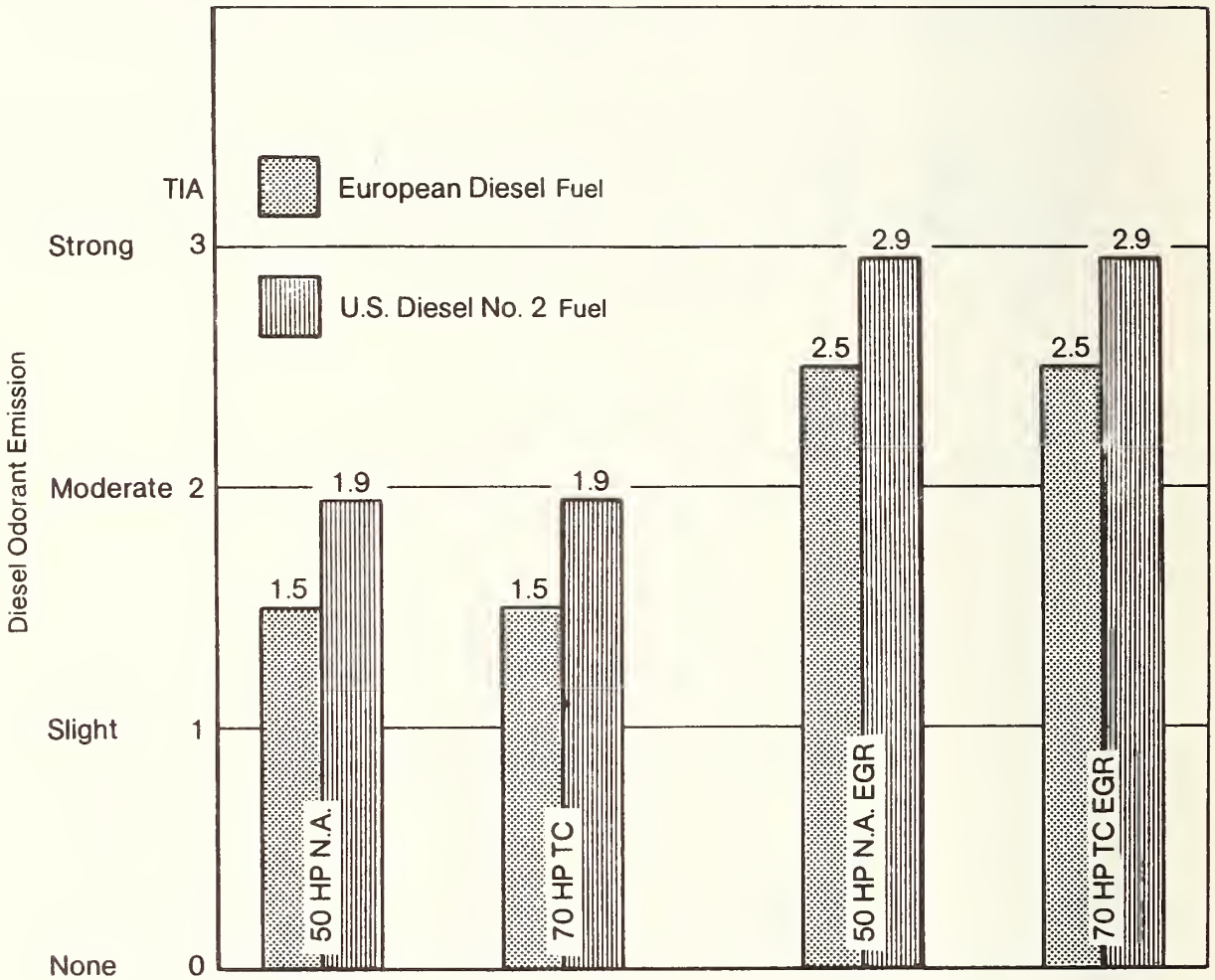

FIGURE 1.3-17: DIESEL ODOR EMISSION AVERAGED OVER A CITY DRIVING CYCLE, INFLUENCED BY FUEL COMPOSITION AND EXHAUST GAS RECIRCULATION
Odor values may vary by $\pm$ 0.25 units.

Figure 1.3-18 shows the emission of sulfates at the two emission levels. Of the total amount of sulfur contained in diesel fuel, a fraction ranging from 1 to 2%, is converted into sulfates, which is equivalent to the conversion rate for spark ignition engines without catalytic converters. Mainly, the differences between the emissions of diesel and gasoline engines are due to the unequal sulfur content of the fuels, which in diesel fuels ranges from 0.1 to 0.5% by weight, and in gasoline corresponds to 0.03% by weight. About 80 to 90% of the sulfur is burned into sulfur dioxide (SO_2), whereas the remaining 10 to 20% is shared by several other sulfur compounds.

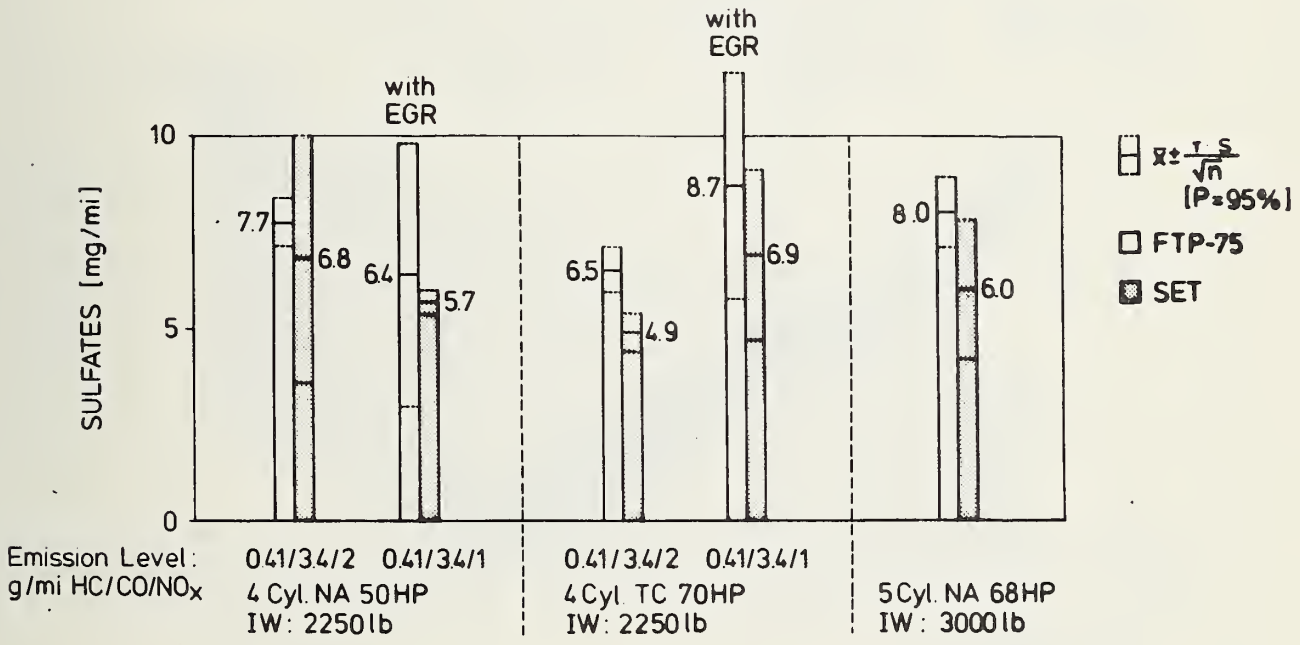

FIGURE 1.3-18: SULFATE EMISSIONS.
The diesel fuel contained 0.225 wt % S.

Figure 1.3-19 shows the aldehyde emissions at the two emission levels. Diesel engines tested emitted aldehydes at a rate of 13 - 55 mg/mile. This is in the range of aldehyde emissions emitted by gasoline engines.

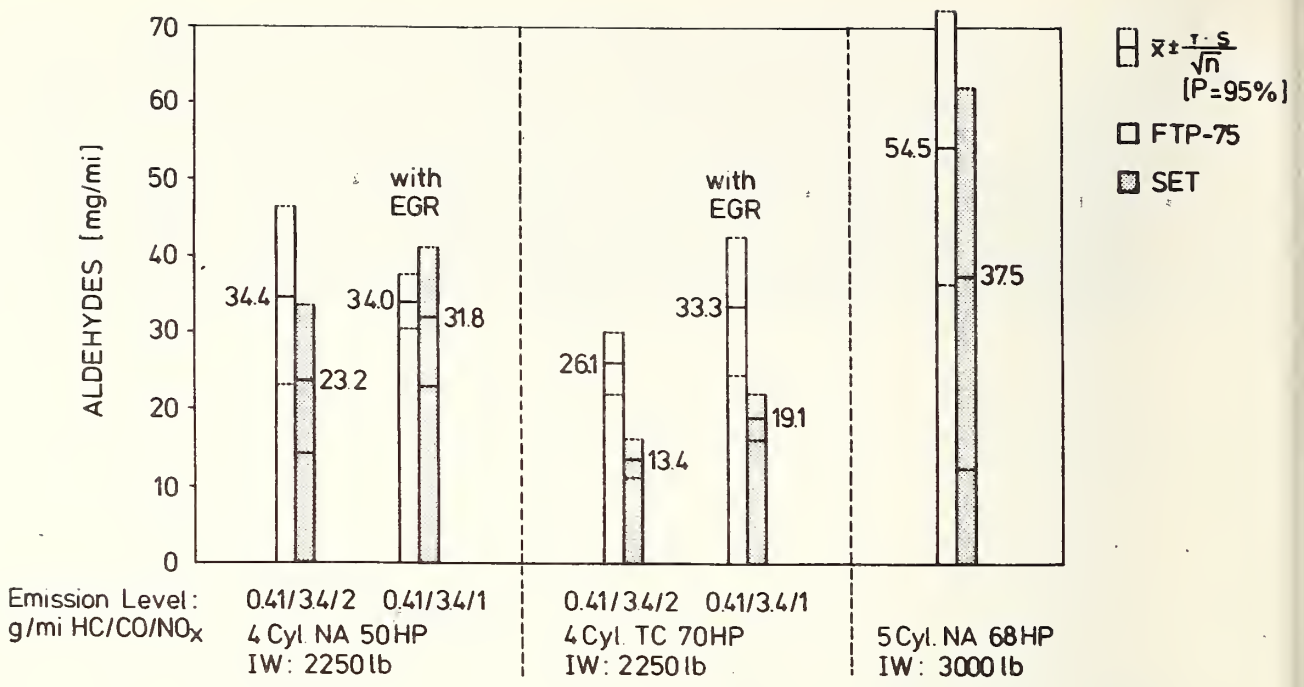

FIGURE 1.3-19: ALDEHYDE EMISSIONS

1.3.4.4 Consumer Acceptability

All engine/vehicle systems had been tested under a wide range of operating environments in order to establish their performance, startability, noise, driveability, durability, fuels and lubricants, and maintenance.

Performance

The performance of the vehicles studied were described by the following parameters (values in parentheses show the assumed restrictions):

- Acceleration time from 0 to 60 mph (less than 20 seconds)
- Time for performing a passing maneuver between 30 and 70 mph (less than 25 seconds)
- Top speed (not less than 75 mph)
- Maximum gradeability in first gear (not less than 30%).

Figure 1.3-20 shows the relationship between fuel economy, vehicle weight, acceleration time from 0 to 60 mph, and drivelines for vehicles with the 70 HP TD diesel engine.

Startability

At extremely low temperatures, the startability of diesel engines is limited by the self-ignition process. Preheating (all engines were equipped with glow plugs) provided good starting at low temperatures and minimum blue-smoke emissions. The engines tested were able to start at any temperature above -25°C (-12°F) provided that proper fuel is used. The so-called Cold Filter Plugging Point (CFPP) indicates the low-temperature properties of diesel fuel. The properties of winter-grade fuels have to be adapted to the prevailing geographical requirements. At temperatures below -25°C, it may be necessary to use auxiliary devices like starting fluids.

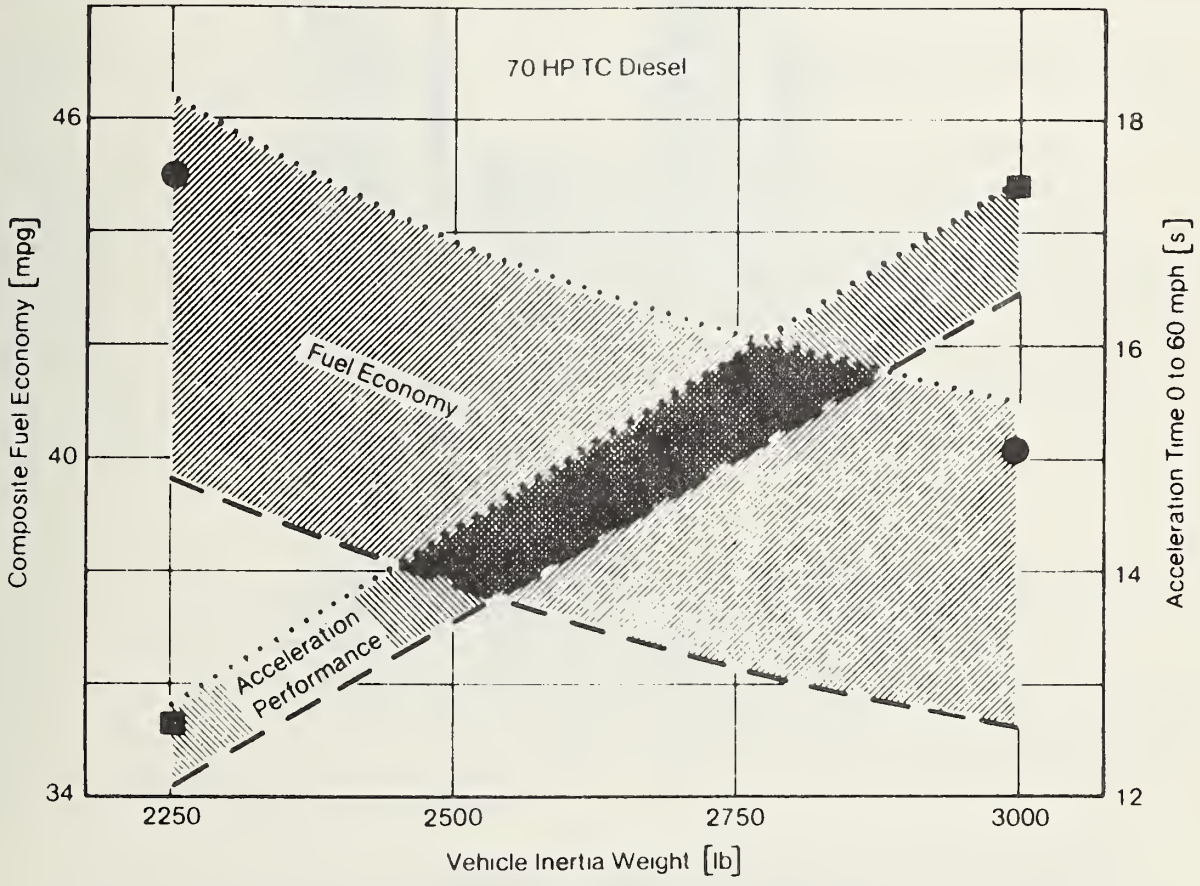

70 HP Turbocharged Research Diesel; Manual Transmission.
——— Limit for max. performance, top speed 75 mph, n/v = 66 rpm/mph.
···· Limit for max fuel economy, acceptable performance, n/v = 38 rpm/mph.
● Fuel economy for recommended n/v = 50 rpm/mph.
■ Acceleration performance for recommended n/v = 50 rpm/mph.
The figures may vary by ± 2 mpg and ± 0 5 sec

FIGURE 1.3-20: FUEL ECONOMY AND ACCELERATION PERFORMANCE AS A FUNCTION OF DRIVETRAIN RATIO AND WEIGHT.

Noise

The main noise emission results are summarized in Figure 1.3-21. Due to the noise reducing property of EGR and the lower engine speed for the turbocharged version, the noisiest engine/vehicle systems are those with naturally-aspirated engines. However, there is no significant difference from gasoline engines during full-load acceleration.

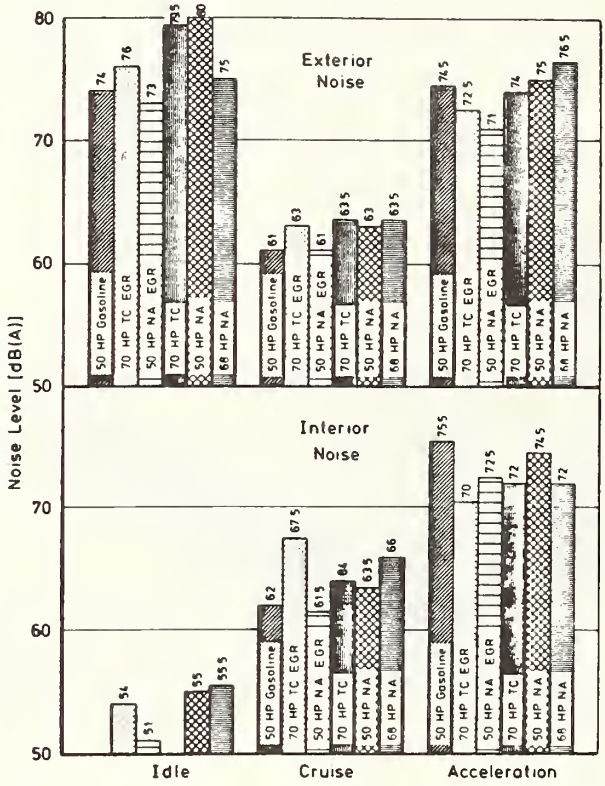

FIGURE 1.3-21: NOISE EMISSION BY VARIOUS ENGINE/VEHICLE SYSTEMS. Exterior noise at 50 ft. distance, 30 mph cruise or full-load acceleration from 30 mph; idle noise at 0.5 m from the vehicle front. The noise tolerance is ± 1 dB(A).

Driveability

Subjective driveability was tested in accordance with an applicable VW test procedure. Each vehicle was tested by a panel of skilled drivers who awarded merit points for the following characteristics:

- Startability: Number of successful cold-starts in proportion to the total number of trials.

- Idling Quality: Assessment of the smoothness of engine operation as judged from the driver's seat.

- Noise: Subjective driver evaluation.

- Surge: Short, abrupt power fluctuations at any speed or load.

- Hesitation: A temporary lack of engine response to accelerator actuation.

- Pick-up Performance: Subjective driver evaluation.

- Acceleration Jolt: Jerks felt in the driver's seat due to excessively rapid engine response.

The scores ranged from 0 to 10 merit points. A minimum of 5 points was required for customer acceptance.

When plotted in the sequence of operating modes, the merit points for each characteristic resulted in a subjective driveability profile. The individual characteristics were evaluated separately because there is no clearly defined interrelationship between them that would permit totaling. Figure 1.3-22 shows driveability profiles resulting from high-altitude tests at 2,150 m (7,200 feet) and a temperature of roughly $0^{o}C$ ($32^{o}F$). It compares the driveability profiles from a diesel and a gasoline engine of the same output. The cold-running performance of the diesel engine was found to be more acceptable than that of the gasoline engine. There was no difference in the warm-up and warm-running phases.

Durability

Results from experiments at Volkswagen and from extensive durability tests performed prior to this contract were analyzed (300 cars equipped with the 50 HP 4-cylinder naturally-aspirated diesel engine, 1977 Rabbit and Dasher) show that diesel engines are, as expected, more durable than spark ignition engines. Volkswagen data from endurance dynamometer tests on engines running at full load over 83% of the test time showed that the service life of the 4-cylinder naturally-aspirated diesel engines could be twice as long as that of the spark ignition engines.

It is possible that the production design of the turbocharged engine versions may require some changes. These changes may include pistons, piston pin, cooling system and lubricants, mainly because of higher operating temperatures and higher peak pressures.

The results of EPA durability tests performed on the above fleet were analyzed in order to determine emission behavior as a function of service life. They established that the fuel economy and emissions of the naturally-aspirated diesel engines will remain relatively stable over 50,000 miles.

Fuels and Lubricants

We tested a broad variety of fuels, compositions differing in cetane number (45.7 to 54.5), aromatics content (17 - 28.4%), CFPP (+0 to -27°C) and end point (FBPP) (310 to 400°C) in cooperation with the oil industry. Based on this, we do not expect commercial U.S. Fuels to cause engine troubles. Using a multigrade lubricant based on SAE W 15 oil guarantees satisfactory cold-start behavior.

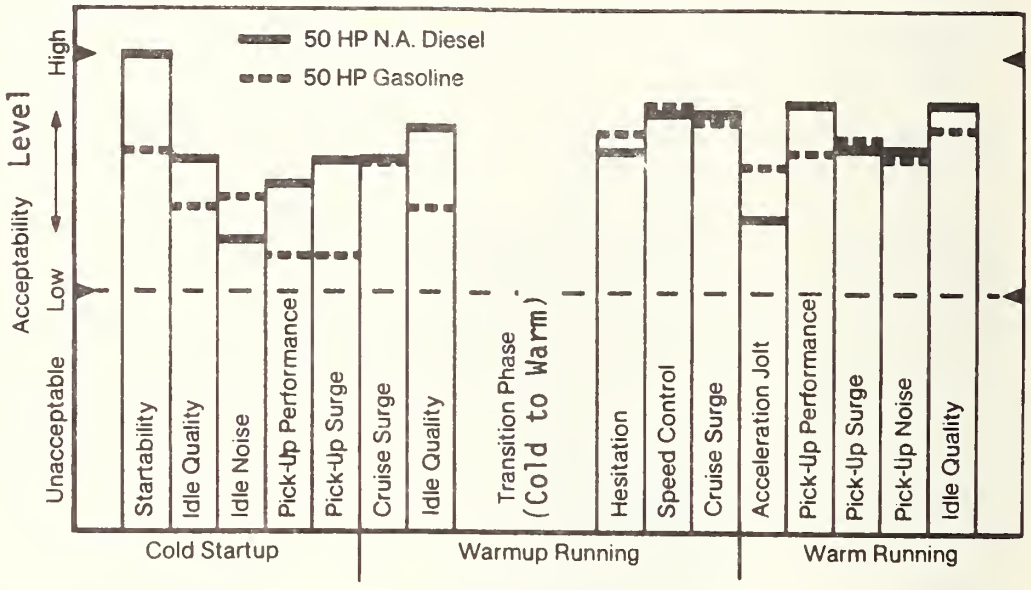

FIGURE 1.3-22: SUBJECTIVE DRIVEABILITY PROFILE.
50 HP diesel versus 50 HP gasoline Rabbit.
(Carbureted, not marketed in the U.S.A.)

The same lubricant can be used for both diesel and spark-ignition engines. Low oil pollution enabled us to set the oil cahnge intervals at 7,500 miles and the oil filter change interval at 15,000 miles. These intervals are the same as those in spark-ignition engines. The analysis of oil-viscosity-changes as a function of mileage indicates that they are minor because of low soot formation.

Maintenance

Compared to current diesel practice, these maintenance requirements are less demanding because of the low quantity of soot passed on to the lubricant.

The teeth-belt-drive design of the VW diesel engines facilitates economical maintenance because it is not elastic and does not need any lubrication.

1.3.4.5 Compatibility of Diesel Engines with Structures of Advanced Crashworthiness

Three typical vehicles were studied to determine the compatibility between light-weight automotive diesel power plants and frontal-impact crashworthiness at three safety levels:

- Current safety practice
- Current safety practice and 40 mph frontal impact
- Current safety practice and 45 mph frontal impact.

The typical baseline vehicles were:

- VW Rabbit (2,250 pounds inertia weight)
- VW Dasher (2,500 pounds inertia weight)
- Audi 100 (3,000 pounds inertia weight).

The approach used in the study was to keep the roominess index of the vehicles constant or variable and to determine the impacts of different engine/vehicle configurations and safety levels on other main vehicle characteristics such as:

- Vehicle weight
- Weight distribution
- Vehicle length
- Location of center of gravity
- Wheelbase
- Luggage capacity.

For our study we used the safety characteristics of the VW Passive Restraint System (shoulder belt and kneebar) for driver and front passenger. The characteristics of a three-point belt system were used for the rear passengers. Pre-loaders and force limiters were added to the restraint system for all tests in which higher impact velocities (40 and 45 mph) were used. It was assumed further that there would be no changes to the passenger compartment configuration. Therefore, there would be no change in the space used for occupant forward displacement. It should be noted that so far there is no documented proof of restraint system reliability in production cars at higher impact velocities (40 and 45 mph).

The selected weights and lengths shown in Table 1.3-4 (selected examples) were calculated on the basis of the above assumptions and reflect only the weight and length changes of the vehicle frontal structure.

TYPICAL VEHICLES / ROOMINESS INDEX	ENGINES	CURRENT SAFETY PRACTICE, GASOLINE ENGINE, BASELINE 30 MPH FRONTAL IMPACT		CURRENT SAFETY PRACTICE, DIESEL ENGINE 30 MPH FRONTAL IMPACT		CURRENT SAFETY PRACTICE, DIESEL ENGINE AND 40 MPH FRONTAL IMPACT		CURRENT SAFETY PRACTICE, DIESEL ENGINE AND 45 MPH FRONTAL IMPACT	
INCH		Length INCH	Weight KG LB	Length INCH	Weight KG LB	Length INCH	Weight KG LB	Length INCH	Weight KG LB
VW-RABBIT 260	FRONT ENGINE TRANSVERSE 4-cyl. naturally aspirated, 50 HP	154.57	825 1819	154.57	829 1828	156.54	831 1833	161.45	837 1846
	4-cyl. turbo-charged, 70 HP	154.57	825 1819	154.57	836 1843	156.54	838 1847	161.45	844 1861
VW-DASHER	FRONT ENGINE LENGTHWISE 4-cyl. turbo-charged, 70 HP	172.43	973 2145	172.43	985 2172	176.17	990 2183	182.07	998 2200
269	5-cyl. naturally aspirated, 66 HP	177.75	1019 2246	177.75	1034 2280	179.72	1037 2286	185.62	1045 2304
AUDI 100 276	FRONT ENGINE LENGTHWISE 5-cyl. naturally aspirated, 66 HP	191.31	1173 2586	191.31	1181 2604	191.31	1181 2604	193.30	1185 2613

TABLE 1.3-4: EFFECTS OF INSTALLATION OF THE STUDIED DIESEL ENGINE IN TYPICAL VEHICLES (CONSTANT ROOMINESS INDEX).

The studies at all three safety levels were based on the assumption that the deformation characteristic of the front structure of the vehicles was rectangular. Because of this assumption, higher impact velocities did not require any additional reinforcements to the sides of the vehicle or to the firewall, but necessitated a longitudinal extension of the energy absorbing zone with no changes to the beam cross sections and material thicknesses.

1.3.4.6 Application

An Integrated Research Volkswagen (IRVW) was built to demonstrate the compatibility and to point out the technical potential of a turbocharged diesel power plant, five-speed manual transmission with a vehicle of advanced safety features, high performance, acceptable emissions, and good fuel economy. The vehicle (Figure 1.3-23) was designed and built on the basis of the so-called ESVW II (Advanced Safety Vehicle). The general specifications of the IRVW are given in Table 1.3-5.

TABLE 1.3-5

IRVW GENERAL SPECIFICATIONS

Body type:	2-door hatchback
Overall length:	153.3 in.
Overall width:	63.4 in.
Overall height:	53.9 in.
Wheelbase:	94.5 in.
Curb weight:	2,070 lb.
Seating capacity:	4 persons
Engine and Drivetrain Specifications:	
Engine:	4-cylinder turbocharged diesel
Bore/stroke:	3.012/3.149 in.
Displacement:	90 cu. in.
Compression ratio:	23
Transmission:	5-speed manual
Gear ratios:	3.45, 1.94, 1.29, 0.97, 0.75
Axle ratio:	3.7

This vehicle integrates the ability to protect occupants in 40 mph frontal barrier crashes, to achieve 60 miles per gallon (composite cycle), to comply with the emission standards of .41/3.4/1.5 gram/mile HC/CO/NOx, and to accelerate from 0 to 60 mph in 13.5 seconds.

Figure 1.3-24 shows the fuel economy of the IRVW compared to the U.S. gasoline fleet of 1977 and Figure 1.3-24 illustrates the IRVW fuel economy at steady-state driving.

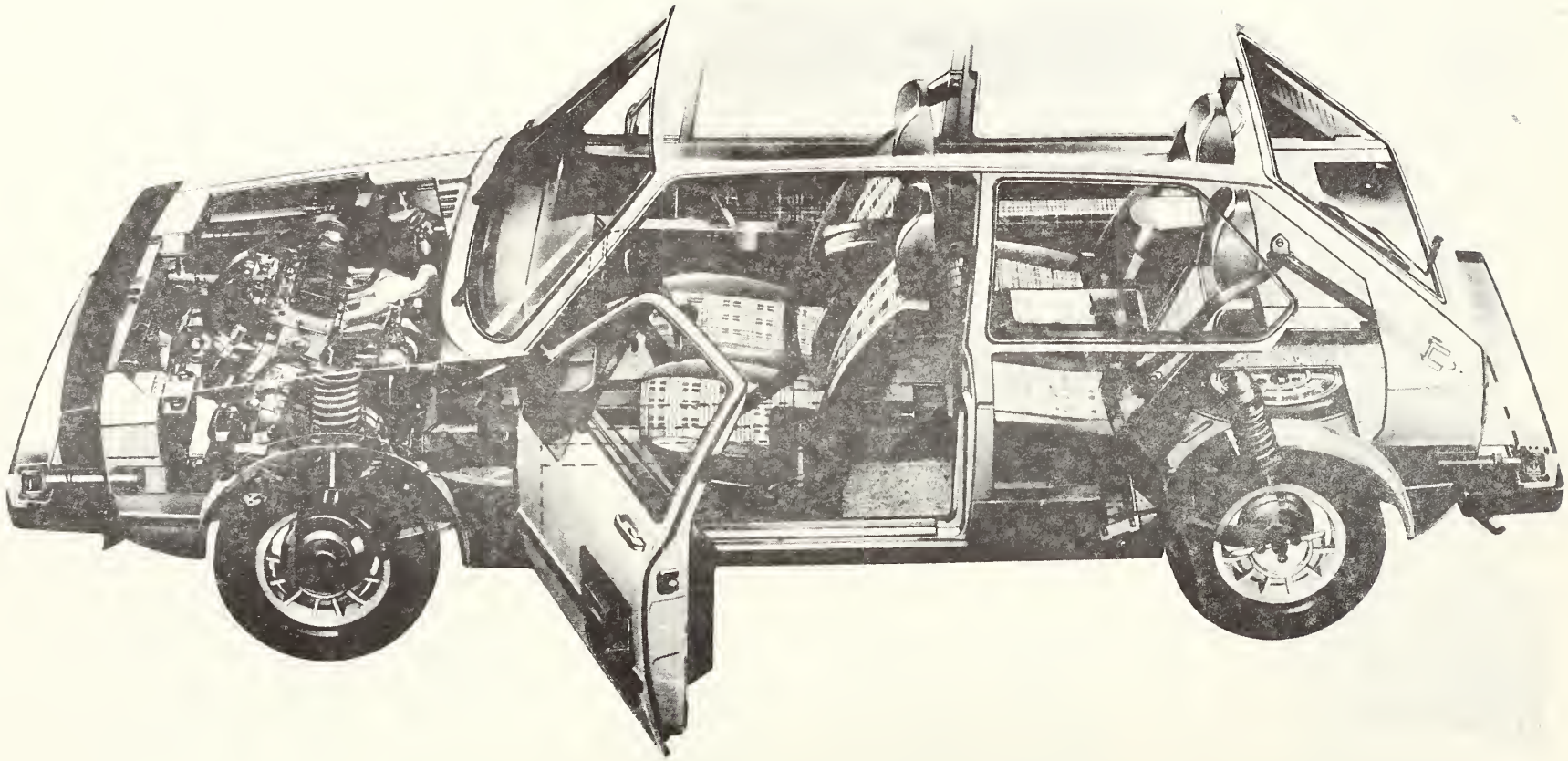

FIGURE 1.3-23: CUTAWAY VIEW OF THE INTEGRATED RESEARCH VEHICLE (IRVW)

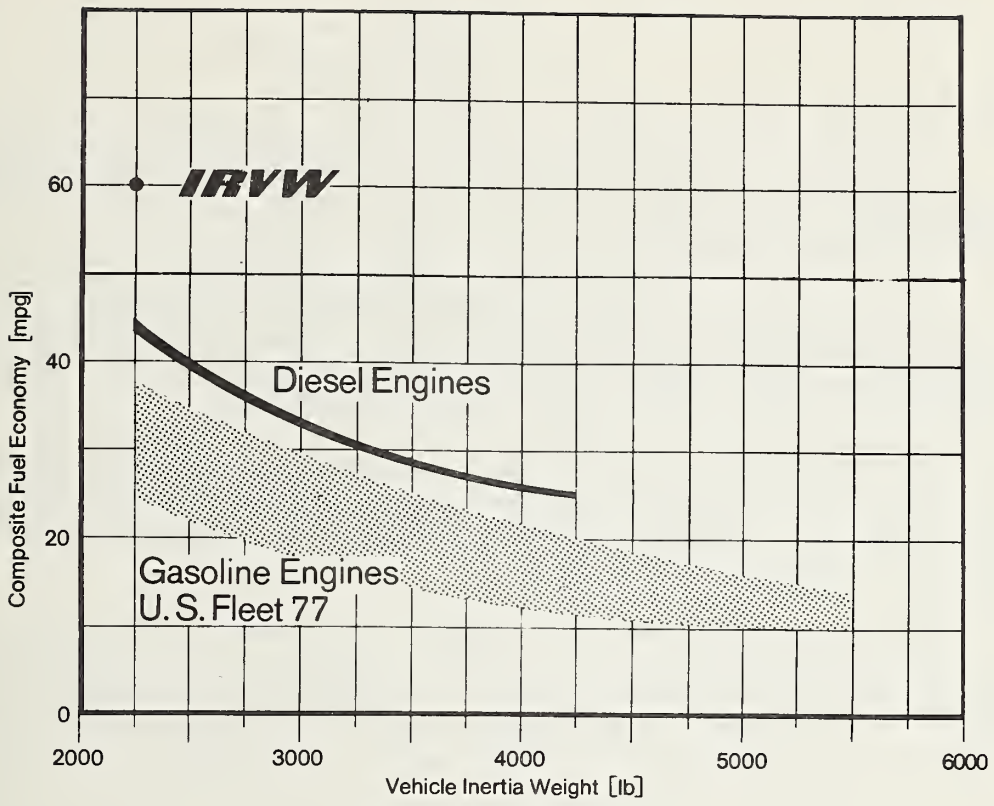

FIGURE 1.3-24: FUEL ECONOMY COMPARISON OF THE IRVW WITH CONVENTIONAL DIESEL ENGINES AND U.S. 1977 GASOLINE FLEET. Typical fuel economy at steady-state driving is shown in Figure 1.3-25.

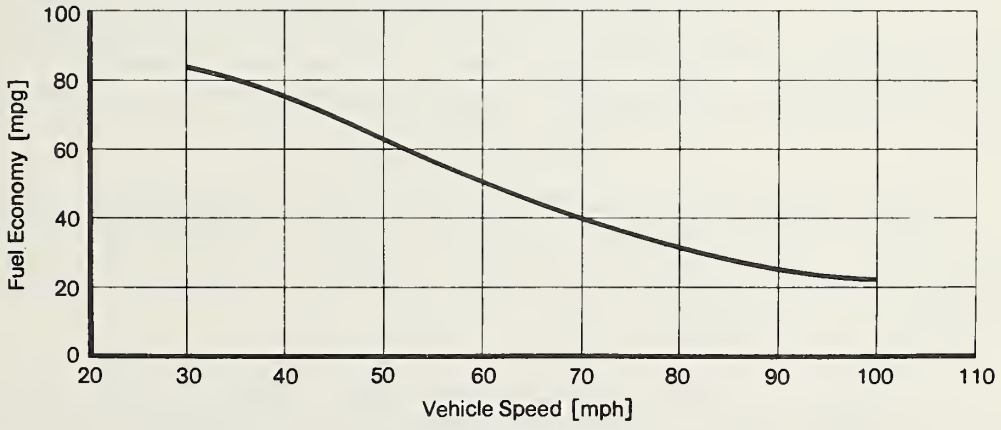

FIGURE 1.3-25: IRVW FUEL ECONOMY AT STEADY-STATE DRIVING.

2. INTRODUCTION

In recent years the conservation of natural resources has become increasingly significant, and the saving of energy is one of the primary objectives in this area.

The automobile is one of the major consumers of energy. This is illustrated by the fact that the U.S. passenger car population consumes roughly 30% of all crude oil used in the country. Therefore, saving energy in automotive applications is an important goal.

Efforts in this direction have led to fuel economy standards that decisively affect present and future automobile development in the U.S. through weight reduction, higher powerplant efficiency, and reduced aerodynamic and rolling resistance.

Futuristic concepts, such as gas turbines or the Stirling engine, are unlikely to meet the requirements for more efficient passenger-car powerplants in the foreseeable future. The conventional reciprocating piston engine will maintain its dominating position throughout the forthcoming decades. The percentage of diesel engines is expected to increase substantially in Europe as well as in the U.S., especially since the development potential for modern diesel engines has not yet been fully exhausted. The increase in the use of diesel engines in the U.S., however, depends on whether the diesel engine concept can ensure compliance with the future exhaust emission standards.

Despite the opposing trends of fuel economy and tighter emission constraints, the introduction of fuel economy standards has not led to any mitigation of emission standards.

The primary objective of the program covered by this report was to characterize the potential for fuel economy and emission reduction in light-weight automotive diesel power plants. Therefore, a family of light-weight diesel engines was established, and trade-offs were made between fuel economy, emissions, and consumer considerations.

The data base which was established covers passenger cars in the 2,000- to 3,000-lb. inertia-weight classes with diesel powerplants in the range of 50 - 100 HP. The effects of emission levels of .41/3.4/2.0 and .41/3.4/1.0 grams/mile of HC/CO/NOx on fuel economy, engine technolgoy, and consumer attributes were studied.

Volkswagen attributed particular significance to this program because it is an opportunity to offer competent and constructive contributions to the solution of the important problem of saving energy.

3. APPROACH

The program was broken down into nine main tasks in order to facilitate project structuring. A brief description of the approach to each task is submitted below:

(1) Preparation of a framework for engine layout and design and for the rationale of the diesel engine family

The framework was prepared with the assistance of Ricardo & Co., Ltd., England. Comparisons were made between direct fuel injection and two-stage combustion systems. The sensitivities and intercorrelations of the individual parameters are shown, and trade-offs are made between the two systems in regard to performance, emissions, fuel economy, noise levels, and startability. It is indicated that according to the present state-of-the-art, the swirl chamber diesel engine is particularly suitable for passenger-car application.

Investigations were conducted on injection timing, exhaust gas recirculation, water injection, and the use of ceramics in order to determine their effects on emissions in swirl chamber diesel engines. The effects were studied of the number of cylinders in a two-stage combustion diesel engine on specific performance levels in order to arrive at, and to offer a rationale for, the structure of the Volkswagen diesel engine family that is evaluated in this program.

(2) Engine Provision

Production, pre-production, and research prototype diesel engines were provided. Two engine families were established; the first one by varying the total displacement (i.e. increasing the number of cylinders), and the second one by varying the total displacement and adding a turbocharger.

The first engine family consists of four engines:

- 4-cylinder naturally-aspirated engine, 50 HP
- 5-cylinder naturally-aspirated engine, 68 HP
- 6-cylinder naturally-aspirated engine, 80 HP
- 8-cylinder naturally-aspirated engine, 100 HP (projections only)

The second engine family consists of two basic engines and two turbocharged versions:

- 4-cylinder naturally-aspirated engine, 50 HP
- 4-cylinder turbocharged engine, 70 HP
- 6-cylinder naturally-aspirated engine, 80 HP
- 6-cylinder turbocharged engine, 100 HP (projections only)

The second engine family permits a comparison between two different engine technologies - the naturally-aspirated and the turbocharged versions. The number of base engines can be minimized by turbocharging.

(3) Development of feasible technologies for compliance with the two gaseous emission levels of .41/3.4/2.0 and .41/3.4/1.0 g/m of HC/CO/NOx

Internal and external engine measures were studied in order to ensure compliance with the two emission levels and to determine the potential for emission reduction. The investigations of internal engine measures primarily deal with the sensitivities of combustion chamber geometry, injection timing and fuel delivery curve.

In the area of external measures, primary significance was attributed to the effects on emissions of exhaust gas recirculation (EGR), water injection, and the matching of the drivetrain to the engine. Technologies for the reduction of emissions, e.g. EGR, were established and evaluated. Steady-state engine maps showing the emissions are provided.

(4) Fuel economy as a function of engine, drivetrain, vehicle, emission levels, and consumer requirements

Three methods were used to generate the fuel economy data:

(a) Steady-state engine maps were prepared to characterize the engines. Investigations of engine/drivetrain/vehicle matches were performed in order to establish fuel economy and performance predictions for these combinations.

(b) Simulated dynamic engine/vehicle tests were conducted on engine dynamometers in order to ascertain the engine-map zones in which the engine operates during a test cycle. Engines were tuned, and projections were made of fuel economy and emissions.

(c) Chassis dynamometer tests were run in compliance with the applicable Federal Test Procedures in order to determine the actual fuel economy.

The fuel economy data is presented in the following formats:

- Steady-state engine maps showing the specific fuel consumption of each test engine

- Predictions of fuel economy and performance data for different engine/drivetrain combinations based on steady-state engine maps

- Fuel economy data from engine dynamometer tests. (Vehicle dynamics characteristics were computer simulated. The resulting engine speed/torque data was fed to AC pendulum-type dynamometers.)

- Dynamic engine maps identifying the fuel consumption at operating states during the test cycles

- Fuel economy data from chassis dynamometer tests in accordance with the applicable U.S. Federal Test Procedures.

(5) Determination of unregulated emissions

The unregulated exhaust emission data was generated for the following components: smoke, particulates, odor, sulfates, ammonia, aldehydes, and noise.

Two different methods were used to measure the smoke visibility: stained filter paper (Bosch numbers) and white-light absorption (Hartridge Smoke Units). The emissions of particulates were measured in the City Driving Cycle and in the Sulfate Emission Test (SET). The exhaust gas was passed through a Fluoropore filter, and the increase in weight of the dried filter element is a measure of the amount of particulate emission.

The odor emission data was obtained with a chemical method of odorant determination. Odorant samples were analyzed by Arthur D. Little, Inc.

Wet-chemical processes were employed in order to determine the amounts of sulfates, ammonia, and aldehydes. The engine/vehicle systems were tested on chassis dynamometers. The EPA City Driving Cycle (cold engine start) and the Sulfate Emission Driving Cycle (warm engine start) were used to obtain the sample.

Noise measurements were performed in accordance with SAE J 986a. In addition, exterior noise levels were measured at constant speed and idle. All measurements included interior noise level readings. Comparisons were made between the noise levels of diesel and gasoline-powered vehicles.

(6) Degree of modification required for the concept and design of diesel-powered automobiles for compliance with current and advanced safety standards

Preliminary design studies were carried out in order to arrive at an evaluation of the compatibility of diesel engines with light-weight vehicle structures of current and advanced crashworthiness. The effects were studied of different engine/vehicle configurations and safety levels on vehicle weight, roominess, and exterior geometry in front-, mid-, and rear-engine concepts at three safety levels (30, 40, and 45 mph frontal impact velocity).

(7) Evaluation of consumer attributes

The following characteristics were investigated, which essentially determine consumer acceptability of passenger cars: acceleration and passing performance, gradeability, startability, noise, driveability, durability, fuels and lubricants, and maintenance requirements, with a particular view to the broad range of operating conditions found in the U.S. The results of world-wide fleet tests and production data were included in the background information for the evaluation of durability, reliability, and maintenance requirements.

(8) Sensitivities, intercorrelations and trade-offs

The sensitivities and intercorrelations of the individual parameters were established. Trade-offs were indicated and performed.

(9) Application of diesel engines

A turbocharged diesel Rabbit with 4-speed manual transmission and an "Integrated Research Volkswagen" (IRVW) were used for the verification and demonstration purposes. The IRVW illustrates the compatibility of a turbocharged diesel engine with a 5-speed transmission with a vehicle of advanced crashworthiness. This combination provides excellent fuel economy, low emissions, good performance, and advanced safety.

4. LAYOUT AND DESIGN OF DIESEL ENGINES

4.1 REVIEW OF COMBUSTION SYSTEMS

The diesel combustion process is characterized by the fact that the injected fuel self-ignites in the compressed air once a sufficiently high temperature has been reached. Complete fuel combustion requires excess air and a thorough mixing of air and injected fuel. Insufficient mixing of fuel and air results in incomplete combustion, which produces smoke in the exhaust gas. The formation of soot during the combustion process limits the diesel engine performance.

We distinguish between direct injection and two-stage combustion depending on the fuel distribution and fuel/air mixture process. There are four basic types of combustion systems that could be considered suitable for passenger-car diesel engines. These types may be described as follows (Figure 4.1.-1):

(1) Direct injection, air distributing

(2) Direct injection, wall distributing

(3) Swirl chamber

(4) Pre-chamber.

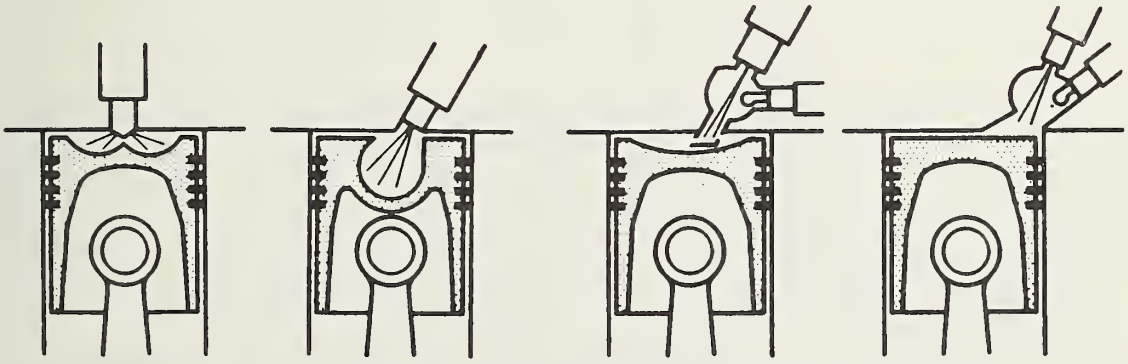

FIGURE 4.1-1: DIESEL COMBUSTION SYSTEMS (from left to right): Direct Injection, MAN-M-System, Prechamber, Swirl Chamber.

4.1.1 Direct Injection

The direct-injection diesel engine concept provides for a high injection pressure of the fuel (180 - 500 bar) into the open combustion chamber. The air-distributing process (Figure 4.1-2) provides for the formation of a combustible fuel/air mixture with the aid of multi-hole nozzles which distribute and atomize the fuel in the combustion chamber. High-speed engines frequently support the fuel/air mixture formation with the creation of an additional air swirl, e.g. by specially designed piston-head configuration,

masked valves, swirl inserts, or specially designed swirl intake ports. The tuning of the air motion with the aid of the air intake duct through the broad engine-speed range of a passenger car poses particular problems because the air swirl leads to a loss of volumetric efficiency, especially in the high-speed ranges.

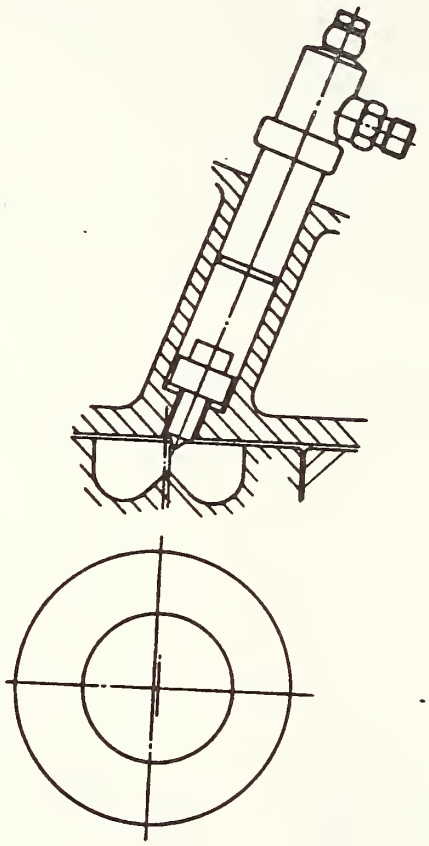

FIGURE 4.1-2: DIRECT INJECTION, AIR DISTRIBUTING

The direct-injecting engine with wall distributing (e.g. MAN-M-System, Figure 4.1-3) provides for the injection of the fuel into an open, spherical combustion chamber in the piston. A small portion of the fuel is atomized immediately in the intake air while the major portion of the fuel forms a film on or near the wall of the combustion chamber. The vaporizing fuel forms a rotating fuel/air mixture which burns completely and uniformly.

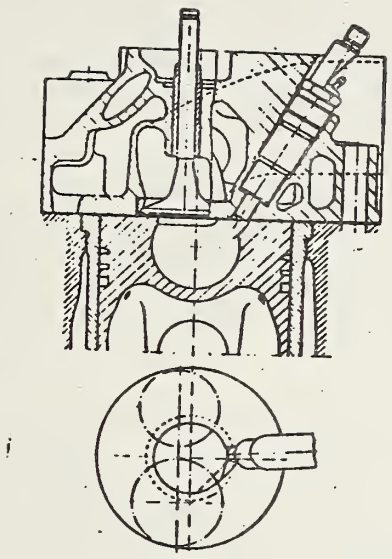

FIGURE 4.1-3: DIRECT INJECTION MAN-M-SYSTEM

4.1.2 Two-Stage Combustion

The design of the two-stage combustion diesel engine provides for a pre-chamber separate from the main chamber. Part of the intake air is moved into the prechamber during the compression process. Combustion starts upon the injection of fuel (at > 120 bar) into the pre-chamber. The combustion pressure forces the prepared and only partially burned fuel/air mixture into the main combustion chamber at high pressure where the unburned or only partially burned portions of the mixture are thoroughly swirled with the residual air in order to achieve complete combustion. This more thorough mixing of fuel with air permits a lower air/fuel ratio, i.e. the power output of two-stage combustion engines is higher than that of direct-injection engines. At the same time, the drive train is exposed to lower loads because the throttling effect of two-stage combustion lowers the peak pressures in the engine. This will lead to a higher fuel consumption, though, because the transfer of the gas from pre-chamber to main chamber entails energy losses, and the higher combustion chamber surface together with the high velocities in the throats lead to higher heat losses.

The swirl-chamber engine design (Figure 4.1-4) provides for a major portion of the air (approximately 50%) to be transferred into the swirl chamber during the compression process. One throat should be located tangentially in order to allow for precisely controlled air motion. This concept results in a well prepared fuel/air mixture during the injection process.

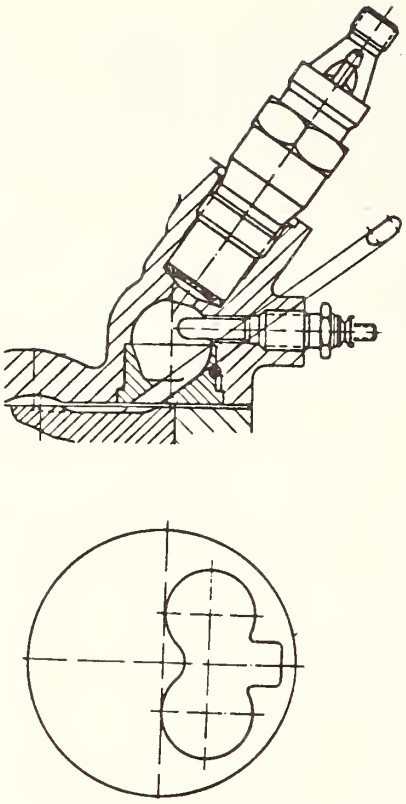

FIGURE 4.1-4: SWIRL CHAMBER

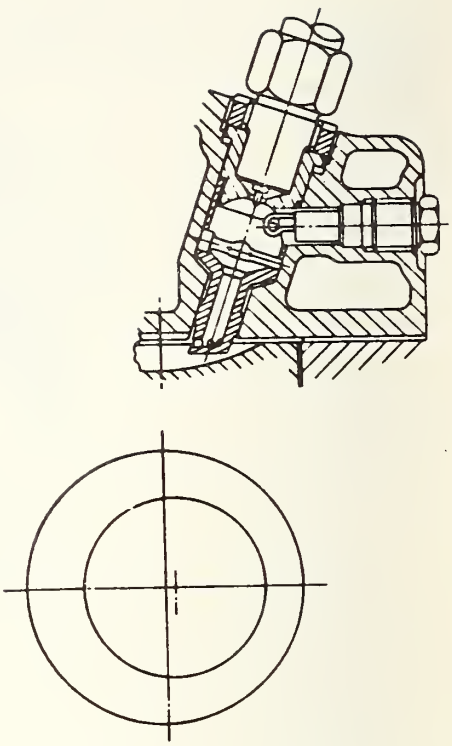

FIGURE 4.1-5: PRECHAMBER

The pre-chamber process (Figure 4.1-5) provides for the transfer of only 20 - 30% of the air into a pre-chamber, which is connected to the main chamber by one or several narrow bores. This system does not have a rotatory motion of air compared with the swirl chamber.

4.1.3 Trade-Off of Possible Combustion Systems

A trade-off between the following main parameters must be found for the selection of the combustion process for the specified application:

- Fuel economy
- Emission levels
- Noise levels
- Startability.

Consideration should also be given to production considerations and further development potential.

4.1.3.1 Performance

The performance restrictions imposed by smoke formation require a comparison between the various combustion processes at the same smoke level with a view to specific output and possible engine speed range. Engine speed ranges of up to 83 rev/sec (5,000 rpm) were reached with direct and indirect injection. It should be borne in mind that the most significant goal is not the engine maximum speed but the brake mean effective pressure (bmep) that is achieved over the entire engine speed range.

Figure 4.1-5 shows the markedly higher specific output produced by the swirl chamber process when compared with direct injection. This applies especially to the higher engine speed ranges. A direct-injection diesel engine would require roughly 15% more displacement in order to produce the same output. A pre-chamber engine, too, would require approximately 8% more displacement because of its lower specific output.

Compared with a direct-injection engine, the swirl-chamber engine provides for a higher degree of swirl. This results in a higher rate of air/fuel mixture preparation and thus a higher rate of burning. Since the swirl-chamber engine provides for better air utilization over a wide engine speed range (Figure 4.1-6), it produces a lower smoke level than the direct injection engine (Figure 4.1-7) and has a less linearly ascending smoke curve. This means that compliance with a given smoke limit entails a higher loss in performance of a direct-injection engine than that of a swirl-chamber engine. Figure 4.1-8 clearly shows the higher degree of smoke sensitivity of a wall-distributing direct-injection system compared with that of a swirl-chamber system. The superior air utilization of the swirl-chamber system indicates that even direct-injection engines with improved volumetric efficiency (e.g. optimized intake ports instead of masked valves) may continue to have an inferior performance level.

4.1.3.2 Fuel Economy

Direct-injection systems have lower compression ratios and thus markedly lower friction losses; pumping and heat transfer losses are lower, too. This advantage outweighs the lower degree of air utilization caused by smoke limitation.

The brake specific fuel consumption (bsfc) direct-injection systems, therefore, is 10 - 15% lower compared with two-stage combustion systems, especially during partial-load operation. Figure 4.1-9 shows a performance comparison made by Ricardo[3,4] between a swirl-chamber engin and an engine modified for indirect injection. Figure 4.1-10 is a comparison between the motoring loss curves of these two engines. It is evident that the friction (fmep) of the direct-injection engine is lower by approximately .35 bar (5 psi) than that of the swirl-chamber engine.

Figure 4.1-11 shows the heat rejection to coolant in terms of heat energy. The heat rejection in swirl-chamber engines tends to be between 1.1 and 1.4 times the maximum engine output, compared with .6 or .7 in direct-injection engines.

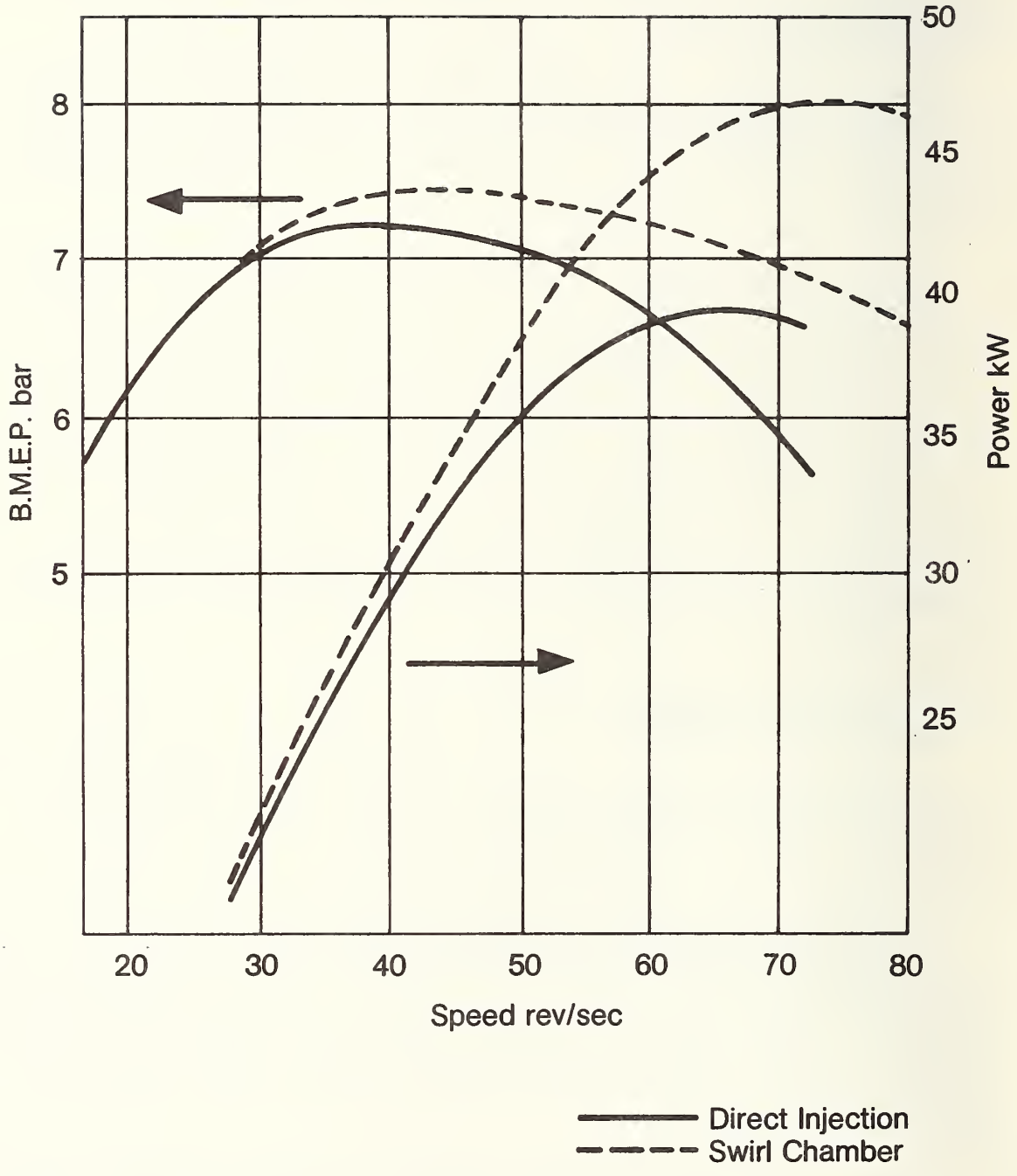

FIGURE 4.1-5: COMPARISON, DIRECT INJECTION VERSUS SWIRL CHAMBER

Source: Ricardo Test Results

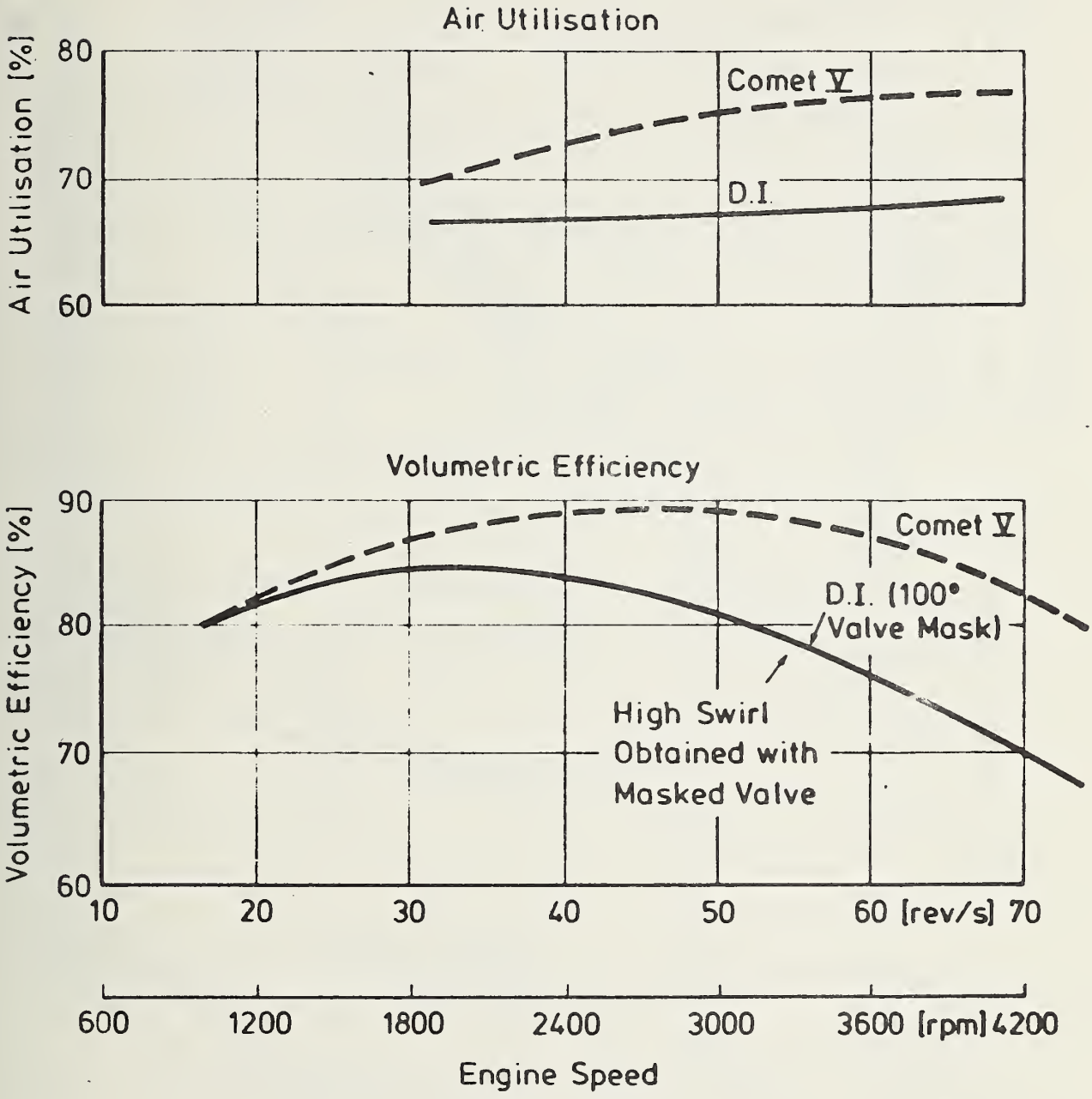

FIGURE 4.1-6: 2-LITER D.I. CONVERSION COMPARISON OF D.I. AND COMET V CHAMBERS ON THE BASIS OF AIR UTILIZATION AT B.S. SMOKE LIMITS

$$\text{Air Utilization} = \frac{\text{Stoichiometric Air/Fuel Ratio}}{\text{Air/Fuel Ratio at B.S. Smoke Level}}$$

Airflow Measured by Viscous Airflow Meter at 4.83 bar B.M.E.P.

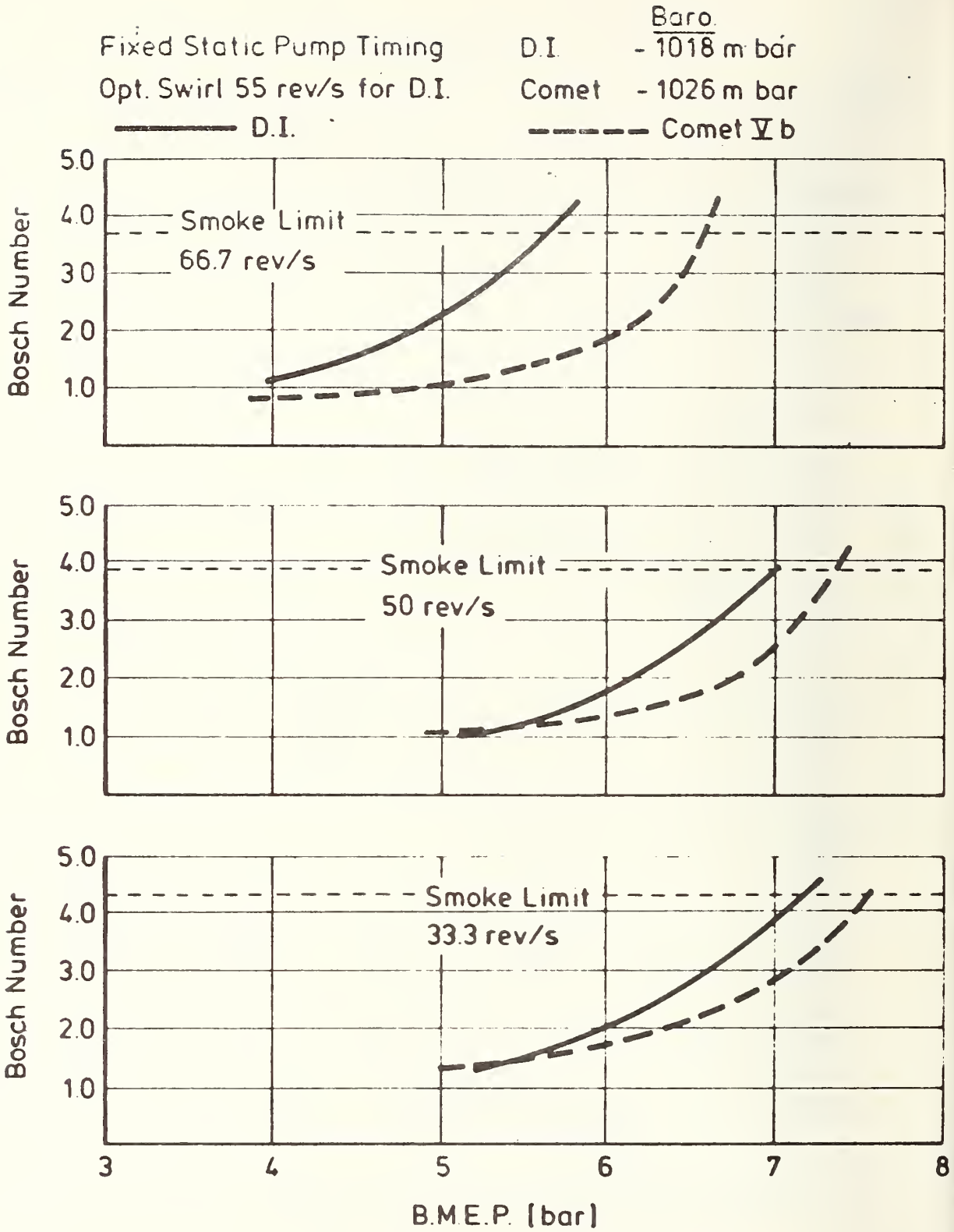

FIGURE 4.1-7: 2-LITER D.I. CONVERSION PERFORMANCE COMPARISON D.I. AND COMET V BUILDS EXHAUST SMOKE DENSITY MEASUREMENTS AT OPTIMUM CONDITIONS

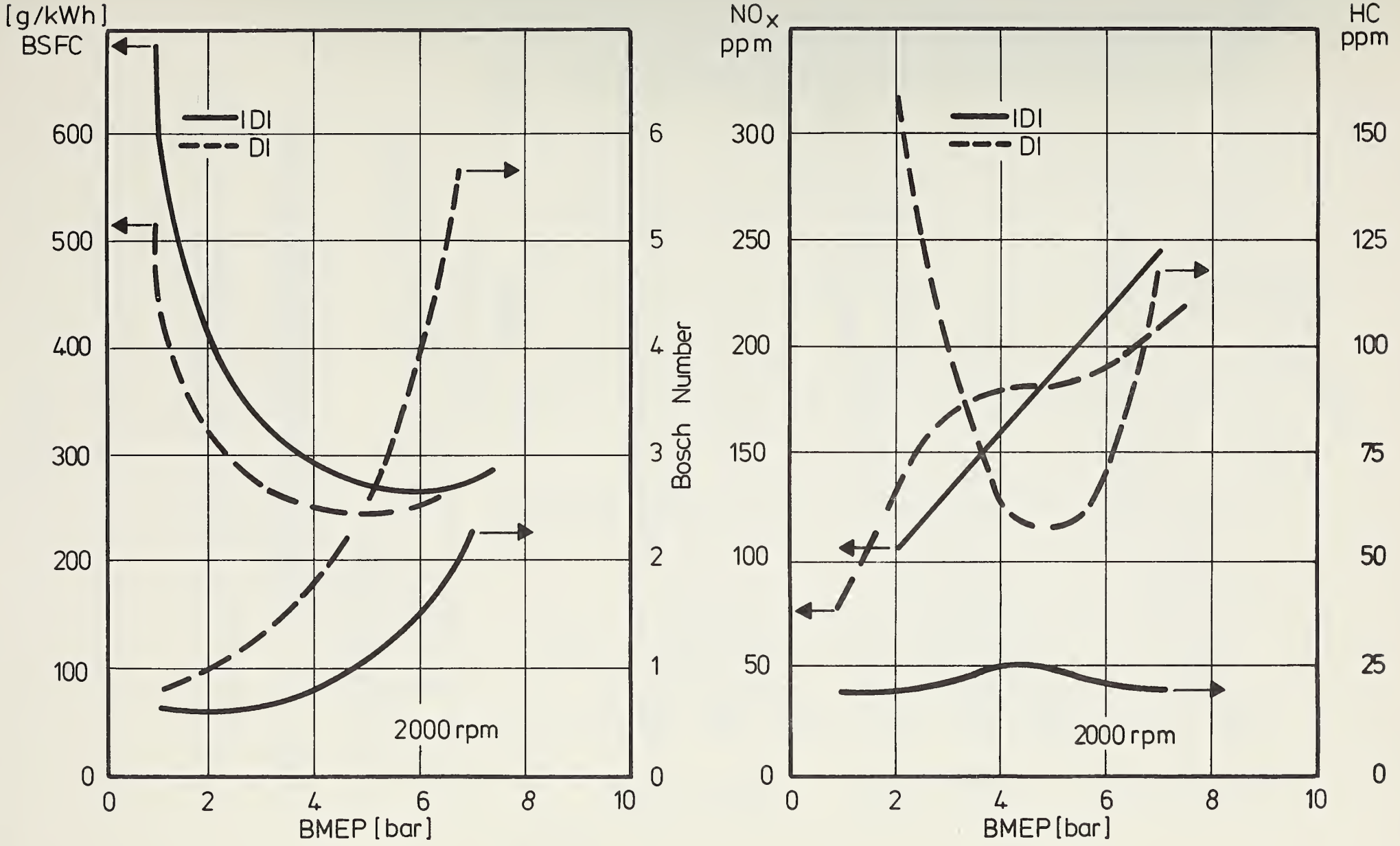

FIGURE 4.1-8: SPECIFIC FUEL CONSUMPTION AND EMISSIONS OF DIRECT INJECTION VERSUS INDIRECT INJECTION

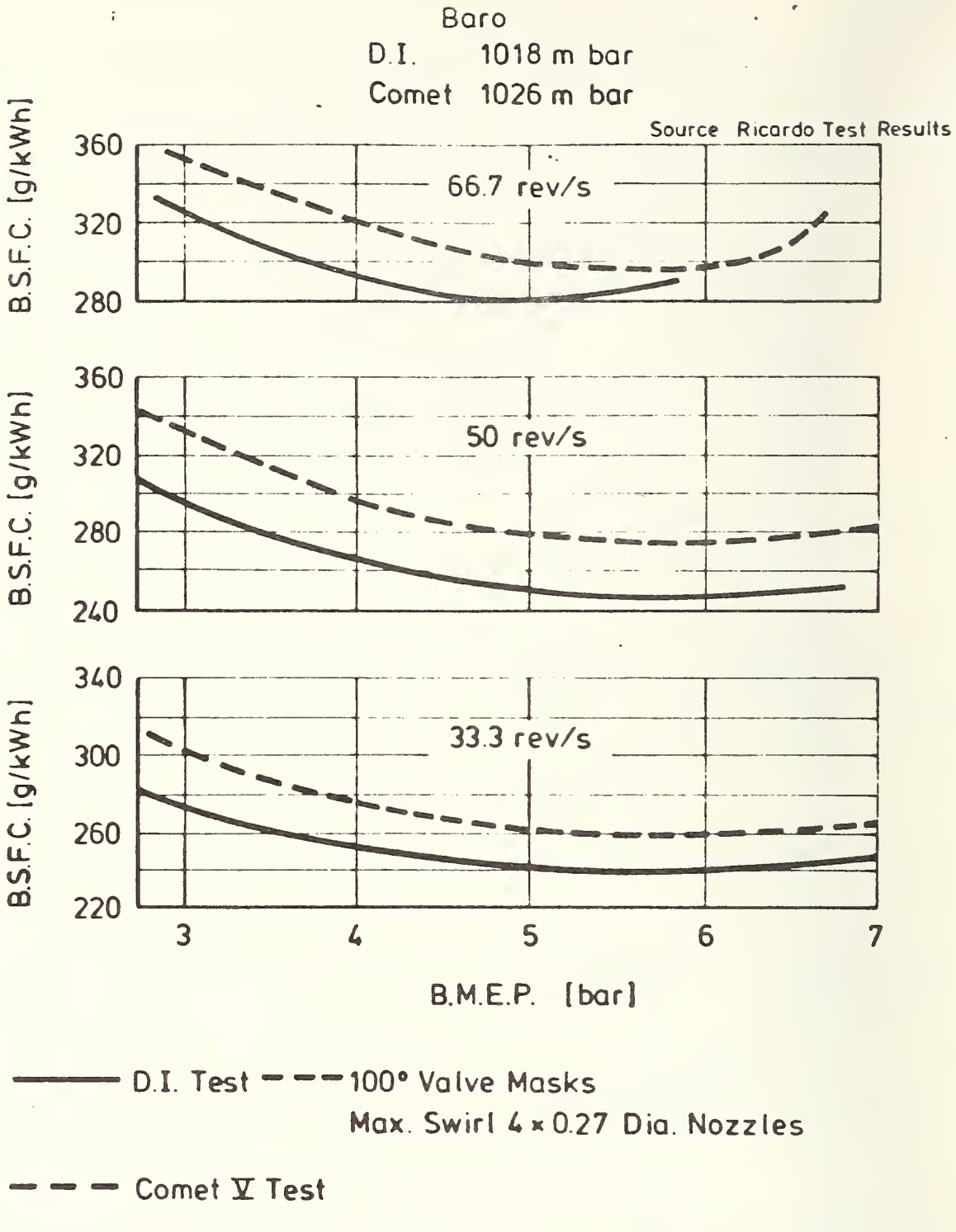

FIGURE 4.1-9: 2-LITER D.I. CONVERSION PERFORMANCE COMPARISON
D.I. AND COMET V BUILDS

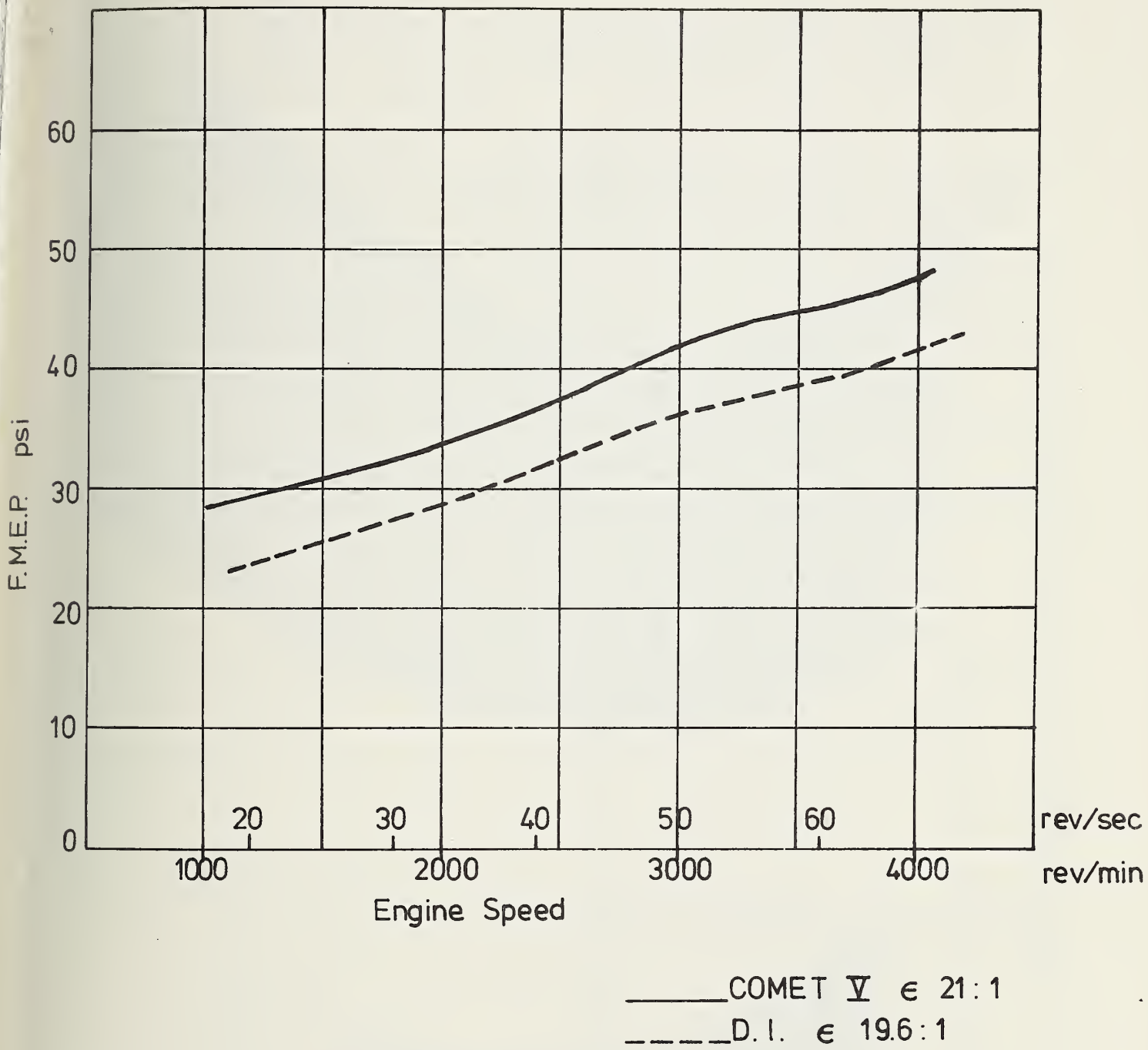

FIGURE 4.1-10: MOTORING LOSS CURVES FOR ENGINE IN SWIRLCHAMBER AND DIRECT INJECTION BUILDS

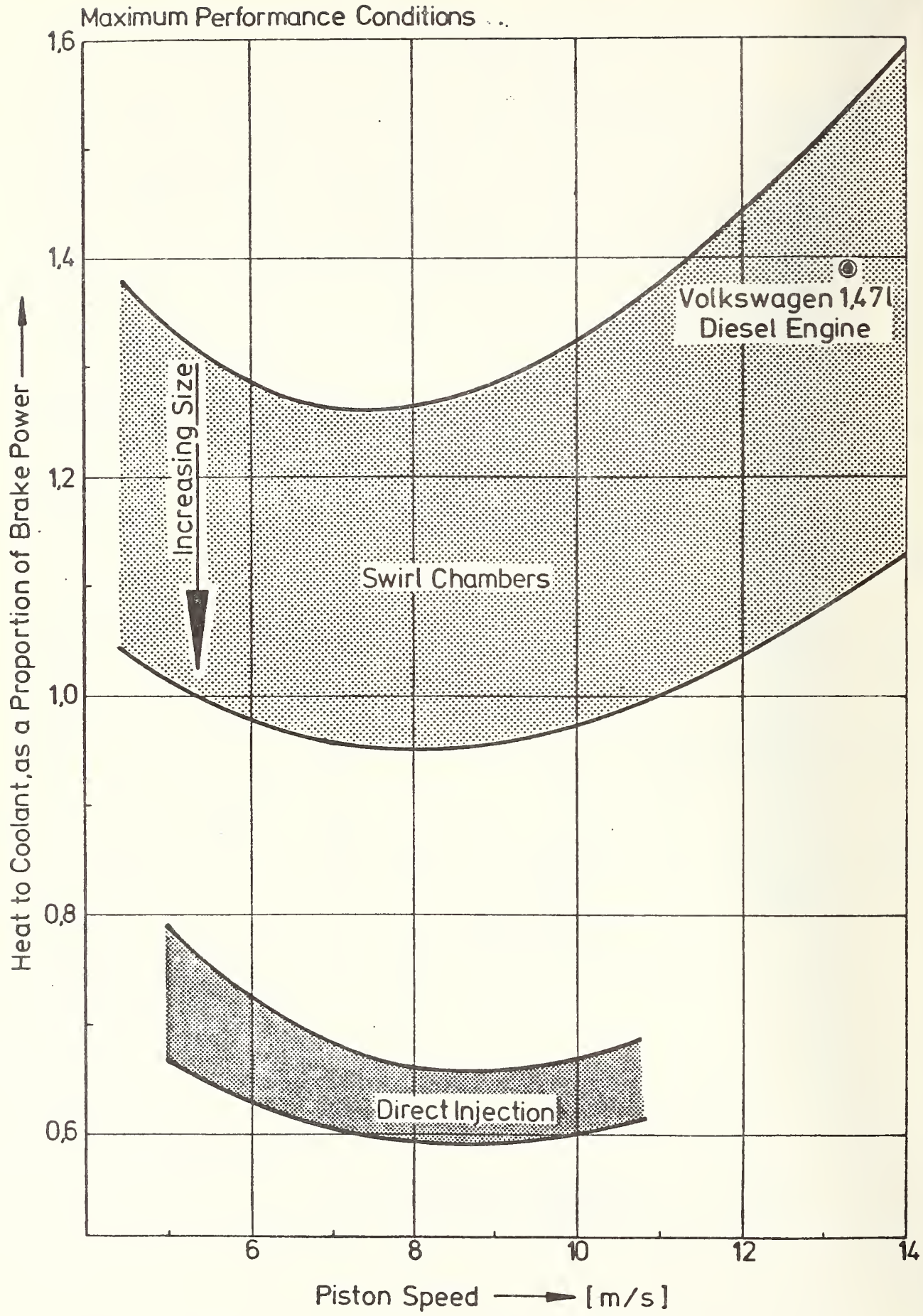

FIGURE 4.1-11: EFFECT OF PISTON SPEED ON HEAT REJECTION COOLANT

4.1.3.3 Emissions

Diesel combustion system emissions are largely determined by peak temperatures and rates of burning. The NOx emissions that have an exponential correlation with the flame front temperature are known to rise along with rising thermodynamic efficiency and thus display an opposing trend to that of the specific fuel consumption.

Swirl chamber engines have significantly lower NOx levels[5,6] than direct-injection engines, especially at lower engine speeds. The NOx concentration in these engines rises along with load and engine speed (Figure 4.1-12), while the NOx emissions of air-distributing direct-injection engines are rather independent of engine speeds but increase along with the load. The higher NOx emission levels from wall-distributing direct-injection engines also rise along with load and engine speed. Problems are posed by the control of HC emissions and odor development at low-load and idle operation because of the low wall temperature and the resulting low combustion temperature[7]. An increase in the share of air-distributed fuel and a more sophisticated injection system may lead to improved mixture formation and a faster rate of burning.

Retarded timing generally reduces NOx emissions in direct injection and two-stage combustion engines, but initially increases and later on decreases smoke formation (see Figures 4.1-13 and 4.1-14).[6]

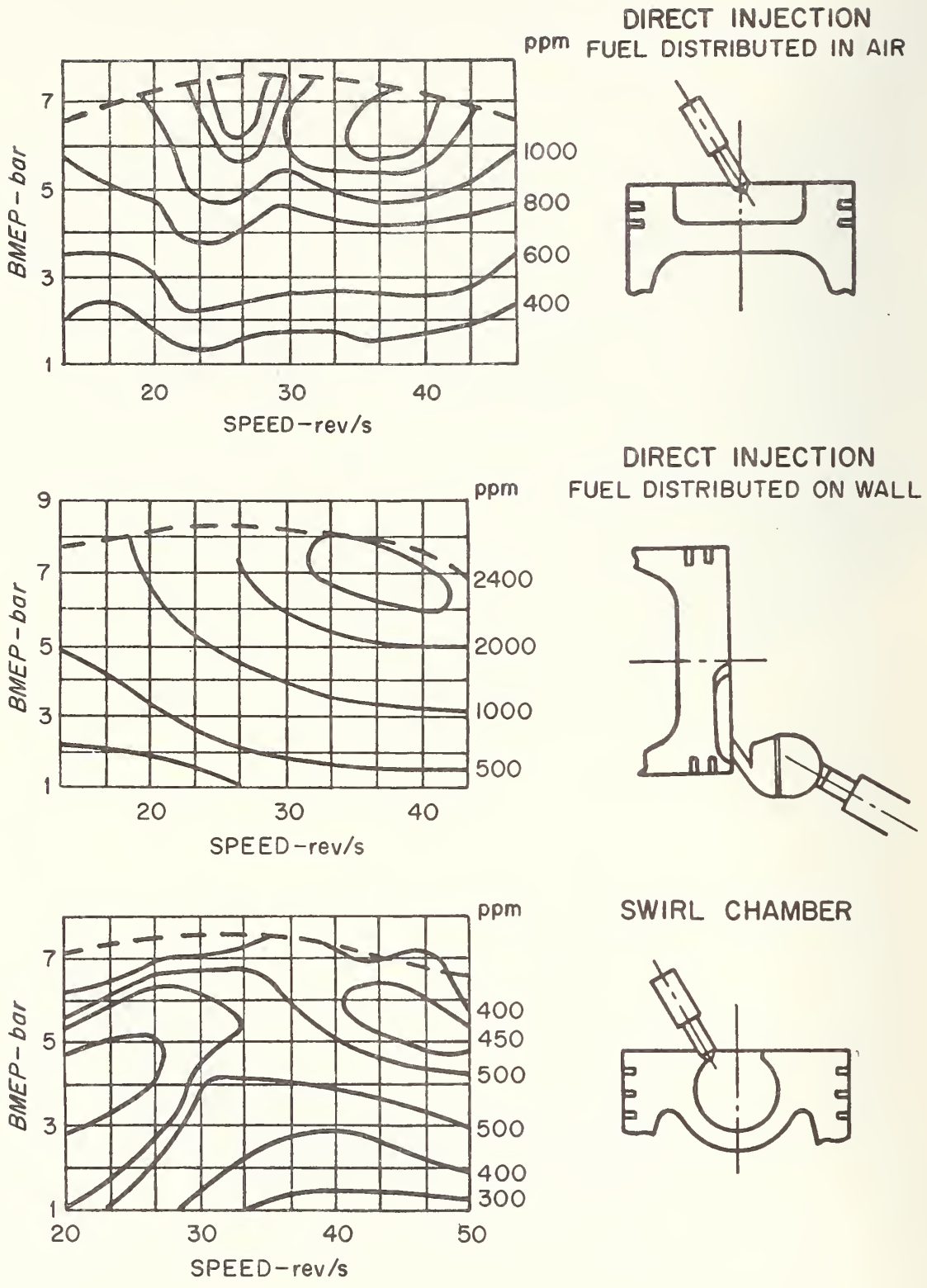

FIGURE 4.1-12: EFFECT OF COMBUSTION SYSTEMS ON NOx LEVELS

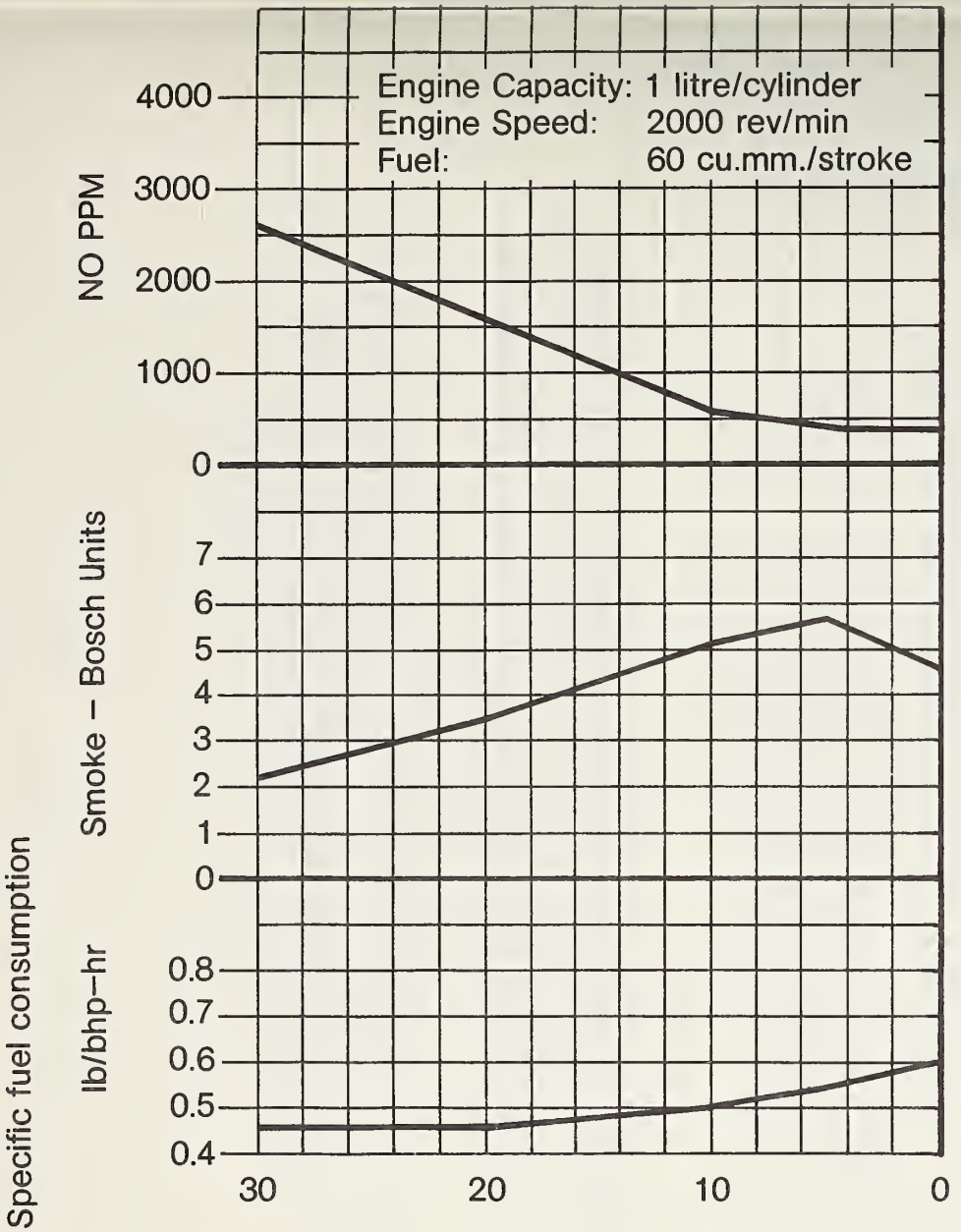

FIGURE 4.1-13: DYNAMIC INJECTION TIMING DEGREES BTDC

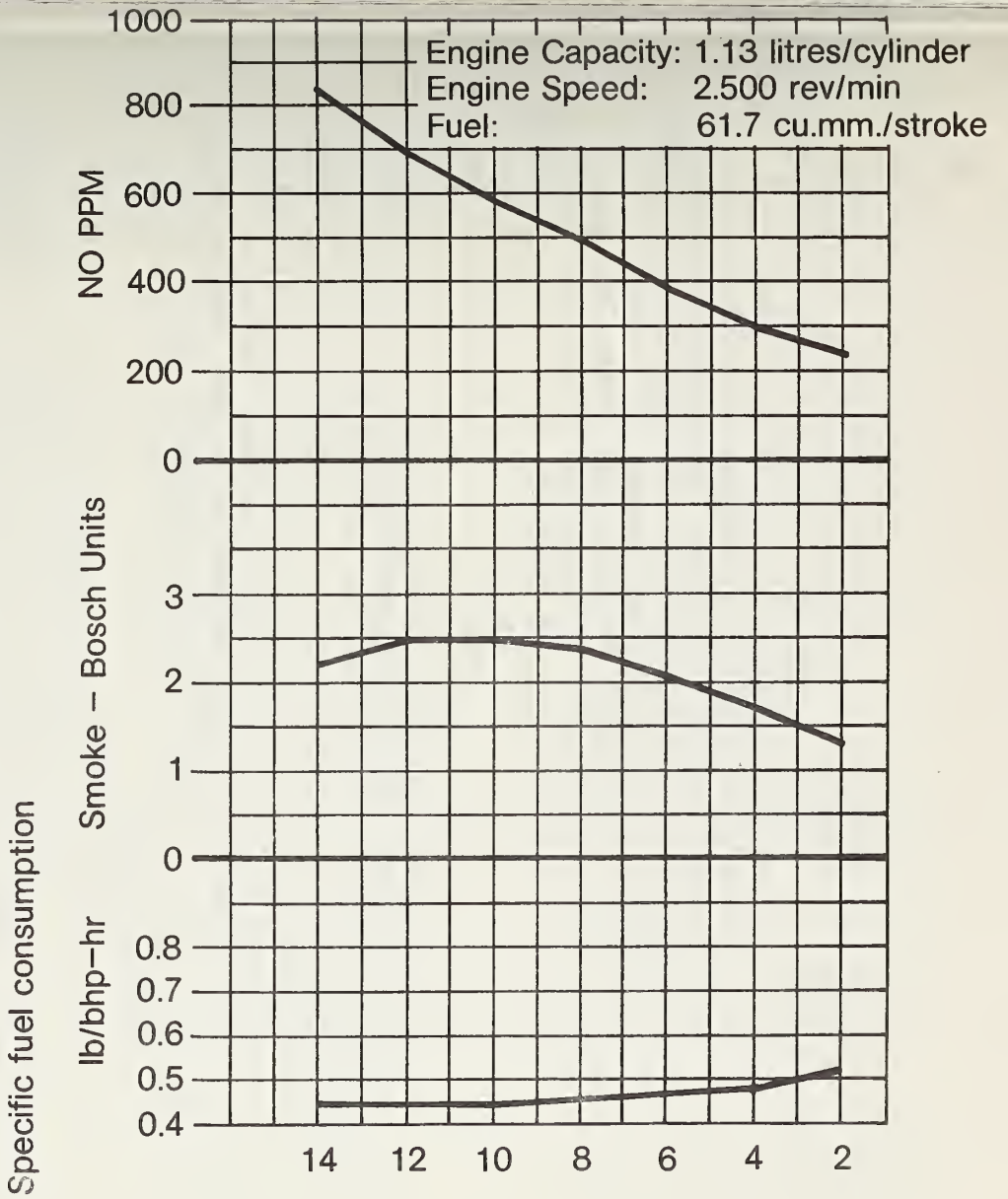

FIGURE 4.1-14: DYNAMIC START OF INJECTION DEGREES BTDC

The difference in smoke behavior between direct-injection and indirect-injection systems is caused by the differences in smoke formation. The smoke formation from direct-injection engines is affected primarily by the various compression temperatures while the smoke formation from swirl chamber engines mainly is affected by the air/fuel ratio. The fuel injection in direct-injection systems is more advanced for optimized specific fuel consumption because of the lower burning rate. Progressive retard reduces the difference in NOx levels due to the lower burning rate but results also in a negligible difference in the fuel consumption of direct-injection and swirl chamber systems (Figure 4.1-15). Recent publications indicate that direct-injection engines may permit low NOx emissions at good fuel economy[2].

4.1.3.4 Noise

Figure 4.1-16 shows the anticipated noise levels for direct- and indirect-injection (swirl chamber) systems[9]. Superimposed on this curve is the noise level of a pre-chamber engine. This last engine was already in a low emission build. The anticipated noise level for both turbocharged and naturally-aspirated versions of direct- and indirect-injection systems in the specified size range are shown in Figure 4.1-17. These curves show that indirect-injection engines run more quietly than direct-injection systems. While turbocharging reduces the noise level of direct-injection engines, it has little effect on swirl chamber systems. Problems are posed by the hard acceleration noise in the direct-injection engine.

Figures 4.1-18 and 4.1-19 show a breakdown of the contributing noise factors. The combustion process in an indirect-injection system is a major noise source at low engine speeds only, while it continues to be a predominant factor throughout the entire engine speed range in direct-injection systems. The strength of combustion noise is a function of the rise in cylinder pressure.

MAN-M system engines are expected to be quieter than conventional direct-injection engines because the fuel is injected against the wall of the piston which results in a lower rate of pressure rise. This is the reason why there is no pinging noise at idle and low load.

4.1.3.5 Startability

The unaided cold-start characteristics of direct-injection engines generally are better than those of indirect-injection engines, even though the former have a lower compression ratio. The adverse cold-start characteristics of the latter are due to the significant thermal losses that take place in the throat of indirect-injection systems.

While the direct-injection engines will start up without starting aids at temperatures as low as $0^{o}C$ ($32^{o}F$), indirect-injection engines require start-up aids such as heater plugs. These devices permit start-up at temperatures as low as $-25^{o}C$ ($-11^{o}F$) after having been energized for up to 30 seconds.

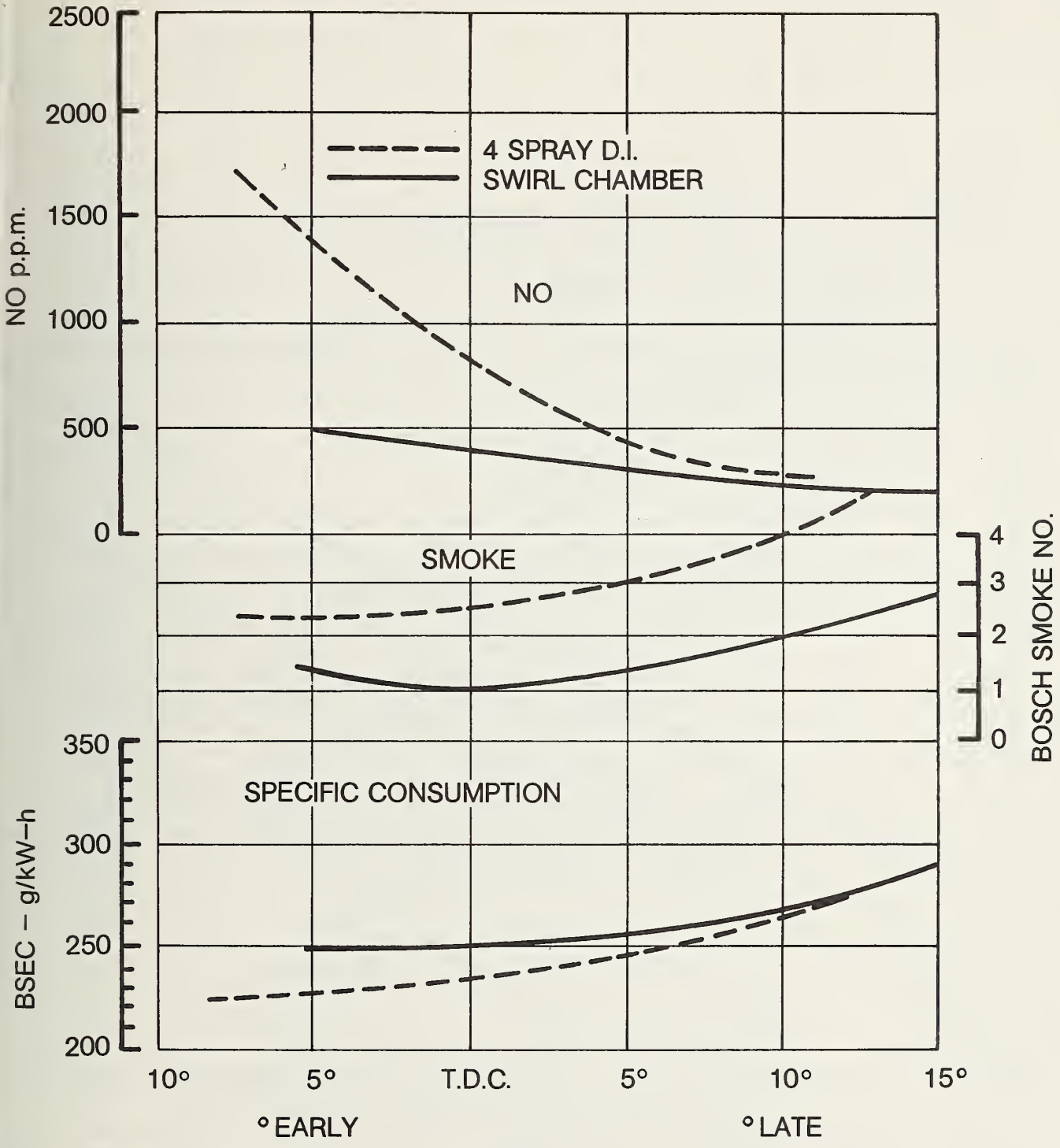

FIGURE 4.1-15: AVERAGE DATA FROM NATURALLY-ASPIRATED ENGINES AT 21:1 AIR/FUEL RATIO AND PISTON SPEED APPROXIMATELY 6.5 M/SEC.

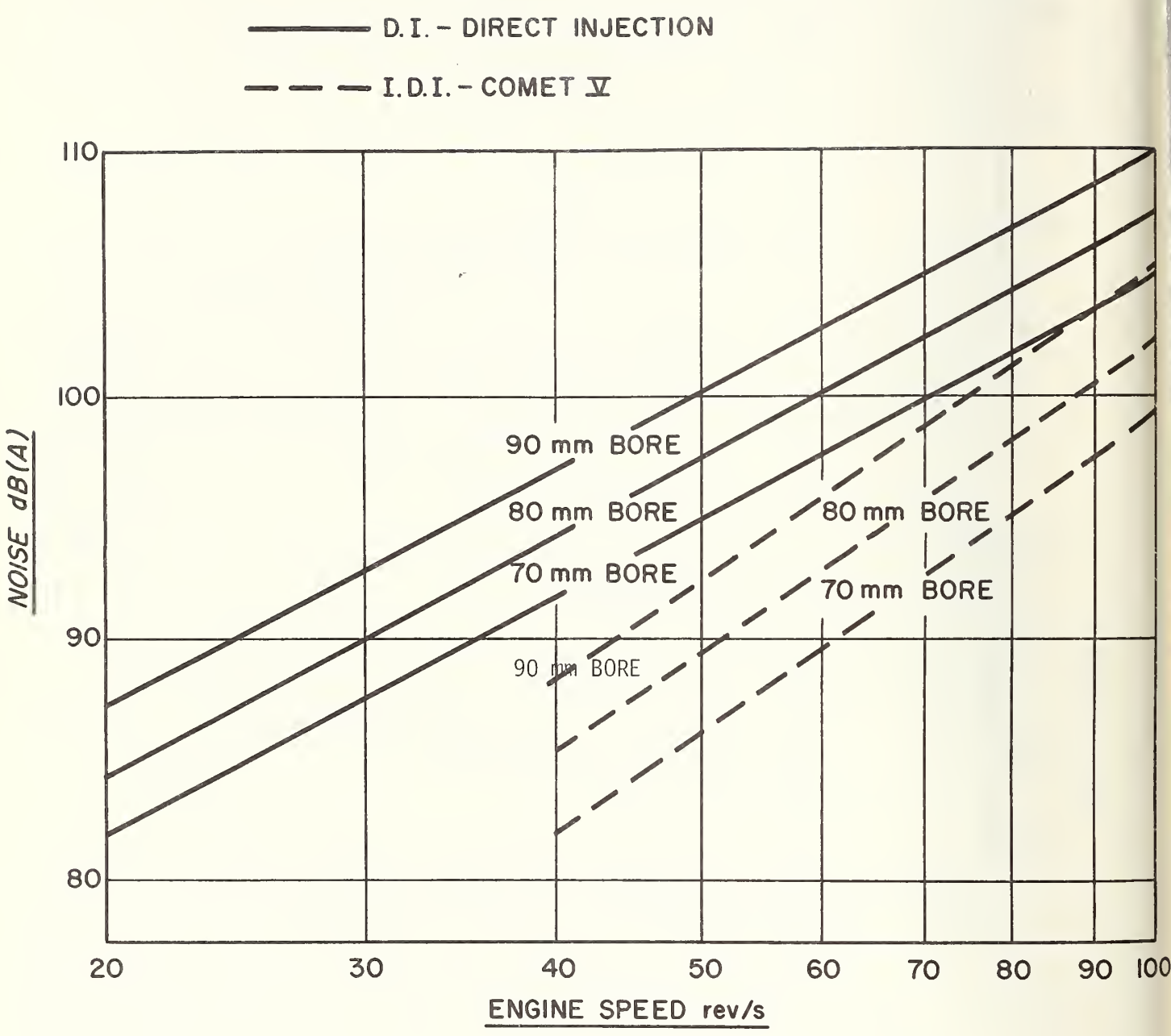

FIGURE 4.1-16: COMPARATIVE NOISE LEVELS FOR VARIOUS COMBUSTION SYSTEMS

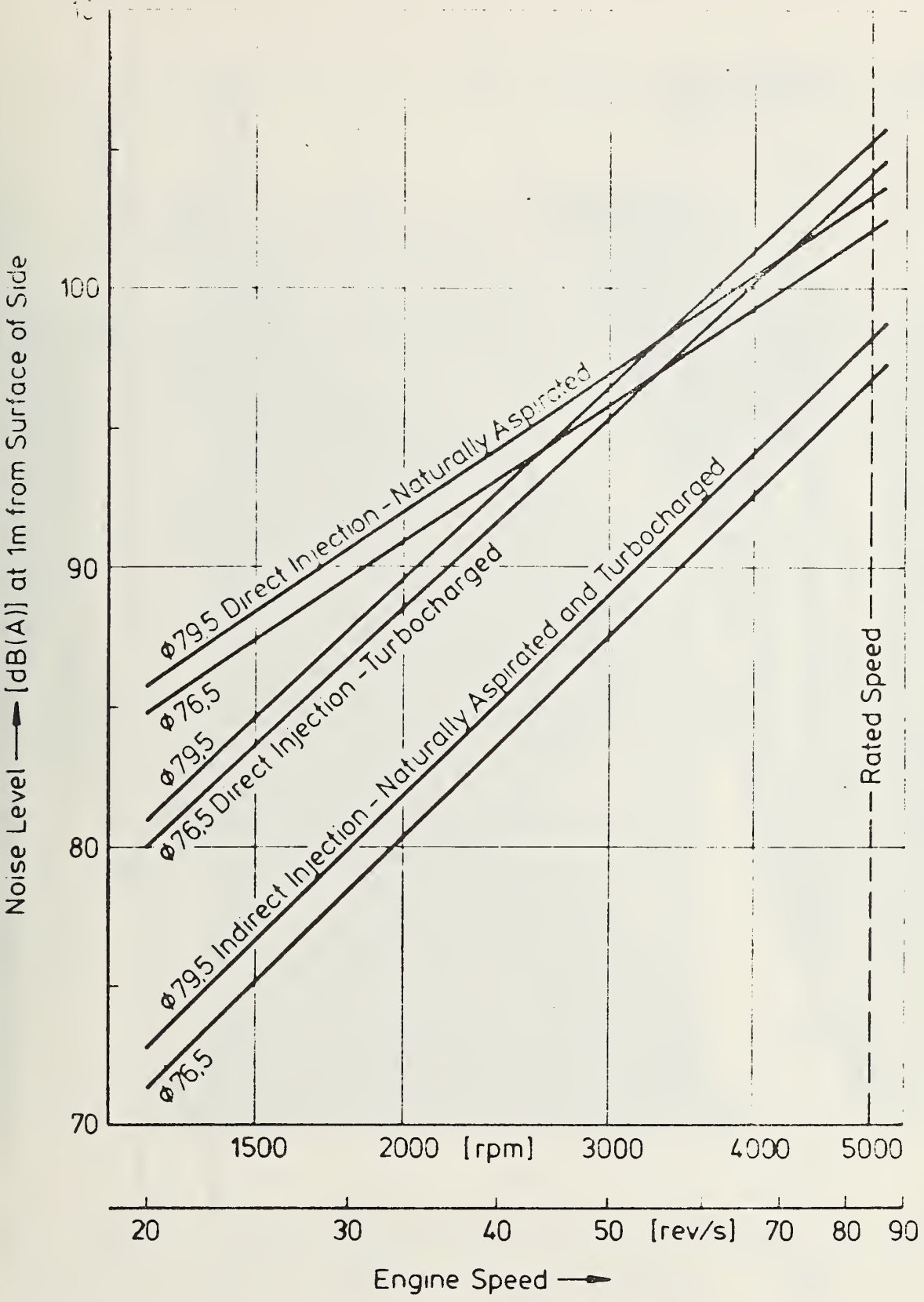

FIGURE 4.1-17: PREDICTED NOISE LEVELS FOR DIESEL ENGINES OF ϕ79.5 x 80 AND ϕ76.5 x 80 IN VARYING BUILDS AND RATINGS

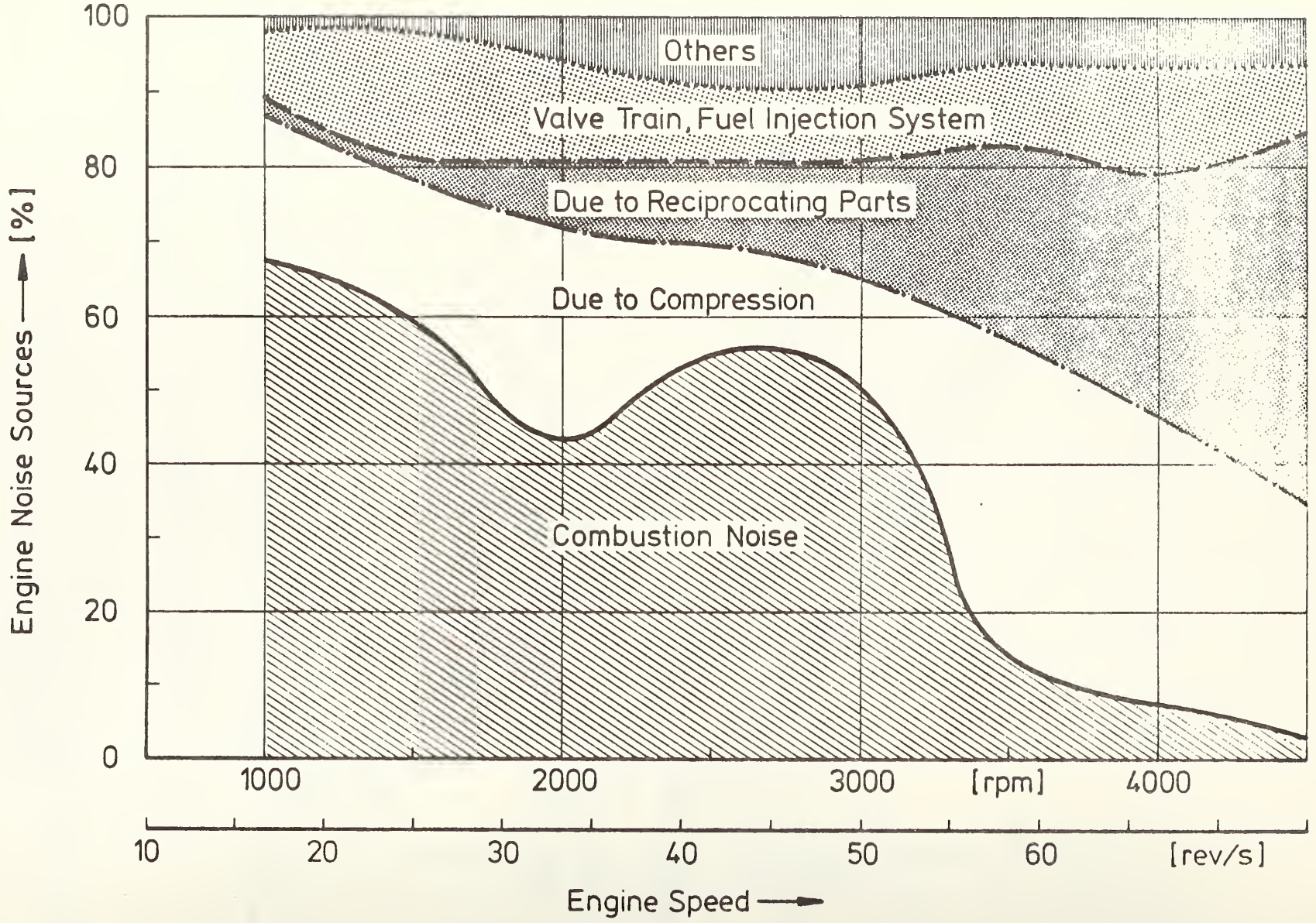

FIGURE 4.1-18: SOURCES OF NOISE IN SWIRL CHAMBER ENGINES

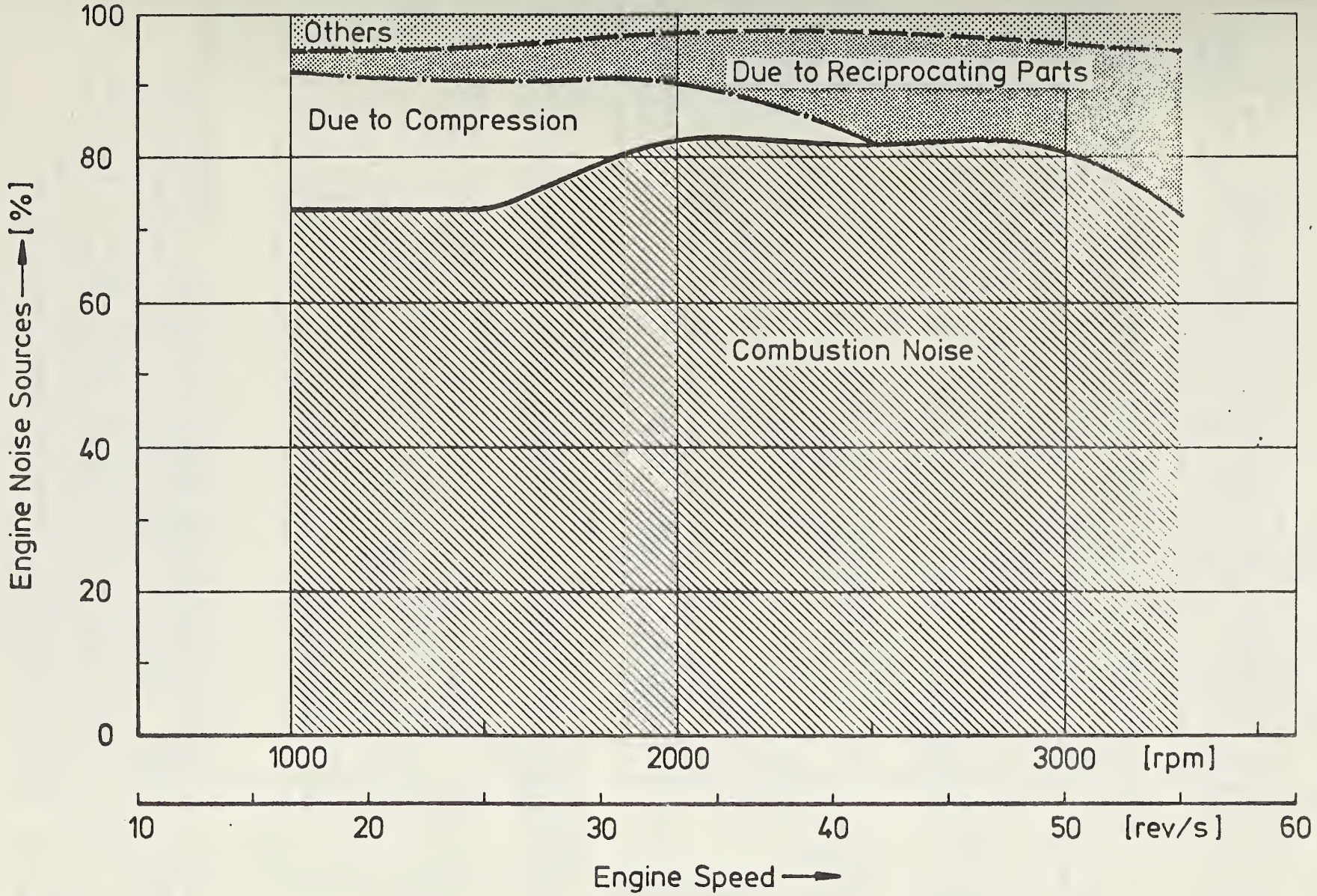

FIGURE 4.1-19: SOURCES OF NOISE IN DIRECT INJECTION ENGINES

4.1.3.6 Design Considerations

Figure 4.1-20 shows the maximum cylinder pressures for the various combustion systems throughout their entire engine speed range. These pressures can be changed by varying the injection timing. The values shown here are representative of engines optimized for performance. They ascend less steeply for engines optimized for emissions.

The higher thermal load of the indirect-injection engine should be controlled by careful design of the cylinder head, thickness of the lower cylinder-head deck, coolant flow through the valve bridge, and swirl-chamber configuration. The design configuration of the tuned intake ports poses problems for indirect-injection engines. Precise compliance with the port shape and position requirements in order to ensure the correct swirl level for the engine poses production problems. Satisfaction of the stringent emission standards also requires additional outlay in the area of injection equipment (e.g. timing, nozzles) in direct-injection systems because of their higher sensitivity to air/fuel mixture formation.

Close control of the compression ratio and piston-to-head clearance in diesel engines is required in order to ensure good startability and good performance and to eliminate contact between piston head and valves. Figure 4.1-21 shows the variances in compression ratios of direct- and indirect-injection engines in relation to tolerance build-up between the bottom face of the cylinder head and piston top. The real-life variances in indirect-injection engines might be greater because of combustion-chamber tolerance build-up. Because approximately 70% of the compression volume in the pre-chamber system is located in the space between piston crown and cylinder head, which compares with 50% in the swirl chamber engine, the piston-to-head clearance is greater; and its control is not so critical in pre-chamber engines.

The evaluation of engines with a cylinder unit displacement of approximately 400 cc resulted in the decision to use indirect-injection systems for the intended application. The findings of the evaluation are presented below.

The emission standards (CO < 3.4; HO < .41; NOx < 1.5) can be satisfied with two-stage combustion systems. Severe problems are posed in regard to compliance with these standards by direct-injection engines. The fuel consumption of a diesel engine can be reduced by 10 to 15% by direct injection if U.S. emission standards are disregarded. This advantage of the direct-injection system over the swirl chamber system is reduced to a mere slight improvement in fuel consumption when compliance with the U.S. emission standards must be ensured. Fuel economy could be improved more easily at low cost and without any development risks by simple gearbox modifications, e.g. the addition of a fifth gear.

It appears highly unlikely that during the next few years mass-produced passenger cars with direct-injection engines will be able to satisfy the stringent emission requirements at better fuel economy than the indirect-injection systems. The specific output of the air-distributing system becomes too low while the noise level rises too high. Wall-distributing systems, too, show a drop in output. Problems are also posed by the comparatively high emission and odor levels which are observed especially during low-load operation. Therefore, the direct-injection system should be used for commercial vehicle application only.

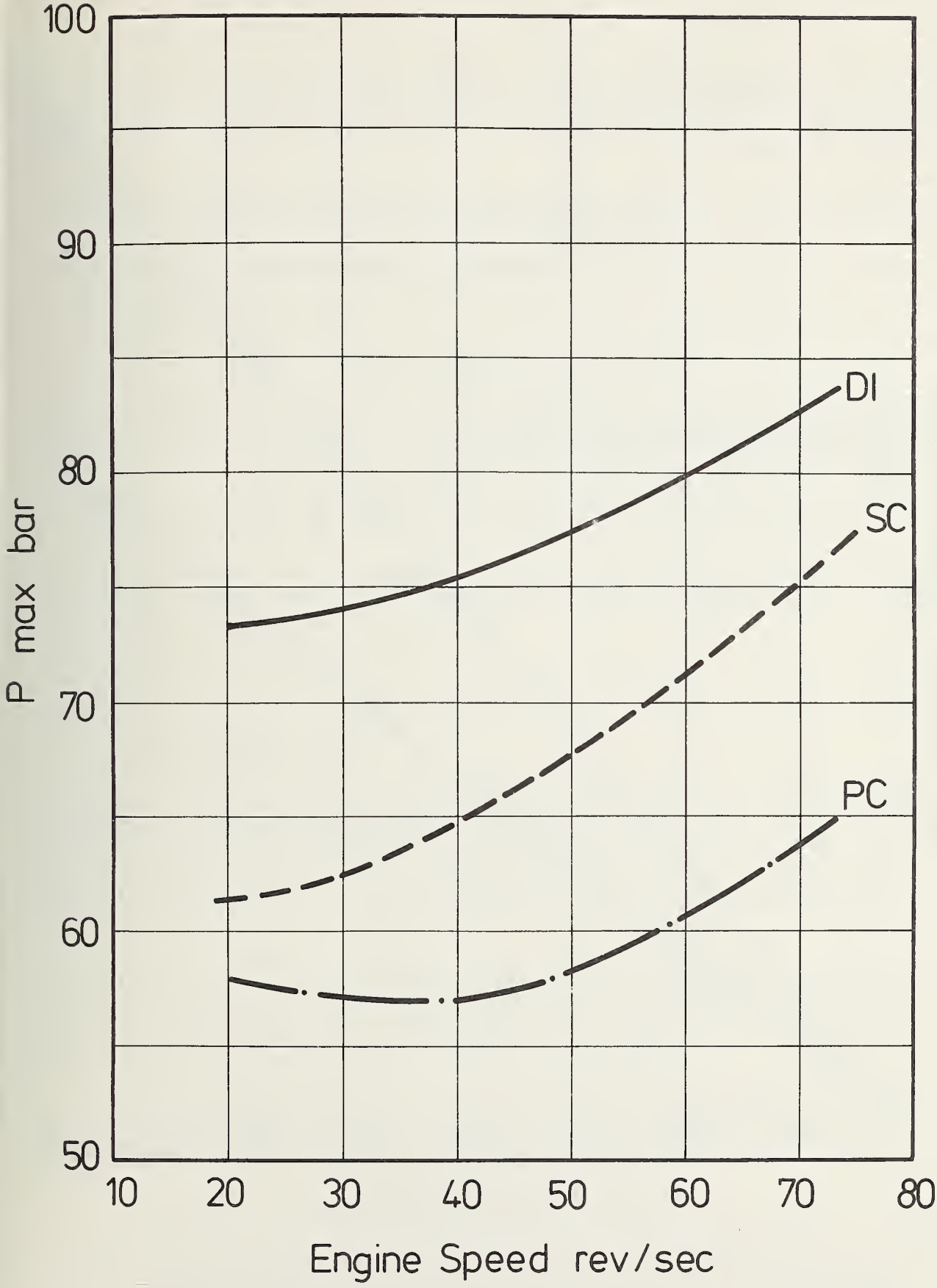

FIGURE 4.1-20: COMPARISON OF CYLINDER PRESSURES

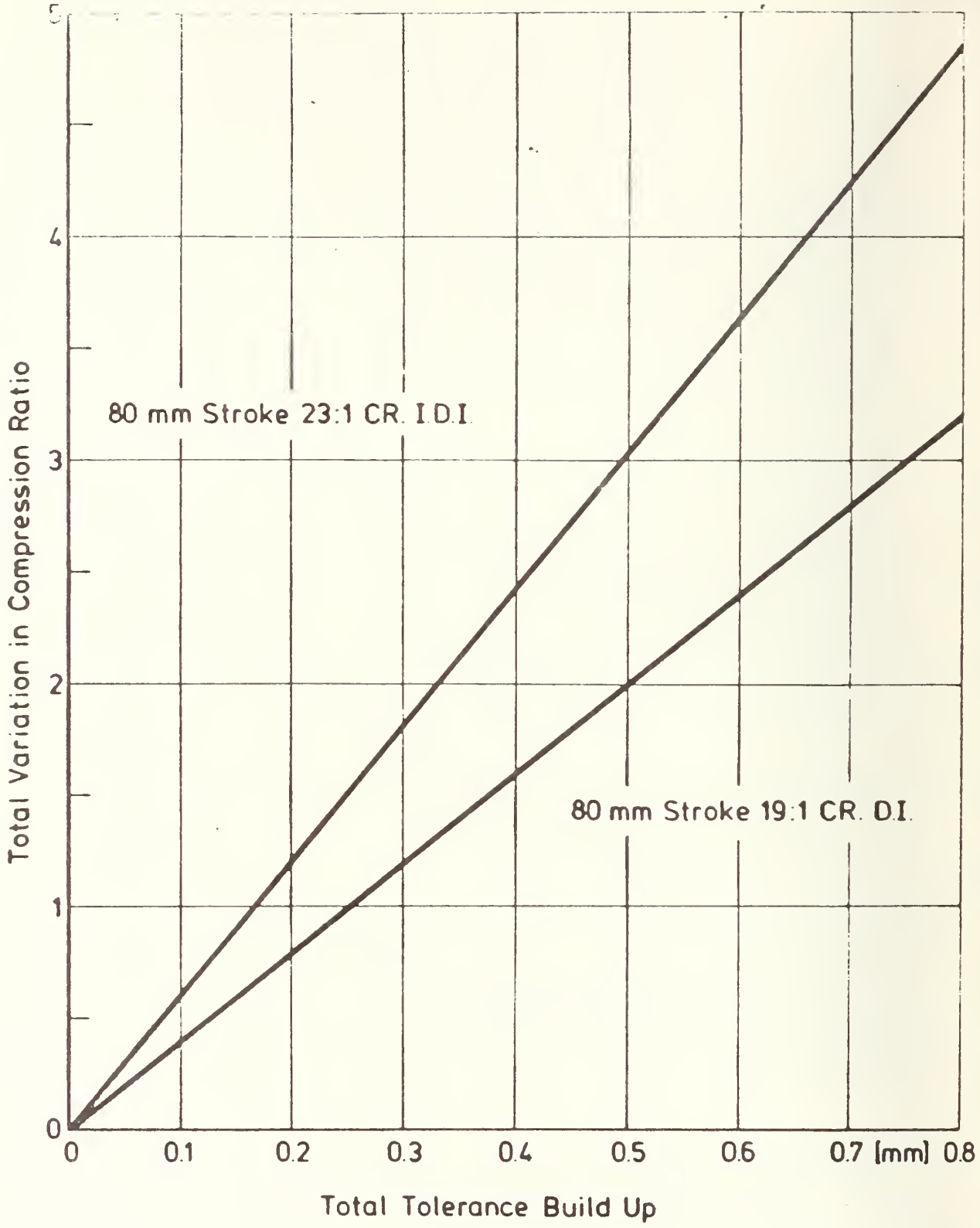

FIGURE 4.1-21: EFFECT OF COMBUSTION SYSTEM ON COMPRESSION RATIO VARIATION DUE TO TOLERANCE STACK-UP

The use of the MAN-M Concept may reduce the idling noise of a diesel engine to the level of a spark-ignition engine. The separate-combustion-chamber concept, however, generates less noise during driving operation which is considered more important.

The decision was made in favor of the swirl chamber concept rather than the pre-chamber concept because of the following priorities:

- Satisfactory fuel economy in all operating modes
- Adequate power output
- Good black-smoke emission behavior.

The swirl chamber concept attains these objectives more easily than the pre-chamber concept. In addition, the fuel economy offered by the swirl chamber system is superior to that of the latter, especially at high engine speeds .

Only swirl chamber systems permit rated engine speeds up to 83 rev/sec (5,000 rev/min) and a specific power output of 35 HP per liter (25 kw).

High altitude tests, furthermore, gave conclusive proof of the fact that pre-chamber engines are far more delicate than swirl chamber engines in regard to the control of black-smoke emissions.

4.2 SWIRL CHAMBER ENGINES

4.2.1 Compression Ratio

Swirl chamber combustion diesel engines for passenger car application should have a high compression ratio (22 : 1) to ensure good cold-start behavior, low noise levels, and low HC emissions under partial load. It is therefore necessary to trade off between these goals and the increase in friction losses. These losses are accompanied by a minimal increase in thermal efficiency.

The effect of the compression ratio on engine performance is shown in Figure 4.2-1. At low engine speeds, highest bmep is obtained with a high compression ratio; but as the speed increases, a lower compression ratio results in higher bmep values. The associated specific fuel consumption loops do not show the same trend with increasing speed.

A rise in the compression ratio raises the internal friction loss in the engine as shown in Figure 4.2-2. An increase by one compression ratio unit usually reduces the bmep of an indirect injection engine by about 0.08 to 0.09 bar.

An increase in compression ratio leads to a slight rise in NOx as shown in Figures 4.2-3 and 4.2-4. The HC levels do not vary significantly with an increase in compression ratio except at a low compression ratio condition with retarded timings when HC levels are very high, probably due to incomplete combustion.

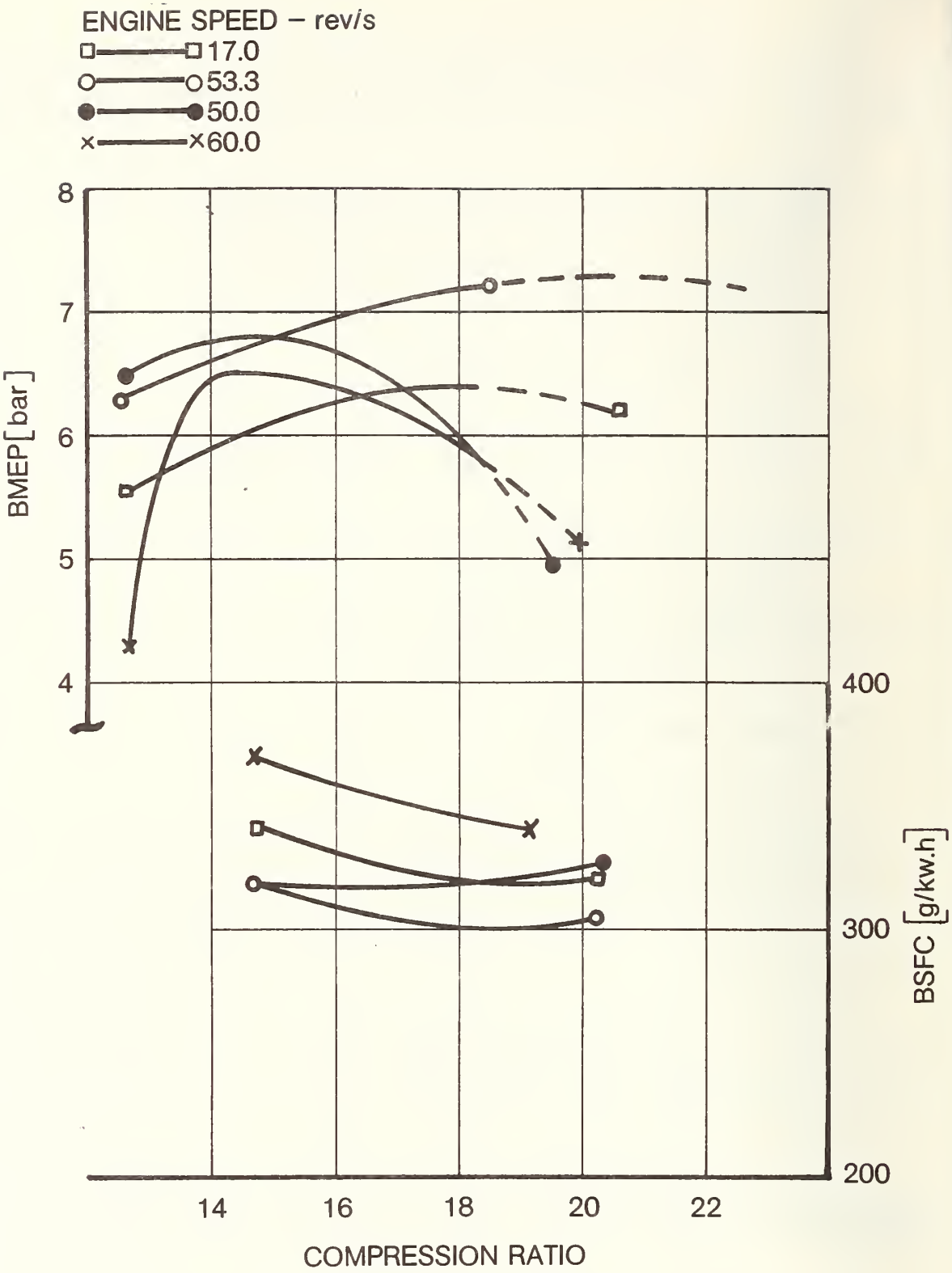

FIGURE 4.2-1: EFFECT OF COMPRESSION RATIO ON PERFORMANCE OVER THE SPEED RANGE IN SWIRL CHAMBER ENGINES - AT SMOKE LEVEL 3 BOSCH

85 ø x 85 Single Cylinder Research Engine

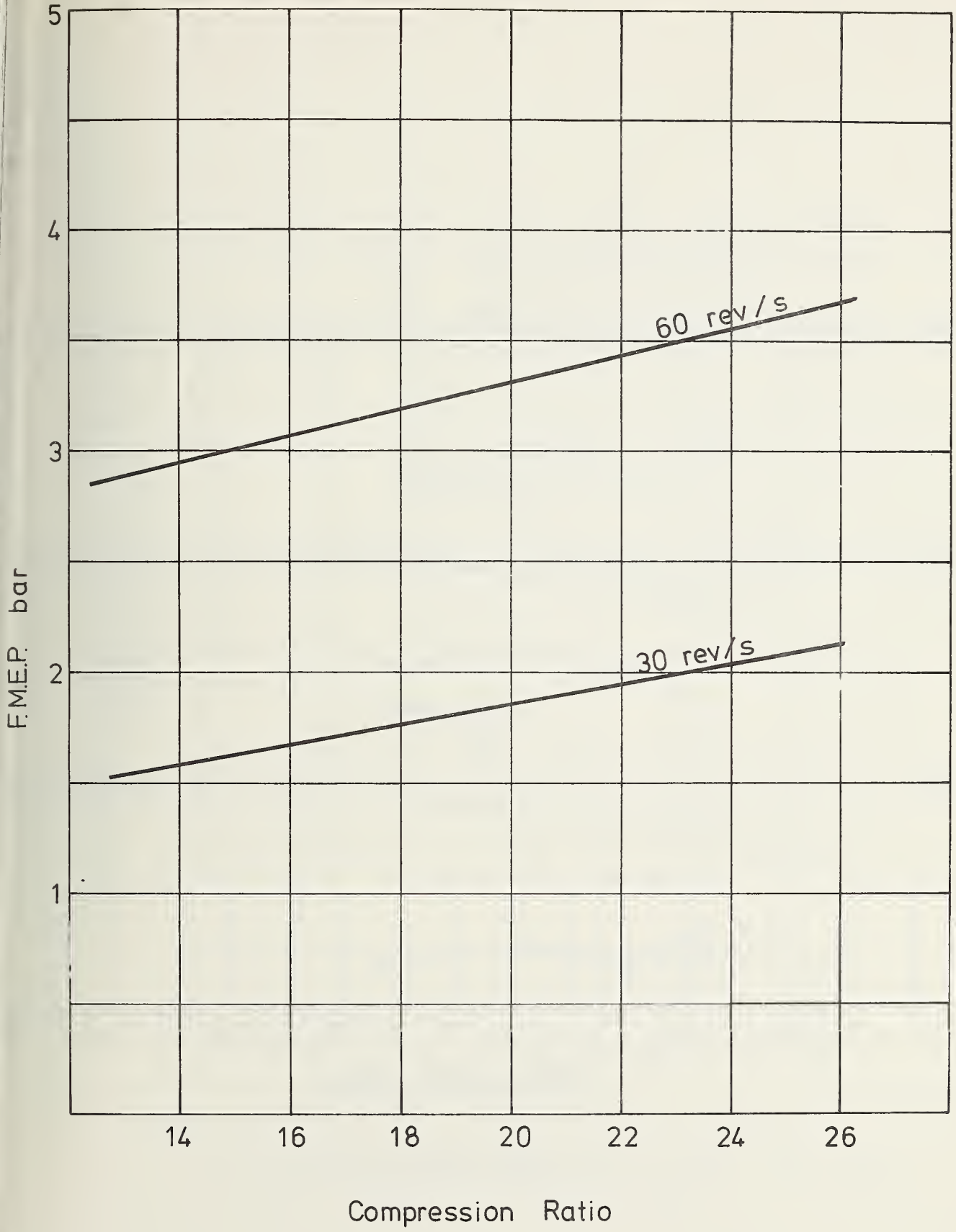

FIGURE 4.2-2: THE EFFECT OF COMPRESSION RATIO ON I.D.I ENGINE FRICTION
Stroke 80 mm, Bore 76.5 mm

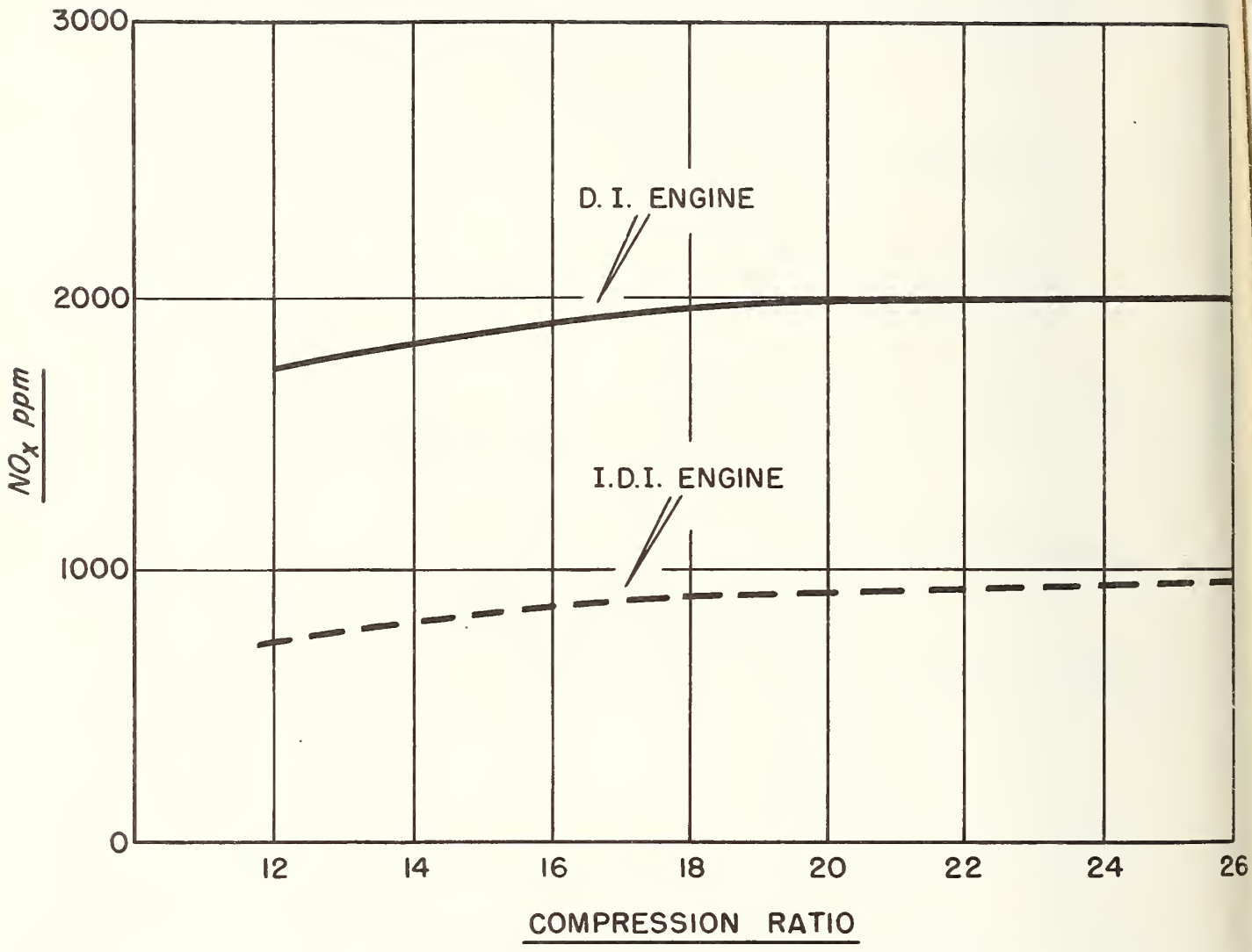

FIGURE 4.2-3: EFFECT OF COMPRESSION RATIO ON NOx FORMATION

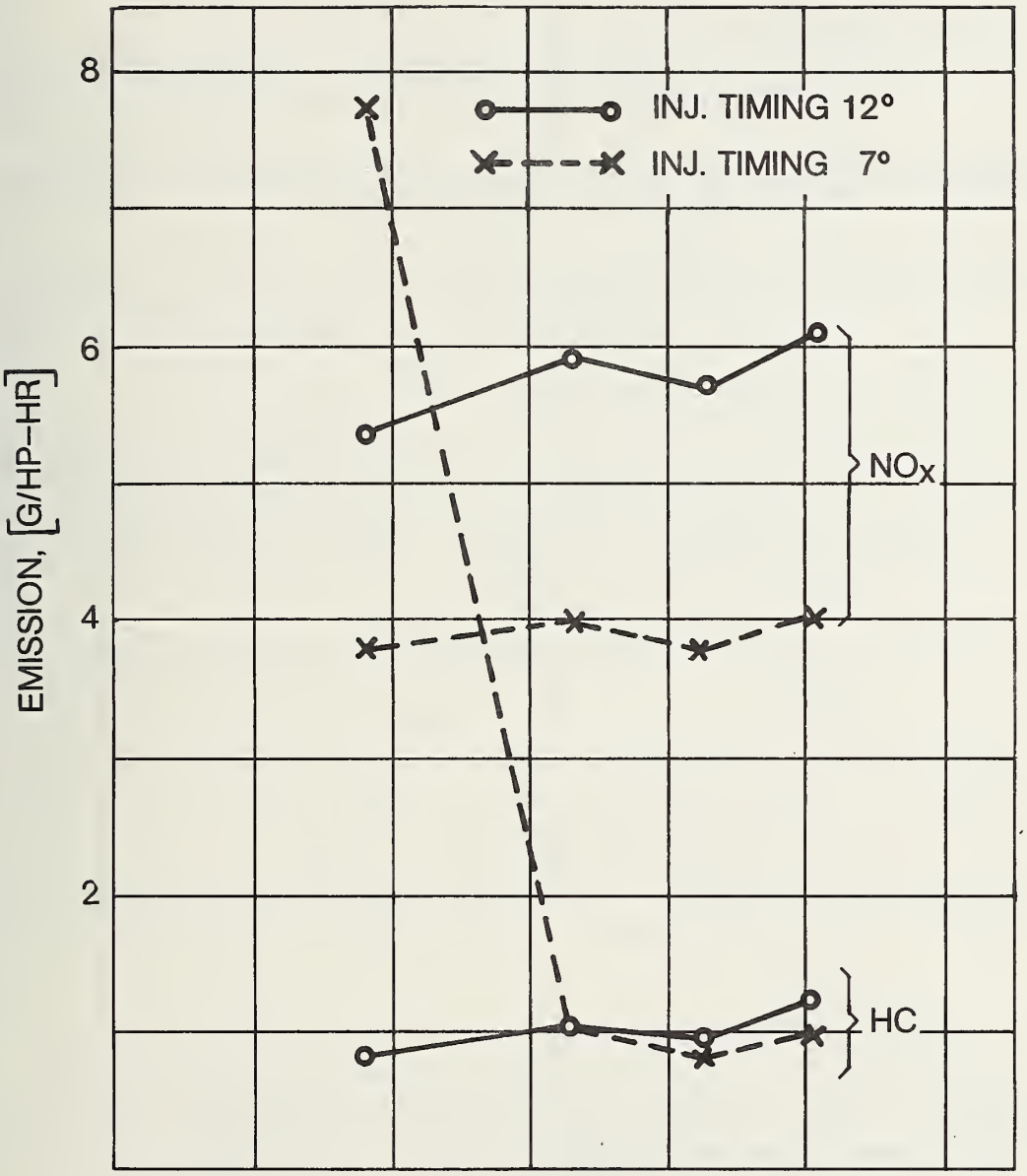

FIGURE 4.2-4: EFFECT OF INJECTION TIMING ON HC EMISSIONS IN SWIRL CHAMBER ENGINES

The limited work on odor suggests that the compression ratio has little effect.

A higher compression ratio reduces noise levels throughout the load speed range as shown in Figure 4.2-5 by about 2 dbA for an increase of two ratio units. Idle noise levels have been reduced by increasing the compression ratio.

As the compression ratio increases, its control in production becomes more difficult. Figure 4.2-6 shows that the variation in compression ratio can be greater as the compression ratio increases for a fixed tolerance build-up.

For small swept-volume cylinder units exact adherence to the compression ratio becomes extremely significant and difficult.

The disadvantages of a high compression ratio are that it precludes optimum fuel economy and makes it difficult to solve the production problems caused by a high compression ratio coupled with a small compressed volume.

The compression ratios which permit optimum fuel consumption in small swirl chamber engines range between $\varepsilon = 16$ and $\varepsilon = 18$ as shown in Figure 4.2-7. However, at the present state-of-the-art it is impossible to produce cold-start and idling characteristics which are satisfactory to the passenger car customer at engine compression ratios of less than $\varepsilon = 20$. Any developments aiming at improving the fuel consumption of small swirl chamber engines should be directed towards optimizing the compression ratio.

All passenger car diesel engines pose problems in the following areas:

- Cold-start behavior
- Warm-up noise
- Idle noise in cold and warm engines.

A mean compression ratio of $\geq$ 22 : 1 was found to be required as a satisfactory solution to these problems.

4.2.2 Combustion Chamber Variables

The entire process of combustion is governed by the swirl chamber and throat geometry (Figure 4.2-8) where heat losses are high (flow speed). Compression ratio, timing, swirl chamber geometry, the ratio between swirl chamber and dead space volume (throat area and cavities), and injection specifications should be optimized for each application[10,11,12] within acceptable manufacturing conditions.

4.2.2.1 Combustion Chamber Volume

The effect of the combustion chamber volume (including the volume of the throat) on bmep levels in a swirl chamber engine is shown in Figure 4.2-9. These bmep contours, obtained from a single cylinder research engine, indicate that a swirl chamber volume of between 45% and 50% of the total clearance volume yields maximum bmep. This result was obtained on a large engine (121 mm bore x 140 mm stroke) running at only 23.3 rev/sec. Results from tests on a smaller

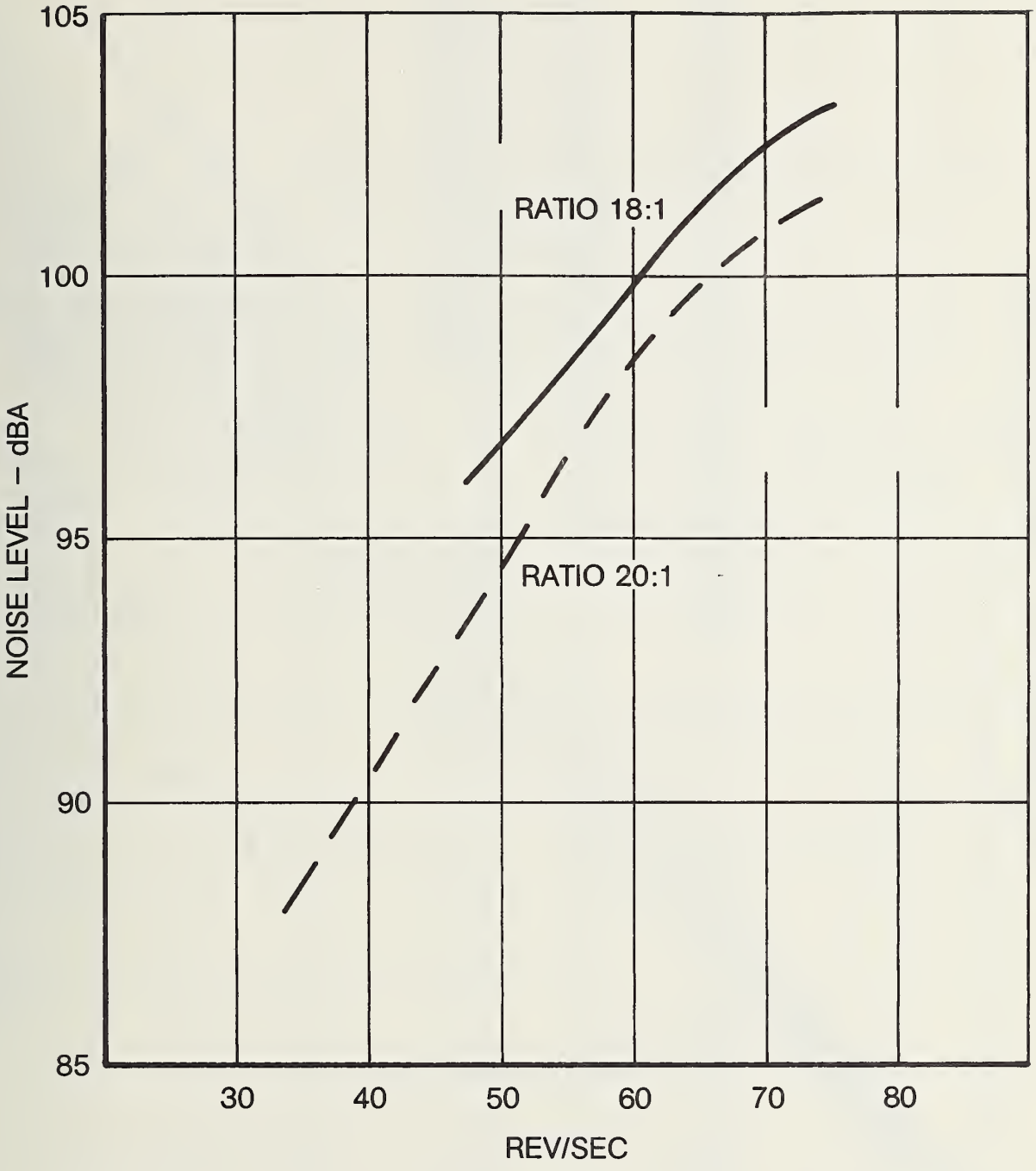

FIGURE 4.2-5: EFFECT OF COMPRESSION RATIO ON NOISE
2.18-l, 4-Cylinder Swirl Chamber Engine
(Maximum Performance Conditions)

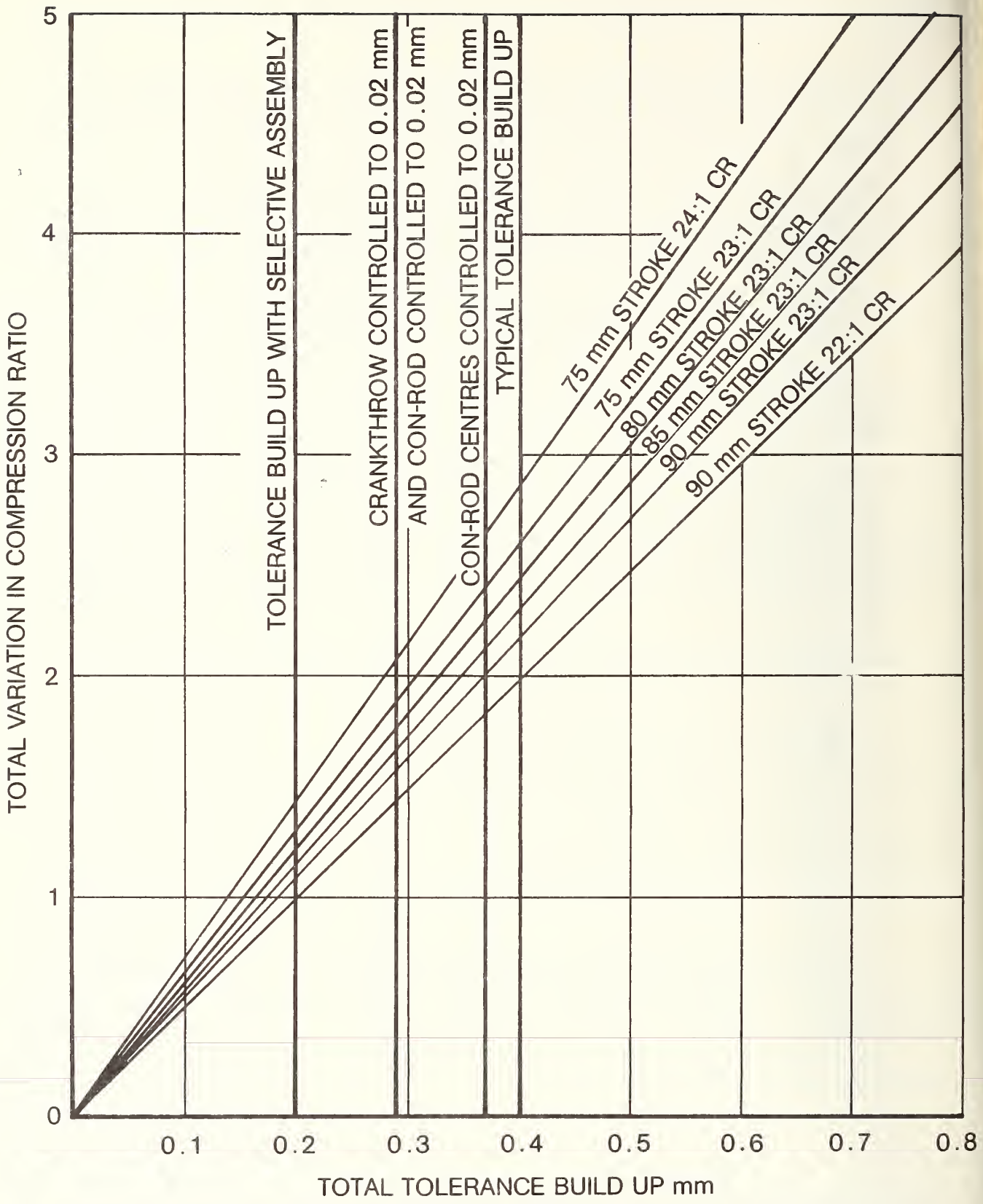

FIGURE 4.2-6: EFFECT OF STROKE ON COMPRESSION RATIO VARIATION IN INDIRECT INJECTION ENGINES DUE TO TOLERANCE STACK-UP

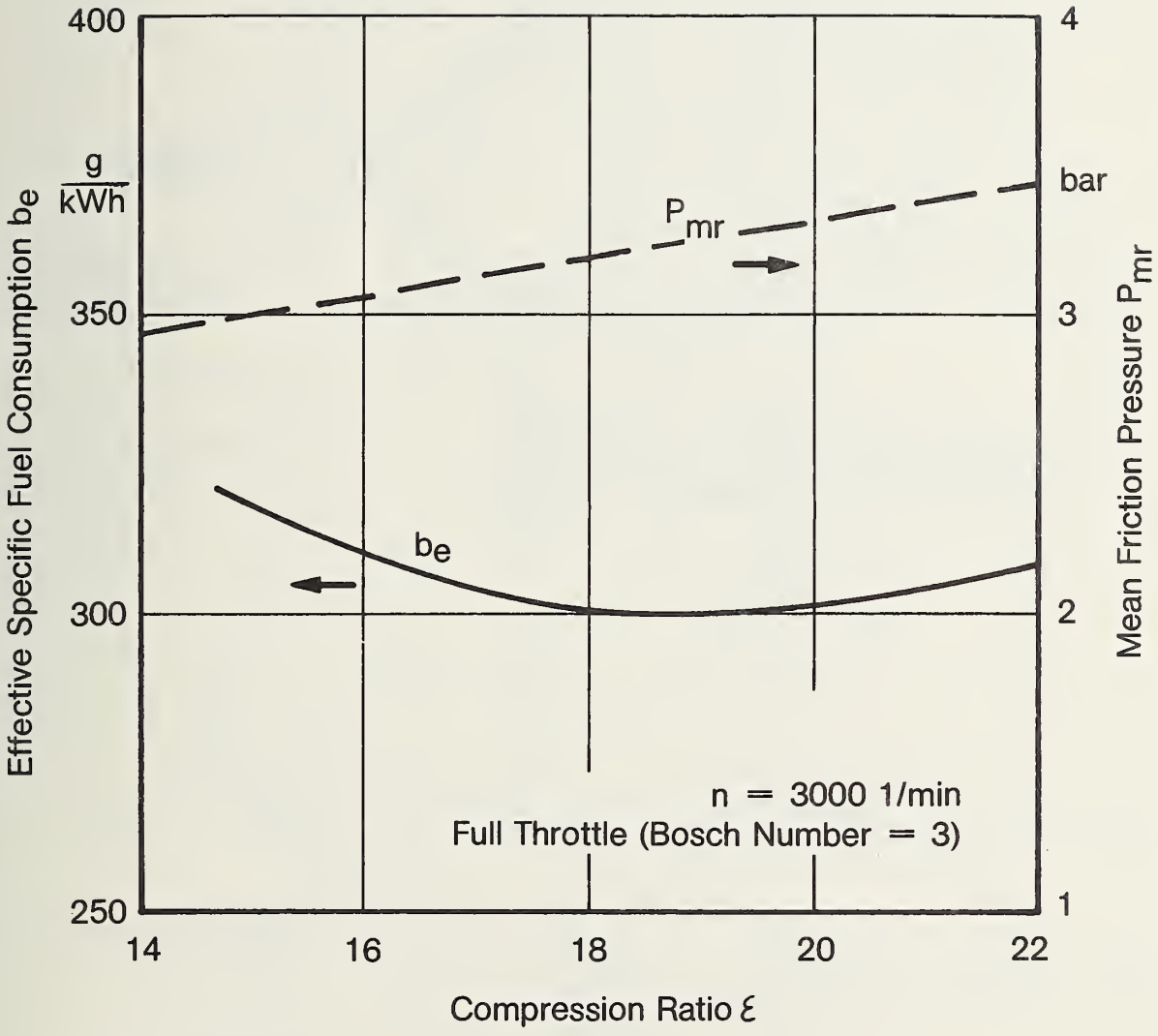

FIGURE 4.2-7: MEAN FRICTION PRESSURE AND FUEL CONSUMPTION OVER COMPRESSION RATIO

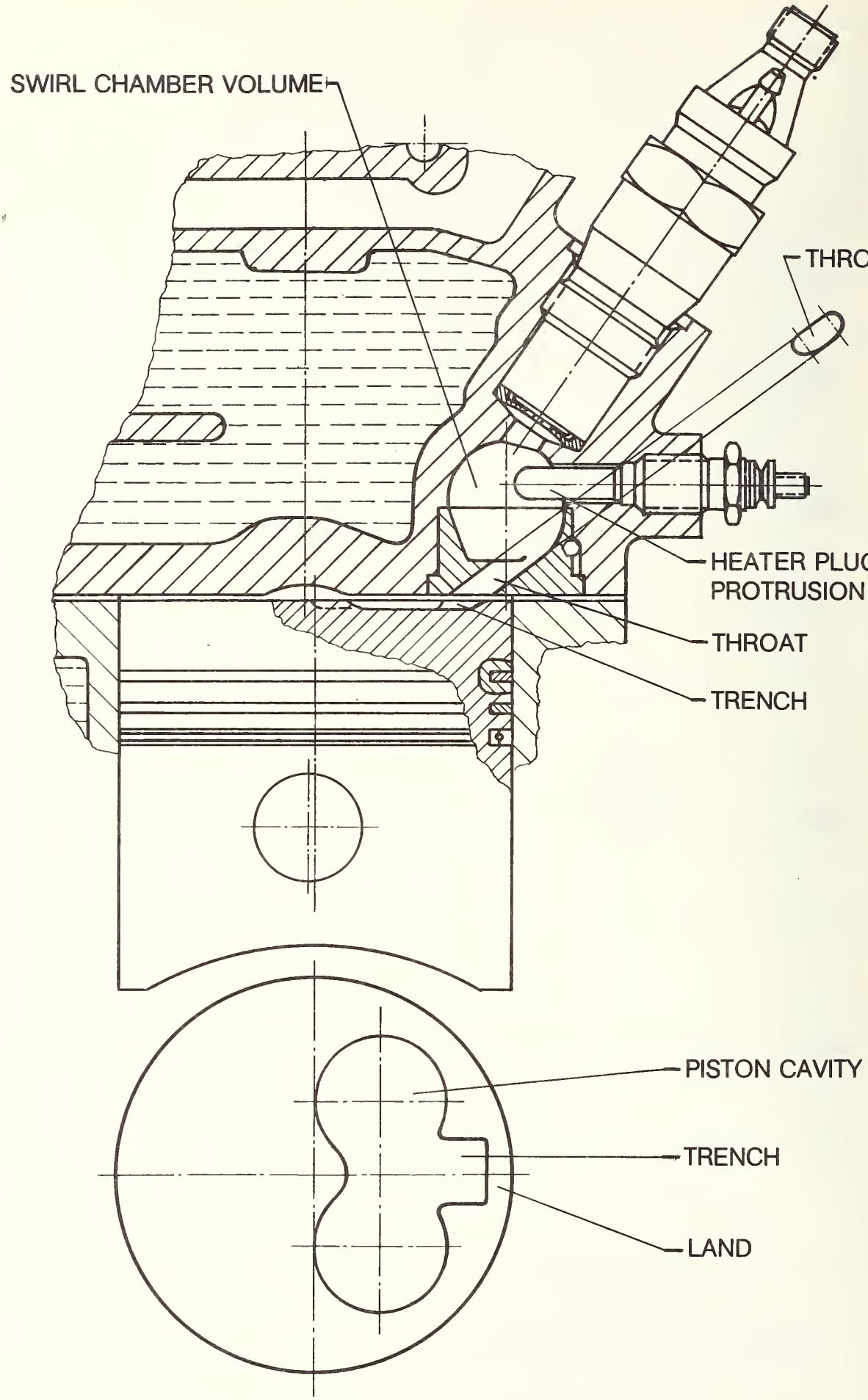

FIGURE 4.2-8: COMBUSTION CHAMBER VARIABLES

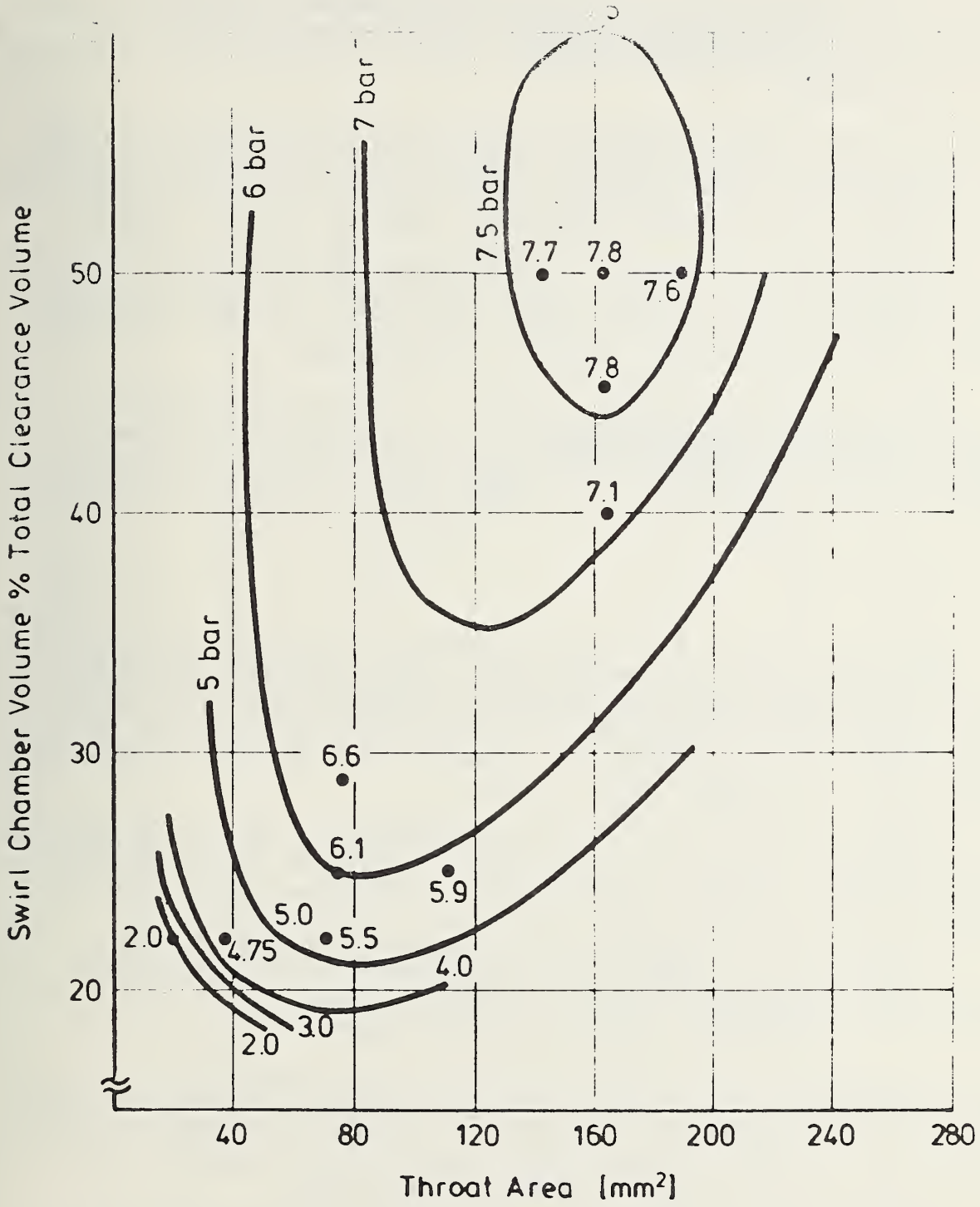

Results from Single Cylinder Engine Bore 120 mm,
Stroke 140 mm Speed 16.7 rev/s Compression Ratio 16:1

FIGURE 4.2-9: THE EFFECT OF SWIRL CHAMBER VOLUME AND THROAT AREA ON PERFORMANCE AT CONSTANT SMOKE LEVEL OF 4% OPALITY

single-cylinder engine with a swept volume of about 680 cc are shown in Figure 4.2-10. The curves indicate that the 50% volume in the swirl chamber produces optimum performance and show that the performance drop is more significant at high engine speeds if the combustion chamber volume is altered in either direction.

Best specific fuel consumption throughout the load range has also been obtained with the standard combustion chamber volume as shown in Figure 4.2-11. With a reduced swirl chamber volume, the specific fuel consumption deteriorates significantly at the high load condition but improves at partial load[13].

Figure 4.2-11 also shows the relationship between NOx emissions and combustion chamber volume. At light loads of less than 5 bar bmep the standard volume is clearly superior, but at higher loads the variation in NOx levels between the various combustion chambers is insignificant.

Figure 4.2-12, obtained from reference 5, shows that a reduction in combustion chamber volume gives better emissions characteristics than the standard value for optimum performance. As this accompanies an increase in compression ratio, the optimum swirl chamber volume for both performance and emissions is still about 50% of the total compression volume.

4.2.2.2 Throat

Figures 4.2-13 and 4.2-14 show the effects of the throat area on the bmep of a swirl chamber engine at various engine speeds. Smaller-than-standard throat areas produce better performance at low speeds and inferior performance at high speeds. A slight increase in throat area produces opposite results. A significant increase in throat area, however, leads to a drop in performance throughout the entire speed range.

In terms of specific fuel consumption the standard throat area represents a good compromise throughout the speed and load range as shown in Figures 4.2-15 and 4.2-16. However, at high speeds an improvement in specific fuel consumption can be obtained with a 50% increase in throat area.

An increase in the throat area in turbocharged engines improves the specific fuel consumption throughout the speed range for the same bmep level as shown in Figure 4.2-17.

The advantage of the larger throat size at high speed results from lower pumping losses through the throat and reduced swirl in the combustion chamber. The relationship between pumping losses and throat size is shown in Figure 4.2-18. At low speeds, the swirl level in the combustion chamber is inadequate with a large throat which reduces combustion efficiency.

The effect of the throat area on HC and NOx emissions over the C.A.R.B.13 mode cycle[5] shows a reduction in both HC and NOx emissions with larger throat areas but an increase in smoke levels (Figure 4.2-19).

SINGLE CYLINDER ENGINE: SWEPT VOLUME @ 0.68 L
BORE/STROKE @ .93
COMPRESSION RATIO 22.5:1

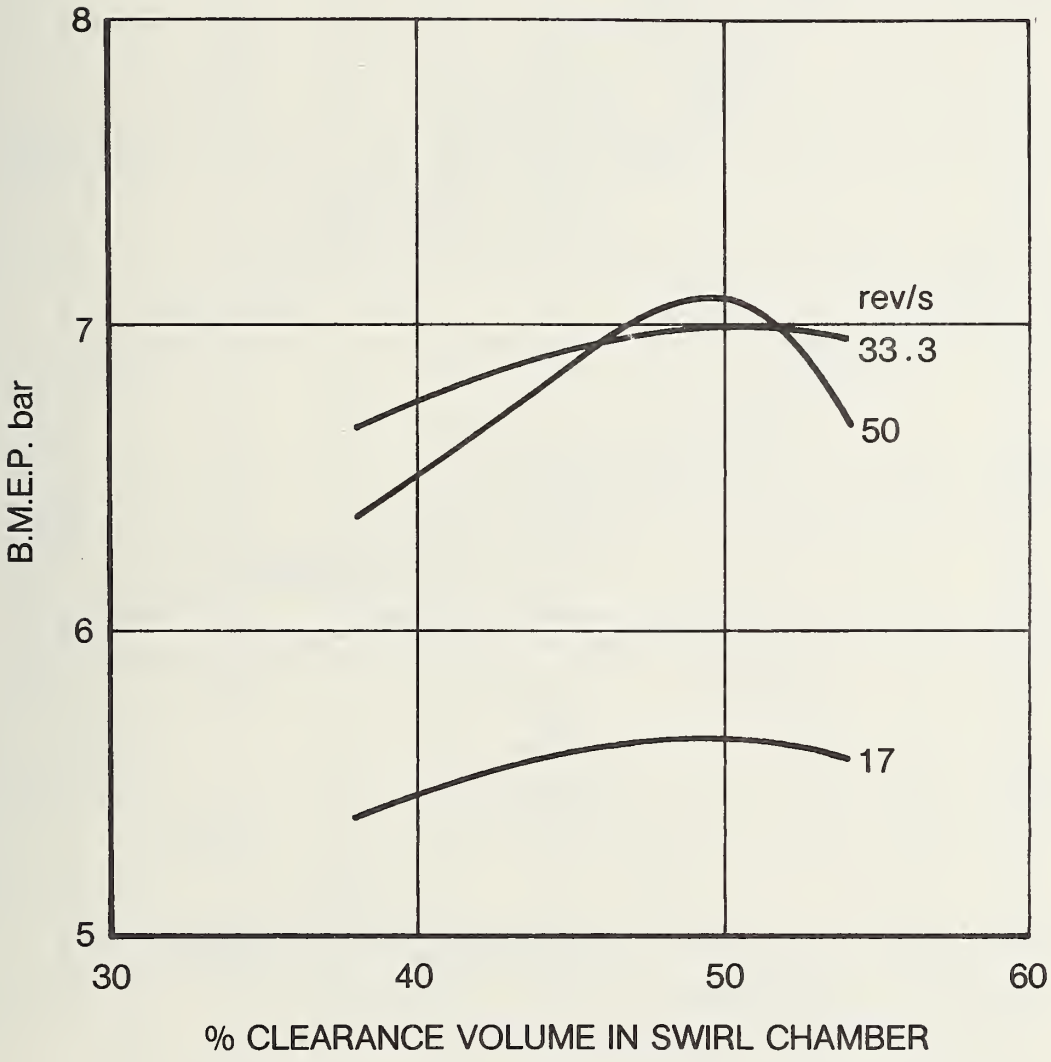

FIGURE 4.2-10: EFFECT ON PERFORMANCE OF % VOLUME IN SWIRL CHAMBER

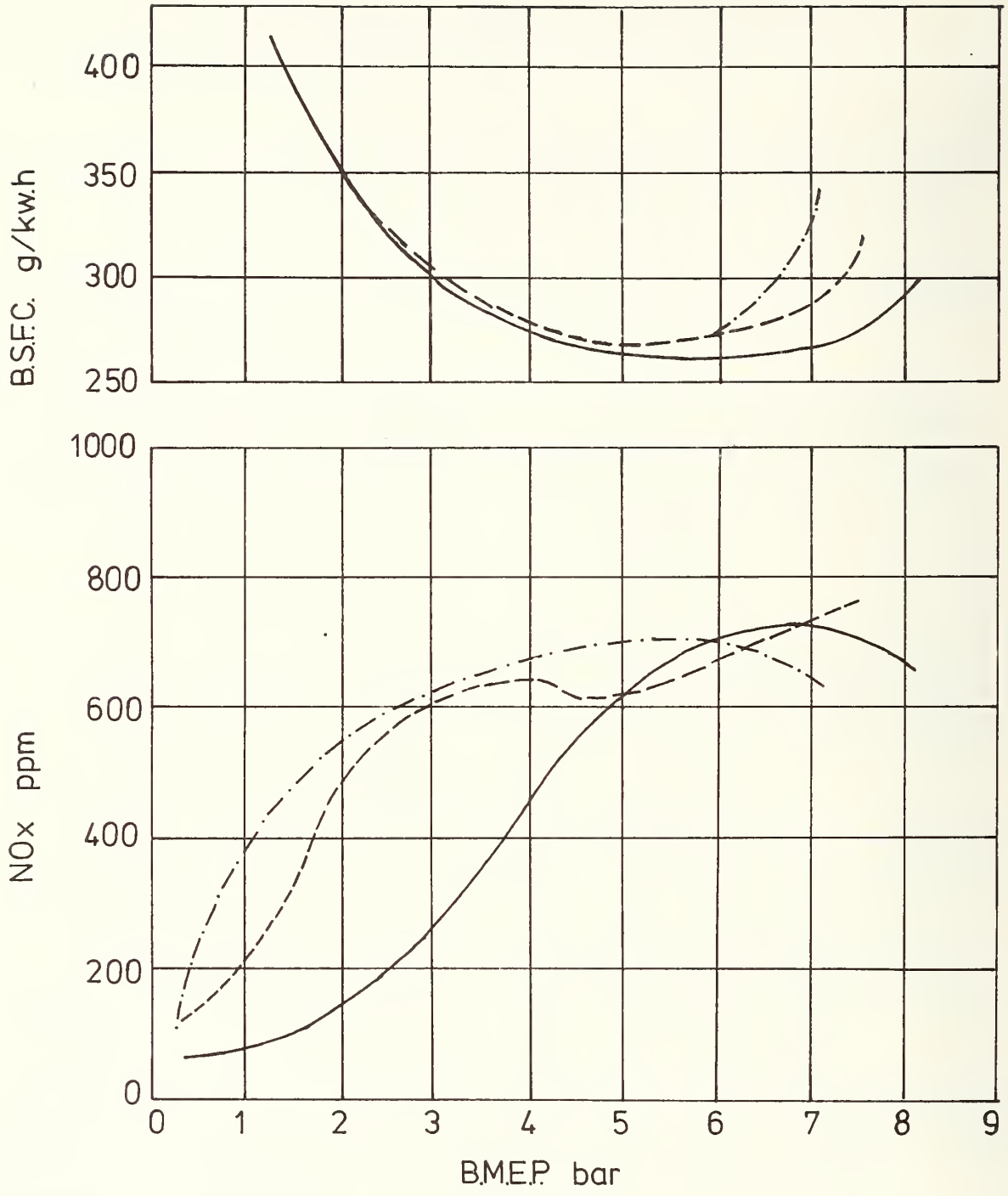

FIGURE 4.2-11: EFFECT OF COMBUSTION CHAMBER GEOMETRY ON NOx EMISSIONS AND B.S.F.C.

_____ Standard COMET V 4^{o} Injection Retard

_·_·_·_ 25% Vol. in COMET Ch. - Flat Top Piston

_ _ _ _ 25% Vol. in COMET Ch. - Cavities in Piston

(Source: I. Mech. E. C124/71)

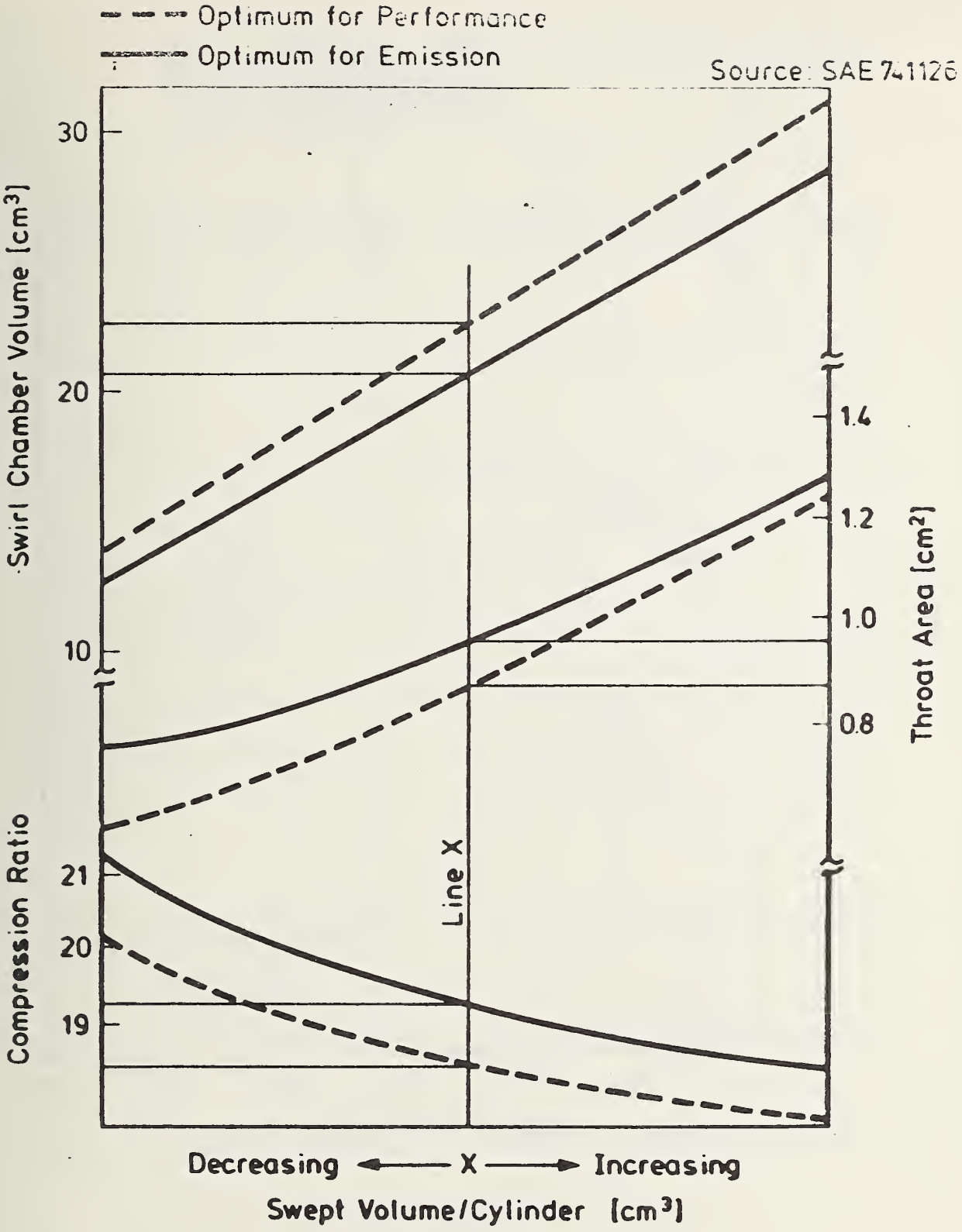

FIGURE 4.2-12: EFFECT OF CYLINDER VOLUME ON IMPORTANT FACTORS IN SWIRL CHAMBER ENGINES WHEN OPTIMIZING FOR EMISSIONS OR PERFORMANCE

SINGLE CYLINDER ENGINE: SWEPT VOLUME 0.68 LITRE
BORE/STROKE RATIO 0.93
COMPRESSION RATIO 22.5:1

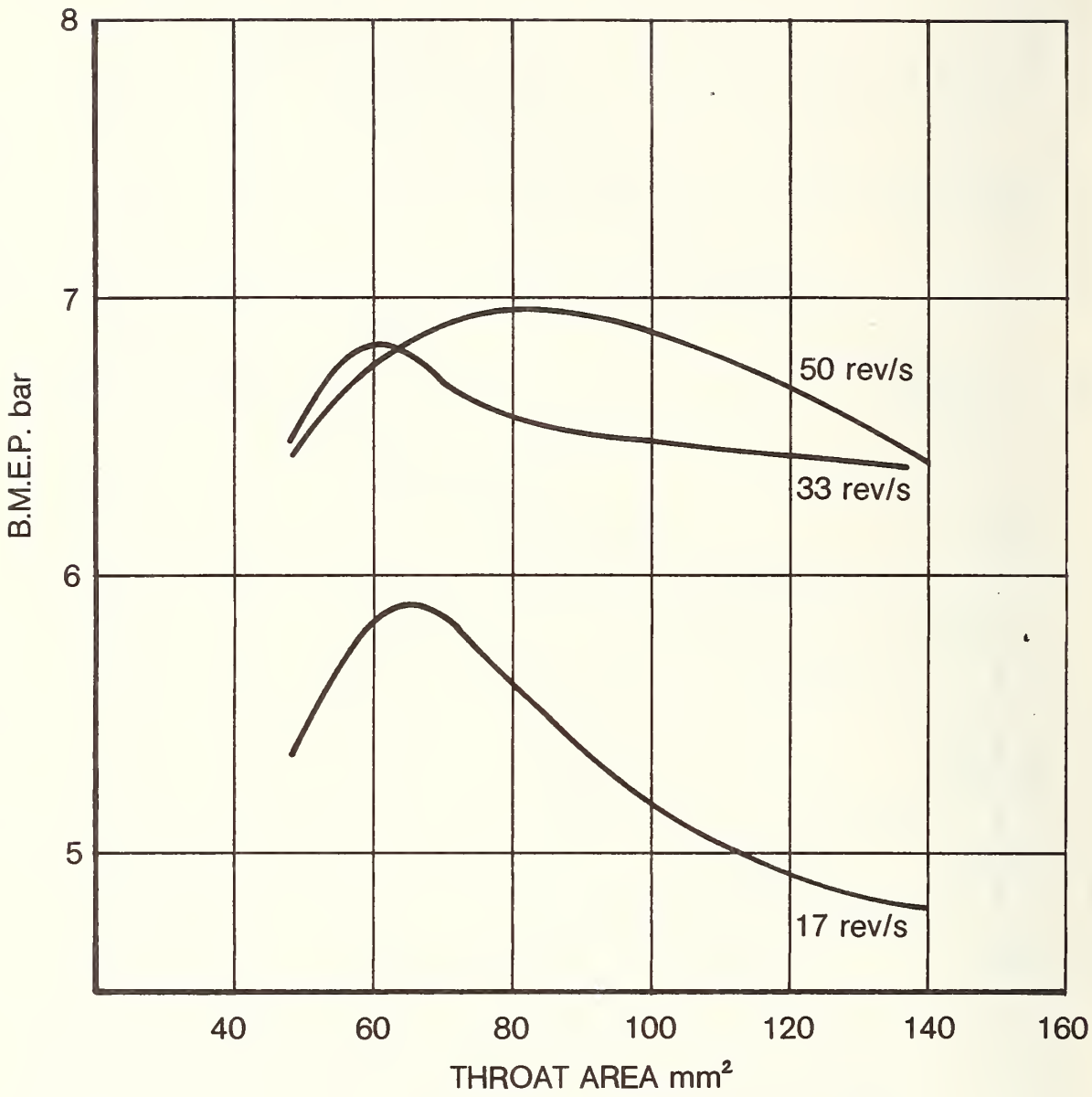

FIGURE 4.2-13: EFFECT OF THROAT AREA ON PERFORMANCE OF A SWIRL CHAMBER ENGINE.

4 CYLINDER ENGINE
ABOUT 2.2 L
BORE/STROKE
RATIO ≃ 0.81:1
SOURCE – RICARDO
TESTS

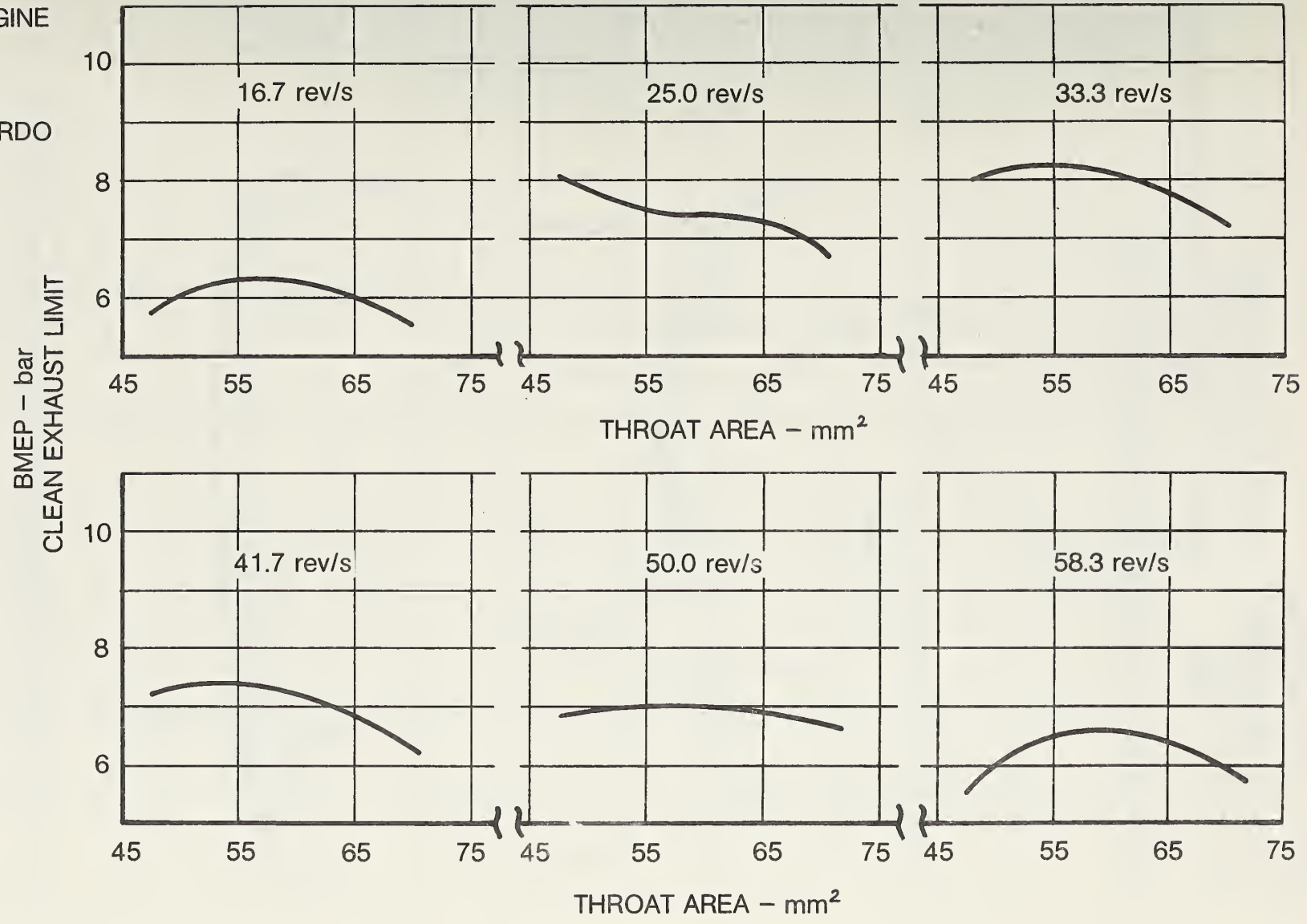

FIGURE 4.2-14: EFFECT OF SWIRL CHAMBER THROAT AREA ON SMOKE LIMITED BMEP OVER SPEED RANGE

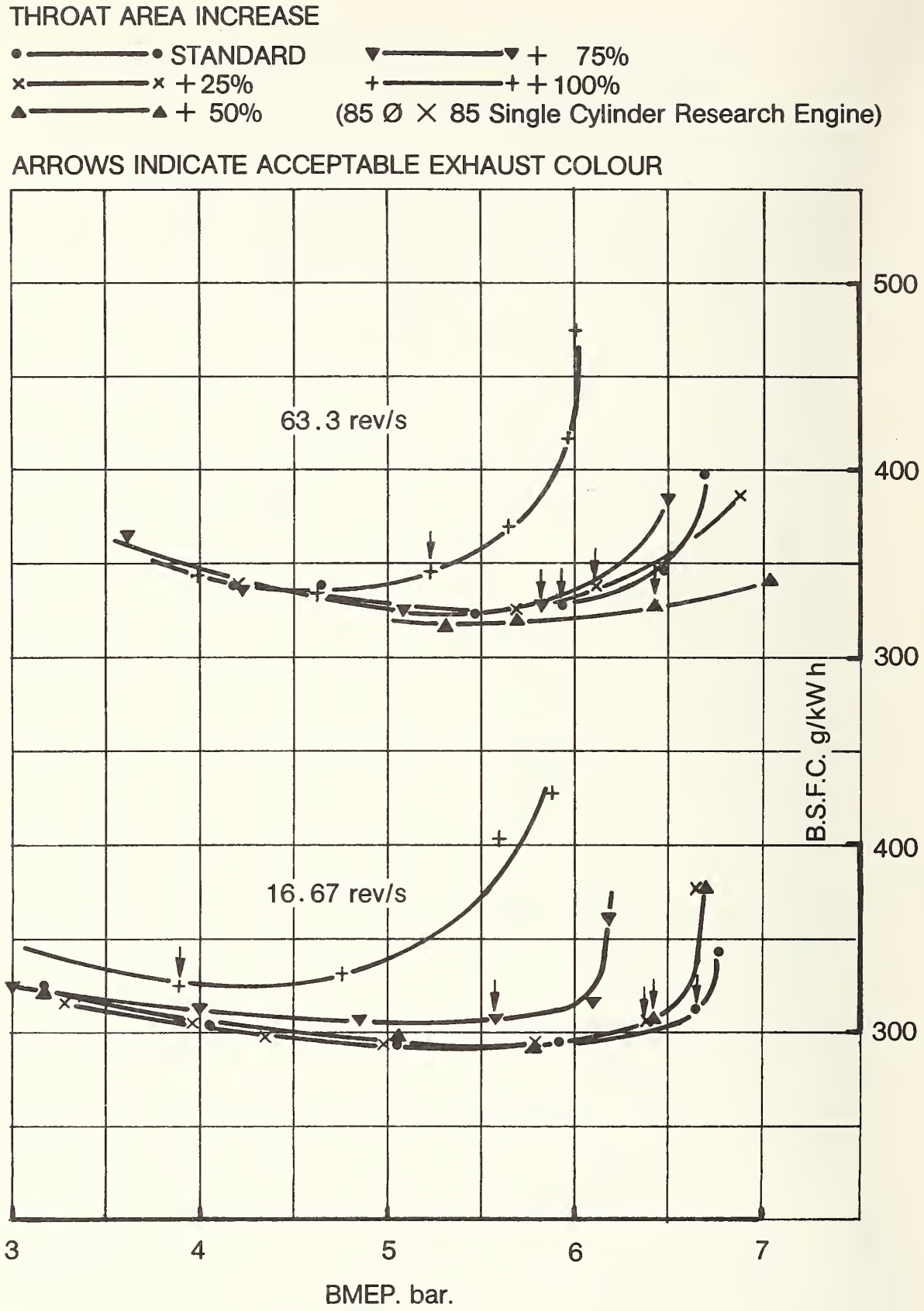

FIGURE 4.2-15: EFFECT OF SWIRL CHAMBER THROAT AREA ON PERFORMANCE

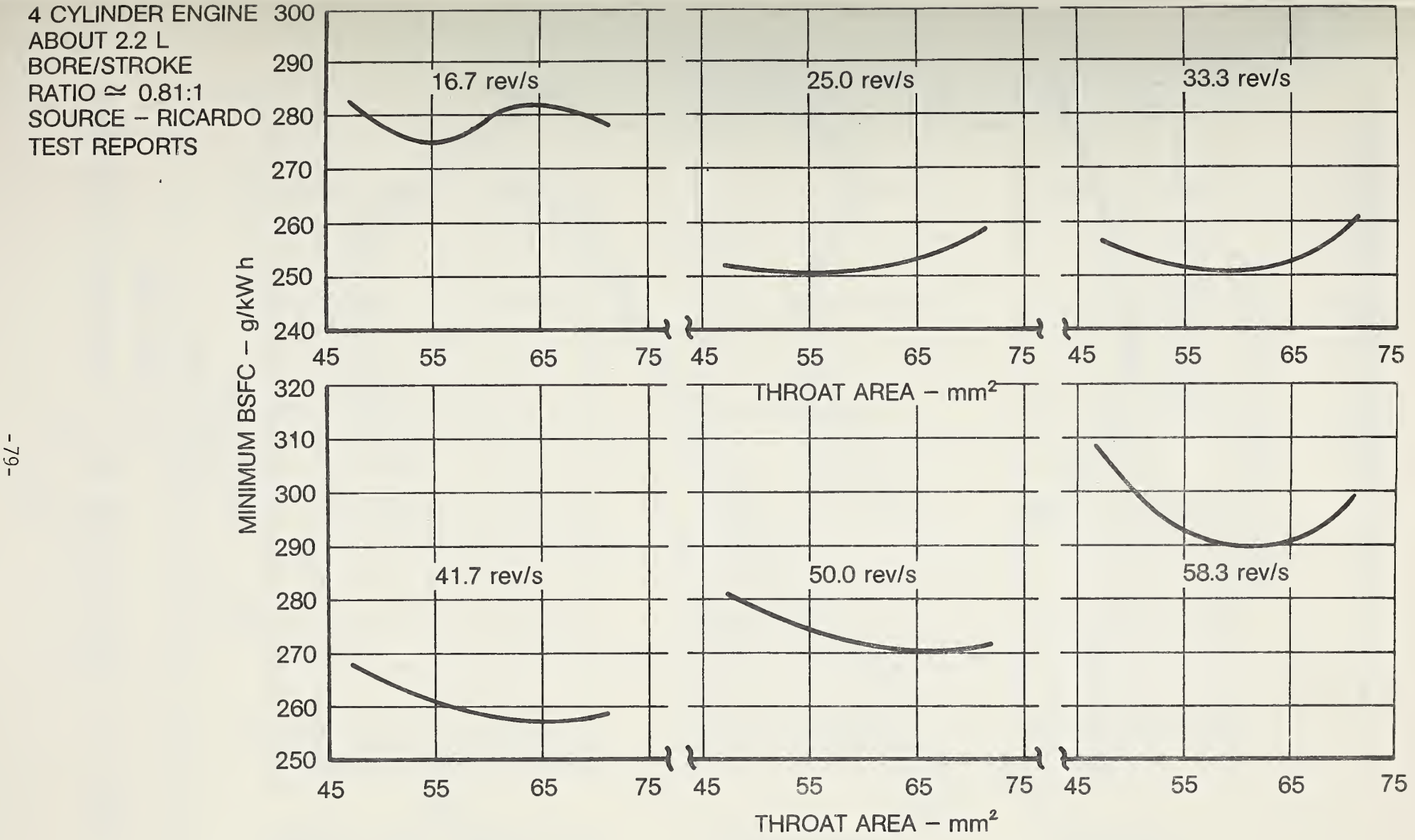

FIGURE 4.2-16: EFFECT OF SWIRL CHAMBER THROAT AREA ON MINIMUM BSFC OVER SPEED RANGE

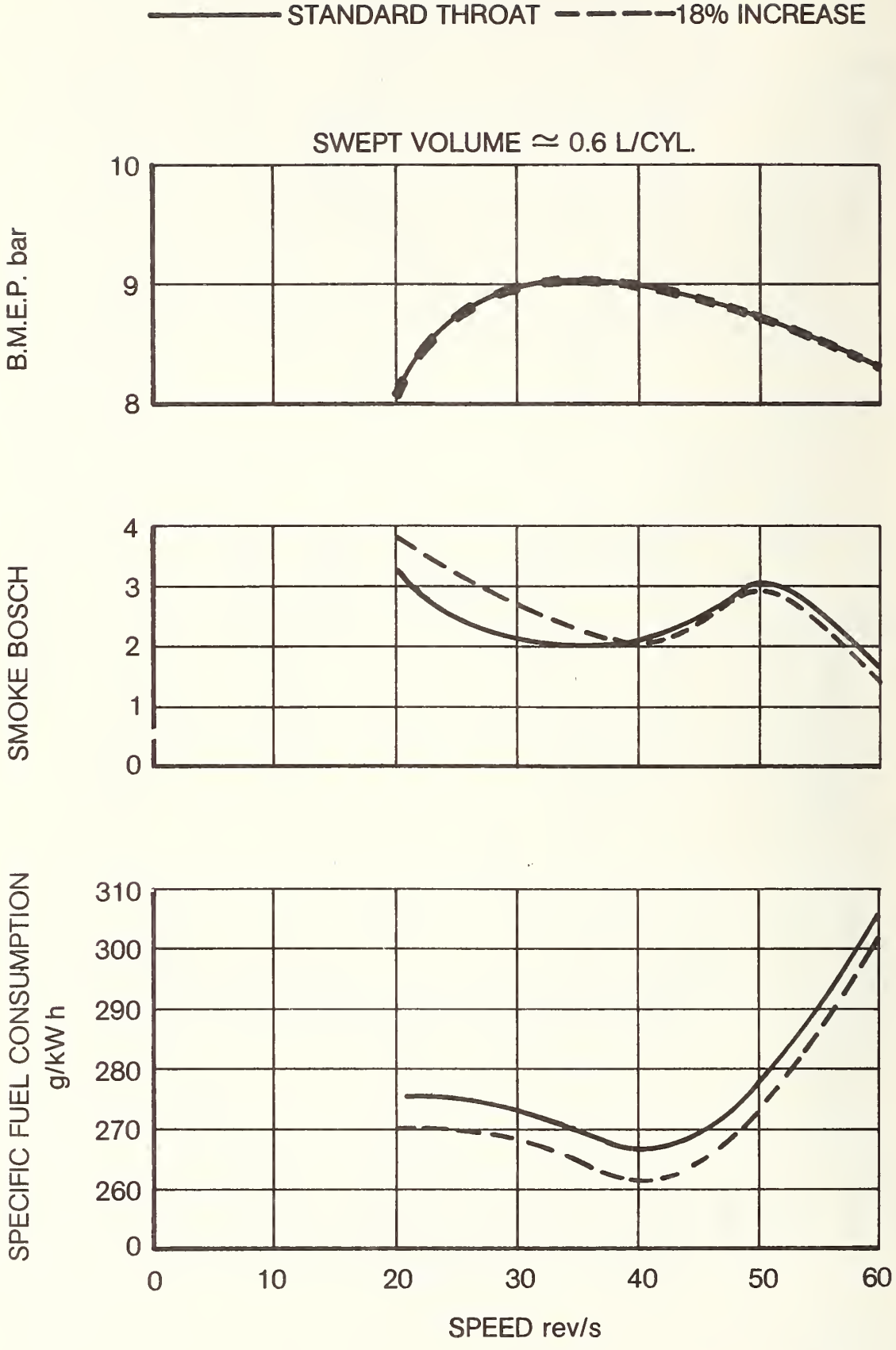

FIGURE 4.2-17: EFFECT OF THROAT AREA ON PERFORMANCE OF TURBOCHARGED COMET Vb ENGINE

4 CYLINDER ENGINE ABOUT 2.2 L
BORE/STROKE RATIO ≃ 0.81:1

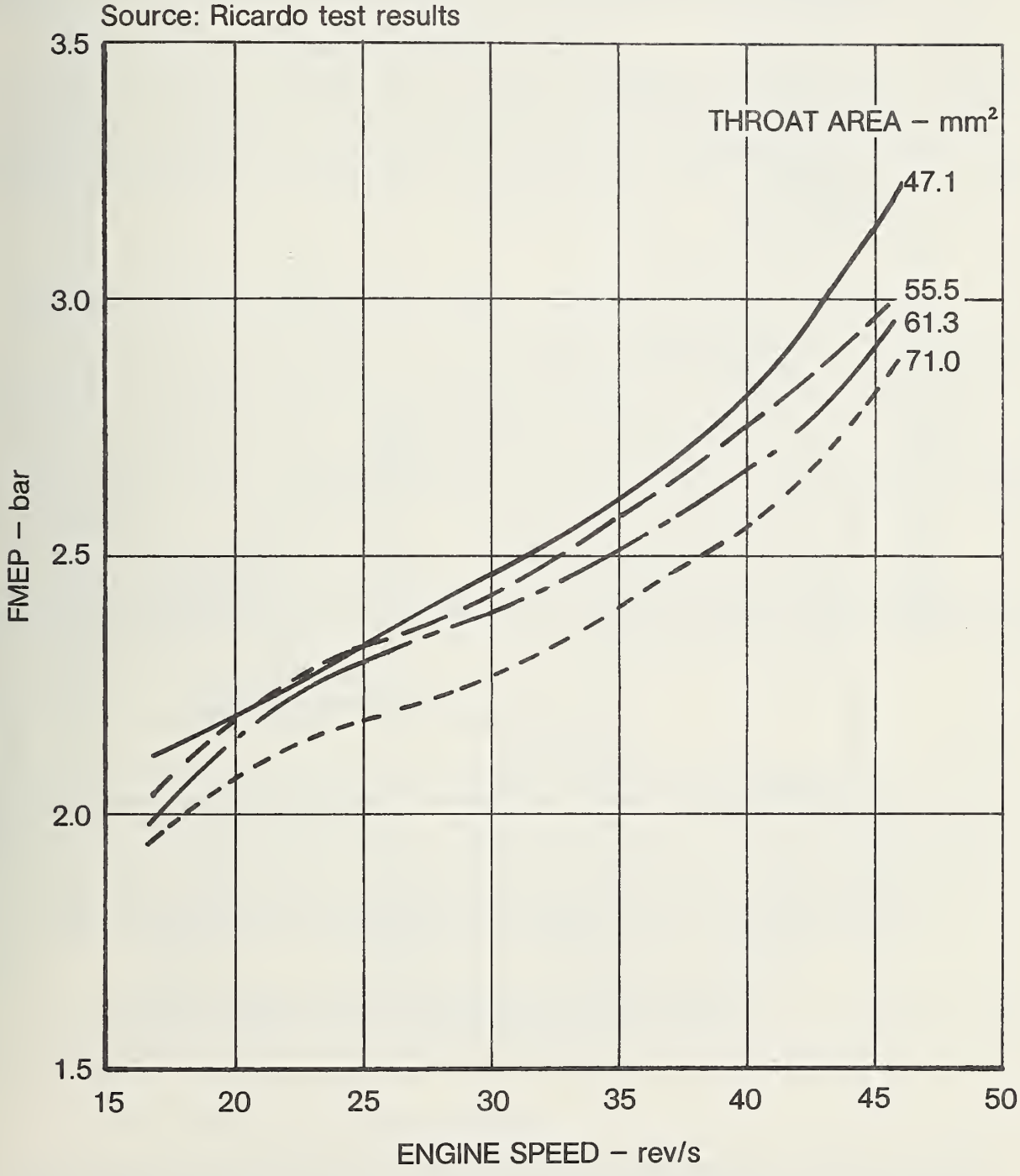

FIGURE 4.2-18: EFFECT OF SWIRL CHAMBER THROAT AREA ON FRICTION LOSSES OVER SPEED RANGE

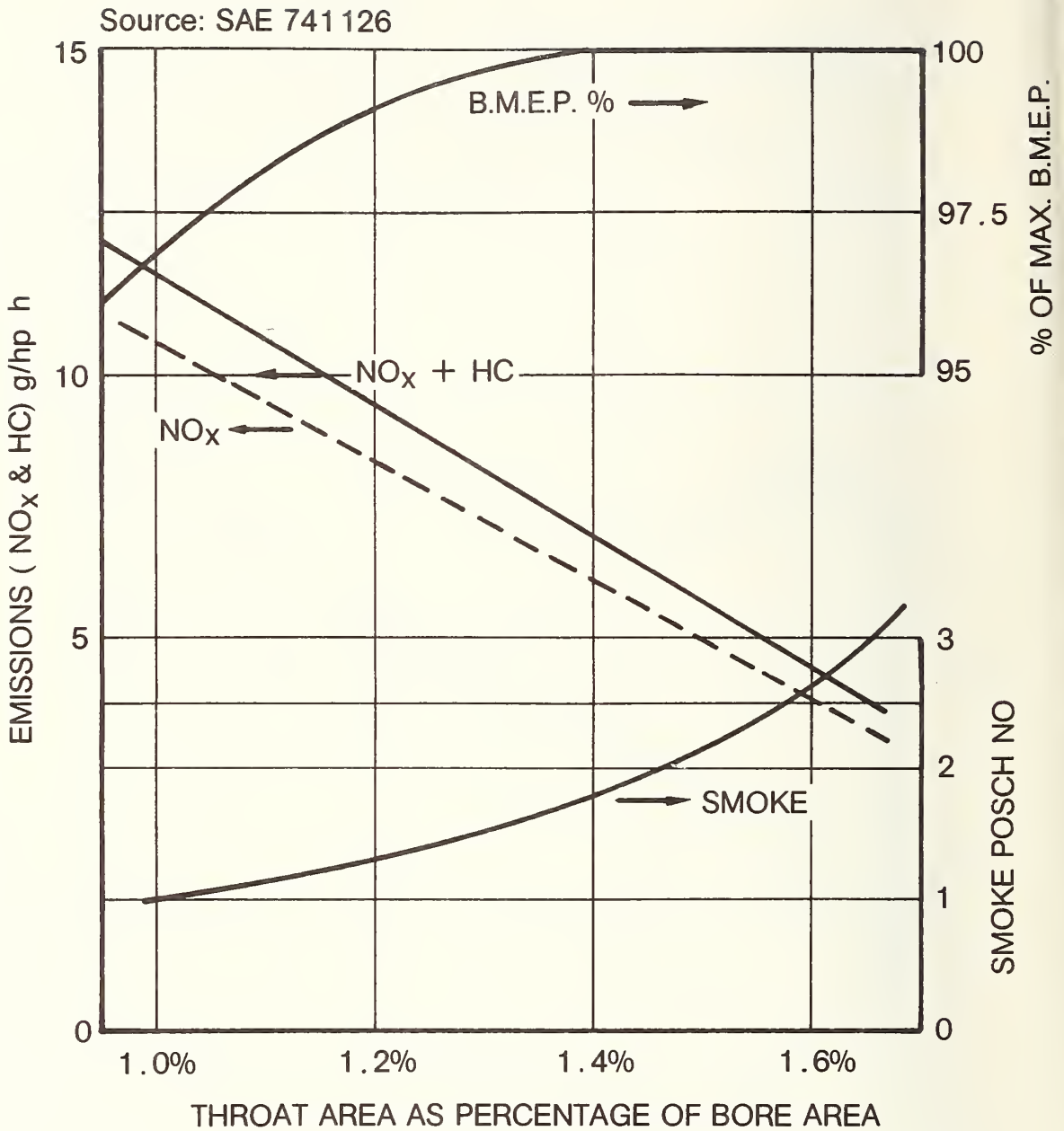

FIGURE 4.2-19: EFFECTS OF THE THROAT AREA ON EMISSIONS AND PERFORMANCE OF SWIRL CHAMBER ENGINES

4.2.2.3 Injector Angle

The effect of injector angle was determined by two methods. A statistical analysis was made of various production and prototype engines correlating a subjective performance level to injector angle. The results in Figure 4.2-20 do not show any clearly defined relationship between performance and injector angles. It is interesting to note, though, that all the engines with an "excellent" performance rating have acute injector angles of between 27^{o} and 36^{o} with the location of spray impact in the lower half of the swirl chamber wall.

Another series of tests were conducted in a single-cylinder swirl chamber engine (121 mm bore x 140 mm stroke) with single-hole nozzles to give spray angles at 10^{o} intervals up to 30^{o} on either side of the injector angle as illustrated in Figure 4.2-21. This test indicates that positions A and F are clearly detrimental to performance. Of the other angles, none proved to offer significantly better performance at both of the speed conditions examined.

4.2.2.4 Heater Plug Protrusion

The results obtained by varying the heater plug protrusion in a Comet Vb combustion chamber are shown in Figure 4.2.-22. Only when the heater plug protrudes into the chamber by about 3 mm is there a noticeable deterioration in bmep and specific fuel consumption. With a greater protrusion, in excess of 6 mm, the bmep increases above the value with zero heater plug protrusion, and the specific fuel consumption is at a similar level. The heater plug should not extend beyond the swirl chamber center in order to avoid disturbance of the fuel spray.

The poor performance recorded with small protrusion is thought to be caused by air being deflected off the tip of the plug which creates uncontrolled swirl and adversely affects the normal swirl characteristics in a swirl chamber.

4.2.2.5 Piston-to-Cylinder-Head Clearance

The piston-to-cylinder-head clearance in a swirl chamber engine is normally designed to be 1% of the stroke in cold condition. It is limited to a minimum to overcome the problem of valve and piston collision in hot condition at maximum speed with adverse tolerance built-up. The maximum piston-to-cylinder-head clearance is restricted by the compression ratio requirement. Even with a completely flat piston crown the maximum real-life value is restricted to about 2% of the stroke with compression ratios in excess of 20 : 1.

The minimum piston-to-cylinder-head clearance should be so designed that a maximum amount of air is available for improved air utilization.

4.2.2.6 Piston Cavity Shape and Size

The effects of piston cavity shape and size on engine performance are determined by comparison tests. These tests pose problems because they invariably involve variations in compression ratio and piston friction. Most

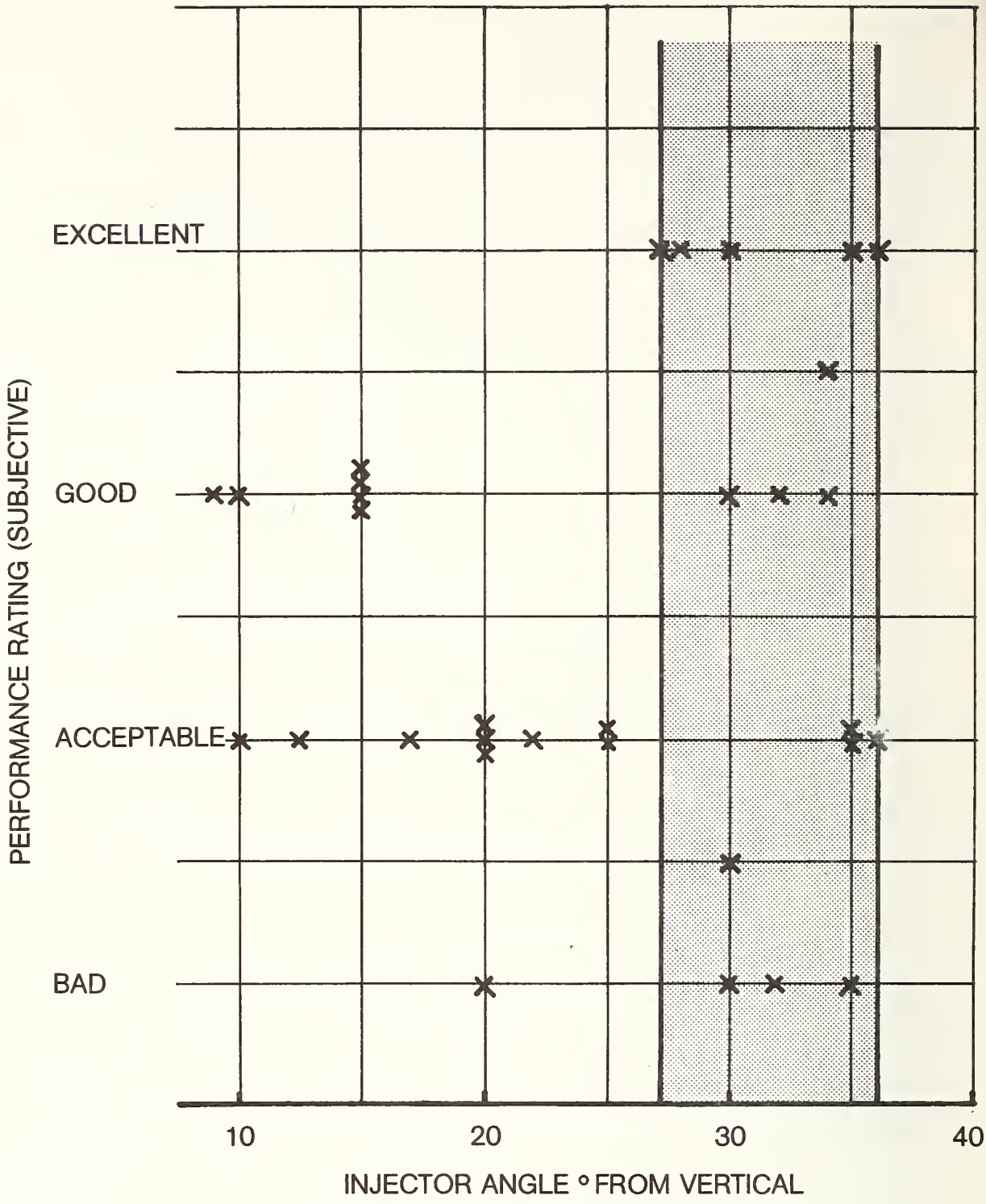

FIGURE 4.2-20: SUBJECTIVE ASSESSMENT OF THE EFFECTS OF INJECTOR ANGLE ON THE PERFORMANCE OF SWIRL CHAMBER ENGINES

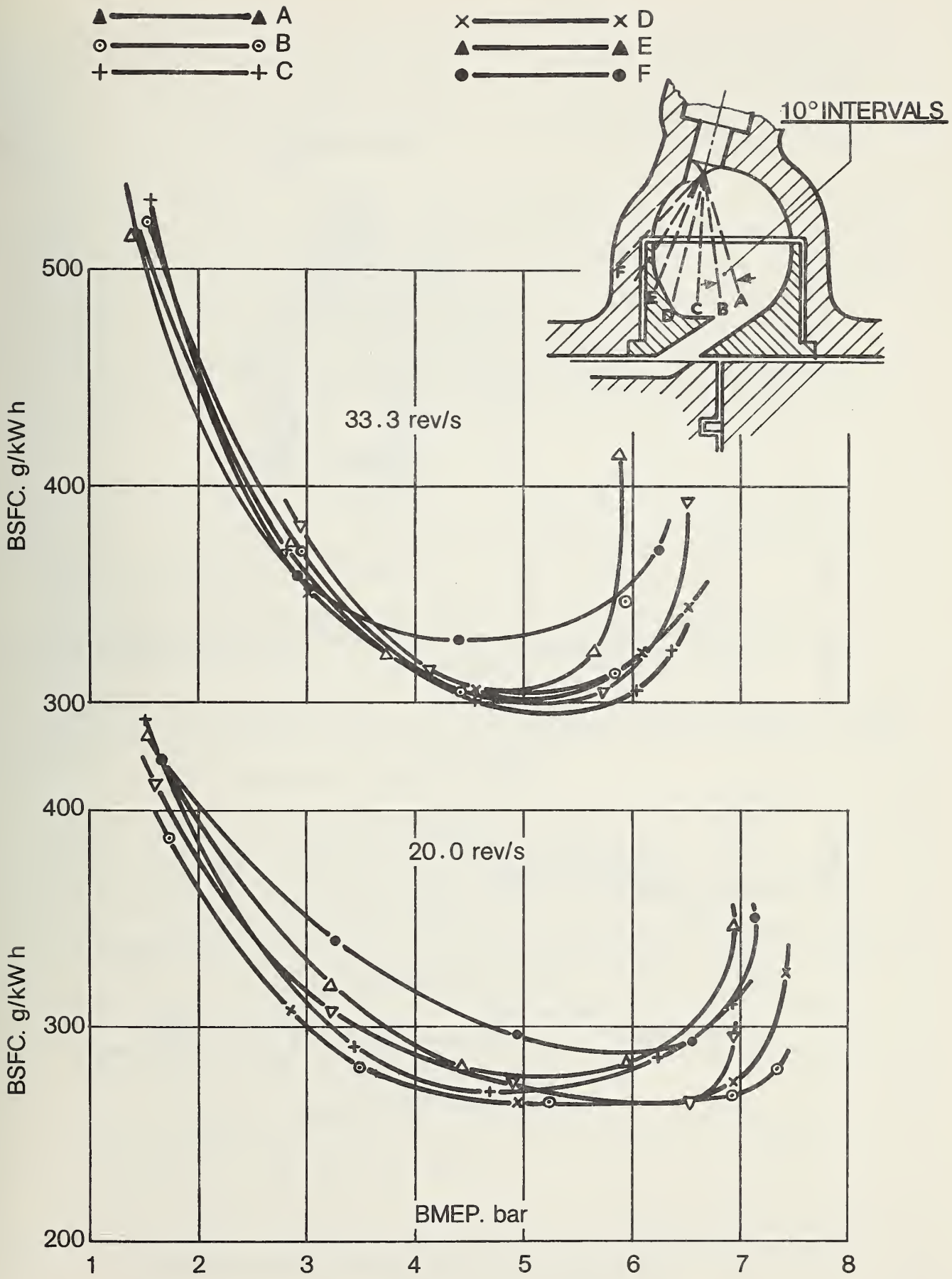

FIGURE 4.2-21: THE EFFECTS OF SPRAY ANGLE ON THE PERFORMANCE OF SWIRL CHAMBER ENGINES - SINGLE CYLINDER 1.6-LITER RESEARCH ENGINE

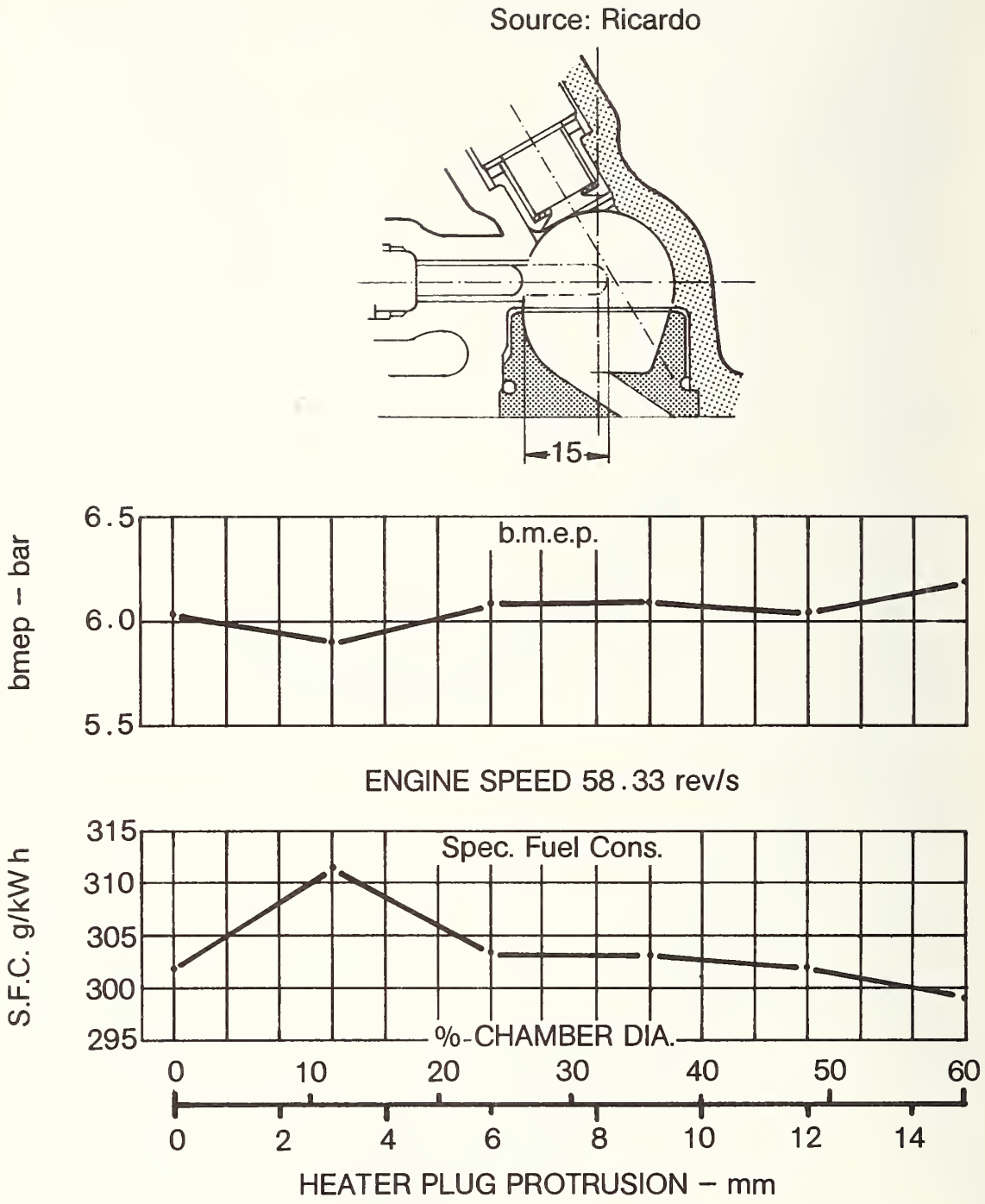

FIGURE 4.2-22: EFFECT OF HEATER PLUG PROTRUSION ON PERFORMANCE AT CONSTANT FUELING LEVEL

results indicate that optimum engine performance and specific fuel consumption is achieved with piston cavities of diameters 1.0 and 1.1 times the combustion chamber diameter. This is shown in Figures 4.2-23 and 4.2-24. It should be noted that the compression ratio in these tests drops as the piston cavity size increases. The combustion chamber volume thus becomes less than 50% of the total compression volume.

A series of tests on the same engine type was run with piston cavities of the same volume in order to keep the compression ratio at a constant level and the swirl chamber at roughly 50% of the total compression volume. The test results in Figures 4.2-25 and 4.2-26 show that the best bmep levels are reached with piston cavities of 25 and 29 mm diameters, or 1.19 and 1.38 times the swirl chamber diameter. The smaller of these two cavities yields higher performance at maximum engine speed, but the larger cavity leads to minor performance improvements at low engine speeds. The specific fuel consumption loops in Figure 4.2-26 also show the advantages offered at high engine speeds by the 25 mm diameter cavities and those offered by the 29 mm cavities at lower speeds.

In order to keep the volume constant, the piston cavity depth should decrease as the cavity diameter increases. Too shallow cavities (i.e. less than roughly 1.5 mm) no longer permit control of the combustion gases which then tend to pass immediately over the piston crown and do not mix with the air trapped in the cavities.

The piston trench should be wider than the throat in the hot plug to allow for misalignment. Its cross-sectional area should be larger than the throat area in order to avoid burning of the piston crown at the land.

Figure 4.2-24 shows the test results produced by a piston with a triangular cutout. This cavity configuration yielded significantly lower performance than conventional cavities.

4.2.2.7 Charge Cycle

The following three objectives determine the development of the charge cycle in passenger-car high-speed diesel engines with small displacement:

- High volumetric efficiency at rated engine speeds (83 rev/sec = 5,000 rpm) to ensure the desired specific output of 24 kw/liter.

- High final compression temperature at starting speed (2 - 2.5 rev/sec = 120 - 150 rpm) and at idle (12 - 15.5 rev/sec = 720 - 810 rpm) to provide for a cold-start and warm-up comfort as well as an idle noise that approximate those of spark-ignition engines.

- Low air-intake noise; this noise does not pose problems in spark-ignition engines, especially at partial-load operation, because of the throttle in spark-ignition engines.

These requirements necessitate careful design of intake system and valve timing. This applies in particular to the inlet valve closing time.

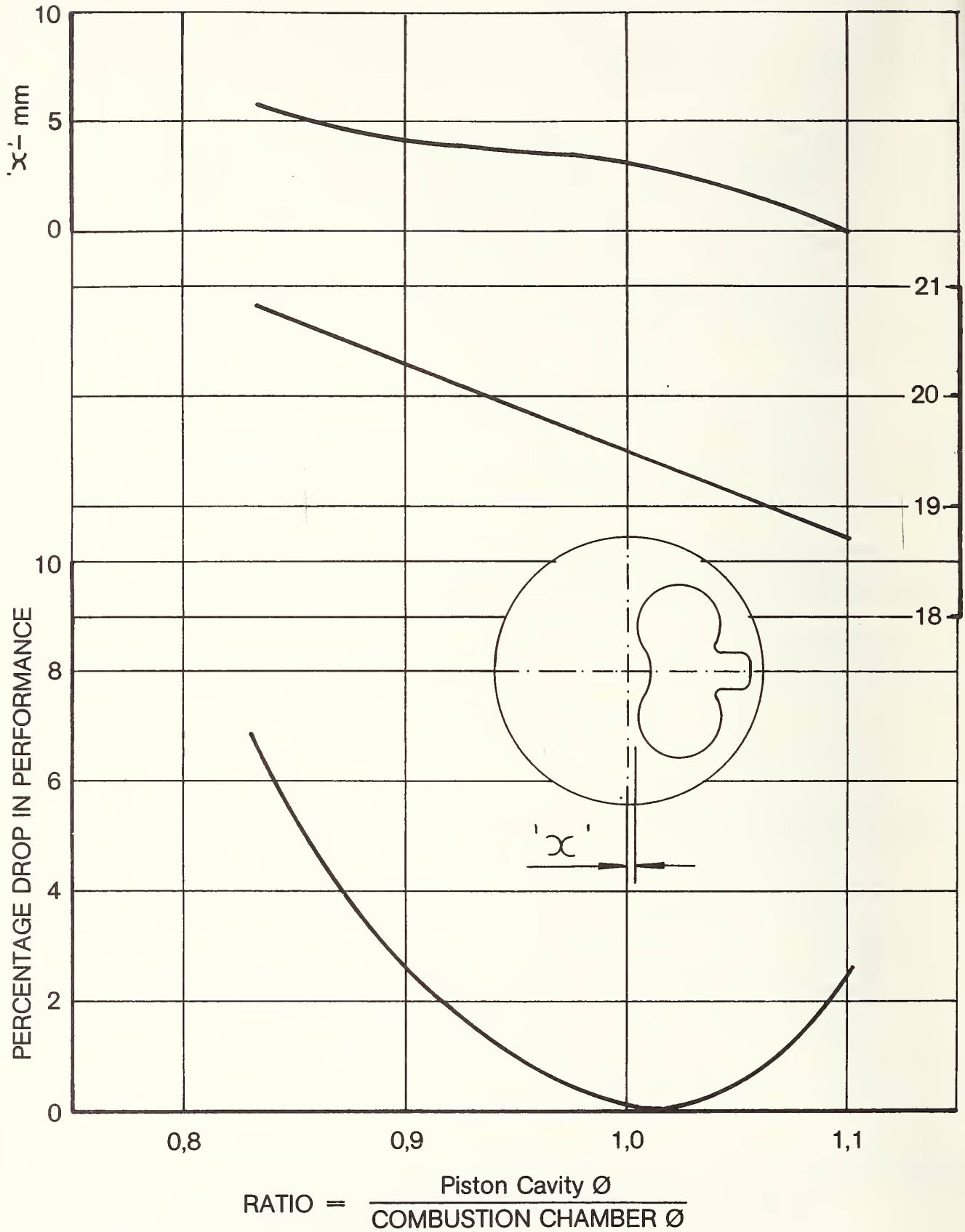

FIGURE 4.2-23: SWIRL CHAMBER ENGINES - EFFECT OF RATIO - PISTON CAVITY : COMBUSTION CHAMBER ø - ON PERFORMANCE OVER SPEED RANGE

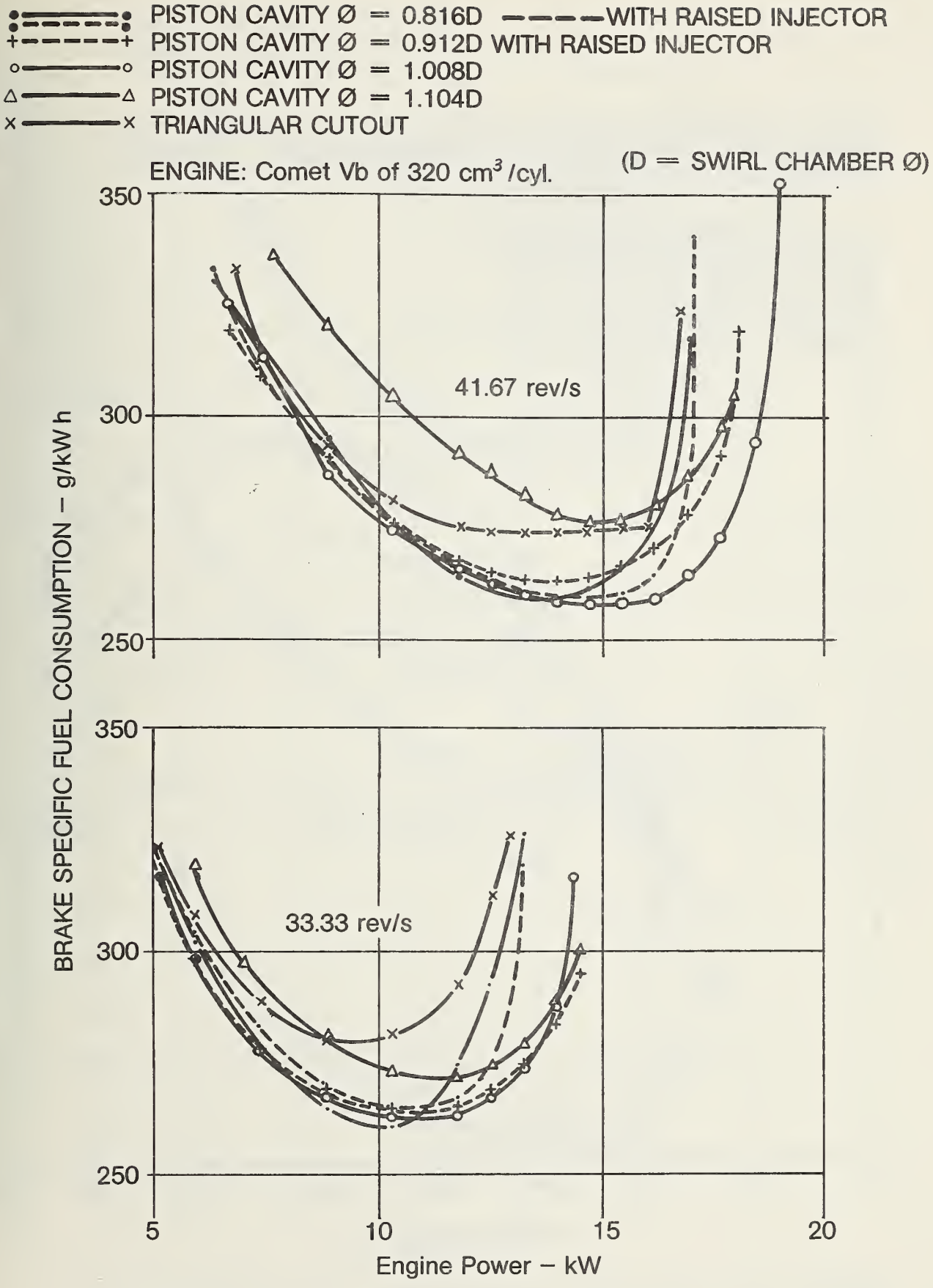

FIGURE 4.2-24: EFFECT OF PISTON CAVITY DIAMETER ON PERFORMANCE OF SWIRL CHAMBER ENGINES

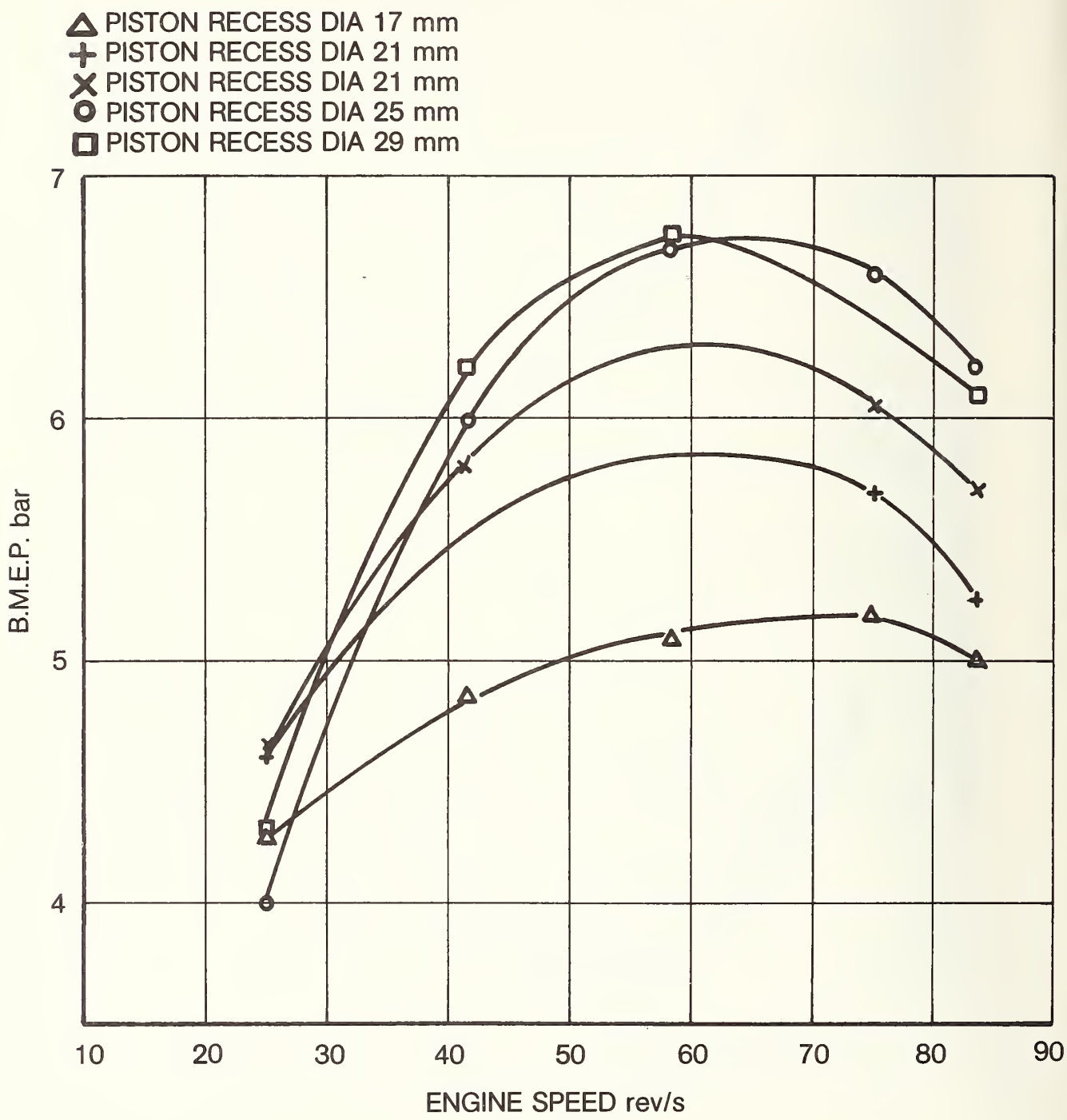

FIGURE 4.2-25: THE EFFECT OF PISTON CAVITY DIAMETER ON PERFORMANCE ON PERFORMANCE OF COMET Vb ENGINE

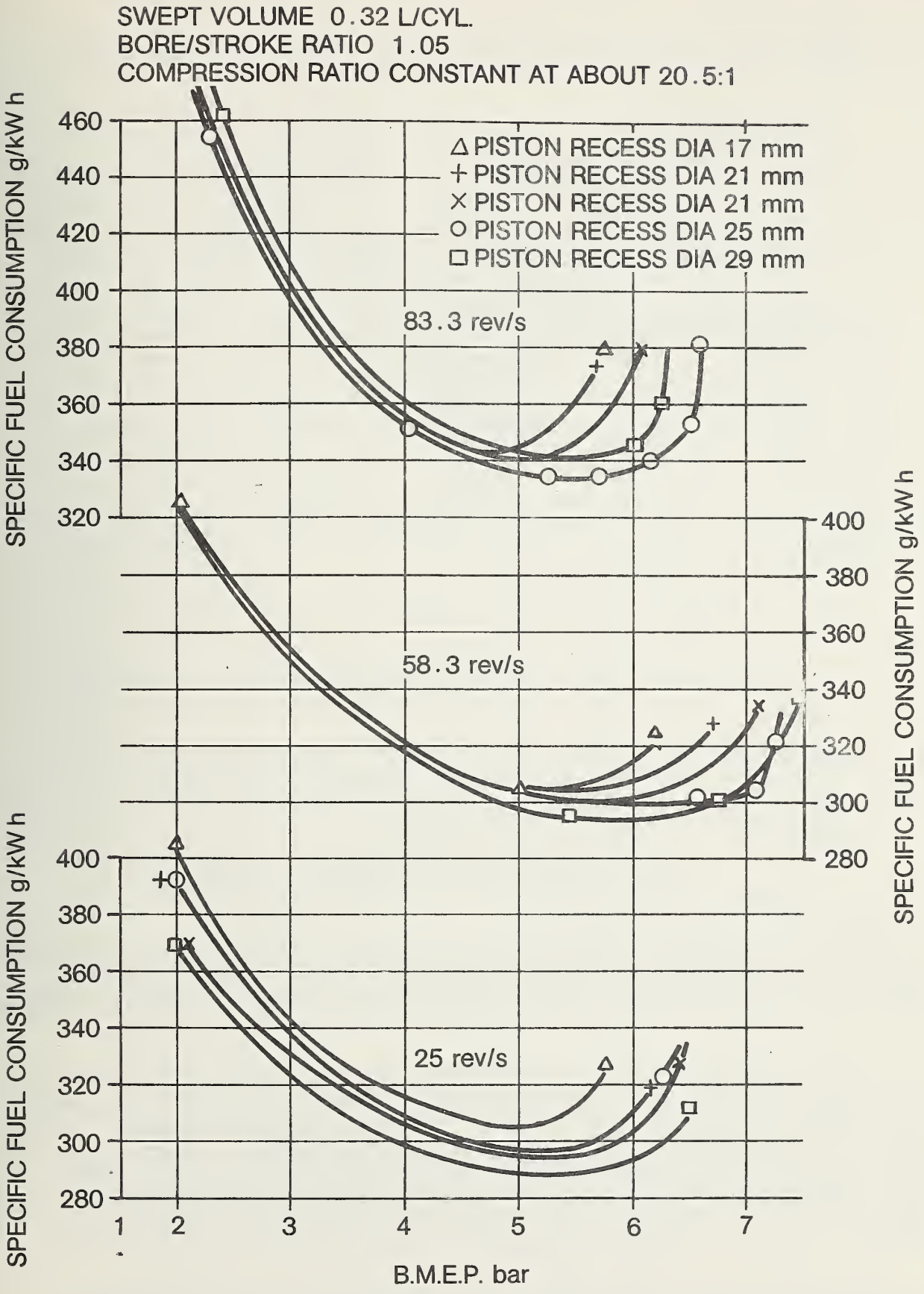

FIGURE 4.2-26: THE EFFECT OF PISTON CAVITY DIAMETER ON SPECIFIC FUEL CONSUMPTION THROUGHOUT THE SPEED AND LOAD RANGE ON A COMET Vb ENGINE

Figure 4.2-27 shows the interdependencies between final compression temperature, inlet valve closing time, and compression ratio.

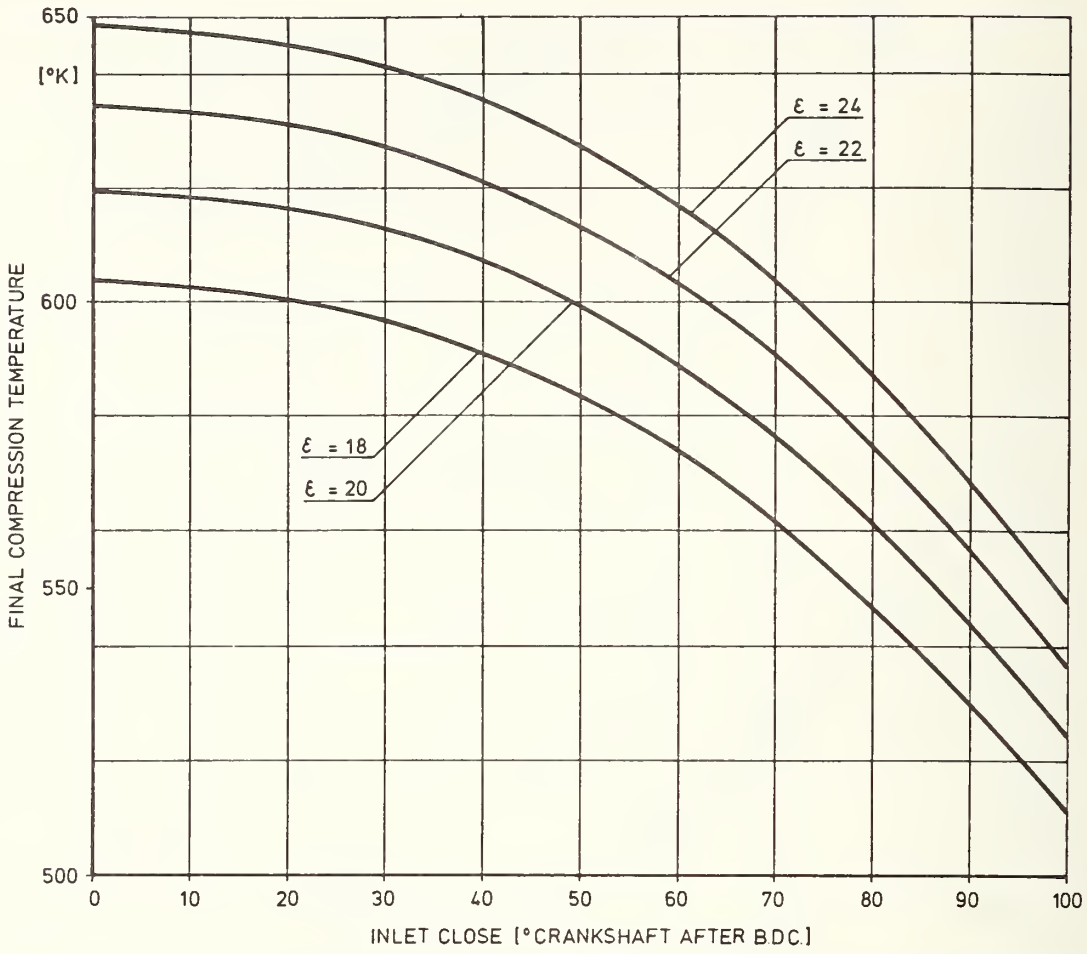

FIGURE 4.2-27: FINAL COMPRESSION TEMPERATURE AS A FUNCTION OF INLET VALVE CLOSING TIME, ENVIRONMENTAL TEMPERATURE 20°C.

The intake valve in modern passenger-car diesel engines closes effectively at 90° BDC. The advancing of this timing by 25° would mean that either the compression could be reduced by six units or that the final compression temperature could be raised by 40°C if the compression ratio remains unchanged.

Efforts are made, therefore, to advance the intake valve closing time as much as possible when the intake cam geometry of a passenger car diesel engine is optimized. On the other hand, there must be sufficient delivery at rated speed in order to ensure the desired output of rated power. Figure 4.2-28 shows the restrictions imposed by the kinematics of the power plant. The space between piston and valve should be minimized for low-capacity diesel engines so that almost 50% of the dead space could be used for the swirl chamber.

The intake cam lift is limited by the piston travel; this condition poses a typical trade-off problem. A compromise was to be found between a narrow cam (earliest possible intake-valve closure time during start-up and idle, and latest possible intake-valve opening because of kinematic requirements) and a broad cam for maximum power output.

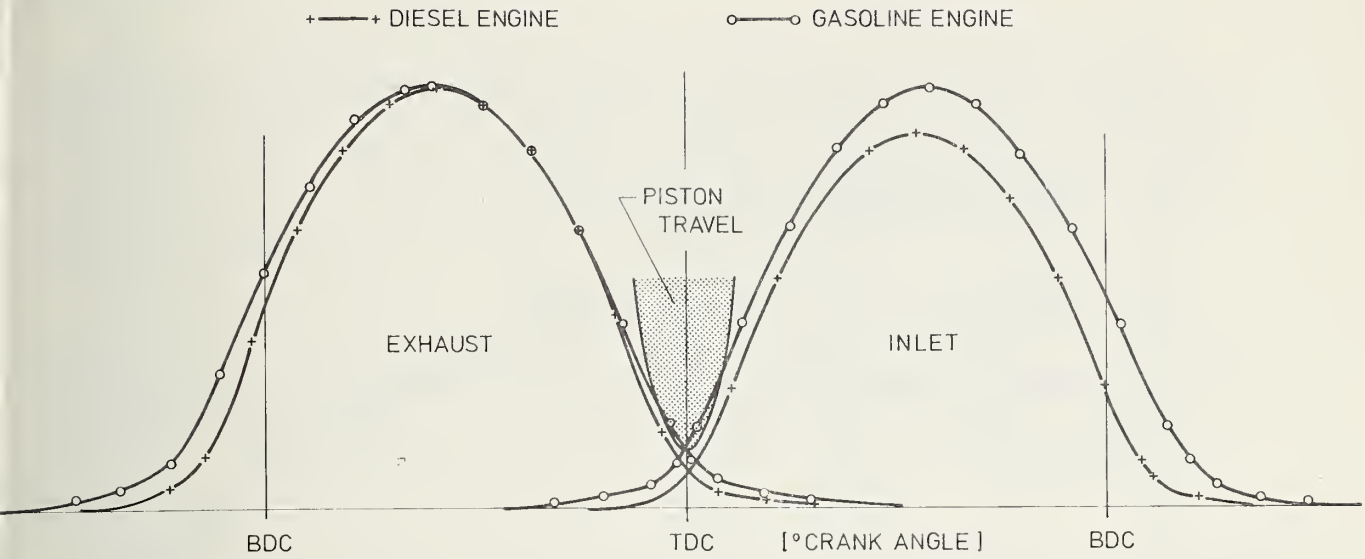

FIGURE 4.2-28: VALVE TRAVEL CURVE

The high compression ratio of the indirect injection diesel engine results in a very narrow clearance between piston and cylinder head. This again restricts valve overlap to roughly 12^{0} on either side of TDC. As a consequence, changes may be made only to the intake valve closing point and the exhaust valve opening.

The performance characteristics are determined by the termination of the intake process. This applies to both the conventional gasoline engine and the diesel concept. An early closing of the intake valve raises the mean effective pressure in the lower rpm range. However, this occurs at the expense of the high mean pressure at higher rpm's (Figure 4.2-29).

4.2.2.8 Injection

Optimized combustion can be obtained only if the injection system and combustion chamber are compatible. The injection characteristic or the beginning of injection and fuel delivery curve, which is determined by the type of injection system, together with the movement of the air in the combustion chamber determines the air/fuel mixture formation and combustion. Therefore, the characteristics of injection pump, nozzles, and injection lines must be matched to the specific requirements of each engine type.

It is essential that not only the injection system is tuned to full-load operation and road-load curve, but that also the collective load is taken into account, which occurs especially in city traffic in the range of up to approximately 50% speed range and up to full load.

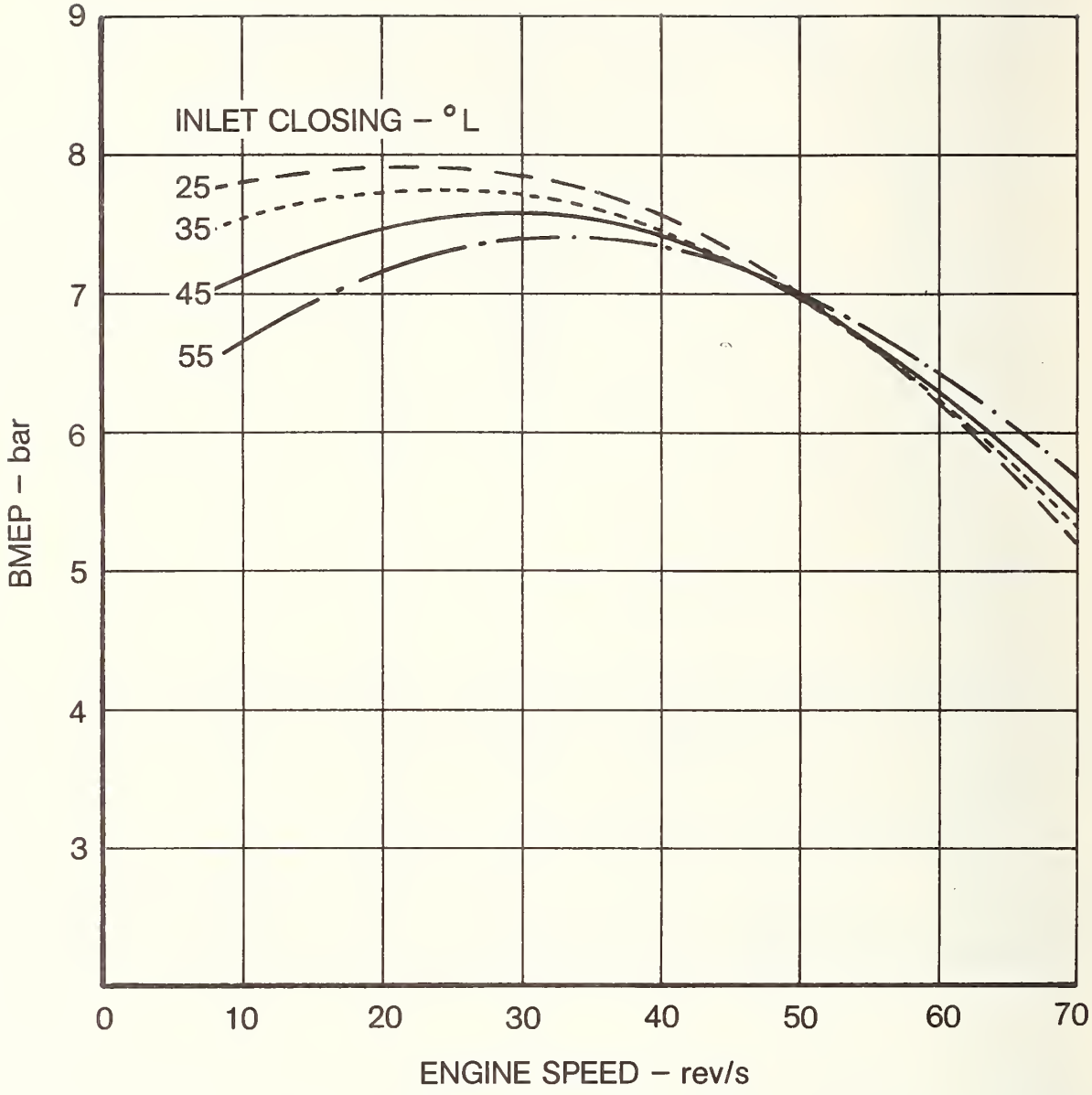

FIGURE 4.2-29: ESTIMATED EFFECT OF INLET VALVE TIMING ON LOW SPEED TORQUE

85 ø x 90 Swirl Chamber Engine

Figure 4.2-30 shows the effects of injection timing on swirl chamber performance. The retard of timing reduces the bmep and increases specific fuel consumption. Both of these effects become more pronounced at high engine speeds.

A retardation of the injection timing from the optimum performance condition reduces the NOx levels (see Figure 4.2-31). A small retard from 12^{o}E to 8^{o}E leads to a maximum reduction of NOx at high and low engine speeds. Any further retard entails only minor decreases in NOx emissions and raises the HC level. This is shown in Figures 4.2-32 and 4.2-33, which illustrate the opposing trends versus the specific fuel consumption with the injection time as a parameter.

The effects of injection timing on the levels of HC/CO/NOx emissions in the urban cycle are shown in Figure 4.2-34. Figures 4.2-35 and 4.2-36 show the injection requirements for a low-emission swirl chamber engine at full- and no-load operation. They indicate an advancement of dynamic injection timing by 3 - 4^{o} crank angle per 1000 rpm (16,7 rev/sec). The advancing of the dynamic injection at low load over the load range improves output and lowers emissions mostly in the lower engine speed range.

The design of the injection system should provide for compliance with the desired fuel delivery curve, while the nozzle should produce a good spray pattern over the entire load and speed range so that a trade-off becomes possible in the narrow range of fuel economy and HC and NOx emissions. Therefore, the tolerances in the fuel delivery curve and the injection timing variances from line to line and from pump to pump must be adhered to as closely as possible also in mass production because fuel economy and emission levels react quite sensitively to these tolerances as may be seen from the preceding figures (also see Section 6.1).

Particular attention should be devoted to two aspects in regard to the tuning of a diesel engine injection system[12]:

- The adaptation of the governor to passenger-care requirements,

- Cold-start and warm-up behavior.

The all-speed governor used in commercial vehicles is also used in the passenger car (see Figure 4.2-37). This type of governor, however, produces an acceleration jerk in vehicles with a high HP/IW ratio. This effect is not acceptable for good driveability. Therefore, the car-application speed governor is used in passenger cars (see Figure 4.2-38), which provides for an acceleration behavior similar to that of a well tuned spark-ignition engine.

The low-speed range of this modified partial-load governor has been expanded. It also governs maximum engine speed. When operating at low speeds, this governor ensures smooth load absorption during start-up and thus provides for maximum utilization of the design advantages.

Figure 4.2-37 shows the operation of the car application governor over the entire speed range, covering

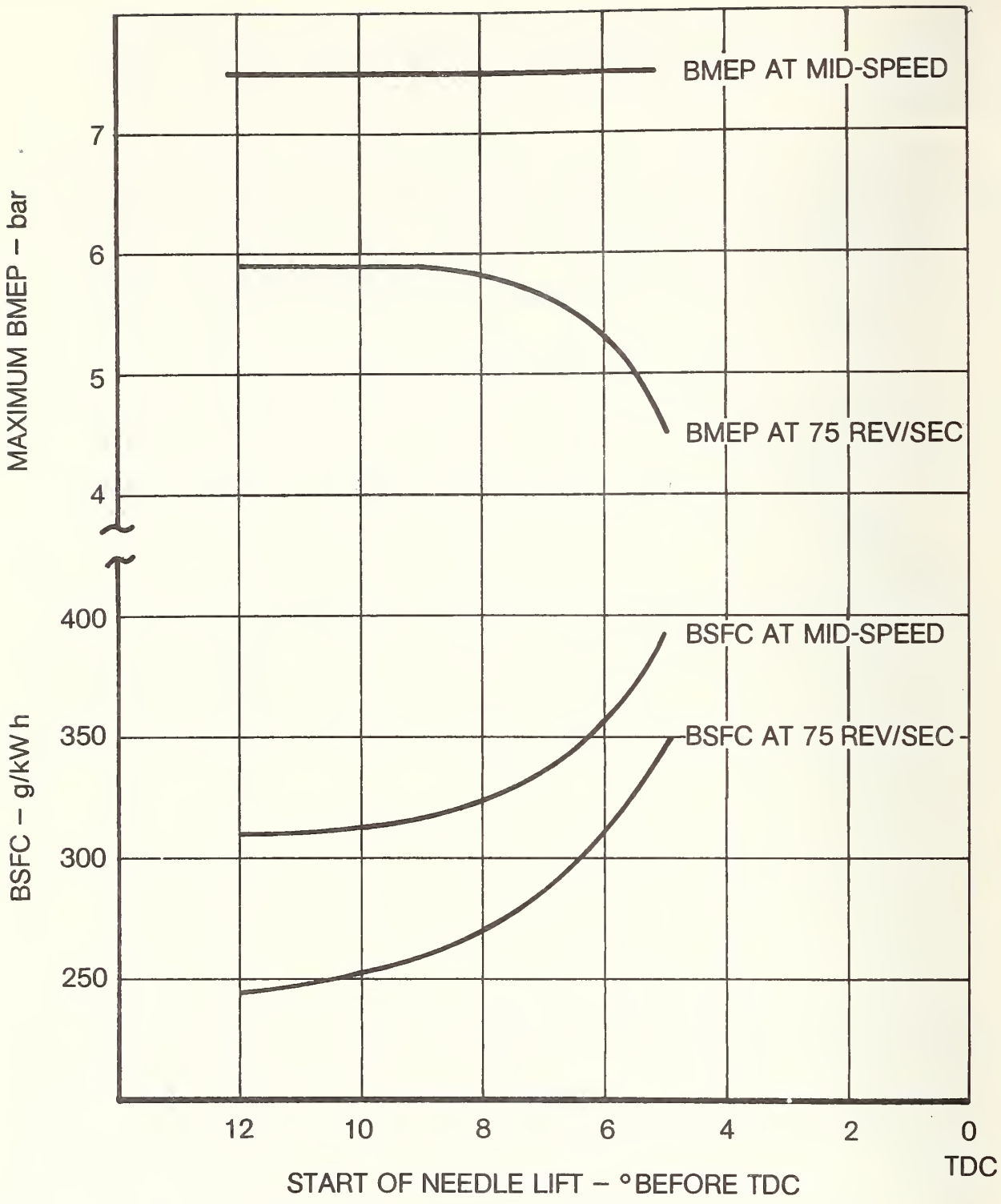

FIGURE 4.2-30: EFFECT OF INJECTION TIMING ON PERFORMANCE OF A SWIRL CHAMBER ENGINE OF APPROXIMATELY 0.4-L/CYL.

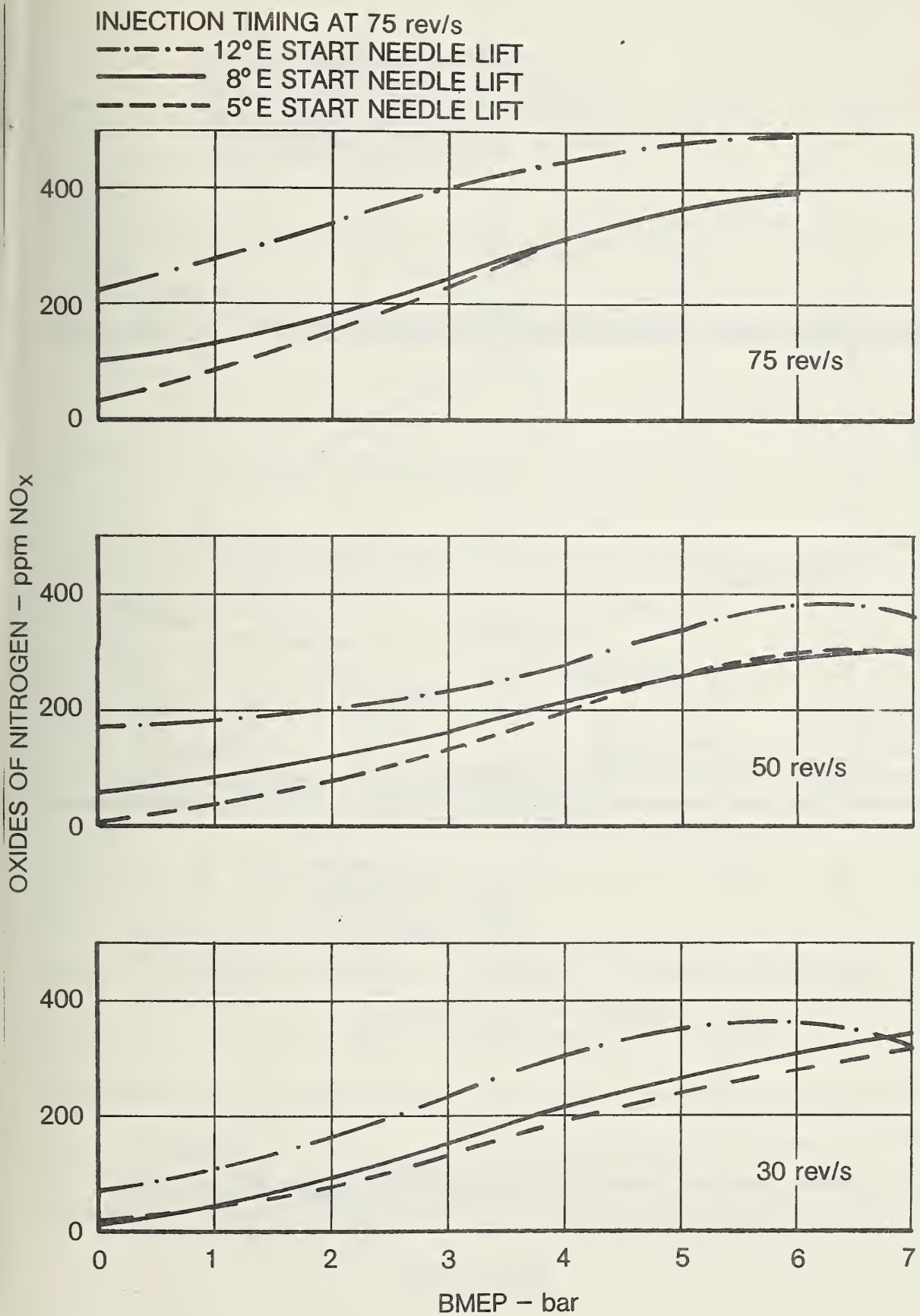

FIGURE 4.2-31: EFFECT OF INJECTION TIMING ON NOx EMISSIONS IN SWIRL CHAMBER ENGINES

Naturally Aspirated COMET Vb, about 0.4L/Cyl.

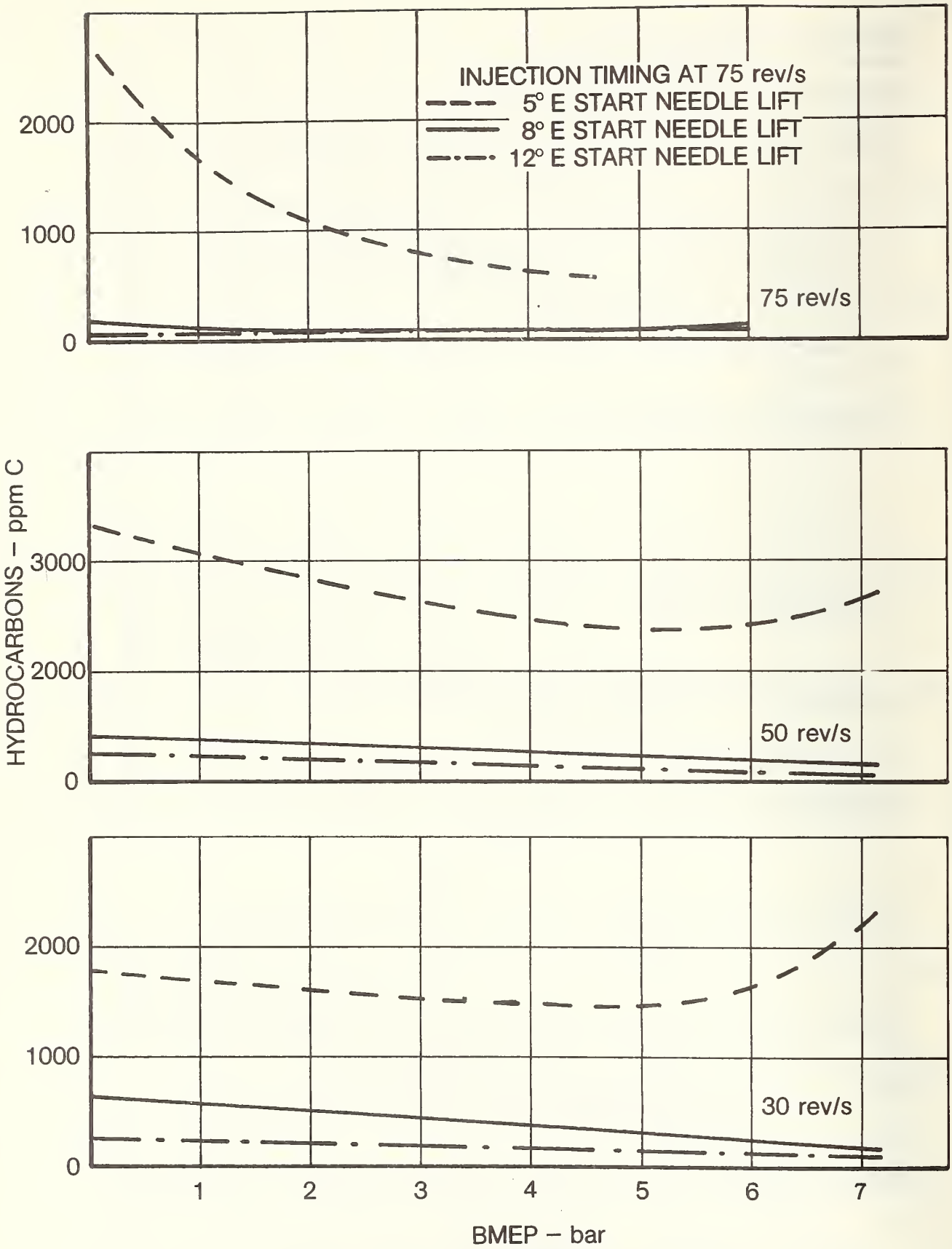

FIGURE 4.2-32: EFFECT OF INJECTION TIMING ON HC EMISSIONS IN SWIRL CHAMBER ENGINES

Naturally Aspirated COMET Vb, about 0.4 L/Cyl.

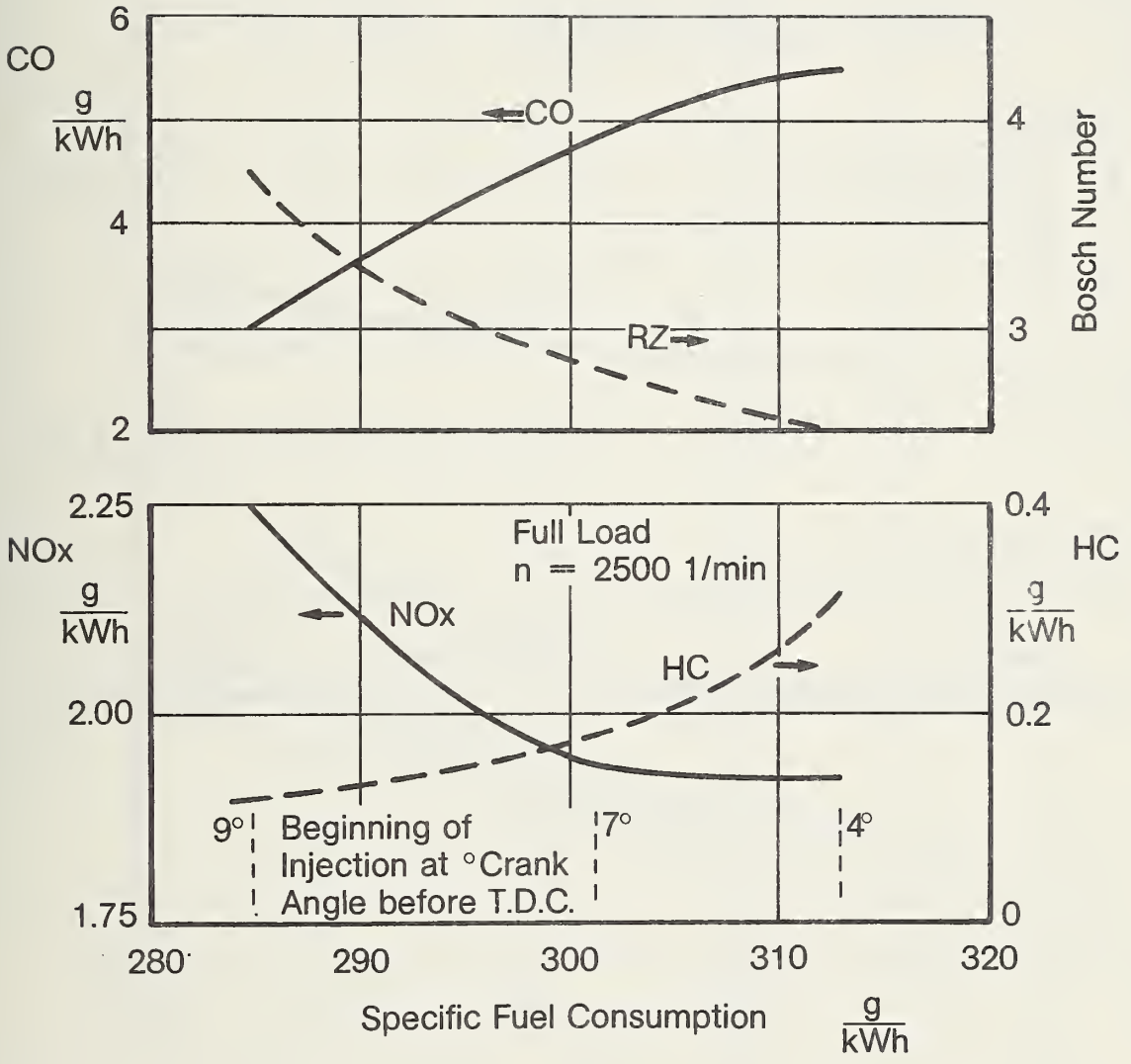

FIGURE 4.2-33: EMISSIONS AND CONSUMPTION VERSUS INJECTION TIMING

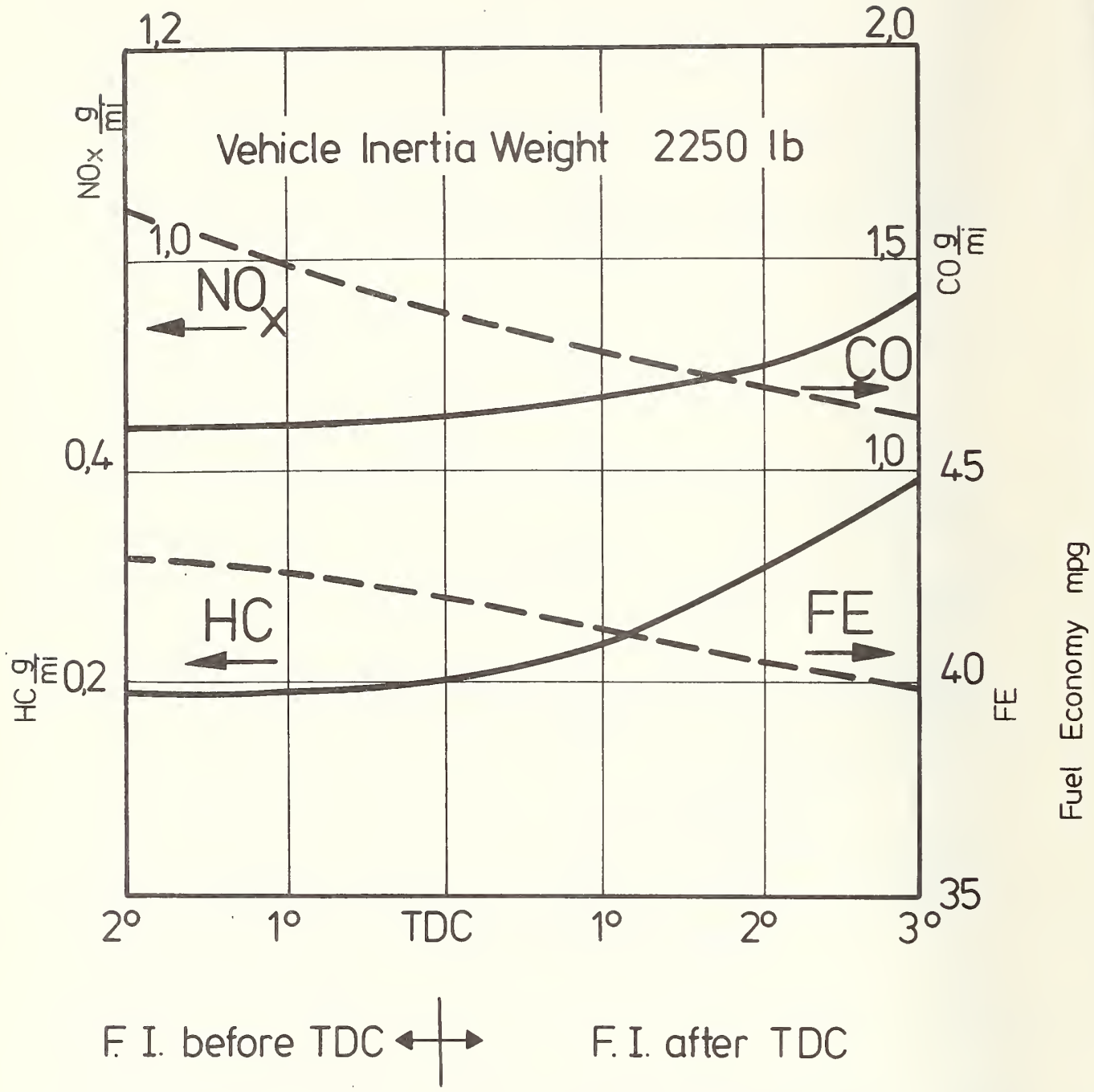

FIGURE 4.2-34: THE INFLUENCE OF FUEL INJECTION TIMING ON EXHAUST EMISSIONS AND FUEL CONSUMPTION IN CVS TESTS

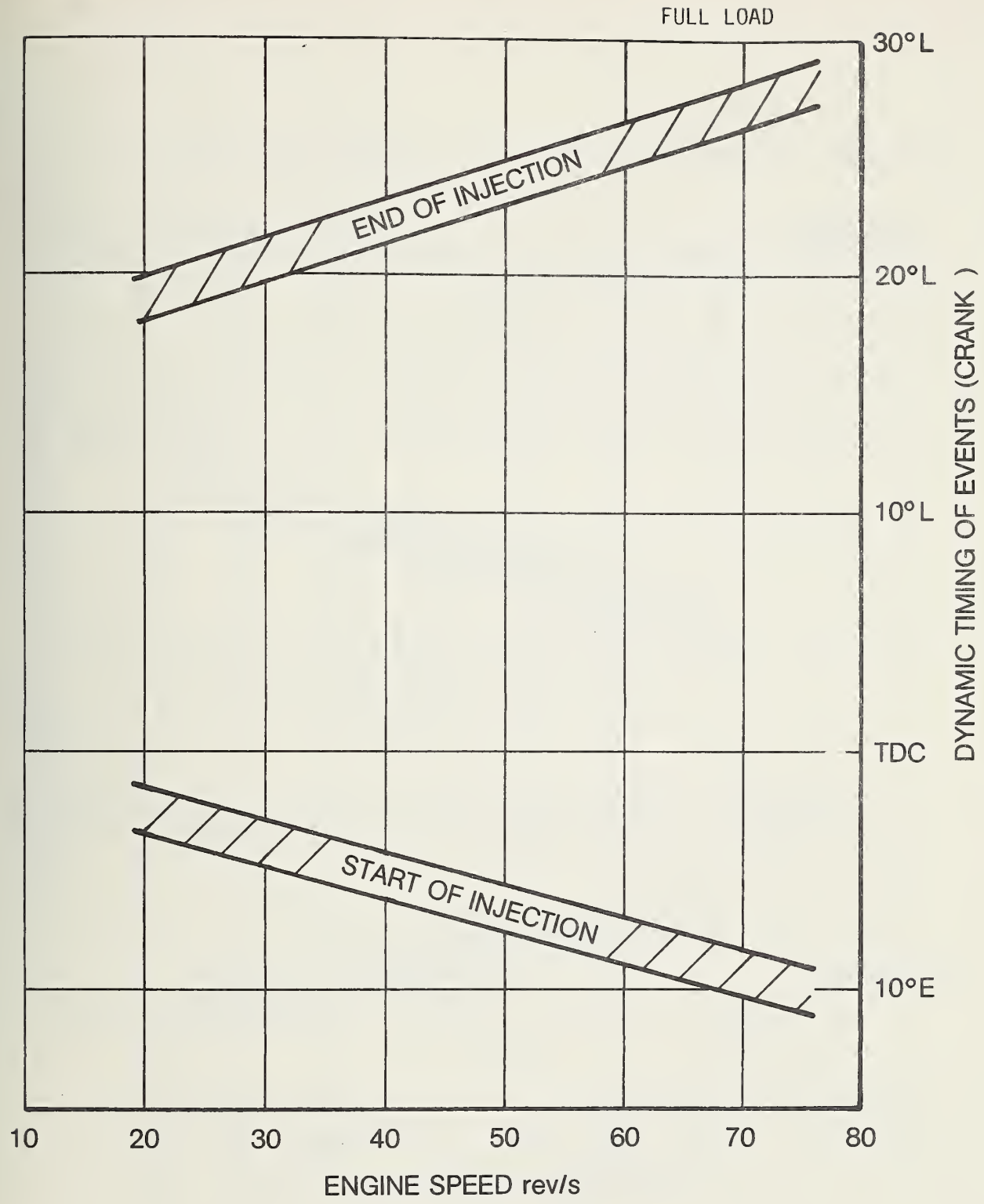

FIGURE 4.2-35: DYNAMIC INJECTION TIMINGS REQUIRED FOR EMISSION- AND NOISE-OPTIMIZED, SMALL HIGH-SPEED NATURALLY-ASPIRATED COMET V ENGINES

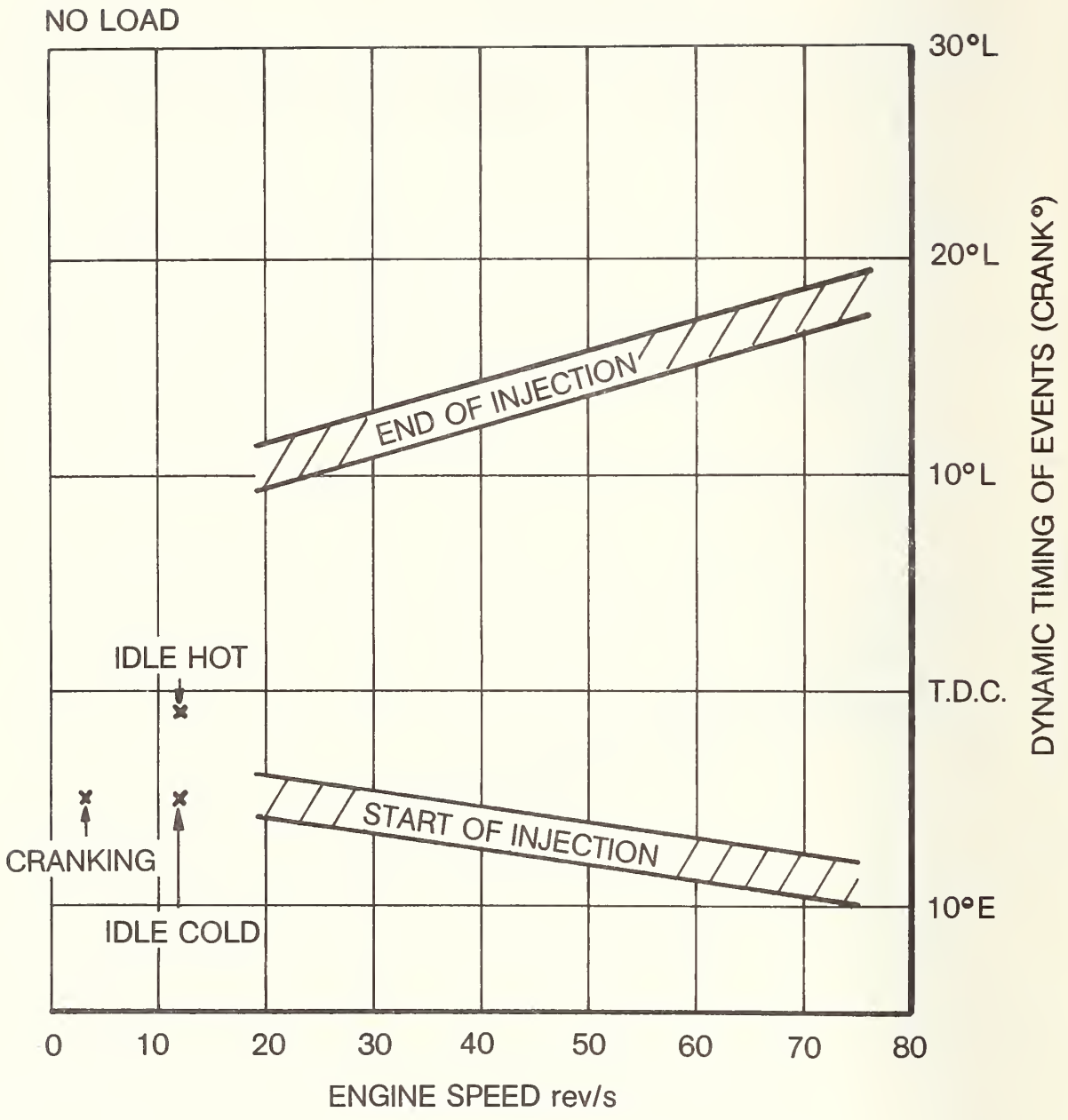

FIGURE 4.2-36: DYNAMIC INJECTION TIMINGS REQUIRED FOR EMISSION- AND NOISE-OPTIMIZED, SMALL HIGH-SPEED NATURALLY-ASPIRATED COMET V ENGINES

- Start-up

- Idle

- Partial load (speed range not affected by the governor and controlled directly by the accelerator)

- Full load (cutoff speed).

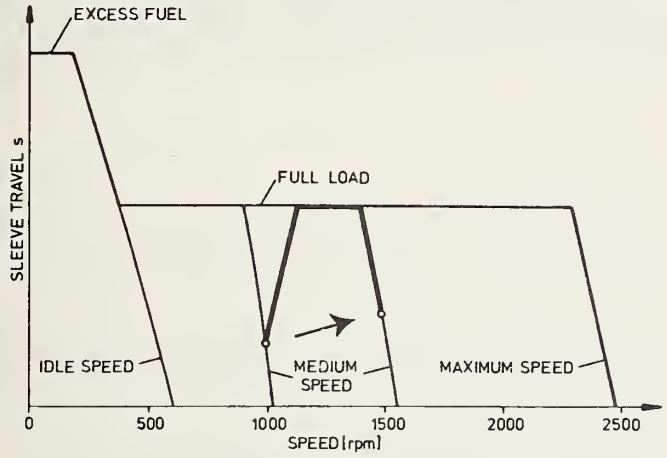

FIGURE 4.2-37: OPERATION OF THE ALL-SPEED GOVERNOR

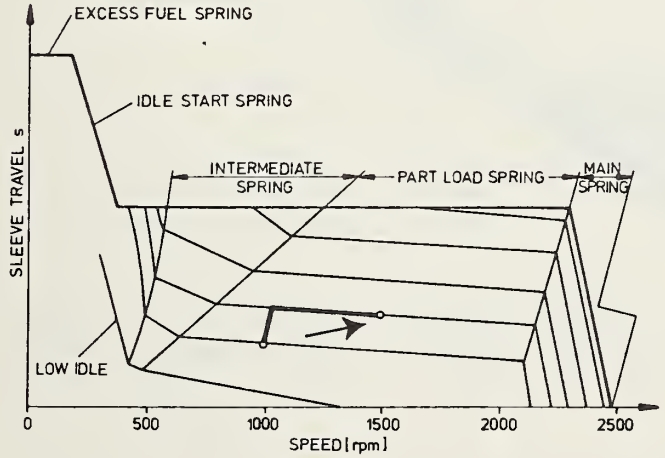

FIGURE 4.2-38: OPERATION OF THE CAR-APPLICATION SPEED GOVERNOR

Two-stage combustion diesel engines pose problems in regard to vehicle driveability and blue-smoke emissions under cold-start conditions at temperatures below 0°C (32°F).

The cold-start device (CSD) advances the ignition timing of the cold engine and thus provides for proper combustion. Upon completion of the warm-up phase the CSD is pushed back and the injection timing is retarded. The resetting of the CSD led to an appreciable cut in engine idle noise. The curves in Figure 4.2-39 show injection timing adjustments with and without CSD. The same graph also contains a curve indicating the injection timer settings for minimum warm-up (a minimum of blue-smoke emissions). When the engine speed exceeds 2,000 rpm, the CSD no longer affects injection timing, and combustion at those higher engine speeds follows a more constant pressure cycle.

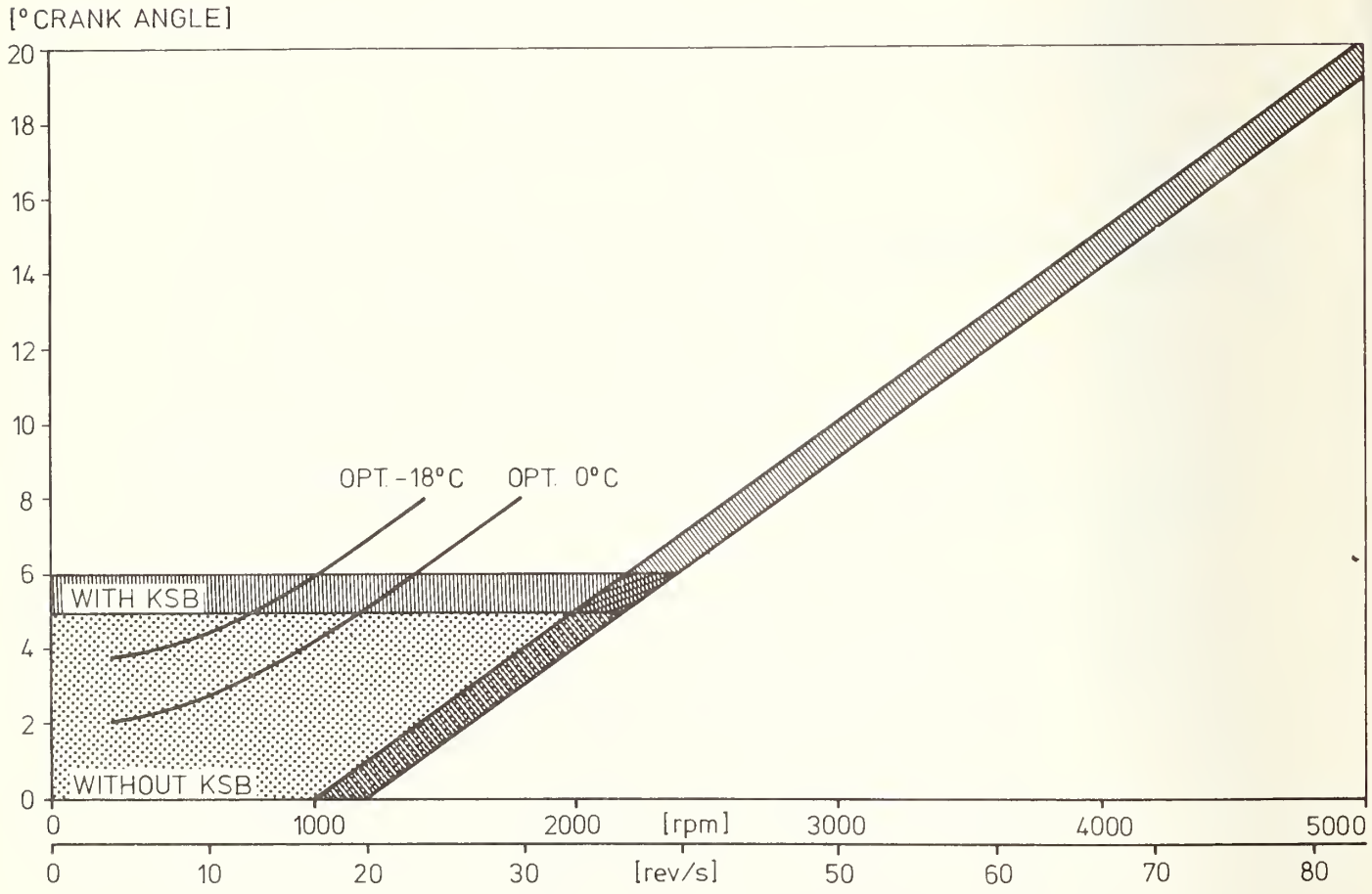

FIGURE 4.2-39: INJECTION TIMING ADJUSTMENT WITH CSD

Pipe wave travel significantly affects injection timing and rate. The fuel moved by the plunger does not flow evenly through the nozzle. There may be a delay of several degrees cam angle between the geometric start of delivery and the onset of injection at the nozzle.

Figure 4.2-40 is a comparison between the geometric feed rate and the rate of injection at the rated pump speed N = 2,500 rpm at the engine speed of 5,000 rpm.

The four diagrams show the following data (top to bottom):

1. Geometric feed rate computed from plunger lift (H) and plunger speed (C)

2. Pressure curve at the injection nozzle intake side

3. Needle lift

4. Actual rate of injection.

The feed wave moves through the injection lines at the speed of sound, and its front generates sufficient pressure at the nozzle to lift the needle for the injection of the proper amount of fuel.

All graphs use the same time scale. The scale quantity is the same for the feed rate graph (top) and the graph showing the injection rate (bottom). The start of the rise in nozzle pressure and the onset of the plunger feed at about 10^{0} cam angle were assumed to occur at the same time in order to facilitate a comparison. The ignition timer must be used to control any retardation of injection which might become necessary because of engine speed.

The distributor pump is particularly well suited for passenger-car application. Contrary to the in-line injection pump concept where one plunger is provided for each cylinder, the rotary pump has only one plunger which works as distributor[15]. While leakage problems increase as the number of cylinders rises, and while it becomes more difficult to maintain the accurate injection rate at high engine speeds and additional measures become necessary to ensure proper spray adjustment, the weight, size, and cost of the distributor pump should be significantly lower because the speed governor, injection timing, and feed pump are combined into one unit.

4.3 THE EFFECTS OF COMBUSTION SYSTEM VARIABLES ON EMISSIONS

Compliance with the stringent emission standards of .41/3.4/1.0 gram/mile of HC/CO/NOx requires modifications. Production tolerances and deterioration factors necessitate a tolerance margin.

The following modifications may be contemplated:

- Fuel injection timing

- Ceramic swirl chamber

- Water injection

- Exhaust gas recirculation (EGR).

Fuel injection timing affects nearly all engine output characteristics including power output, fuel economy, HC/CO/NOx emissions, smoke visibility and noise. The optimization of each of these characteristics requires a number of injection timing adjustments. Only a limited range of crank angles is available in which this optimization can be accomplished (see Section 6).

A trade-off between injection timing and various engine-output characteristics would lead to lower emissions. Prototype NOx emission values of .75 gram/mile were obtained by starting the injection later than at 3^{o} after TDC.

However, this lowered fuel economy by about 10% and pushed the HC emission in the range of .41 gram/mile. In addition, power output dropped. Therefore, this trade-off was disregarded.

4.3.1 Exhaust Gas Recirculation

Exhaust gas recirculation is one way to significantly lower the NOx emissions of diesel engines. Up to 50% exhaust gas can be recirculated at low engine loads because of the large fraction of excess air in the exhaust gas of a diesel engine. The effective EGR which takes into account the dilution of the exhaust gas by the excess air is defined as follows:

$$\text{Effective EGR} = \frac{\text{EGR}}{\text{Air-to-Fuel Ratio}}$$

Figure 4.3-1 shows the effects of exhaust gas recirculation at 25 rev/sec (1,500 rpm). The tests were conducted with hot and cold exhaust gas at standard timings and with cold exhaust gas at a 4^{o} injection retard.

The results of these tests showed a considerable reduction of the NOx levels associated with a reduction in smoke-limited performance. Little change in specific fuel consumption or NOx levels was observed at low load factors below 3 bar bmep. The gains in NOx reduction were significant at higher load factors. Figure 4.3-2 shows the effects of the proportion of exhaust gas recirculation on performance and NOx emissions. Significant reductions in NOx levels were obtained with hot exhaust gas recirculation. Exhaust gas recirculation of 15% reduced the NOx levels by 44% and lowered the performance by roughly 22%. A 20% EGR reduced the NOx levels to approximately 48% only and dropped the performance more rapidly by more than 30%.

Cooling of the recirculated exhaust gases leads to a lesser performance drop because of better volumetric efficiency while the reduction of NOx emissions increases. A 5% cold EGR lowers the NOx levels by almost 30% and the maximum smoke-limited bmep by roughly 1%. Any further increases of cold EGR up to 20% produces a consistent reduction in NOx levels by 60% with a performance drop of 15%. Cold EGR in an engine with retarded injection timing continues to produce significant increases in the reduction of NOx levels with lesser performance penalty than with standard timing. A 5% EGR reduced the NOx levels by 26% with a performance drop of less than 1%. Again, further increases in EGR led to smaller gains in NOx level reduction and a deterioration in performance.

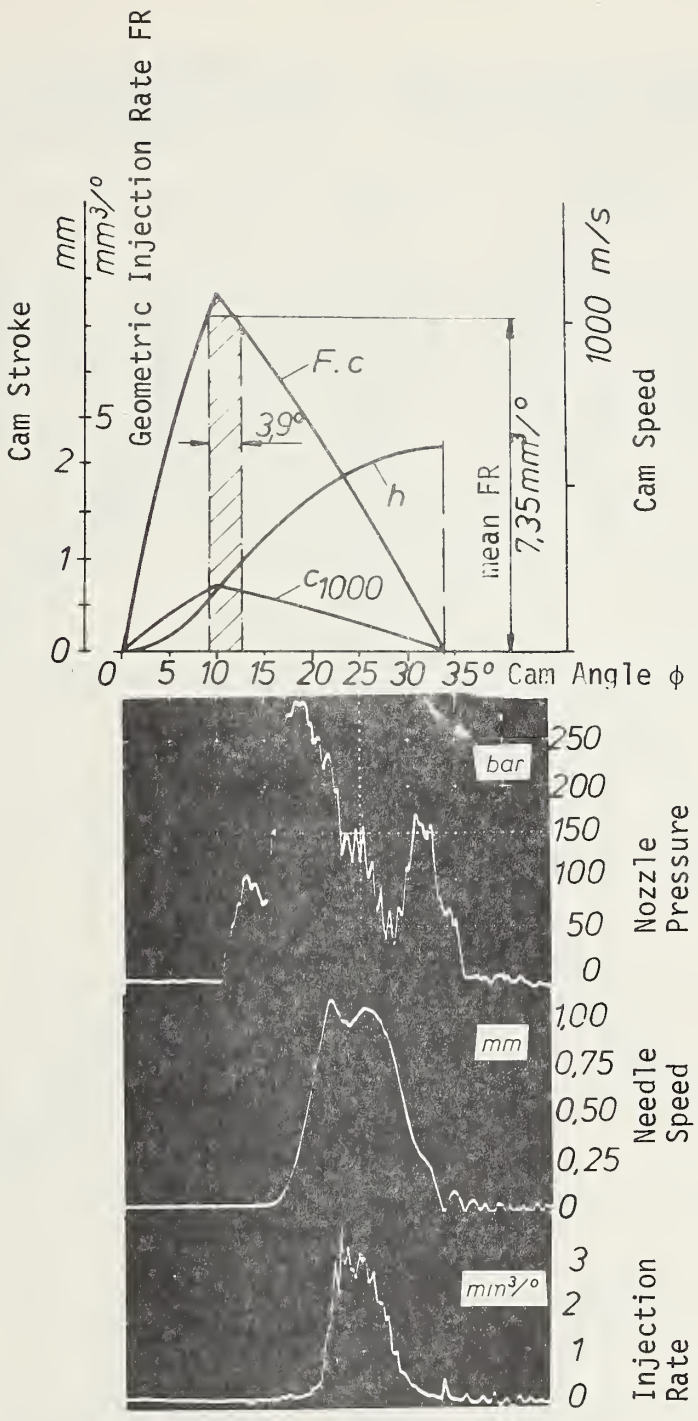

FIGURE 4.2-40: DISTRIBUTOR PUMP, TYPE VE 419F 2500R16
Nozzle: DNO SD 193
Opening Pressure: 130 bar
Inj. Tubing: $\phi 6 \times \phi 2.25 \times 340$ mm

$n = 2400\ min^{-1}$
$Q = 29\ mm^3$ per Stroke

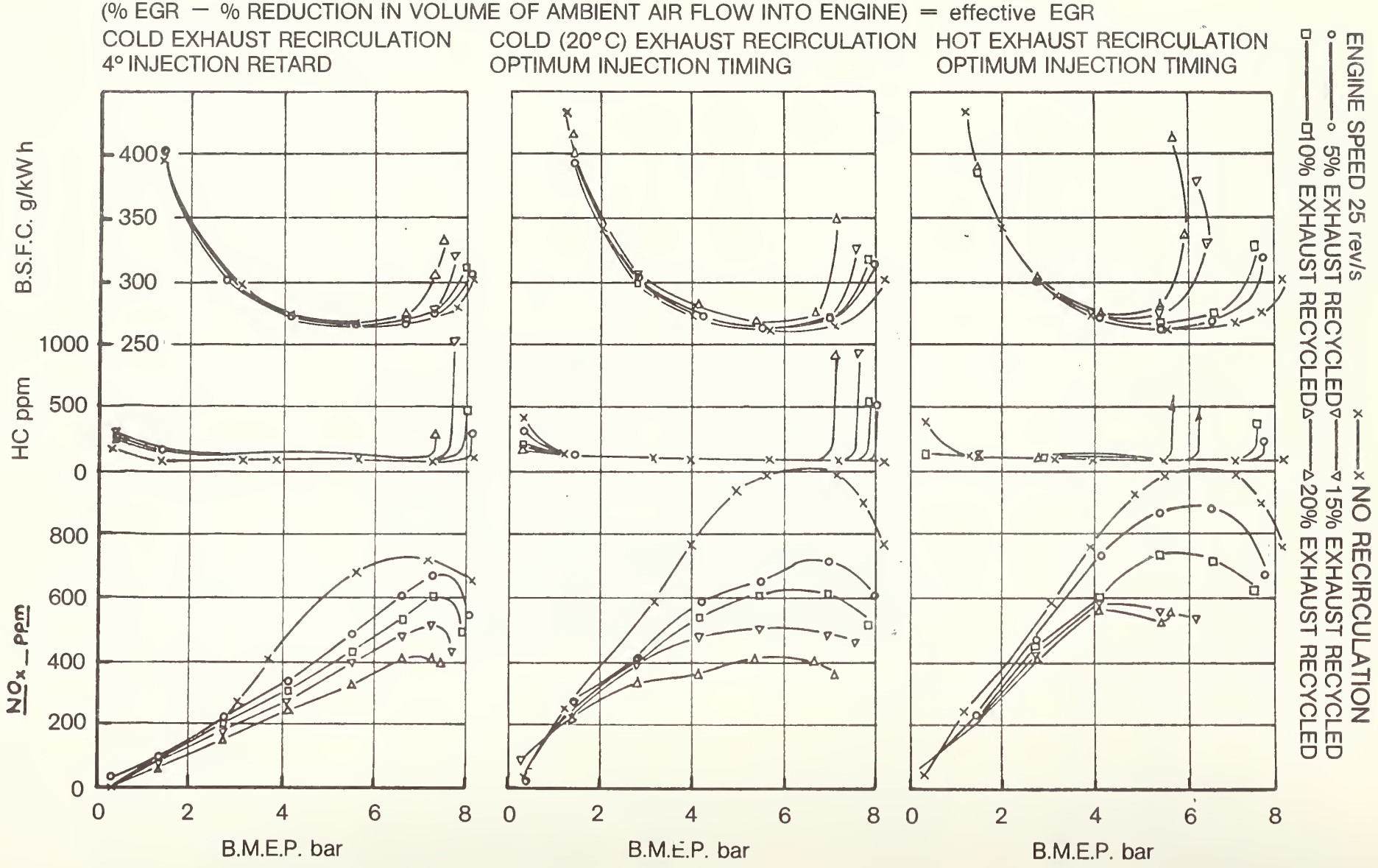

FIGURE 4.3-1: EFFECT OF EXHAUST GAS RECIRCULATION

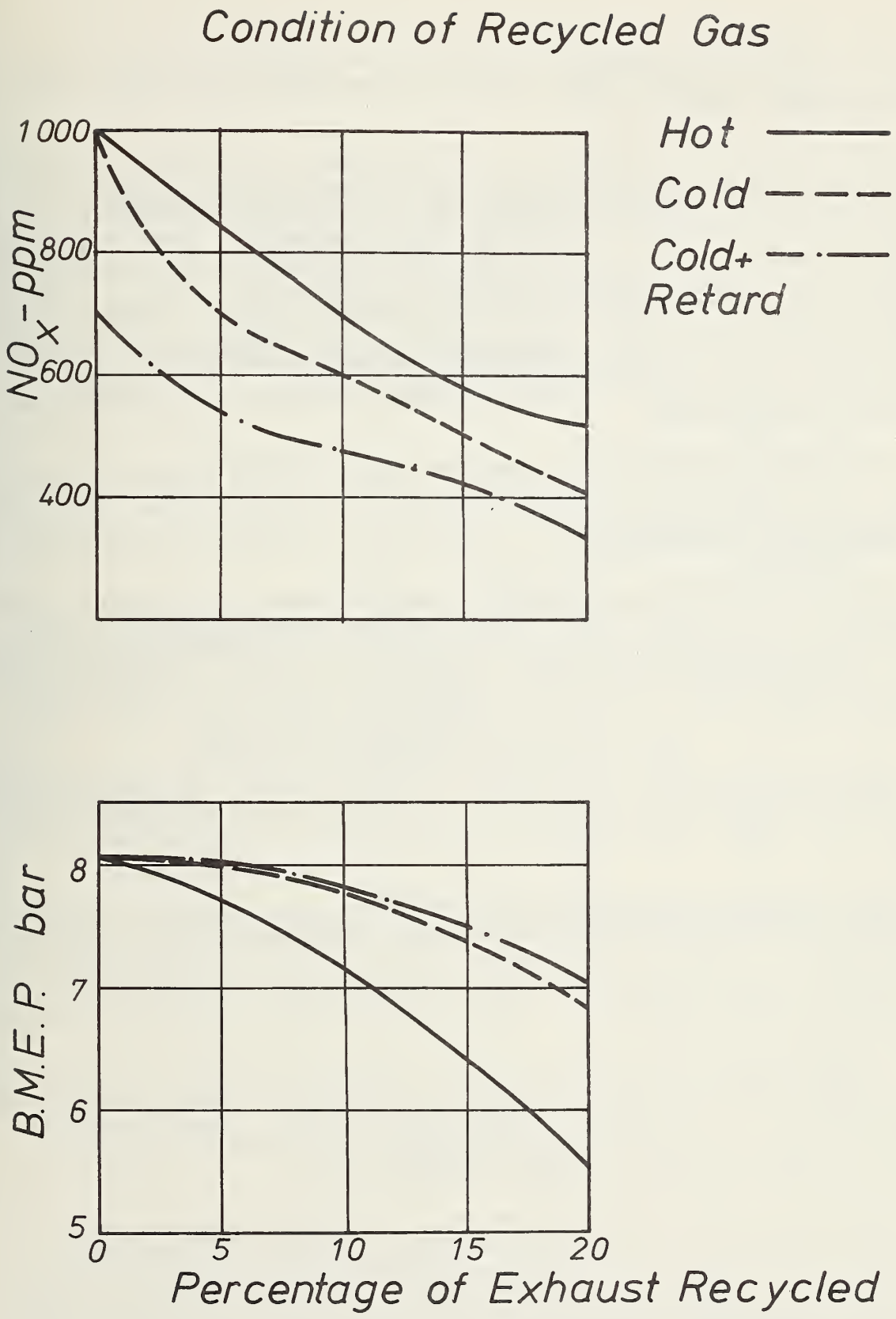

FIGURE 4.3-2: EFFECT OF EXHAUST GAS RECIRCULATION ON NOx EMISSIONS AND PERFORMANCE

The specific fuel consumption virtually is unaffected except at high load condition which increases fuel consumption significantly and raises smoke and HC levels (see Figure 4.3-1).

The reason for this behavior is the high amount of excess air in the lower load range. The recirculation of hot exhaust gas rapidly compensates for the too low operating temperatures that occur in the lowest load range which then leads to a drop in thermal efficiency (higher temperature level, higher heat losses to the wall, and dropping volumetric efficiency). The reduction of NOx emissions, which occurs despite the higher temperatures, is due to a decrease of the oxygen and nitrogen content in the cylinder charge and the resulting change in the burning rate. This condition is also reflected in the markedly lower noise level of diesel engines with EGR during cold start-up and idle. Figure 4.3-3 shows the drop of smoke-limited performance as a function of recirculated exhaust gas.

The recirculation of cold exhaust gas can be used to reduce the performance drop. However, the high outlay required for an effective exhaust gas cooler together with the problems involved would make a passenger-car application of the system appear impractical.

Therefore, the influence of EGR, without any additional cooling, on fuel consumption, air-to-fuel ratio, temperature in the intake manifold, smoke visibility, and HC/CO/NOx emissions was investigated, operating the engine in a steady-state mode on an engine dynamometer. Figures 4.3-4 through 4.3-6 show the results for a grid of 3 x 3 speed/torque points 1000, 2000, and 3000 rpm, and 0, 3, and 6 bar for a turbocharged 70 HP engine.

The results for zero power output are given in g/h. The specific emissions are shown at positive power outputs. A remarkable reduction of NOx emission occurs at all engine operating points up to a factor of 10 for loads below 3 bar.

Smoke visibility and HC/CO emissions show a small minimum at low EGR EGR rates and a steep increase at large EGR rates where the air-to-fuel ratio λ drops below 1.5. The fuel consumption rises very slowly to the inflection point where λ roughly equals 1.5. This points out that the air-to-fuel ratio λ determines the EGR upper limit. Figures 4.3-4 through 4.3-6 clearly show the smoke limitation over load.

A second limiting factor occurred at idle and zero torque. The minimum oxygen content in the combustion chamber must be higher than 10% or heat absorption of the non-oxygen gases in the resulting inert atmosphere will quench any flame produced by a small quantity of fuel.

The extent to which fuel economy and NOx emissions are affected by EGR is shown in Figure 4.3-7 at one operating point of the 50 HP naturally-aspirated diesel engine. The fuel consumption increase and the NOx emissions decrease for the naturally-aspirated and the turbocharged engine are shown in Table 4.3-1. A substantial reduction of the NOx levels was achieved without any severe performance penalty.

(Source: SAE 730214)

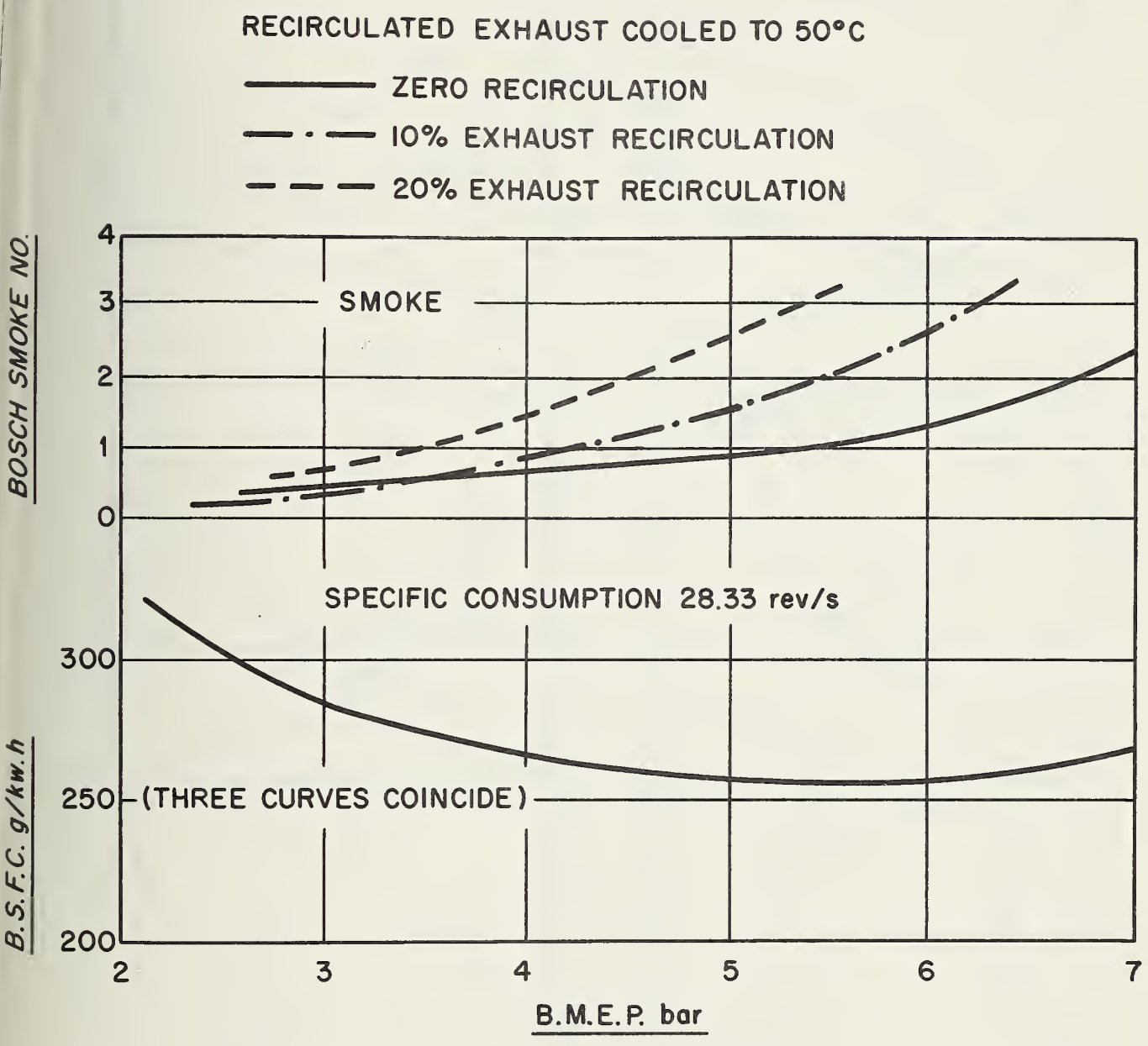

FIGURE 4.3-3: EFFECT OF EXHAUST GAS RECIRCULATION ON PERFORMANCE AND SMOKE OF A 6-CYLINDER SWIRL CHAMBER ENGINE OVER LOAD RANGE AT 28.33 rev/s (110 Bore x 120 Stroke)

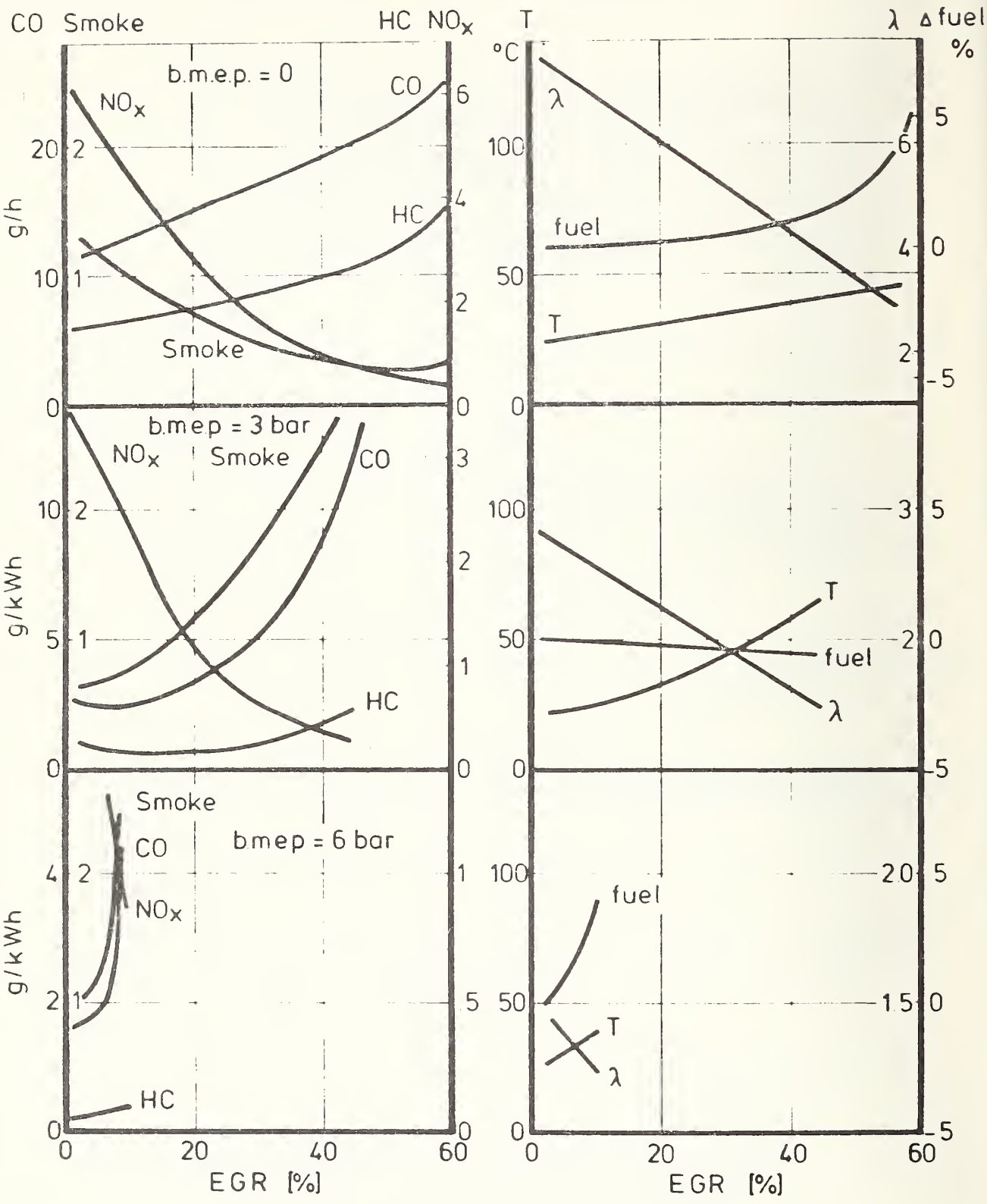

FIGURE 4.3-4: EFFECTS OF EXHAUST GAS RECIRCULATION (EGR) ON VARIOUS ENGINE OUTPUT CHARACTERISTICS

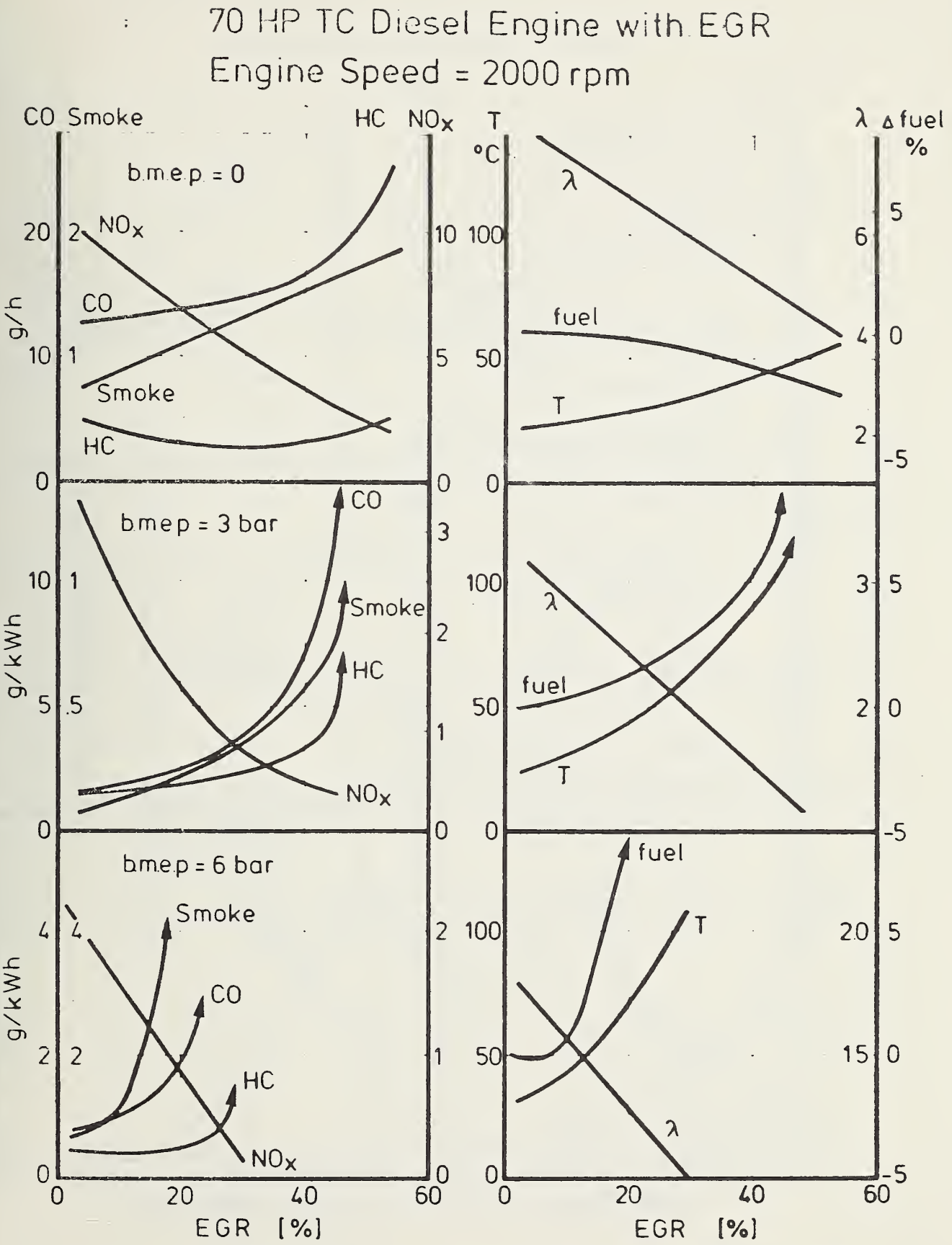

FIGURE 4.3-5: EFFECTS OF EXHAUST GAS RECIRCULATION (EGR) ON VARIOUS ENGINE OUTPUT CHARACTERISTICS

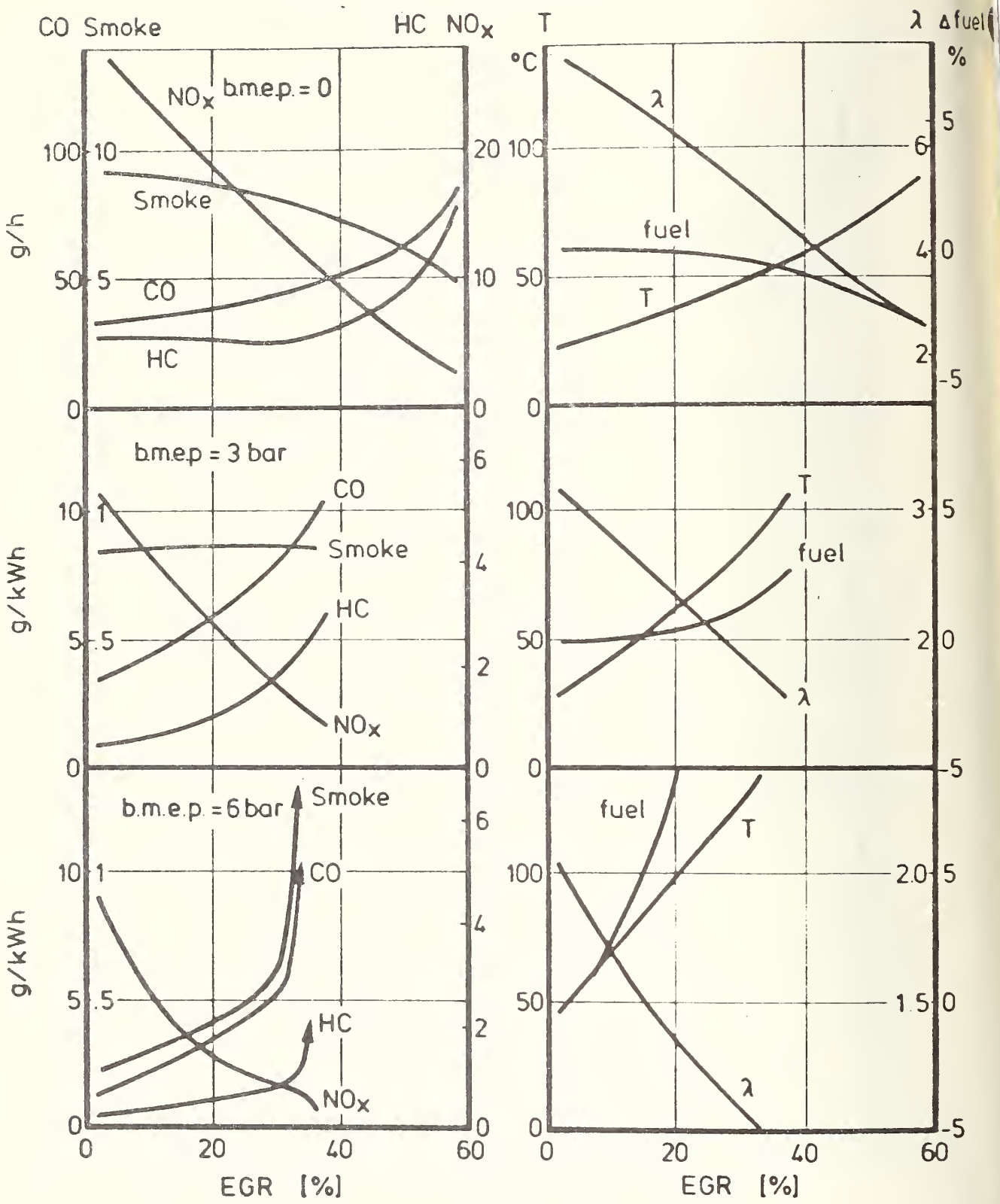

FIGURE 4.3-6: EFFECTS OF EXHAUST GAS RECIRCULATION (EGR) ON VARIOUS ENGINE OUTPUT CHARACTERISTICS.

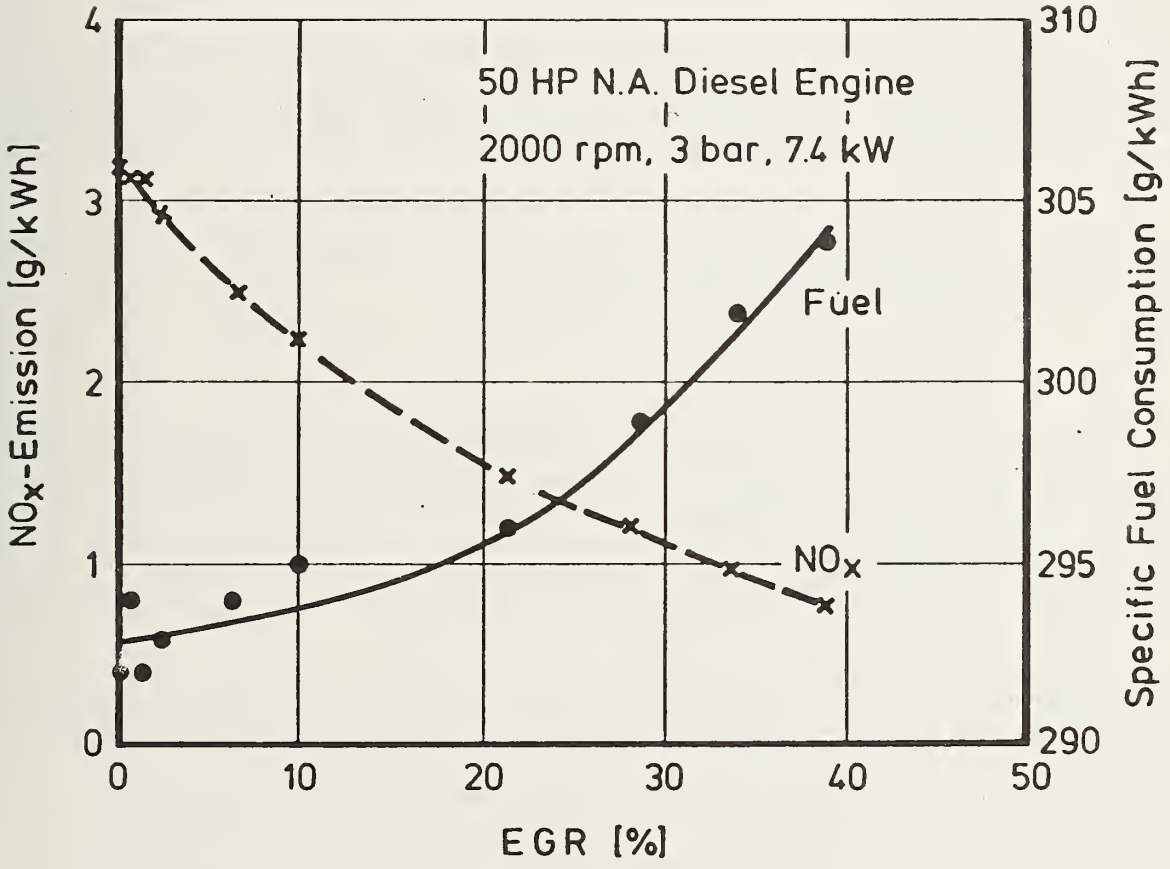

FIGURE 4.3-7: FUEL CONSUMPTION AND NOx EMISSION AS A FUNCTION OF THE AMOUNT OF RECIRCULATED EXHAUST GAS

TABLE 4.3-1:

INFLUENCE OF EGR ON NOx AND FUEL CONSUMPTION

Engine	Characteristics	Change
2000 rpm, 3 bar	EGR	0 → 40%
50 HP N-A	Fuel	0 → 4%
70 HP TC	Fuel	0 → 5%
50 HP N-A	NOx	3.2 → 0.7 g/kwh
70 HP TC	NOx	4.0 → 0.5 g/kwh

The use of a modulated EGR device leads to a substantial reduction in NOx levels without any severe performance penalty. The amount of EGR can be a maximum (up to 50%) at low engine loads because of the large amount of excess air. It should be reduced to zero at full load in order to avoid any power loss.

Figure 4.3-8 shows the effective EGR that was achieved for 1.5-l naturally-aspirated engines with modulated EGR device.

4.3.2 Water Injection

Water injection lowers the peak temperature and thus reduces the NOx level. Significant NOx reductions are achieved with injected water quantities of up to three times the injected fuel quantity[16]. Water quantities like that would require a complex direct injection system in the cylinder head because the intake air cannot carry the necessary amount of water. These large quantities of water, furthermore, are not practical for automotive engines.

Figure 4.3-9 shows the effects of introducing water into the manifold of a naturally-aspirated engine. The results obtained with varying quantities of water from .5 to 3.0 times the fuel supply show very significant reductions in the NOx levels at standard and retard timings without any excessive increase in fuel consumption and HC levels. A water/fuel ratio of .5 produces significant reductions of the NOx level (i.e. to the order of 30%). Figure 4.3-10 shows that water/fuel ratios of more than 1.5 produce only minor reductions in the NOx levels. Stable operation is possible up to a ratio of 2. However, the performance drops by some 25% because some of the water evaporates and displaces the incoming air. The resulting overall effect is a reduction in volumetric efficiency.

Water injection requires a pump and control system that shuts off the water supply shortly before engine shut-off in order to avoid corrosion problems[17]. Such a control system can be realized comparatively easily in turbocharged engines by water injection between air filter and turbocharger with the aid of the turbocharger pressure. This method provides water supply without any additional control device and water shut-off prior to engine shut-off. At the same time, there is a slight improvement of the thermal efficiency. Figure 4.3-11 shows the water-to-fuel ratio that was achieved in a 70 HP turbocharged engine.

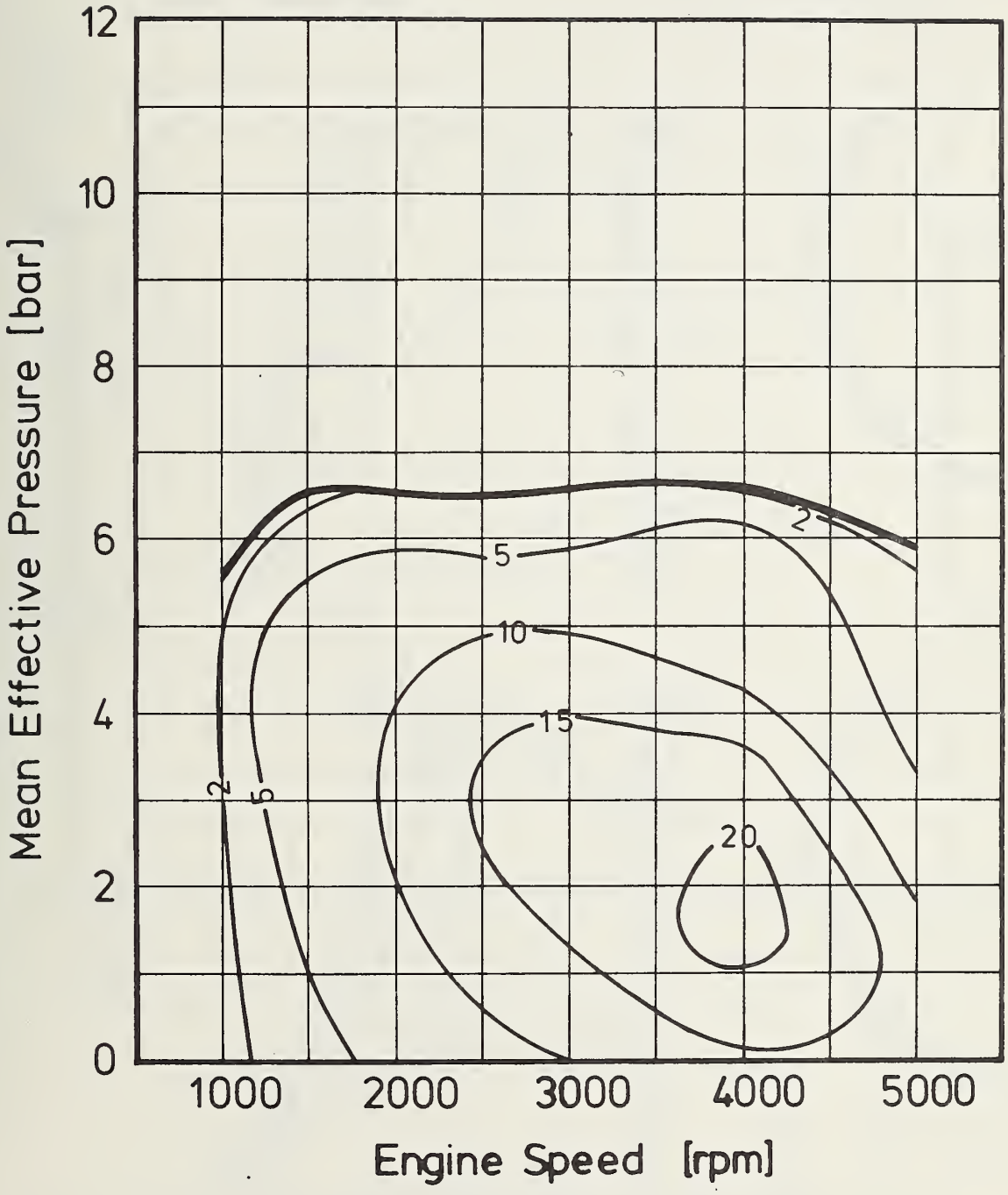

FIGURE 4.3-8: EFFECTIVE EGR (%) - 50 HP N.A. DIESEL ENGINE WITH MODULATED EGR

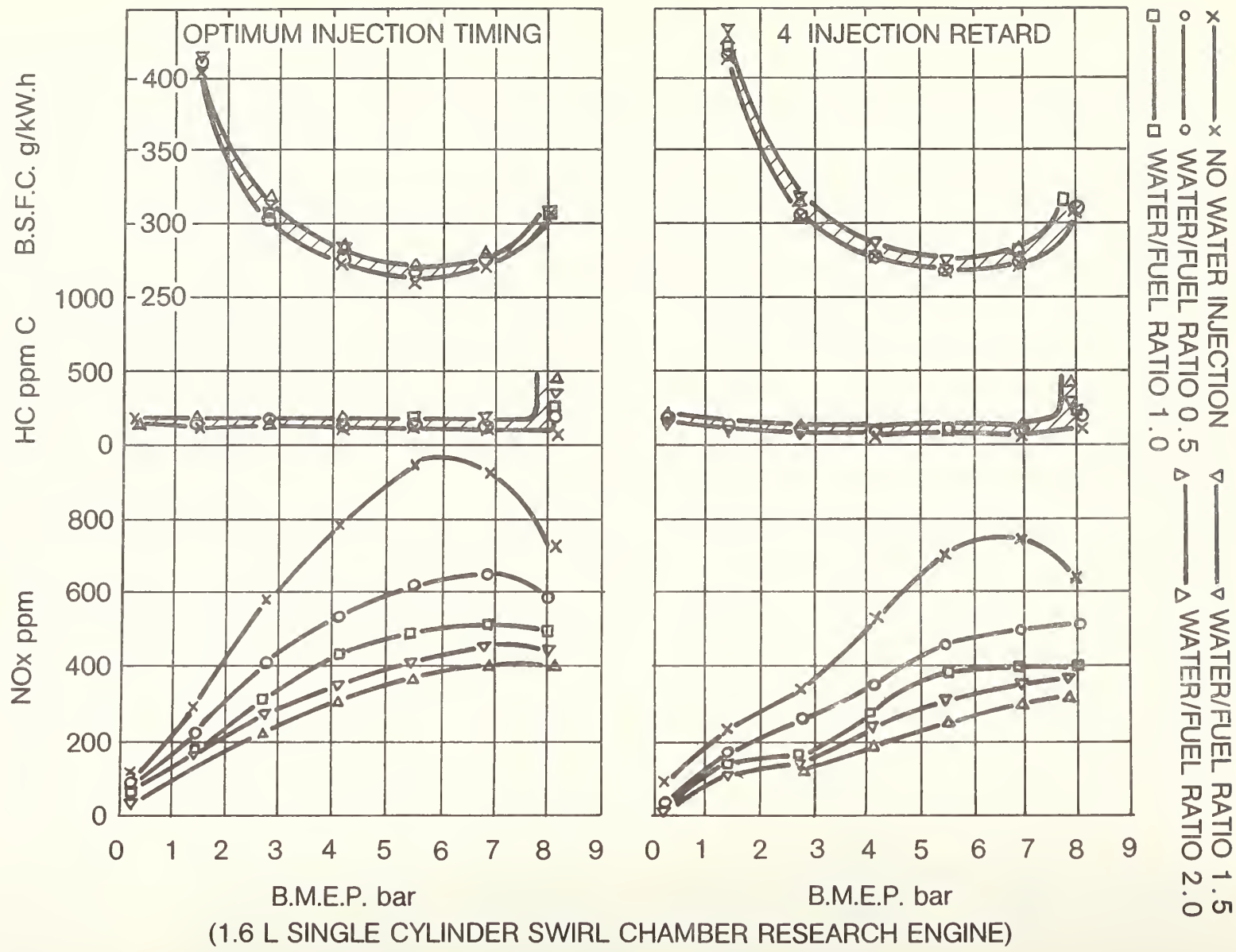

(1.6 L SINGLE CYLINDER SWIRL CHAMBER RESEARCH ENGINE)

FIGURE 4.3-9: EFFECT OF INLET MANIFOLD WATER INJECTION

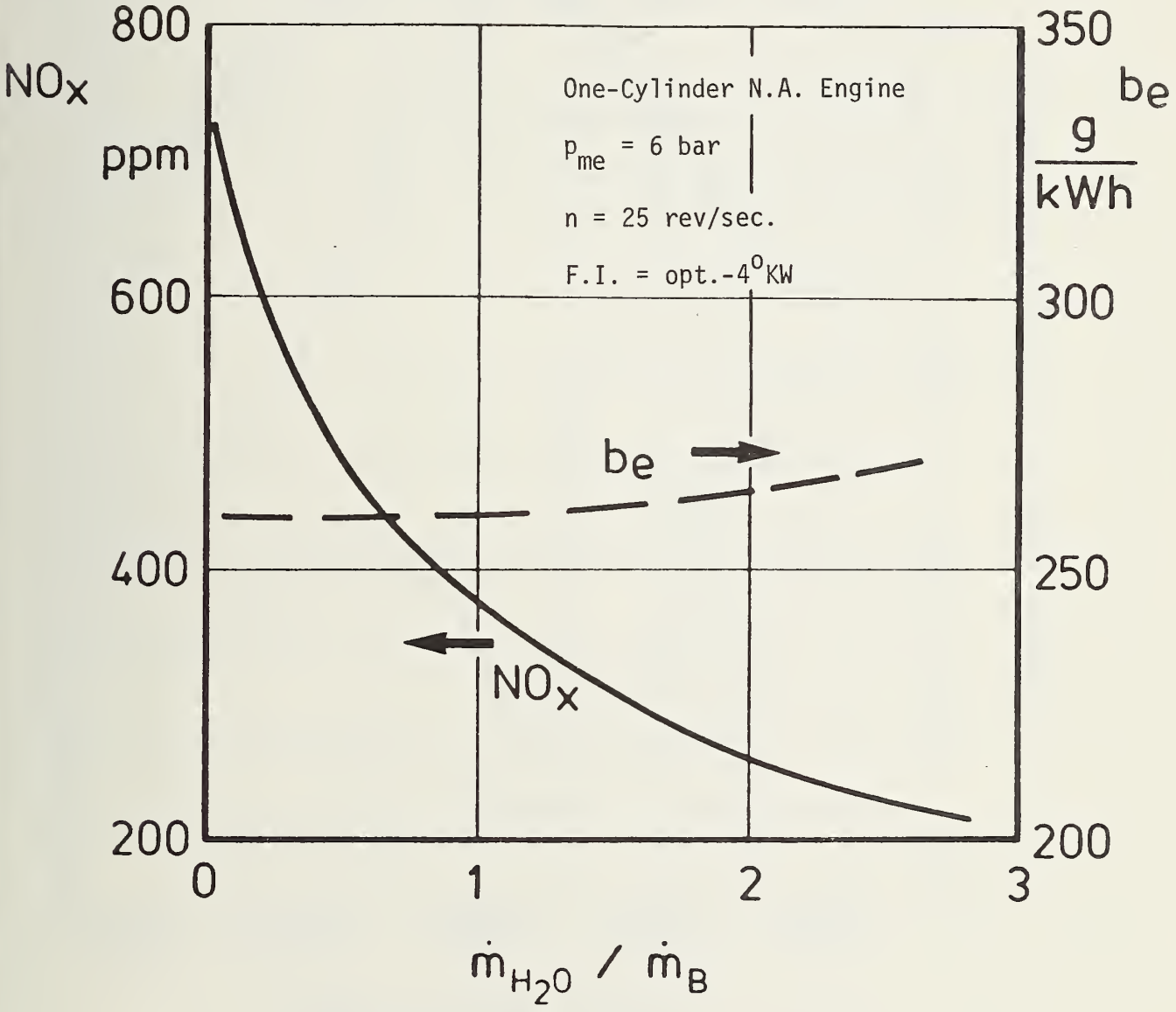

FIGURE 4.3-10: THE EFFECTS OF INTAKE PIPE WATER INJECTION ON NOx EMISSIONS AND FUEL CONSUMPTION.

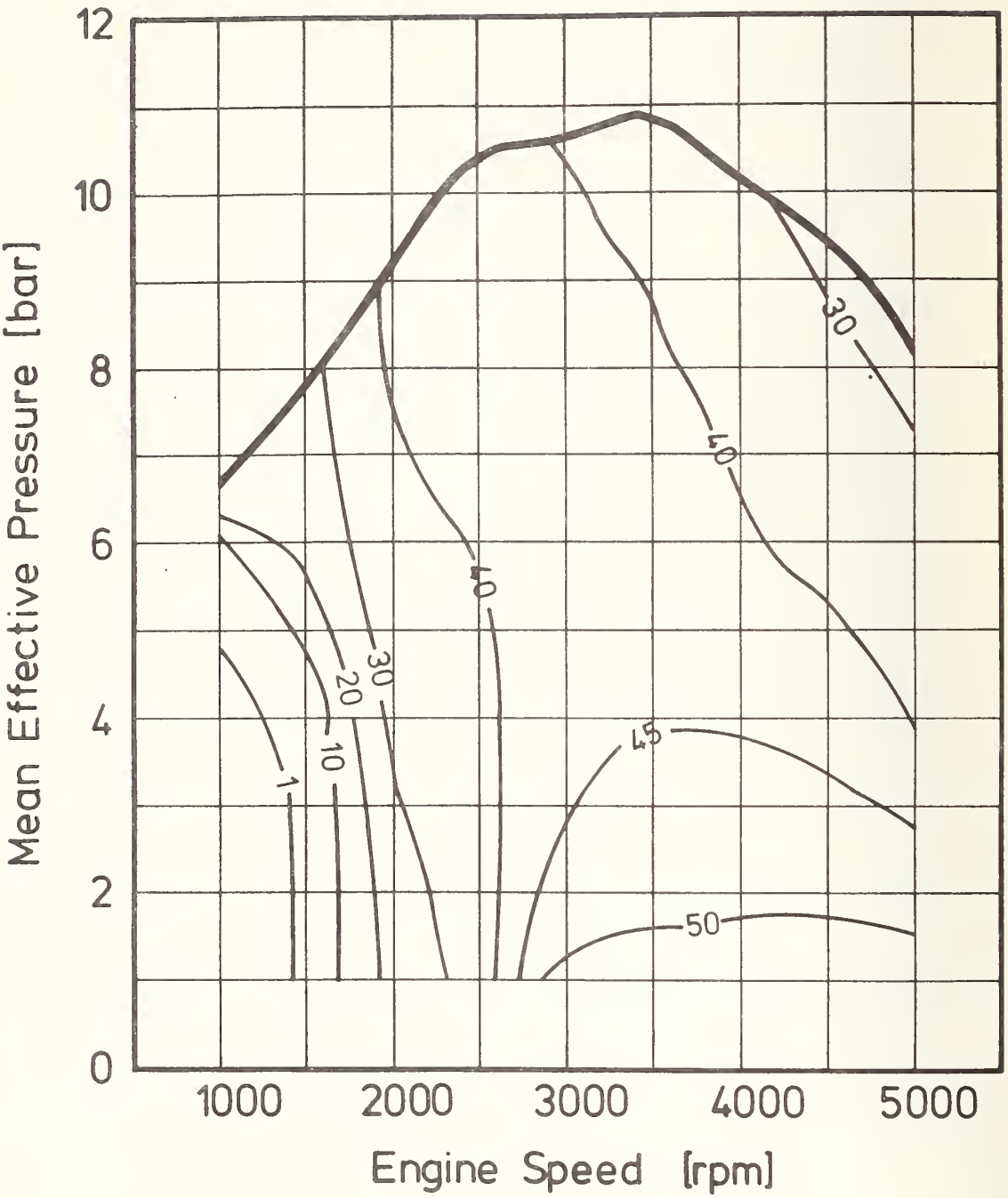

FIGURE 4.3-11: WATER-TO-FUEL RATIO (%) - 70 HP TC DIESEL WITH WATER INJECTION

So far, water injection has been considered for specific applications only. The relative reduction by water injection of NOx emissions in modern emission-optimized diesel engines with already low NOx emissions might not be very substantial. Furthermore, water injection would adversely affect the power plant bulk and weight because the size of the required water tank together with the water supply and control system would be equal to that of the fuel tank. Problems are anticipated because of the dual fuel system, corrosion, icing, and the additional cost for a second injection system.

4.4 ENGINE DESIGN CHARACTERISTICS

Passenger-car engine design is characterized by the following basic parameters:

- Performance
- Engine weight
- Engine dimensions.

These characteristics are affected by displacement, engine speed, number and arrangement of cylinders, boosting, and material. The investigation of the performance range studied (50 - 100 HP) was performed on the current 1.5 l, 4-cylinder VW production diesel engine. This engine ensures compliance with all applicable emission and fuel economy standards and satisfies such consumer attributes as good driveability and cold-start behavior.

4.4.1 Performance

The engine performance is given by:

$$P_e = P_{me} \cdot \frac{n}{2} \cdot i \cdot V_i$$

where

P_{me} = Mean effective pressure

n = Engine rpm

i = Number of cylinders

V_i = Displacement per cylinder unit

4.4.1.1 Combustion System

Figure 4.4-1 shows the assumed mean effective pressure P_{me} for the swirl chamber engines under consideration. This figure also shows the specific fuel consumption and smoke versus engine speed.

4.4.1.2 Engine Speed

Engine performance increases in direct proportion to the engine rpm to that point where the decrease in volumetric efficiency and the steeply increasing friction losses become predominant and specific fuel consumption rises (Figure 4.4-2). The indicated output rises less than in direct proportion to the engine speed and thus to the piston speed at high rpm's because of the low volumetric efficiency. On the other hand, the friction losses increase more than in direct proportion to the rpm. Therefore, the share of the friction losses in the indicated output reduces the actual output. This effect is particularly pronounced during partial-load operation

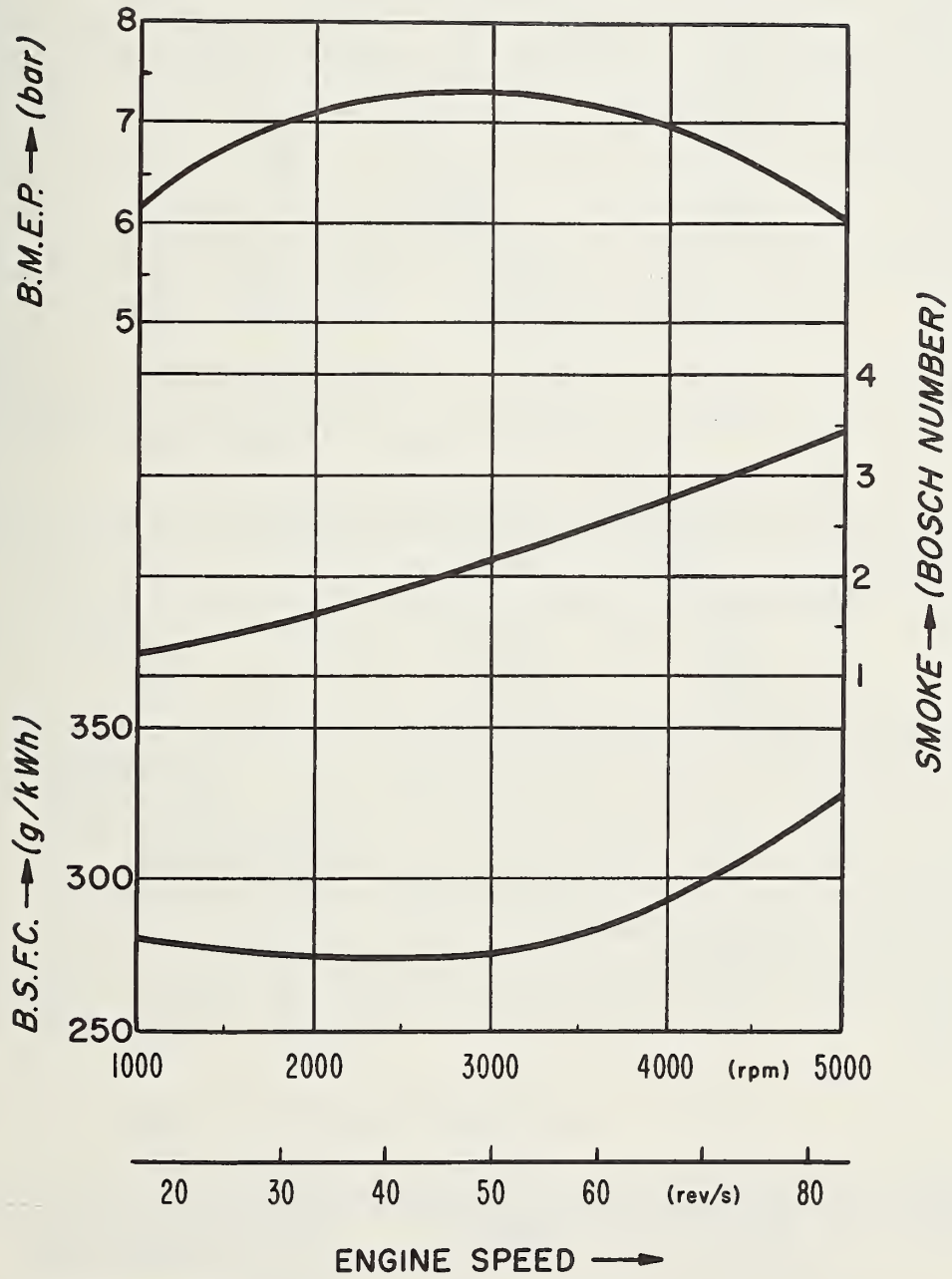

FIGURE 4.4-1: B.M.E.P., SMOKE AND FUEL CONSUMPTION OF SWIRL CHAMBER ENGINES

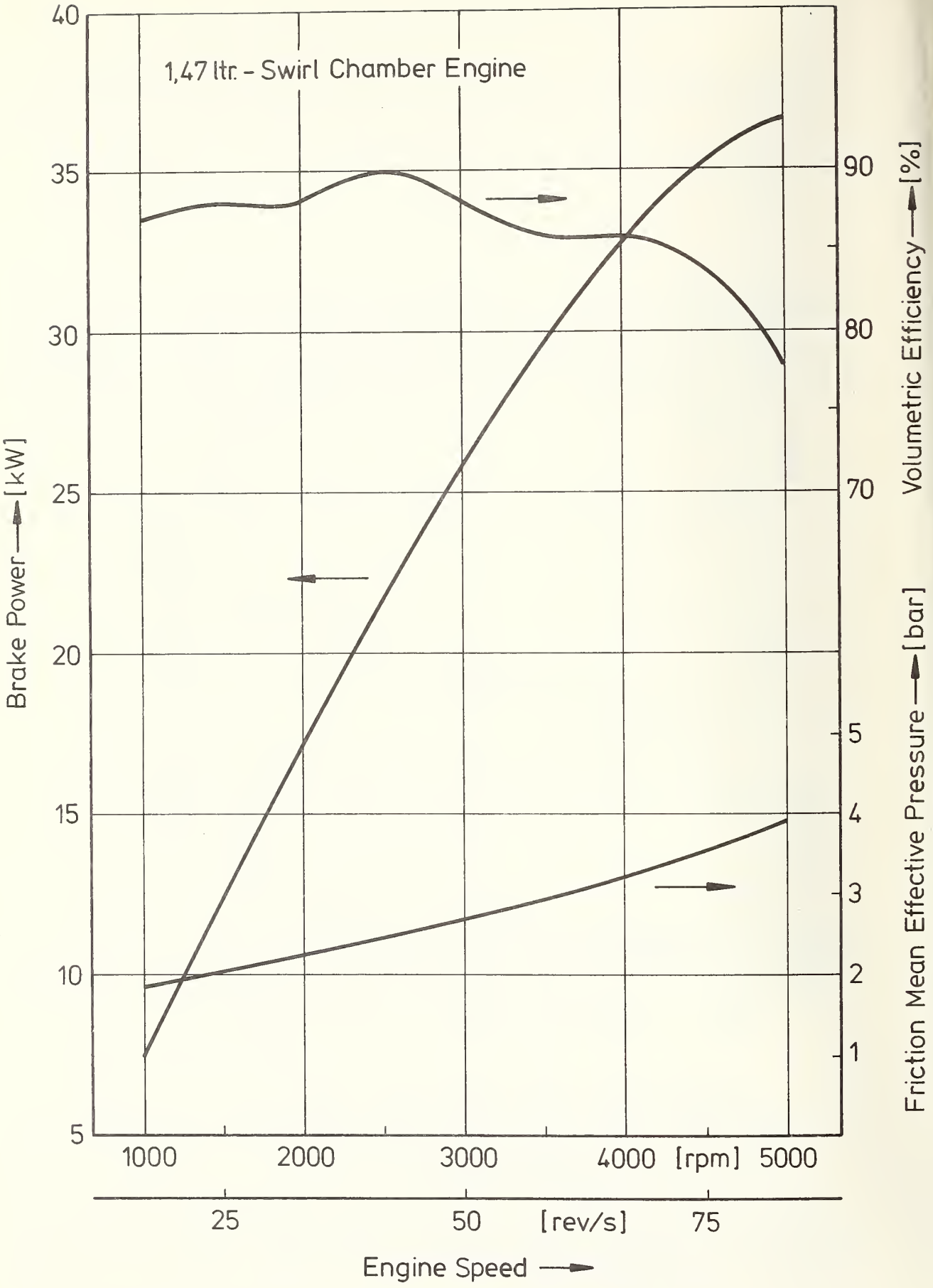

FIGURE 4.4-2: EFFECT OF ENGINE SPEED ON VOLUMETRIC EFFICIENCY, FMEP AND PERFORMANCE

where the friction losses rise even higher. The mean piston velocity should not exceed 13.5 m/s because of the friction losses (Figure 4.4-3) and mass forces and not so much for reasons of wear.

Because the effectiveness of combustion decreases at high engine speeds due to the lack of time available for the mixture formation and preparation, the nominal rpm of swirl chamber engines should not exceed 5,000 rpm (83 rev/sec).

With these restrictions, the possible rated output of an engine is a function only of the displacement, number of cylinders and, in some cases, arrangement of cylinders, if the rpm is limited by the dynamic behavior of the engine. This interrelation is illustrated in Figures 4.4-4 and 4.4-5. Engine output rises in direct proportion to the displacement, while the specific output can be raised for large total displacements by increasing the number of cylinders. The potential advantage in choosing a 6-cylinder version over a 4-cylinder version for an engine of approximately 2.4 liters swept volume is an increase by approximately 5 kw in maximum output. The higher output is accompanied by smoother running characteristics. On the other hand, the engine with the larger number of cylinders will be heavier and have a higher specific fuel consumption. This will be shown later.

Figure 4.4-4 shows the potential maximum performance of the possible turbocharged and naturally-aspirated derivatives of the 4-cylinder base engine. The engines were divided into two engine families.

The radiator fan in VW passenger cars is powered electrically. This is an economic method for this particular application because of the very low "on" time. There is no waste of energy for fan operation during those vehicle operating states where the air stream provides for sufficient heat exchange. Mechanically powered fans reduce the nominal output by 2 - 4%.

The output data are averages that have been reached or can be reached by production units. Figure 4.4-6 shows the production scatter band of the most significant characteristics for the 4-cylinder engine. The maximum deviation from the nominal output is approximately $\pm$ 3%. Engine performance may be further increased at the expense of other characteristics, e.g. fuel consumption, soot formation, and start-up behavior. We feel, however, that the performance data achieved in the VW diesel engine are the best possible compromise. At this time, only the 4-cylinder version is a VW production unit. The performance data of the VW 5-, 6-, and 8-cylinder engines were based on prototype engines and estimates. Special consideration has to be given to their different states of development when the analysis is performed.

4.4.1.3 Effects of Cylinder Dimensions

Trade-offs for different displacements per cylinder unit indicate that cylinder units of 300 to 400 cc produce the highest specific output in terms of kw/l (see Figure 4.4-5) because of the following reasons:

- The effects of cylinder sizes smaller than 300 cc:

  The ratio between surface and volume of the combustion chamber increases. This leads to lower combustion effectiveness.

  The effects of component part tolerances become increasingly severe (compliance with the target compression ratio).

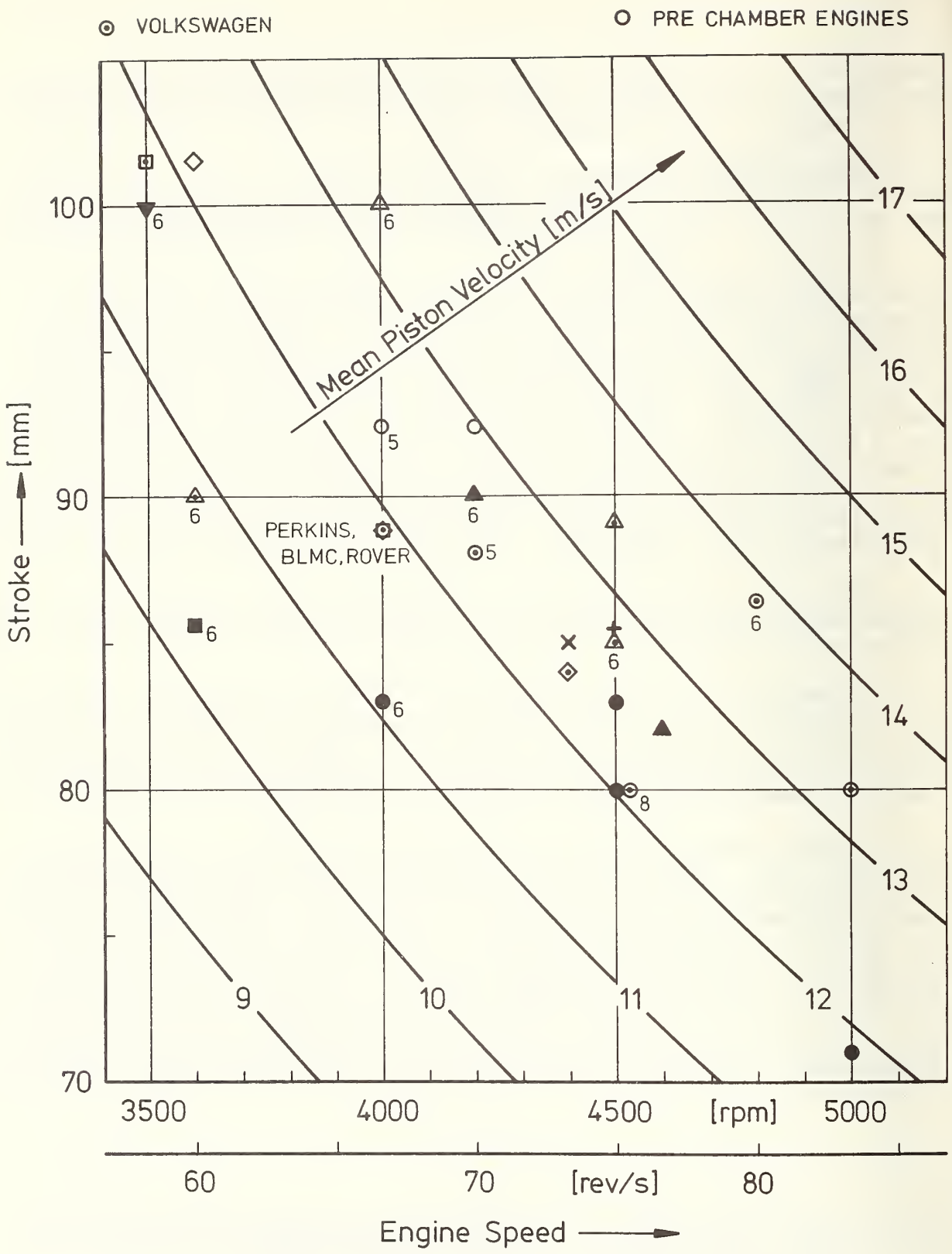

FIGURE 4.4-3: MEAN PISTON VELOCITY AT RATED SPEED FOR SWIRL CHAMBER ENGINES

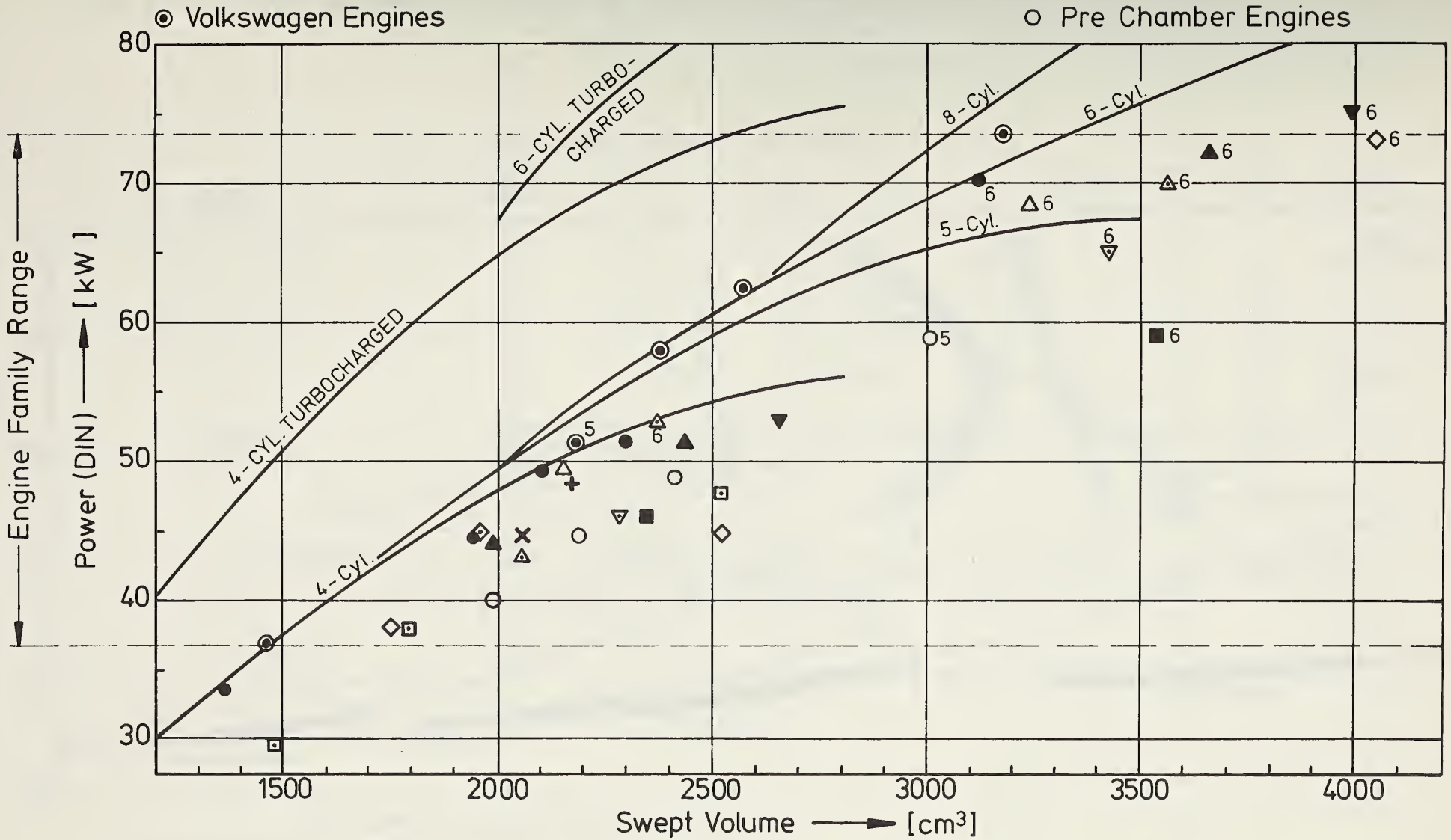

FIGURE 4.4-4: RELATIONSHIP BETWEEN MAXIMUM PERFORMANCE AND SWEPT VOLUME FOR AUTOMOTIVE SWIRL CHAMBER DIESEL ENGINES

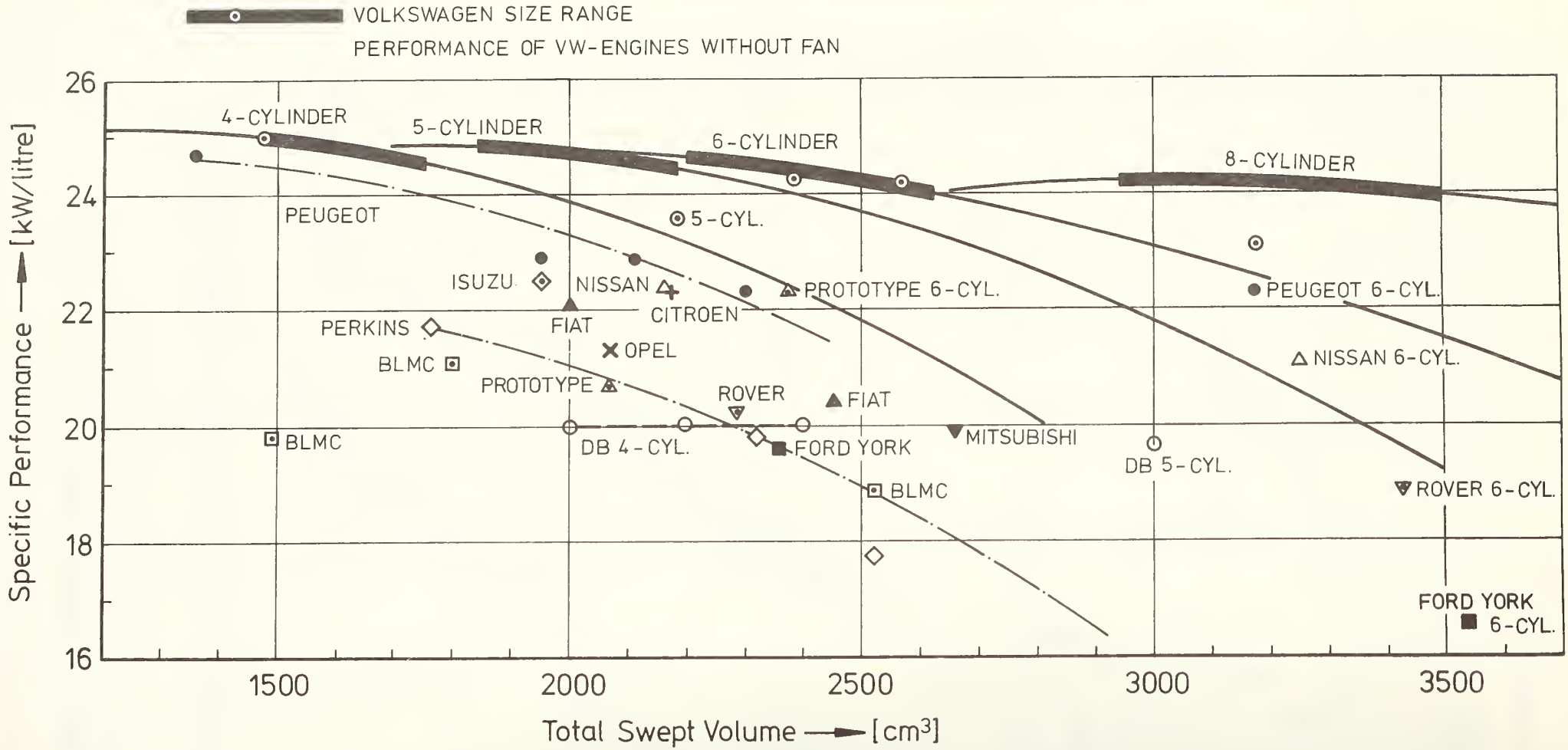

FIGURE 4.4-5: EFFECT OF NUMBER OF CYLINDERS ON SPECIFIC PERFORMANCE LEVELS OF TWO-STAGE COMBUSTION DIESEL ENGINES

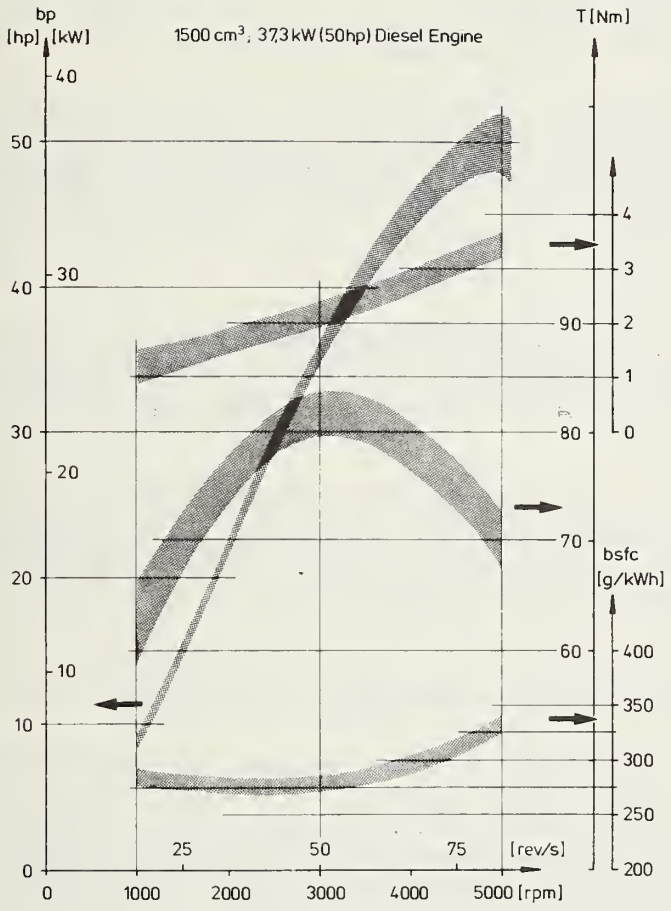

FIGURE 4.4-6: PRODUCTION SCATTER BAND

The specific output is not raised by an increase of the nominal rpm, which would be entirely possible because of the decreasing mass forces. The reason is the drop in volumetric and thermal efficiency and the rapid increase of internal friction losses and fuel consumption (see Figure 4.4-2).

- The effects of cylinder sizes larger than 400 cc:

  Assuming a bore dimension restriction, it is not advisable to maintain the high nominal rpm of 5,000 which is required for the high specific output of 25 kW/l because this entails too steep an increase of the mean piston velocities and friction losses. In addition, the mass forces in engines with cylinders larger than 500 cc require a reduction of the nominal engine speed.

  While the smaller ratio between surface and volume of the combustion chamber results in higher thermal efficiency, which cannot compensate for the drop in engine speed, the HC emissions are lowered, and the wall effects decrease.

Therefore, the nominal engine speed is limited by the combustion process in smaller cylinder units and by the mean piston velocity in larger units. A deviation from the range of the optimum cylinder size (300 ... 400 cc) thus leads to a reduction of the specific output.

4.4.1.4 Effects of Number and Arrangement of Cylinders

Any increase in the number of cylinders reduces the volume of the individual cylinder for a given total volume. This means that 4-, 5-, 6-, and 8-cylinder engines with the optimum cylinder size of between 300 and 400 cc suffice for the total displacement volume range of between 1.2 and 3.2 liters (see Figure 4.4-5). These configurations cover the performance range from 30 to 75 kW (41 through 102 HP) with naturally-aspirated engines, and from 41 through 100 kW (56 through 138 HP) with turbocharged engines (Figure 4.4-4).

4-Cylinder Engines

Four-cylinder in-line engines and 4-cylinder V 60^{o} with balancing shaft[18] should not have a total displacement higher than 2.4 liters because of the unbalanced mass forces of the second order. This places the output limit (Figure 4.4-4) in the neighborhood of 53 kW (72 HP).

Four-cylinder opposed-piston engines have a very good interior mass balance. Therefore, they permit somewhat larger cylinder units. However, a 10% increase of the total displacement to more than 2.4 liters leads only to an increase in output of roughly 5% (Figure 4.4-4) because the nominal engine speed in this range is determined by the permissible piston velocity. The maximum output per liter is obtained with total displacements of between 1.2 and 1.6 liters.

5-Cylinder Engines

The data in Figures 4.4-4 and 4.4-5 are based on the performance data produced by VW prototypes.

The piston rod of the prototypes was comparatively short. This caused an unfavorable piston-rod ratio $\lambda = r/\ell = 0.324$, which led to high rectangular piston forces and entails high friction losses at high engine speeds. Therefore, the nominal engine speed was limited to 4,500 rpm.

This engine speed produced a specific output of 23.6 kW/liter. An improvement is possible in order to match the curves shown in Figures 4.4-4 and 4.4-5.

The upper limit of a practical 5-cylinder engine is in the range of 3 liters displacement and 65 kW (88.4 HP) output. The optimum range is between 1.5 and 2 liters displacement.

6-Cylinder Engine

The 6-cylinder in-line and opposed-piston engine concepts have ideal mass balance. Mass balance is acceptable with V-60° and V-90° 6-cylinder engines[19]. The nominal output is not affected by the cylinder arrangement. It is limited by the permissible piston velocity.

Therefore, a 73.5kW engine would have to have a displacement of 3.3 liters (Figure 4.4-5). This would result in a specific output of 22.3 kW/l. The nominal rpm would be 4,100 at a mean pressure of 6.6 bar. This would result in a mean piston velocity of 13 m/sec at a stroke/bore ratio of 1.1.

The range of maximum specific output for a 6-cylinder engine is in the total displacement of 1.8 to 2.4 liters.

8-Cylinder Engine

The crankshafts in 8-cylinder in-line engines offer comparatively little resistance to torsion. The high target rpm's can be controlled only with power take-off between the fourth and fifth cylinder. This again increases production outlay. V-90°, V-180° and opposed-piston design yield acceptable to very good mass balance[19].

The nominal output of 73.5 kW requires a displacement of 3.1 liters (Figure 4.4-4). The speed, and thus the nominal output, of an 8-cylinder diesel engine was designed for slightly lower values because of the ratio between cylinder distance and bore of 1.1, which is an extremely low ratio for V-engines.

Maximum specific output is reached in total displacement configurations between 2.4 and 3.2 liters.

4.4.2 Engine Weight

4.4.2.1 Definition

At this time, there is no national nor international standard vehicle weight definition.

The weight data in this project were obtained from different sources and are not uniformly defined. Weight data from some other source for a certain engine may differ from those in the graphs.

The following definition was used to determine the engine weight:

Engine weight including:

Flywheel
Intake manifold
Exhaust manifold
Air filter
Generator
Starter

excluding:

Radiator
Water
Oil.

4.4.2.2 Engine Weight as a Function of Engine Power Output

Figure 4.4-7 shows the increase in engine weight as a function of engine power output. However, the specific weight in kg/kW decreases in direct proportion to the increase in power output (Figure 4.4-8). The specific weight increases steeply as the power output decreases. This is attributed to the following facts:

- The weight of engine accessories (especially generator, injection pump, and starter) is affected by the engine output to a comparatively small extent only.

- The minimum wall thicknesses are determined by foundry technology.

The use of a turbocharger permits a distinct decrease in the weight of an engine with a given output (Figure 4.4-8).

Cylinder outputs of between 11 and 13 kW permit the lowest power-to-weight ratio. This applies to naturally-aspirated and turbocharged engine configurations. Depending on the number of cylinders, this means that the individual cylinder displacement ranges between 450 and 550 cc.

4.4.2.3 Engine Weight as a Function of Displacement

Engine weight generally increases in direct proportion to the increase in displacement (Figure 4.4-9), while there is a drop in the specific weight (kg/liter) as shown in Figure 4.4-10. The steep increase of the specific weight along with the decrease in displacement is attributed to the causes described above.

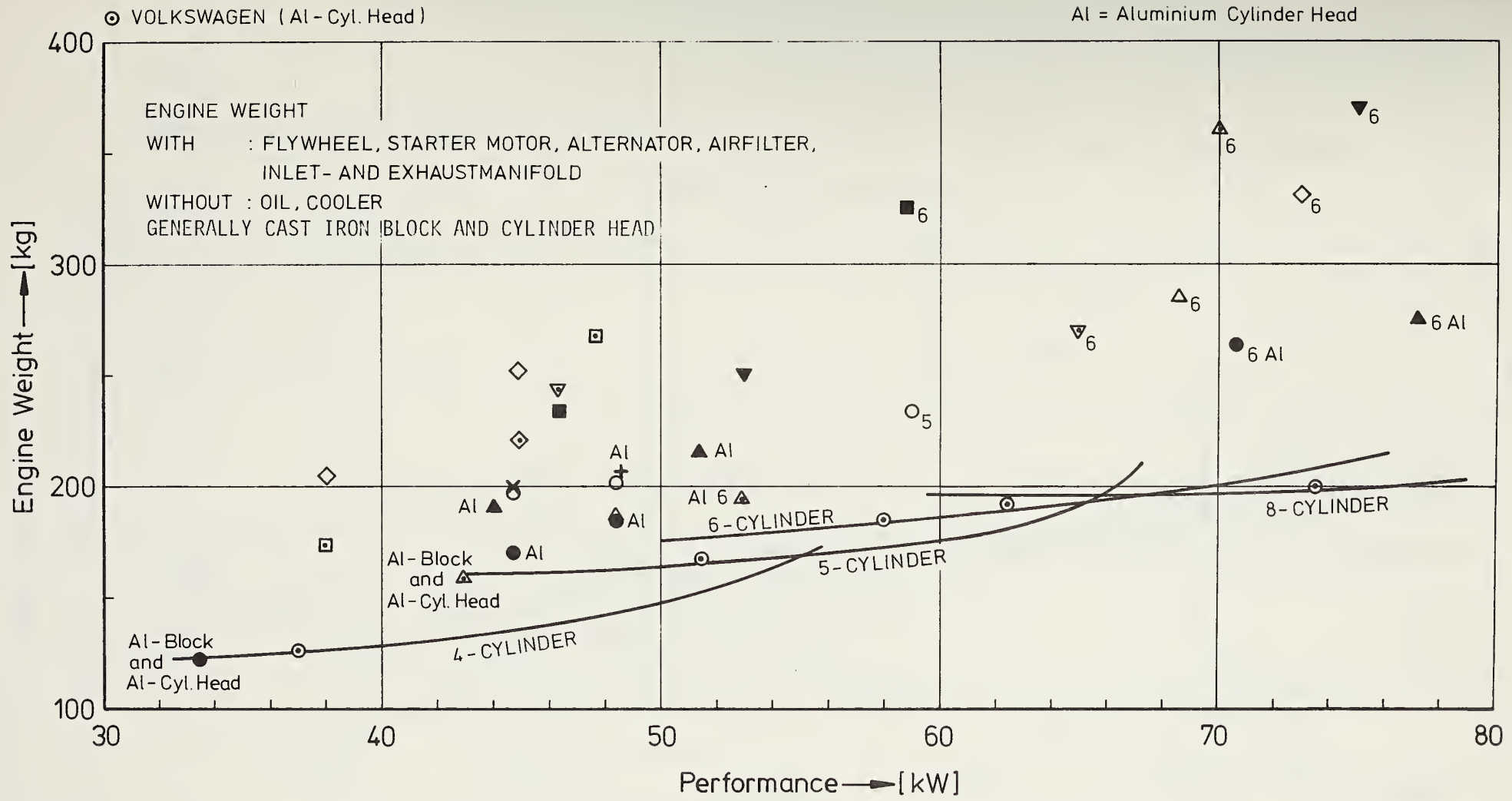

FIGURE 4.4-7: CORRELATION BETWEEN ENGINE WEIGHT, PERFORMANCE AND NUMBER OF CYLINDERS FOR TWO-STAGE COMBUSTION DIESEL ENGINES

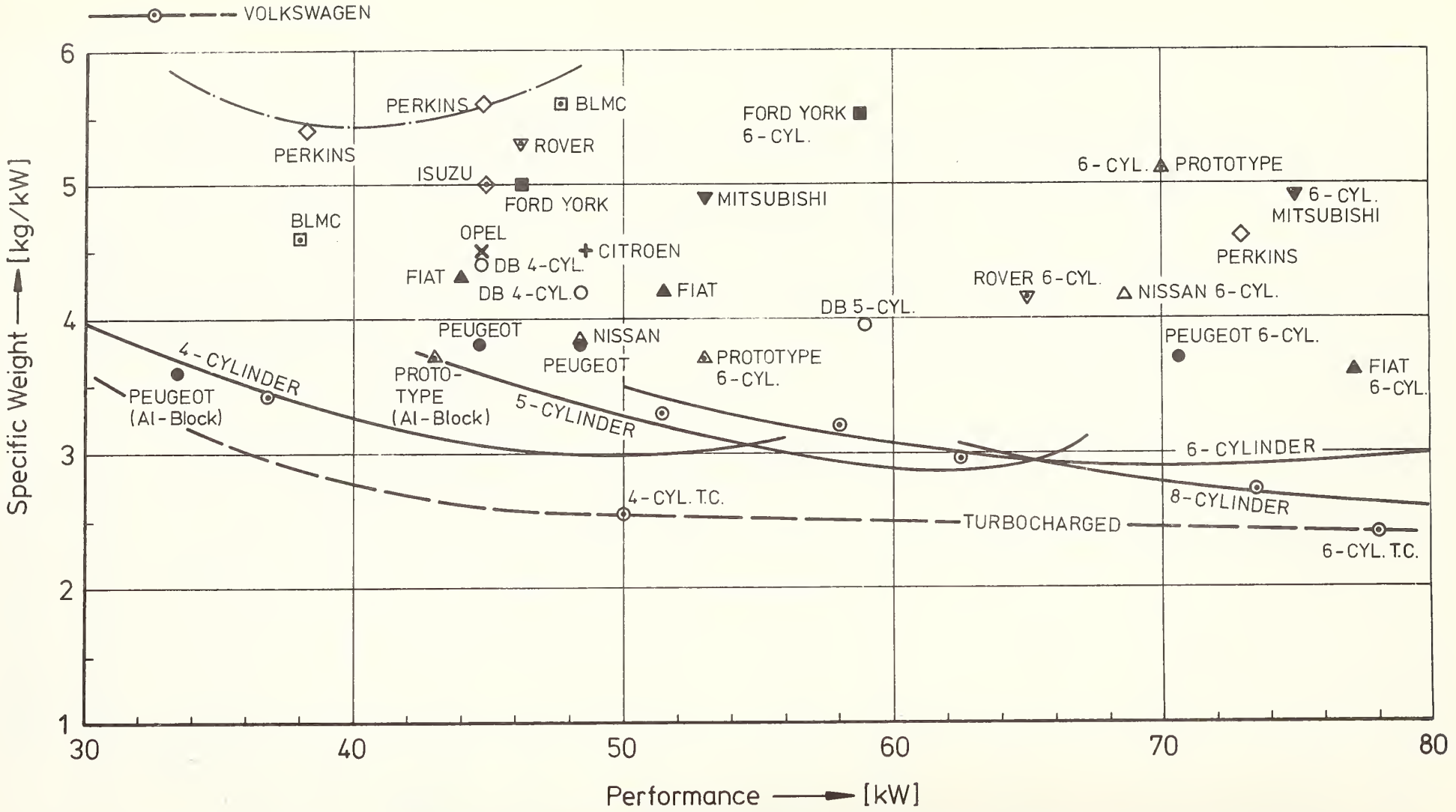

FIGURE 4.4-8: EFFECT OF NUMBER OF CYLINDERS ON SPECIFIC WEIGHT OF TWO-STAGE COMBUSTION DIESEL ENGINES

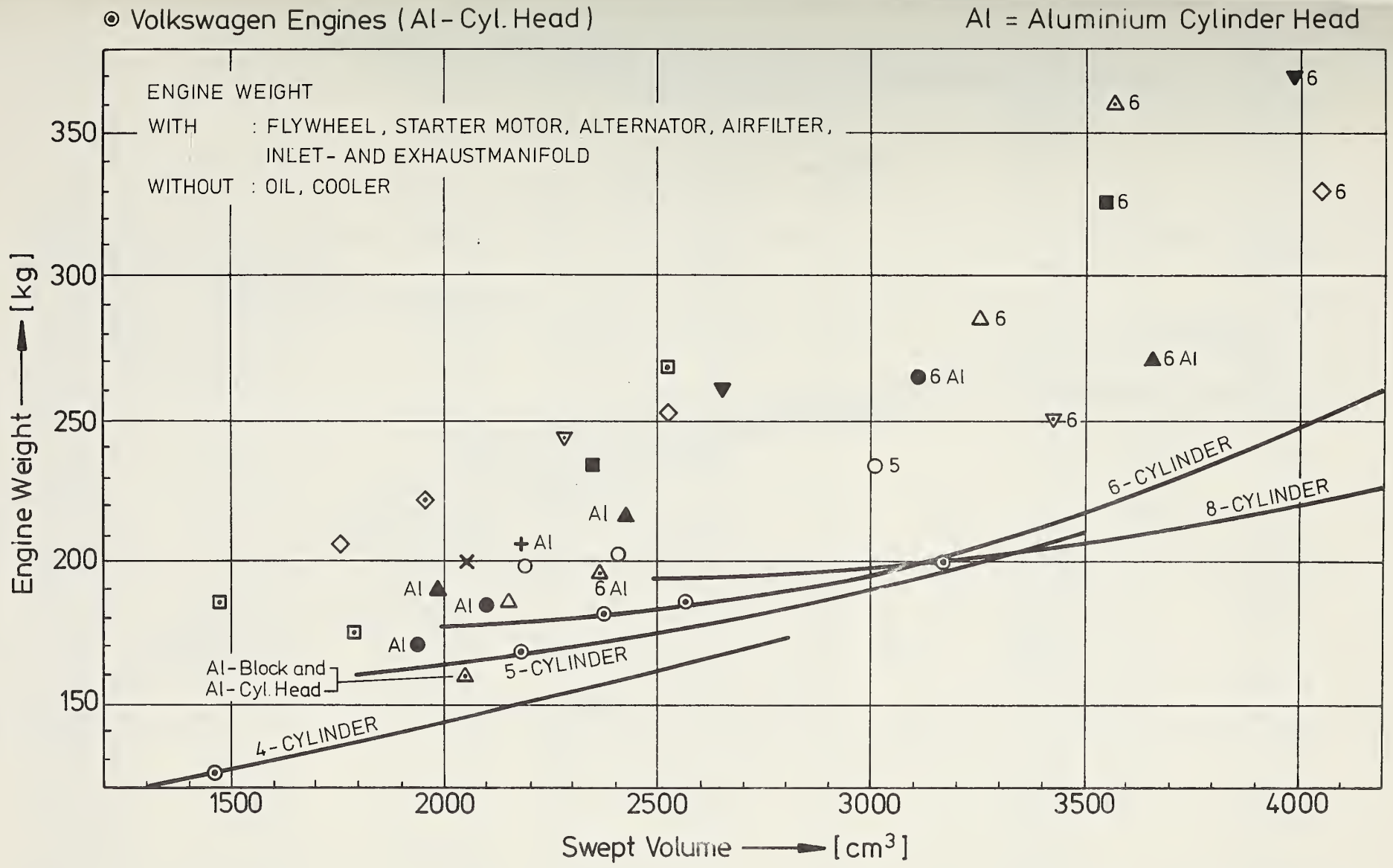

FIGURE 4.4-9: CORRELATION BETWEEN ENGINE WEIGHT, SWEPT VOLUME AND NUMBER OF CYLINDERS FOR TWO-STAGE COMBUSTION DIESEL ENGINES

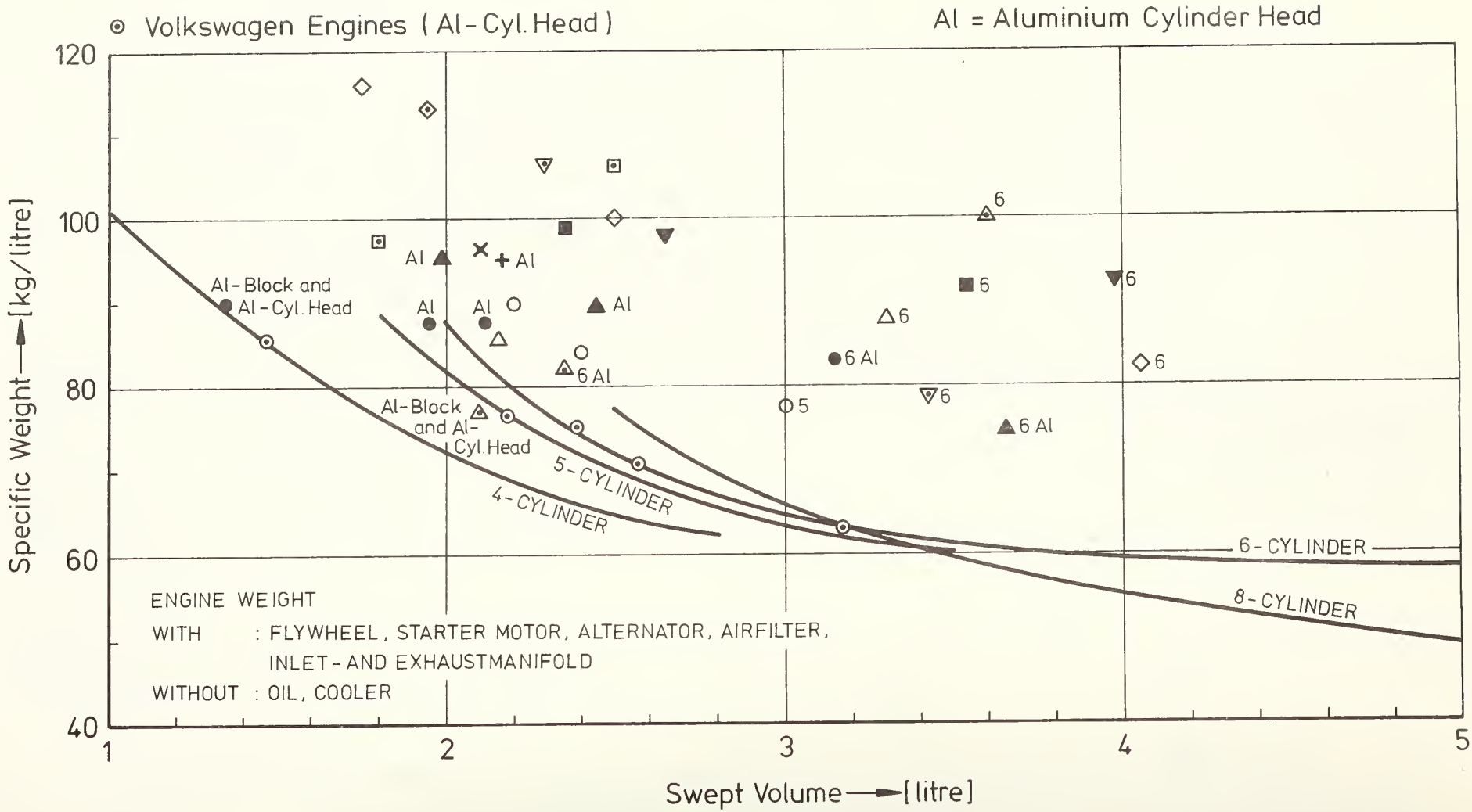

FIGURE 4.4-10: EFFECT OF SWEPT VOLUME AND NUMBER OF CYLINDERS ON SPECIFIC WEIGHT FOR TWO-STAGE COMBUSTION DIESEL ENGINES

The weight-to-power ratio in kg/kW (Figure 4.4-11) shows similar trends as the specific weight in kg/liter (Figure 4.4-10), considering the interrelationship described in Figure 4.4-4. The lowest weight-to power-output ratio is reached with cylinder sizes of between 500 and 600 cc (Table 4.4-1).

TABLE 4.4-1:

OPTIMUM CYLINDER UNIT FOR LOWEST WEIGHT-TO-POWER RATIO

Number of Cylinders	Optimum Cylinder Unit	Lowest Weight-to-Power Ratio	Power per Cylinder Unit
-	cc	kg/kW	kW
4	500 ... 575	3	12 ... 13
5	500 ... 600	2.85	12 ... 13
6	470 ... 570	2.9	11 ... 12.5

4.4.2.4 Engine Weight as a Function of Number of Cylinders

The engine weight is almost independent of the number of cylinders in the displacement range between 3.0 and 3.5 liters. This is illustrated in Figures 4.4-9 and 4.4-10. An increase in the number of cylinders in engines below this displacement range leads to higher engine weight. An increase in the number of cylinders above this displacement range may decrease the engine weight. This is illustrated quite clearly in the presentation of the specific weight data in Figure 4.4-10 because an increase in the number of cylinders in that displacement range, e.g. from six to eight, produces an increase in output (Figure 4.4-4).

The specific weight curves (kg/kW) show distinct minima (Figure 4.4-8). The specific weight increases in the output and displacement range above the minimum because the specific output in kW/liter decreases in that range (Figure 4.4-5).

4.4.2.5 Engine Weight as a Function of Material

The weight of engines with cast iron cylinder block and crankcase and cylinder head is markedly higher than that of engines with aluminum head (Figures 4.4-7 and 4.4-9). The weight may be further reduced by the use of aluminum for the cylinder block and crankcase. Both designs are close to the lower scatter band limit in Figures 4.4-7 through 4.4-11.

All VW diesel engines have cast-iron cylinder blocks and crankcases and aluminum cylinder heads. A highly sophisticated light-weight design permits substantially lower engine weights than those offered by competitors. The VW diesel engine weights have reached the weight ranges of pure aluminum engines. An aluminum crankcase may reduce the weight of VW engines by another 15%.

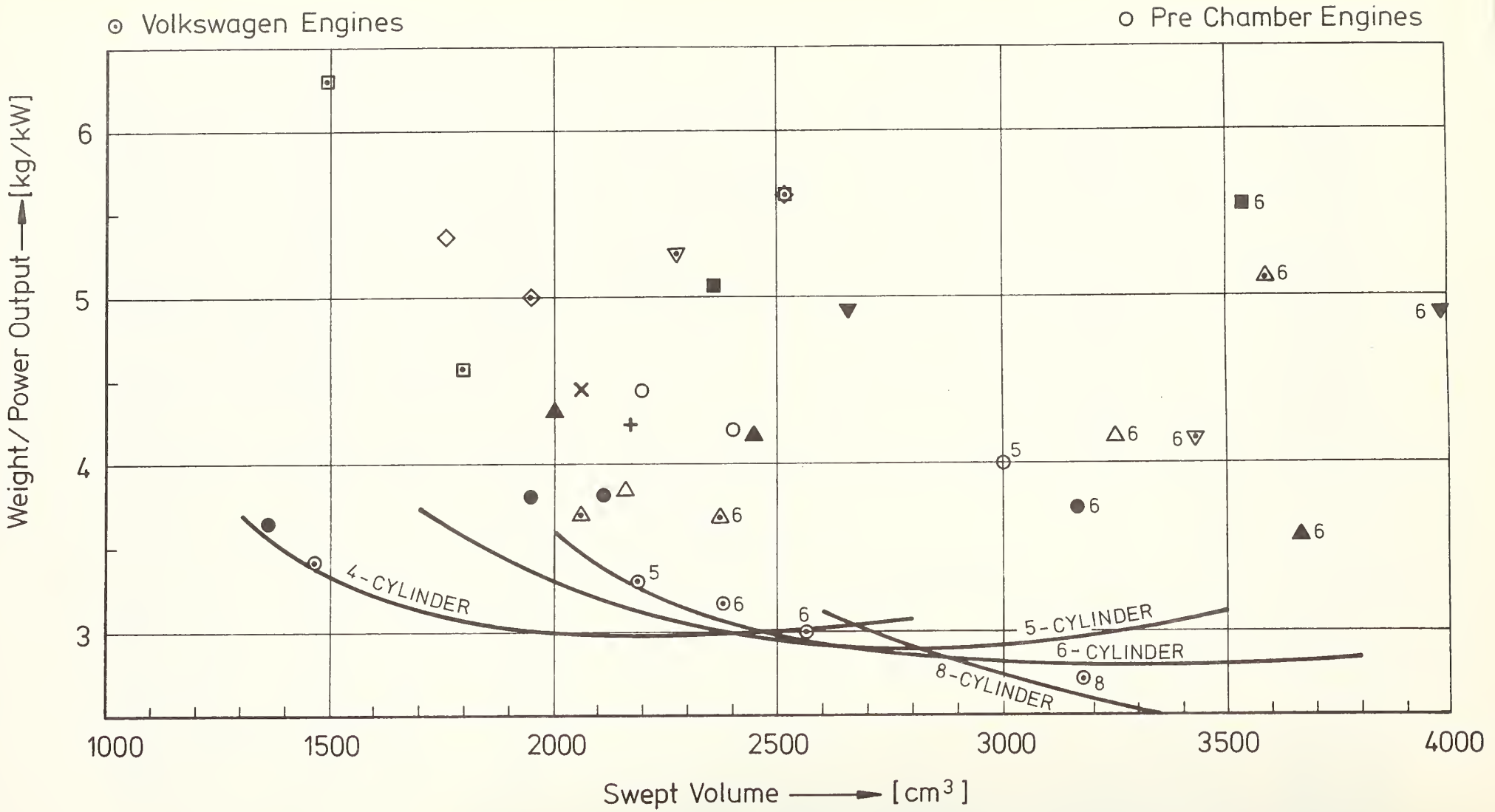

FIGURE 4.4-11: RELATIONSHIP BETWEEN SPECIFIC WEIGHT AND SWEPT VOLUME FOR AUTOMOTIVE SWIRL CHAMBER DIESEL ENGINES

4.4.3 Box Dimensions

4.4.3.1 Definition

The box dimensions are length, width, and height of the smallest box that can accomodate the engine with all accessories.

Again, there are variances in the definition similar to those of the engine weight. Some engines are equipped with an air filter that is mounted to the vehicle body in the engine compartment and has a hose connection to the engine air intake. In those cases, air filter and hose are not taken into account when the box dimensions are determined. This results in smaller dimensions for those engines.

Some engines are installed at a certain angle to minimize the height of the engine system. Also, there are occasions where height and width are computed for the installed engine position. The VW engine data refer to a vertical engine position.

Although the box dimension is a well-suited criterion for engine compactness, box dimensions alone should not be used to determine the installation suitability of an engine. The appearance of the engine compartment in the vehicle body shows a large number of gaps and spaces. The designer of a compact vehicle engine tries to pack this engine space as effectively as possible, which may lead to a different box dimension.

4.4.3.2 Effects of Engine Power Output, Displacement, and Number of Cylinders

There is an almost linear relationship between displacement and box dimensions (Figure 4.4-12). The most compact engines reach 0.09 m^3/liter, less compact ones 0.14 m^3/liter. Displacements up to approximately 2.6 liters result in an advantage in the case of 4-cylinder engines. An increase in the number of cylinders in units beyond this displacement range makes the engine more compact. The V-configuration offers increasing advantages.

The situation is similar when the box dimension is plotted versus the output (Figure 4.4-13). The drop in specific output in the kW/liter displacement causes the progressive increase in the case of larger cylinder units (Figure 4.4-5).

The combination of the graphs in Figures 4.4-4 and 4.4-12 leads to the relations shown in Figure 4.4-14, which shows the power-to-volume ratio in kW/m^3 versus displacement. The broad scatter does not indicate any trend.

The maximum power-to-volume ratio is reached with the following cylinder sizes, depending on the number of cylinders (Table 4.4-2).

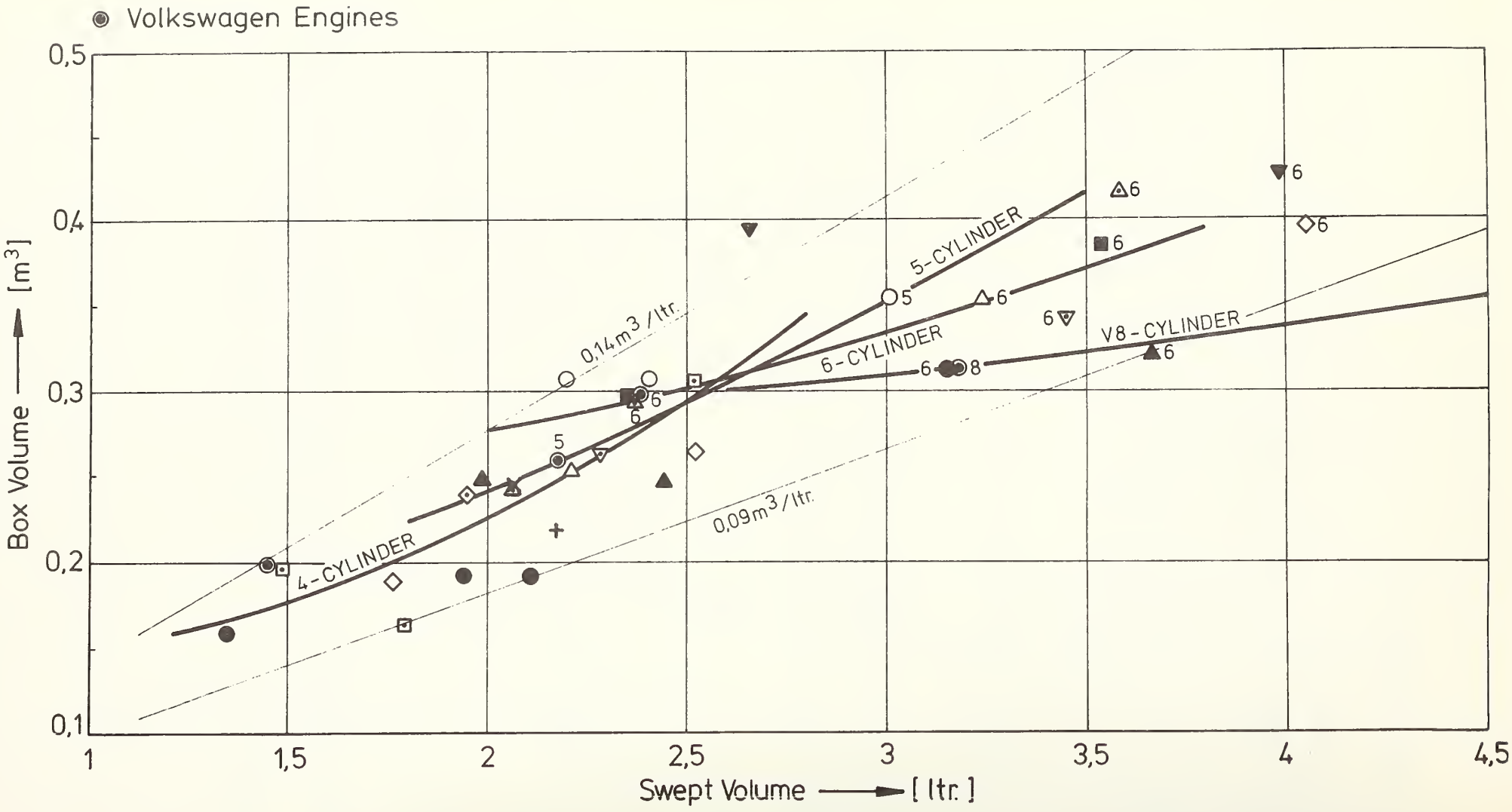

FIGURE 4.4-12: VARIATION OF BOX VOLUME WITH SWEPT VOLUME FOR AUTOMOTIVE DIESEL ENGINES

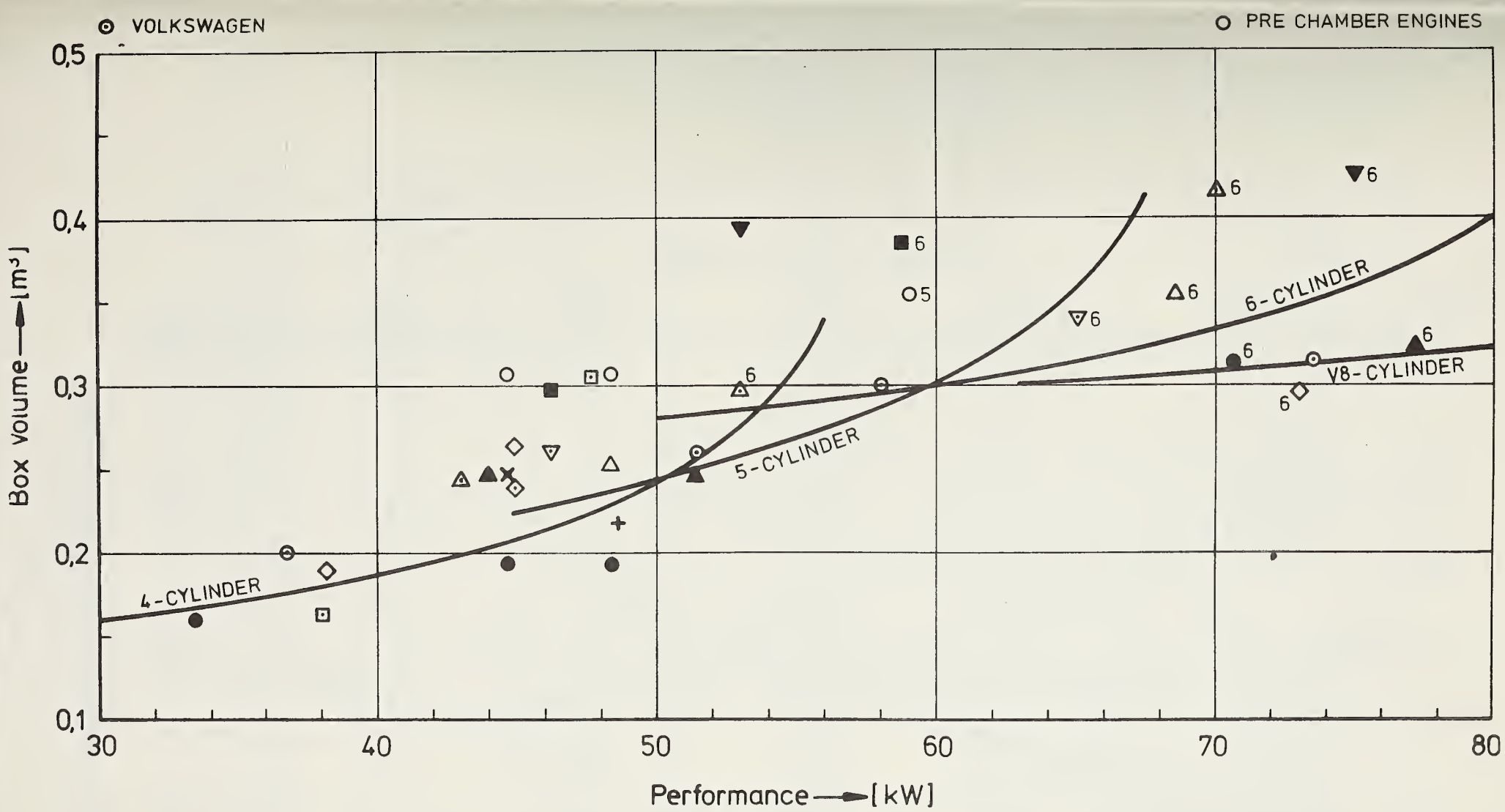

FIGURE 4.4-13: RELATIONSHIP BETWEEN BOX VOLUME AND PERFORMANCE FOR AUTOMOTIVE SWIRL CHAMBER DIESEL ENGINES

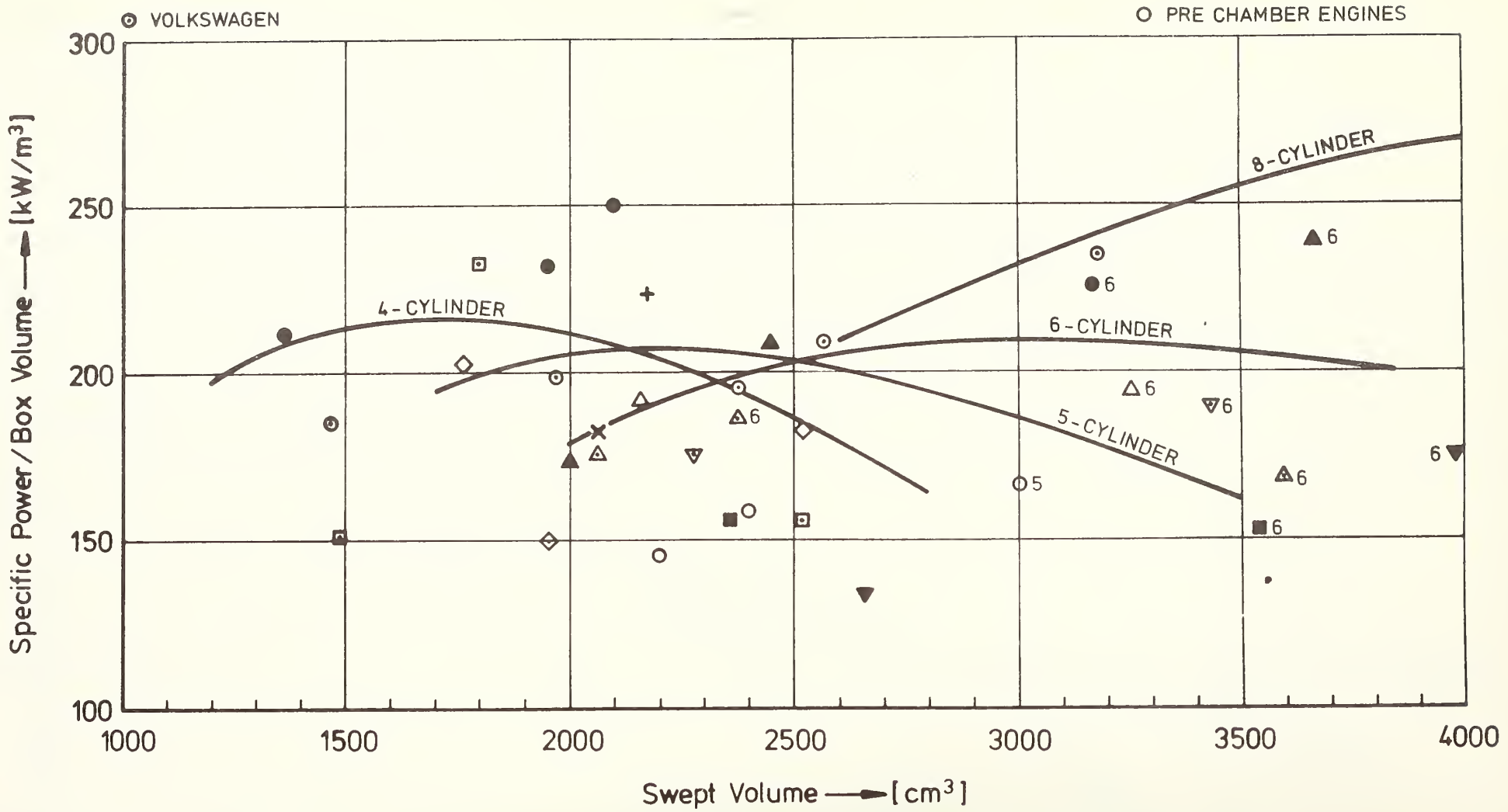

FIGURE 4.4-14: RELATIONSHIP BETWEEN SPECIFIC POWER AND SWEPT VOLUME FOR AUTOMOTIVE SWIRL CHAMBER DIESEL ENGINES

TABLE 4.4-2:

OPTIMUM CYLINDER UNIT FOR MAXIMUM POWER-TO-VOLUME RATIO

Number of Cylinders	Swept Volume per Cylinder Unit cc	Maximum Power-to-Volume Ratio kW/m^3
4	375 ... 500	230
5	400 ... 500	210
6	430 ... 580	215
V8	500 ... 650	ca. 270

It may be seen that the displacement of maximum power-to-volume ratio increases in direct proportion to the increase in the number of cylinders. The V-configuration offers increasing advantages with larger displacement.

4.4.4 Optimized Cylinder Unit

Sections 4.4.1 through 4.4.3 describe the effects of the displacement of each cylinder on engine performance, weight, and volume. Table 4.4-3 is a summary of the most favorable cylinder sizes for optimum engine characteristics.

TABLE 4.4-3:

SWEPT VOLUME PER UNIT FOR OPTIMIZED ENGINE CHARACTERISTICS

Engine Characteristics	Optimum	Optimum Swept Volume (cc)
Specific Output (kW/l)	24.3 ... 25.2	300 ... 400
Weight-to-Power-Ratio (kg/kW)	2.5 ... 3	500 ... 600
Power-to-Volume-Ratio (kW/m^3)	210 ... 270	375 ... 650

Table 4.4-4 shows the compromise suitable for passenger-car diesel engines considering the following three characteristics: specific output, power-to-weight ratio, and power-to-volume ratio. However, the individual characteristics may be weighed differently for a particular compromise in individual cases.

TABLE 4.4-4:

CYLINDER UNIT FOR PASSENGER CAR DIESEL ENGINES

Number of Cylinders	Optimum Swept Volume per Cylinder Unit (cc)
4	350 ... 480 (1.4 ... 1.9 l)
5	400 ... 500 (2.0 ... 2.5 l)
6	420 ... 520 (2.5 ... 3.1 l)
V8	450 ... 550 (3.6 ... 4.4 l)

4.5 DESIGN PARAMETER VARIATIONS

Section 4.4 describes the effects of cylinder dimension, number, and arrangement on performance, engine weight, and box dimensions. This section present the effects of the following design parameters:

- Engine speed
- Stroke/bore ratio
- Connecting rod ratio
- Compression ratio
- Valve-diameter/cylinder-bore ratio
- Valve timing
- Production tolerances

on the characteristics mentioned earlier and their impacts on data such as

- Performance
- Specific fuel consumption
- Emissions
- Noise
- Startability

4.5.1 Engine Speed

A rise in engine speed raises the output to that point where the increases in friction losses and the lower volumetric efficiency caused by throttling losses result in a drop in power output. Fuel consumption and Bosch number increase along with the engine speed (Section 4.4.1). The nominal engine speed of passenger-car diesel engines should not exceed 5,000 rpm.

The piston velocity and the oscillating masses rise in direct proportion to an increase in the cylinder size. The mean piston velocity should not exceed 13.5 m/s in order to prevent exceedingly steep increases in friction losses and mass forces. Figure 4.5-1 shows the possible rpm as a function of the cylinder displacement and stroke/bore ratio at a constant mean piston velocity of 13.4 m/s.

The relationship between cylinder displacement and available nominal engine speed for constant mean piston velocity and constant stroke/bore ratio is

$$n \sim v_i^{-\frac{1}{3}}$$

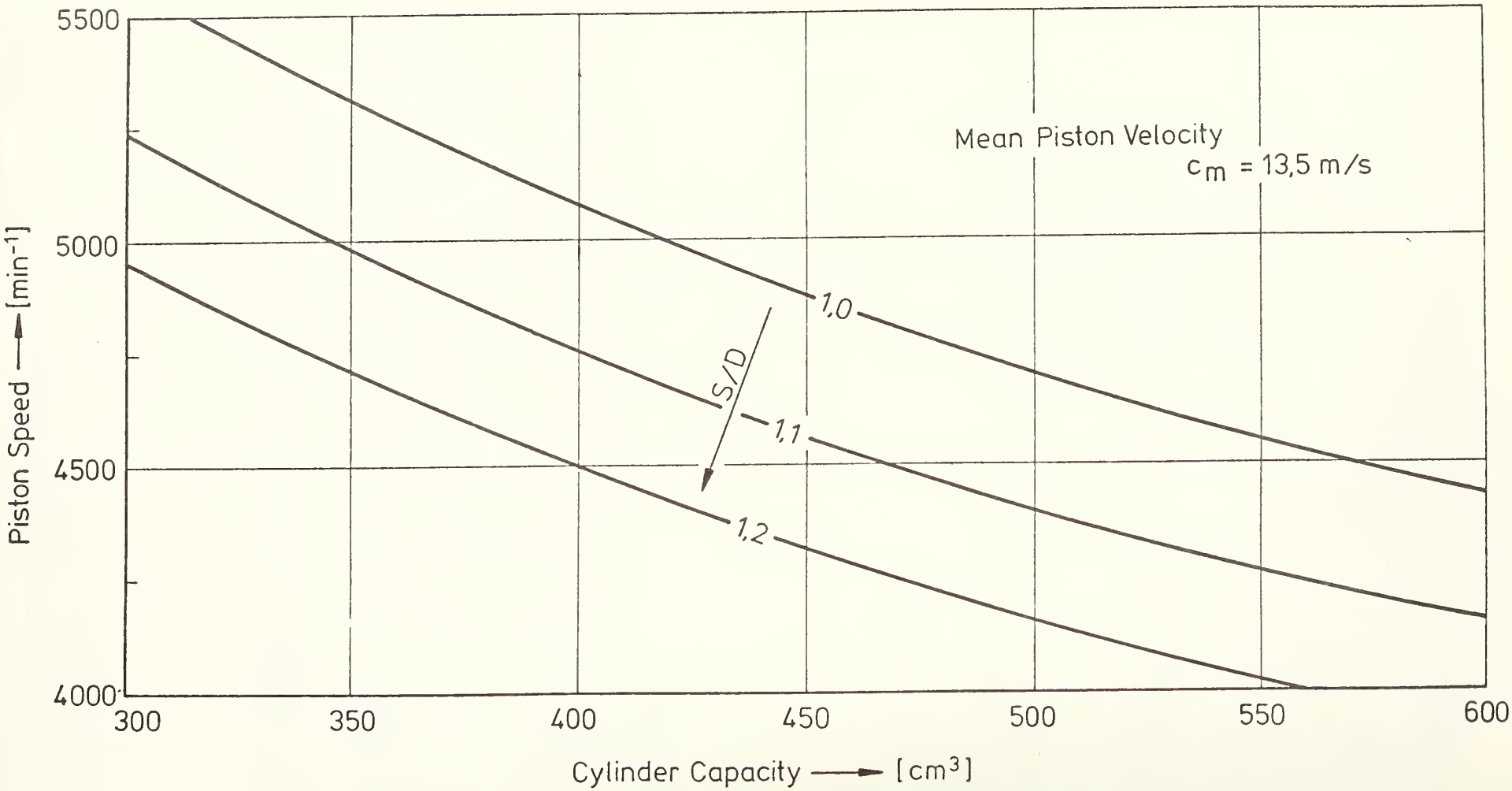

FIGURE 4.5-1: ENGINE SPEED AS A FUNCTION OF CYLINDER CAPACITY AND STROKE/BORE RATIO AT CONSTANT MEAN PISTON VELOCITY

4.5.2 Stroke/Bore Ratio

The stroke/bore ratio essentially affects the following parameters:

- Charge cycle
- Mean friction pressure
- Mean effective pressure
- Heat transfer
- Final compression pressure
- Specific fuel consumption
- Piston velocity
- Torsional behavior
- Power plant stresses
- Engine weight
- Engine dimensions
- Engine volume

The range of the optimum stroke/bore ratio for passenger-car diesel engines is established with particular consideration of these parameters.

4.5.2.1 Charge Cycle

The short-stroke engine permits larger valve cross sections in relation to the displacement in those cases where there is an optimum match of valve sizes and distances and cylinder bore. The following relation between stroke S and bore D applies to the gas velocity C in the valve cross section:

$$C \sim \sqrt{S/D}$$

A 20% decrease of the stroke/bore ratio thus lowers the gas velocity by roughly 10%. This decreases the throttle losses during gas exchanges and results in an improved charge at high engine speeds. Figure 4.5-2 shows the relationship between volumetric efficiency and mean gas velocity. Figure 4.5-3 shows the efficiency versus the engine speed for various stroke/bore ratios.

The gas velocity is determined by the valve stroke at a stroke/bore ratio < 0.9. The valve stroke is restricted by the stresses on the valve drive. The effects of the channel cross section clearance in the space between valve seat ring and valve shaft becomes increasingly significant at an S/D ratio of 0.9. An increase in the valve stroke does not lead to a better charge but merely raises the valve drive stresses.

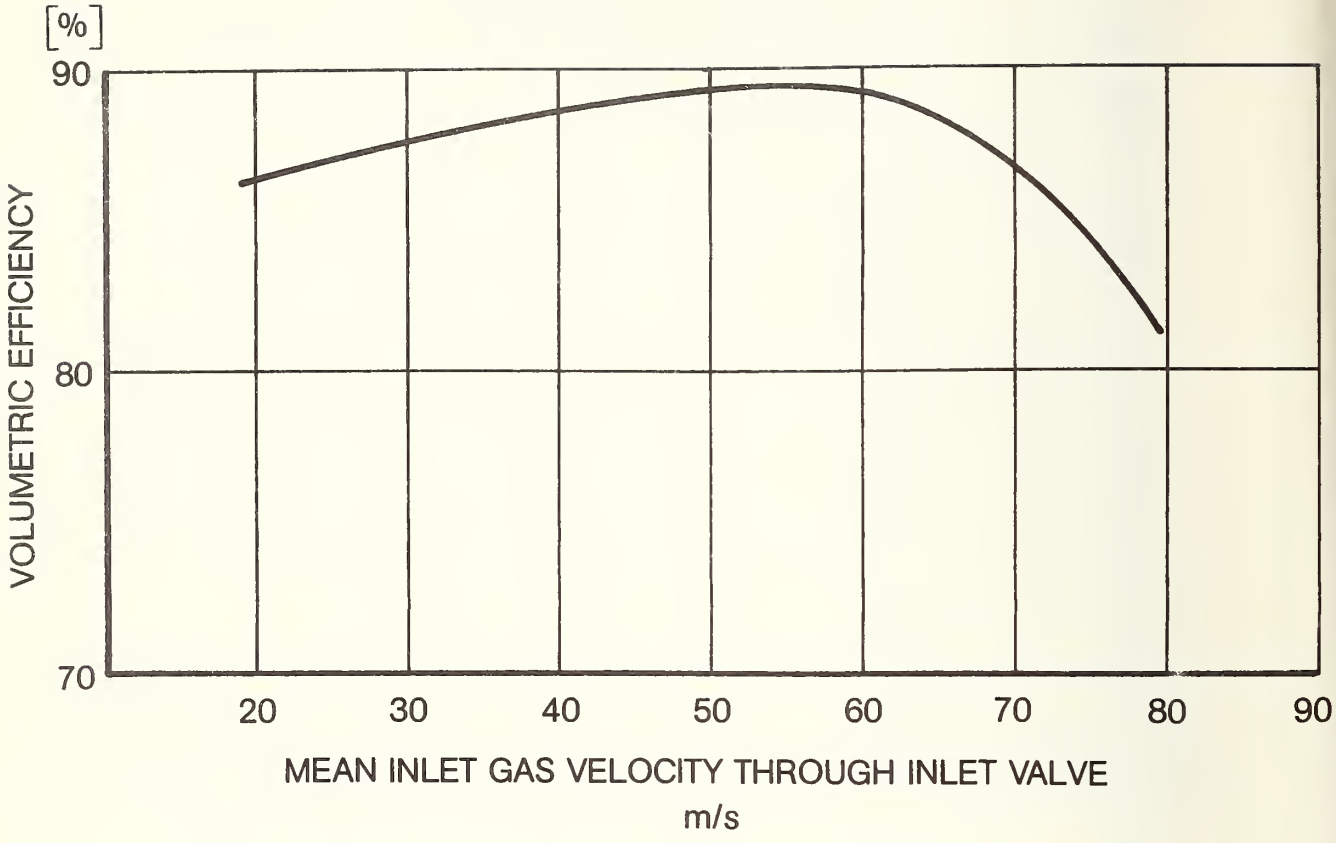

FIGURE 4.5-2: RELATIONSHIP BETWEEN VOLUMETRIC EFFICIENCY AND MEAN GAS VELOCITY ASSUMED FOR PERFORMANCE CALCULATIONS
Mean gas velocity measured through inlet valve inner seat diameter.

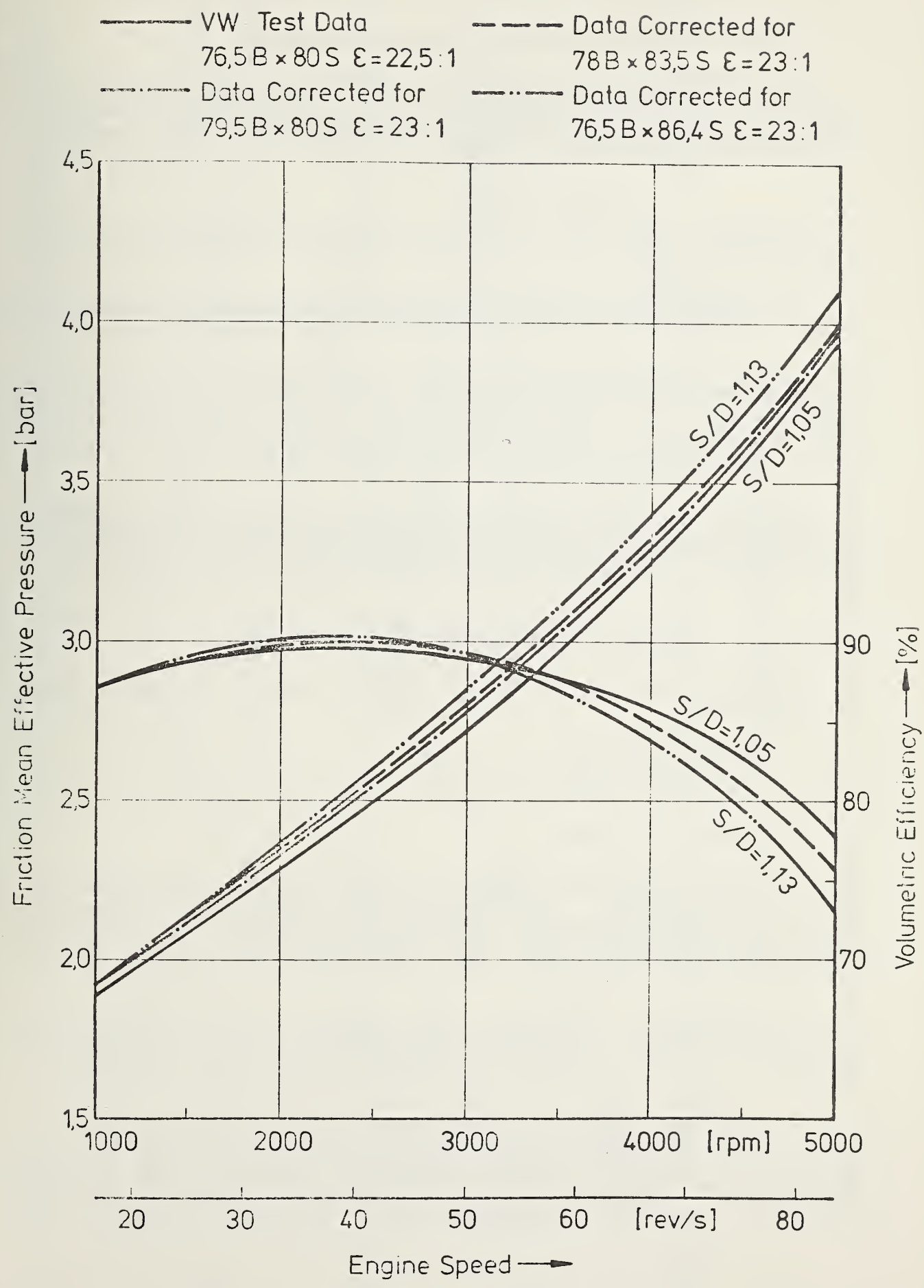

FIGURE 4.5-3: MOTORING LOSS AND VOLUMETRIC EFFICIENCY OF VW ENGINE WITH CHANGE OF BORE/STROKE

4.5.2.2 Effects on the Final Compression Pressure

The following equation defines the relationship between the possible compression ratio and the stroke/bore ratio at a given minimum distance between piston and cylinder head and a ratio given between swirl chamber folume and the total clearance volume:

$$\varepsilon = \text{Constant } (S/D)^{\frac{2}{3}}$$

Reference shows this function and includes the cylinder volume as an additional parameter.

The compression ratio, too, affects the final compression pressure, which in turn is also a function of engine efficiency and thus of engine speed.

Figure 4.5-4 shows the final compression pressure for a variety of piston velocities versus the stroke/bore ratio. The final compression pressure drops steeply for $S/D < 1$. This is caused by the increase in heat losses at rising surface/volume ratios of the combustion chamber and by the higher mass losses due to larger sealing surfaces at larger piston diameters.

The final compression pressure drops along with the efficiency when S/D is higher than 1.1 because of the decreasing cross section of the channel in the space between valve seat ring and valve shaft. The final compression pressure versus the engine speed follows the volumetric efficiency.

4.5.2.3 Effects on the Brake Mean Effective Pressure

The brake mean effective pressure (bmep) at constant compression ratios is a function of

- internal efficiency
- volumetric efficiency
- mechanical efficiency

The internal efficiency is severely affected by the surface/volume ratio of the combustion chamber. The effects of the stroke/bore ratio on the surface/volume ratio become increasingly significant as the compression ratio rises Long-stroke engines have a more compact combustion chamber and thus offer a better internal efficiency.

The stroke/bore ratio has very little effect on the efficiency and the mean friction pressure at low engine speeds (Figure 4.5-3). The short-stroke design offers definite advantages in the engine speed range from 3,200 rpm and up.

The lower heat losses of the long-stroke engine outweigh the lower friction losses of the short-stroke engine below engine speeds of 4,000 rpm. This may be seen from the curves of output, mean pressure, and specific fuel consumption in Figure 4.5-5. The ratio between valve size and cylinder bore is the same in both cases. The volumetric efficiency curve is the same for each engine with

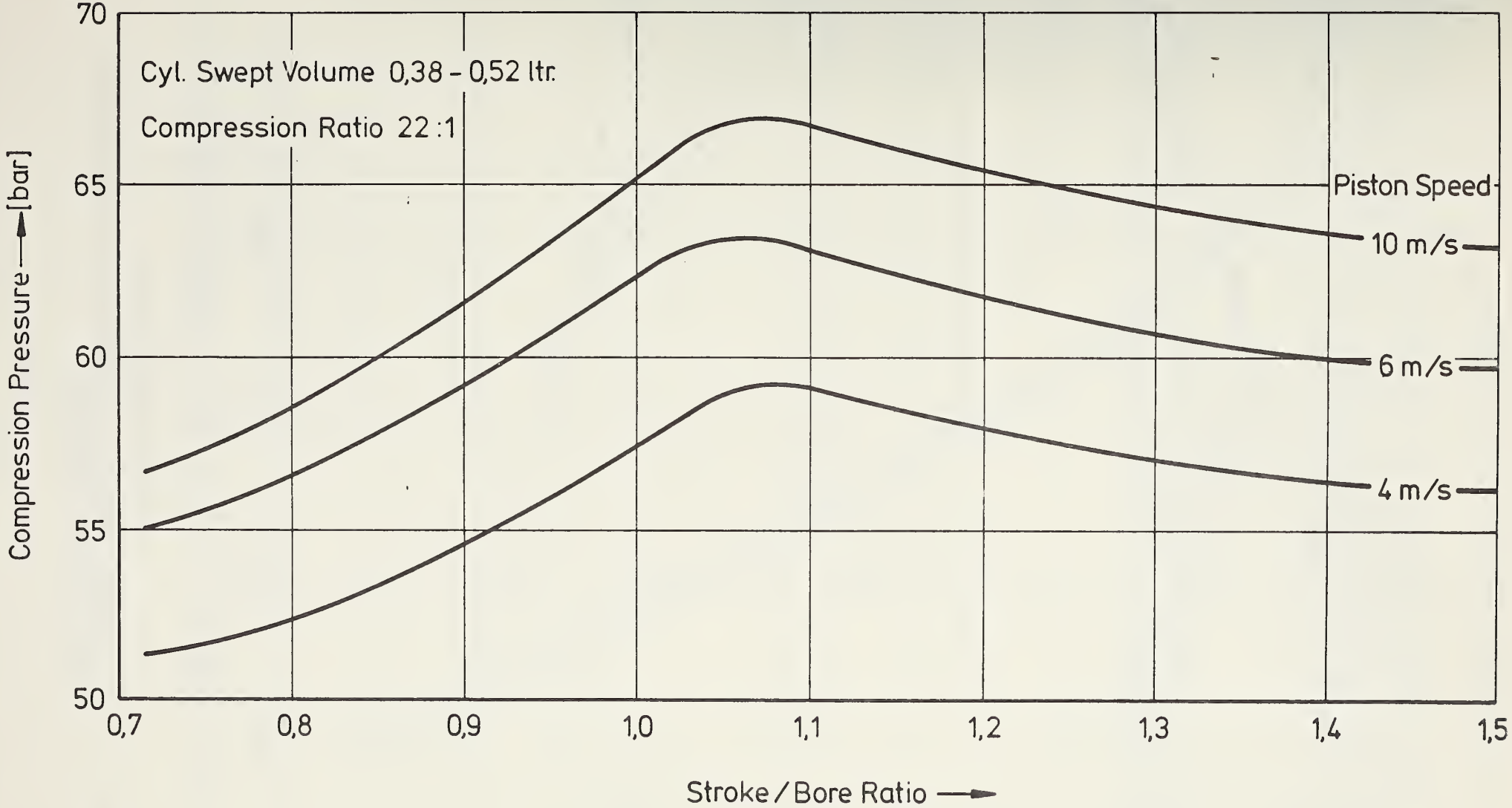

FIGURE 4.5-4: EFFECT OF STROKE/BORE RATIO ON COMPRESSION PRESSURE AT VARYING PISTON SPEEDS

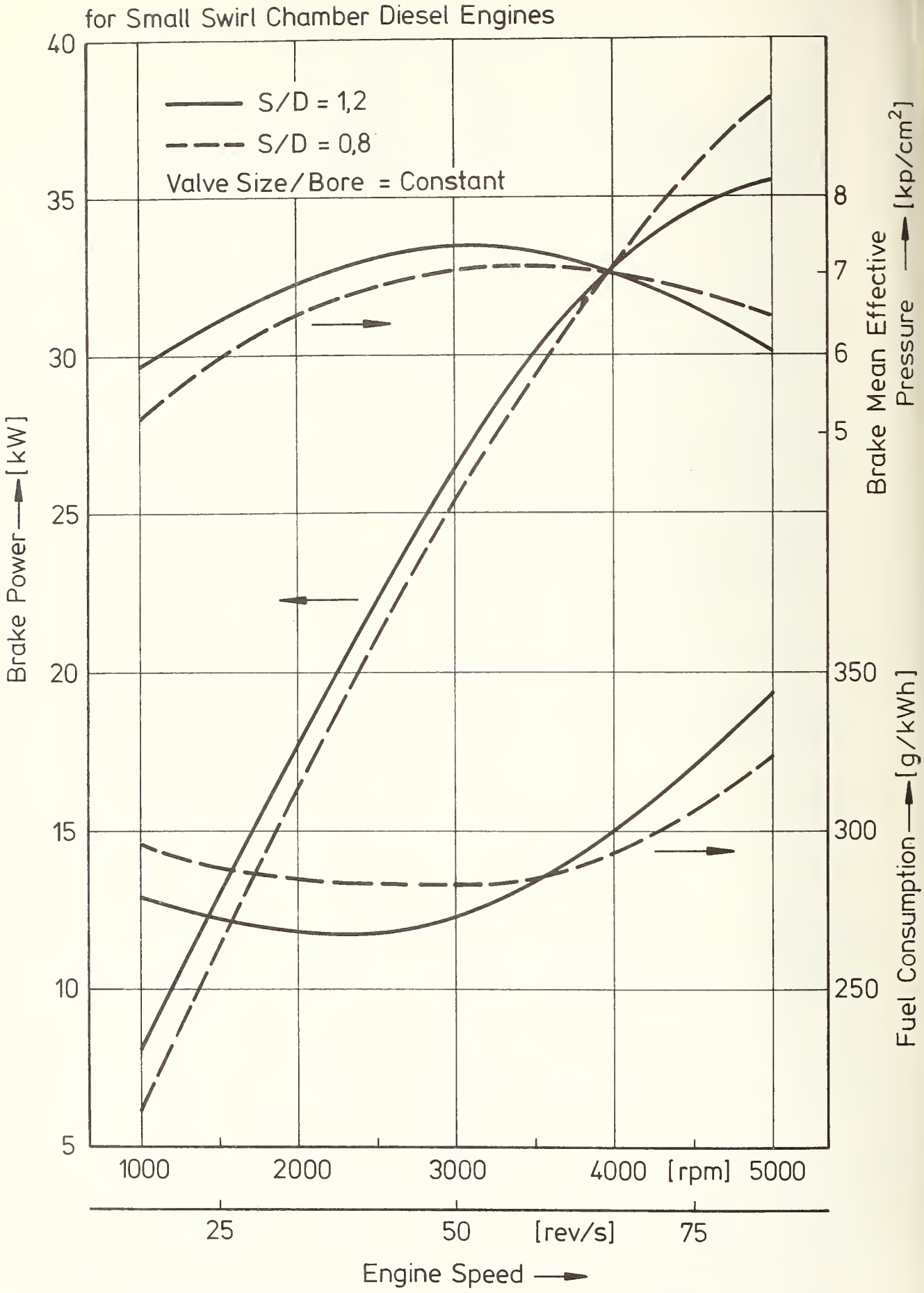

FIGURE 4.5-5: ESTIMATED EFFECT OF STROKE/BORE RATIO ON PERFORMANCE, BMEP AND FUEL CONSUMPTION

respect to gas velocities through the valves. The motoring losses were adjusted for the higher piston speed of the long-stroke engine. Both of these relationships are shown in Figure 4.5-3. The volumetric efficiency of long-stroke engines drops noticeably while motoring losses increase at high engine speeds. The combustion efficiency was assumed to remain constant within the investigated range of bore/stroke ratios.

4.5.2.4 Effects on Power Plant Stresses

The mean piston velocity alone does not suffice to permit an estimate of the power plant stresses. Consideration should also be given to the effects of the forces resulting from combustion pressure and oscillating masses as a function of the stroke/bore ratio.

Mean piston velocity

The mean piston velocity

$$c_m = 2S \cdot n$$

results for constant engine speed in

$$c_m = \text{Const.} \cdot S$$

The equation for the displacement of one cylinder

$$V_i = D^2 \cdot \frac{\pi}{4} \cdot S$$

results for constant V_i in

$$D \sim (1/S)^{\frac{1}{2}}$$

Therefore,

$$\frac{S}{D} \sim S^{\frac{3}{2}}$$

The mean piston velocity is a function of the stroke/bore ratio:

$$c_m \sim (S/D)^{\frac{2}{3}}$$

A 50% increase of the stroke/bore ratio from S/D = 0.8 to 1.2 raises the mean piston velocity by 31.2% at constant rpm.

A given maximum piston velocity results in

$$n \sim (S/D)^{-\frac{2}{3}}$$

A 50% increase in the stroke/bore ratio causes a 23.7% decrease in engine speed at constant mean piston velocity.

Combustion Pressure

The combustion pressure p_G versus the crank angle is assumed to be constant and independent of the stroke/bore ratio. This results in the piston force for the piston area A_K.

$$F_K = p_G \cdot A_K$$

where

$$A_K \sim D^2$$

and

$$S/D \sim \frac{1}{D^3}$$

$$F_K \sim (S/D)^{-\frac{2}{3}}$$

The connecting rod force, piston normal force, radial force, and tangential force are not affected by the stroke/bore ratio at constant connecting rod ratio $\lambda = r/\ell$

The following requirement must be met in order to obtain constant bearing loads

$$A_{proj} \sim (S/D)^{-\frac{2}{3}}$$

where

A_{proj} = the projected bearing surface.

Mass Forces

The maximum oscillating mass force at constant $\lambda = r/\ell$ is

$$F_{OSZ} \sim m_{OSZ} \cdot r \cdot \omega^2$$

where

F_{OSZ} = Force oscillating

m_{OSZ} = Mass oscillating

ω = Angular speed

The oscillating mass is approximately in direct proportion to the third power of the bore diameter . This results in

$$F_{OSZ} \sim D^3 \cdot s \cdot n^2$$

$$F_{OSZ} \sim (S/D)^{-\frac{1}{3}} \cdot n^2$$

In those cases where the bearing surfaces are selected in accordance with

$$A_{proj} \sim (S/D)^{-\frac{2}{3}}$$

the speed for constant bearing loads is

$$\frac{F_{OSZ}}{A_{proj}} \sim D \cdot s \cdot n^2$$

where

$$n \sim (S/D)^{-\frac{1}{6}}$$

The mean piston velocity at constant power plant stresses is

$$c_m \sim (S/D)^{\frac{1}{2}}$$

An increase of the stroke/bore ratio from 1 to 1.2 requires a 3% decrease in engine speed. The mean pistong velocity continues to rise by 9.5%.

4.5.2.5 Effects on Engine Dimensions

The space for installation of the engine in the vehicle does not have an ideal rectangular configuration but is severely split by wheel wells, steering system, axle assembly, etc. Many accessories are adapted to the contours of the engine compartment, such as intake pipe, exhaust manifold, oil sump, generator mounting, power-assist pumps, etc.

The individual dimensions have different degrees of significance in relation to the entire vehicle configuration.

The engine should require as little longitudinal space as possible. This produces favorable effects on the vehicle crash behavior. In transverse installations, engine and transmission fill the space between the wheel wells and thus determine the possible steering angle and the total vehicle width.

A flat, wedge-shaped front end lowers the drag coefficient. Therefore, the engine should be as flat as possible.

The engine width in transverse installations is significant in view of the vehicle crash safety. The width of longitudinally installed units is of minor significance if there is sufficient space available between the wheel wells. This generally holds true for in-line engines.

The adaptation of engine contours to a specific vehicle reduce the effects of the stroke/bore ratio on the exterior engine dimensions. Therefore, the investigation was to cover only the dimensions of those components that are not affected by the configuration of the specific engine compartment, i.e. cylinder block and crankcase with cylinder head, oil pan, and flywheel, without accessories. The engine width is expressed in terms of crankcase width, which is determined by the envelope of the connecting rod. It is not determined by the flywheel diameter because the latter is independent of the stroke/bore ratio.

Engine dimensions that are functions of the stroke/bore ratio

The following dimensions are used to determine the effect of the stroke/bore ratio.

Length: Center-to-center of the exterior crankshaft bearings.

Height: From upper edge of piston in TDC to center of crankshaft journal in BDC.

Width: Envelope curve of piston rod.

Length

The length of the crankcase is determined by the space between the cylinder units.

The space between the cylinders of an in-line engine is in direct proportion to the bore diameter. This results in

$$1 \sim D$$

$$D \sim (S/D)^{-\frac{1}{3}}$$

$$L \sim (S/D)^{-\frac{1}{3}}$$

A 20% increase in the stroke/bore ratio reduces the length of the crankcase by 6%.

Height

The height of the in-line engine is determined by the crank radius, the length of the piston rod, and the compression height of the piston:

$$H = S + 1 + h_K$$

where H is the engine height affected by the stroke/bore ratio

$r = S/2$ = crank radius

ℓ = length of piston rod

h_k = compression height of piston

$K = h_k/D$ = constant

$\lambda = r/l$ = crank ratio

D = cylinder bore

$$S = \left(S/D \right)^{\frac{2}{3}} \left(\frac{4}{\pi} V_n \right)^{\frac{1}{3}}$$

$$D = \left(S/D \right)^{-\frac{1}{3}} \left(\frac{4}{\pi} V_n \right)^{\frac{1}{3}}$$

$$H = \left(S/D \right)^{\frac{2}{3}} \left(\frac{4}{\pi} V_n \right)^{\frac{1}{3}} \left(\frac{2\pi + 1}{2\pi} \right) + K \left(S/D \right)^{-\frac{1}{3}} \left(\frac{4}{\pi} V_n \right)^{\frac{1}{3}}$$

Example:

$V_h = 400$ cc

where $\lambda = 0.29$

$K = 0.6$

An increase of 20% in the stroke/bore ratio leads to a 9.5% increase in engine height.

Width

The width of an in-line engine crankcase is determined by the envelope curve of the piston rod. The following relation has been determined empirically:

$$B \sim \left(S/D \right)^{0.27}$$

Engine Dimensions without Accessories

An investigation of the base engine without accessories showed a reduction of the effects of the stroke/bore ratio on engine length, height and width. The design of the valve drive, camshaft drive and crankcase faces with seals is not affected by the stroke/bore ratio.

Figure 4.5-6 presents the dimensions of the base engine as a function of the stroke/bore ratio.

Figure 4.5-7 shows the resulting engine volume. This volume was obtained by multiplying the above-mentioned factors. Figure 4.5-7 also includes the volume of the cylinder block which is affected by the stroke/bore ratio to a higher degree.

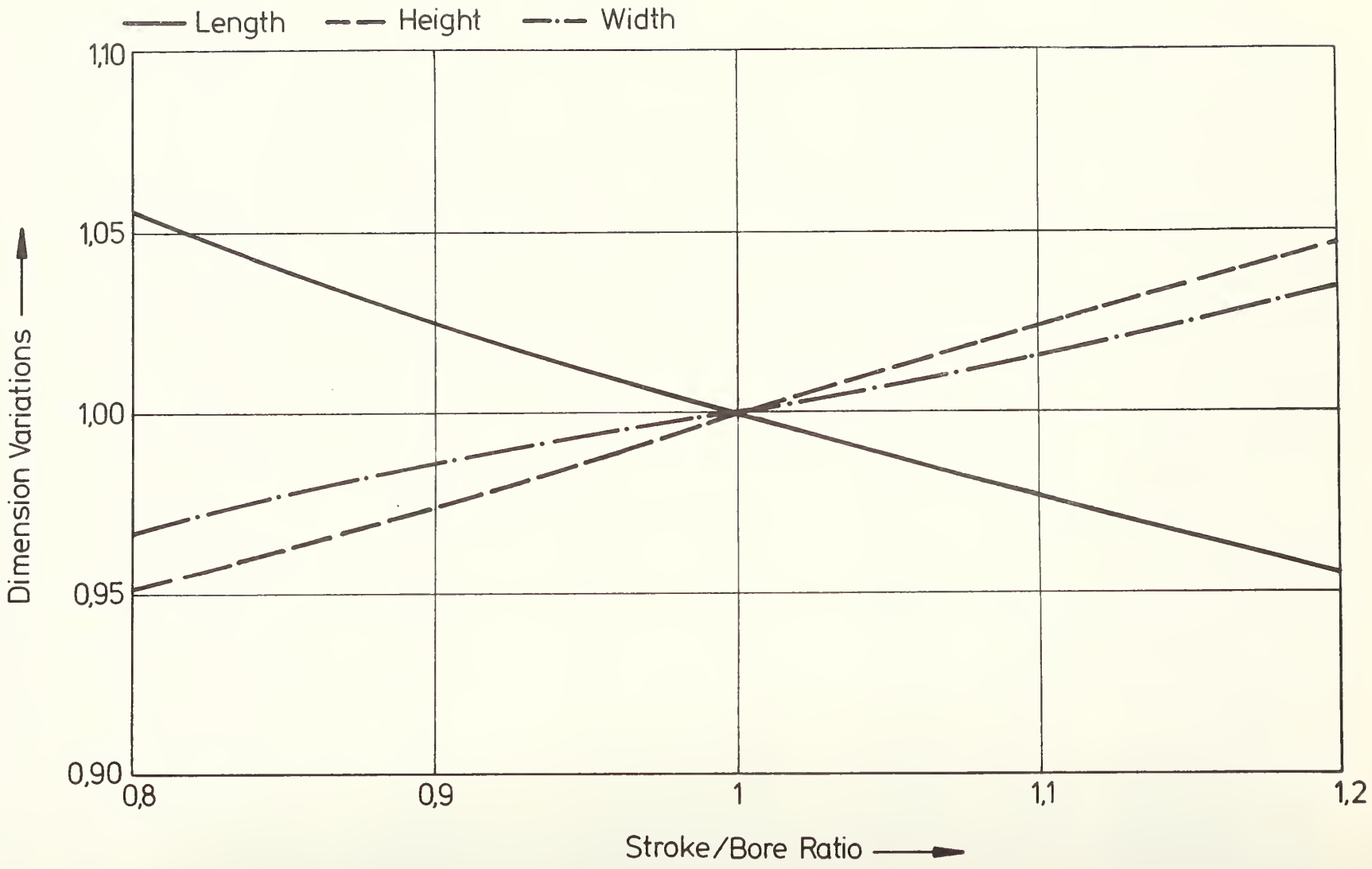

FIGURE 4.5-6: THEORETICAL RELATIONSHIP BETWEEN STROKE/BORE RATIO AND MAJOR DIMENSIONS FOR INLINE ENGINES WITHOUT ACCESSORIES

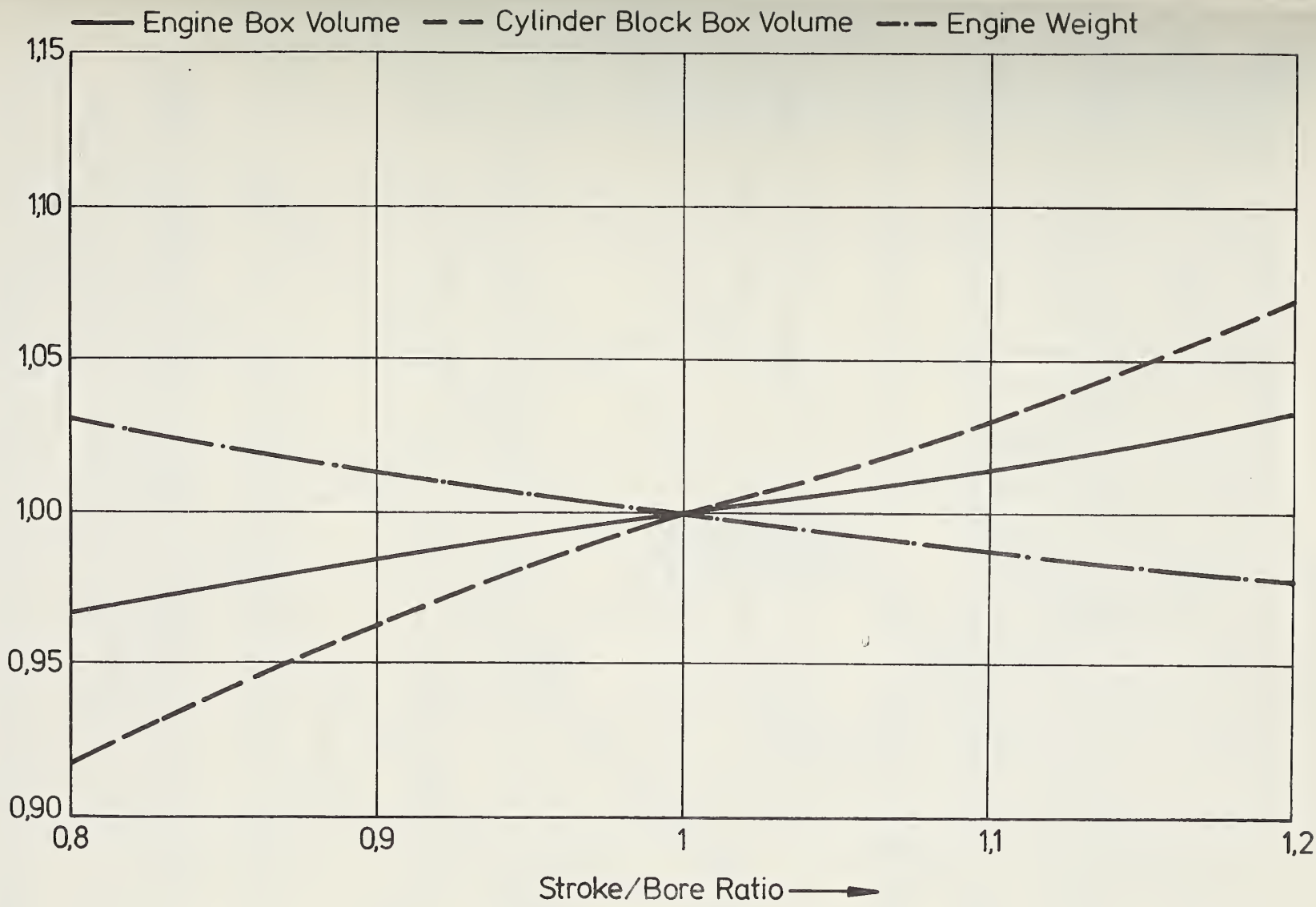

FIGURE 4.5-7: EFFECT OF STROKE/BORE RATIO ON WEIGHT AND BOX VOLUME FOR INLINE ENGINES WITHOUT ACCESSORIES

4.5.2.6 Effects on Engine Weight

The total engine weight consists of one constant portion not affected by stroke/bore ratio and displacement, e.g. generator, starter, water pump, oil pump, injection pump, etc., and one portion that is determined by the stroke/bore ratio, such as cylinder crank case, crank drive, cylinder head, and valves.

Various authors determine the engine weight by the box volume. This means that an increase in the stroke/bore ratio would lead to an increase in engine weight. However, the larger dimensions of the crank drive that become necessary as the stroke/bore ratio decreases were not taken into consideration.

Engine length is the dimension that determines the weight of the engine. This results in the relation shown in Figure 4.5-7 where the engine weight is a function of the stroke/bore ratio.

An increase in the stroke/bore ratio from 1 to 1.2 leads to a 2.3% decrease in engine weight.

4.5.2.7 The Optimum Stroke/Bore Ratio for Passenger-Car Diesel Engines

The short-stroke design concept offers the following advantages at high engine speeds:

- Higher output
- Better fuel economy
- Lower drivetrain stresses.

In addition, engine height, width, and box dimensions are smaller.

The long-stroke concept presents the following advantages in the low- and medium-engine-speed ranges:

- Higher torque
- Less fuel consumption.

This concept has a better cold-start behavior due to the higher compression pressure, and engine length and weight are reduced.

Figure 4.5-8 shows the stroke/bore ratios of present production passenger car diesel engines and VW prototypes. It is interesting to note that almost half of all engines have a stroke/bore ratio between 0.9 and 1. It should be borne in mind, though, that most of these engines were derived from short-stroke spark-ignition engines. Efforts were made to provide for a maximum displacement in the available cylinder blocks in order to compensate at least in part for the lower output of the diesel compared with the conventional spark-ignition combustion system. These efforts led to a stroke/bore ratio which is not favorable for diesel engines.

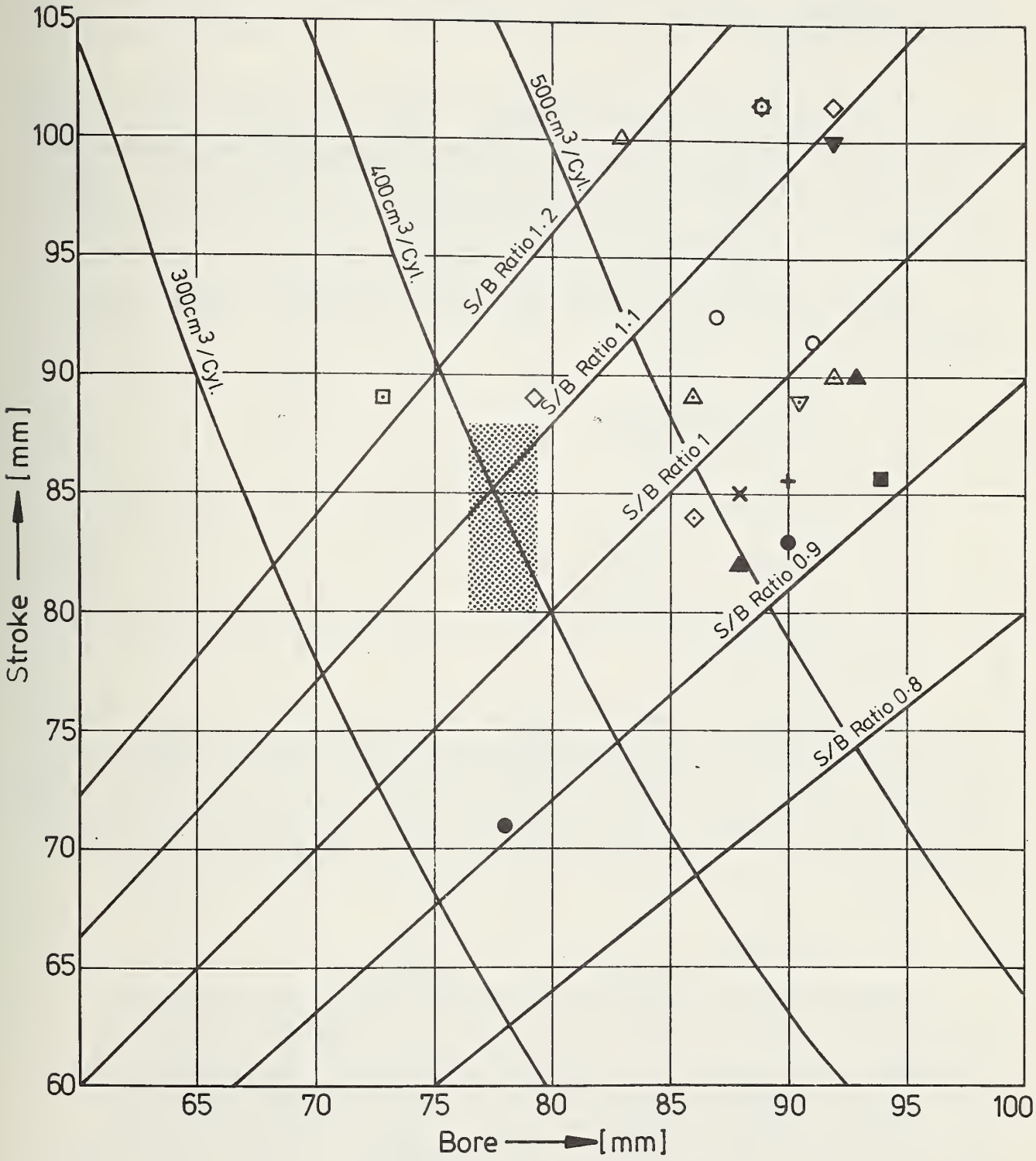

FIGURE 4.5-8: RELATIONSHIP BETWEEN BORE AND STROKE FOR VARIOUS SWEPT VOLUME AND STROKE/BORE RATIOS

The optimum stroke/bore ratio is between 1 and 1.2 for small, high-revving passenger-car diesel engines with cylinder unit displacements of between 300 and 500 cc.

The final compression pressure drops steeply in the lower ranges. This, again, detrimentally affects the cold-start behavior because of the too low final compression temperature. Furthermore, the engine weight increases and thus leads to higher production costs. The achievable output drops in the ranges above a stroke/bore ratio of 1.2 because of lower efficiency, higher friction and the loss in engine speed due to higher power plant stresses. Furthermore, fuel consumption rises too steeply at higher engine speeds.

Engine units in a V-configuration become increasingly compact as the stroke/bore ratio decreases. The optimum stroke/bore ratio ranges roughly between 1 and 1.1.

4.5.3 Connecting Rod Ratio

The connecting rod ratio $\lambda = l/r$ affects

- The friction losses
- The rotating and oscillating masses
- The engine weight
- The engine height.

Volkswagenwerk's studies have shown that at least up to $\lambda = 3.15$ friction losses are affected by the connecting rod ratio to a very minor extent only. A minimum connecting rod length should be the design objective because of the advantages offered by the short connecting rod in lower rotating and oscillating masses, the lower engine weight and engine height. Restrictions are imposed by the length of the piston shaft, which is determined by wear and noise factors.

4.5.4 Valve Size

The necessity of an adequate space between intake and exhaust valve (valve bridge) restricts the valve diameters at a given cylinder bore. In practice this means that the sum of the valve inner seat diameters is restricted to about 80% of the cylinder bore diameter. This results in an inlet valve inner seat of about 42 - 45% of the bore. Increasing valve size and lift increases performance. Valve lifts in excess of about 28% of the inner seat diameter generally are unnecessary . Figure 4.5-9 shows the pump losses as a function of the gas velocity in the valve cross section.

This data was used to determine the mean pressure and output curves shown in Figure 4.5-10 and 4.5-11. The mean pressure and output rise at high rpm's. There is no significant drop in bmep and power at low rpm's if the ratio between intake valve diameter and cylinder bore is lower than 0.45. The intake pipe should have a sufficiently large cross section with

SOURCE: SAE PAPER 680 590

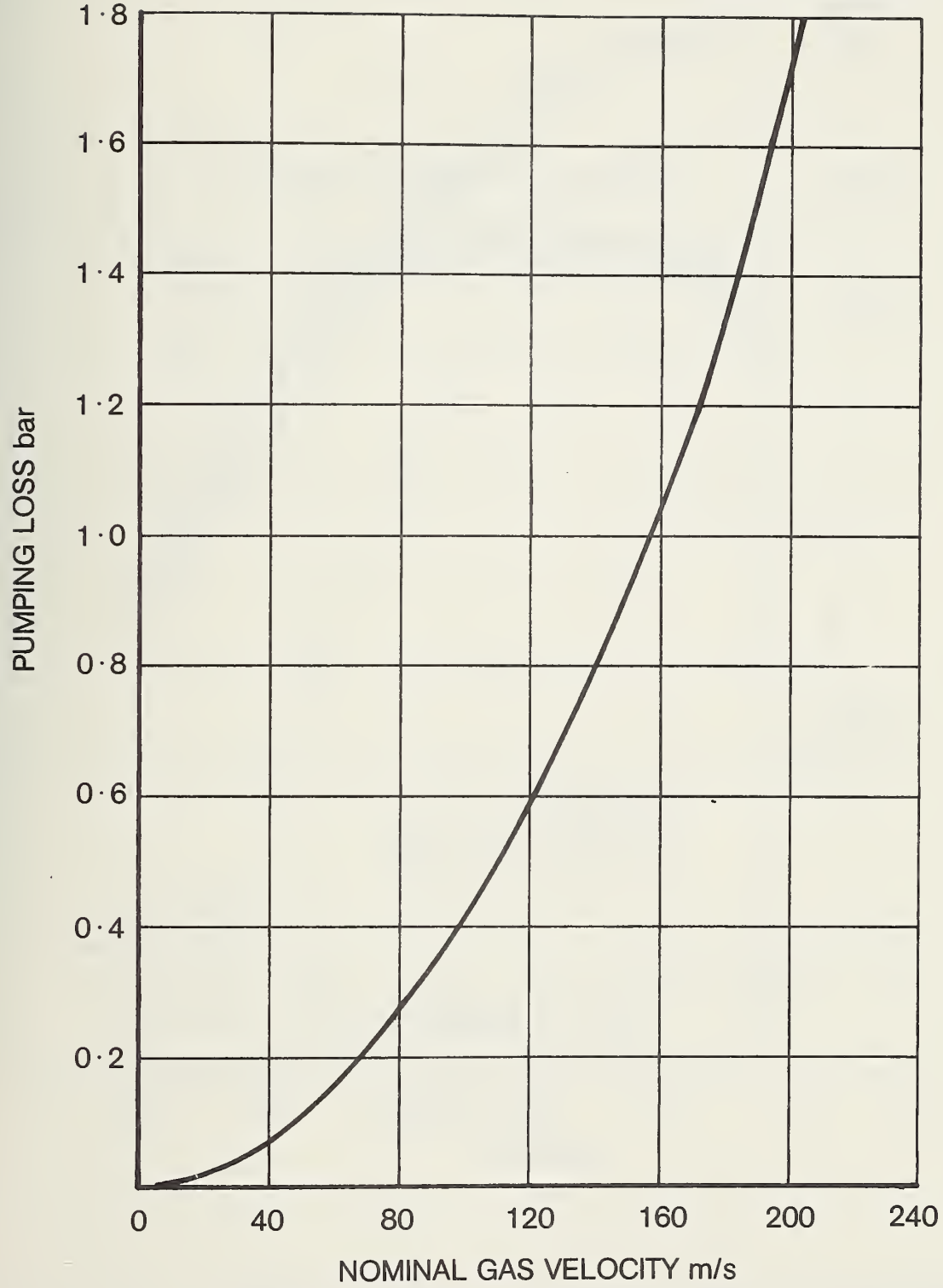

FIGURE 4.5-9: EFFECT OF GAS VELOCITY ON PUMPING LOSSES THROUGH INLET AND EXHAUST VALVES

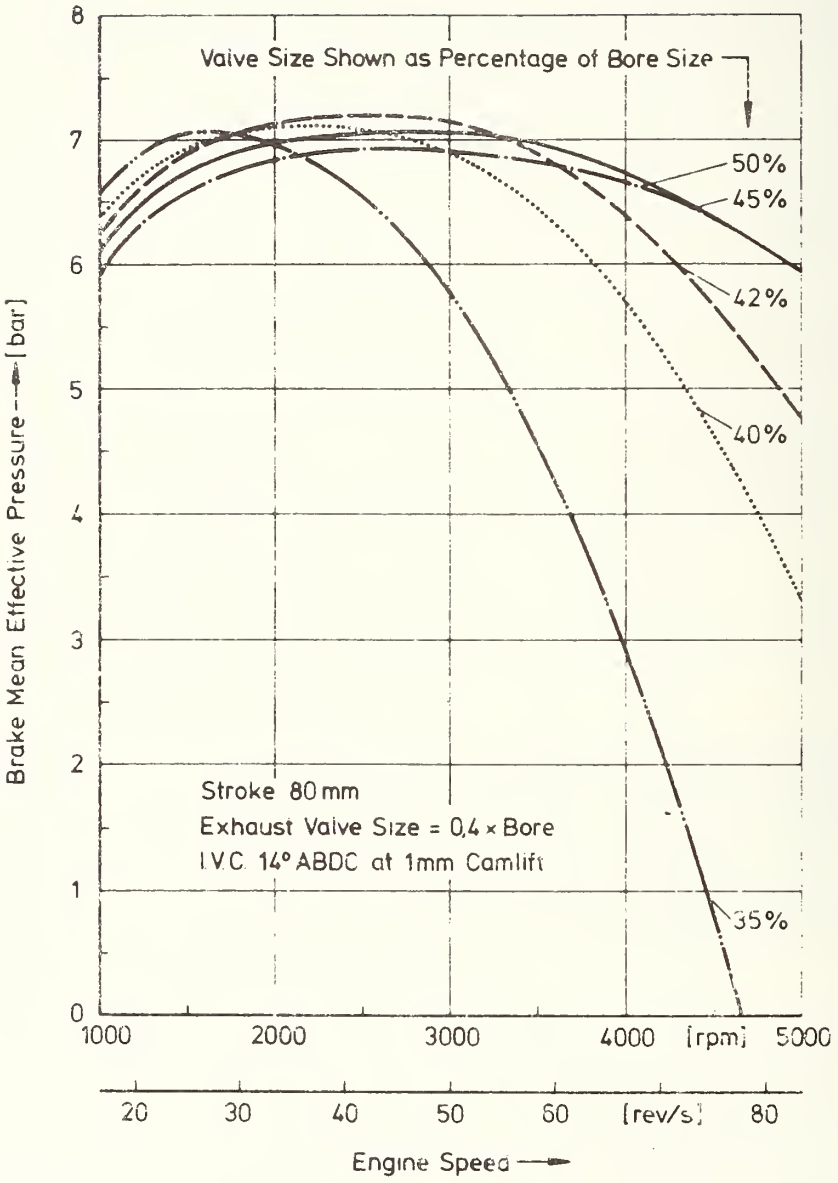

FIGURE 4.5-10: ESTIMATED EFFECT OF INTAKE VALVE SIZE ON THE PERFORMANCE OF A SWIRL CHAMBER ENGINE

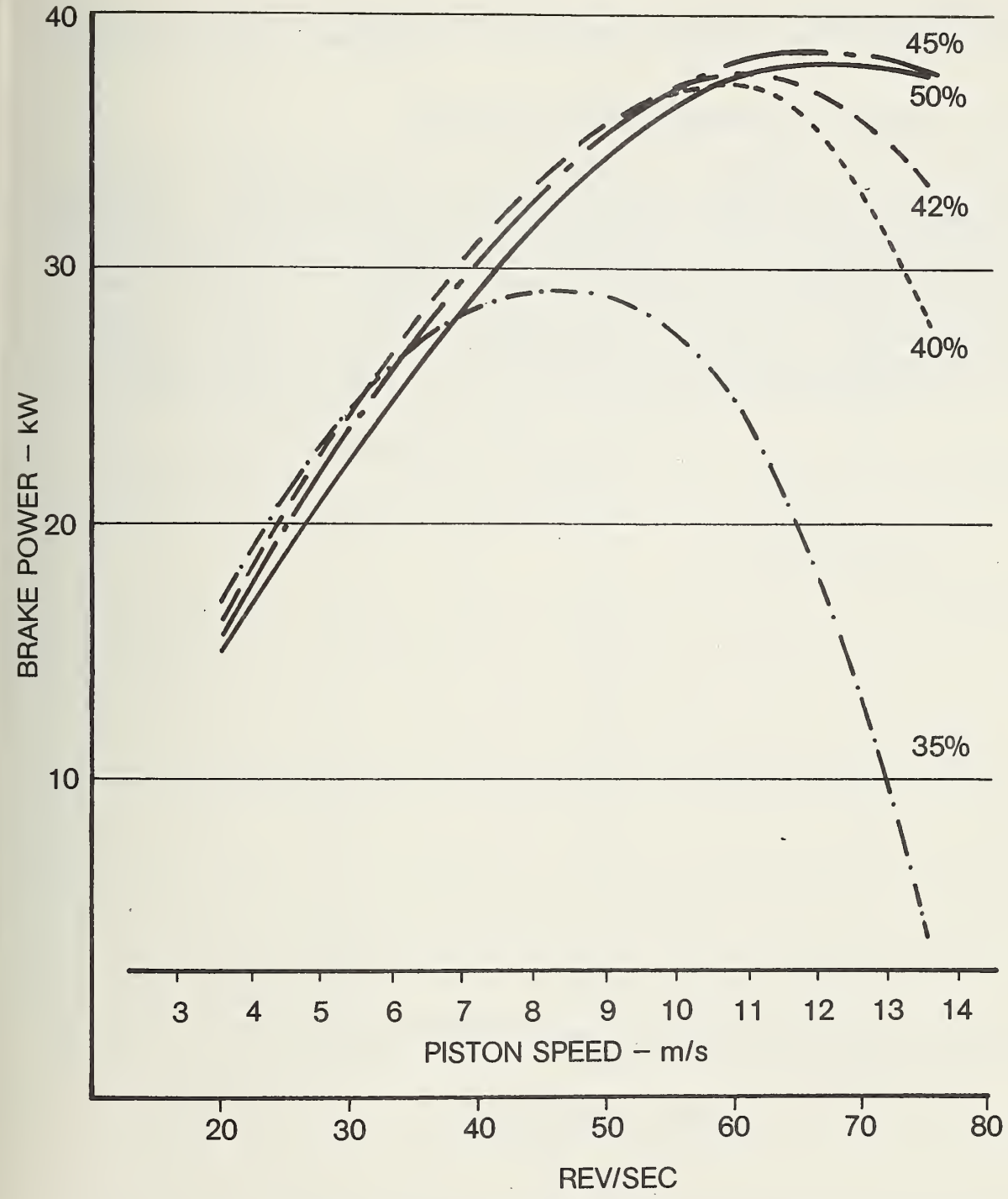

FIGURE 4.5-11: THEORETICAL EFFECT OF INTAKE VALVE SIZE ON PERFORMANCE OF A SWIRL CHAMBER ENGINE

85 ø x 90
Valve size shown as percentage of bore size

a large valve diameter because the length and the diameter of the intake pipe exert significantly stronger effects on the performance characteristics.

4.5.5 Control of Compression Ratio Variation

The control of compression ratio variation due to tolerance stack-up becomes easier as the stroke increases as shown in Figure 4.5-11. The effect of stroke/bore ratio is shown in Figure 4.5-12. With a constant swept volume and compression ratio (Case a), the possible variation in the compression ratio becomes worse and the stroke/bore ratio decreases. A constant stroke and compression ratio (Case b) with a varying bore does not cause changes in tolerance build-up. A variance in the compression ratio in order to adjust to the increased swept volume reduces the possible swept volume reduces the possible compression ratio along with the decrease in bore/stroke ratio.

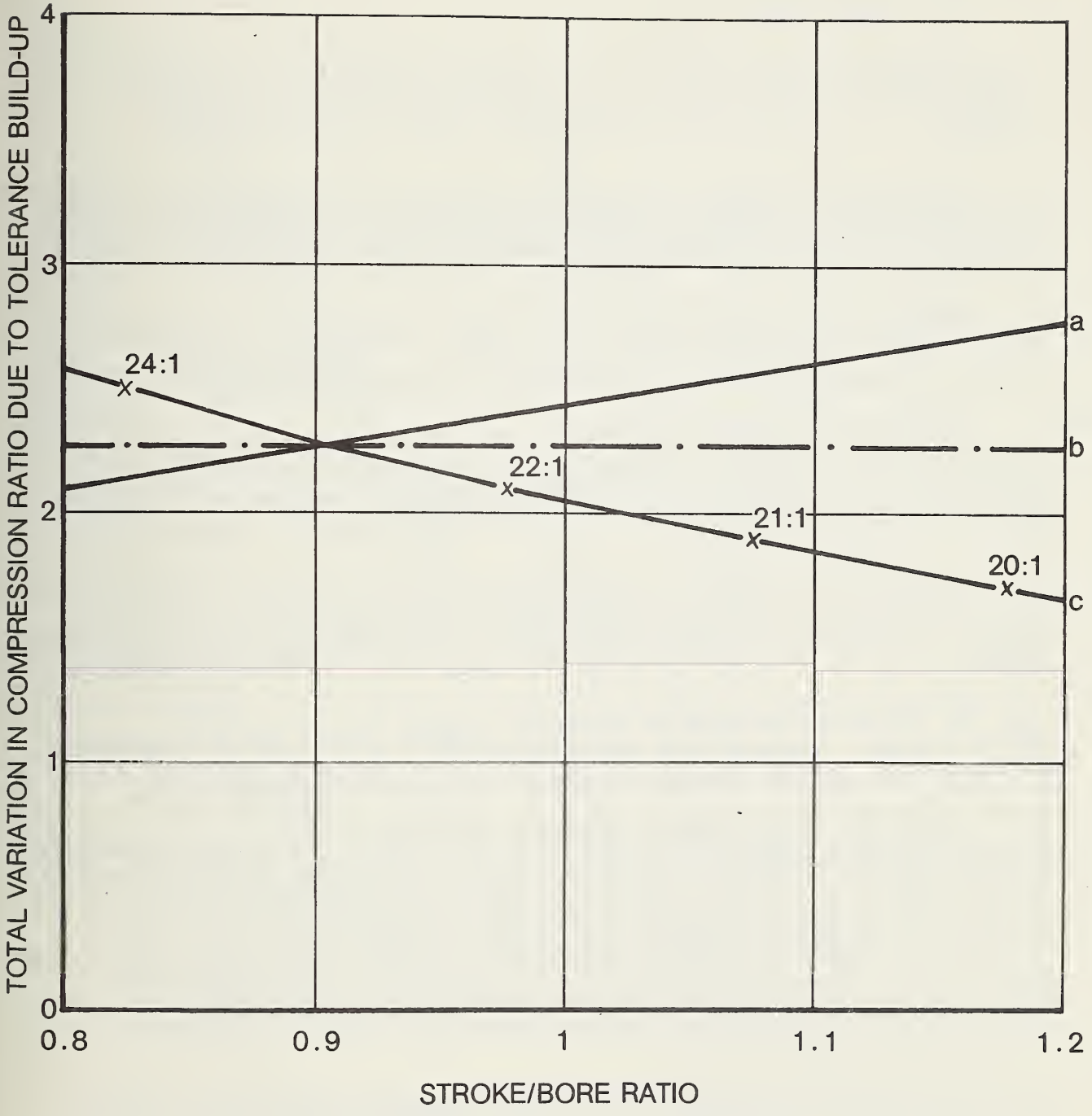

FIGURE 4.5-12: EFFECT OF BORE/STROKE RATIO ON COMPRESSION RATIO VARIATION FOR A 4-CYLINDER COMET V ENGINE UNDER THREE CONDITIONS

1) Constant swept volume (1.59 L) and constant compression ratio (23:1)
2) Constant stroke, constant CR, bore changing
3) Constant stroke, compression ratio changing to suit change in swept volume

4.6 ENGINE FAMILY

The project task called for a diesel engine family for light- and medium-weight passenger cars in the inertia-weight class of 1,750 to 3,000 lbs. with a powerplant output range from 37 to 73.5 kW (50 to 100 HP).

Preliminary investigations showed that the cost of production and parts inventory could be lowered by using a modular-system concept which would provide for some interchangeable components in diesel and spark-ignition engines.

The optimum cylinder unit size for small, high-speed passenger car diesel engines is in the range of 350 to 450 cc. This range yields a high specific output (kW/liter) at a favorable specific engine weight in kg/liter.

Engine configurations with 4-, 5-, 6-, and 8-cylinders with the above displacement are required in order to cover the target output range from almost 37 to 73.5 kW almost completely, as shown in Figure 4.4-1. This objective can also be achieved with naturally-aspirated and turbocharged 4- and 6-cylinder engines.

The torsion resistance of the crankshaft decreases as the number of cylinders rises, and thus limits the number of cylinders in an in-line engine to six. Five- and 6-cylinder crankshafts can be controlled only with torsion dampers.

The 90^{o} V-configuration of an engine suggests itself for an 8-cylinder engine concept. Compared with the opposed-piston design and the 180^{o} V-configuration, the 90^{o} concept results in a taller but narrower engine.

A family of in-line diesel engines offers distinct production advantages. The same internal components, such as valves, pistons, and connecting rods can be used, and the line facilities can be adapted to accommodate units with varying numbers of cylinders. New castings are required for the cylinder block, cylinder head, crankshaft and camshaft for each number of cylinders. The design characteristics and especially the cylinder bank configuration make in-line engines particularly well suited for an engine family. V-engines may pose production problems, particularly where the facilities are laid out for in-line engines.

The investigations were conducted on Volkswagen diesel engine concepts with two different bore dimensions and three different strokes.

The combination of these two factors led to five different cylinder-unit displacements in the range from 367.7 cc to 436.8 cc. The combination of these displacements and engines with 4-, 5-, 6-, and 8-cylinders results in 20 engines in the total displacement range from 1.5 through 3.5 liters (Table 4.6-1) in an output range of 37 to 80 kW (50 - 108 HP).

Four engines cover the output range from 37 to 73.5 kW (50 - 100 HP). Two engine families were selected to accomplish this purpose. Figure 4.6-1 shows the output that can be provided by engines with cylinder-unit displacements from 367.7 to 436.8 cc. Family A includes naturally-aspirated engines

BORE	mm	76.5	76.5	79.5	79.5	79.5
STROKE	mm	80	86.4	80	86.4	88
STROKE/BORE RATIO	-	1.05	1.13	1.01	1.09	1.11
CONNECTING ROD RATIO L/R	-	3.4	3.2	3.4	3.2	3.09
CYLINDER VOLUME	cm^3	367.7	397.1	397.1	428.9	436.8
4-CYLINDER	Swept Volume (cm^3) / Power (DIN) (kW)	1471 36.8	1588 40	1588 40	1716 42.5	1747 43
5-CYLINDER		1839 44.4	1986 47.7	1986 47.7	2145 51	2184 51.5
6-CYLINDER		2206 54.5	2383 58	2383 58	2573 62.3	2621 63
8-CYLINDER		2942 68	3177 73.5	3177 73.5	3431 78.6	3494 80

TABLE 4.6-1: VOLKSWAGEN DIESEL ENGINE FAMILY - ENGINE SIZE RANGE

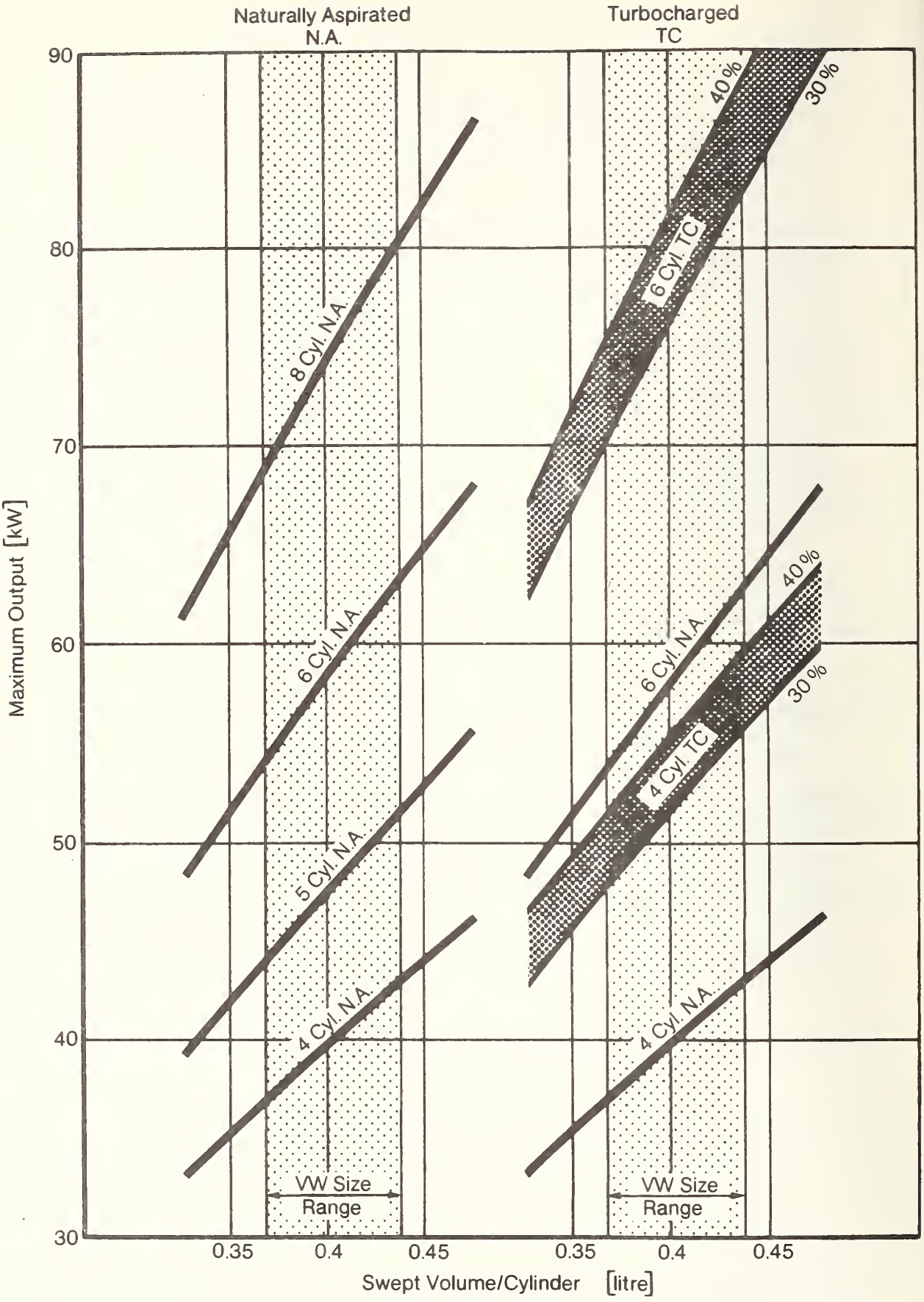

FIGURE 4.6-1: PERFORMANCE OF ENGINE FAMILIES

only. Family B includes two naturally-aspirated engines and their tubocharged variances. The turbocharged engines were d-signed for a 30 to 40% increase in power and thus reach the upper limit for swirl chamber engines without charged-air cooling.

The output of the engines in one family should form a geometric progression with a factor of approximately 1.25. Four engines in the range from 37 through 73.5 kW result in a factor of 1.26 with the selected cylinder-unit dimensions.

Table 4.6-2 shows the displacement and output data of the naturally-aspirated engine family. Table 4.6-3 shows the output grouping of the family consisting of naturally-aspirated and turbocharged engines. The increase in output from one engine to the next substatially deviates at times from the target value of 26%.

The output data of the B Family shows the maximum possible values which can be achieved by the turbocharged versions. Changes in turbocharger system design may lead to an increase in the bmep in the lower rpm range at the expense of the nominal output. Table 4.6-4 shows the major dimensions of the evaluated engines.

4.6.1 Modular Unit System

The objective was to establish a diesel engine family with varying numbers of cylinders. The modular-unit system should be used in order to permit the production of this engine family at a minimum of cost. The base of the diesel engine family is the present line of production gasoline engines. This product line consists of 4- and 5-cylinder in-line engines.

A large number of interchangeable parts reduces inventory costs. The economically optimal volume of interchangeable parts is determined by the number of parts in the intended modular system. Compliance with the closer diesel tolerances can be ensured at lower cost if parts are selected from a larger number of engine components with the aid of normal distribution.

The acquisition of expensive production equipment frequently is not justifiable in the case of small parts volumes. The application of the modular unit system permits mass production of a large number of parts. This again makes the entire production process more economical.

The major portion of the production cost is incurred for cylinder block and crankcase manufacturing. Minor modifications at some stations may permit the production on the same line of cylinder blocks and crankcase units for engines with different numbers of cylinders.

Major problems, however, are posed by differing cylinder arrangements. Installation problems can be solved by adaptors in those situations where cylinder block and crankcase units are made on the same line for in-line and V-engines. This solution requires an assembly line which is especially designed for this purpose. However, this would pose problems in regard to the production of other engine configurations. Consequently, such a mixed production method should be employed only in special cases and for small unit volumes.

Family A				
Number of Cylinders	4	5	6	8
Stroke S [mm]	80	88	86,4	80
Bore D [mm]	76,5	79,5	79,5	79,5
Swept Volume V_H [ltr.]	1,471	2,184	2,573	3,177
ΔV_H [ltr.]	0,713	0,389	0,604	
ΔV_H [%]	48,5	17,8	23,5	
Power P_e [kW]	37	51,5	62,3	73,5
ΔP_e [kW]	13,5	10,8	11,2	
ΔP_e [%]	36,5	20,9	18	

TABLE 4.6-2: FUNDAMENTAL DATA OF DIESEL ENGINE FAMILY A

Family B				
Number of Cylinders	4		6	
Naturally Aspirated NA Turbocharged TC	NA	TC	NA	TC
Stroke S [mm]	80		86,4	
Bore D [mm]	76,5		76,5	
Swept Volume V_H [ltr.]	1,471		2,383	
Power P_e [kW]	37	51,5	58	78
ΔP_e [kW]	14,5	6,5	20	
ΔP_e [%]	39,2	12,6	34,5	

TABLE 4.6-3: FUNDAMENTAL DATA OF DIESEL ENGINE FAMILY B

Volkswagen Diesel Engine Family							
Engine Type	Major Dimensions [mm]						Weight [kg]
	Cylinder-Block			Engine overall			
	Length	Width	Hight	Length	Width	Hight	
I4-NA	378	336	278	514	555	700	126
I4-TC	378	336	278	514	572	645	133
I5	475	369,4	282	680	490	780	170
I6-NA	563	369,4	278	780	490	780	184
I6-TC	563	369,4	278	780	638	800	193
V8	385	410	265	610	750	685	200

TABLE 4.6-4: MAJOR DIMENSIONS OF THE EVALUATED DIESEL ENGINES

It should also be borne in mind that the distance between cylinders in in-line engines is determined by the bore diameter and by the location of the bearings and side walls on the crankshaft in V-engines. This results in larger water spaces between the cylinders. The compactness of the in-line engine is realized by long-stroke design characteristics and that of the V-engine by short-stroke characteristics. A combination within one family is practical only if the design of the crankshaft drive reduces the distance between cylinders in the V-engine to that of the in-line engine. In those cases, V-8 engine cylinder heads require only minor modifications so that they can be used in the 4-cylinder in-line engine.

The cost of amortization and labor become less significant when the production volume exceeds 1,500 units per day. This is the production volume where the cost of material is the predominant factor that affects the cost of production. It should be determined, therefore, whether interchangeable parts should be used or whether the optimum solution is presented by two different of optimum design for the particular application. This is illustrated by the fact that the significance of a standard connecting rod frequently is over-rated. The fact that some engines in the engine family may require a stronger piston pin does not mean that all the other engines, too, should be equipped with the same pin. The excess dimension can be accepted only if the low production volume of these engines does not justify a special connecting rod.

The consistent application of the modular unit system permits the standardization of the following parts:

Piston with pin and rings
Connecting rod with bearing bushes
Main bearing bushes and caps
Crankshaft sealing flanges, front and rear
Valves with springs and plates
Valve seat rings
Valve guides
Tappets (or rocker levers)
Swirl chamber inserts
Injection nozzles
Glow plugs
Toothed-belt drive with pulleys
Water pump bearing and drive unit
Oil pump drive components.

4.6.2 Comparison of the Engine Families

37 kW Engine

The only reasonable solution was felt to be a 4-cylinder naturally-aspirated engine. An engine with fewer cylinders would not offer the necessary comfort because of its higher degree of irregularity. A design providing for more than 4-cylinders would increase the cost of production, internal friction and fuel consumption, engine unit weight and length. The current VW production engine reflects the present state-of-the-art.

46 kW Engine

This required output can be accomplished with a 5-cylinder naturally-aspirated or turbocharged 4-cylinder engine. Both of the selected engines for this application permit a nominal output of 51.5 kW at different rpm's (Figure 4.6-2).

The decrease of the cylinder unit dimensions to 76.5 mm bore and 86.4 mm stroke can lower the 5-cylinder engine output to 48 kW (see Table 4.6-1). The turbocharged design can be used to vary the output characteristics of the turbocharged engine.

The output versus engine rpm (see Figure 4.6-2) shows that the 5-cylinder curve matches the curve of the turbocharged 4-cylinder unit. Both engines have the same maximum output. This means that these engine configurations used in one vehicle produce the same vehicle velocity. The engine with the smaller nominal rpm needs a longer gear ratio. When the engine characteristics are plotted versus the vehicle velocity in fourth gear, the output of the turbocharged engine is higher than that of the 5-cylinder engine starting with an rpm of approximately 1,300. At the same time, there may be a more favorable fuel consumption in the 5-cylinder engine at speeds higher than approximately 3,000 rpm.

The turbocharged 4-cylinder engine (Table 4.6-4) offers advantages in regard to the total dimensions as well as to the engine length. This is significant for the vehicle crash behavior.

58 kW Engine

A 6-cylinder naturally-aspirated engine was selected in both families for this output group. The required output, however, could also be obtained with a turbocharged 4-cylinder engine of 1.747 liters displacement or with a turbocharged 5-cylinder engine of 1.839 liters displacement.

73.5 kW Engine

This performance group again includes a turbocharged engine and a naturally-aspirated unit with higher displacement and a greater number of cylinders (Figure 4.6-3). The turbocharged 6-cylinder engine has a higher output capacity. This becomes even more pronounced when the different nominal rpm's are taken into consideration. The 8-cylinder engine may then be competitive in full-load fuel economy at engine speeds higher than 3,000 rpm.

Another advantage of the V-8 engine is the more compact design. While it is only slightly wider than the 6-cylinder in-line engine, it is markedly shorter and flatter. The 6-cylinder engine could be made more compact by a V-configuration of the cylinder block. This, however, would affect the good mass balance as well as the cost of production. Weight advantages are offered by the turbocharged 6-cylinder engine (see Table 4.6-4).

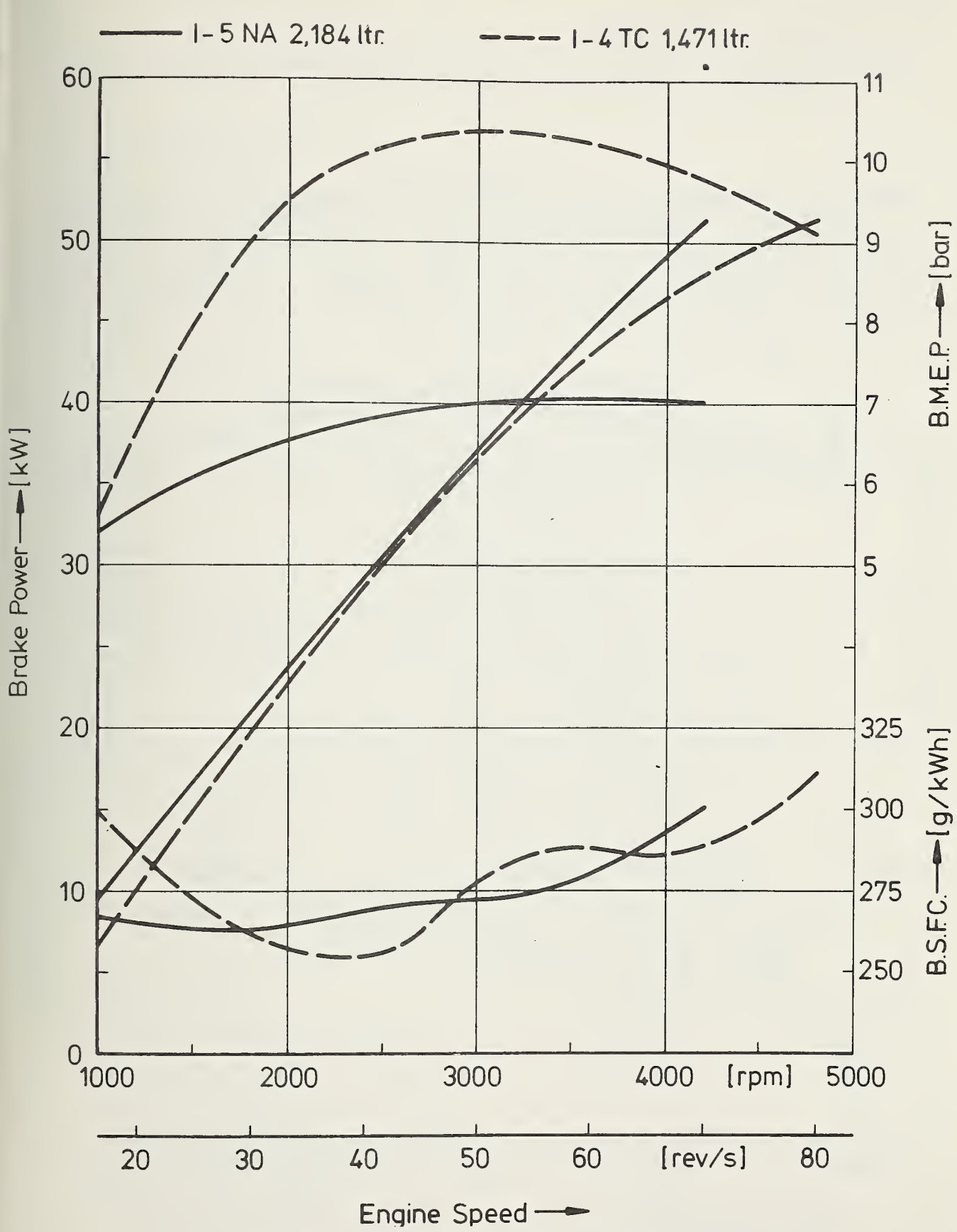

FIGURE 4.6-2: COMPARISON BETWEEN AN INLINE-5 NATURALLY-ASPIRATED AND AN INLINE-4 TURBOCHARGED DIESEL ENGINE

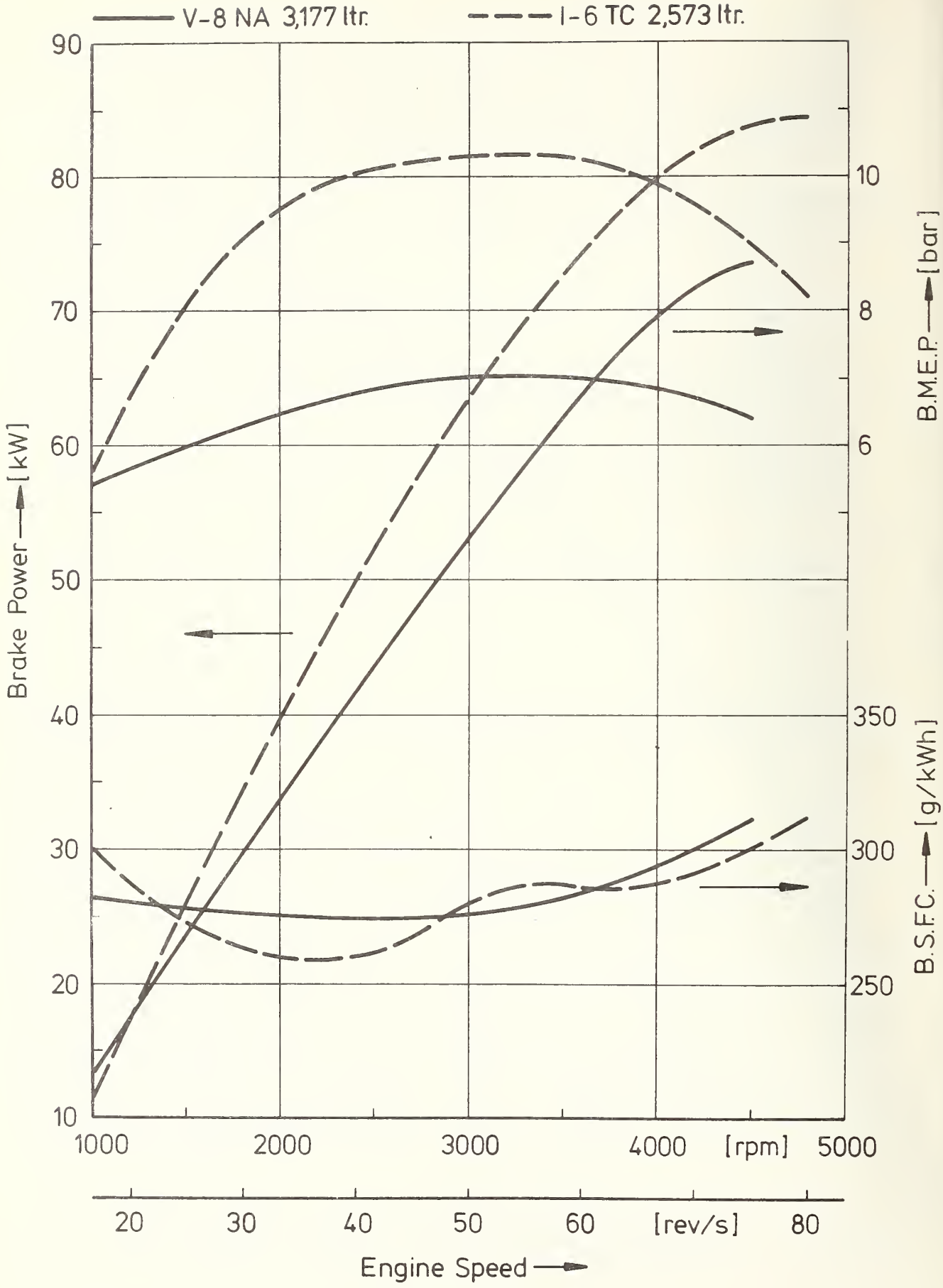

FIGURE 4.6-3: COMPARISON BETWEEN A V8 NATURALLY-ASPIRATED AND AN INLINE-6 TURBOCHARGED DIESEL ENGINE

5. DESCRIPTION OF THE ENGINE/VEHICLE SYSTEMS UNDER INVESTIGATION

5.1 DIESEL ENGINES

This section describes two diesel engine families that were established on the basis of two technologies, i.e. displacement variations and turbo-charging. The investigations on performance ranges were conducted on engines based on the current 1.5-liter 4-cylinder Volkswagen production diesel engine. Each of the two engine families consists of four engines that are intended to cover the output range from 37 to 73.5 kW (50 - 100 HP).

5.1.1 The 4-Cylinder Naturally-Aspirated Engine

The design base of the 4-cylinder diesel engine (Figures 5.1-1 through 5.1-7) is the 1.5-liter gasoline engine, which is presently used in various Volkswagen and Audi models. A reference description of the base engine is provided in

5.1.1.1 Technical Data, 4-Cylinder NA Diesel Engine

Four-Cylinder In-Line Engine

Swept volume	1.471 l
Bore	76.5 mm
Stroke	80 mm
Stroke/Bore Ratio	1.05
Cylinder Volume	367.7 cm^3
Compression Ratio	23
Firing Sequence	1 - 3 - 4 - 2
Power (DIN)	37 kW (50 BHP)
Rated Speed	5,000 min^{-1}
Specific Power Output	25 kW/l (34 BHP/l)
Maximum Torque	82.4 Nm (8.4 kpm)
at Max. Mean Effective Pressure	7.7 bar
Mean Piston Velocity at Rated Speed	13.3 m/s
Weight (including clutch, intake- and exhaust manifold, airfilter, oil, generator; excluding cooling system, coolant, starter motor)	125 kg
Weight-to-Horsepower Ratio	3.3 kg/kW (2.4 kg/BHP)
Length, Width, Height	514 x 555 x 700 mm
Power-to-Volume Ratio	185.3 kW/m^3 (250.4 BHP/m^3)
Oil Capacity	3.5 l

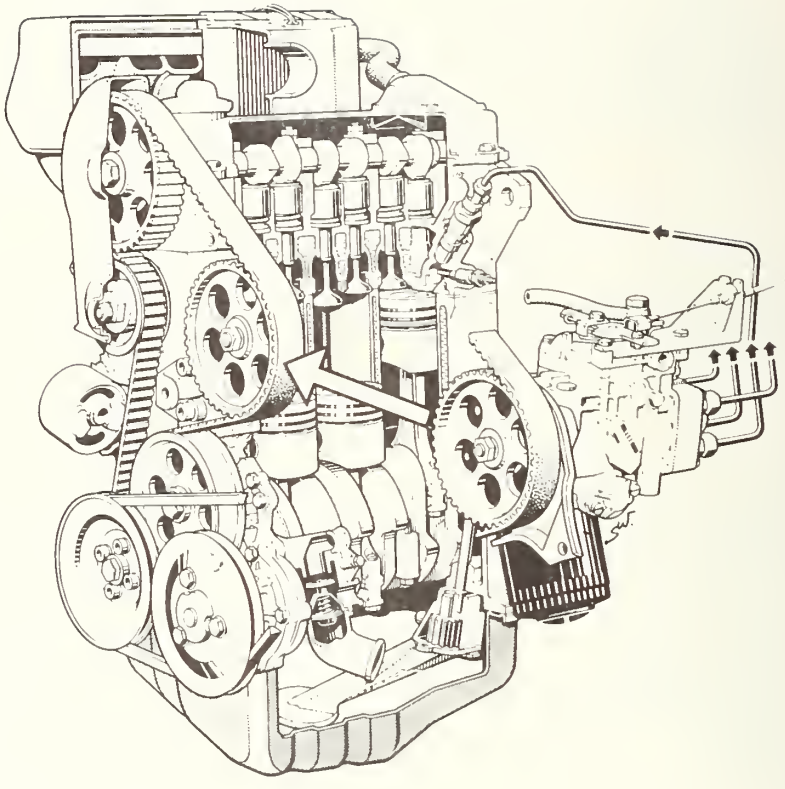

FIGURE 5.1-1: VOLKSWAGEN 1.5-LITER DIESEL ENGINE

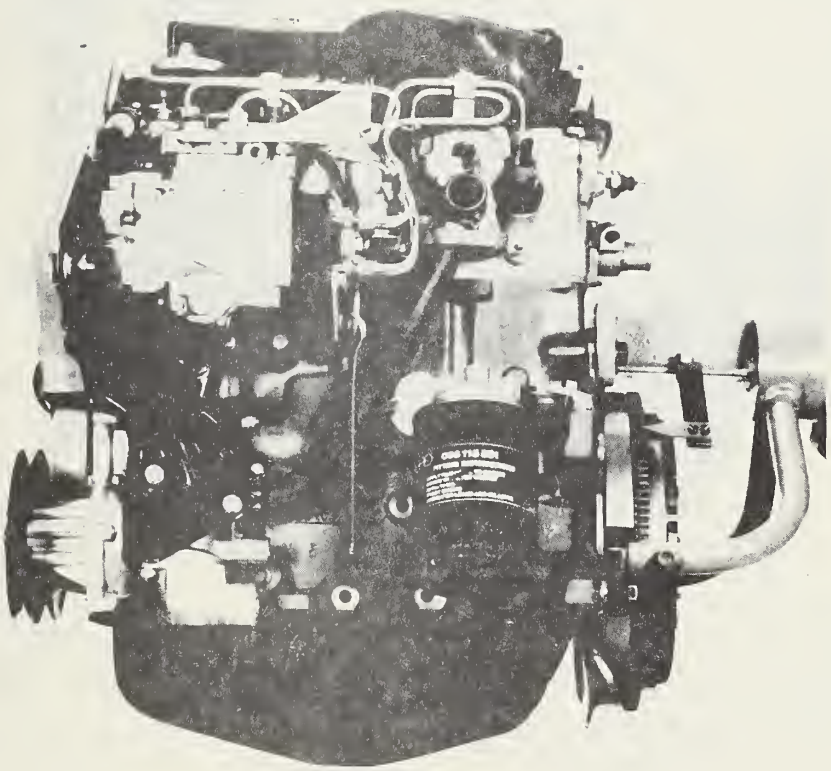

FIGURE 5.1-2: 4-CYLINDER NATURALLY-ASPIRATED ENGINE SIDE VIEW - INJECTION PUMP

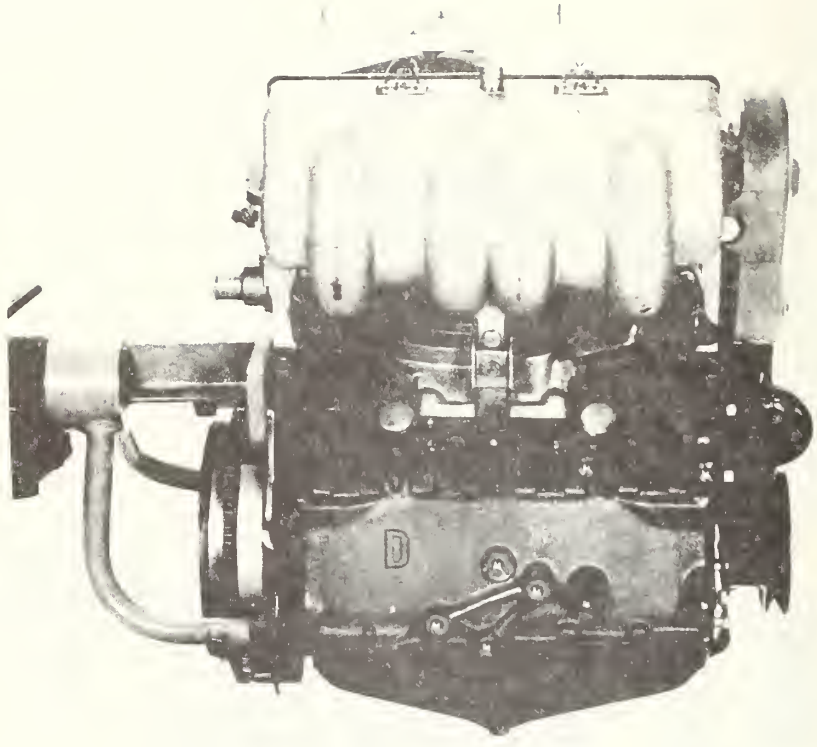

FIGURE 5.1-3: 4-CYLINDER NATURALLY-ASPIRATED DIESEL ENGINE SIDE VIEW - INLET MANIFOLD

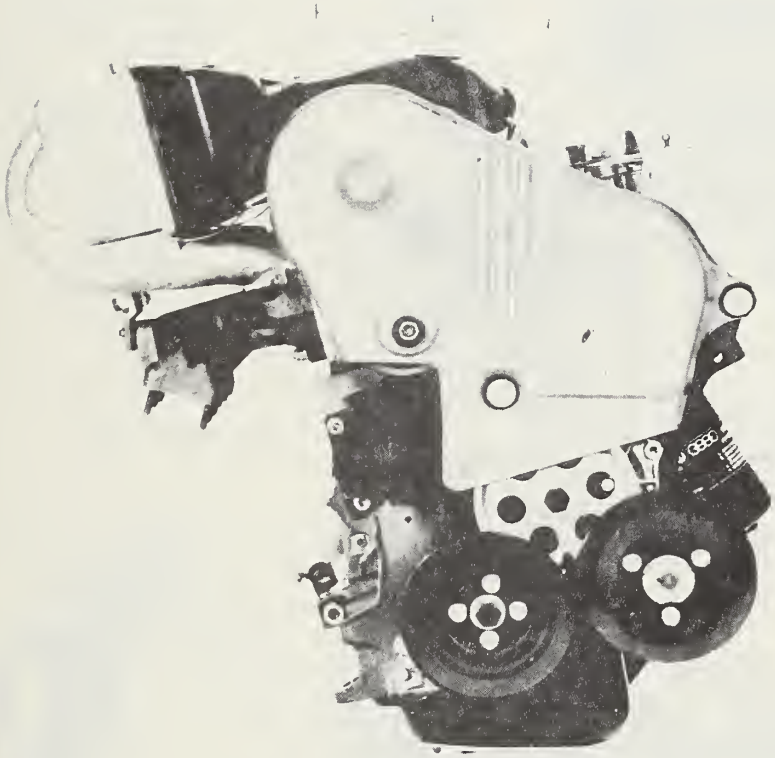

FIGURE 5.1-4: 4-CYLINDER NATURALLY-ASPIRATED DIESEL ENGINE
FRONT VIEW

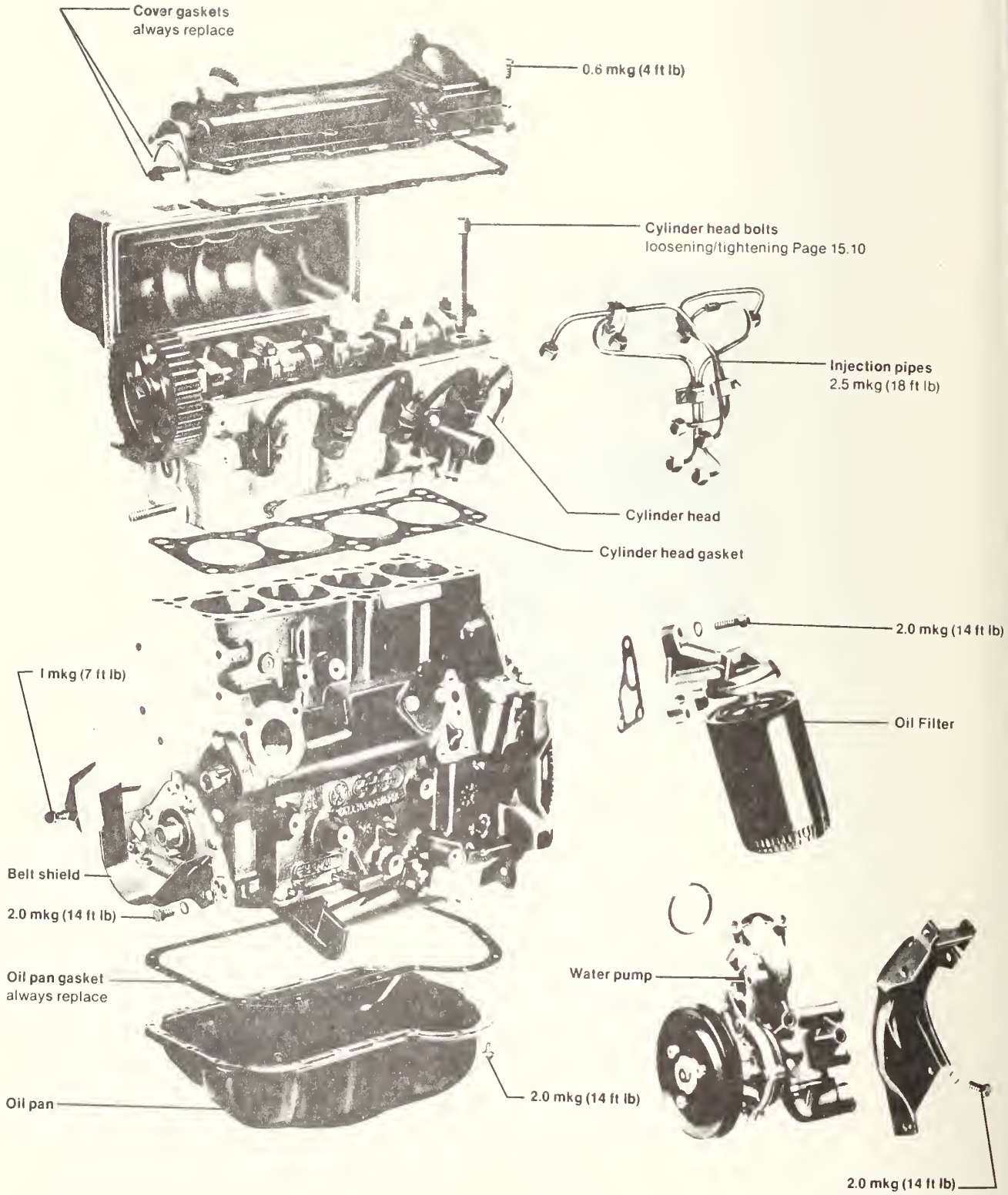

FIGURE 5.1-5: 4-CYLINDER NATURALLY-ASPIRATED ENGINE - EXPLOSION VIEW

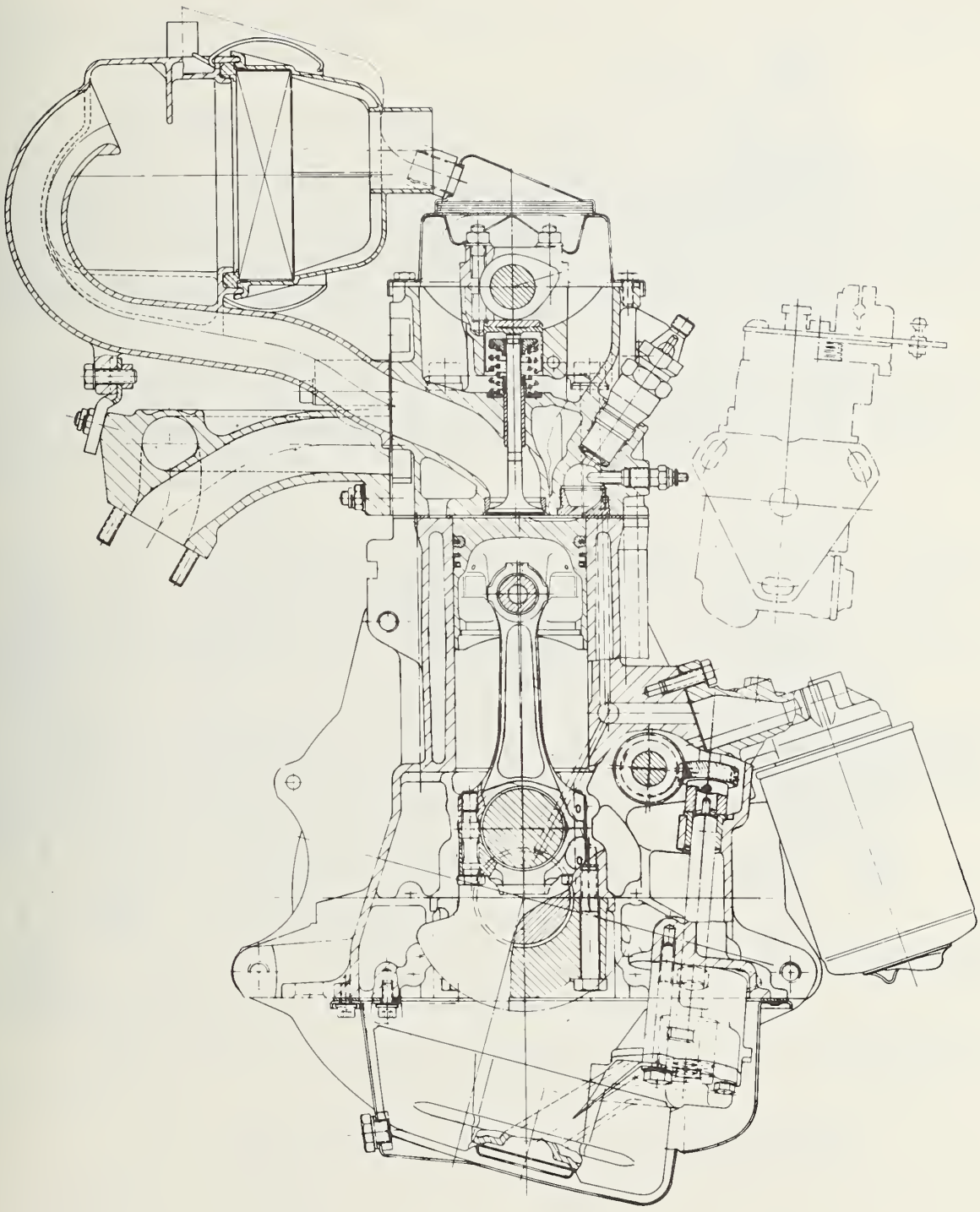

FIGURE 5.1-6: CROSS SECTION OF VW 1.5-L ENGINE

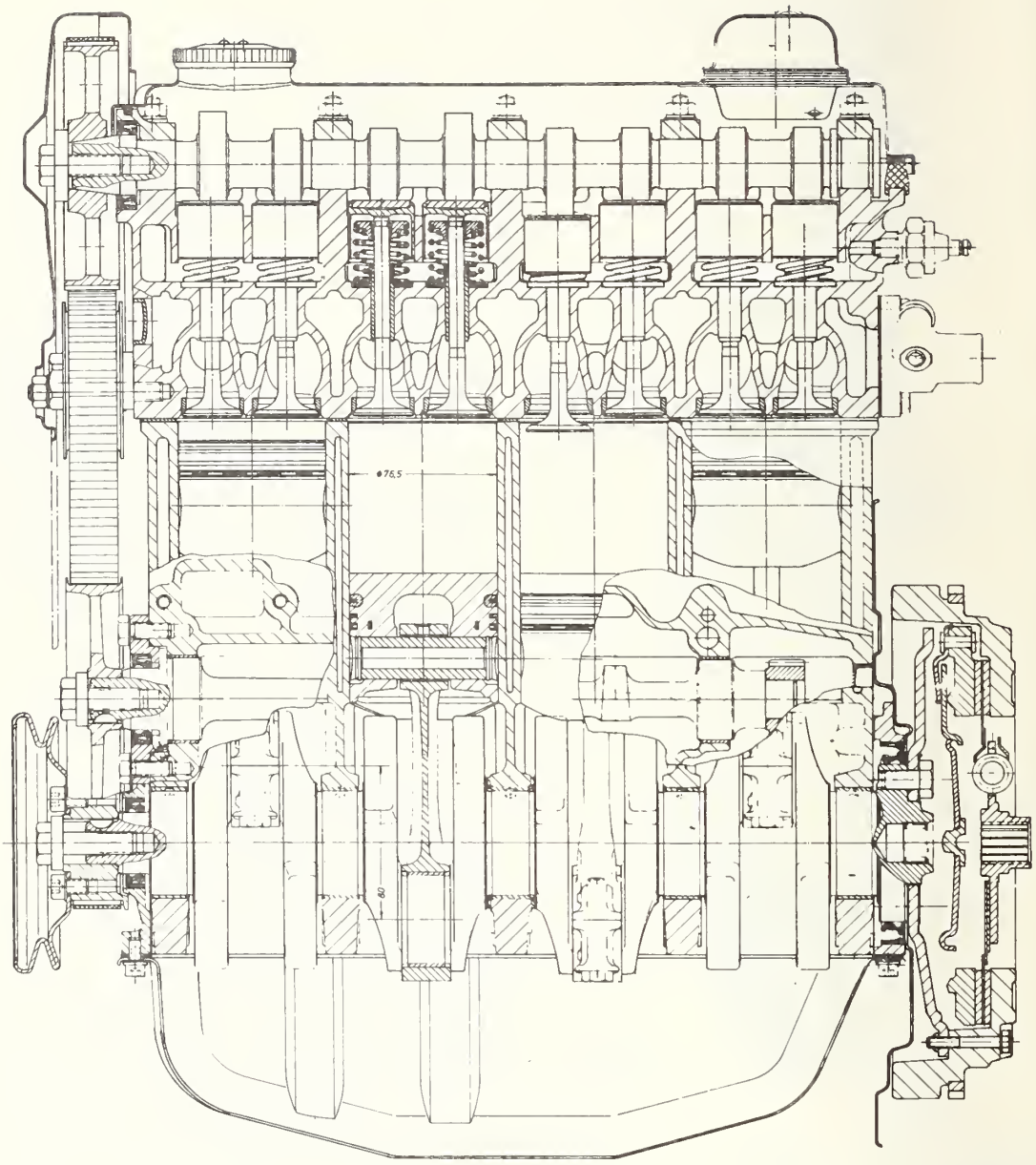

FIGURE 5.1-7: LONGITUDINAL SECTION OF THE 1.5-L ENGINE

5.1.1.2 Crankcase and Crankshaft Drive

The crankcase and crankshaft (Figure 5.1-8) drive are exposed to gas and mass forces and to vibrations.

5.1.1.2.1 Stresses and Dimensions

There are no significant differences between the mechanical stresses in this diesel engine and in the gasoline engine. The maximum ignition pressures are approximately the same. The statistical scatter of the peak pressure of the individual cycles in the gasoline engine is approximately three times as much as that in the diesel engine. The peak pressures of the gasoline engine occur at maximum efficiency where they reach 75 bar.

The mass forces at maximum rpm are higher in the gasoline engine because of the higher engine speed despite small oscillating mass of the gasoline engine. Therefore, the mechanical stress results in the same drivetrain dimentions for small, high-speed diesel engines. The results of the endurance test confirmed these findings.

The thermal stress on those components that confine the combustion chamber in the diesel engine exceed that in the gasoline engine. In order to limit the thermal effects, care should be taken to ensure sufficient heat transfer. The particularly endangered zones (piston head, cylinder head, valve bridge, and head gasket) require component reinforcements and design modifications.

The Volkswagen diesel engine design did not require any changes to the crankshaft, connecting rods and bearings. The cylinder block and crankcase and the piston pins of the gasoline engine required only minor modifications. The piston was redesigned for diesel operation.

5.1.1.2.2 Crankshaft

The forged crankshaft has eight counter-weights to reduce bending stresses. This configuration balances 38% of (m_{rot}* + 1/2 m_{OSZ}**). A 100% balance would lead to an unnecessary increase of the powerplant weight.

The crankshaft is supported by 5 bearings. The bearing dimensions are as follows:

	Main Bearing	Connecting Rod Bearing
Diameter	54 mm	46 mm
Width	18.5 mm	19 mm

*m_{rot} = rotating masses
**m_{OSZ} = oscillating masses

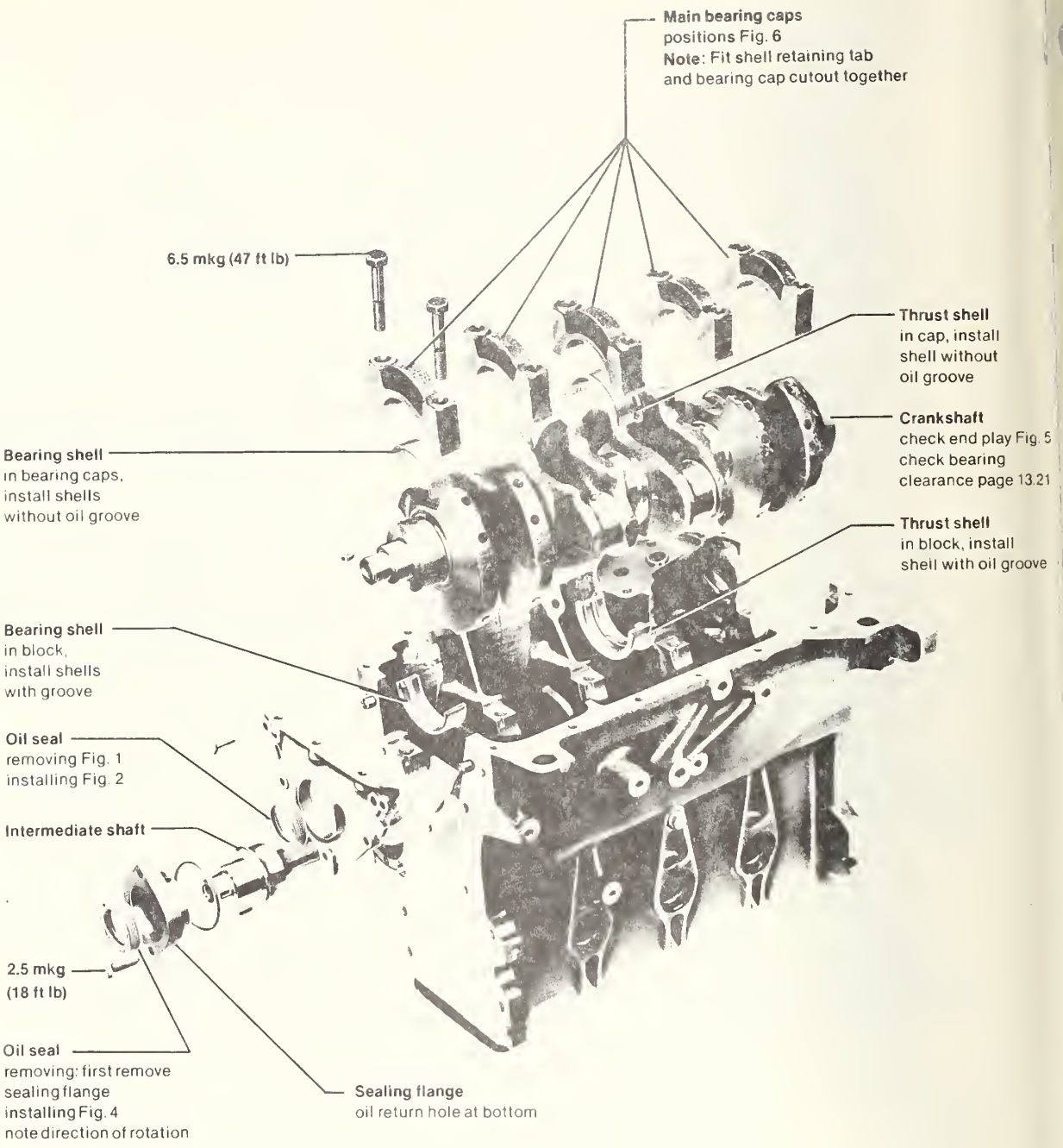

FIGURE 5.1-8: CYLINDER BLOCK AND CRANKCASE WITH CRANKSHAFT, BEARING SHELLS, MAIN BEARING CAPS, INTERMITTENT SHAFT, FRONT FLANGES (EXPLODED VIEW).

5.1.1.2.3 Connecting Rod

The connecting rod is drop-forged of heat-treated steel and has a distance between bosses of 136 mm. It is a standard component element used in the Volkswagen gasoline and diesel engine production. The connecting rod ratio $\lambda = 4/1 = 0.294$.

5.1.1.2.4 Piston

The thickness of the piston top land in the diesel engine was increased from 8.3 mm (gasoline engine) to 13.5 mm in order to permit realization of the high compression and to provide protection of the top piston ring from the higher thermal loads in the diesel engine. The exterior diameter of the piston pin is 22 mm and equals that in the gasoline engine. The interior diameter was reduced from 15 mm to 11 mm.

The following piston requirements were to be met:

- Long service life

- Low noise

- Uniform low oil consumption, minimal blow-by, no seizure.

Recent developments in high-speed diesel engine pistons have shown that service life greatly depends on the wear of the upper ring and groove. Under favorable conditions, single-metal pistons may have a useful life of up to 100,000 km. These pistons, though, cannot be used for heavy duty applications, nor do they have a longer service life. Ring-carrier pistons wear much more slowly because they are equipped with cast-in Ni-Resist ring carriers with punched-in upper groove.

These carriers also reduce wear on the piston ring flanks. An Alfin process is used to fuse ring carrier and piston. Details may be seen from Figures 5.1-9.

Comparison tests of ring-carrier and standard pistons confirmed the above findings. Figure 5.1-10 shows the wear measured in the course of endurance tests at the upper rings groove. Rings and grooves of standard pistons will wear about 0.1 mm after only 500 or 1,000 hours bench tests. The wear of ring-carrier pistons amounted to approximatley 12 micron at the upper and lower flank of the upper groove after 1,500 hours (see Figure 5.1-11). Axial ring wear, in this case, amounted to about 25 micron. Roughness-height measurements have shown the wear on the piston skirt to amount to a diameter reduction of about 20 micron (Figure 5.1-12).

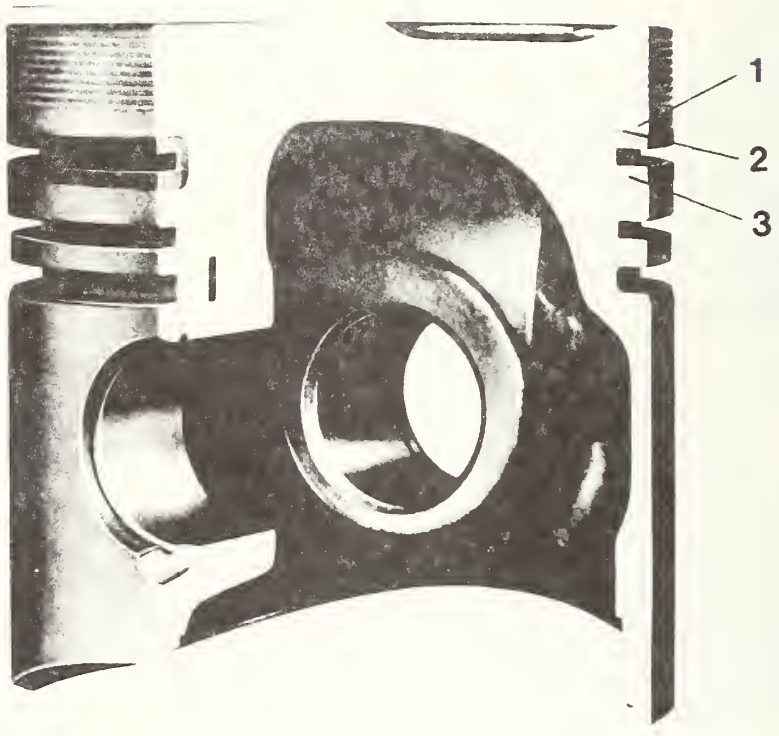

FIGURE 5.1-9: AUTOTHERMATIK PISTON WITH RING CARRIER

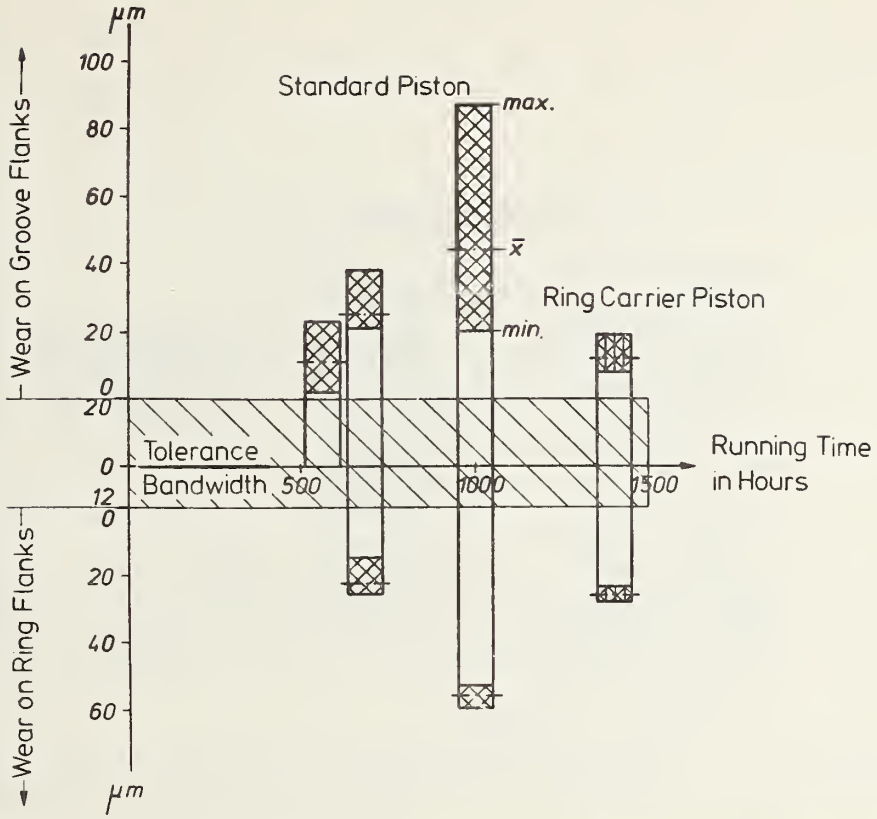

FIGURE 5.1-10: AXIAL UPPER GROOVE AND RING WEAR IN STANDARD AND RING CARRIER PISTONS

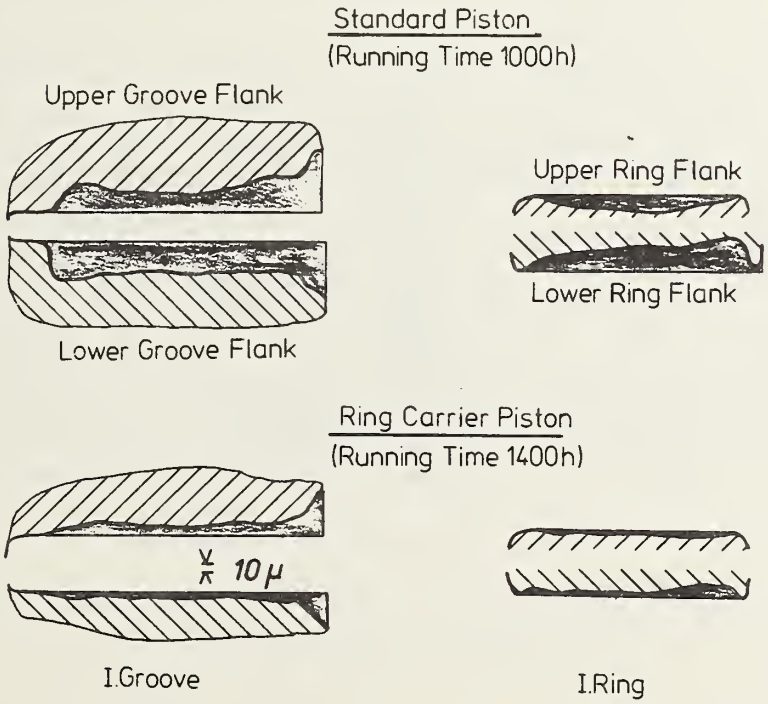

FIGURE 5.1-11: WEAR OF GROOVES AND RING FLANKS

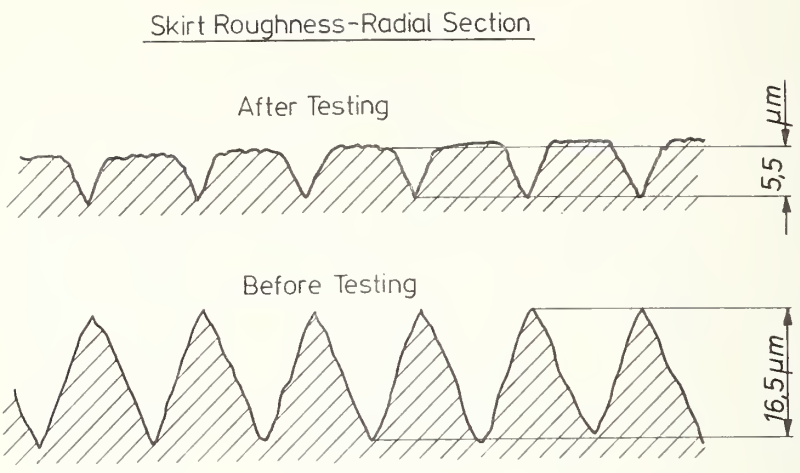

FIGURE 5.1-12: PISTON SKIRT ROUGHNESS BEFORE AND AFTER TESTING

Noise level reduction was achieved by specially developed steel-strutted pistons with low clearance and favorable deformation behavior.

Figure 5.1-13 shows piston expansion under heat. The effect of the strut reaction to pressure in the skirt ($a_K = 16.10^{-6}$) is such that more than 50% of the expansions caused by heat build-up in the piston and cylinder is eliminated. Therefore, the engine will work with very little play through its entire load range. The clearance of smooth-skirted pistons is designed for maximum power only, so that it exceeds the one which is actually required by a cold engine at partial-load operation. Figure 5.1-14 shows the contours of the piston together with some installation clearances at various levels. The broken line in the region of the skirt indicates the clearance required by smooth-skirted pistons. Skirt deformation is one of the major factors that affect the long-term behavior and service life of a piston. A skirt must be sufficiently resilient to accept deformation forces caused by load and temperature variations. However, to ensure a low risk of seizure a cerain certain amount of stiffness is needed to avoid plastic skirt deformation.

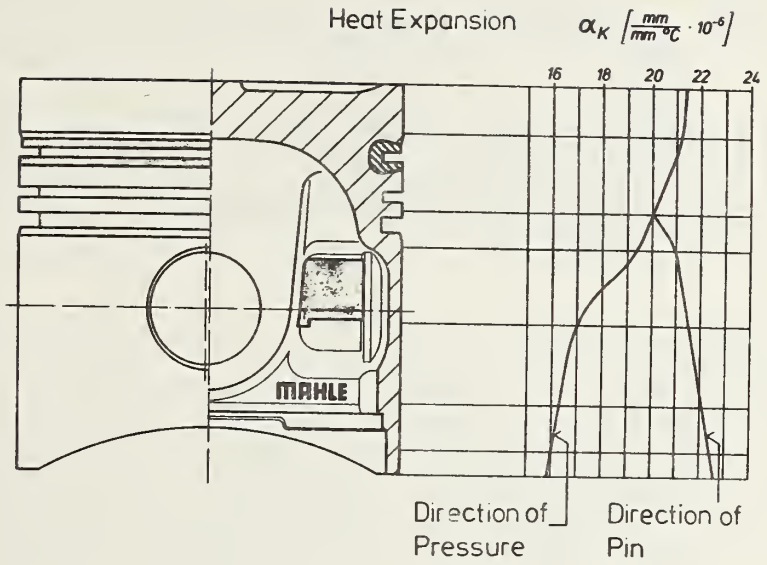

FIGURE 5.1-13: SELF-REGULATING EFFECT OF AUTOTHERMIC PISTON

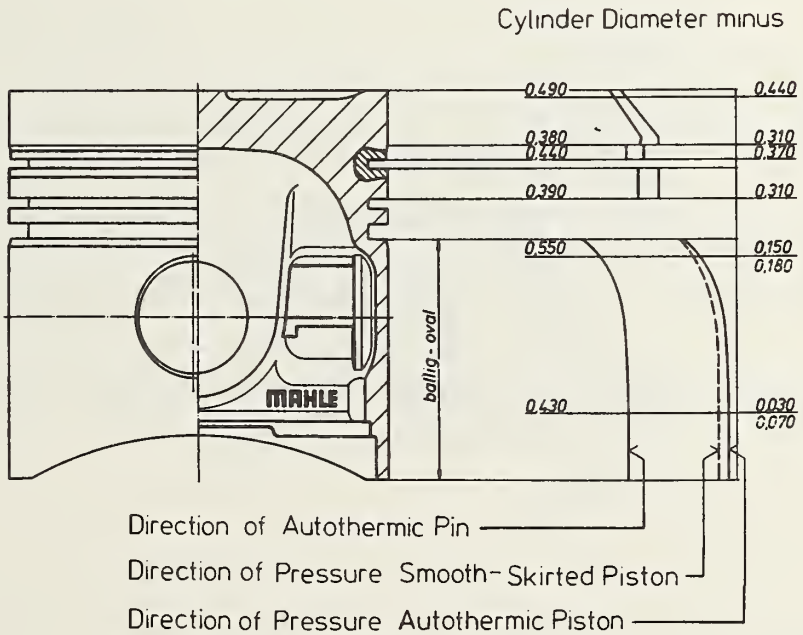

FIGURE 5.1-14: CONFIGURATION, CLEARANCE, AND OVALITY OF AUTOTHERMIC PISTON

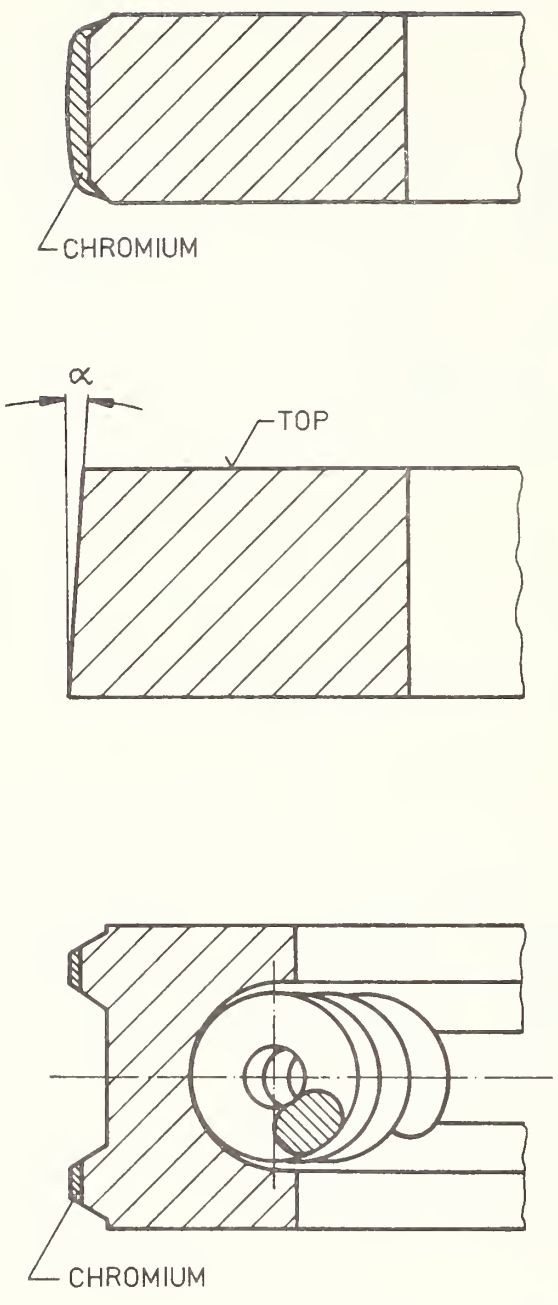

FIGURE 5.1-15: PISTON RING CROSS SECTIONS
The piston is equipped with compression rings and one oil ring.

First groove: Plain compression ring, axial width 1.75 mm, hard chromium-plated and barrel-lapped running surface; ring made from high-strength spheroidal graphite cast-iron, type Goetze KV1. The hard chromium-plated running surface of the ring ensures low wear over a long operating period, and the barrel-lapped running surface provides good compatibility by improving lubrication.

Second groove: Taper-faced compression ring axial width 2.0 mm. Taper angle of the running surface a = 45' $\pm$ 15', ring entirely phosphated and made from special piston ring cast-iron Goetze K2 standard. The tapered running surface of this ring not only provides adequate gas sealing but also contributes to the control of engine-oil consumption.

Third groove: Bevelled spring-loaded oil ring, axial width 3.0 mm, hard chromium-plated and profile-ground contact lands; ring made from special piston ring cast-iron Goetze K1 standard. The narrow axial width and small cross section make this ring very flexible. The coil-type expander spring ensures good conformability and effective oil scraping action. The hard chromium-plated contact lands are highly wear-resistant. Their narrow width, which is obtained by using small machining tolerances, as well as their defined shape, which is obtained by profile grining, are maintained during long running periods.

This design of pistons and piston rings leads to the average oil consumption of 0.5 g/PSh, whereas blow-by amounts to 0.4 - 0.5% of the theoretical air throughput.

5.1.1.3 Cylinder Block

The cast-iron cylinder block extends by 58 mm below the crankcase center to provide for high strength (Figure 5.1-16). The minimum wall thickness is 4 mm because of casting limitations.

In order to ensure the long service life generally expected of diesel engines we decided to use the 1.5-liter cylinder block. The 76.5 mm bore allows the flow of coolant between the cylinder bores, and the distance between the bores is sufficient to ensure long cylinder head gasket life.

An 88-mm cylinder spacing leaves a water gap of approximately 3.5 mm between the cylinders. The ratio between cylinder distance and cylinder bore is 1.1.

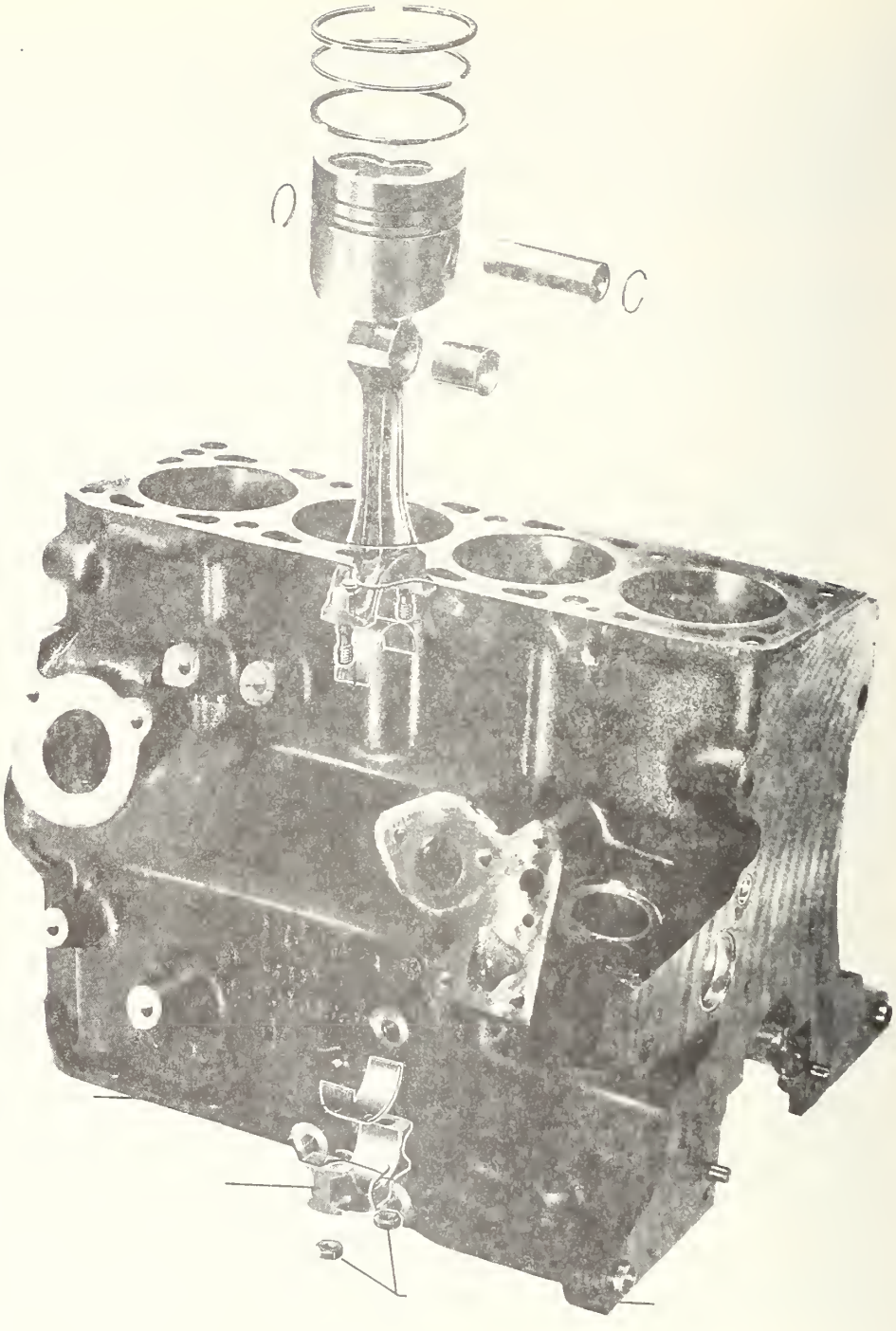

FIGURE 5.1-16: CYLINDER BLOCK

5.1.1.4 Cylinder Head

The cylinder head is a permanent-mold aluminum alloy casting. It is very stiff because of its 133 mm height (Figures 5.1-17 and 5.1-18). The basic gasoline engine cylinder head has intake and exhaust ports on the same side. It was found to be highly suitable for conversion to diesel operation. The opposite side of the cylinder head provides adequate space for the swirl chamber. The injection nozzles are arranged at the same angle ($34^{o}30"$) as the gasoline engine spark plugs. It was possible to minimize the gasoline engine transfer line modifications required for the production of the diesel heads.

The thickness of the cylinder head at the sealing surface was increased from 8 mm to 10 mm, and the water ports in the cylinder head were adapted to satisfy the spcific diesel engine requirements. The cylinder blocks and crankcases for gasoline and diesel engines are processed on the same line.

5.1.1.4.1 Cylinder Head Cooling

The diesel engine is exposed to higher thermal loads than gasoline engines. Therefore, clearly defined measures had to be taken to provide for heat transfer from specially critical zones, such as the combustion chamber and the space between valves. The cooling water from the cylinder block and crankcase unit enters the cylinder head from the bottom through calibrated ports for accurately controlled water distribution. Approximately 75% of the water volume is directed to the swirl chamber by ribs between the inlet and ports in the casting (Figure 5.1-19).

It was not found necessary to provide for water flow around the injection nozzles. The lateral water outlet had to be moved from the front to the rear for the diesel engine because this space is taken up by the injection pump (Figure 5.1-17).

5.1.1.4.2 Valve Drive

The valves are arranged in parallel (Figure 5.1-6). They are 6.1 mm longer than those of the gasoline engine. The diameter of the intake valve is 34 mm, and that of the exhaust valve 31 mm. The distance between valves is 38.5 mm, and the space between valve seats is 4.5 mm. The valves are closed by 2 concentric valve springs each. The tangential forces of the cams are accommodated by valve tappets.

The valve clearance is adjusted by washers of various thicknesses between cam and tappet. The clearance is 0.25 mm for the intake and 0.40 mm for the exhaust valve in cold engines. Low oil consumption is provided by valve shaft seals.

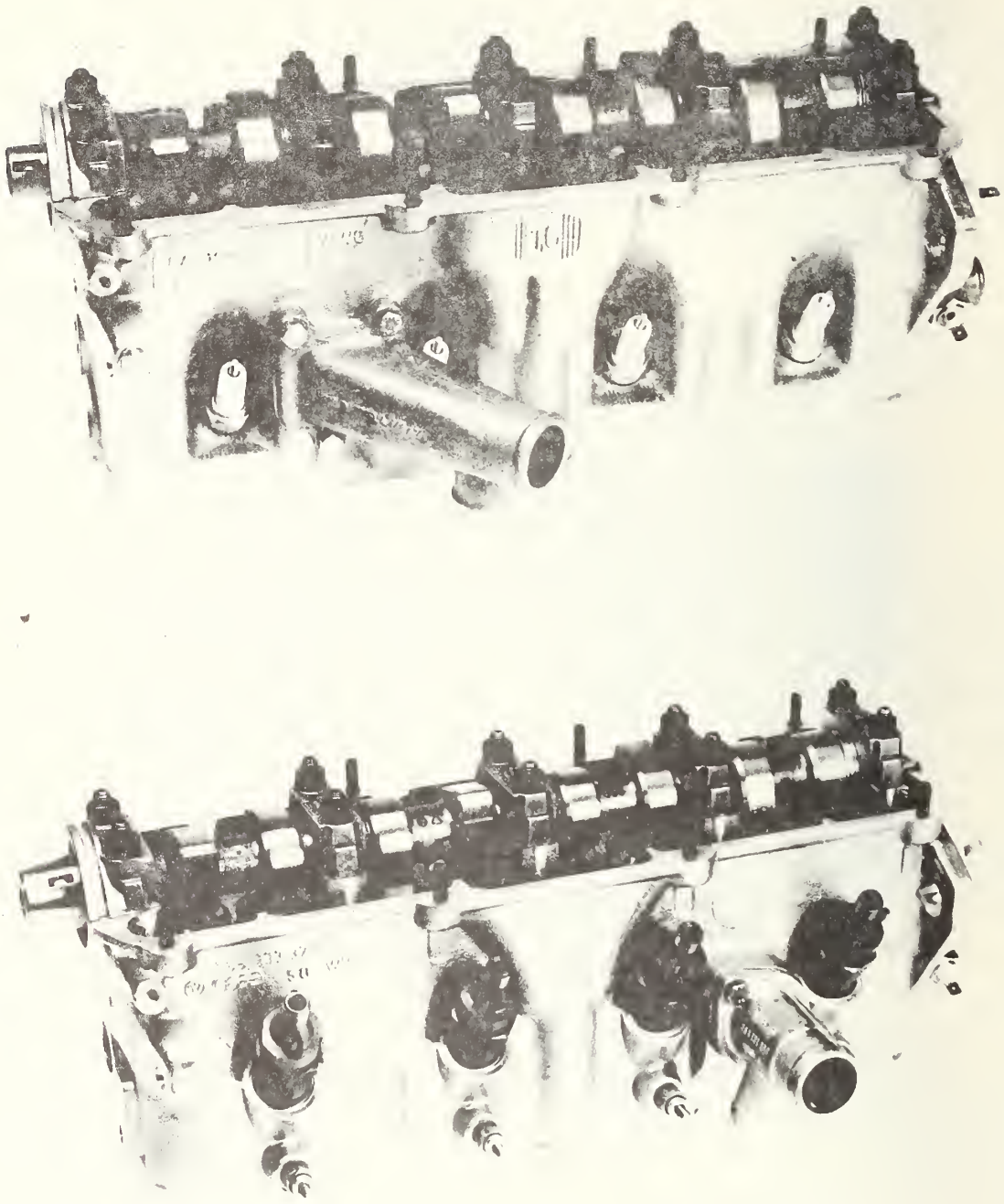

FIGURE 5.1-17: DIESEL AND SPARK-IGNITION ENGINE CYLINDER HEAD

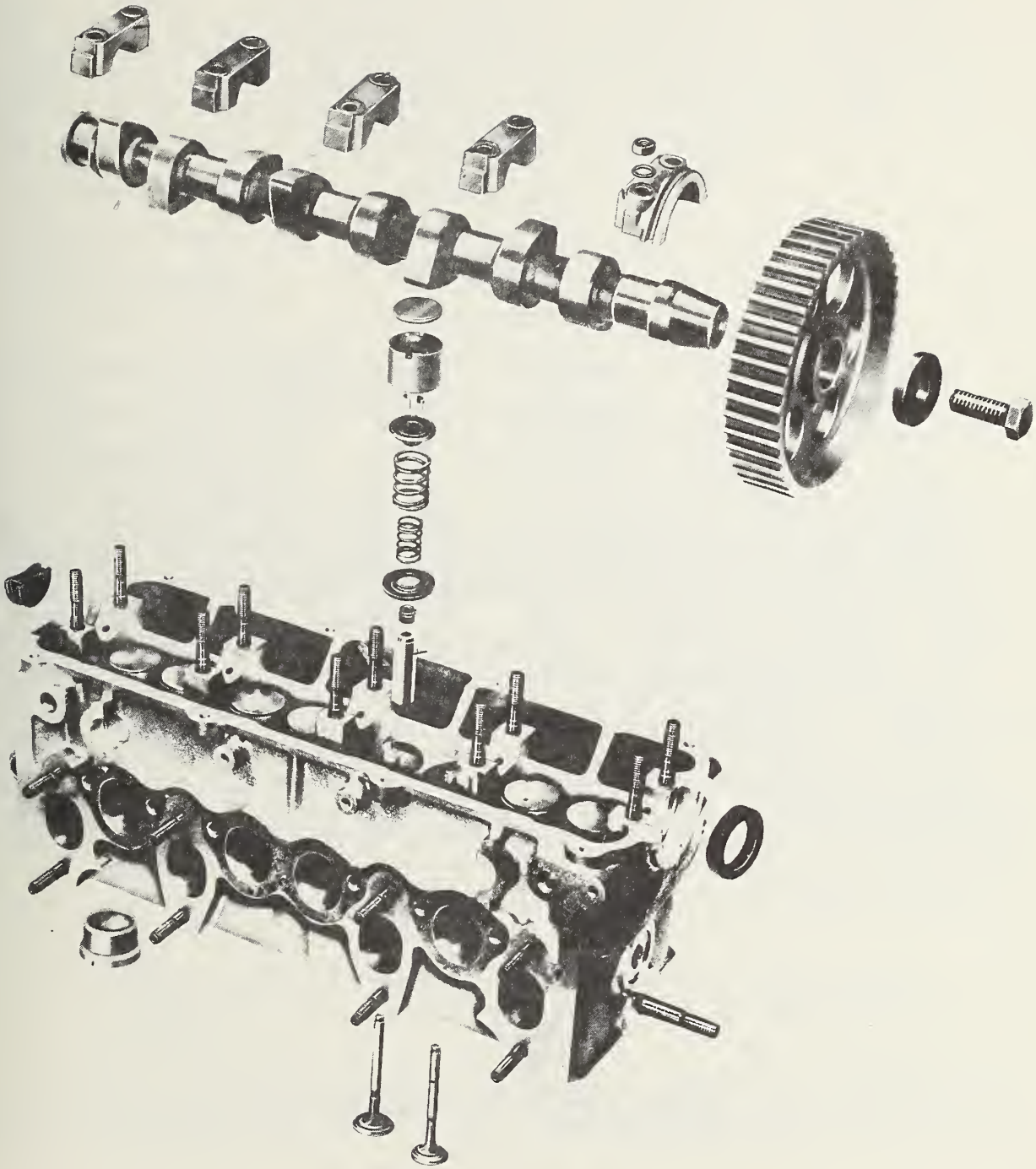

FIGURE 5.1-18: 4-CYLINDER DIESEL CYLINDER HEAD

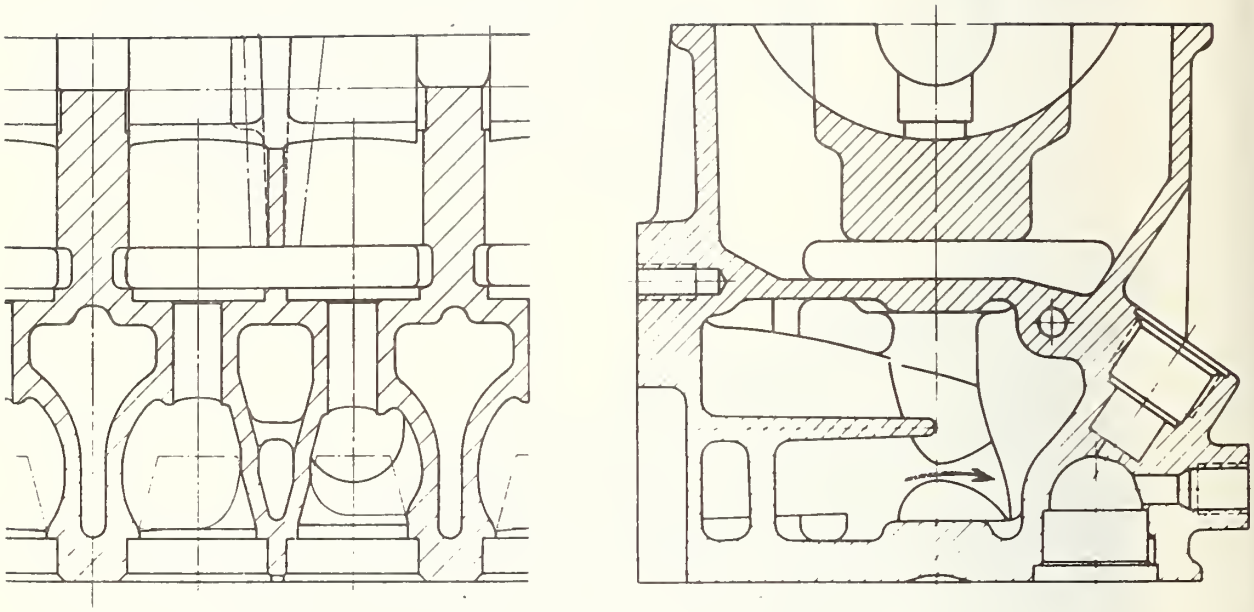

FIGURE 5.1-19: PARTIAL LONGITUDINAL AND CROSS SECTION OF THE CYLINDER HEAD

The chilled cast-iron camshaft runs in five split aluminum bearings without bushings. The cams are displaced by 1.5 mm from the valve and tappet center in the longitudinal direction of the engine. This provides a rotatory pulse to the valves during each stroke and thus substantially improves valve sealing during component life. The cams have a base radius of 19 mm. The intake cam has a stroke of 8 mm and the exhaust cam 9 mm. Valve timing at 1 mm valve clearance is as follows:

- Intake opens 5^{o} after TDC
- Intake closes 14^{o} after BDC
- Exhaust opens 27^{o} before BDC
- Exhaust closes 5^{o} before TDC

- Intake opening angle 189^{o} crank angle
- Exhaust opening angle 202^{o} crank angle
- Cam spread 205^{o} crank angle

The valve lift curves are shown in Figure 5.1-20. The valves in the gasoline engine with its combustion chamber configuration were set back so that there is no contact between them and the piston in top dead center position when the valves are fully opened.

Developing the charge cycle of low-capacity high-speed passenger car diesel engines is always governed by the following three objectives:

(1) High volumetric efficiency at full rated speeds (83 r/s = 5,000 rpm) to guarantee the desired power output (50 BHP = 37 KW),

(2) High final compression temperature at starting speed (2 - 2.5 r/sec = 120 - 150 rpm) and at idle speed (12 - 15.5 r/s = 720 - 930 rpm) to ensure favorable cold-start and warm-up behavior as well as idle noise approximately equal to the standards set by spark-ignition engines

(3) Damping the air intake noise, not a problem in spark-ignition engines, espcially at part load, because of the existence of a throttle.

To comply with these objectives we designed a special air intake system and carefully adjusted the valve timing, especially the intake valve closing time.

Figure 5.1-21 shows the interdependence existing between final compression temperature, intake valve closing time and compression ratio.

In modern passenger car diesel engines the inlet valve closes effectively at 90^{o} after BDC. Advancing this timing by 25^{o} would mean that either compression could be reduced by 6 units or that, with the compression ratio remaining the same, the final compression temperature could be increased by 40^{o} C.

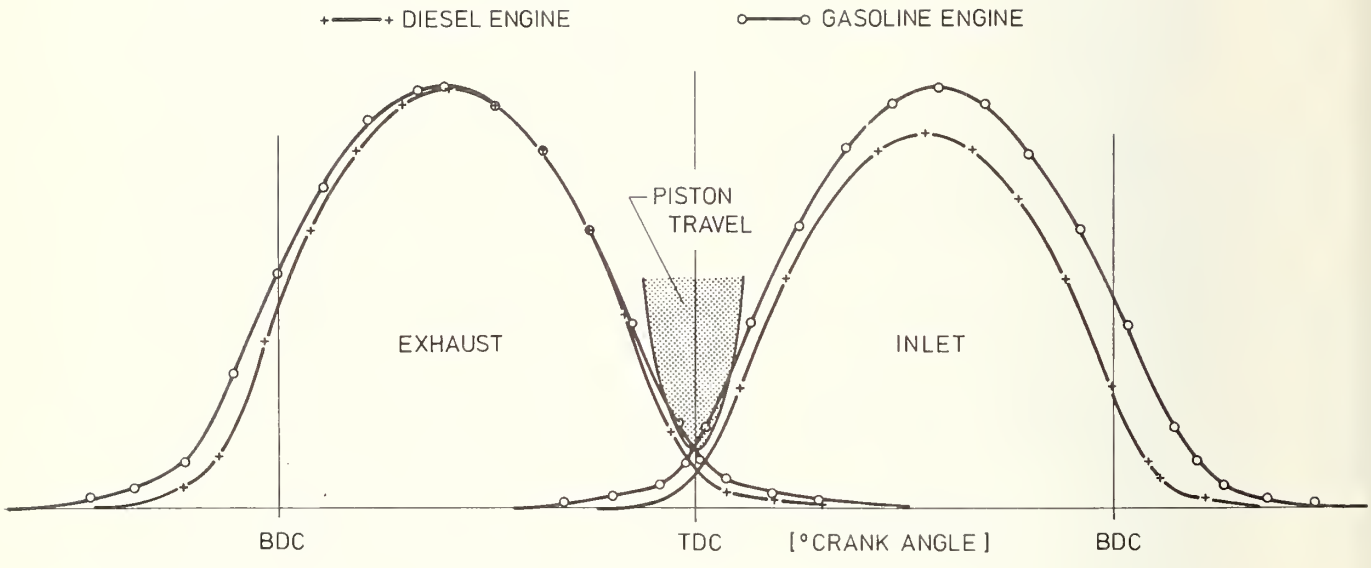

FIGURE 5.1-20: VALVE LIFT CURVE

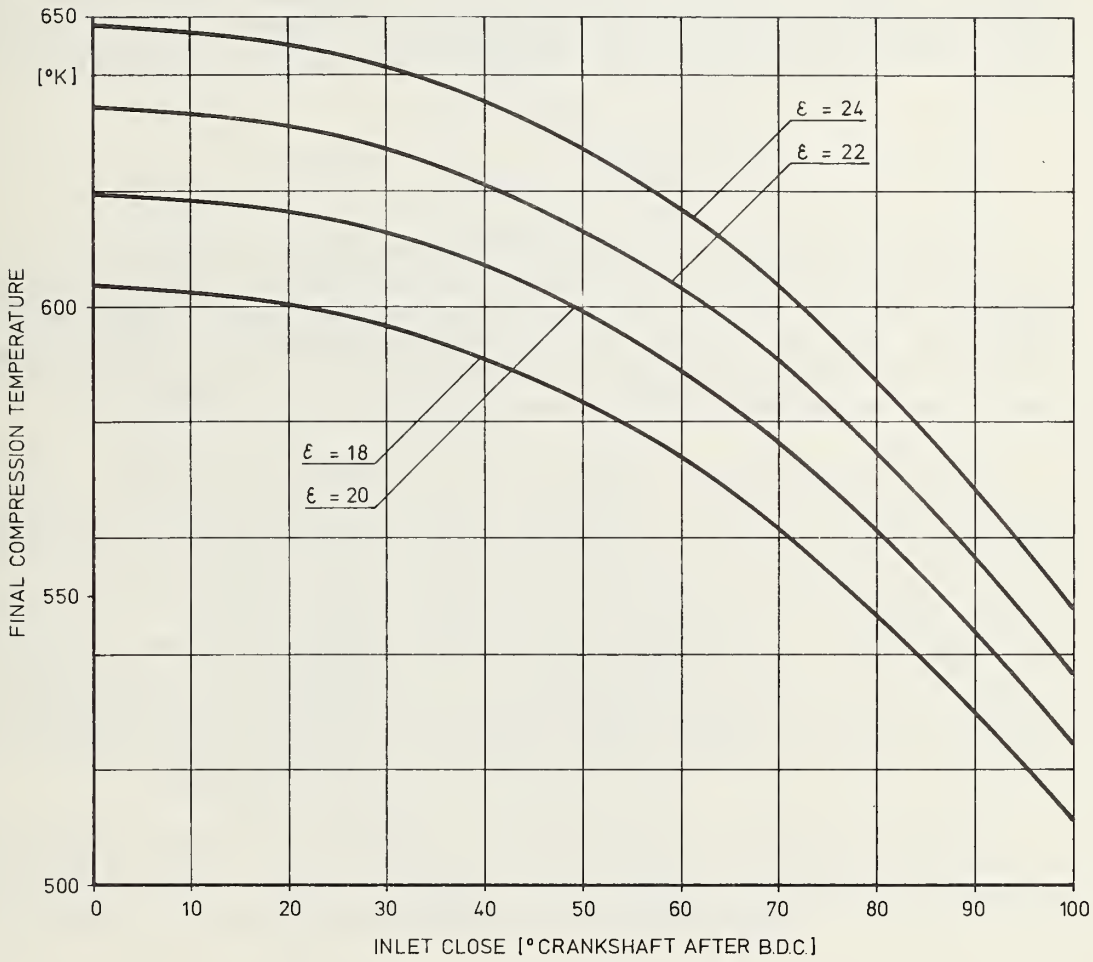

FIGURE 5.1-21: FINAL COMPRESSION TEMPERATURE AS A FUNCTION OF INTAKE VALVE CLOSING TIME, AMBIENT TEMPERATURE 20°C

Therefore, an effort is made to advance the intake valve closing time as much as possible when optimizing the inlet cam geometry for a passenger car diesel engine. On the other hand, airflow at full rated speed must be sufficient to ensure the desired power output. Figure 5.1-20 shows the restrictions imposed by the kinematic conditions of the powerplant. In this low-capacity engine, we minimized the gap between piston and valve so as to be able to use nearly 50% of the dead space for the swirl chamber. For this reason, intake valve lift is limited by piston travel.

This posed a typical trade-off problem: A compromise had to be reached between a short duration cam (as early as possible intake valve closing during starting and idle; and due to kinematic requirements, intake valve opening as late as possible) and long duration cam (to ensure maximum possible power output).

5.1.1.4.3 Cylinder Head Gasket

Three different thicknesses of cylinder head gaskets (1.2, 1.3 and 1.4 mm) are used in the production of the diesel engines. In order to keep close compression ratio tolerances and to ensure that under present production conditions the gap between piston and cylinder head is kept at a minimum while avoiding any contact between valves and pistons. Figure 5.1-22 shows the statistical distribution of compression ratios in production.

Extensive tests were carried out for gasket tightening. The pressure distributions occurring at various tightening torques were determined statistically. These experiments showed that an increase of the tightening torque will improve the static distribution of pressure but will decrease the resistance of the assembly to extreme thermal shocks. The dynamic setting behavior of released gaskets was determined by means of the lead-block method. It was found that with the engine operating, gaskets will set with a variation of 0.03 mm due to differences in measurement locations. Tolerances can be closely adhered to by using gaskets of a thickness compatible with the prevalent degree of piston protrusion.

Proper functioning of the gasket (Figure 5.1-23) was most difficult in the area around the outlet ports (low pressure). This condition was relieved by partially extending the flange.

5.1.1.5 Toothed-Belt Drive

The camshaft, injection pump, and auxiliary shaft are powered by a crankshaft-driven toothed belt (Figure 5.1-24). The advantages offered by this type of drive system are minimal stretching, no lubrication requirements, light weight, durability, compactness, and low noise level. Maintenance is easy and economical.

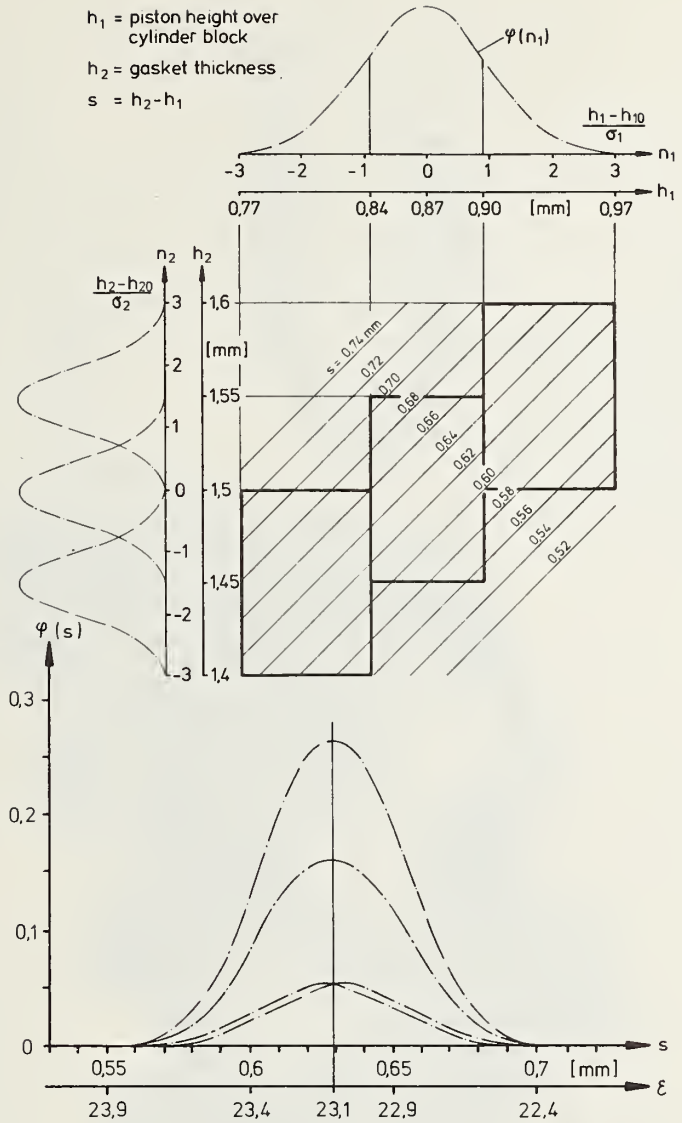

FIGURE 5.1-22: COMPRESSION RATIO DISTRIBUTION CURVE

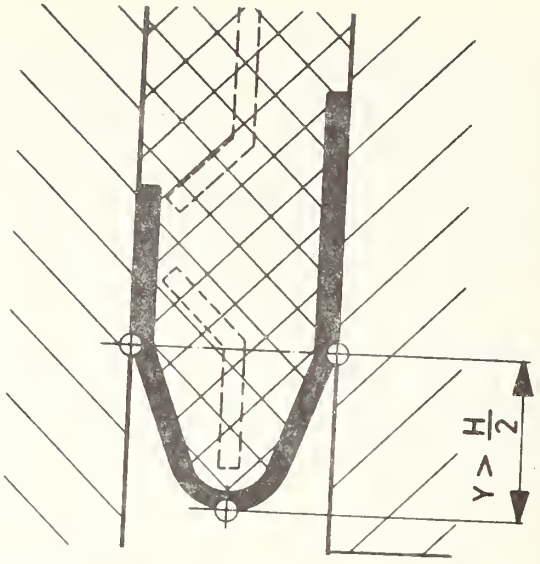

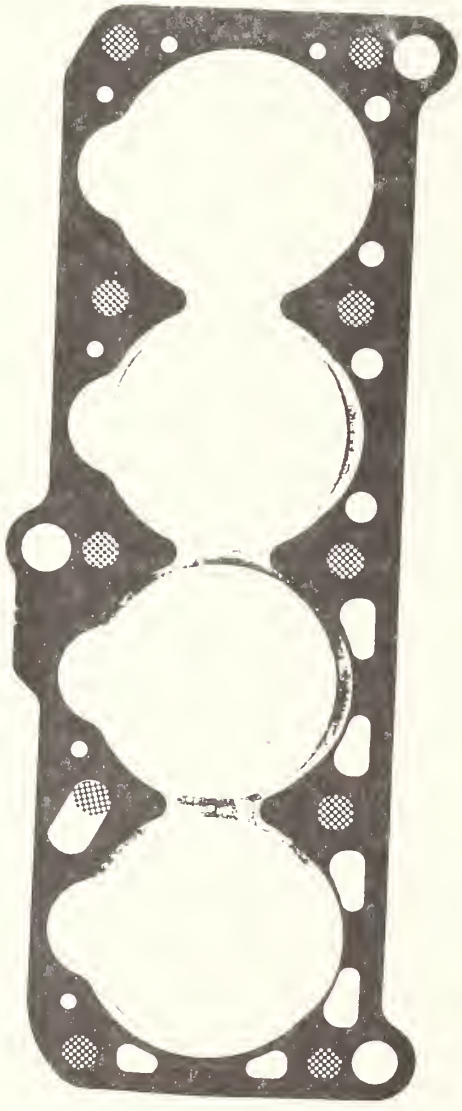

FIGURE 5.1-23: CYLINDER HEAD GASKET

FIGURE 5.1-24: TOOTHED-BELT DRIVE

To achieve the high compression needed in the diesel engine, the space between the piston at TDC and the head is kept as small as possible. This means that the space between piston and valves will also be small. In the case of belt failure, e.g. breakage or jumping, the piston will strike the valves and the engine will be destroyed.

Spark-ignition engines with normal combustion chambers in the cylinder head are not affected by this phenomenon. This is the reason for the significant improvements to the toothed-belt drive system for the diesel engine.

The objective of the research in this area was the elimination of any possible belt slip. This was accomplished by the following measures (Figure 5.1-25):

- The belt is wrapped 215^{o} around the very critical crankshaft pulley (rather than 135^{o} as on the gasoline engine) because the back of the belt drives the intermediate shaft pulley.

- The little space remaining above the crankshaft pulley is blocked by a wedge.

- The entire toothed-belt drive is protected by metal covers.

- We used a wider belt - 25 mm instead of 3/4 in.

- Toothe geometry was changed from R to RH.

- The entire structure of the belt was improved.

Figure 5.1-26 shows that these improvements permit the transfer of 100% more torque. The toothed belt used in VW diesel engines is made by Pirelli (ISORAN RH) (Figure 5.1-27). Its structure proved to be best suited to our requirements. In addition to the ISORAN R type usually installed by the automobile industry, this type of belt was developed specifically for heavy-duty purposes.

Most of the strain on the toothed belt is caused by peak torques originating from the fuel injection pump (6 mkp max.).

The ISORAN RH belt differs from the R type belts (Figure 5.1-27) in profile configuration, material, and structure. Its teeth are spaced 3/8" (9.525 mm) apart, similar to the distance between the teeth of the R-type belts. This permitted the design of belt drives with pulleys and axial distances similar to those of spark ignition engines. The teeth of the RH-type belt are stronger and higher. Its structural characteristics are:

- Fiberglass core

- Teeth and belt body of synthetic rubber of great shore hardness

- Double-toothe protection by reinforced nylon fabric and a dry, self-lubricating medium on the surface.

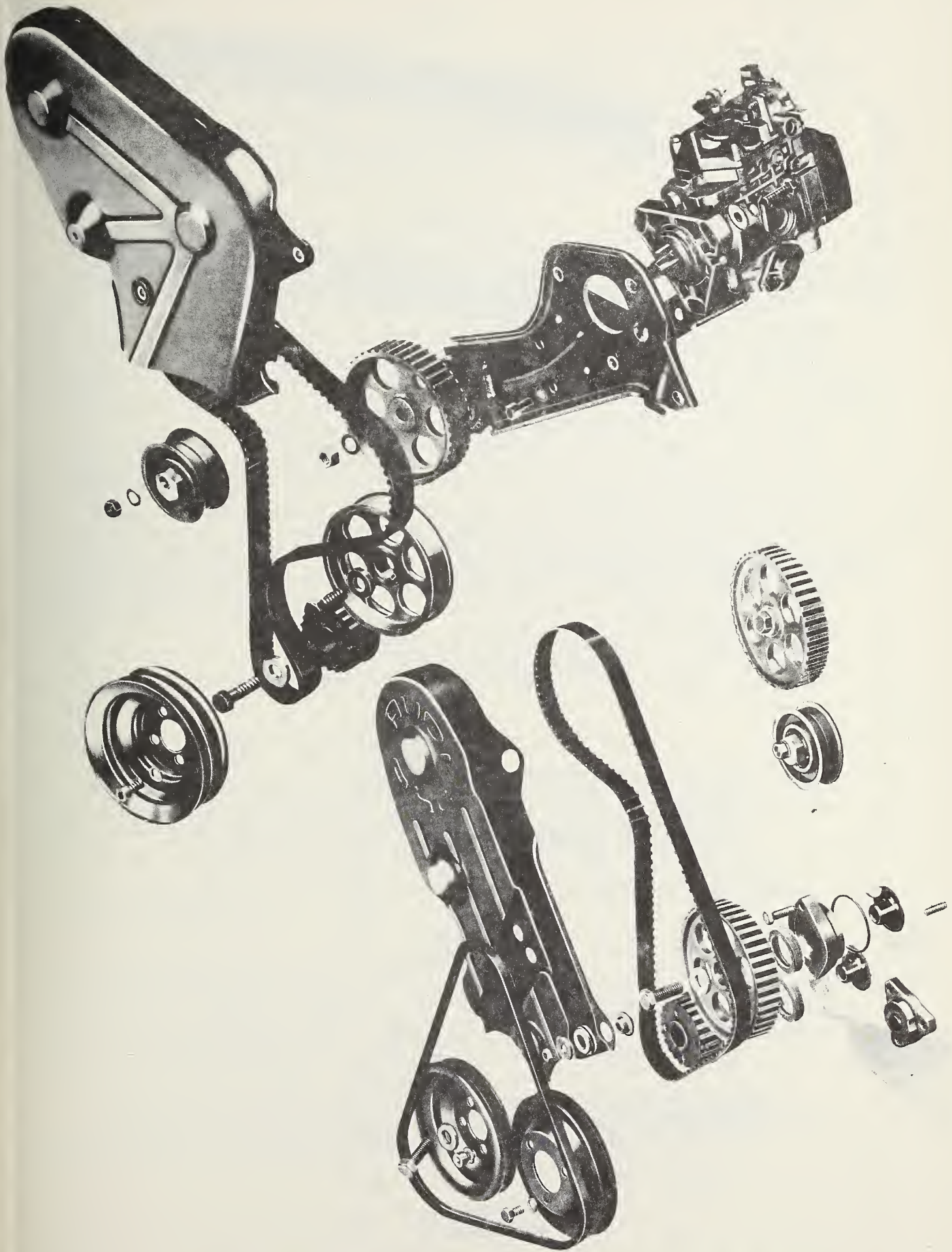

FIGURE 5.1-25: ARRANGEMENT OF TOOTHED-BELT DRIVE: SPARK-IGNITION VW DIESEL

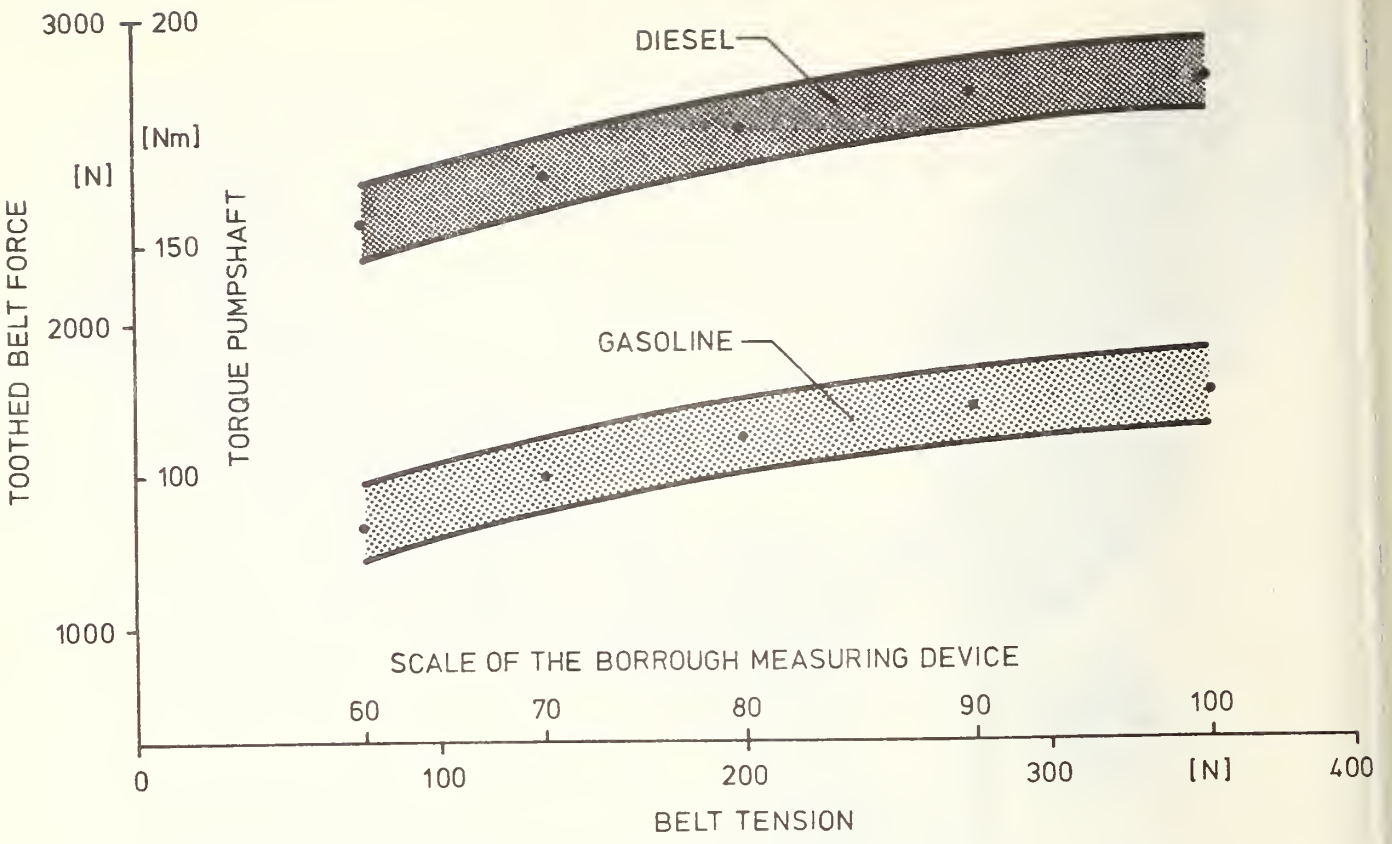

FIGURE 5.1-26: TOOTHED-BELT FORCE AS A FUNCTION OF BELT TENSION

CODE		R	RH
	width-pitch ratio b_b/P_b	0,33	0,46
	height-pitch ratio h_b/P_b	0,19	0,24

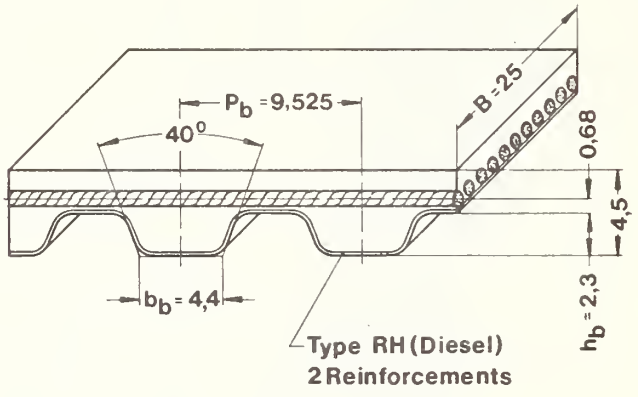

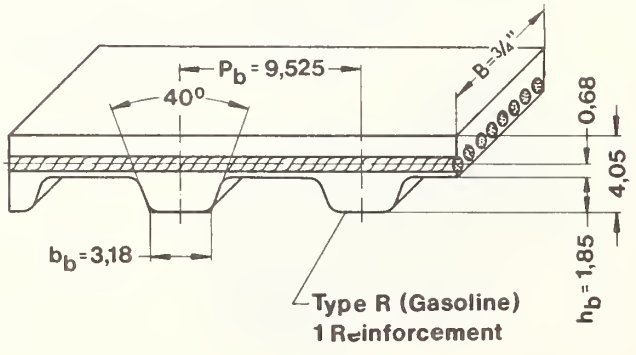

FIGURE 5.1-27: STRUCTURE OF TOOTHED BELT

Both camshaft and injection pump have to be adjusted with cylinder No. 1 at TDC. The rough injection pump timing is set by a mark on its pulley. The camshaft is correctly positioned by a setting bar which is inserted in a slot in the back of the camshaft and supported by the cylinder head. After the belt is correctly tensioned with the excentric roller, the pulley is locked onto the tapered end of the camshaft by tightening the mounting bolt.

5.1.1.6 Oil Circulation

The gear-type oil pump is driven by a worm gear on the intermediate shaft. Instead of a distributor for the gasoline engine the VW diesel engine is equipped with a thrust cover which eliminates the axial forces of the worm gear. A thrust cover or a vacuum pump is located above the worm gear in the position occupied by the distributor on the spark ignition engine. The oil is drawn from the oil pan via the oil pump cover, which doubles as a suction tube, and is then forced through the oil filter and into the main oil gallery.

The oil filter has been enlarged in comparison to the gasoline engine because of the higher engine oil contamination.

The main bearing supports and the main oil gallery in the cylinder crankcase are connected via bores. One bore supplies oil to the cylinder head through the cylinder head gasket and through lateral bor in the cylinder head to the camshaft bearings. Cam lobes, lifters, and valves are splash lubricated from the camshaft bearings. Oil returns to the oil pan through three large bores in the cylinder head and block.

5.1.1.7 Cooling System

5.1.1.7.1 Water Circulation System

A crankshaft-driven V-belt powers the alternator and water pump. The water pump housing is die-cast aluminum. It is mounted off-center at the front side of the engine. The pump housing contains a thermostat in addition to the pump impeller bearings and seals.

The engine coolant leaves the cylinder head through a duct between cylinders 3 and 4.

While the engine is cold, the coolant circuit through the radiator is bypassed (Figure 5.1-28). The pump draws the coolant from the outlet duct in the cylinder head and pumps it back into the cylinder block. As soon as the water has reached a temperature of 80^{o}C, the thermostat begins opening the main cooling circuit. All the coolant is flowing through the radiator by the time the temperature reaches 86^{o}C.

A manually-operated valve allows coolant to flow through the heat exchanger for the car's heating system. A transparent expansion tank has been provided to facilitate coolant level monitoring and fill-up.

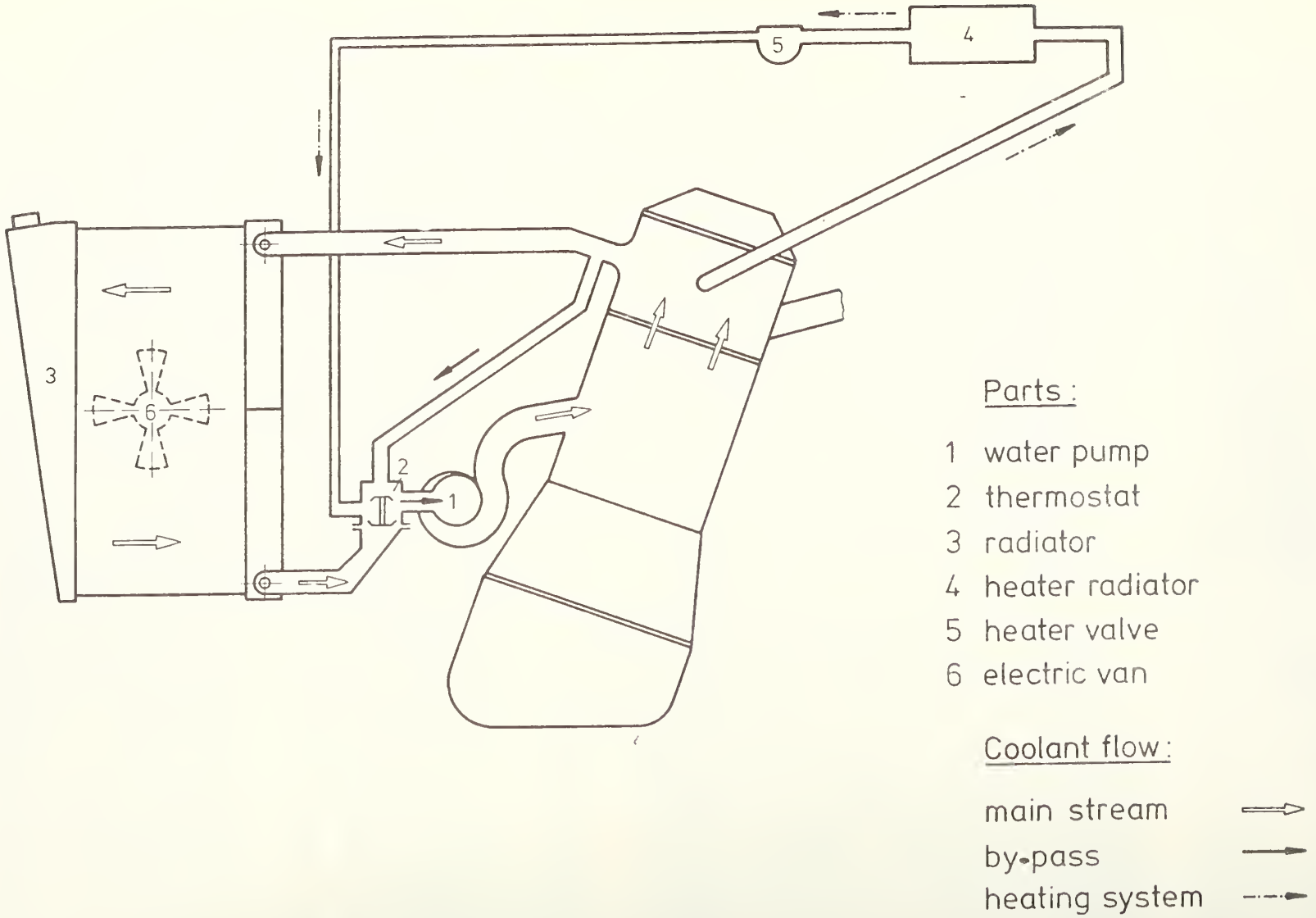

FIGURE 5.1-28: COOLING SYSTEM CONFIGURATION

5.1.1.7.2 Coolant

Tests have shown that the coolants commonly used in spark-ignition engines may be used also in diesel engines. There were no detrimental effects to the coolant after 100,000 km. Both pH-index and alkalinity still conformed to our requirements even after this mileage.

Coolant samples drawn from several vehicles of different mileages were subjected to anti-corrosion tests according to ASTM D 1384-70. The results show that even after high mileage the anticorrosion effect still meets VW requirements.

Coolant samples were drawn from several diesel-powered vehicles of varying mileage in order to determine any changes in the coolants. The samples were tested for coolant additive concentration (density test), pH-index, and alkalinity. The latter was measured according to ASTM D 1121 for 100 ml of a 10% coolant solution.

The coolant additive concentration level remained at between 40 and 50% by volume independent of mileage.

While decreasing slightly after relatively low mileage, the pH-index in all vehicles remained somewhere in this region for the entire duration of the test.

Many metals including aluminum are amphoteric. This means that they corrode and dissolve in an acid as well as in an alkaline environment (low and high pH-indexes). Every corrosion inhibitor will work only within a limited pH index range. Once these relatively narrow limits are exceeded, a corrosion inhibitor may become entirely ineffective and may even help to increase corrosion.

The results of our modified ASTM D 1384-70 tests show that the anti-corrosion properties of the coolant additives after a mileage of 75,000 km satisfy the requirements.

The corrosion rate of all metals used in the ASTM test shows a mere 10% increase compared to a newly charged radiator. The only exception is lead, which showed a 30% increase in its corrosion rate after 75,000 km (see Figure 5.1-29).

5.1.1.8 Air Intake System

The air intake system (Figure 5.1-30) makes use of the dynamic ram effect to increase volumetric efficiency in the lower speed range. Long separate ram pipes terminate in the air filter housing, which doubles as an air intake silencer. Its volume is 7 liters.

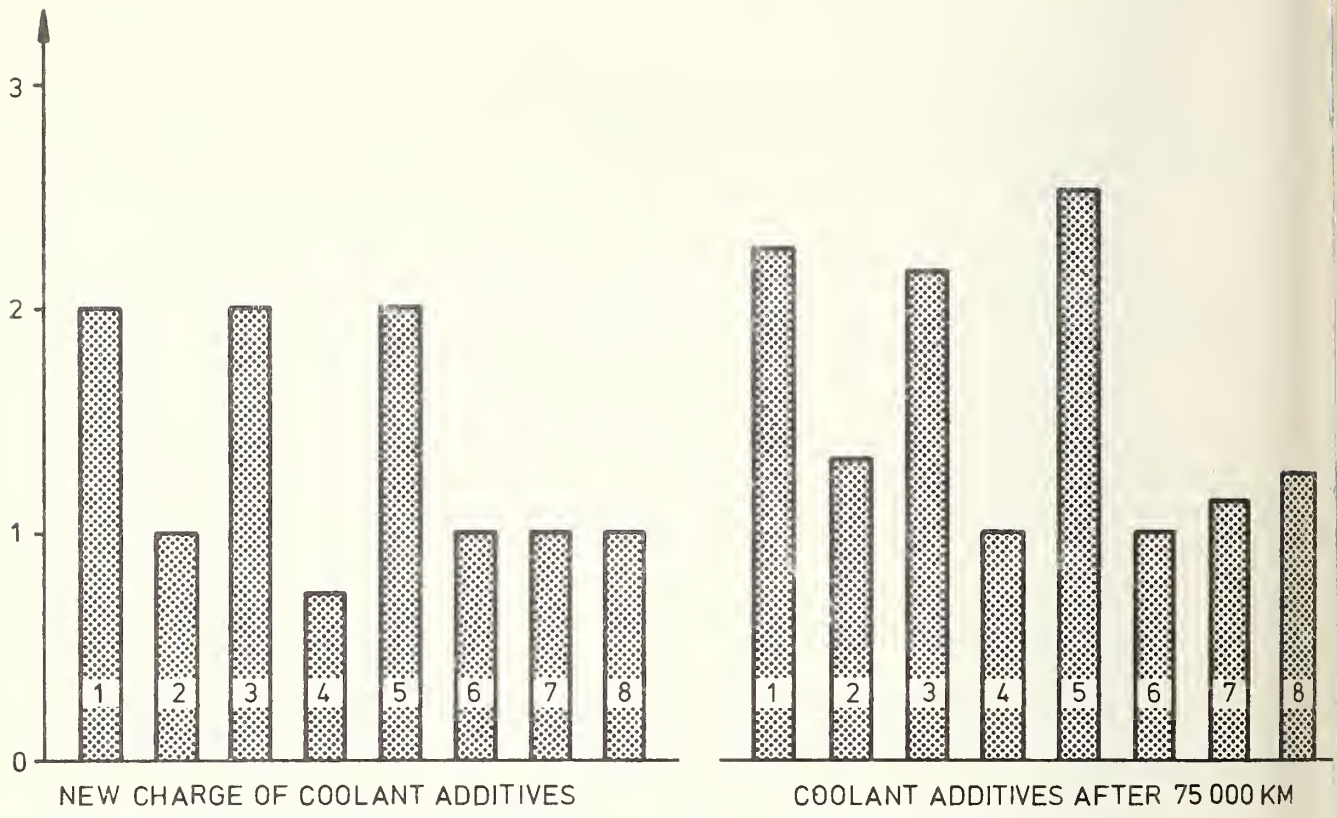

1. Copper DIN 1787
2. Solder L-Pb Sn 30 (Sb) DIN 1707
3. Brass Cu Zn 33 DIN 17 660
4. Steel St 37 DIN 1623
5. Cast-iron GG 25
6. Al Si 6 Cu 4
7. Al Mn DIN 1725
8. Al Si 12 DIN 1725

FIGURE 5.1-29: CHANGES IN COOLANT ADDITIVES AFTER 75,000 KM

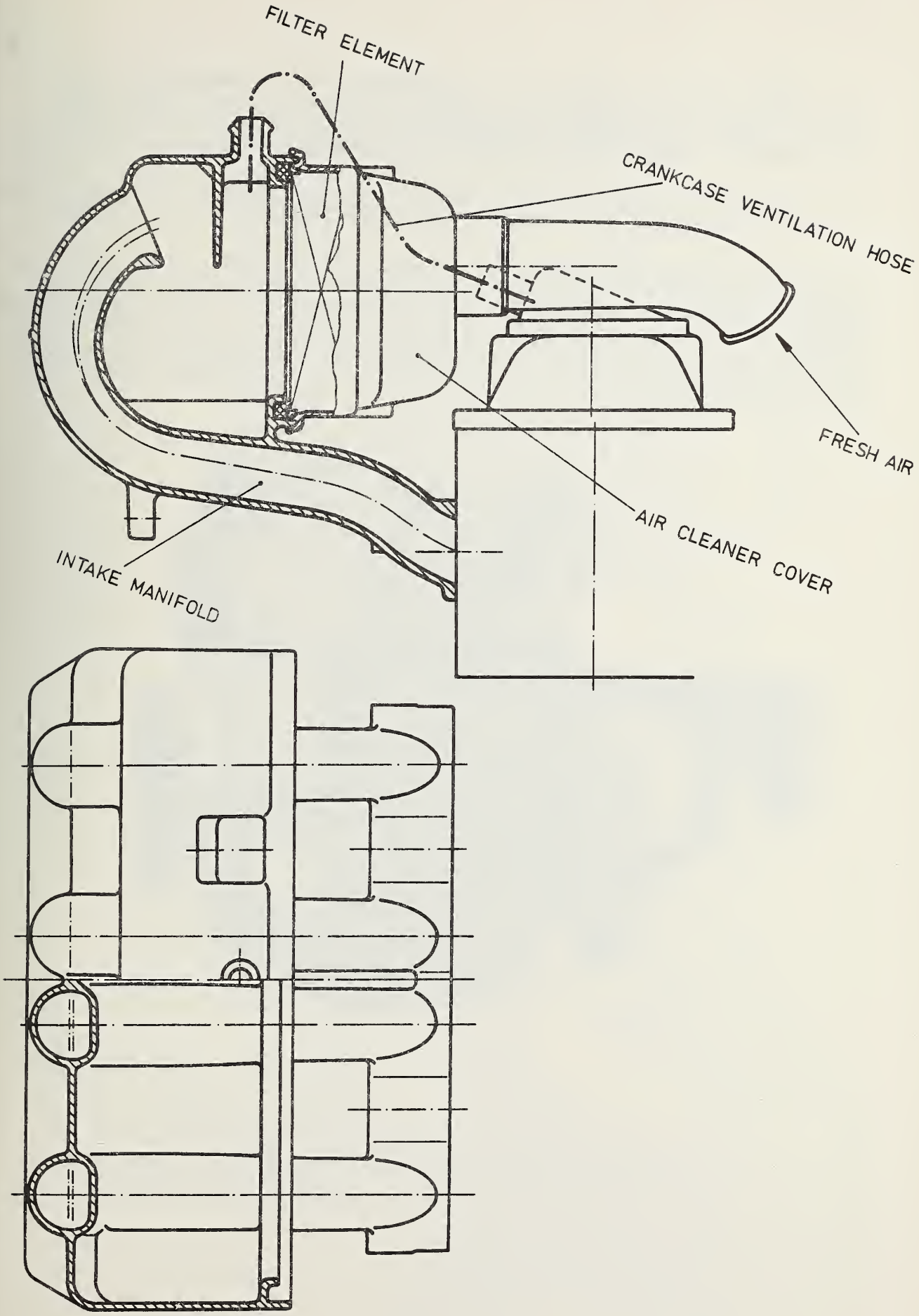

FIGURE 5.1-30: INLET MANIFOLD

Often, dynamic effects like these result in flow losses caused by bends which are required because there is no room for long intake pipes. The VW diesel intake pipes are bent only slightly, and their flattened cross-section is optimally adapted to their bending radius.

All four ram pipes are part of the air intake silencer wall, reinforcing it considerably and reducing both weight and noise.

Diesel engines are troubled by quickly wearing intake valve seats. By adjusting the blow-by carefully it is possible to tackle this problem so successfully that valve lash checks are required only at 15,000 km intervals. Valve readjustments are required even more rarely. A rib cast into the air filter casing distributes the blow-by uniformly. Oil droplets are received by the lower part of the filter, and conducted directly into the ram pipes by way of 1 mm holes.

5.1.2 4-Cylinder Turbocharged Engine

The turbocharged 4-cylinder diesel engine is based on the 37-kW naturally-aspirated production engine. Turbocharging raised the power output by a factor of 1.35.

Figures 5.1-31 through 5.1-35 show the design of the engine.

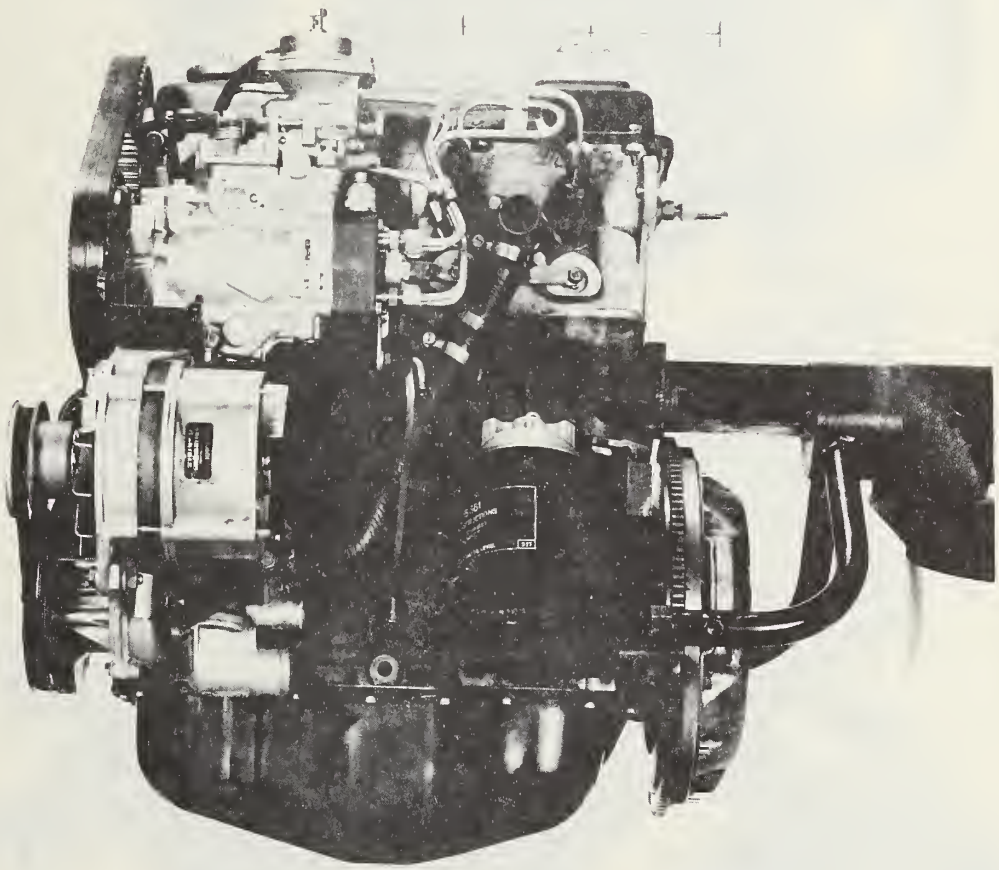

FIGURE 5.1-31: 4-CYLINDER TURBOCHARGED ENGINE - SIDE VIEW - INJECTION PUMP

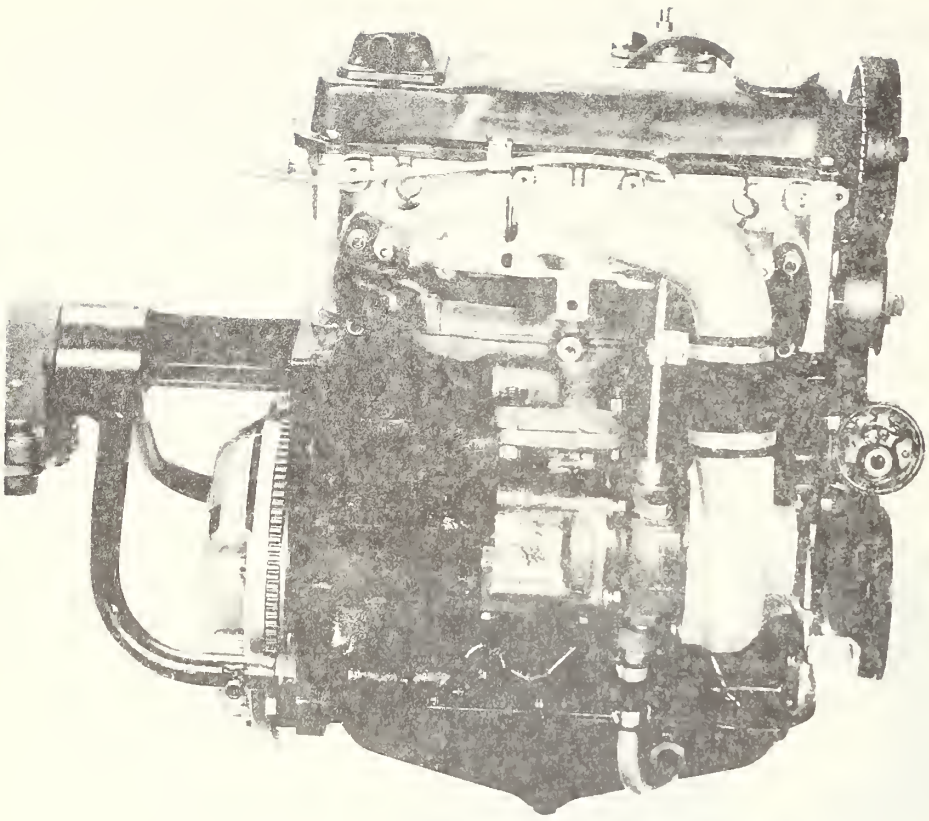

FIGURE 5.1-32: 4-CYLINDER TURBOCHARGED ENGINE - SIDE VIEW - INLET MANIFOLD

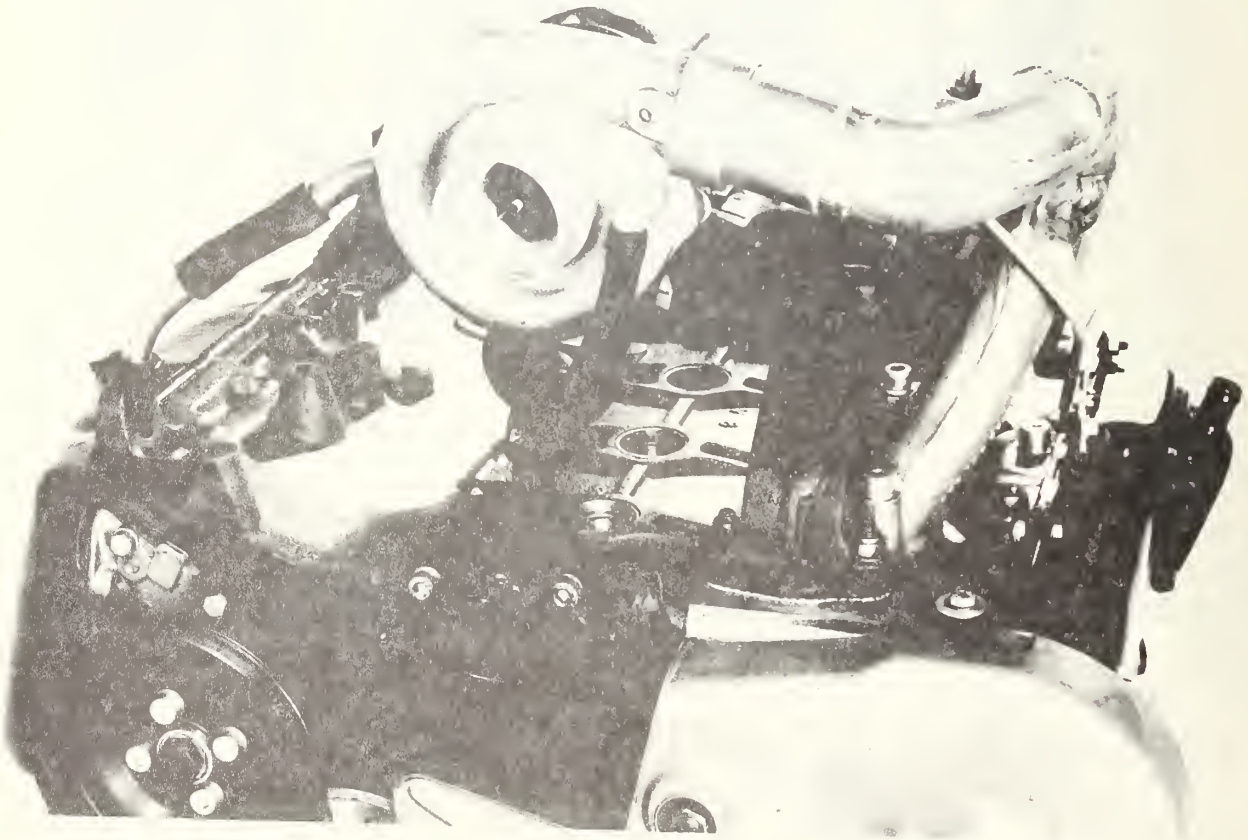

FIGURE 5.1-33: 4-CYLINDER TURBOCHARGED ENGINE - FRONT VIEW - COMPRESSOR INLET

FIGURE 5.1-34: 4-CYLINDER TURBOCHARGED ENGINE - REAR SIDE VIEW - TURBINE OUTLET

5.1.2.1 Technical Data

4-Cylinder TC In-Line Engine

Swept Volume	1.471 l
Bore	76.5 mm
Stroke	80 mm
Stroke/Bore	1.05
Cylinder Volume	367.7 cm^3
Compression	23.5
Maximum Boost Pressure	0.6 bar
Firing Sequence	1 - 3 - 4 - 2
Power (DIN)	51.5 kW (70 BHP)
Rated Speed	4,800 rpm
Specific Power Output	35 kW/l (47.6 BHP/l)
Maximum Torque	118 Nm (12 kpm) at 3,000 rpm
Maximum Mean Effective Pressure	10.3 bar
Mean Piston Velocity at Rated Speed	12.8 m/s
Weight*	132 kg
Weight-to-Horsepower Ratio	2.56 kg/kW (1.9/BHP)
Length, Width, Height	514 x 572 x 645 mm
Power-to-Volume Ratio	272 kW/m^3 (369 BHP/m^3)
Oil Capacity	3.5 l

*including clutch, intake and exhaust manifold, airfilter, oil, generator; excluding cooling system, coolant, starter motor.

5.1.2.2 Power Plant and Cylinder Head

The prototype of this engine used the unchanged engine and cylinder head of the naturally-aspirated engine. The results of endurance tests showed sufficient durability. Production engines may require modifications to the crank drive, especially to the piston (cooled piston) and to the cooling system.

Compressor and intake pipe first were connected by a short hose. The considerable heat radiation from the exhaust manifold soon rendered the rubber porous. Therefore, the intake pipe was extended and sealed with an O-ring (see Figure 5.1-33).

5.1.2.3 Cylinder Head Gasket

The metal rings at the cylinder head gasket in the cylinder bore area were reinforced in order to ensure tight sealing against the higher cylinder pressures compared with the NA engine.

5.1.2.4 Intake Manifold

The air filter is integrated in the intake manifold of the naturally-aspirated engine. The intake manifold of the turbocharged engine was to be re-designed because the filter element must be located upstream from the compressor.

The cross sections of the intake manifold and of the hose to the compressor were enlarged in order to accommodate the higher volume of air throughflow. The turbocharger compressor forces the air into the newly designed intake pipe. Tests showed that long ram pipes in the turbocharged engine do not lead to a significant rise of the brake mean effective pressure (bmep). Improved volumetric efficiency can be achieved only by a complex re-design of the intake system. Therefore, preference was given to the more compact design with short ram pipes.

5.1.2.5 Crankcase Ventilation

The crankcase ventilation flange connection is located in the valve chamber cover. The naturally-aspirated engine has a hose connection to the vacuum intake pipe. The intake pipe pressure in the turbocharged engine is the charge pressure. Therefore, the crankcase ventilation flange connection was to be positioned at an intake manifold location where the pressure is lower than the ambient air pressure.

A connection upstream of the air filter element would result in rapid contamination by oil mist and soot. The only location where the connection can be made is the zone between air filter and compressor. The selected location is in the immediate neighborhood of the compressor intake. This solution permits a comparatively short hose where only small amounts of condensate can precipitate. Condensates from the crankcase ventilation are passed through a curved pipe to the intake orifice of the compressor where they are picked up by the intake air flow.

5.1.2.6 Exhaust System

The exhaust flange of the exhaust manifold was to be modified in order to match the turbine intake flange. This flange is not affected by material thermal expansion and contraction, while the air-intake and exhaust-gas connection can move. The exhaust-pipe diameter of 42 mm is largely the same as that of stronger gasoline engines.

5.1.2.7 Injection Pump

The delivery volume of the Bosch distributor injection pump was adapted to the higher air flow of the turbocharged engine. A charge-pressure-controlled smoke-limiting device prevents smoke emission in excess of the Bosch Number 3.5.

The smoke-limiting device is mounted in the location of the lever stop. The charge pressure is applied to a diaphragm that adjusts the governor slide through an adjustment linkage (see Figures 5.1-35 and 5.1-36). Increasing charge pressure adjusts the slide plate for higher injection volume. The full-load delivery rises in proportion to the charge pressure up to 29 mg/stroke, as shown in Figure 5.1-37.

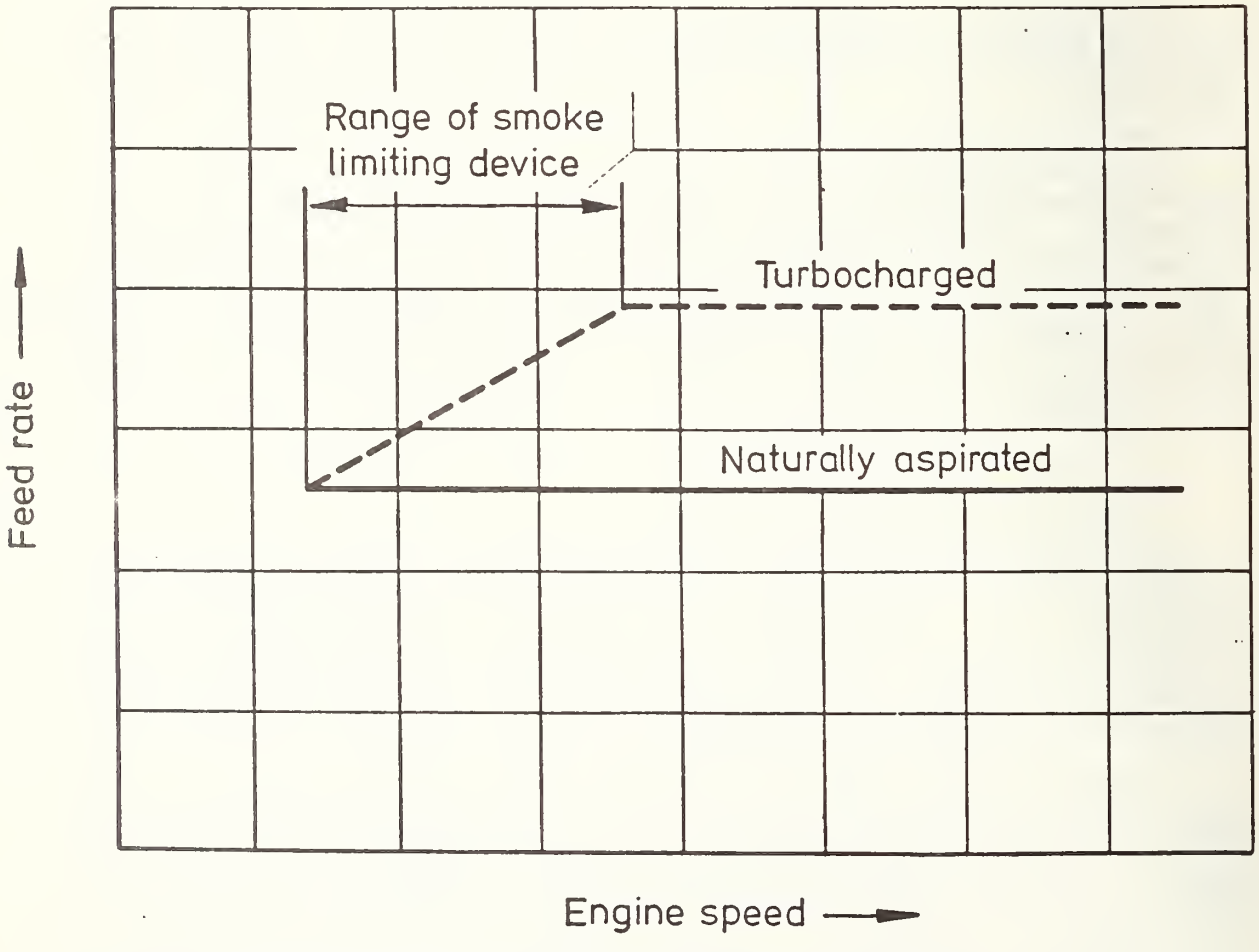

FIGURE 5.1-35: CHARACTERISTIC OF SMOKE LIMITING DEVICE

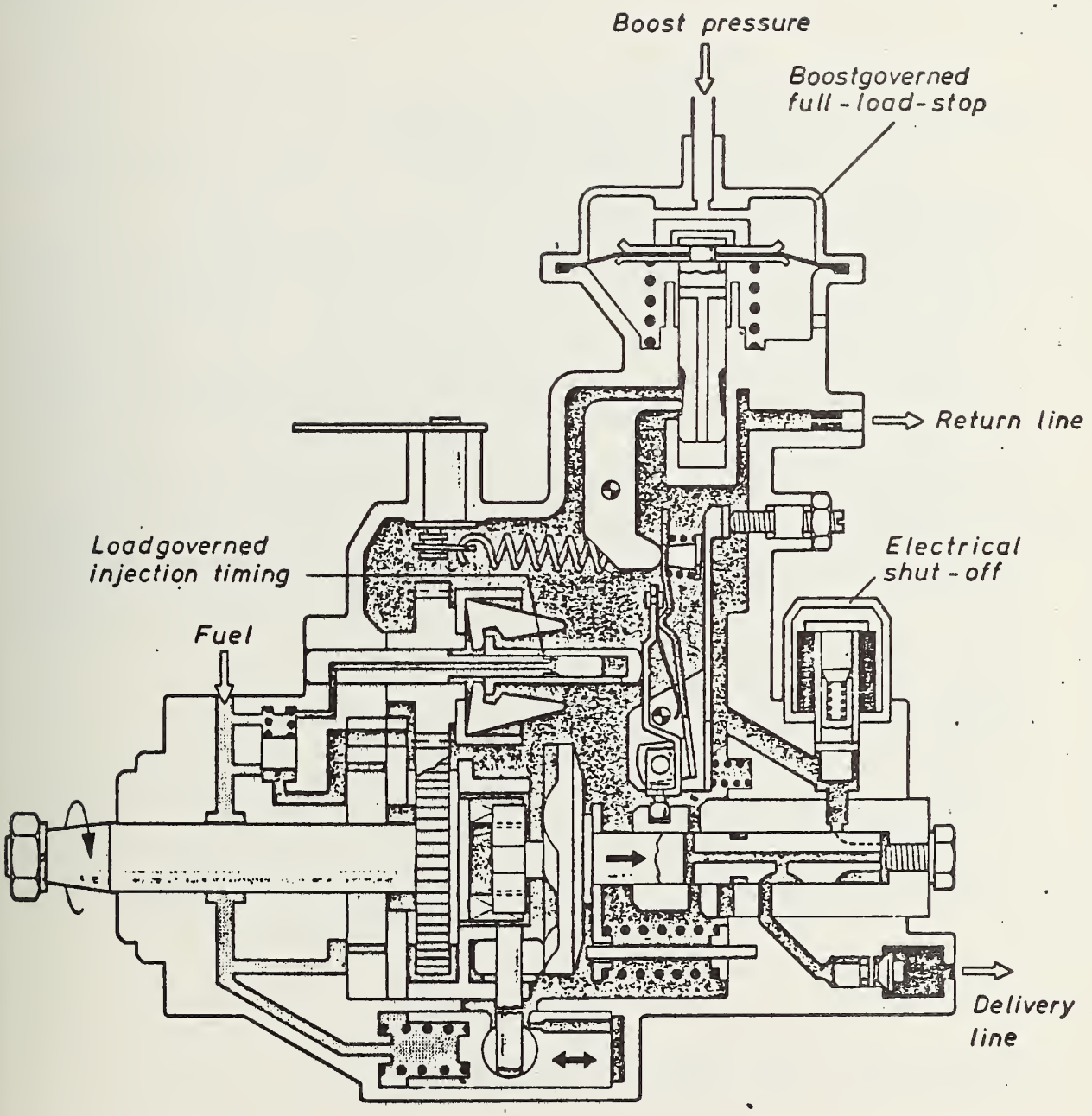

FIGURE 5.1-36: INJECTION PUMP WITH SMOKE-LIMITING DEVICE

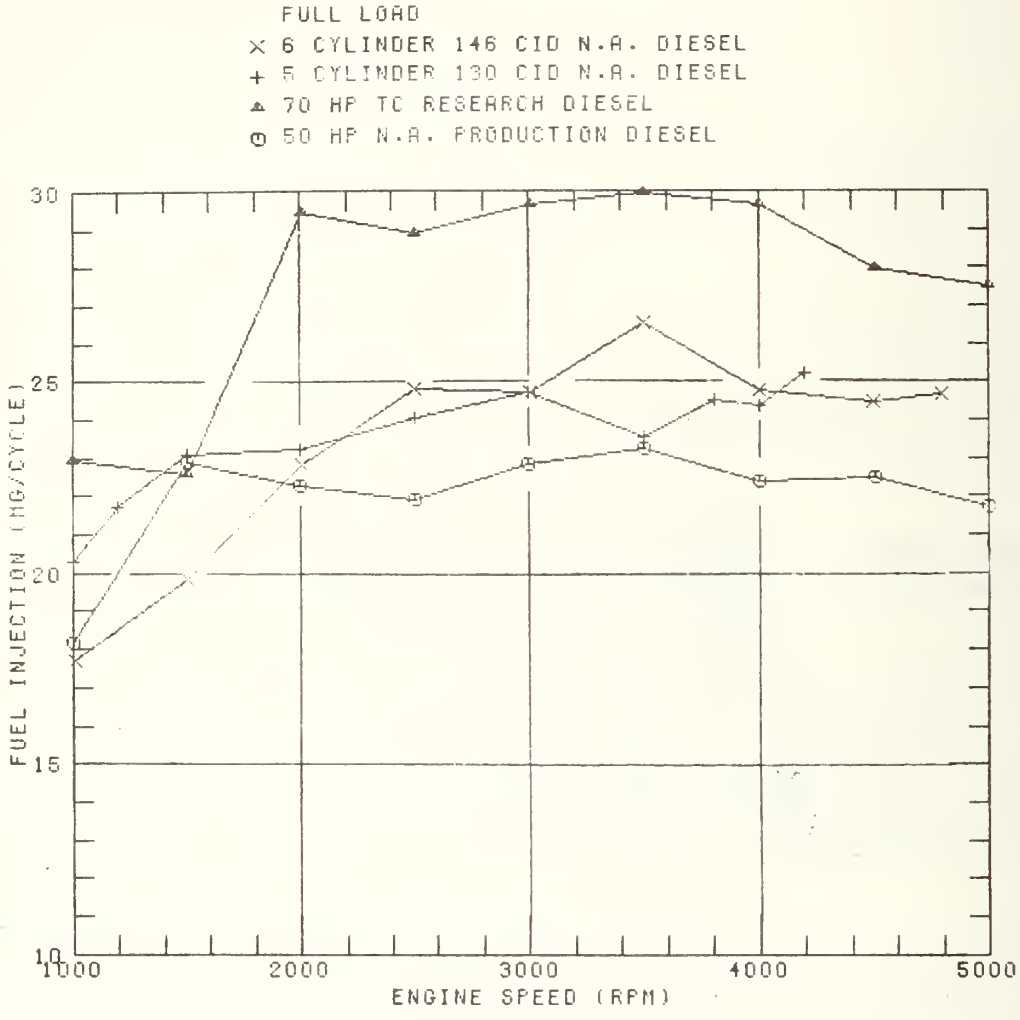

FIGURE 5.1-37: FUEL INJECTION VERSUS SPEED

5.1.2.8 Cooling System

The radiator of the naturally-aspirated engine has a face area of 1.536 cm^2. This radiator was exchanged for a radiator with a face area of 1.664 cm^2. An oil cooler was added.

5.1.2.9 Turbocharger

Investigations were performed on exhaust gas turbochargers with integrated wastegate, made by the AirResearch and Holset companies.

Early charger response is secured by the comparatively narrow turbine nozzle cross section of 3 to 5 cm^2 (ratio between cross section and radius of turbine housing 0.25...0.36) in order to generate charge pressure at low engine speeds, while blow-off is provided through the wastegate at high engine speeds. The bmep of the turbocharged engine exceeds that of the naturally-aspirated engine beginning at engine speeds of 1,300 rpm. A double-flow turbine system is not advisable because of the unfavorable ratio between surfaces and flow cross-section.

The shaft of the turbocharger is supported by forced-oil-lubricated plain bearings. The engine oil flow through the turbocharger provides for cooling. The engine oil is delivered from the cylinder head gallery through a pipe of an interior diameter of 1.9 mm. A flexible hose passes the oil back into the pan. The turbocharger section and wastegate are shown in Figures 5.1-38 and 5.1-39.

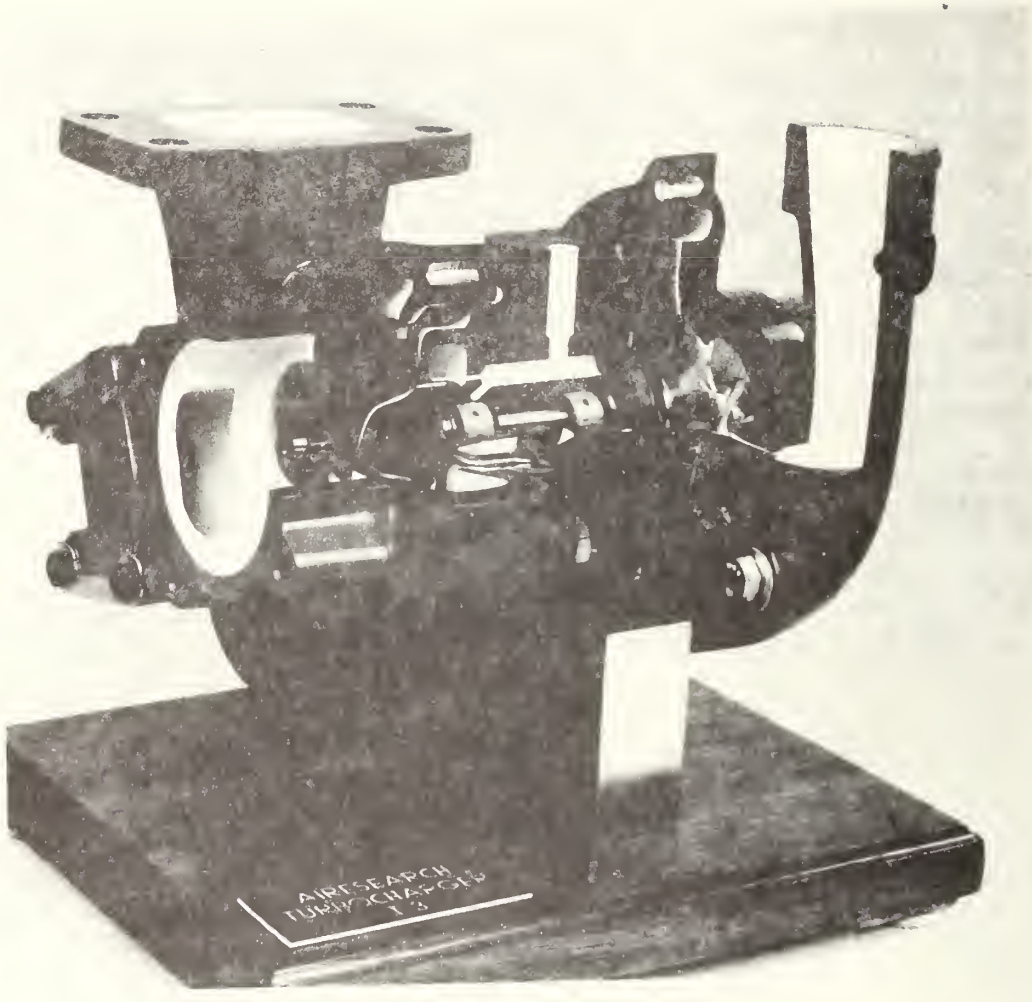

FIGURE 5.1-38: TURBOCHARGER CROSS SECTION

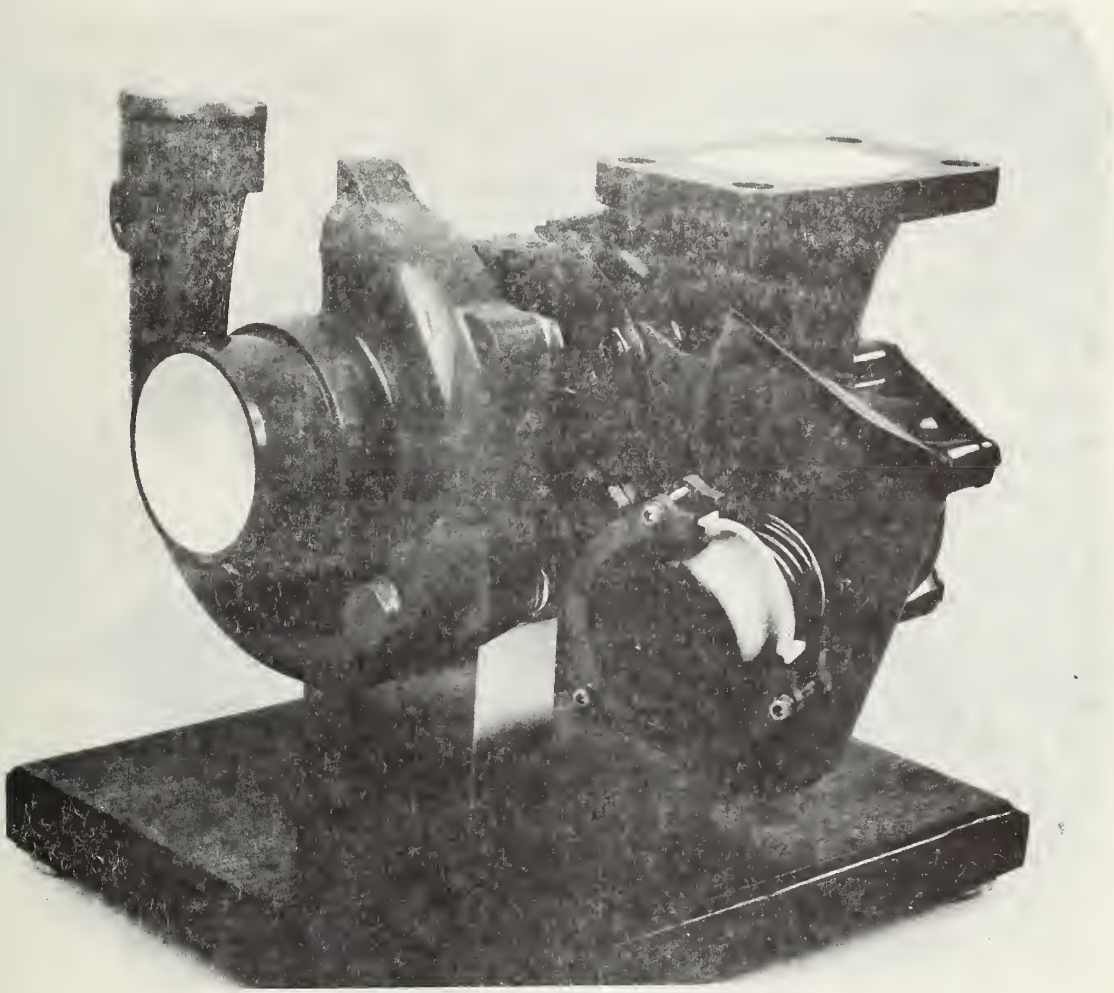

FIGURE 5.1-39: WASTEGATE CONTROL OF TURBOCHARGER

5.1.3 5-Cylinder Naturally-Aspirated Engine

The 5-cylinder prototype diesel engine is based on the 5-cylinder gasoline engine. The design uses the combustion process of the 4-cylinder engine which was tuned to the cylinder unit displacement. Figures 5.1-40 through 5.1-41 illustrate the design concept.

5.1.3.1 Technical Data

5-Cylinder In-Line Naturally-Aspirated Diesel Engine

Swept Volume	2.184 l
Bore	79.5 mm
Stroke	88 mm
Stroke/Bore Ratio	1.107
Cylinder Volume	436.8 cm^3
Compression Ratio	23
Firing Sequence	1 - 2 - 4 - 5 - 3
Power (DIN)	51.5 kW (70 BHP)
Rated Speed	4,500 rpm
Specific Power Output	23.6 kW/l (32 BHP/l)
Maximum Torque	132 Nm (13.5 kpm) at 3000 rpm
Maximum Mean Effective Pressure	7.7 bar
Mean Piston Velocity at Rated Speed	13.1 m/s
Weight*	171 kp
Weight-to-Horsepower Ratio	3.3 kp/kW (2.4 kp/PS)
Length, Width, Height	680 x 490 x 790 mm
Power-to-Volume Ratio	198 kW/m^3 (269 PS/m^3)
Oil Capacity	6 l

*including clutch, intake and exhaust manifold, airfilter, oil, generator; excluding cooling system, coolant, starter motor

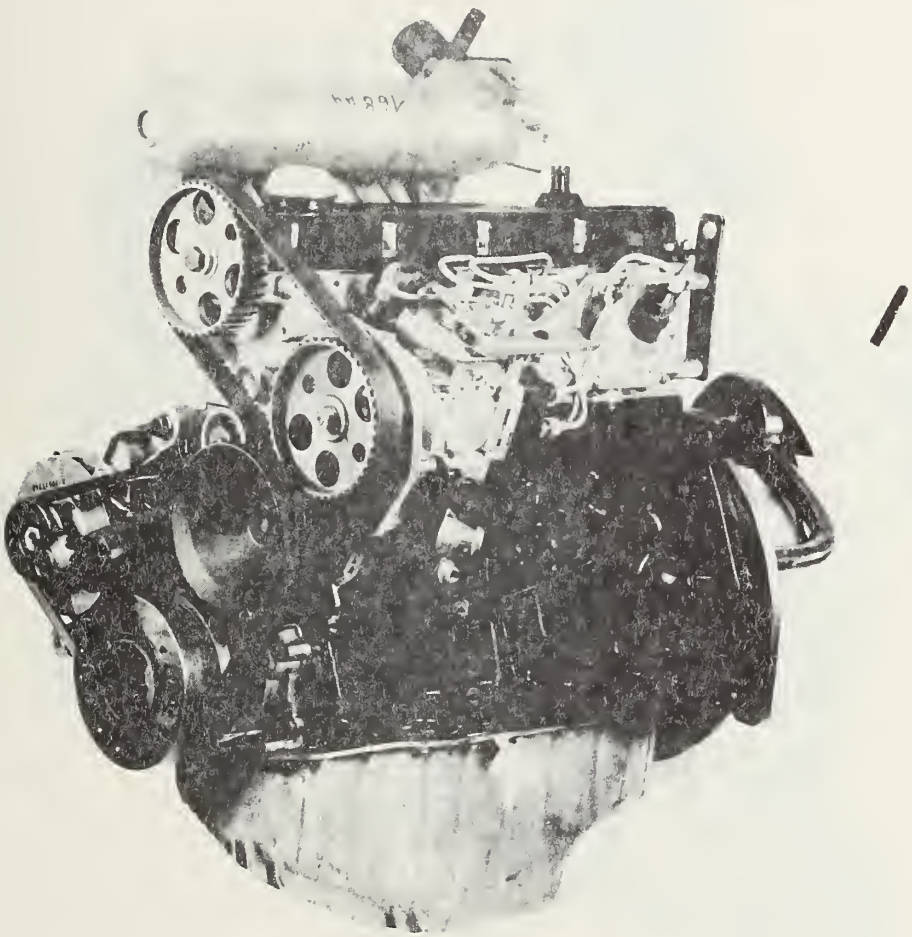

FIGURE 5.1-40: 5-CYLINDER NATURALLY-ASPIRATED ENGINE - SIDE VIEW - INJECTION PUMP

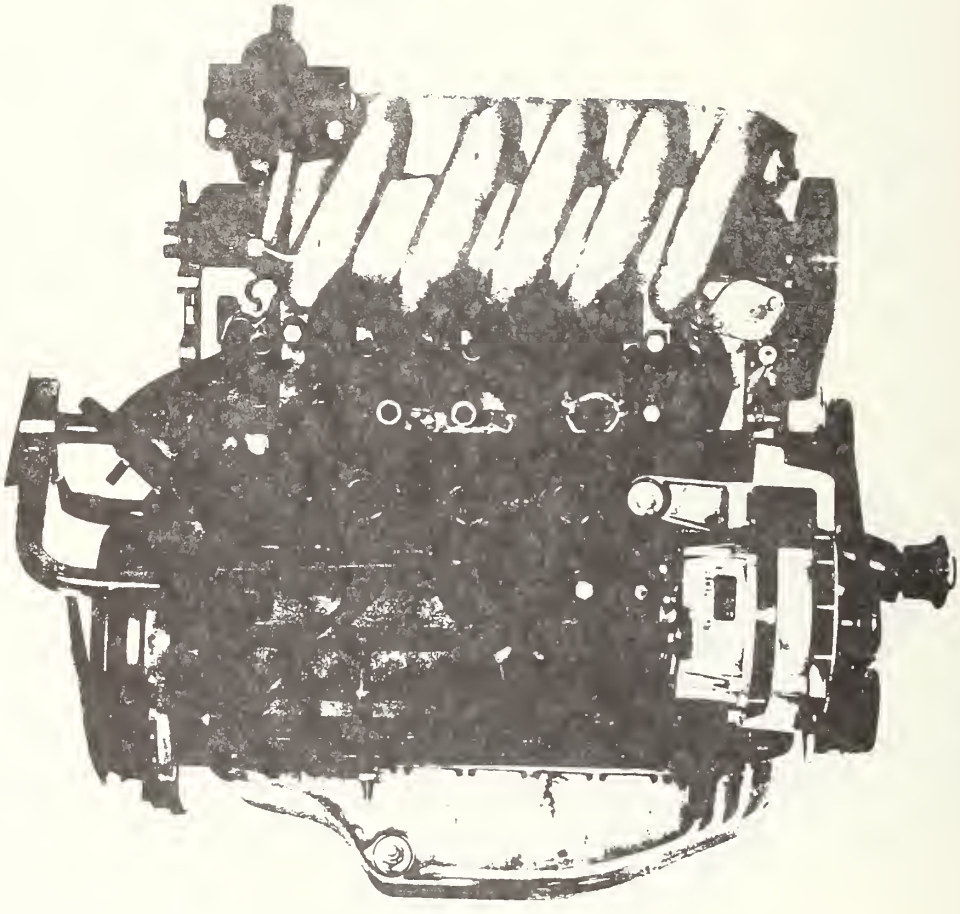

FIGURE 5.1-41: 5-CYLINDER NATURALLY-ASPIRATED ENGINE - SIDE VIEW - INTAKE MANIFOLD

FIGURE 5.1-42: 5-CYLINDER NATURALLY-ASPIRATED ENGINE - FRONT VIEW

5.1.3.2 Crankshaft Drive

5.1.3.2.1 Mass Balancing

The following factors were significant in regard to the selection of the crankshaft throws:

- short unit length
- low unit weight
- low production cost
- satisfactory mass balance
- uniform ignition intervals.

In the case of the Schroen throw arrangement with non-uniform cylinder distances, a twist moment of the first order affects the exterior. However, the powerplant is no longer than a 6-cylinder engine with the same dimension of cylinder units.

By using different throw angles, defined imbalances on both crankshaft ends and two additional balancing shafts, Hasselgruber achieved complete balance of the first and second order. The required balancing shaft drive increases the engine length and width. The irregular ignition intervals result in a free torque of the 0.5 order and higher. Other disadvantages of this layout are higher weight and increased cost of production.

Different cylinder distances within an engine and within the engine family are not useful for a modular unit system for in-line engines with different number of cylinders. Therefore, a throw arrangement was selected with uniform cylinder distances of 88 mm. The crank throws are offset by 72^{o}. This results in uniform ignition intervals of 144^{o}. The rotating masses result in a momentum that rotates around the longitudinal axis in the direction of the crankshaft rotation. The oscillating masses produce twist moments of the first and second order around the transverse axis (Figure 5.1-43).

Sixty percent of the rotating masses are balanced by the counter-weights on the crank throws and 40% by the imbalances in flywheel and vibration damper. This design prevents the occurrence of any exterior effects.

The moment of the first order produced by the oscillating masses can be balanced by two shafts that rotate in opposite directions. This solution, however, entails an engineering outlay that is not justifiable for high volume production engines.

A satisfactory mass balance can be obtained by compensation of the vector of M_I that rotates in the same direction as the crankshaft. This is accomplishe by attaching imbalances to the flywheel and vibration damper.

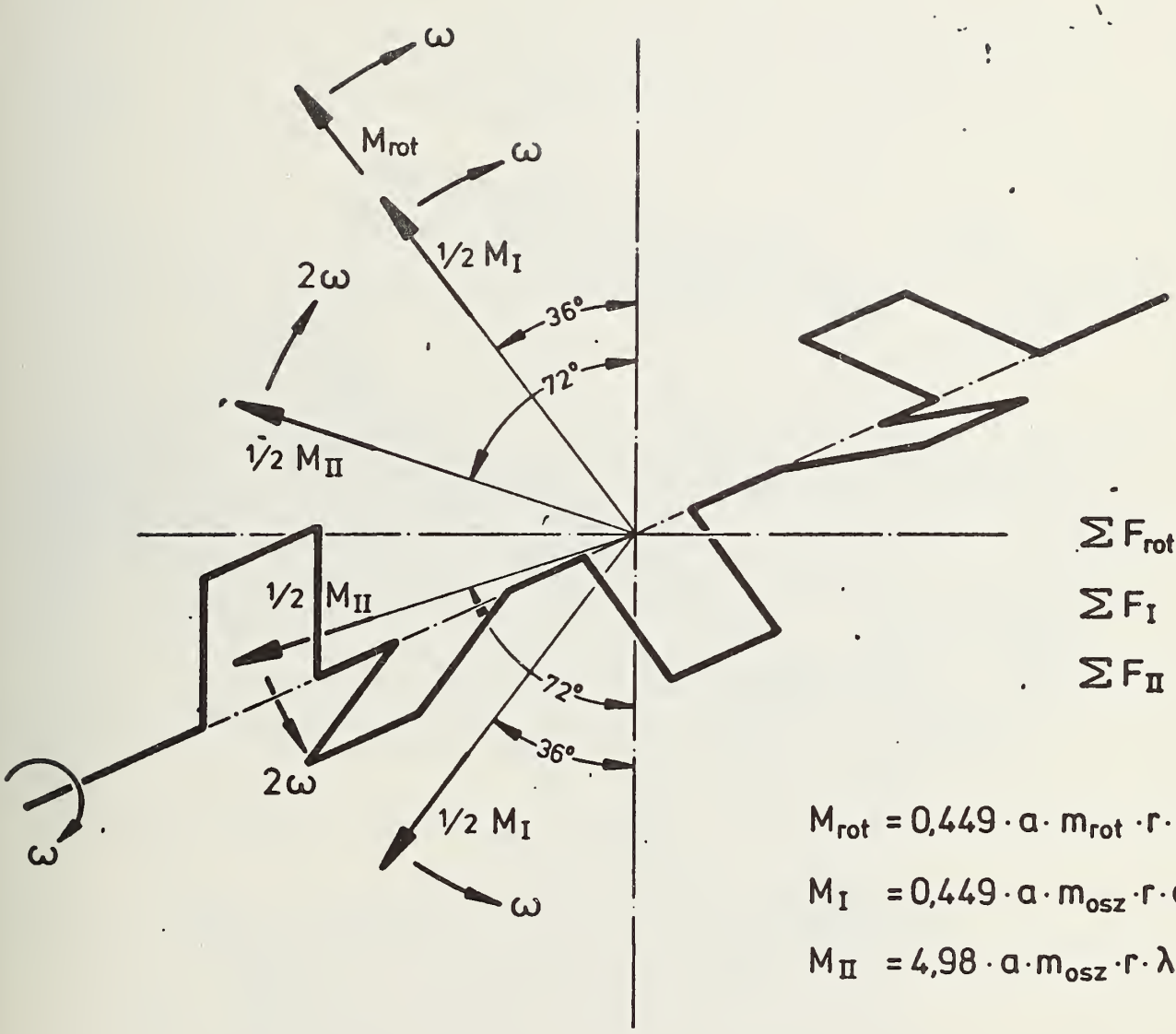

FIGURE 5.1-43: MOMENTS CAUSED BY THE MASS FORCES FOR A 5-CYLINDER ENGINE

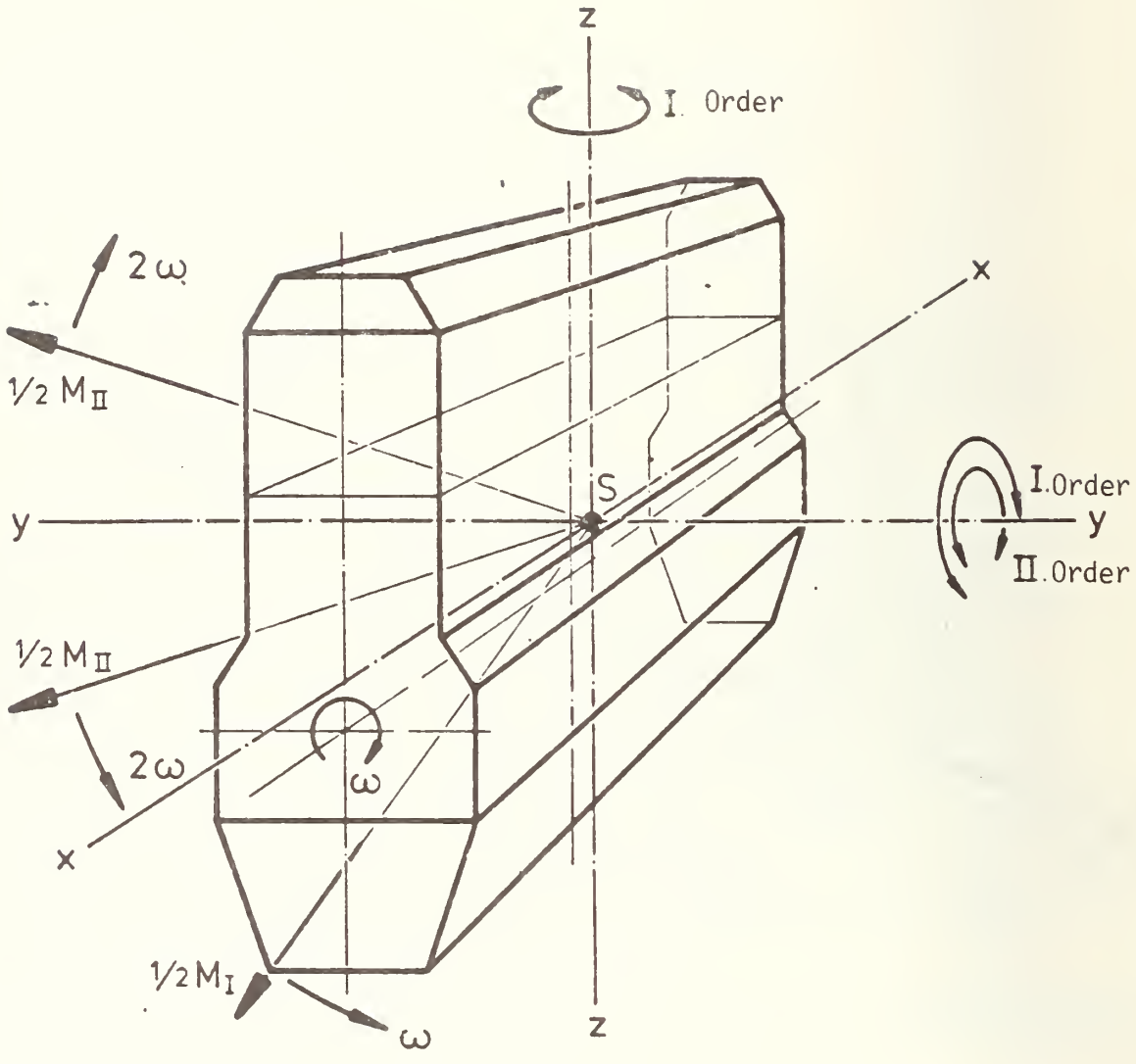

FIGURE 5.1-44: UNBALANCED MOMENTS IN THE 5-CYLINDER ENGINE

The total balancing moment produced by counter-weights on the crankshaft throws and imbalances to both crankshaft ends (flywheel and vibration damper) thus is:

$$M_A = 0.449 \, (m_{rot} + 1/2 \, m_{OSZ}) \, a \cdot r$$

$$m_{rot} = 866 \text{ g}$$

$$m_{OSZ} = 875 \text{ g}$$

$$M_A = 22{,}662 \text{ g cm}$$

This leaves the following imbalances:

- The vector of M_T that rotates in a direction opposite to the direction of the crankshaft
- The moment of the second order.

The moment of the second order leads to torsional vibrations around the transverse axis. The rotating moment of the first order causes torsional vibrations around the vertical and the perpendicular axis. The moment of the second order could be balanced completely by two shafts rotating in opposite directions at double the angular velocity of the crankshaft. This solution, however, requires too high an engineering outlay. This is the same problem that is posed by the complete balancing of the moment of the first order.

During the counter-balancing of the balanced engine shown in Figure 5.1-44 the same magnitudes of imbalances are measured horizontally and vertically, i.e. in the flywheel plane

$$\frac{1}{2 \times a_{sR}} \; 0.449 \times a \times 1/2 \; m_{OSZ} \cdot r = 152 \text{ g cm}$$

and in the plane of the vibration oscillator

$$\frac{1}{2 \times a_{SD}} \; 0.449 \times a \times 1/2 \; m_{OSZ} \cdot r = 116 \text{ g cm}$$

The measured values arrived at during careful balancing show only minor deviations from these hypothetical data.

5.1.3.2.1 Crankshaft

The crankshaft is forged from Cm45 (Figure 5.1-45). It is equipped with counter-weights of the same imbalance on all throws. Counter-weights 1 and 2 and 9 and 10 are asymmetrical because of the forging operation involved (split die). The crankshaft runs in six main bearings. The inserts for main and connecting rod bearings are the same ones as those in the 4-cylinder engine.

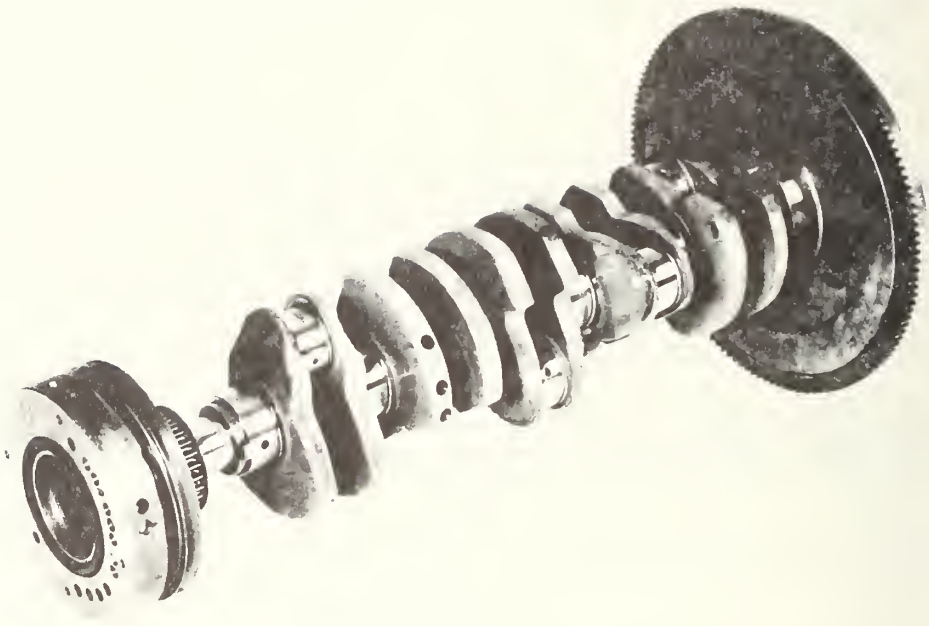

FIGURE 5.1-45: 5-CYLINDER ENGINE CRANKSHAFT

A torsional vibration balancer (Freudenberg Co.) is mounted to the front end of the crankshaft. This unit reduces the torsional vibrations in the range of 450 to 500 Hz. The secondary mass is a v-belt pully.

5.1.3.2.2 Connecting Rod

The design concept uses the 4-cylinder engine connecting rod with a distance between bosses of 136 mm. The longer crank radius results in a connecting rod ratio of $\lambda = r/l = 0.324$ (4-cylinders $\lambda = 0.294$).

5.1.3.2.3 Pistons

The compression height of 44.3 mm and the 1.8-mm cavities in the piston head were taken from the 4-cylinder diesel engine.

5.1.3.3 Cylinder Block

The distance between cylinders is 88 mm throughout the entire engine family. The cylinder bore has a 79.5 mm diameter like the 1.6-liter 4-cylinder gasoline engine. The ratio between cylinder distance and bore is 1.107. The cylinder bores are castings. This design allows for a short, stiff, and light cylinder block.

The height of the cylinder block was raised by 4 mm (half of the increased stroke) to accommodate the larger stroke, which has been increased by 8 mm compared with the base engine at the given connecting rod length and piston height. The water pump housing, thermostat housing, and oil filter support are integrated in the cast-iron cylinder block (Figure 5.1-46). The design requires four additional reinforcement ribs.

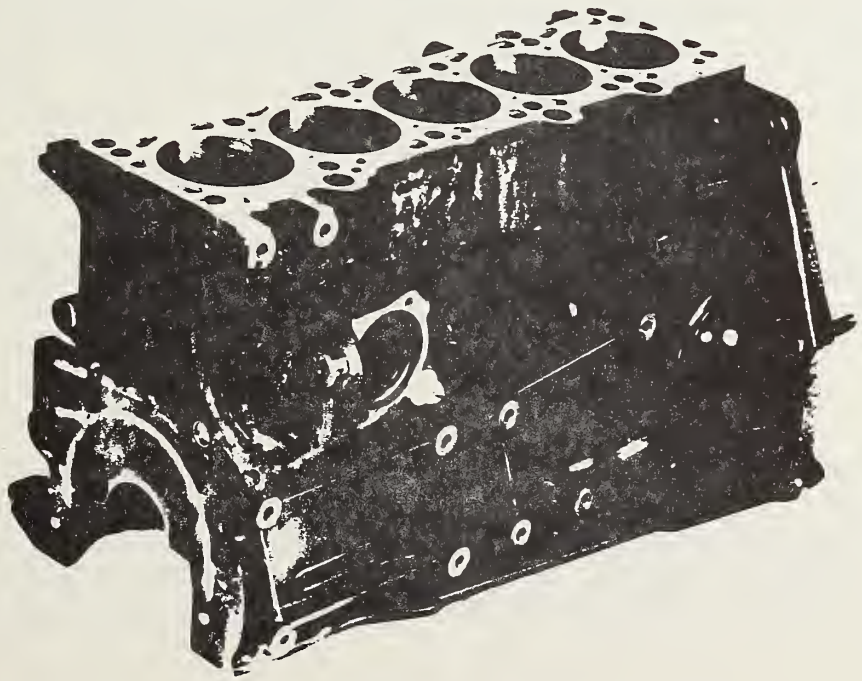

FIGURE 5.1-46: 5-CYLINDER ENGINE, CYLINDER BLOCK

5.1.3.4 Cylinder Head

The cylinder head is shown in Figure 5.1-47. The camshaft runs in four bearings. The toothed-belt pulley is pressed on the camshaft taper. Camshaft timing is adjusted with a bridge that engages in a slot on the back of the camshaft. The camshaft data are the same as in the 4-cylinder engine.

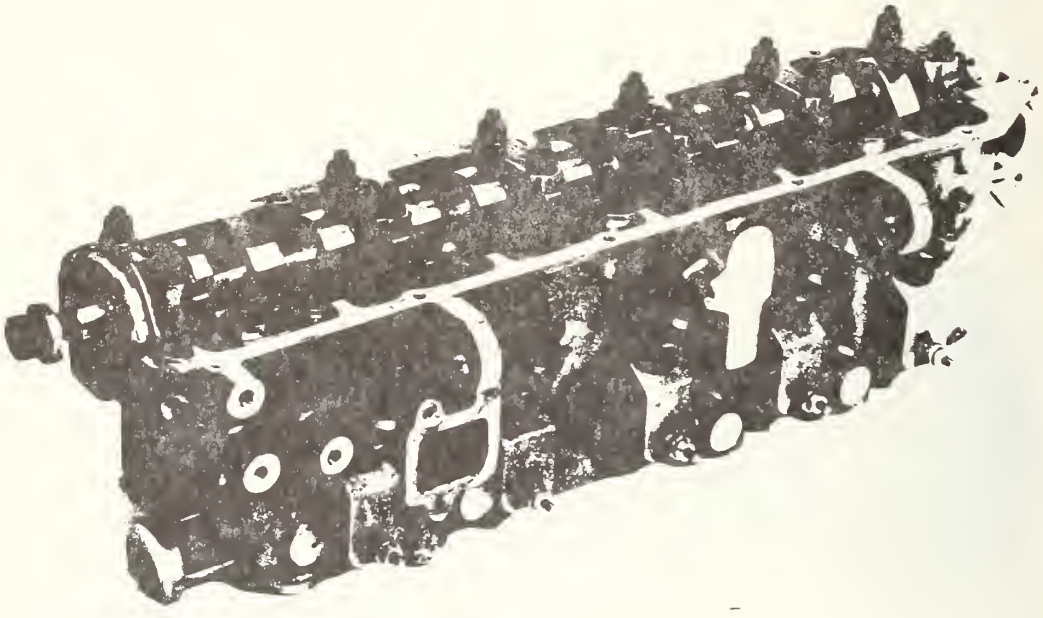

FIGURE 5.1-47: 5-CYLINDER ENGINE, CYLINDER HEAD

5.1.3.5 Auxiliary Unit Drive

The camshaft and injection pump was driven by one toothed-belt as in the 4-cylinder diesel engine. The water pump could not be driven by the toothed-belt as in the gasoline 5-cylinder engine. The water pump is V-belt driven together with the generator by the vibration damper (Figure 5.1-48).

The following looping angles were realized at the toothed-belt pullies:

Crankshaft	161^{o}
Injection pump	96^{o}
Camshaft	198^{o}

Tolerance balance is implemented by a tension roller as in the 4-cylinder engine.

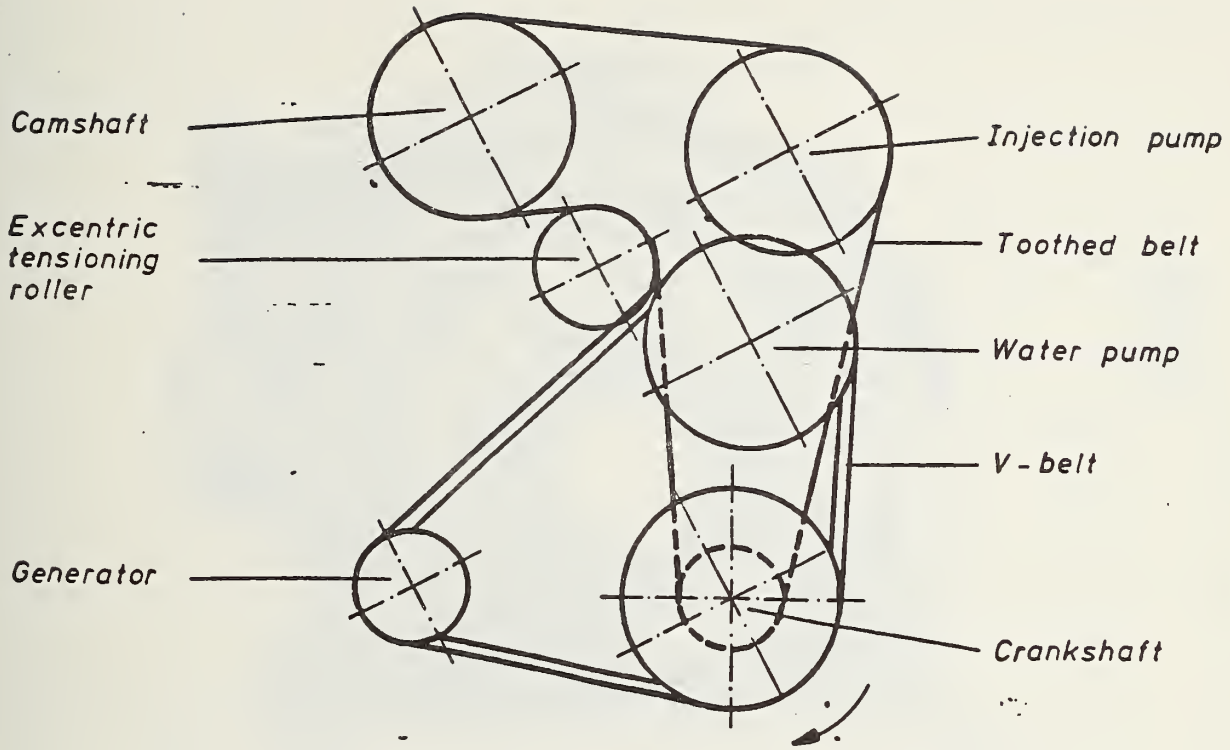

FIGURE 5.1-48: AUXILIARY UNIT DRIVE

The Pirelli ISORAN RH toothed-belt has 134 teeth spaced at 3/8" intervals and a belt width of 1".

The crescent-vane oil pump (Figure 5.1-49) has good delivery characteristics and can be produced at low cost. The die-cast aluminum housing is flanged to the front face of the cylinder block and crankcase and also accommodates the front sealing ring. The external gear is driven by an engaging piece that is pressed on the crankshaft.

5.1.3.6 Inlet Manifold

The 5-cylinder engine uses the gasoline fuel injection intake pipe. The intake filter is a separate unit, other than in the 4-cylinder engine.

5.1.3.7 Exhaust Manifold

The cast-iron manifold combines the ports of cylinders 1 and 5 in one section and those of cylinders 2, 3, and 4 in another one. This results in only minor effects of the charge changes of cylinder 2 by cylinder 4. There is no interaction between all other cylinders (Figure 5.1-50).

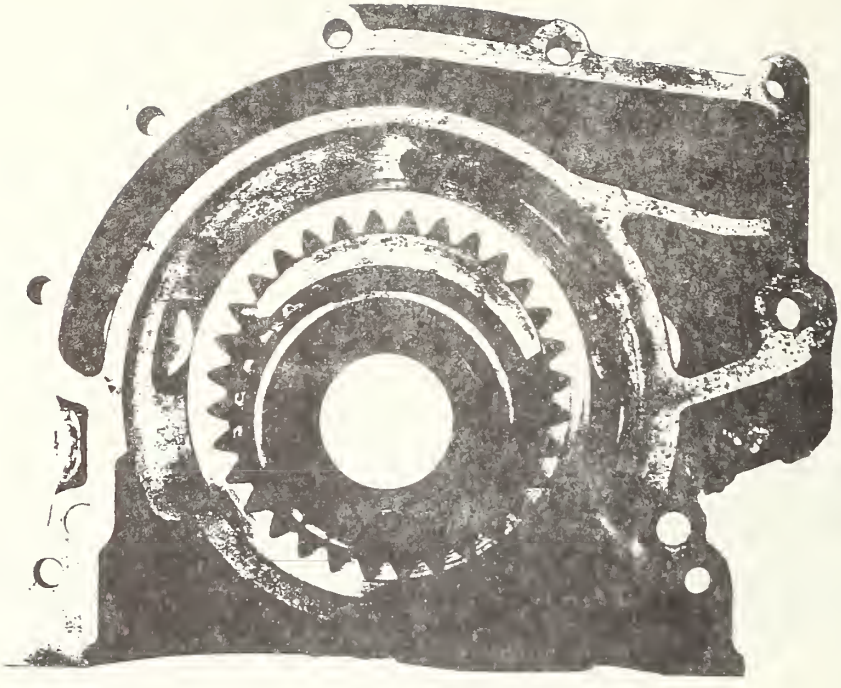

FIGURE 5.1-49: CRESCENT-VANE OIL PUMP

5.1.3.8 Injection Pump

The 5-cylinder engine injection pump design is based on that of the pump in the 4-cylinder engine. It is a Type VE Bosch pump. The prototype pump was not equipped with a cold-start device.

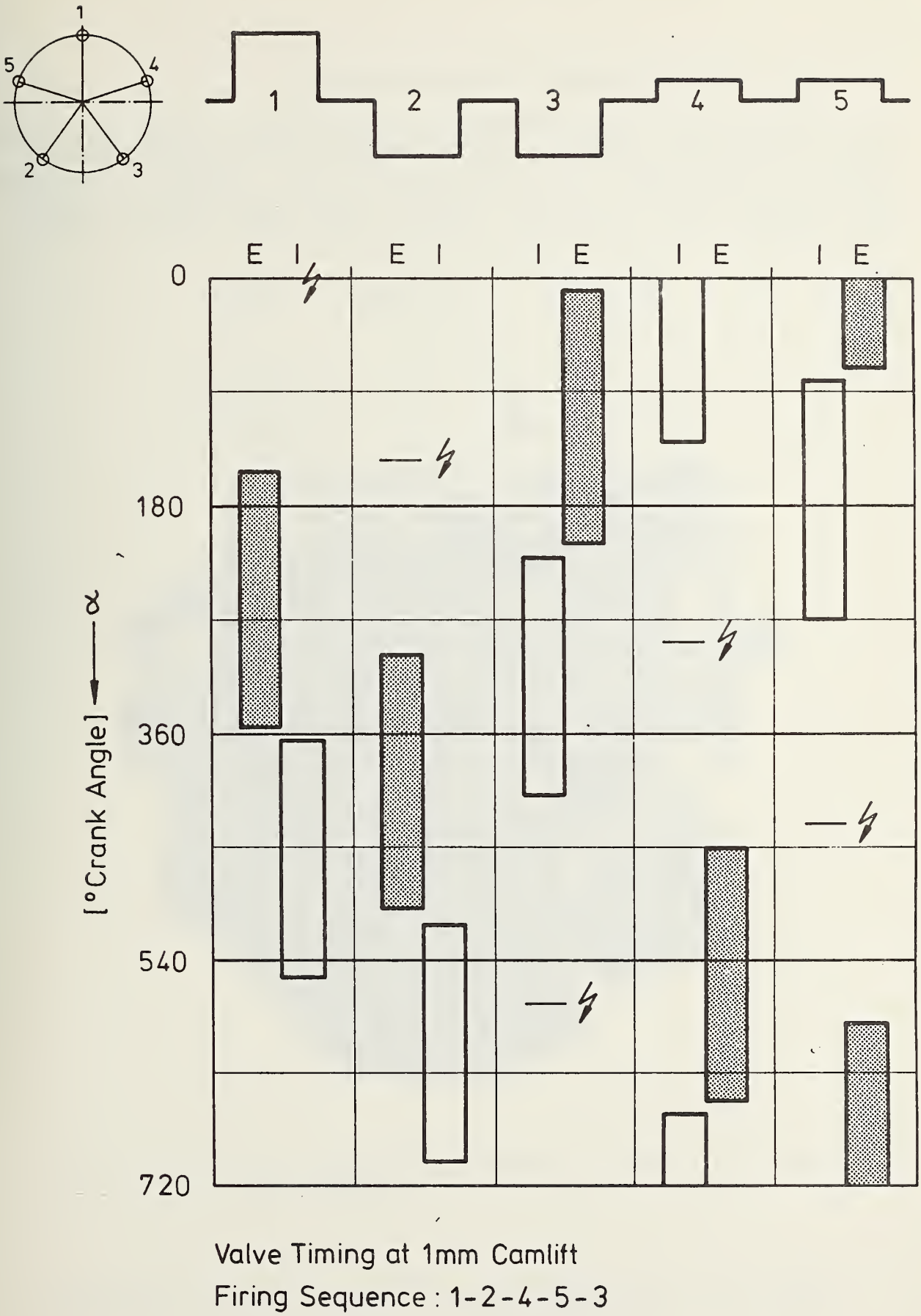

FIGURE 5.1-50: FIRING SEQUENCE AND VALVE TIMING OF THE 5-CYLINDER ENGINE

5.1.4 6-Cylinder Naturally-Aspirated Engine

Similar to the 5-cylinder engine, the 6-cylinder prototype diesel engine has the larger 79.5 mm bore. Like the 5-cylinder engine, the combustion process was optimized for the larger cylinder size. Figures 5.1-51 through 5.1-53 show the cylinder design. Unlike in the 4- and 5-cylinder engine, the injection pump is driven by a separate toothed belt from the back of the camshaft.

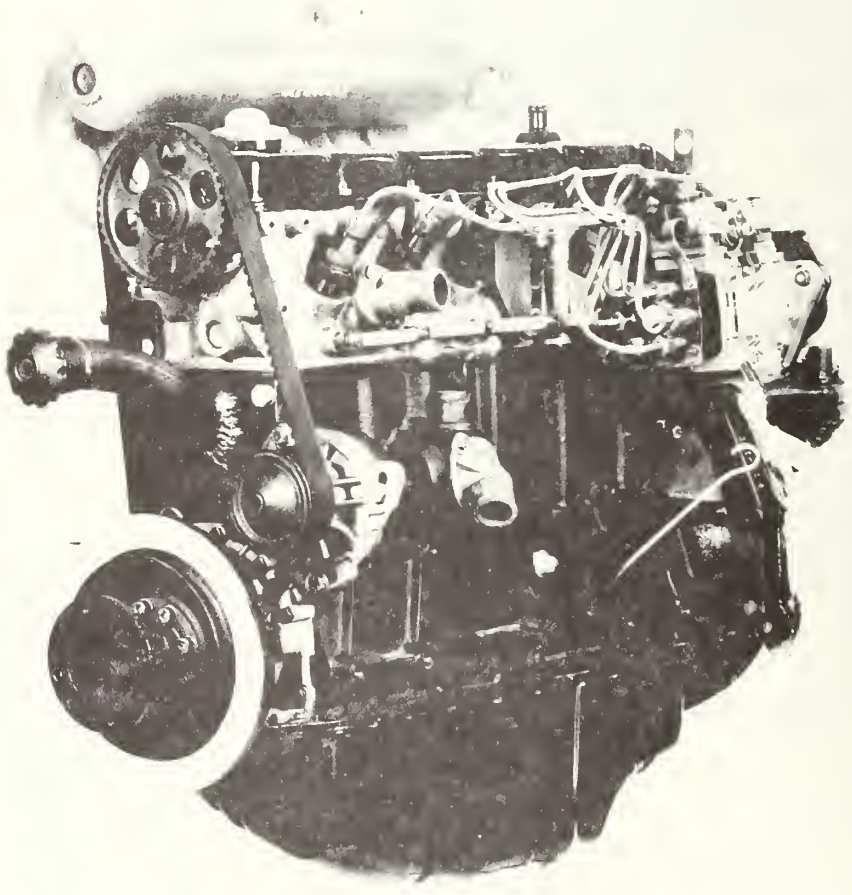

FIGURE 5.1-51: 6-CYLINDER NATURALLY-ASPIRATED ENGINE - SIDE VIEW - INJECTION PUMP

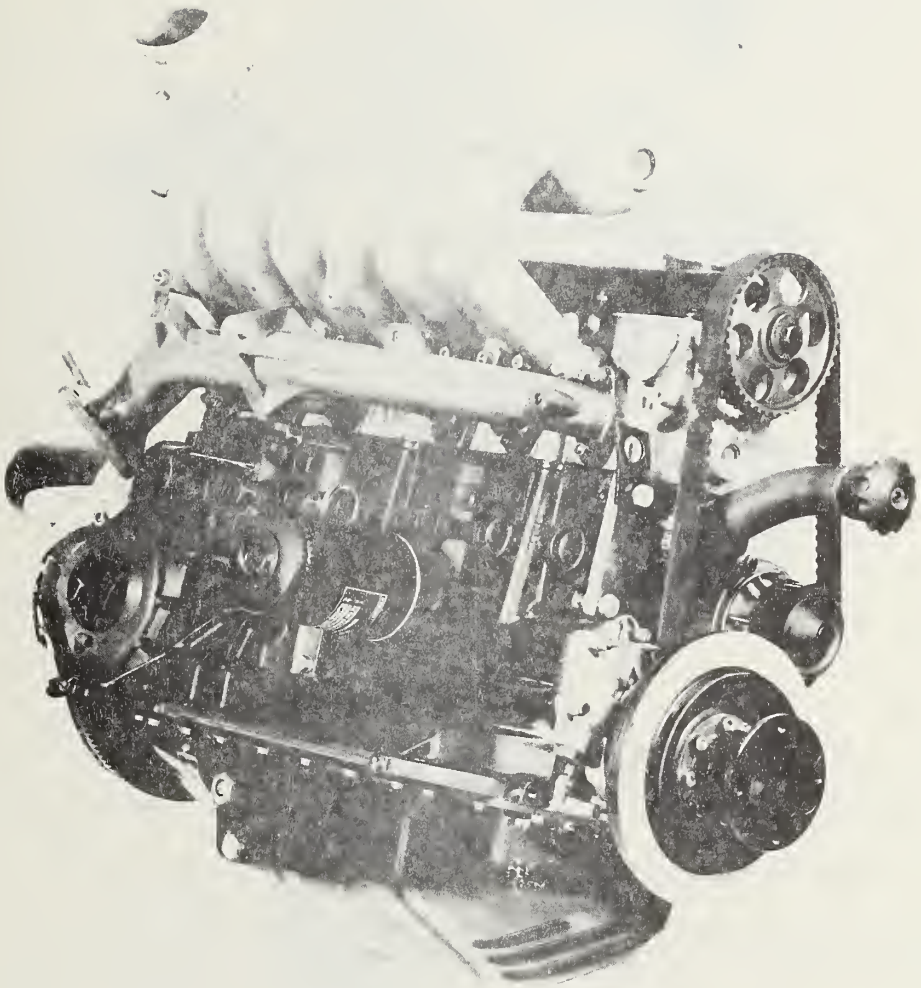

FIGURE 5.1-52: 6-CYLINDER NATURALLY-ASPIRATED ENGINE - SIDE VIEW - INLET MANIFOLD

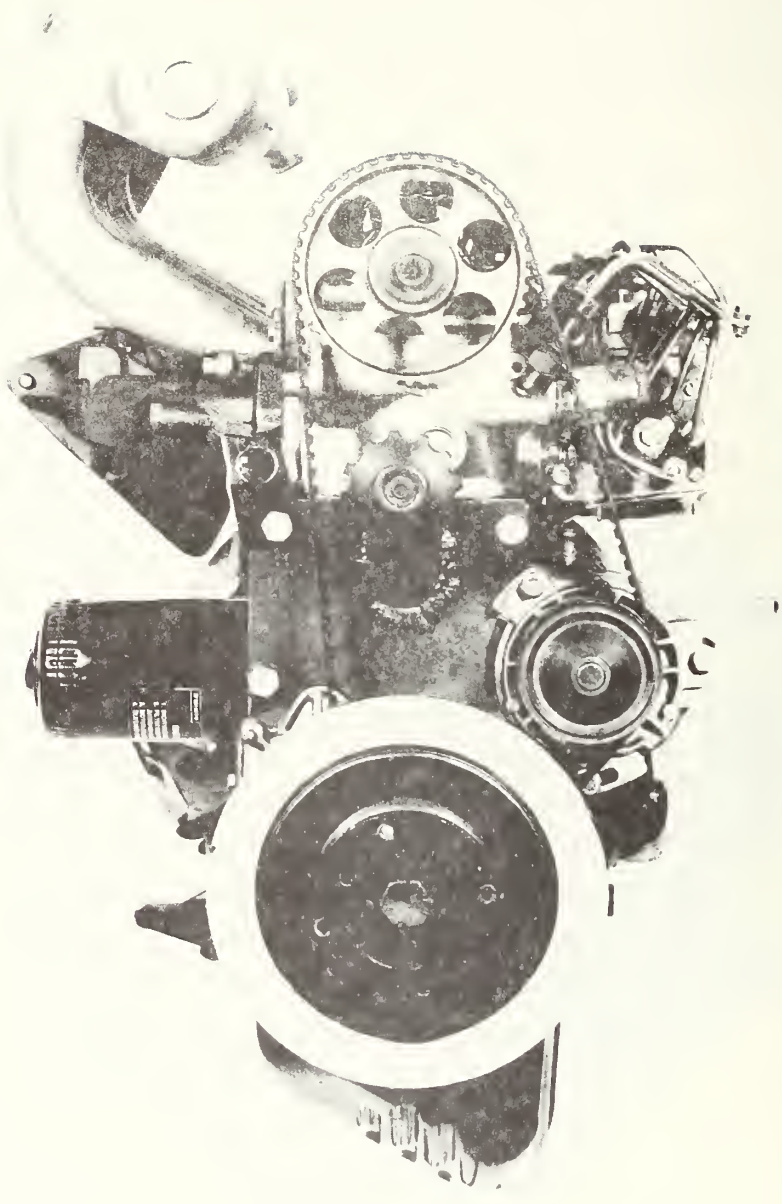

FIGURE 5.1-53: 6-CYLINDER NATURALLY-ASPIRATED ENGINE - FRONT VIEW

5.1.4.1 Technical Data

6-Cylinder In-Line Naturally-Aspirated Engine

Swept Volume	2.387 l
Bore	76.5 mm
Stroke	86.4 mm
Stroke/Bore Ratio	1.13
Cylinder Volume	397 cm^3
Compression Ratio	23
Firing Sequence	1 - 5 - 3 - 6 - 2 - 4
Power (DIN)	58.8 kW (80 HP)
Rated Speed	4,800 rpm
Specific Power Output	24.5 kW/l (33.3 HP/l)
Maximum Torque	147 Nm at 2,800 rpm
Maximum Mean Effective Pressure	7.7 bar
Mean Piston Velocity at Rated Speed	13.8 m/sec
Engine Weight*	187 kg
Weight-to-Horsepower Ratio	3.18 kg/kW (2.33 kg/HP)
Length, Width, Height	780 x 490 x 780 mm
Power-to-Volume Ratio	197.7 kW/m^3 (268.9 HP/m^3)
Oil Capacity	7.7 l

*including clutch, intake and exhaust manifold, airfilter, oil, generator; excluding cooling system, coolant, starter motor.

5.1.4.2 Cylinder Block and Crankshaft Drive

The crankshaft of the 6-cylinder diesel engine has 6 journals in three planes with uniform ignition spacing of 120^{o}. There are no exterior effects of free mass forces or moments. All crank journals are fully counter-weighted to reduce bending stresses. The crankshaft runs in seven main bearings.

The main bearing diameter was increased from 54 to 58 mm compared with the 4-cylinder engine in order to provide for sufficient torsion resistance of the comparatively long crankshaft. A torsional vibration damper is mounted on the front crankshaft journal. The piston pin diameter was increased from 22 mm (4-cylinder engine) to 24 mm.

The connecting rod length of 136 mm and the crankcase height of 220 mm are the same as those in the 4-cylinder engine. This design feature permits production on the same line as the 4-cylinder unit. Therefore, the compression height of the piston was to be decreased by 3.2 mm in line with the increase of the crank radius. The crank ratio λ is 0.318.

The cylinder block casting (Figure 5.1-54) contains the following components:

- Water pump housing
- Thermostat housing
- Bypass system
- Oil filter support.

This eliminates some hoses and seals and thus reduces the cost of production and susceptibility to trouble.

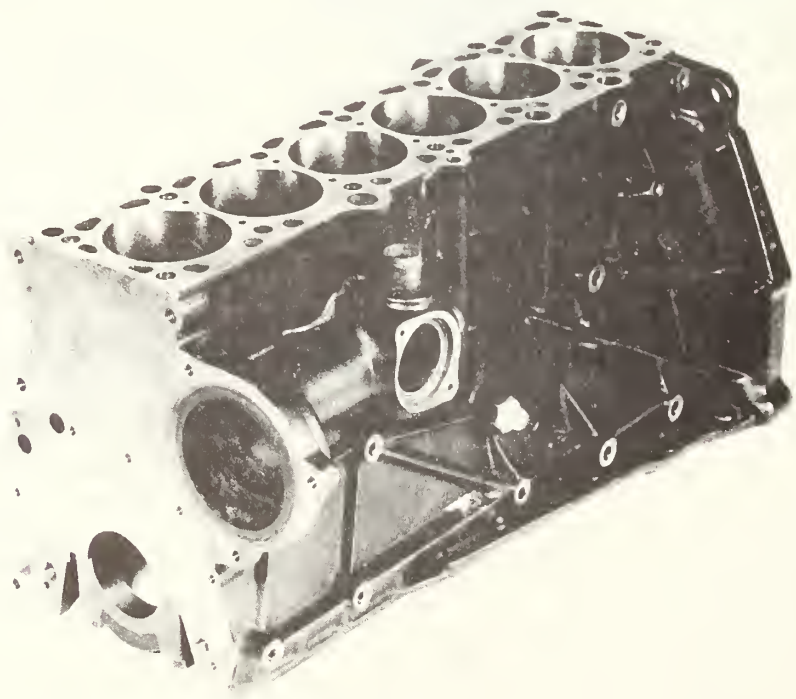

FIGURE 5.1-54: CYLINDER BLOCK

5.1.4.3 Cylinder Head

The cylinder head of the 6-cylinder engine is largely identical with that of the 5-cylinder. Both heads can therefore be processed on one transfer line. Figure 5.1-55 shows the cylinder with the intake manifold.

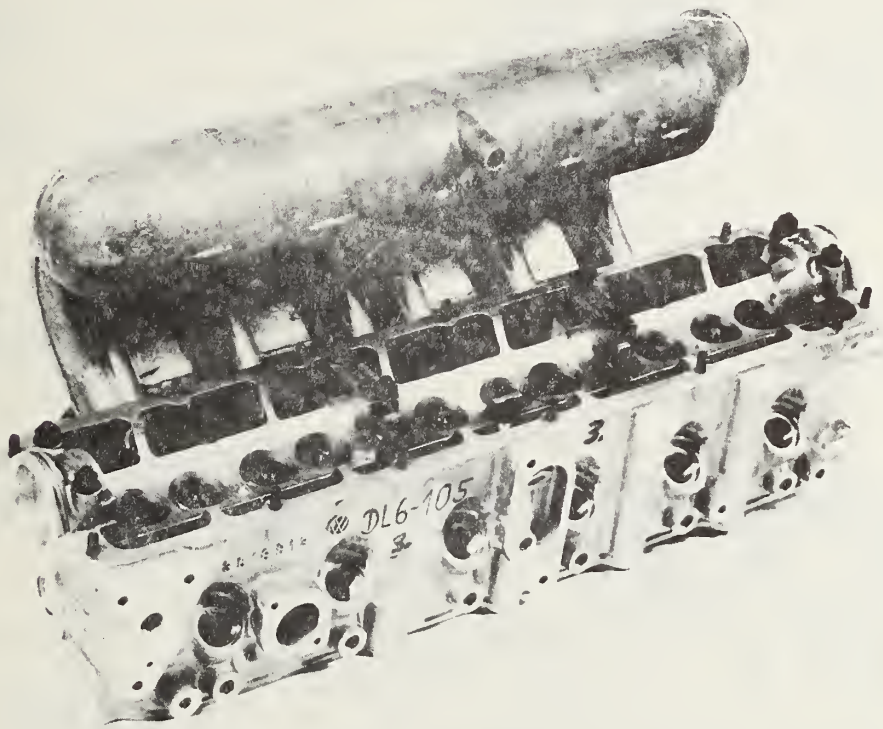

FIGURE 5.1-55: CYLINDER HEAD FOR 6-CYLINDER ENGINE

5.1.4.4 Toothed-Belt Drive

The injection pump was placed at the rear of the 6-cylinder diesel engine in order to leave enough space up front for auxiliary units, such as air conditioner compressor, vacuum pump, and hydraulic pump for power-assisted steering system. The number of auxiliary units required in the vehicle size class that is powered by a 4-cylinder engine is less, e.g. the Rabbit does not need a power-assisted steering system.

Tests on the 6-cylinder engine have shows that no adverse vibrations occur in the toothed-belt drive despite the comparatively long camshaft. The higher production cost caused by the additional toothed-belt and one gear were accepted because of the comparatively large number of required auxiliary units in the vehicle size that can be powered by this engine. Those auxiliary units generally run at speeds that are equal to or higher than the crankshaft speed. This is the reason why the camshaft is not so well suited to drive these auxiliary units. Another advantage of the location at the rear end of the engine is that the gasoline variation of this unit can have an identical front toothed-belt drive.

Figure 5.1-56 is a schematic of the toothed-belt drive. The camshaft is adjusted with a bar that is inserted in a groove at the rear end of the camshaft. The same procedure is used for the 4- and 5-cylinder engine. Cambelt tension is adjusted by the eccentrically-mounted water pump. A guide pulley is installed near the crankshaft so that the cambelt is wrapped further around the crankshaft gear. This ensures that the cambelt does not jump a tooth.

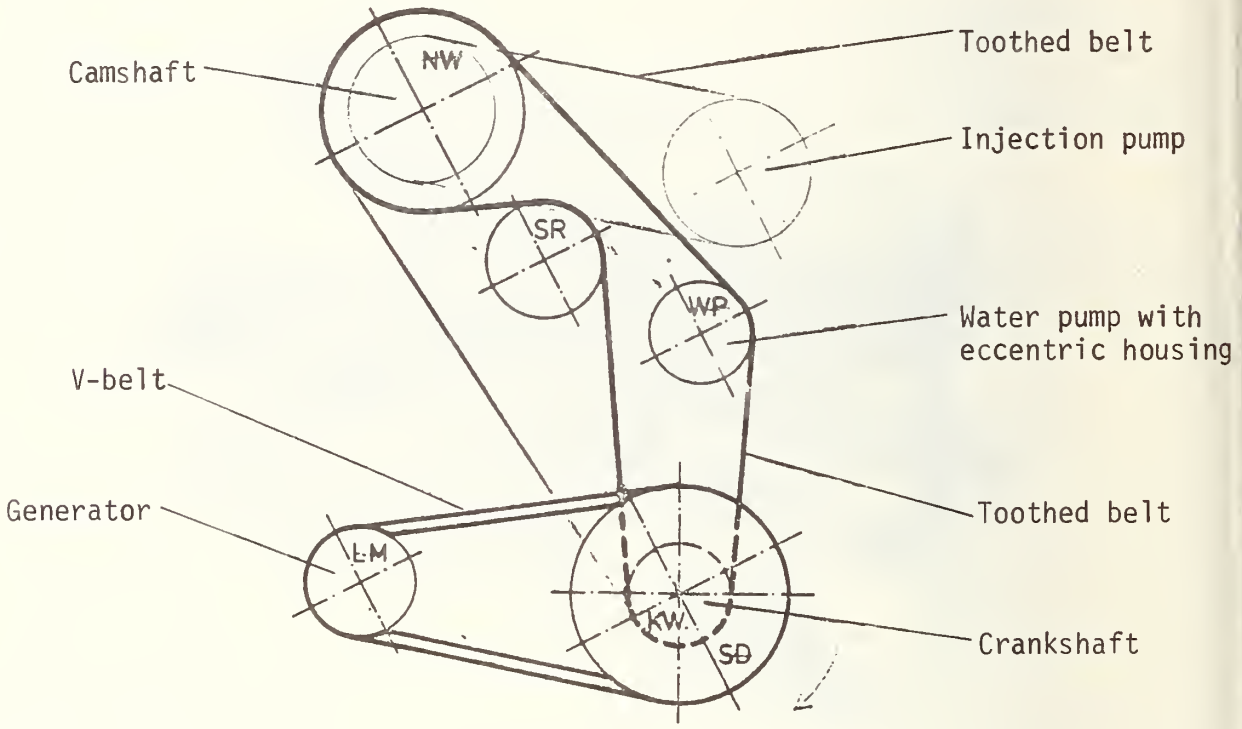

FIGURE 5.1-56: TOOTHED-BELT DRIVE, 6-CYLINDER ENGINE

The injection pump is driven from the camshaft by a toothed belt that engages two pulleys of equal diameter with 33 theeth each. The injection pump is supported by a cast-iron bracket on the side of the cylinder block and crankcase. An additional support is located at the distributor body. Longitudinal holes permit vertical adjustment of the pump to allow for production tolerances.

5.1.4.5 Accessories

The oil pump is the crescent vane pump used in the 5-cylinder gasoline engine.

The distributor-type injection pumps for various numbers of cylinders are made by the Bosch Co. in accordance with the modular unit system. The EP/VA6-pump with cold-start accelerator is described in reference .

The secondary mass of the vibration damper is the V-belt pulley. There are other 2 V-belt grooves for additional auxiliary units. A 1.8 kW starter was installed to ensure safe cold-start behavior at low exterior temperatures.

The aluminum intake manifold basically is the same as that in the 5-cylinder diesel engine. It has a plenum chamber from where the individual ram pipes connect to the cylinders. The performance characteristics of the engine are affected by the length, diameter, and curvature of the ram pipes.

Three exhaust ports run into one exhaust manifold. Cylinders 1, 2, and 3 are combined, as well as cylinders 4, 5, and 6 (Figure 5.1-57). There is an interval of 240^{o} between the firing of the cylinders for each exhaust manifold when the firing sequence is 1 - 5 - 3 - 6 - 2 - 4. This means that there is no interference between the individual exhaust gas streams.

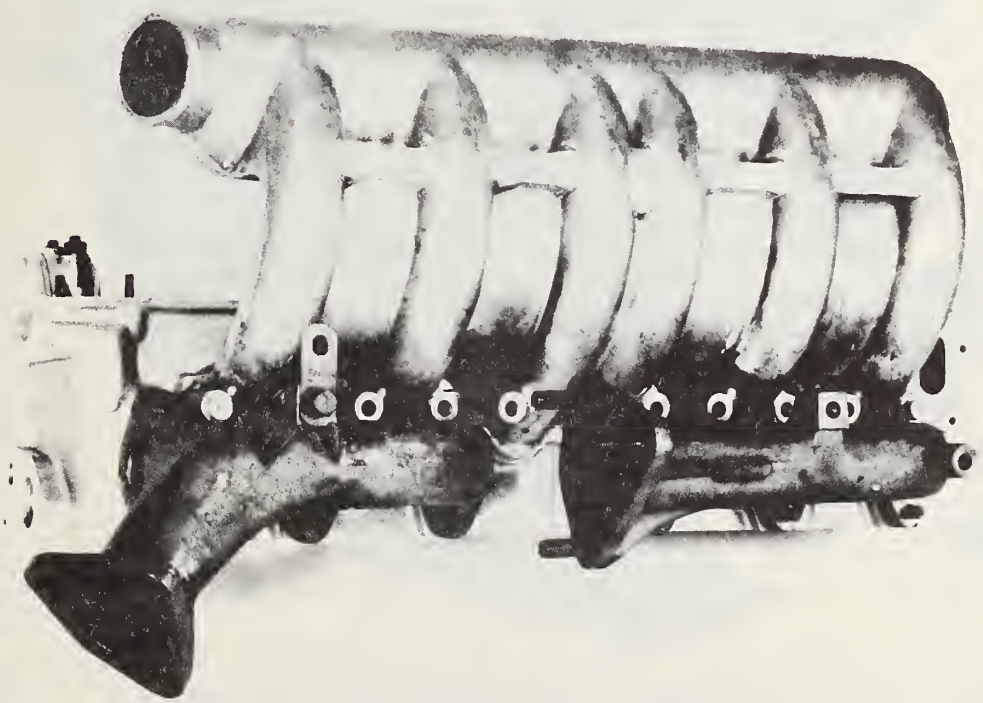

FIGURE 5.1-57: 6-CYLINDER ENGINE - INTAKE AND EXHAUST MANIFOLD

5.1.5 6-Cylinder Turbocharged Engine

The performance level of the 6-cylinder naturally-aspirated engine was raised by turbocharging. This required the same modifications that had been made to the 4-cylinder TC version of the engine. Figures 5.1-58 and 5.1-59 show the design of the prototype engine.

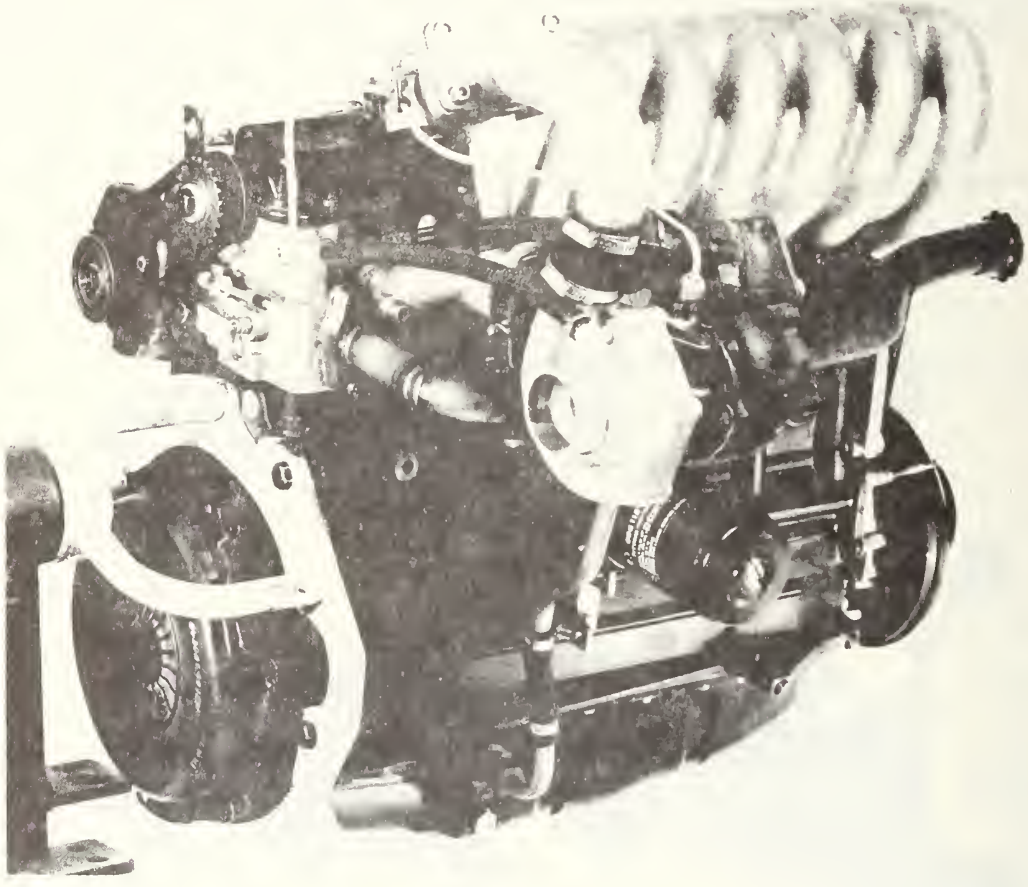

FIGURE 5.1-58: 6-CYLINDER TURBOCHARGED PROTOTYPE ENGINE
Side view showing compressor inlet

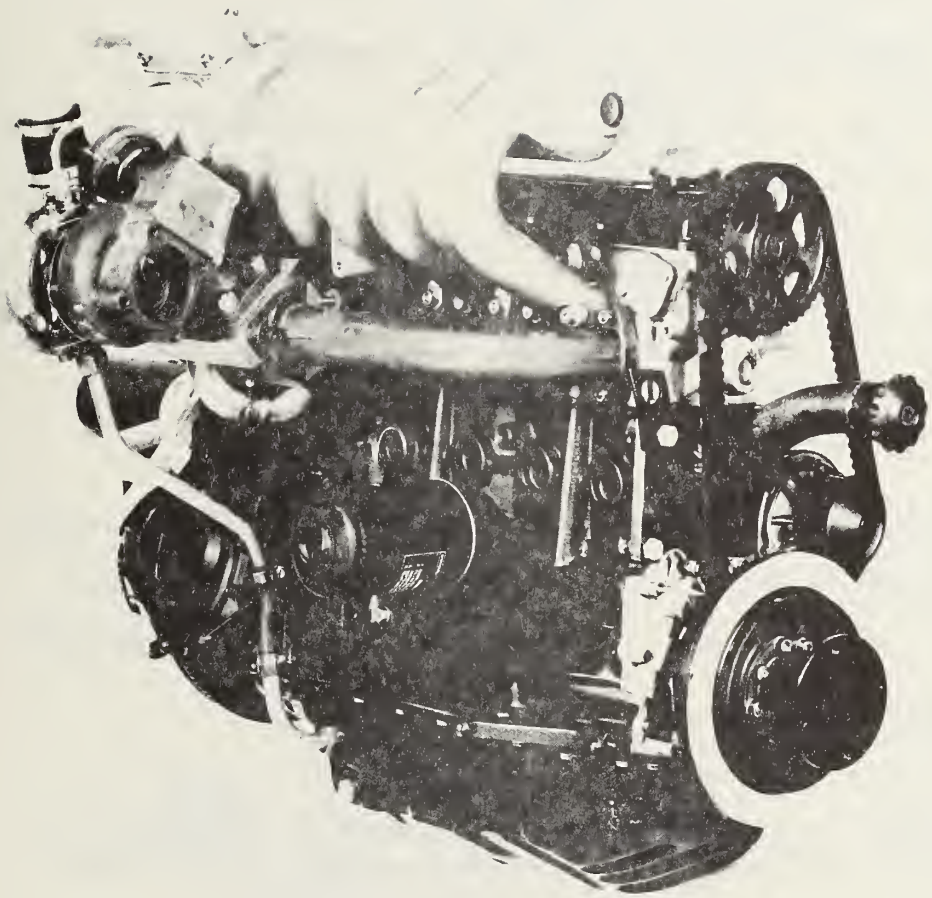

FIGURE 5.1-59: 6-CYLINDER TURBOCHARGED ENGINE - FRONT VIEW

Technical Data: 6-Cylinder In-Line Turbocharged Engine

Swept Volume	2.387 l
Bore	76.5 mm
Stroke	86.4 mm
Stroke/Bore Ratio	1.13
Cylinder Volume	397 cm^3
Compression Ratio	23
Firing Sequence	1 - 5 - 3 - 6 - 2 - 4
Power (DIN)	78 kW (106 HP)
Rated Speed	4,800 rpm
Specific Power Output	56.1 kW/l (41.2 HP/)
Maximum Torque	210 Nm (21.5 kpm) at 3,300 rpm
Maximum Mean Effective Pressure	10.3 bar
Mean Piston Velocity at Rated Speed	13.8 m/s
Engine Weight*	195 kg
Weight-to-Horsepower Ratio	2.45 kg/kW (1.8 kg/HP)
Length, Width, Height	780 x 638 x 800 mm
Power-to-Volume Ratio	192 kW/m^3 (267 HP/m^3)
Oil Capacity	7.7 l

*including clutch, intake and exhaust manifold, airfilter, oil, generator; excluding cooling system, coolant, starter motor

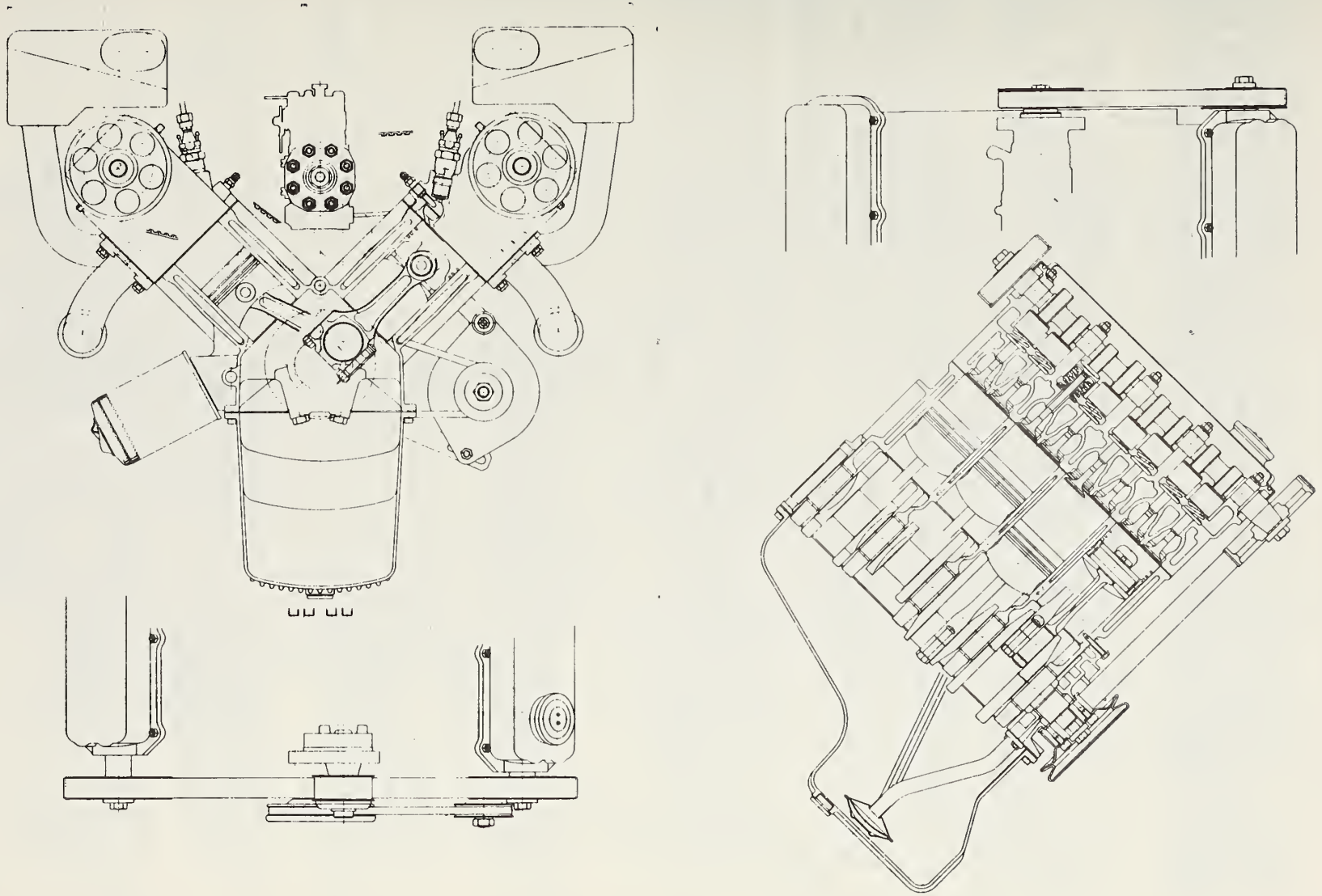

FIGURE 5.1-60: V-8 NATURALLY ASPIRATED DIESEL ENGINE 100 HP

5.1.6 V-8 Naturally-Aspirated Engine

The drawing in Figure 5.1-60 shows a water-cooled light-weight V-8 diesel engine. The engine has a V-angle of 90° and is designed on the basis of the present 1.5-liter four-cylinder engine with overhead camshaft and a cylinder spacing of 88 mm. The production of the individual engine components was to make the largest possible use of the production facilities of the present 4-cylinder engines.

The injection nozzles and glow plugs point towards the middle of the engine. Intake and exhaust manifolds are located on the outside. Each intake manifold is equipped with an air filter element. The distributor injection pump is located in the V formed by the two banks of cylinders. It is driven by a toothed belt from one of the overhead camshafts.

The two overhead camshafts are driven by a toothed belt. The back of the toothed belt drives the water pump pulley. A roller-type tensioner is used to provide belt tension. A special high-strength toothed belt is used to prevent belt breaking and jumping. This is particularly important because of the narrow space between valve and piston at TDC which is caused by the high compression in the diesel (23.5 : 1). The alternator is driven by a V-belt.

5.1.6.1 Technical Data, V-8 Engine

Displacement	2942 cm^3
Bore	76.5 mm
Stroke	80 mm
Stroke/Bore Ratio	1.05
Cylinder Volume	367.7 cm^3
Cylinder Spacing	88 mm
V-Angle	90°
Compression Ratio	23
Ignition Order	1 - 5 - 8 - 3 - 7 - 4 - 2 - 6
Output	73.5 kW (100 HP)
Specific Output	24.5 kW/l (33.3 HP/l)
Rated Engine Speed	4500 rpm
Mean Piston Velocity	12 m/s
Max. Ignition Pressure	75 bar
Weight (Estimated)	200 kg
Length, Width, Height	512 x 775 x 712 mm
Required Space	0.28 m^3
Weight-to-Horsepower Ratio	2.72 kg/kW (2.0 kg/HP)
Power-to-Volume Ratio	263 kW/m^3 (357 HP/m^3)

5.1.6.2 Crankshaft

The draft design calls for a forged, heat-treated crankshaft which is nitrided for 50% increased life. Because of the 88-mm cylinder spacing which means that production cylinder heads can be used, the design includes a short crankshaft with paired connecting rod journals at 90^{o} offset.

5.1.6.3 Connecting Rod

The design uses the forged connecting rod from the 5- and 6-cylinder diesel engine with a length of 176 mm and a stroke-connecting-rod ratio of 40/176 = 0.294. The piston pin bore was enlarged to 24 mm, and the connecting rod bearing bore was enlarged to 48 mm. The width of the connecting rod journal was reduced to 19.6 mm because each crank pin accommodates two connecting rods.

5.1.6.4 Piston

The design includes autothermatic pistons from the 4-cylinder engine. The piston skirt was adapted to the larger radius (76 mm) of the crankshaft. The upper ring is mounted in a cast-in ring carrier. The piston pin has a diameter of 24 mm. The upper ring is lapped to provide for better sealing.

5.1.6.5 Cylinder Block

An oil pump (crescent pump) is mounted on the front end of the crankshaft at the cylinder block. The oil is drawn from the pan via a suction pipe and is then forced through the oil filter into the mail oil gallery from where it reaches the main bearings.

One bore supplies oil to the cylinder head through the cylinder-head gasket and through a lateral bore in the cylinder head to the camshaft bearings. Cam lobes, lifter, and valves are splash-lubricated from the camshaft bearings. Oil returns to the oil cast-aluminum pan through three large bores in the cylinder head and block.

The cast-iron cylinder block extends by 58 mm below the crankcase center. It is reinforced by fins. The left cylinder bank of the cylinder block is offset by 19 mm versus the right cylinder block towards the vehicle front. The rear of the cylinder block has five bores for the transmission.

The main bearing caps are fastened with two bolts. The machined surfaces on the sides of the cap and on the block absorb the lateral forces introduced into the caps. The center main bearing is also the thrust bearing. Small notches must be provided in the lower cylinder bores to provide clearance for the crank throws.

5.1.6.6 Cylinder Head

The cylinder head design is based on the four-cylinder production engine of the Rabbit diesel. It is made of cast aluminum and has pressed-in valve seat rings, valve guides, and swirl chamber inserts that are fixed by a ball mounting. The overhead camshaft actuates the valves view bucket tappets with adjustment shims. The valves are closed by two concentric valve springs. The intake valve disc has a diameter of 34 mm, and the diameter of the exhaust valve disc is 31 mm. The valves are mounted in parallel.

The production cylinder head is mounted to the right cylinder bank of the V-8 engine. The cylinder head on the left bank is reversed and has a second exit. The flange for the second exit is reinforced. This means that both cylinder heads can be made from the same blank, and that the only difference between the two cylinder heads is the second exit.

5.1.7 Exhaust Gas Recirculation Device

The recirculated exhaust gas is introduced into the exhaust system through a throttle valve. The throttle valve is connected to the accelerator pedal through a bowden cable. This application is especially suited for the passenger-car speed governor because it increases fuel injection in direct proportion to the accelerator travel. However, problems are posed in the idle range. Figures 5.1-61 through 5.1-64 show the 4-cylinder TC engine with EGR device. The two inlet ports in the mixing chamber upstream of the compressor intake are the air-intake port and blow-by recirculation port. The recirculated exhaust gas is introduced from the rear into the mixing chamber.

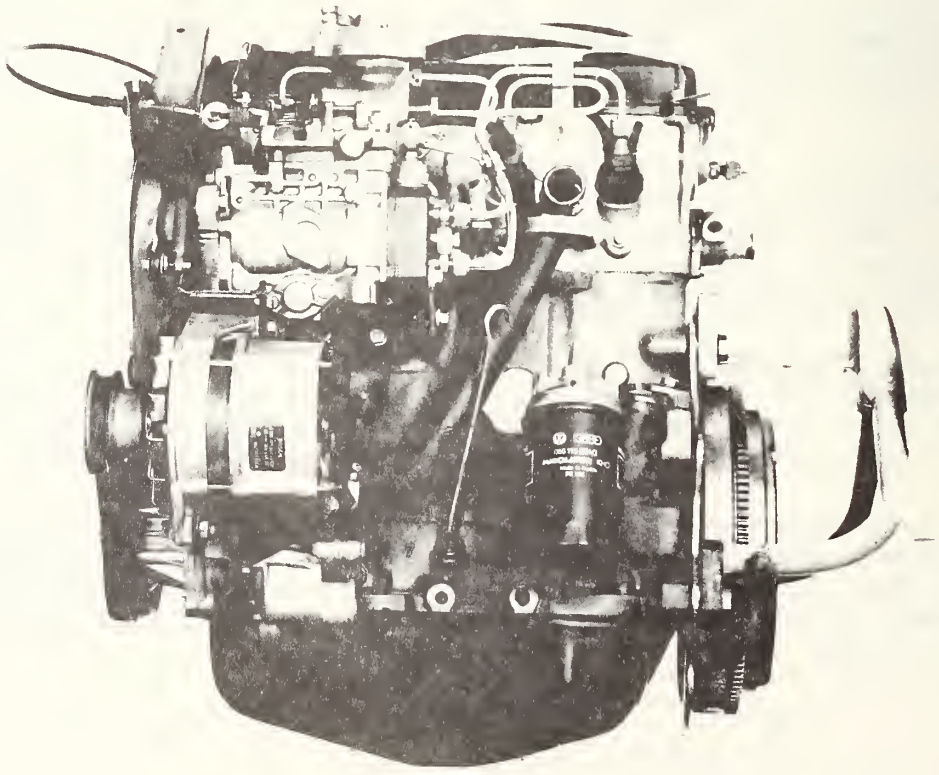

FIGURE 5.1-61: 4-CYLINDER TURBOCHARGED EGR ENGINE - SIDE VIEW - INJECTION PUMP

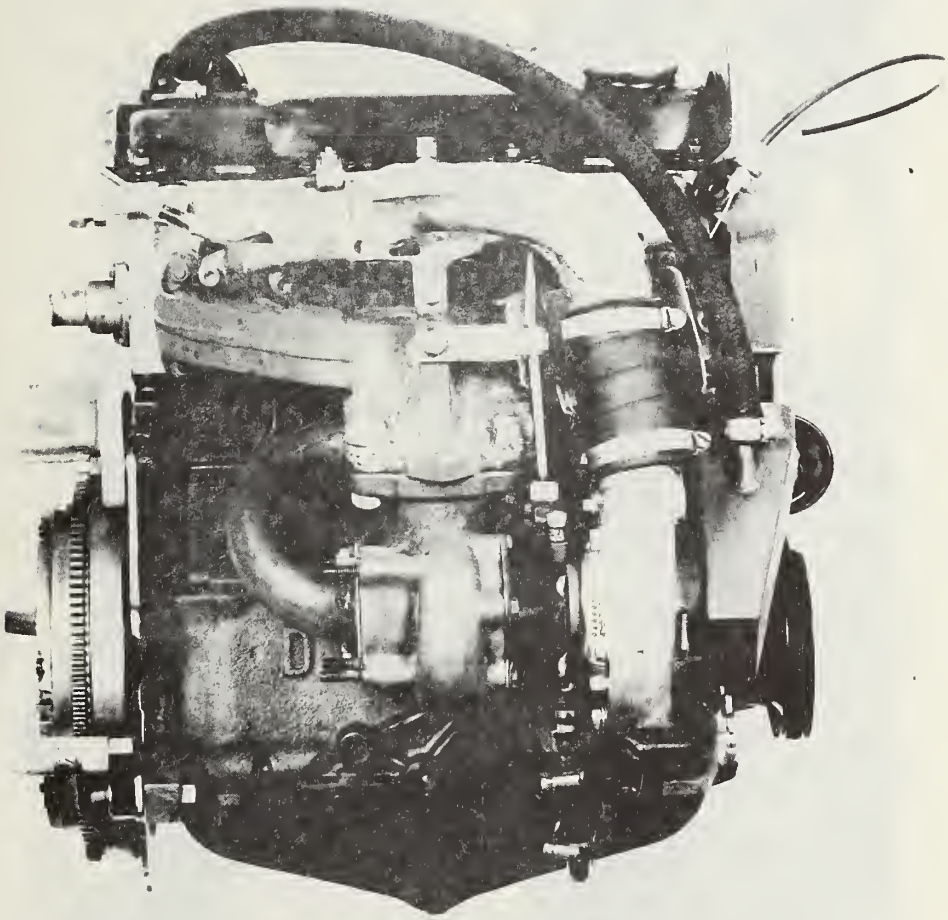

FIGURE 5.1-62: 4-CYLINDER TURBOCHARGED EGR ENGINE - SIDE VIEW - TURBOCHARGER AND EGR DEVICE

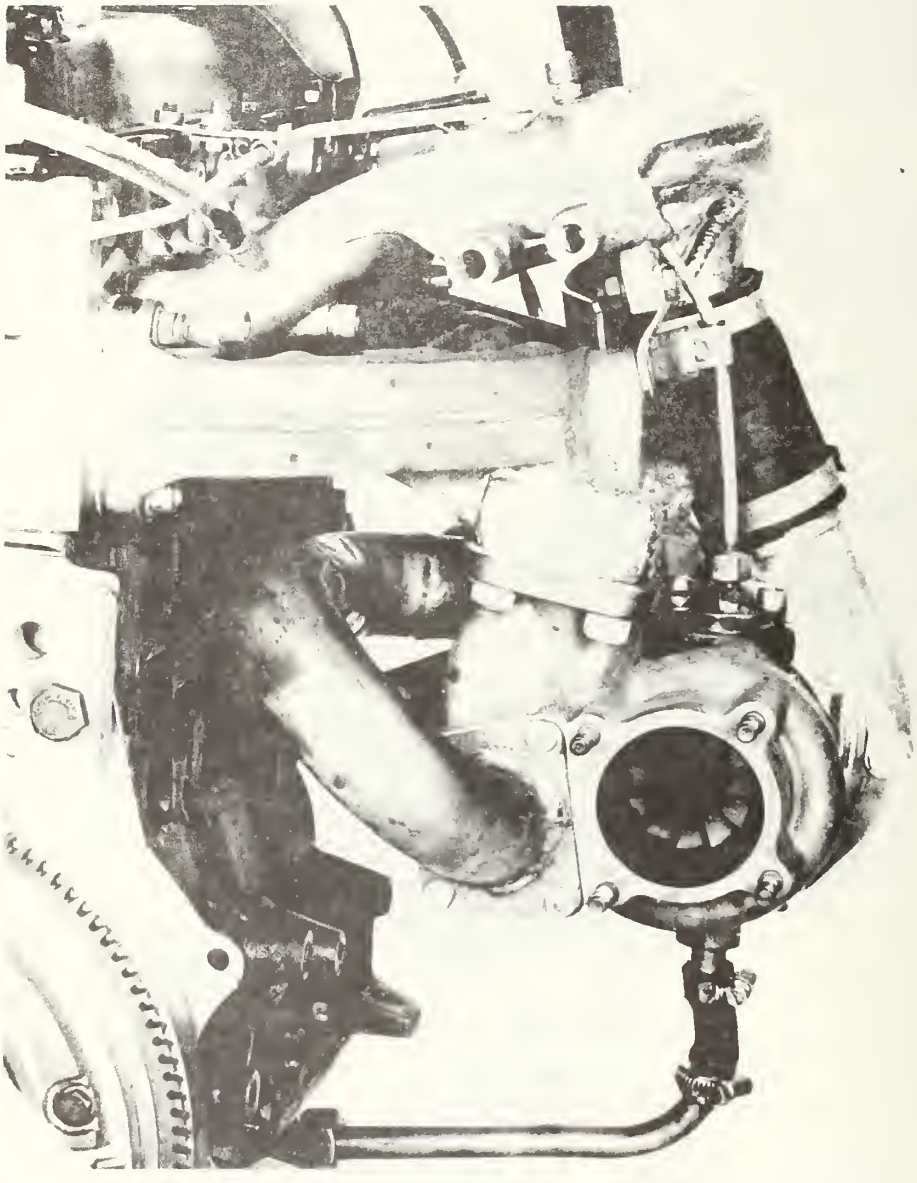

FIGURE 5.1-63: 4-CYLINDER TURBOCHARGED EGR ENGINE DETAIL: GAS CIRCULATION

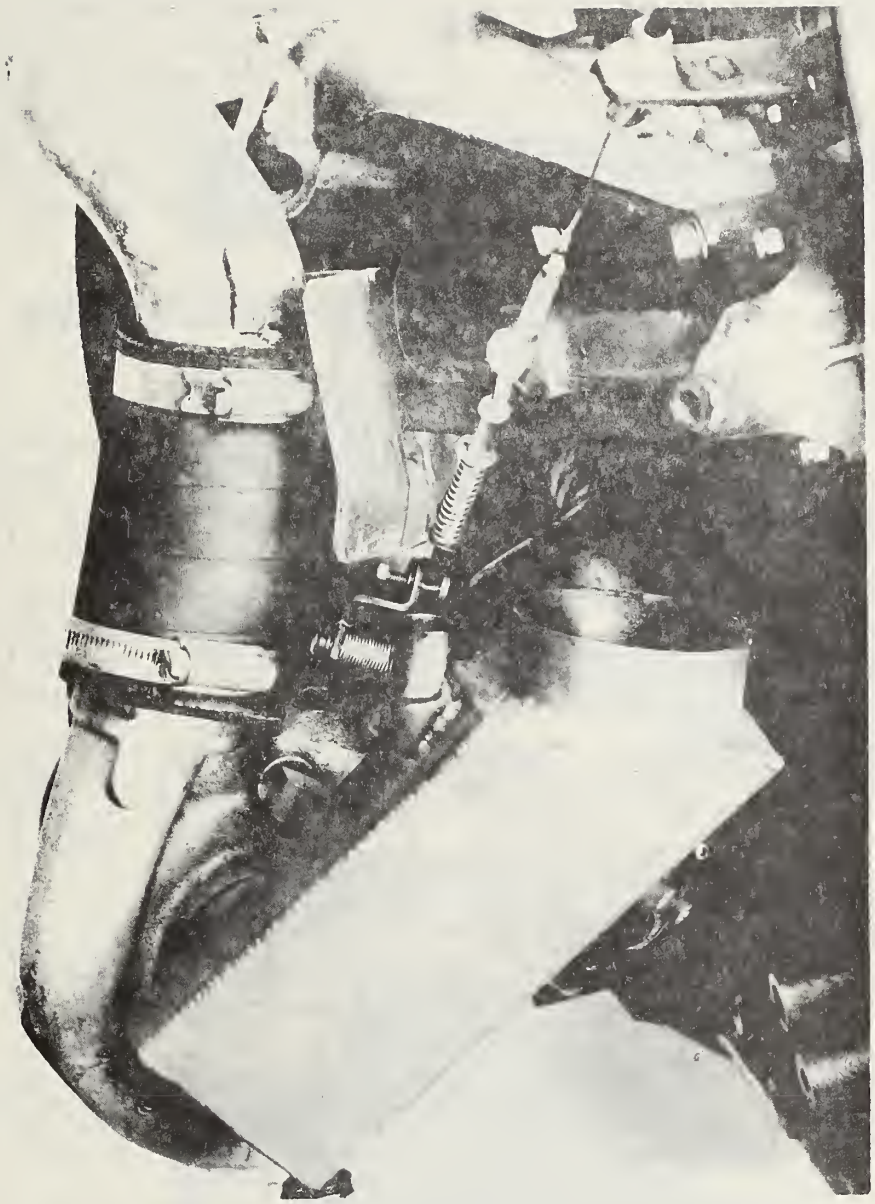

FIGURE 5.1-64: 4-CYLINDER TURBOCHARGED EGR ENGINE, MIXING CHAMBER AND CONTROL

The distribution of the recirculated exhaust gas to the individual cylinders does not pose any problems if the turbocharger is used as a mixer for exhaust gas and air. A uniform distribution poses problems in the NA engine with EGR. A satisfactory solution could not be found in the short time available for this project. Figure 5.1-65 shows the measured distribution for a mesh of speed/torque operating points. Each square is located at a corresponding speed/torque position on a steady-state engine map. The abscissa of the squares shows the 4-cylinders (from 1 to 4). The ordinates show the deviation from the mean EGR within -50% and +50%. Uniform distribution was achieved at idel only. A reduced amount of exhaust gas was introduced into the fourth cylinder in all other operating points.

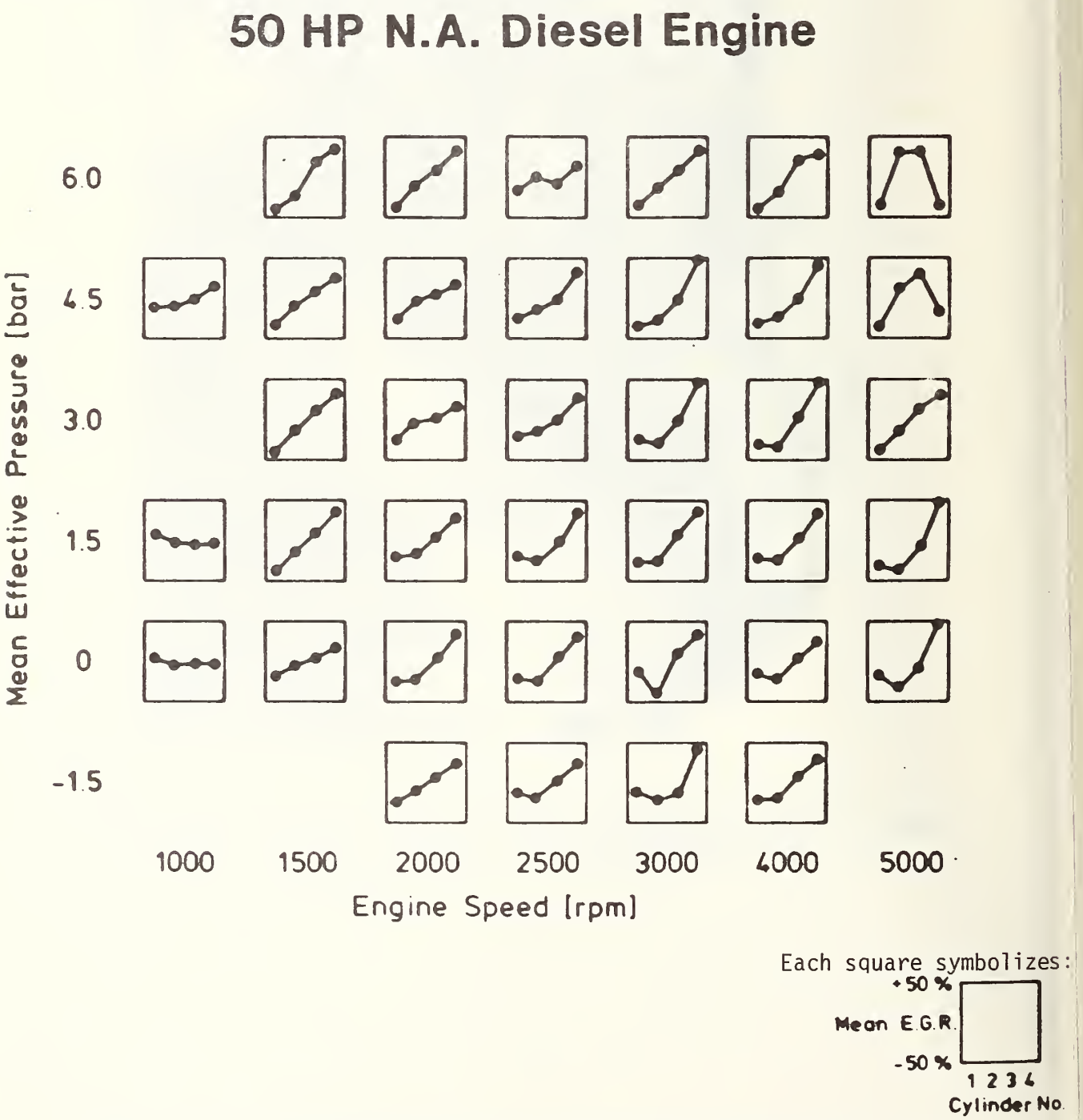

FIGURE 5.1-65: DISTRIBUTION OF THE RECIRCULATED EXHAUST GAS TO THE 4 CYLINDERS AT VARIOUS ENGINE SPEEDS AND TORQUES.

The pictures in Figure 5.1-66 show the EGR device of the naturally-aspirated engine. The exhaust gas enters the intake manifold from the left side (cylinder 1). The illustrations show an air filter after 600 miles.

Before

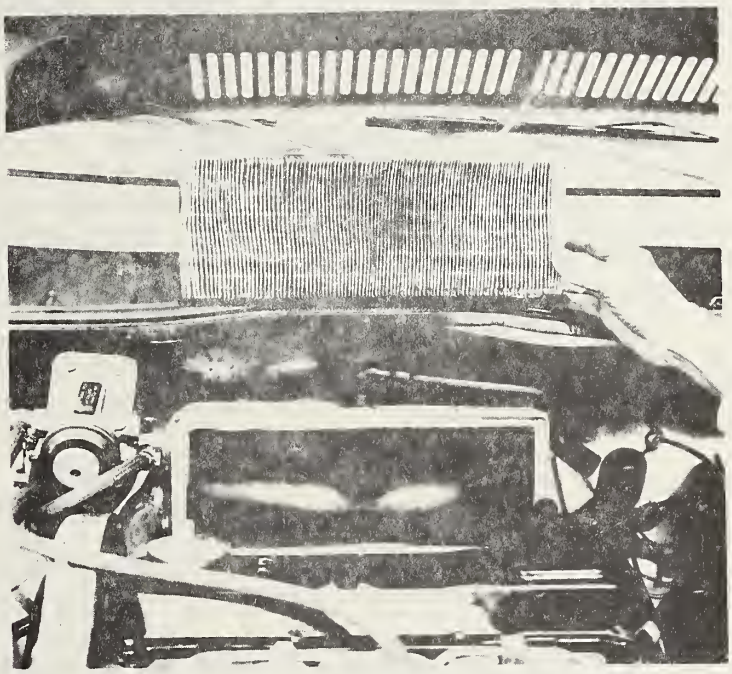

After 600 miles

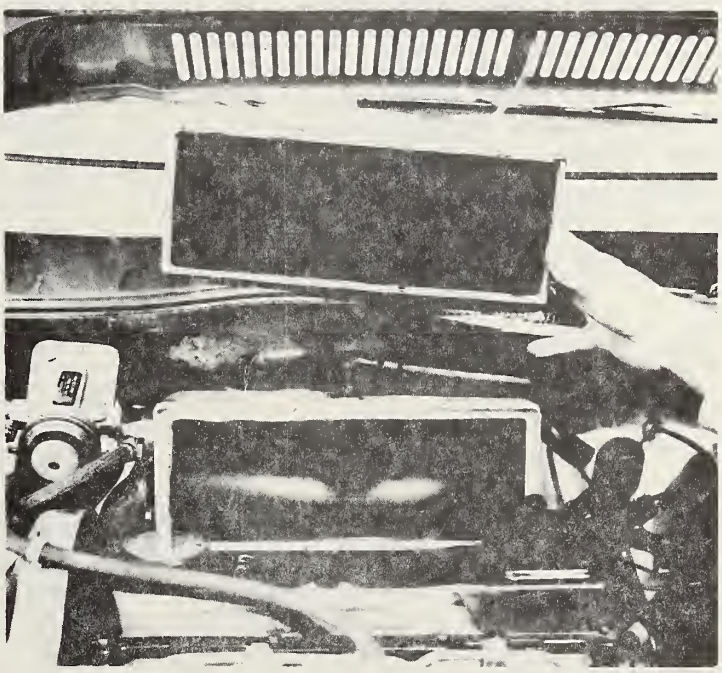

FIGURE 5.1-66: 4-CYLINDER NATURALLY-ASPIRATED ENGINE WITH EGR

5.2 TEST VEHICLES

The VW Rabbit, VW Dasher and Audi 100 were used as test vehicles for the engine/vehicle systems analyses.

VW Rabbit

The VW Rabbit is in the 2,250-lb. inertia-weight category. The vehicle dimensions are shown in Figure 5.2-1.

The vehicle has an all-steel unitized body/chassis configuration with bolt-on front fenders. The occupant compartment is designed as a safety cell, and the front and rear ends of the car are energy-absorbing elements. The vehicle is equipped with rack-and-pinion steering with energy-absorbing steering wheel and column. The front-wheel suspension consists of independent MacPherson struts with negative kingpin offset. The rear-wheel suspension system consists of an independent stabilizer axle with coil springs and shock absorbers. The tires are steel-belted, tubeless radial-ply tires. The power plant is a water-cooled, 4-cylinder transverse front-mounted engine. The vehicle has front-wheel drive and can be equipped with manual or automatic transmission.

VW Dasher

The VW Dasher is in the 2,500-lb. interia-weight class. The vehicle dimensions are shown in Figure 5.2-2.

The vehicle has an all-steel unitized body/chassis with bolt-on fenders. The occupant compartment is designed as a safety cell. The front and rear ends are energy-absorbing elements. The front-wheel suspension consists of independent MacPherson struts with stabilizer bar and negative kingpin offset. The car is equipped with rack-and-pinion steering with energy-absorbing elements. The rear-wheel suspension consists of a torsion crank axle with Panhard rod for lateral stability, and coil springs with shock absorbers. The tires are steel-belted, tubeless radial-ply tires. The power plant is a water-cooled, 4-cylinder in-line engine which is longitudinally mounted in front of the front axle and slanted at an angle of 20^{o}. The vehicle can be equipped with automatic or manual transmission. The car has front-wheel drive.

Audi 100

The Audi 100 is in the 3,000-lb. inertia-weight category. The vehicle dimensions are shown in Figure 5.2-3.

The vehicle has an all-steel unitized body/chassis with bolt-on front fenders. The occupant compartment is designed as a safety cell and the front and rear ends are energy-absorbing elements. The vehicle has independent front-wheel suspension arms, stabilizer, coil springs and telescopic shocks, and negative kingping offset. The rear-wheel suspension consists of a torsion crank axle, panhard rod for lateral stability, stabilizer and coil/shock absorbers. The car has rack-and-pinion steering with energy-absorbing elements. The engine is a 4-cylinder, water-cooled in-line engine and is longitudinally mounted in front of the front axle. The vehicle can be equipped with automatic or manual transmission. The car has front-wheel drive.

Vehicle dimensions:

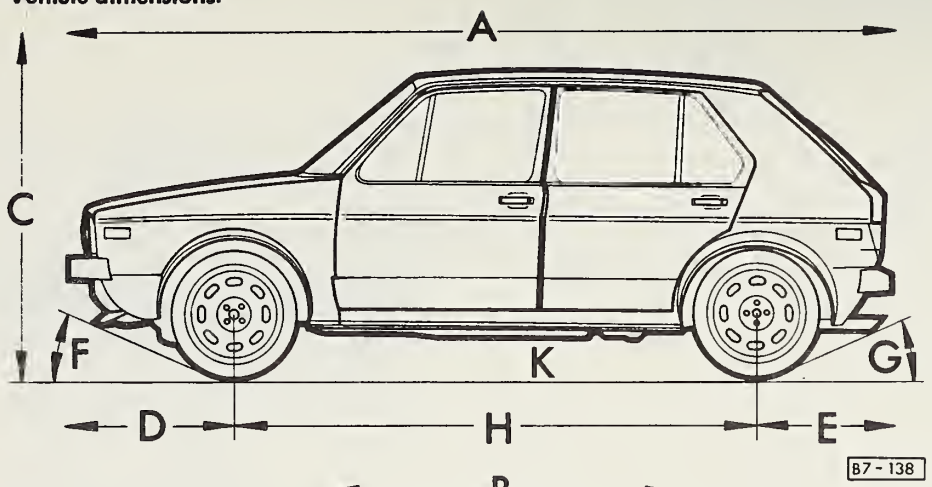

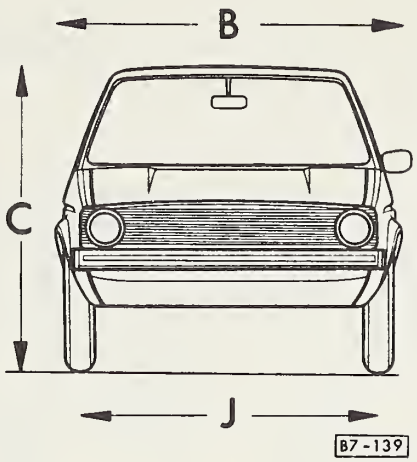

A — Length	155.3 in.	(3945 mm)
B — Width	63.4 in.	(1610 mm)
C — Height (unloaded)	55.5 in.	(1410 mm)
D — Overhang, front	32.9 in.	(830 mm)
E — Overhang, rear	27.2 in.	(693 mm)
F — Ramp angle, front	24°	
G — Ramp angle, rear	22.5°	
H — Wheelbase	94.5 in.	(2400 mm)
J — Front track	54.7 in.	(1390 mm)
Rear track	53.1 in.	(1350 mm)
K — Ground clearance	4.8 in.	(122 mm)

Measured at gross vehicle weight, except item C, which is measured at unladen weight.

Turning circle diameter — approximately 34.4 ft. (10.5 m) curb to curb.

FIGURE 5.2-1: VEHICLE DIMENSIONS (VW RABBIT)

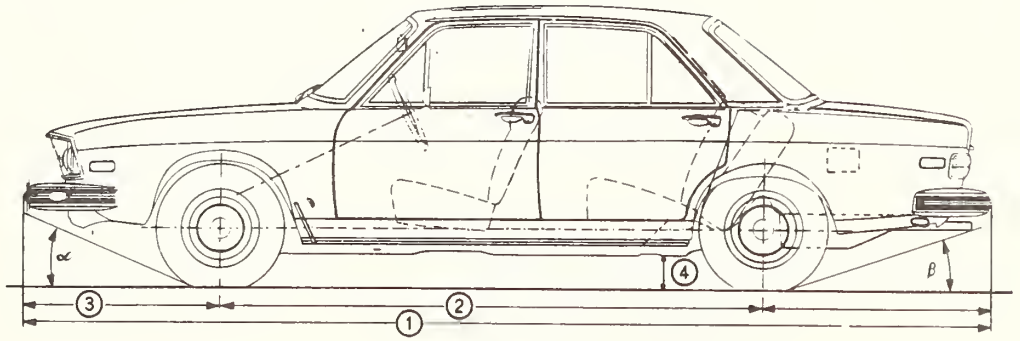

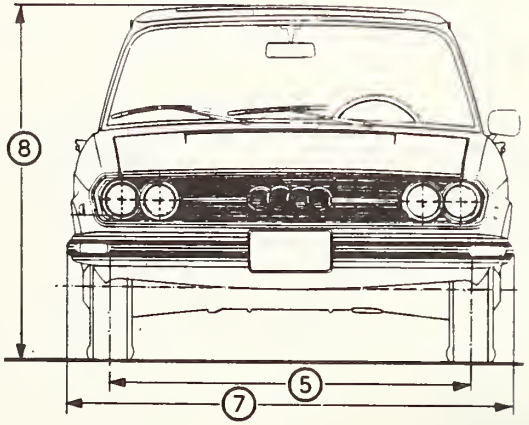

1 = 188.0 in./4774 mm
2 = 105.3 in./2675 mm
3 = 37.7 in./ 959 mm
4 = 5.8 in./ 147 mm*
5 = front 57.0 in./ 1448 mm
rear 56.1 in./ 1425 mm
7 = 68.0 in./1728 mm
8 = 53.2 in./1352 mm*

α = 26°*
β = 14° 30'*

FIGURE 5.2-3: VEHICLE DIMENSIONS (AUDI 100)

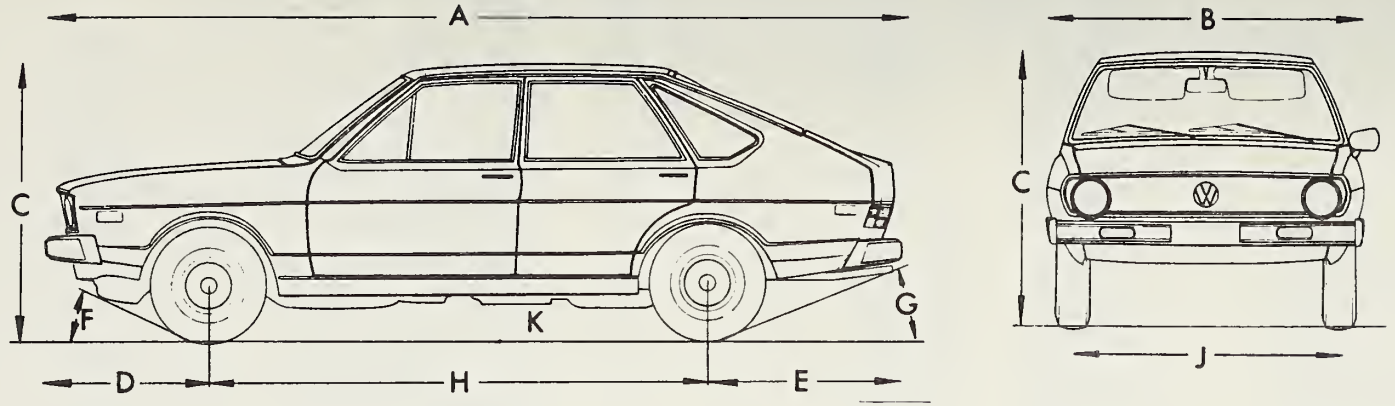

A – 172.4 in. (4380 mm)
B – 63.0 in. (1600 mm)
C – 53.5 in. (1360 mm)
D – 34.1 in. (865 mm)
E – 41.1 in. (1045 mm)
F – 26°
G – 13°
H – 97.2 in. (2470 mm)
J – 52.7 in. (1340 mm) Track at front
52.5 in. (1335 mm) Track at rear
K – 4.2 in. (107 mm) Sedan
4.8 in. (122 mm) Wagon

Measured at gross vehicle weight, except item C, which is measured at unladen weight.

Turning circle, curb to curb . . 31.2 ft. (9.5 m)

FIGURE 5.2-2: VEHICLE DIMENSIONS (VW DASHER)

6. PRESENTATION AND DISCUSSION OF TEST RESULTS

The following section presents the results of the tests performed on the two engine families and the various engine/vehicle systems. Results are shown on engine and vehicle levels. The results are discussed, sensitivities are analyzed, and trade-offs are made between fuel economy, emissions, and consumer attributes.

6.1 FUEL ECONOMY

Fuel economy is affected by several parameters which may be categorized by two groups. The first group includes engine, drivetrain, and vehicle. The second group consists of consumer requirements and legal constraints.

6.1.1 Measurement Procedures and Prediction Methodology

On engine level, steady-state engine maps were prepared which show the specific fuel consumption and other relevant variables for the different engines in order to

- indicate the full-load characteristics
- indicate the road-load characteristics
- predict the fuel economy values for the City Cycle and Highway Driving Cycle (HDC) for different engine/vehicle systems.

The predictions on the basis of steady-state data are especially suited for diesel engines. There is a negligible difference with respect to fuel injection and combustion process between a dynamically and steady-state operated engine. This means that the effects from the speed/torque history may not be taken into account. An appraisal of the errors due to this assumption will be obtained later when the projections are compared with the test results. To compute the average values, the speed and torque axes of an engine map are divided into intervals of 50 rpm and 5 Nm. A time matrix is then computed which contains the time spent by the engine on each of the speed/torque meshes of the network. The engine speed values are defined by the vehicle speed during the driving cycle and the gear ratios. The engine torque is defined by the road-load cycle of the investigated vehicle for constant speed and vehicle acceleration. The products of the time matrix elements and the corresponding steady-state values of fuel consumption or exhaust emissions are totaled. The resulting figures are the projected averages.

Dynamic City and HDC Tests were performed on real-life engines with a computer-controlled engine dynamometer which simulated vehicle characteristics. These dynamic tests on engine level are a prediction method which also takes into account the dynamic behavior of the engine/vehicle system (combustion process and temperature in accordance with the speed/torque history). In this process, the dynamometer is controlled by a computer to the required speed/torque figures for each test vehicle in accordance with the various test cycles. The following parameters can be varied for this simulation:

- Vehicle inertia weight

- Rolling resistance coefficient

- Drag coefficient times frontal area ($C_D \cdot A$)

- Gear ratios and different axles

- Driving schedules.

The measured values of engine speed and torque, air and fuel intake, oil temperature, and the concentrations of NOx, HC, CO, CO_2, and O_2 are sampled eight times per second each and recorded on mass storage. These data are finally analyzed by batch programs. Two consistency checks are performed before and during the dynamic tests in order to reduce errors in the experimental set-up:

- The rate of air intake is compared to the corresponding rate computed from the fuel intake rate and the air/fuel ratio derived from the exhaust gas concentrations.

- The CO_2 concentration (or the O_2 concentration if it is larger than the CO_2 concentration) is compared with the corresponding computed values from air/fuel combustion.

More details of these engine dynamometer techniques may be found in References and .

On vehicle level, chassis dynamometer tests were conducted on selected engine/vehicle systems in accordance with the procedures in the Federal Register, Vol. 41, No. 177, September, 1976, "Fuel Economy Testing, Calculation and Exhaust Emissions Test Procedures for 1977 through 1979 Model Year Automobiles." Because of the relatively small statistical errors of the tests on the engine dynamometer in both steady-state and dynamic engine operation, these tests were used to establish the sensitivity of the fuel economy and regulated emissions on the various measures on the engine and vehicle level.

6.1.2 Specific Fuel Consumption Maps

Steady-state engine maps were prepared for the different engines. These maps show the brake mean effective pressure (bmep) versus speed (rpm) with different variables, such as fuel consumption, as well as Bosch Numbers, temperatures, and emissions. The use of the brake mean effective pressure is known to permit a comparison of the different engines, which is independent of the number of cylinders and displacement. The contour lines for the different variables are presented as an example in Figures 6.1-1 through 6.1-8 for the turbocharged 4-cylinder diesel engine. The steady-state maps for all investigated engines are included in the Appendix.

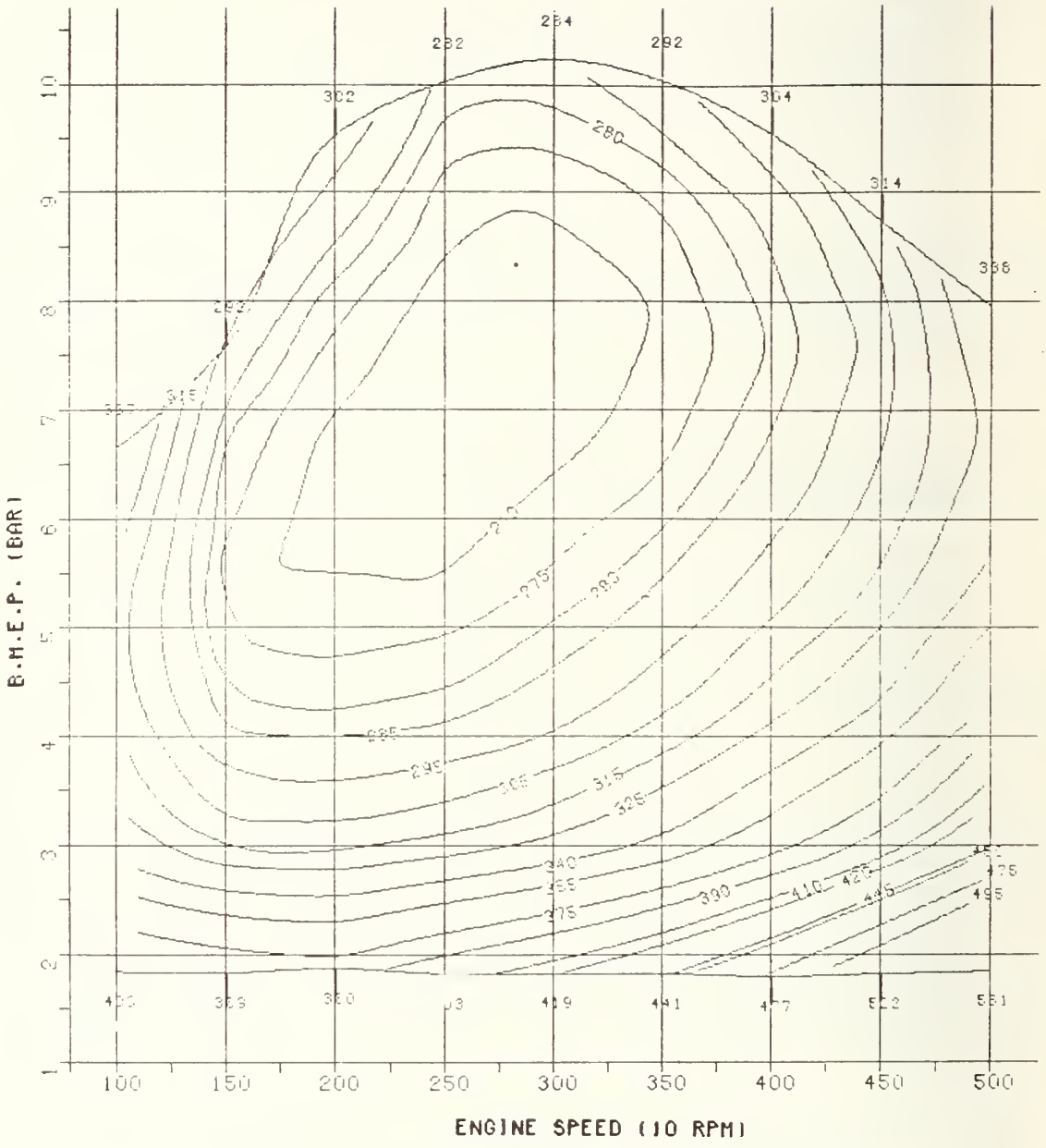

FIGURE 6.1-1: SPECIFIC FUEL CONSUMTPION (g/kWh)
70 HP TURBOCHARGED RESEARCH DIESEL ENGINE

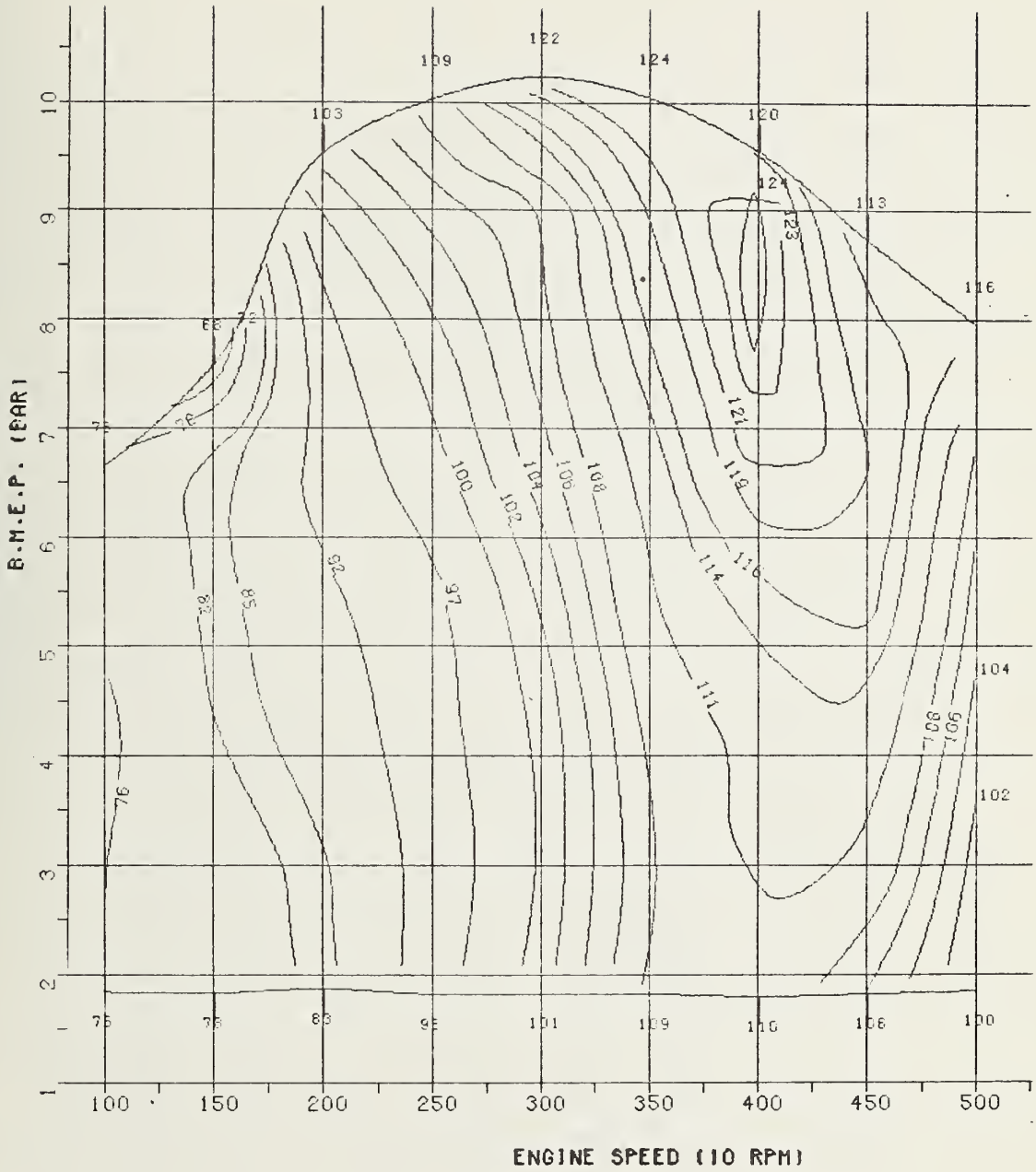

FIGURE 6.1-2: OIL TEMPERATURE (CELSIUS)
70 HP TURBOCHARGED RESEARCH DIESEL ENGINE

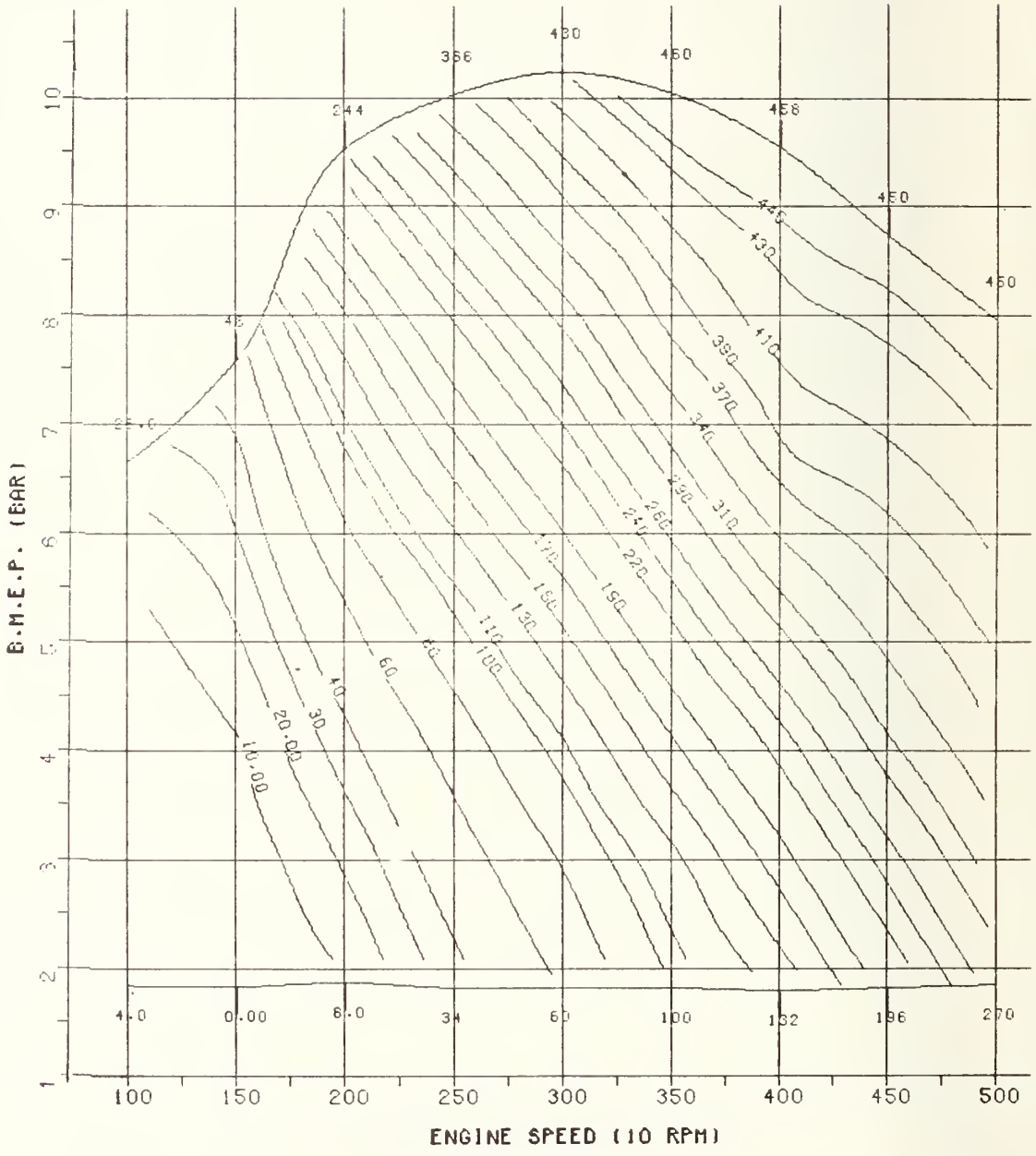

FIGURE 6.1-3: TURBOCHARGER PRESSURE (Torr)
70 HP TURBOCHARGED RESEARCH DIESEL ENGINE

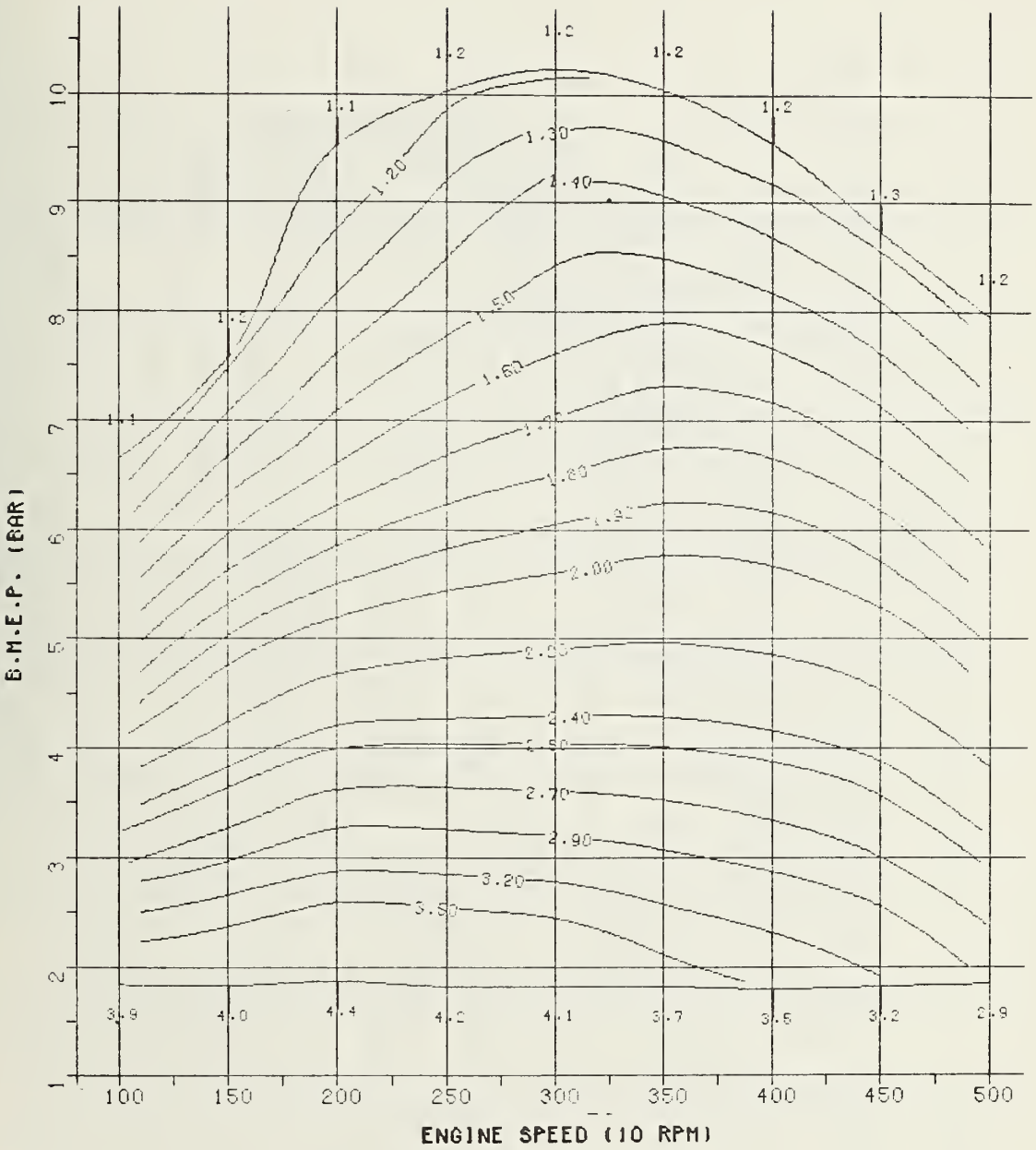

FIGURE 6.1-4: AIR-TO-FUEL RATIO - 70 HP TURBOCHARGED RESEARCH DIESEL ENGINE

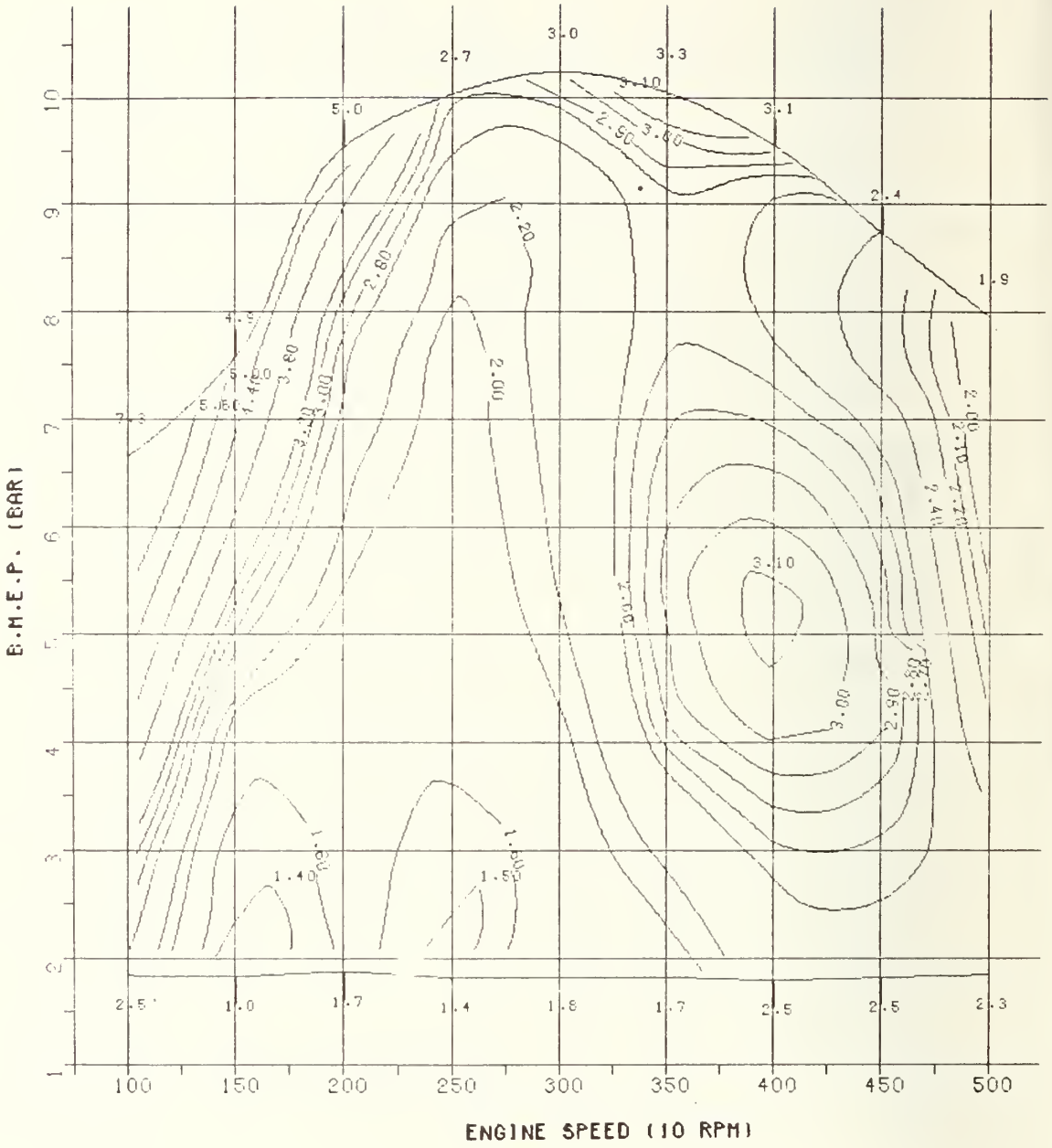

FIGURE 6.1-5: SMOKE (BOSCH NUMBER) - 70 HP TURBOCHARGED RESEARCH DIESEL ENGINE

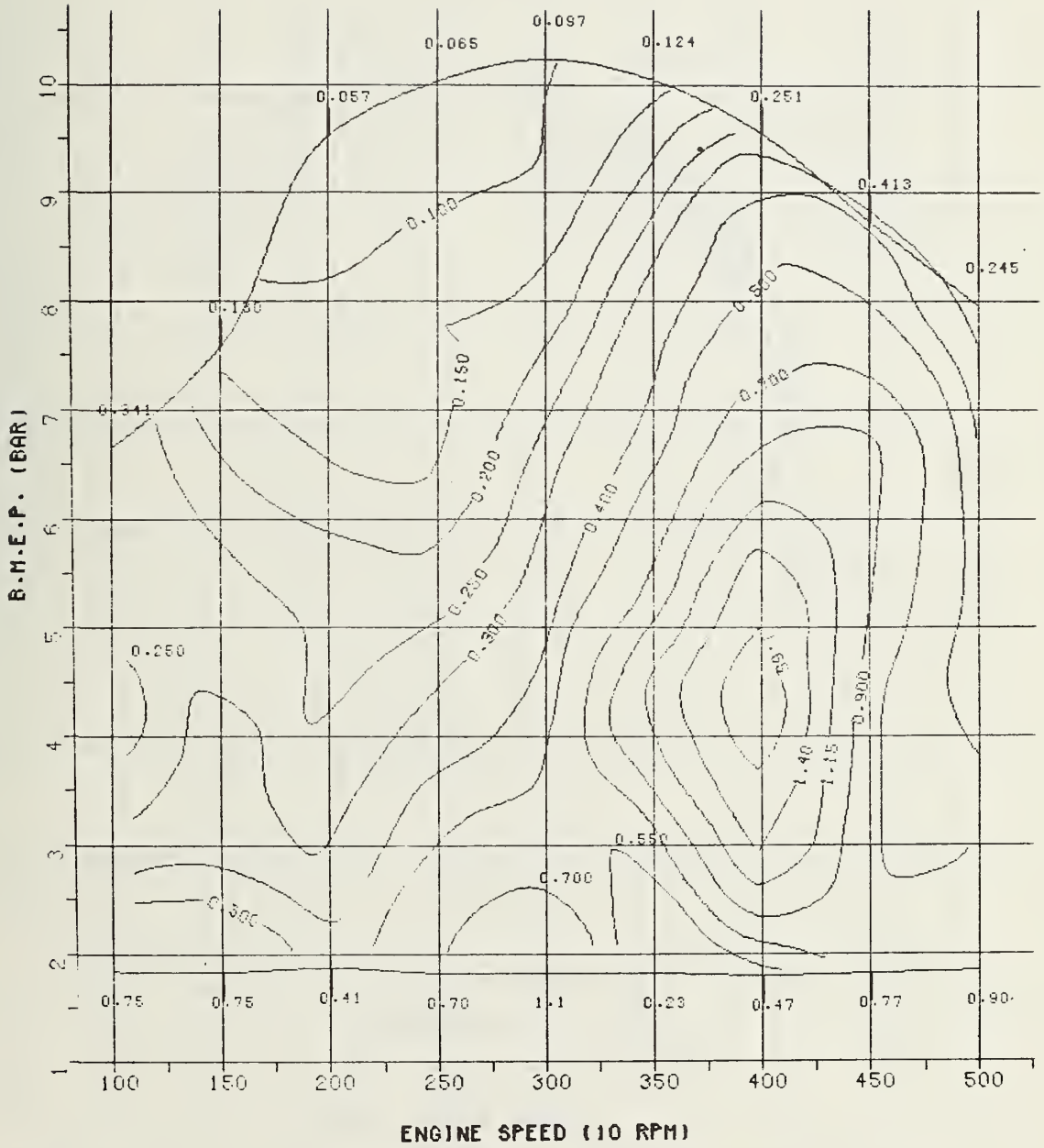

FIGURE 6.1-6: HC EMISSION (g/kWh) - 70 HP TURBOCHARGED RESEARCH DIESEL ENGINE

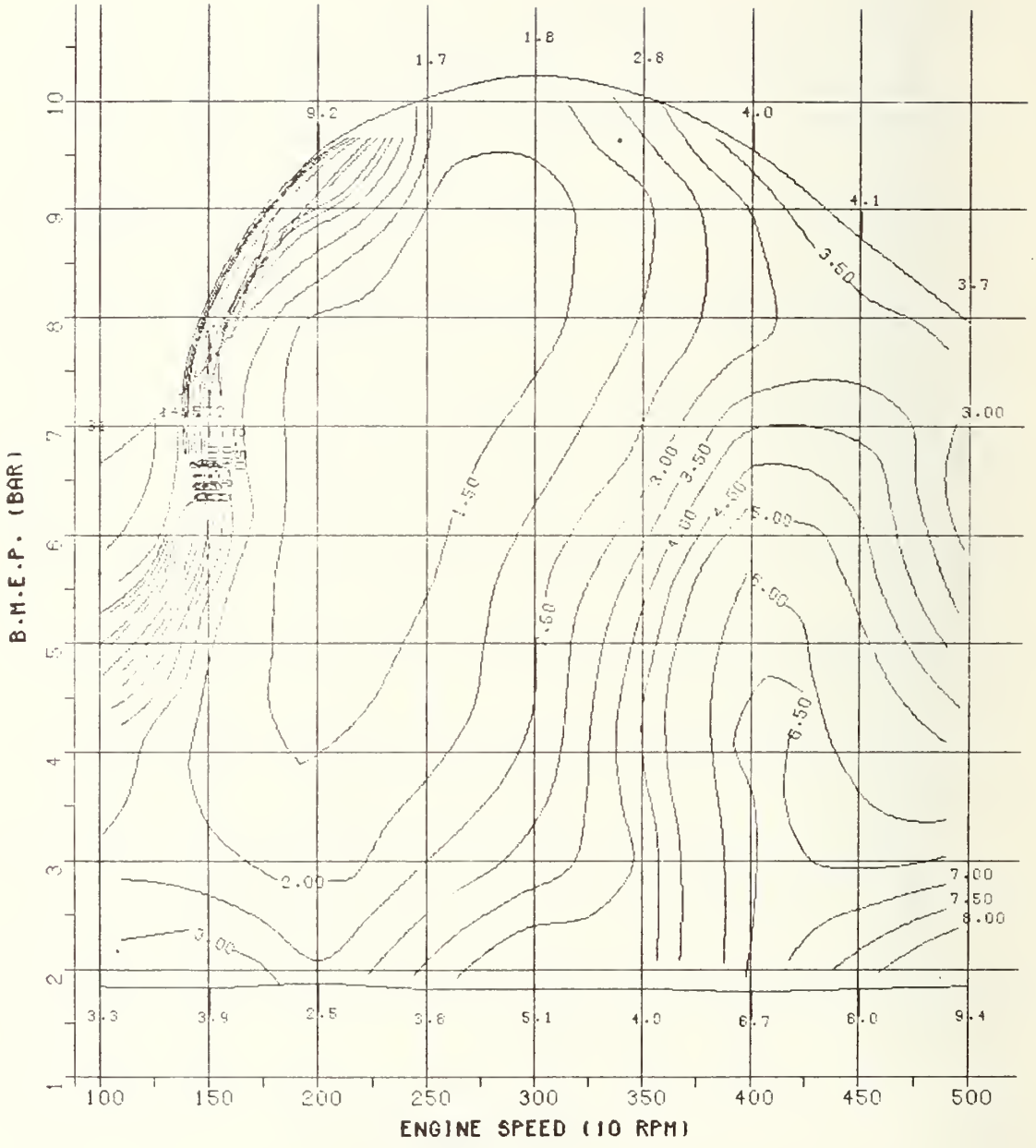

FIGURE 6.1-7: CO EMISSION (g/kWh) - 70 HP TURBOCHARGED RESEARCH DIESEL ENGINE

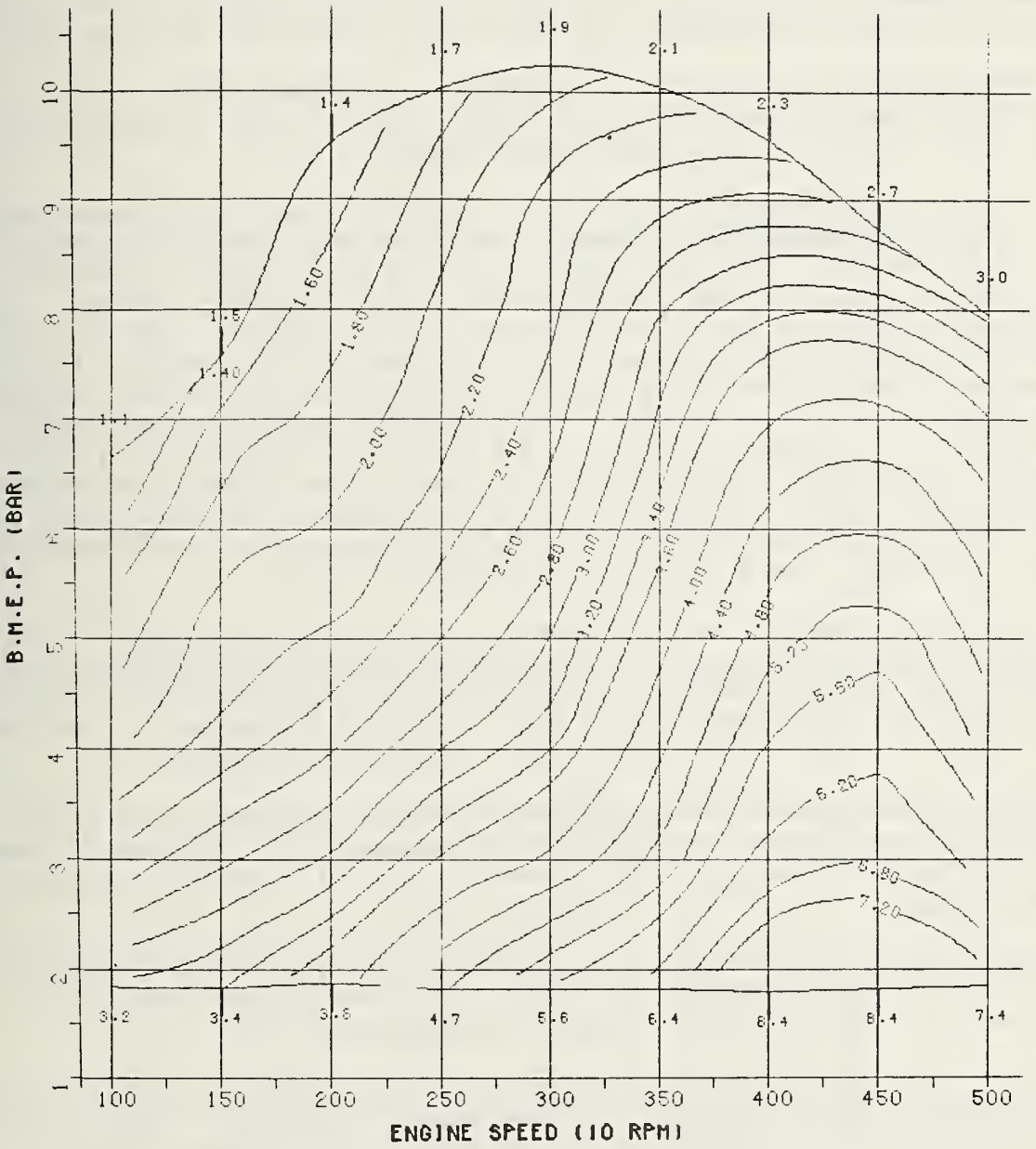

FIGURE 6.1-8: NOx EMISSION (g/kWh) - 70 HP TURBOCHARGED RESEARCH DIESEL ENGINE

Figures 6.1-9 through 6.1-11 are specific fuel consumption maps for the naturally-aspirated 4-cylinder basic engine and the 5- and 6-cylinder versions. Figure 6.1-1 shows the specific fuel consumption map of the turbocharged 4-cylinder engine and Figures 6.1-12 and 6.1-13 the variations with water injection and exhaust gas recirculation. Figure 6.1-14 is the specific fuel consumption map for the naturally-aspirated 4-cylinder basic engine with modulated EGR.

The increase in consumption at low bmep's and higher engine speeds is caused by the proportionally higher friction losses, while the fuel consumption rises at low engine speeds due to insufficient combustion.

The 4-cylinder engine is a production engine without special adjustments. The 5- and 6-cylinder engines, however, are prototypes, some characteristics of which, e.g. smoke and emissions, markedly deviate from those of production units. The 5-cylinder engine reaches the same bmep as the 4-cylinder version. Its engine-speed range of 4,200 rpm is distinctly lower than the 5,000 rpm of the latter. This means a drop in specific output from 25.8 kW/l to 22.5 kW/l. Compared with the 4-cylinder engine, the 6-cylinder version yields a pronouncedly higher bmep at better fuel economy. The 6-cylinder unit was a hand-tuned, optimized version that was operated at a slightly higher smoke level (see Appendix). This engine clearly shows the potential for improved tuning that could be accomplished with advanced injection equipment (see Section 4.2.2). However, the specific output drops along with a decrease in displacement and number of cylinders (see Figure 4.4-4 in Section 4.4.1.3).

The maximum possible bmep is limited to a rather narrow range. It is essentially determined by the air/fuel ratio. The map for a constant air-to-fuel ratio for the turbocharged 4-cylinder engine (Figure 6.1-15) at higher loads shows distinctly higher values than the map of the naturally-aspirated engine (Figure 6.1-16). The maximum bmep is accordingly higher.

Compared with the 5-cylinder naturally-aspirated engine, the broader speed range of the turbocharged engine may improve consumption by different transmission matching for constant output. This is shown in the City and HDC fuel economy data in Section 6.1.4.

The fuel consumption maps of the naturally-aspirated and the turbocharged engine with exhaust gas recirculation show a distinctly lower bmep (by 10 - 13%), i.e. a significant drop in output of approximately 5 kW.

The differences in the constant specific fuel consumption curves for engines without and with EGR essentially are determined by two facts. Figures 6.1-17 and 6.1-18 show that the air-to-fuel ratio decreases as the effective EGR rate rises (see Figures 6.1-19 and 6.1-20). The engines reach the smoke limit earlier and have a markedly higher smoke level at partial load operation. At the same time, the higher intake temperature of the cylinder charge improves combustion in the lower engine-speed range. This is shown especially by a comparison of the turbocharged engines without and with EGR (Figures 6.1-1 and 6.1-13). The curves of constant specific fuel consumption rise for the turbocharged engine with EGR only when the rpm is much lower compared with the engine without EGR. The EGR fuel consumption figures indicate that a sophisticated device permits EGR within certain limits (EGR rate, low load, low rpm) which hardly deteriorates the specific fuel consumption. The effects on other factors such as smoke and driveability will be dealt with later. The slightly lower specific fuel consump-

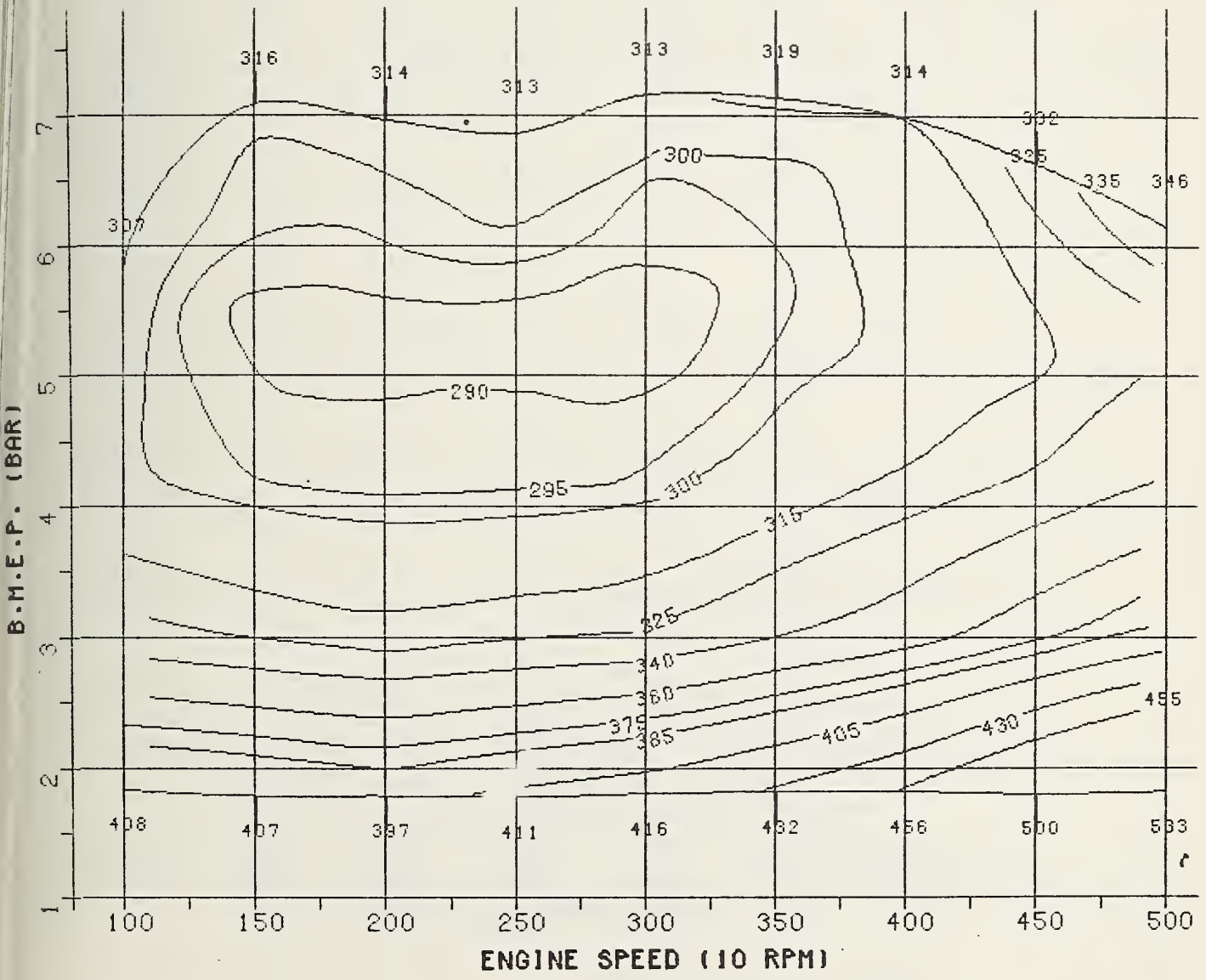

FIGURE 6.1-9: SPECIFIC FUEL CONSUMPTION (g/kWh) - 50 HP N.A. 90 CID PRODUCTION DIESEL ENGINE

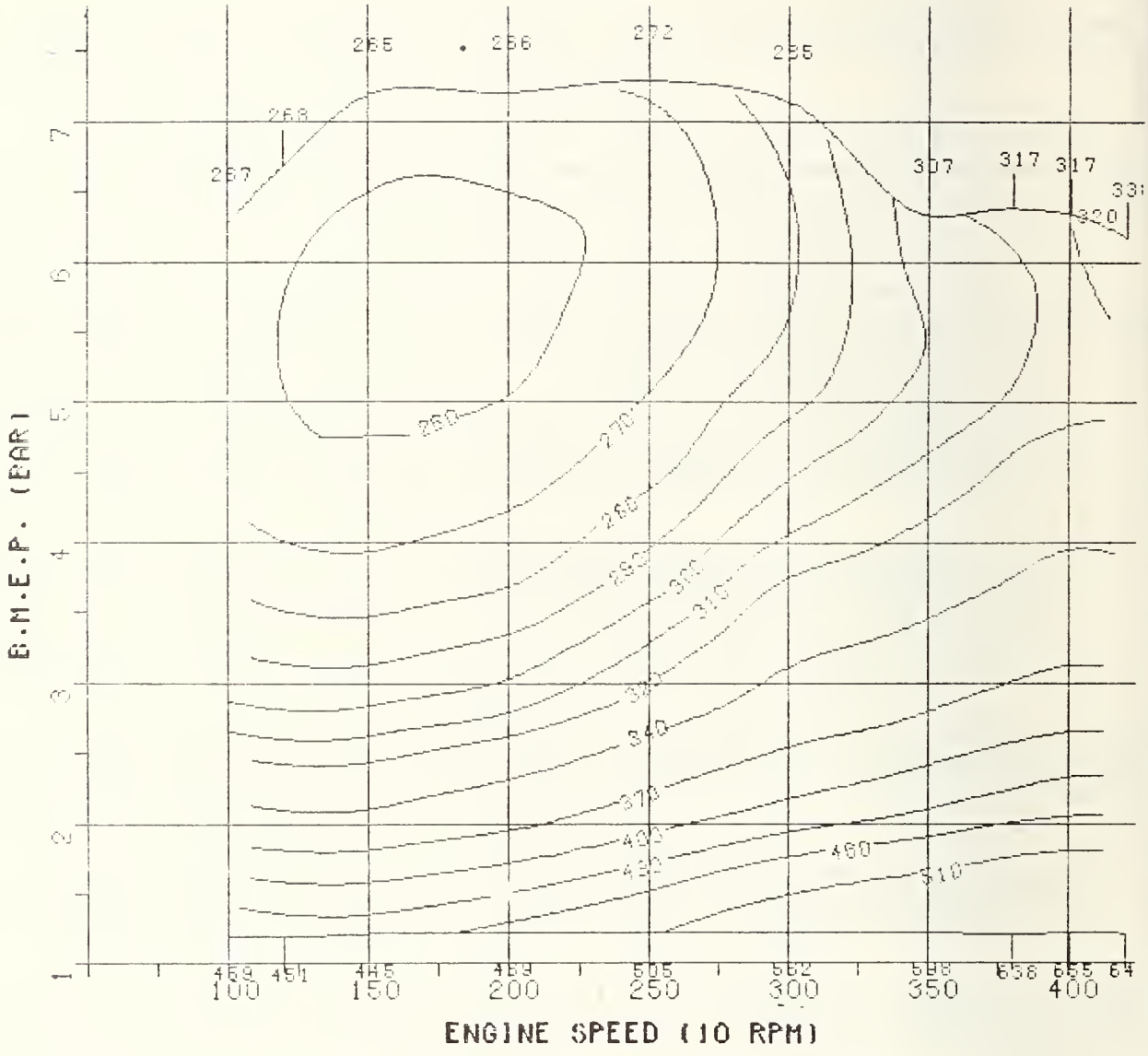

FIGURE 6.1-10: SPECIFIC FUEL CONSUMPTION (g/kWh) - 5-CYLINDER 130 CID N.A. DIESEL ENGINE

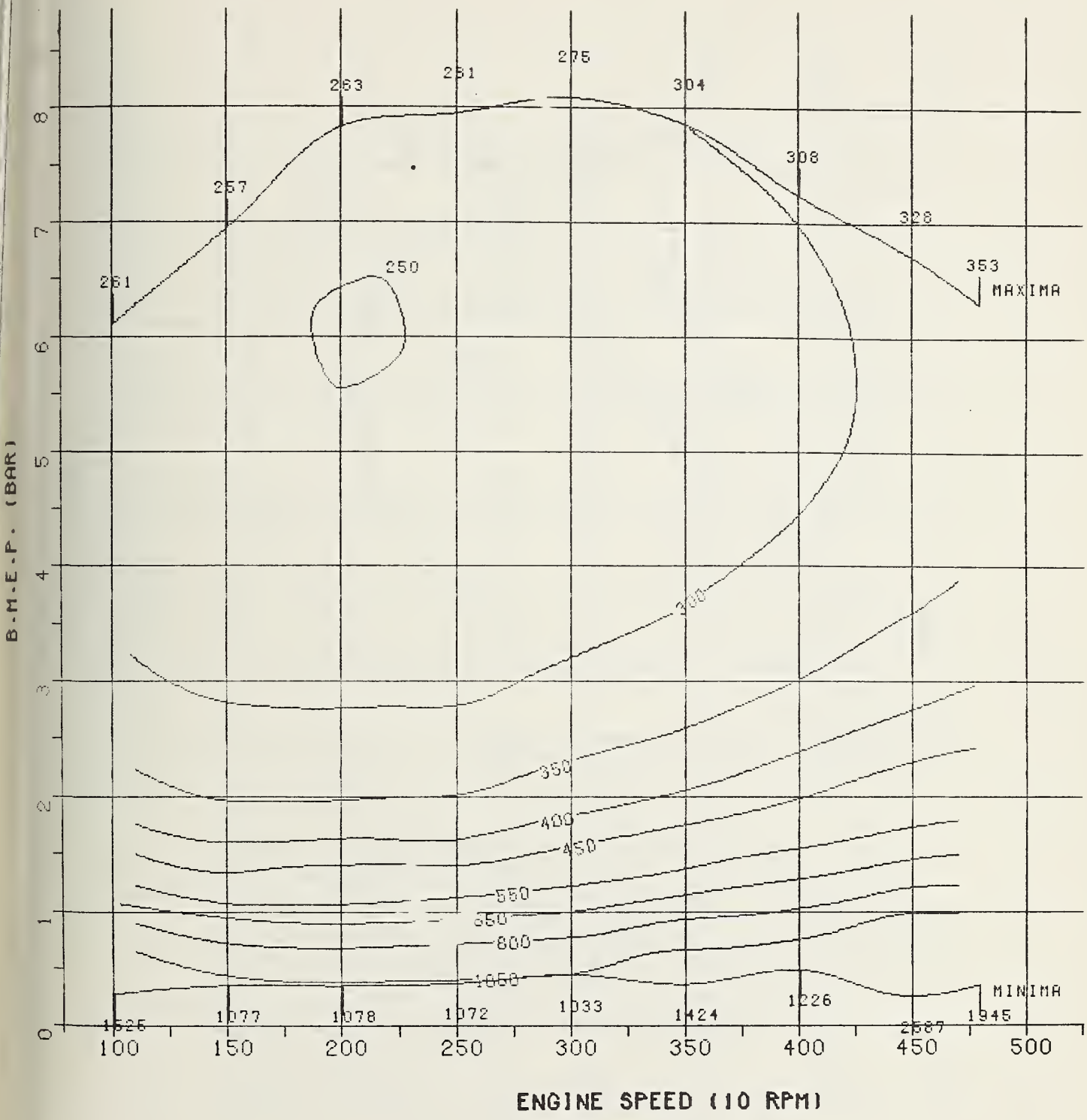

FIGURE 6.1-11: SPECIFIC FUEL CONSUMPTION (g/kWh)
6-CYLINDER 146 CID N.A. DIESEL ENGINE

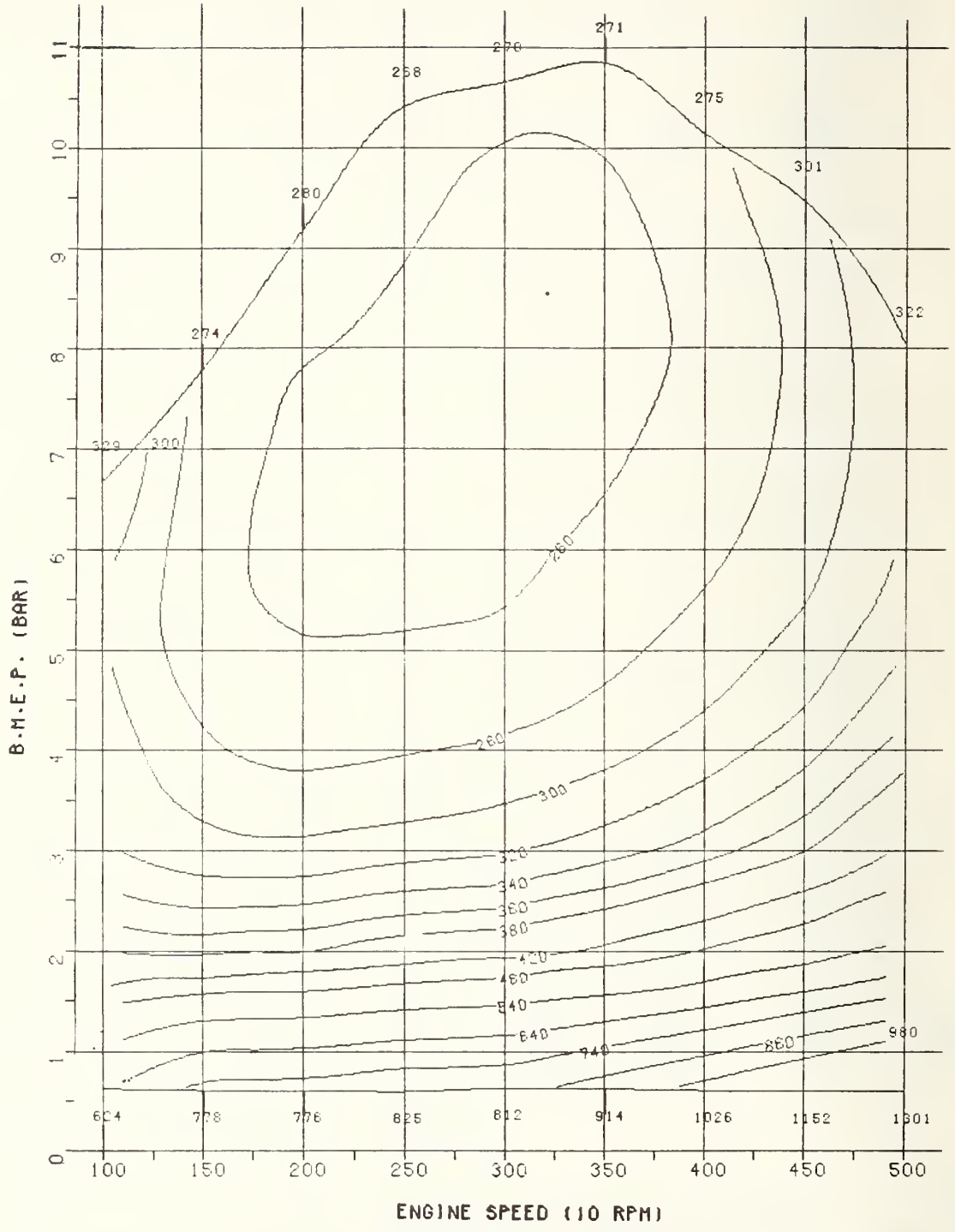

FIGURE 6.1-12: SPECIFIC FUEL CONSUMPTION (g/kWh)
70 HP DIESEL WITH WATER INJECTION

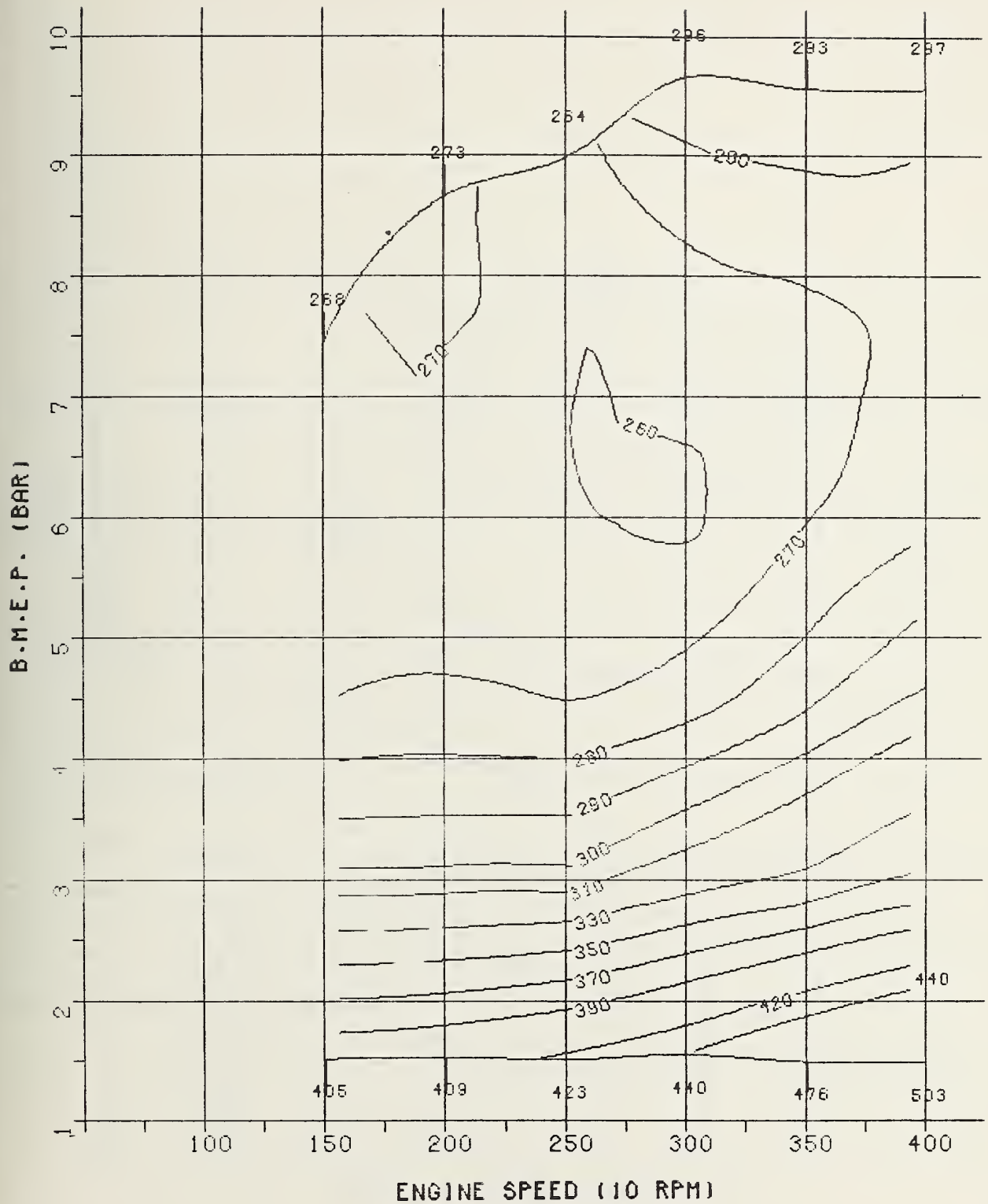

FIGURE 6.1-13: SPECIFIC FUEL CONSUMPTION (g/kWh)
70 HP TC DIESEL ENGINE WITH MODULATED EGR

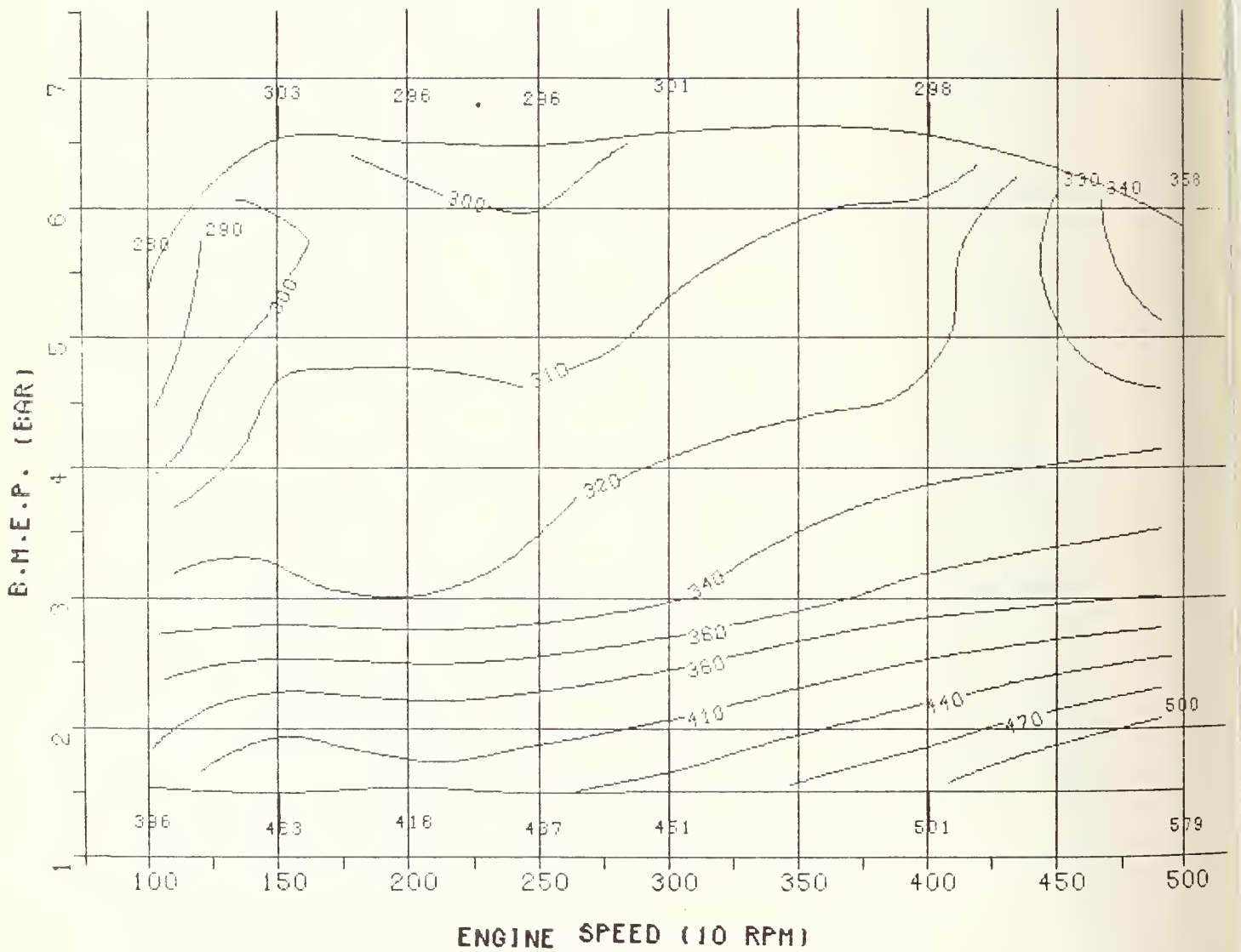

FIGURE 6.1-14: SPECIFIC FUEL CONSUMPTION (g/kWh)
50 HP N.A. DIESEL ENGINE WITH MODULATED EGR

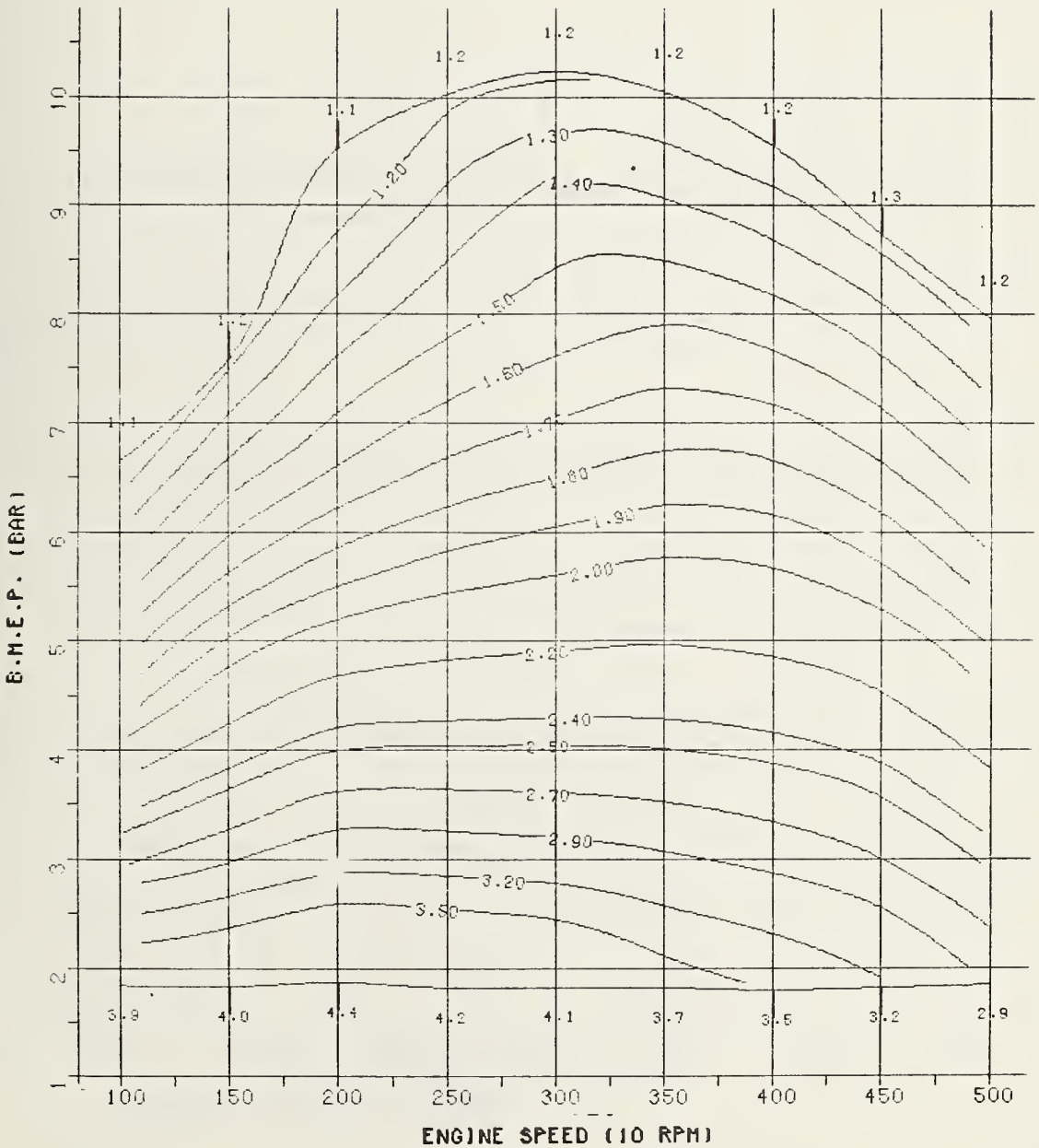

FIGURE 6.1-15: AIR-TO-FUEL RATIO
70 HP TURBOCHARGED RESEARCH DIESEL ENGINE

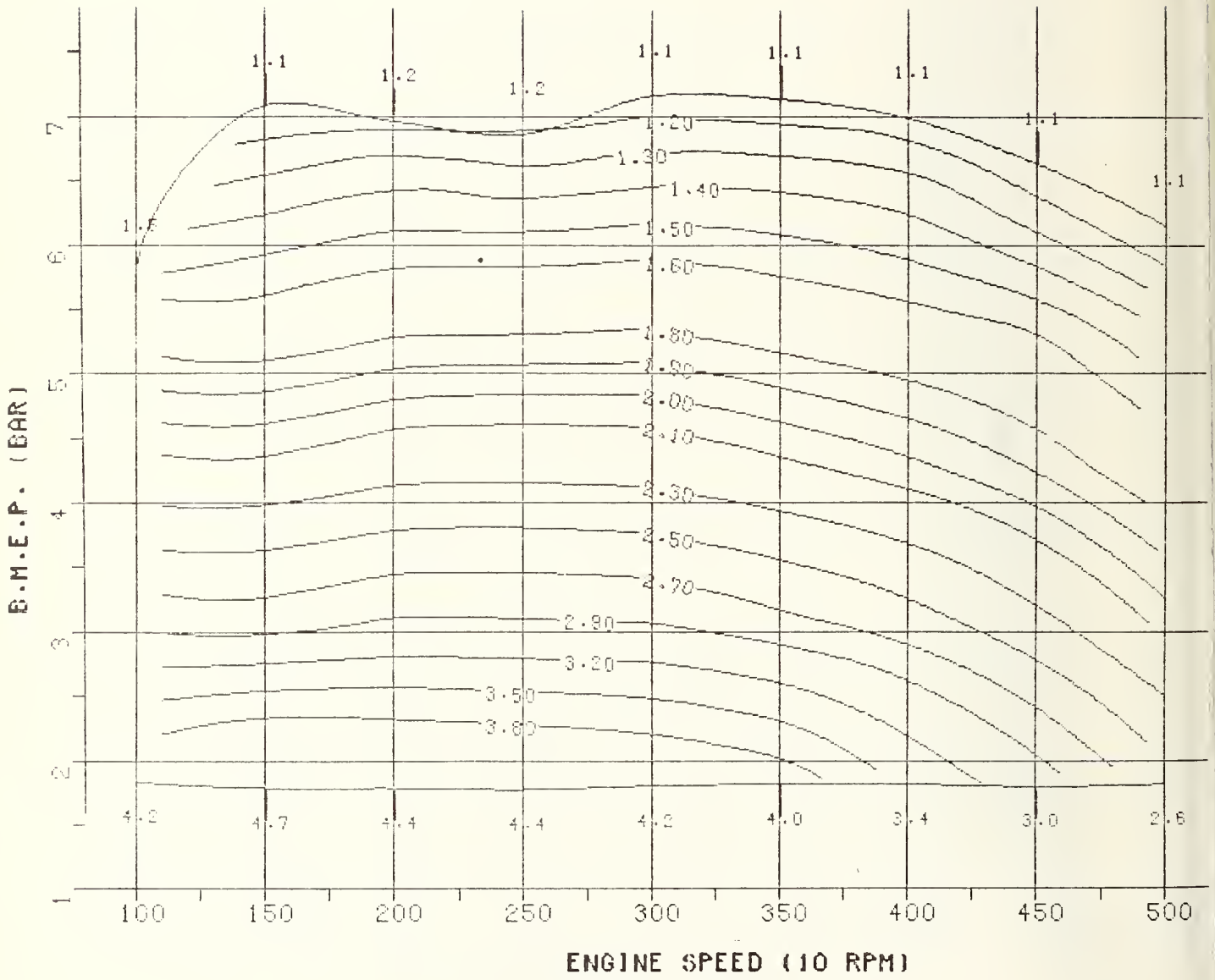

FIGURE 6.1-16: AIR-TO-FUEL RATIO
50 HP N.A. 90 CID PRODUCTION DIESEL ENGINE

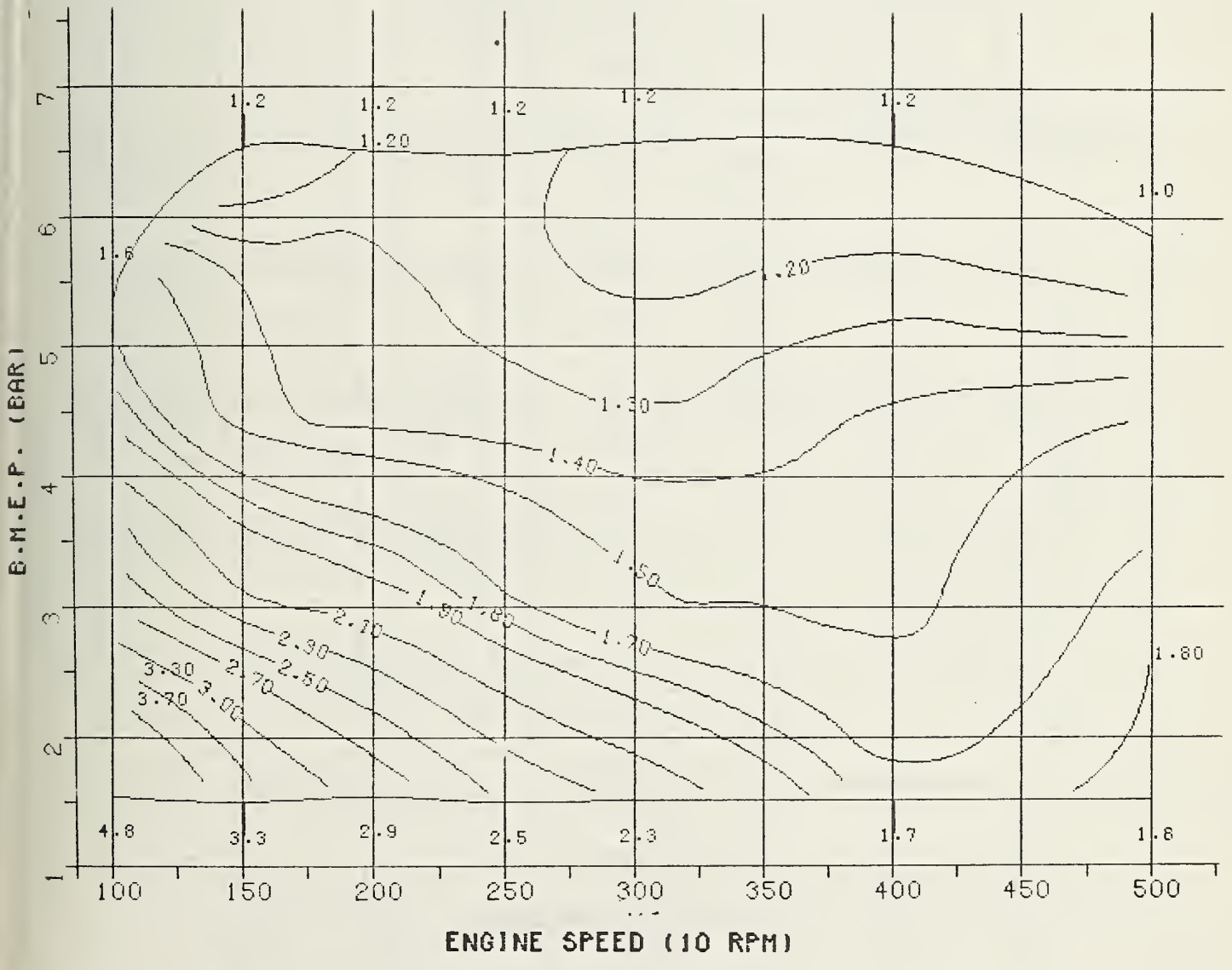

FIGURE 6.1-17: AIR-TO-FUEL RATIO
50 HP N.A. DIESEL ENGINE WITH MODULATED EGR

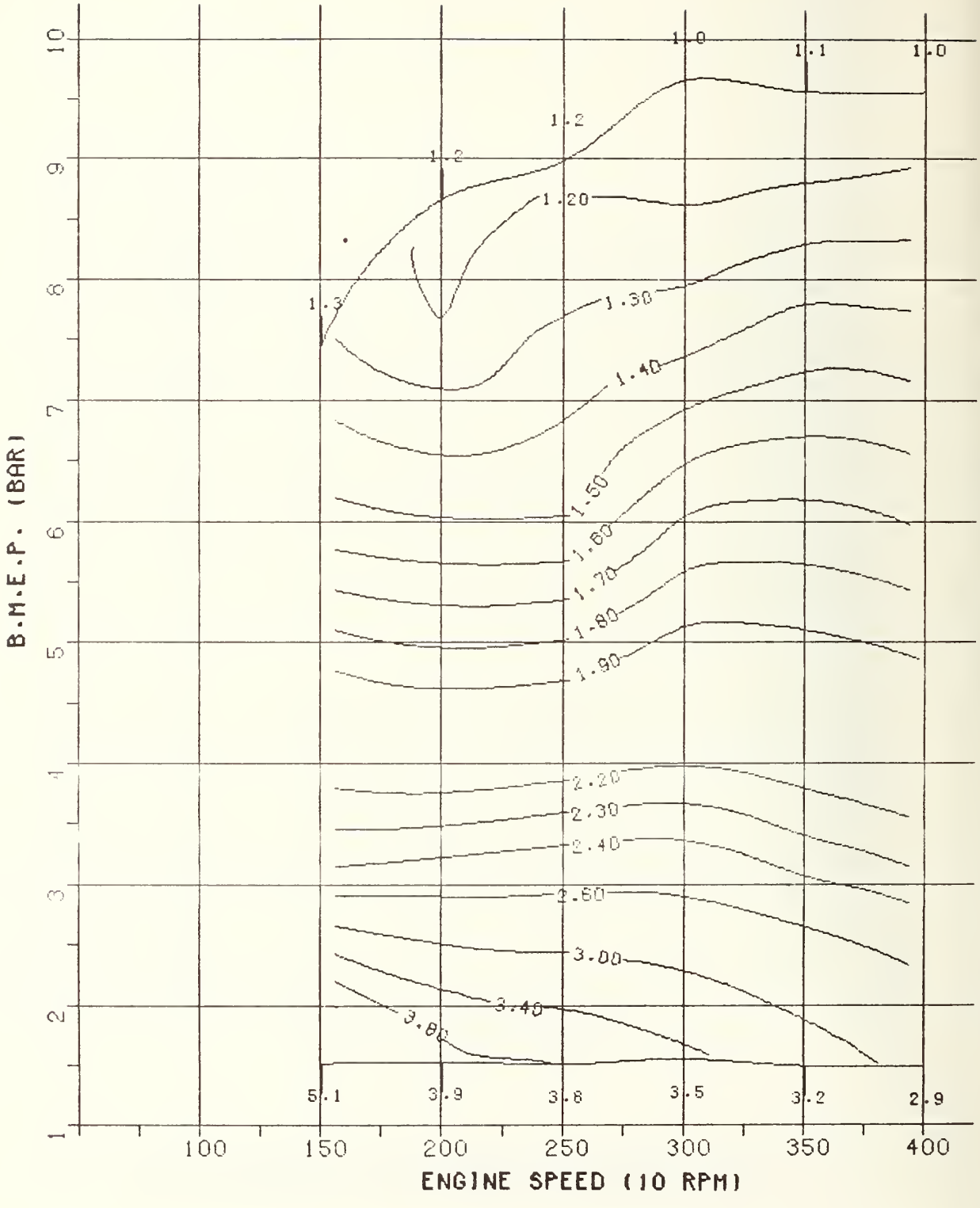

FIGURE 6.1-18: AIR-TO-FUEL RATIO
70 HP TC DIESEL ENGINE WITH MODULATED EGR

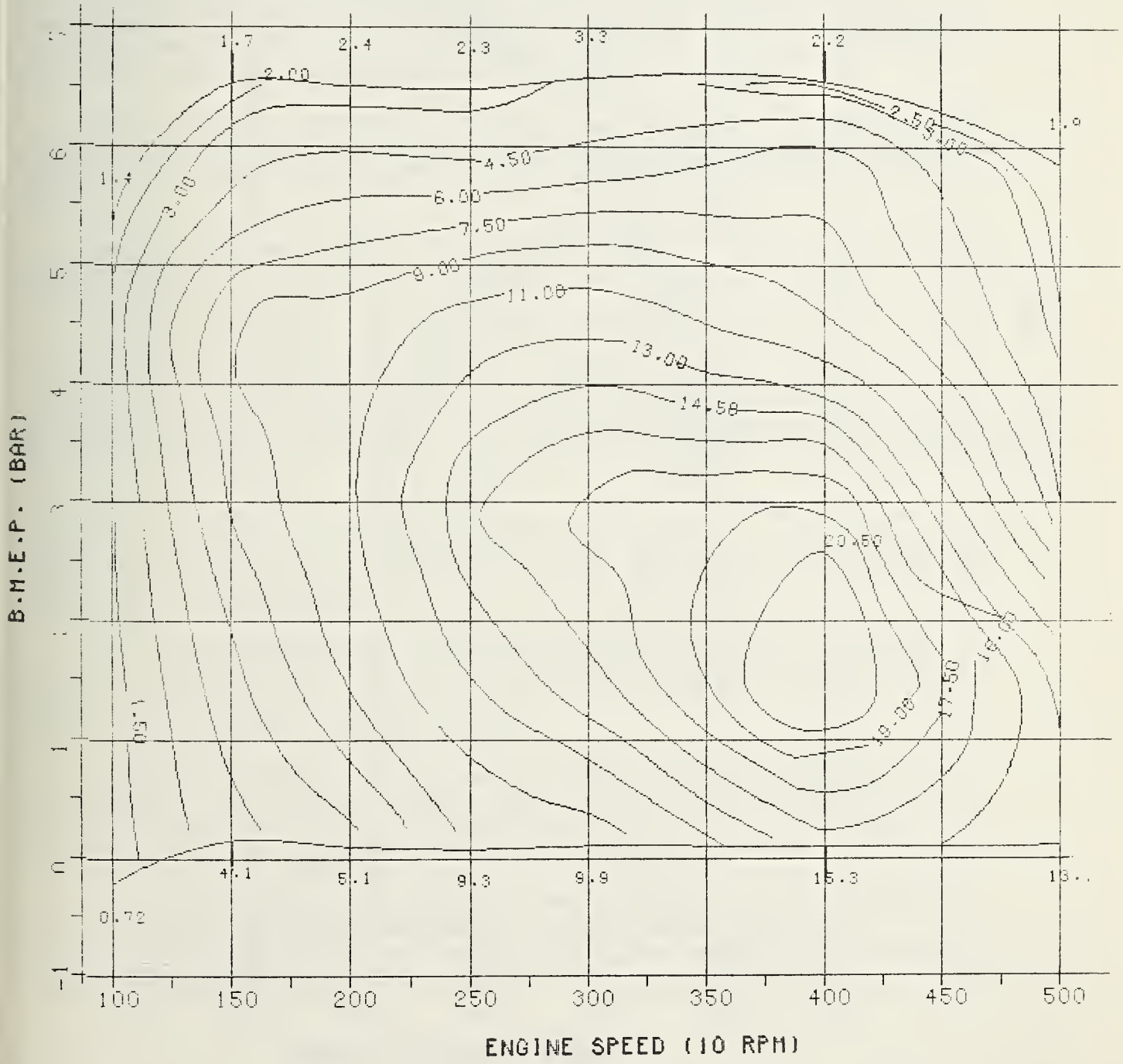

FIGURE 6.1-19: EFFECTIVE EGR (%)
50 HP N.A. DIESEL ENGINE WITH MODULATED EGR

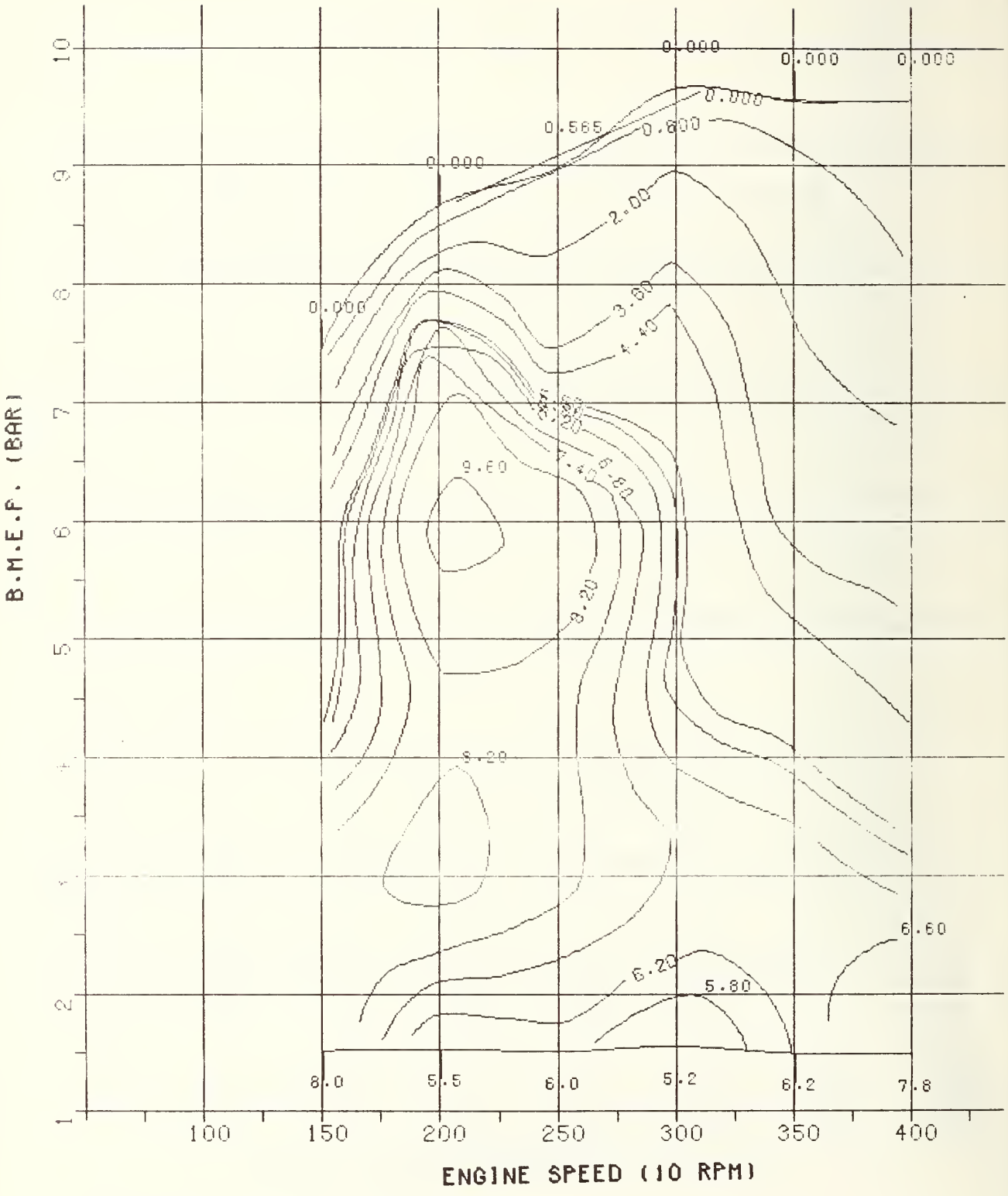

FIGURE 6.1-20: EFFECTIVE EGR (%)
70 HP TC DIESEL ENGINE WITH MODULATED EGR

tion shown in Figure 6.1-13 depends on the engine and is atypical because re-investigations had shown that this engine had extremely low friction losses (tolerances and high mileage). Therefore, these values should be used qualitatively only. The tight program schedule did not leave sufficient time to verify these findings by running comparison tests on another engine within the presently typical tolerance fields.

Figure 6.1-21 is a comparison between the injection quantities per cycle. The markedly broader range between idle and full load operation of the turbocharged engine indicates the higher demands that apply to the fuel injection equipment, especially to the nozzles which must comply with the requirement for a large turn-down ratio in fueling for full-load and idle.

The road-load curves (Figure 6.1-22) show a frequently used partial-load range for the VW Rabbit and the Audi 100. It characterizes the required output versus cruise speed (engine speed) for driving on a level surface in direct gear.

The fuel economy (Figure 6.1-23) was compared at road loads for these two vehicles:

- VW Rabbit, 2250-lb. IW, drag coefficient times frontal area = 0.77 m^2
- Audi 100, 3000-lb. IW, drag coefficient times frontal area = 0.80 m^2

A rolling resistance coefficient of 1.75% (of the inertia weight) was assumed for both vehicles at low speeds. The coefficient increases at higher pseeds as

$$c = 1.75\% + 0.184\% \cdot (V/100\ km/h)^2$$

This rolling resistance is obtained with radial steel tires on average concrete roads and includes friction losses due to shock absorbers, toe-in and road configuration characteristics.

The overall transmission was matched to achieve top vehicle speed at maximum engine power. The resulting vehicle speed V_{1000} at an engine speed of 1,000 rpm with the transmission in high gear is shown in Table 6.1-1 for various vehicle weights and engine types.

Drivetrain efficiency is assumed to be 90%. Now, the specific fuel consumption at any constant vehicle speed is read off by interpolation from the steady-state engine maps. The resultant fuel economy data is shown in Figure 6.1-23.

Fuel economy ranges from roughly 60 mpg at 25 mph to 25 mpg at 80 mph. The effects of different engine/vehicle systems (weight, powertrain, etc.) on the fuel economy during steady-state driving are less pronounced than those of the vehicle velocity.

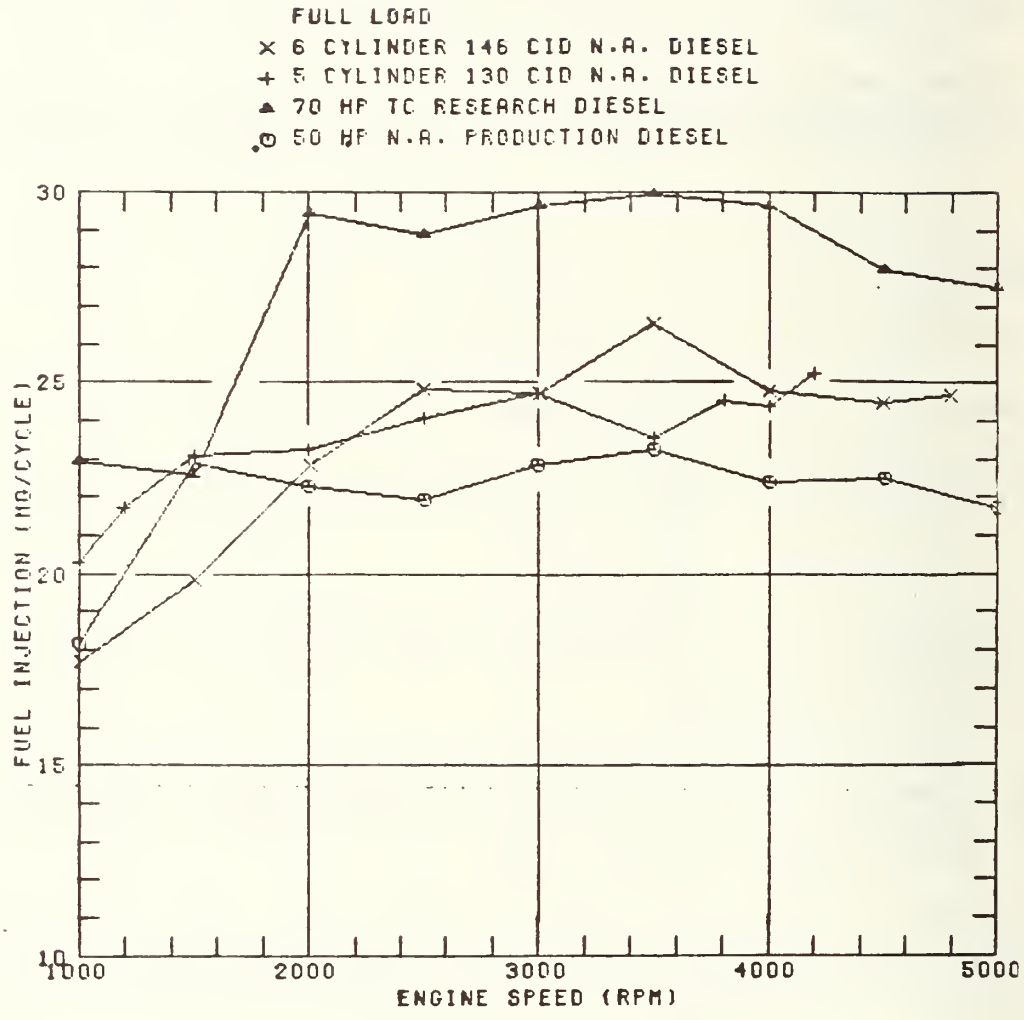

FIGURE 6.1-21: COMPARISON OF INJECTION QUANTITIES PER CYCLE

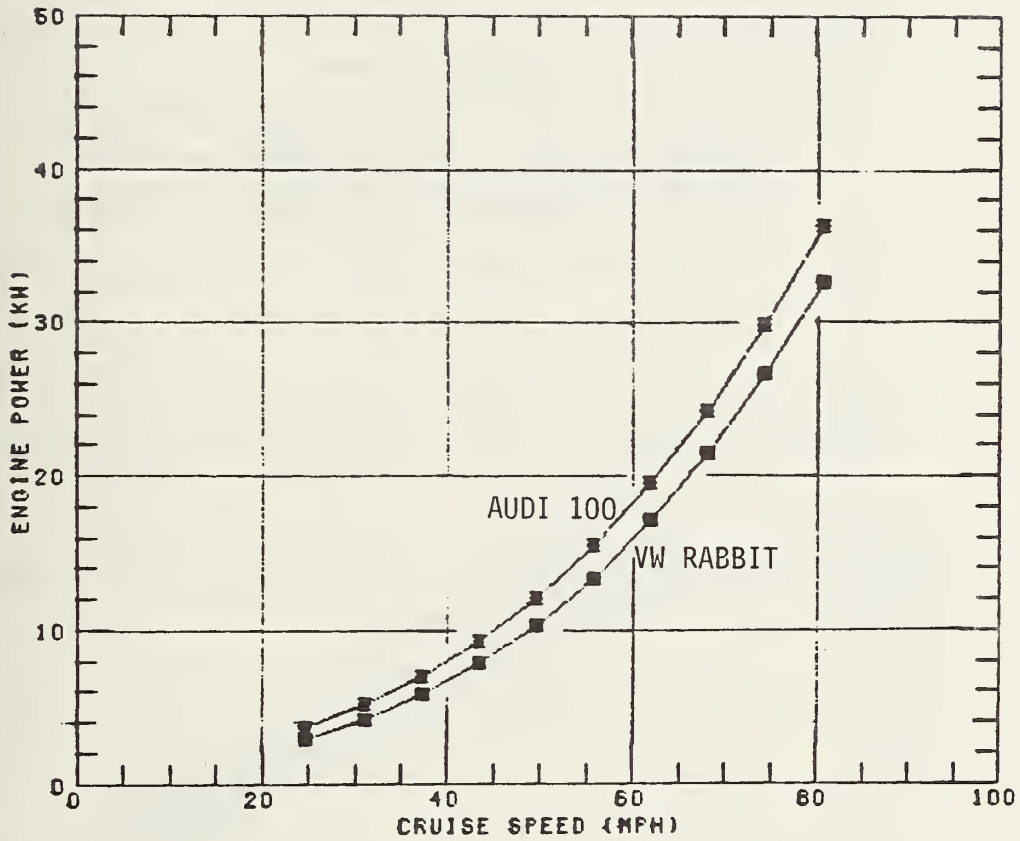

FIGURE 6.1-22: PARTIAL-LOAD RANGE FOR THE VW RABBIT AND AUDI 100

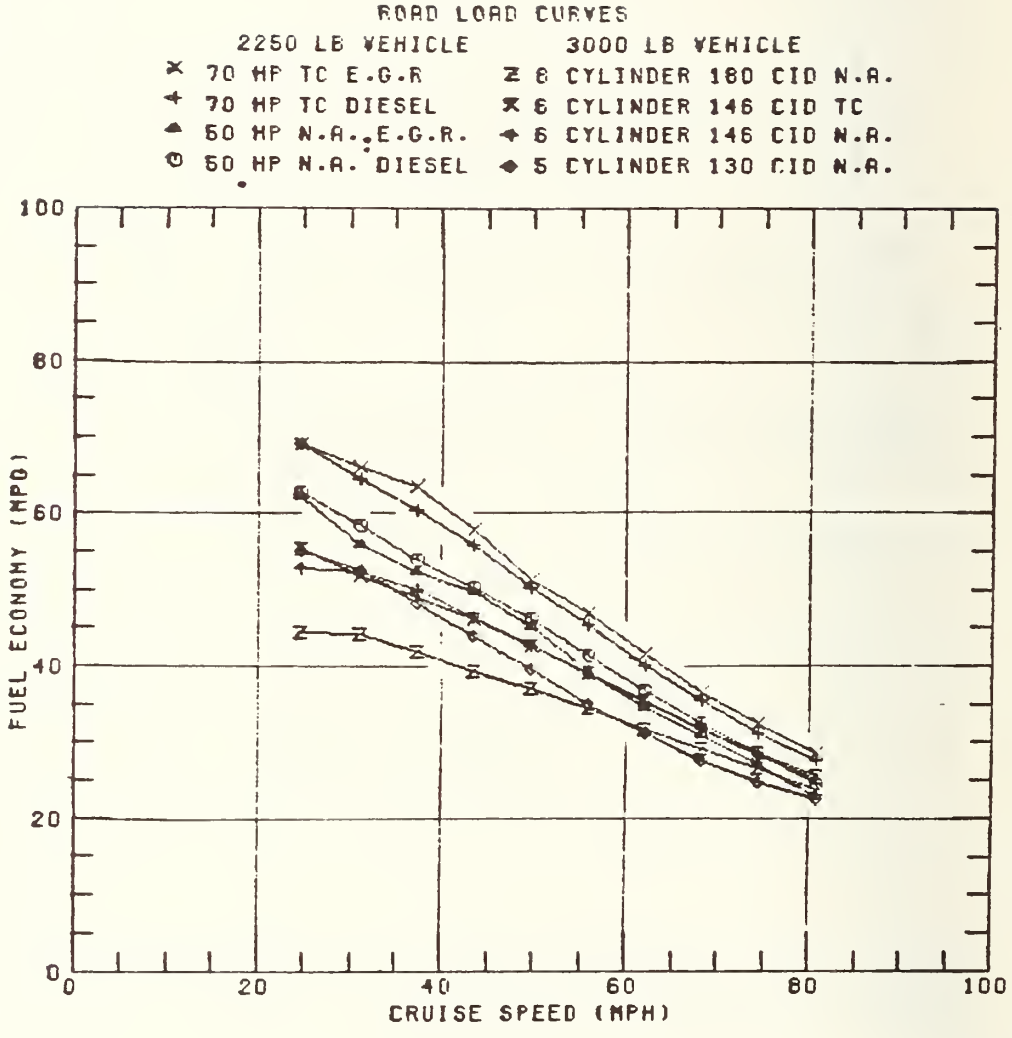

FIGURE 6.1-23: COMPARISON OF FUEL ECONOMY AT ROAD LOADS FOR VW RABBIT AND AUDI 100 DURING USING DIFFERENT ENGINES

Vehicle Weight lb.	Engine Type	V_{1000} km/h
2,250	50 HP NA	27.8
2,250	70 HP TC	33.1
3,000	5-Cylinder NA	33.1
3,000	6-Cylinder NA	36.0
3,000	6-Cylinder TC	40.0
3,000	8-Cylinder NA	40.0

TABLE 6.1-1: VEHICLE SPEED V_{1000} AT ENGINE SPEED OF 1000 RPM.

6.1.3 Fuel Economy Test Results on Chassis Dynamometer

To determine the interdependence between fuel economy, vehicle weight, performance described by the horsepower-to-intertia-weight ratio, engine concept, and the two emission levels (.41/3.4/2.0 and .41/3.4/1.0 gram/mile HC/CO/NOx), the different engine/vehicle systems were tested on vehicle level in the 1,750 to 3,000-lb. inertia-weight range. All tests are listed in the Appendix.

The 50 HP naturally-aspirated 4-cylinder diesel engine was tested in the 1,750 to 2,500-lb. inertia-weight classes. Its fuel economy was found to range from 43 to 40 mpg in the Composite Driving Cycle (Figure 6.1-24).

The 68 HP naturally-aspirated 5-cylinder research diesel engine was tested in the 2,250 to 3,000-lb. inertia-weight classes; the resultant fuel economy ranged from 36 to 33 mpg. According to the experience with the 4-cylinder engine now in production, a potential improvement of 2 mpg is projected for this engine.

The 70 HP turbocharged 4-cylinder research diesel engine was tested in the 2,250 to 3,000-lb. inertia-weight classes. This engine has an improved fuel economy of between 45 and 40 mpg when compared with the naturally-aspirated 5-cylinder diesel engine. The fuel economy of the 100 HP N.A. diesel engine was projected on the basis of the 50 HP N.A. diesel engine.

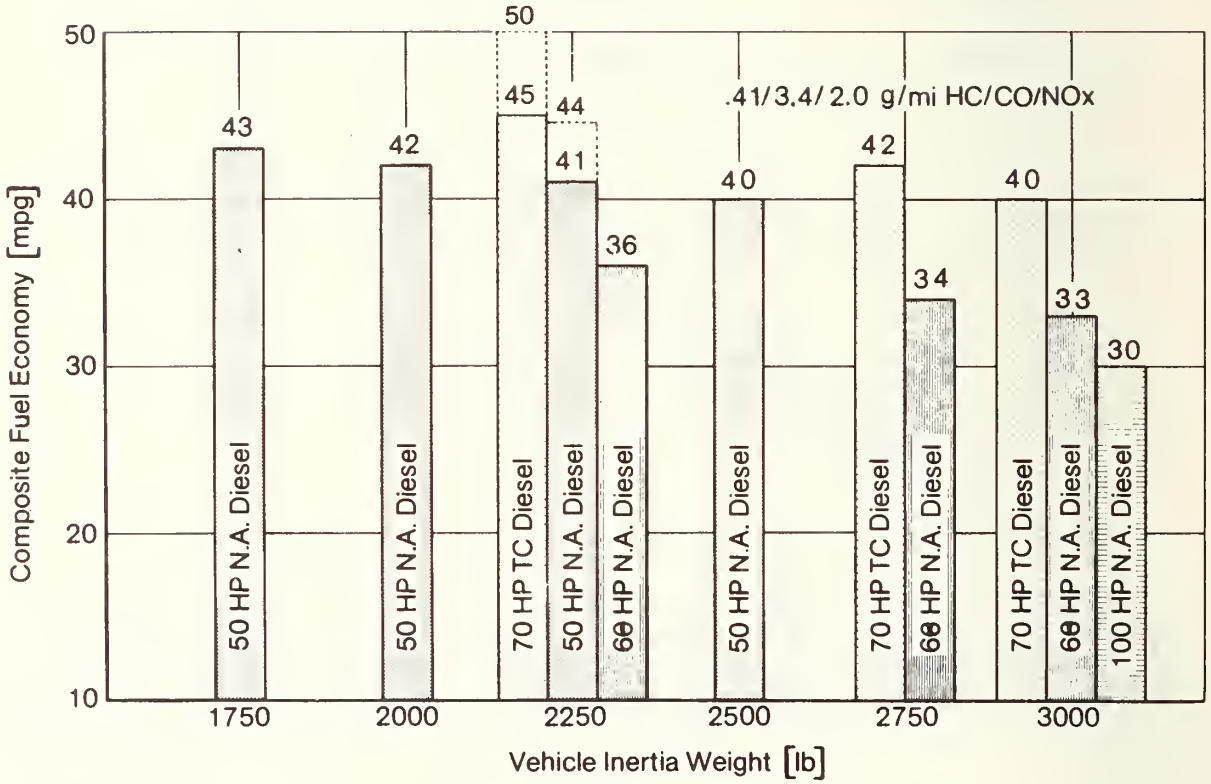

FIGURE 6.1-24: COMPOSITE FUEL ECONOMY OF VARIOUS DIESEL ENGINES AVERAGED OVER THE CITY AND HIGHWAY DRIVING CYCLES.
The fuel economy is given in terms of No. 2 diesel fuel based on nominal EPA road-load setting. The figures given may vary by $\pm$ 2 mpg.

------- EPA obtained results at actual road-load setting.

6.1.4 The Effects of Engine Concept and Performance on Fuel Economy

The sensitivity studies were mainly performed at the engine level in order to limit the number of uncontrolled parameters and statistical errors otherwise present in vehicle testing. These studies include predictions from steady-state engine maps and dynamic dynamometer tests. Figure 6.1-25 shows the computed fuel economy values for several engines as installed in two vehicles.

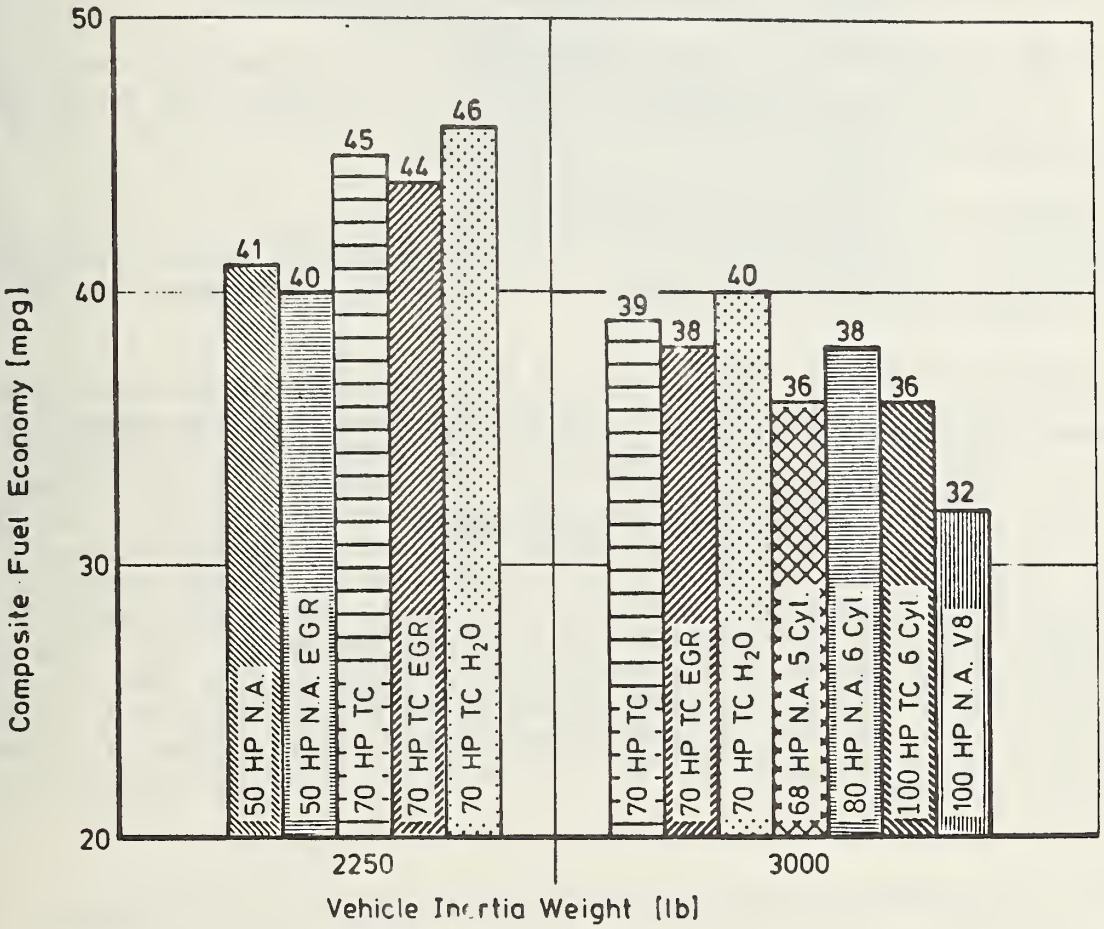

FIGURE 6.1-25: COMPUTED FUEL ECONOMY FROM STEADY-STATE ENGINE MAPS, COMPARISON OF VARIOUS ENGINE TECHNOLOGIES.

The turbocharged (TC) engine offers 10% better fuel economy in vehicles of the 2,250-lb. IW class than naturally-aspirated (NA) engines in this class because of the different transmission ratios in the TC engine, while fuel economy improves by only 3% if both engines use the same transmission (see Table 5, Appendix).

Exhaust gas recirculation (EGR) lowers fuel economy by 3% in the 90 CID 4-cylinder engines 50 HP (NA) and 70 HP (TC). Water injection raises fuel economy by 3%.

Higher performance (HP/IW) in the 3,000-lb. inertia-weight class deteriorates fuel economy of the naturally-aspirated engine. The lowest fuel economy is obtained by the projected 100 HP 180 CID 8-cylinder engine. A straightforward projection was used which does not take into account the comparatively lower friction losses of the V8 engine: two production engines operating in parallel. That means that the engine maps of the 4-cylinder 50 hp engine were used for an engine version of 180 CID. The low fuel economy results from the low degree of engine full-load-torque utilization during the test.

The 80 HP NA 6-cylinder engine has a better fuel economy than the 5-cylinder engine. This somewhat surprising result was achieved because the 6-cylinder engine is a carefully tuned prototype, while the 5-cylinder unit was still in the development stage at the time of the program.

Turbocharging improves fuel economy despite higher output. This is shown by comparisons between the 4-cylinder turbocharged and the naturally-aspirated 5-cylinder diesel engines, and between the 6-cylinder turbocharged and the naturally-aspirated V8 diesel engines.

A comparison between the 68 and 70 HP diesel engines in simulated vehicles of the same weight and with the same transmission shows that the naturally-aspirated engine consumes 10% more fuel than the turbocharged engine. The higher fuel consumption of the 68 HP NA engine is caused by its larger swept volume and increased friction losses at the same power output, and its different speed range. Further development of the 68 HP NA engine may improve fuel economy. Similar trends are observed in a comparison of the 100 HP engines. It should be borne in mind that the results of the simulated 6-cylinder TC engine appear more favorable than those of the real hardware engine. The 100 HP TC 6-cylinder diesel engine fuel economy data was obtained with the aid of the steady-state engine maps of the 70-HP TC engine with the displacement increased by a ratio of 6:4. The drop in specific output at a higher number of cylinders was not taken into account, while the friction losses of the V8 engine were set slightly too high.

6.1.5 The Effects of Vehicle and Drivetrain Design on Fuel Economy

The fuel economy of an engine/vehicle system essentially is affected by the following factors:

- Weight, aerodynamic resistance, rolling resistance (of vehicle)
- Bmep, speed range, specific fuel consumption (of engine)
- Overall ratio, number of gears, axle ratio (of transmission) for the required acceleration, passing performance, gradeability and top speed.

These engine/vehicle system component should be designed for the applicable operation cycle, legal constraints, and consumer requirements. The fuel economy may be shown as a function of vehicle inertia weight (Figure 6.1-26). It may be seen that fuel economy decreases when the vehicle weight and the HP-to-inertia-weight ratio increase. The decrease is due to the increased mechanical energy required during dynamic testing.

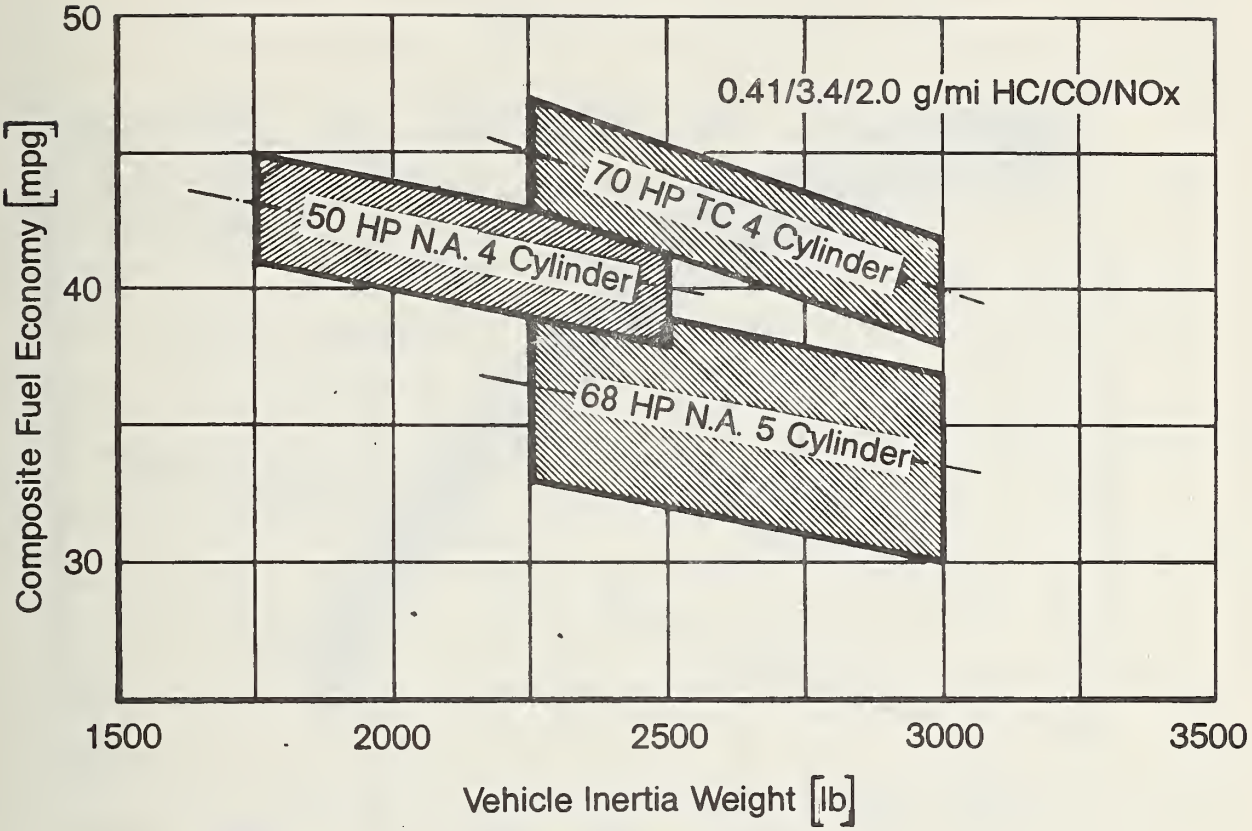

FIGURE 6.1-26: COMPARISON OF FUEL ECONOMY OF THREE DIFFERENT DIESEL ENGINES
The scatter band of the 68-HP engine is wider because of its state of development.

It should be noted, though, that this difference in fuel economy is covered by a scatter band width. Also, the difference may vary significantly depending on the type of engine/vehicle system because of the possible occurence of two opposing effects:

- an increase in the required mechanical energy (inertia weight)
- an increase in the mean thermal efficiency (the engine must be operated at increased bmep in order to produce higher output at the same rpm for a vehicle of higher inertia weight).

Figure 6.1-27 shows the computed thermal engine efficiency for three different drive ratios in the 70 HP turbocharged diesel engine. The engine speed for a given drive ratio is the same in each weight class and thus shifts the operating ranges toward higher thermal efficiency.

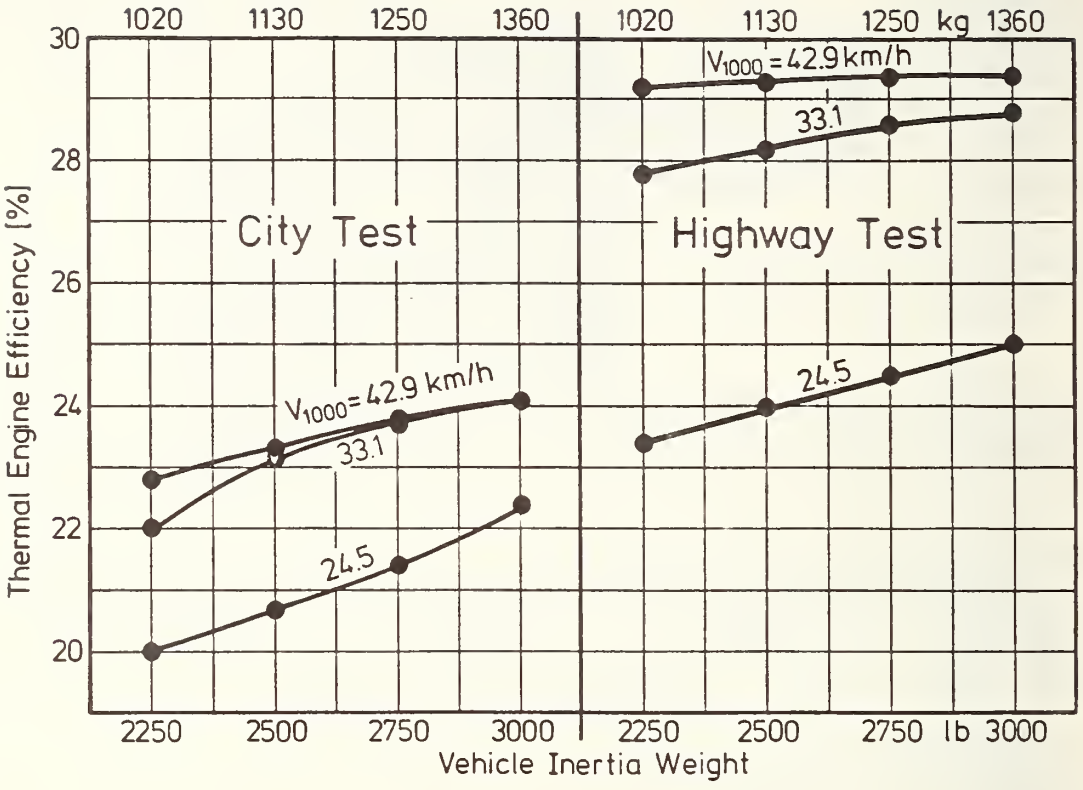

FIGURE 6.1-27: COMPUTED THERMAL ENGINE EFFICIENCY OF A 70 HP TC DIESEL FOR VARIOUS TRANSMISSIONS AND VEHICLE WEIGHTS.

These marked differences show that the fuel economy sensitivity to the various variables must be seen as a complex quantity which cannot be adequately covered by the simplified graph in Figure 6.1-26. Particular importance should be attributed to the drivetrain which is the connecting link between engine and vehicle.

The operating points with the lowest specific fuel consumption can be determined for each engine in the steady-state map on the lines of constant performance. This results in the optimum fuel consumption line (Figure 6.1-28).

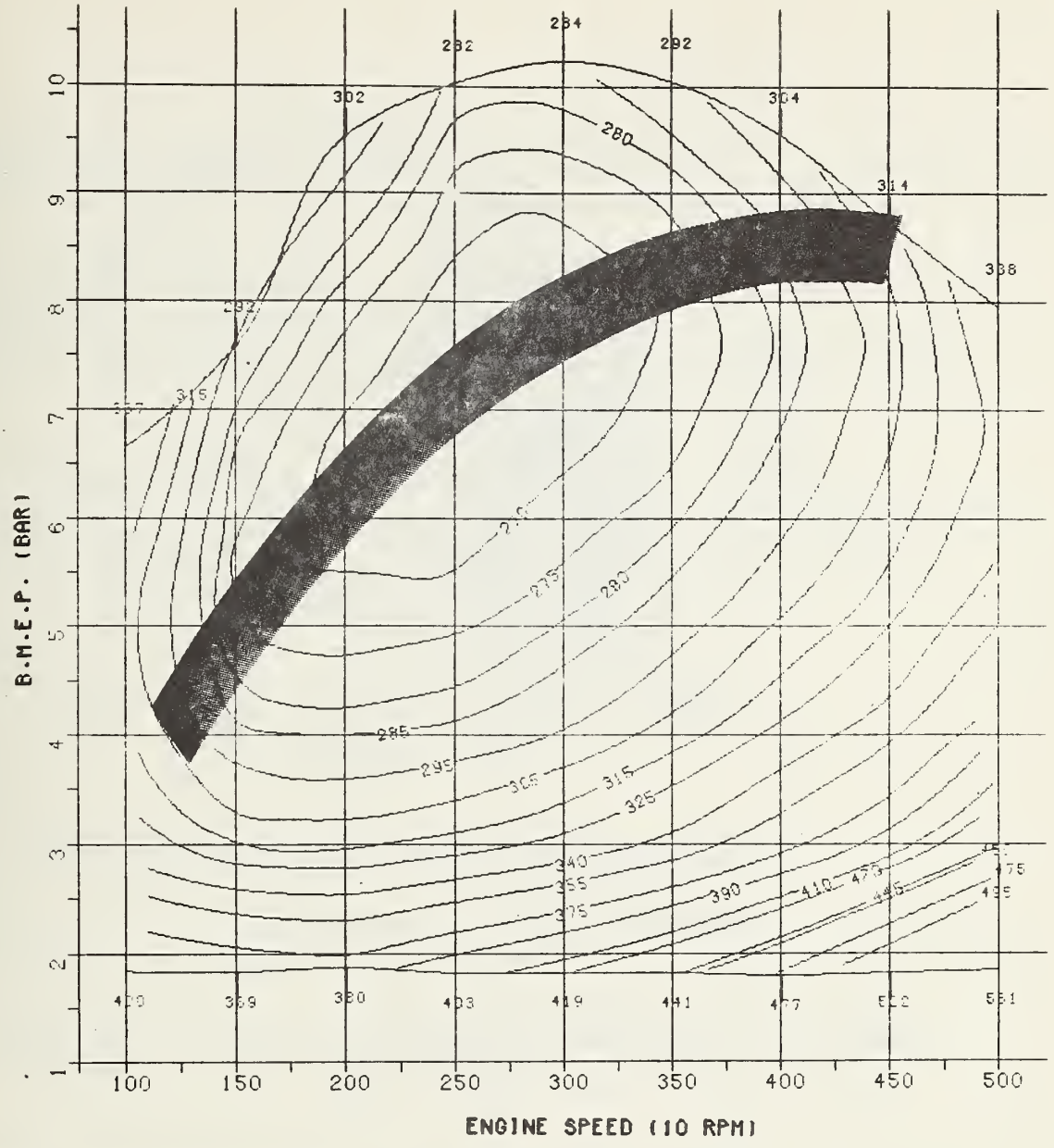

FIGURE 6.1-28: OPTIMUM FUE ECONOMY RANGE

The lowest fuel consumption would be achieved if the engine were operated on this line (invariable transmission). However, significant deviations from this line become necessary because of the limited number of gears in a manual transmission system. The higher maximum output, furthermore, mostly is required for acceleration purposes (tractive power surplus) and also leads to improved driveability. The best possible fuel economy results if the most frequent operation in the load cycle can be positioned on the ideal line with the various load points as close together as possible.

Figure 6.1-29 shows the engine operating regions in the Federal Driving Cycle in a specific fuel consumption map. The graph includes the full-load torque curve and the curves for constant-engine-power output.

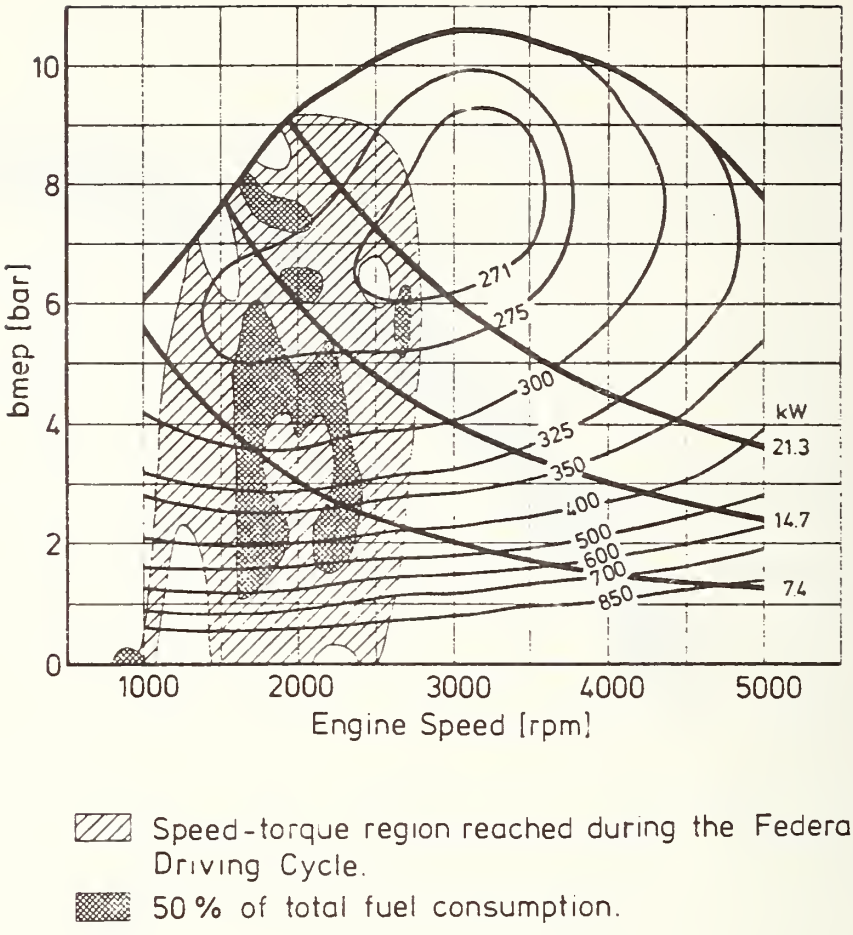

FIGURE 6.1-29: ENGINE OPERATING REGIONS IN THE U.S. 1975 DRIVING CYCLE 70 HP TC DIESEL ENGINE FOR A 3000 LB. VEHICLE

Figure 6.1-30 is a comparison of fuel consumption data for engines with 4- and 5-speed manual transmissions. The brake mean effective pressure in bar is plotted versus the engine speed. The solid black lines show the specific fuel consumption in g/kWh. The shaded areas show engine speeds and torque ratios in the Federal Driving Cycle. Two characteristic points are shown for the Highway Driving Cycle.

The sensitivity of fuel economy to transmission design was arrived at by projections from steady-state engine maps. The computed values were verified by chassis/dynamometer tests on the available engine/vehicle systems.

Tables 6.1-2 through 6.1-4 constitute a classification of the axle/gearbox combinations for the vehicle velocity V_{1000} and high gear. The so-called effective transmission radius R for the city and highway cycles is included. The effective transmission radius is defined by the ratio of travelled test distance to the number of engine revolutions during the test and divided by 2π.

The gear boxes have five speeds. They may be used as four-speed gear boxes by omitting the fifth speed. One of the gear boxes is designed for good acceleration and has small increments in the gear ratios. The other one has large increments for fuel-economy optimization. The transmission data is itemized in Table 5 of the Appendix.

Axle No.	1	2	3
Ratio	3.89	3.60	3.27
Teeth ratio	74/19	72/20	72/22

TABLE 6.1-2: GEAR RATIOS OF THE TWO GEAR BOXES OF 5-SPEEDS

Gear Box No.	Speed 1	2	3	4	5
1	3.45 38/11	1.94 35/18	1.29 36/28	0.97 31/32	0.75 27/36
2	3.45 38/11	1.94 35/18	1.37 37/27	1.10 33/30	0.91 30/33

TABLE 6.1-3: GEAR RATIOS OF THE TWO GEAR BOXES OF FIVE SPEEDS USED

Combi-nation	Axle	Gear-box	Speeds	R City	R Highway	V_{1000}
1	1	2	4	43.12	63.95	24.5
2	2	2	4	46.18	69.15	26.5
3	1	1	4	45.09	72.22	27.8
4	3	2	4	50.21	76.15	29.2
5	1	2	5	44.26	76.30	29.6
6	2	1	4	48.17	77.91	30.0
7	2	2	5	47.37	82.49	32.0
8	3	1	4	52.39	85.91	33.1
9	3	2	5	51.40	90.68	35.2
10	1	1	5	46.62	91.84	36.0
11	2	1	5	49.84	99.17	38.9
12	3	1	5	54.14	109.28	42.9

TABLE 6.1-4: TRANSMISSION DATA RESULTING FROM THE COMBINATION OF 3 AXLES, 2 GEARBOXES USING 4 OR 5 SPEEDS, AND TIRE RADIUS OF 279 mm

Figure 6.1-31 shows the fuel economy values computed for the 12 axle/gearbox combinations given in Tables 6.1-3 through 6.1-5. Each curve for the city fuel economy represents the results with one gear box. The three points on each curve indicate the results for the three axles. All highway fuel economy points may be connected by one smooth curve.

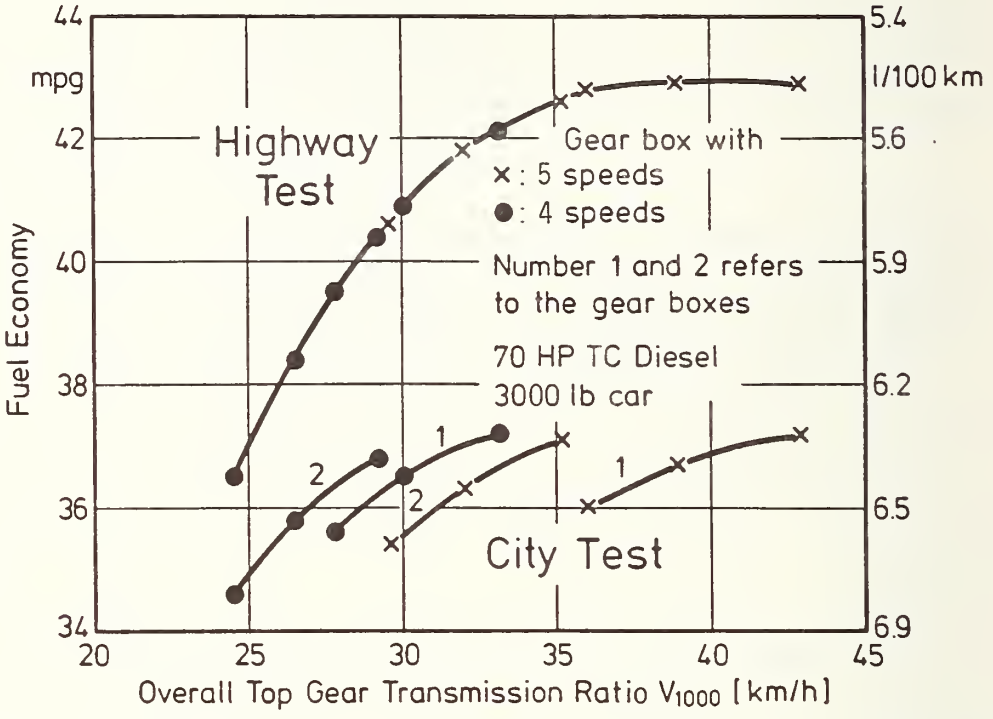

FIGURE 6.1-31: COMPUTED FUEL ECONOMY AS A FUNCTION OF THE OVERALL TOP GEAR TRANSMISSION RATIO V_{1000}. STEADY-STATE DATA OF A 70 HP TURBOCHARGED DIESEL ENGINE ARE USED.

Figure 6.1-32 shows the fuel economy values of 96 different projections versus the effective transmission radius (R) instead of the speed V_{1000}. The fuel economy rises steadily with increasing R, even in the city driving cycle. This means that the fuel consumption is determined primarily by the number of engine revolutions per vehicle mile.

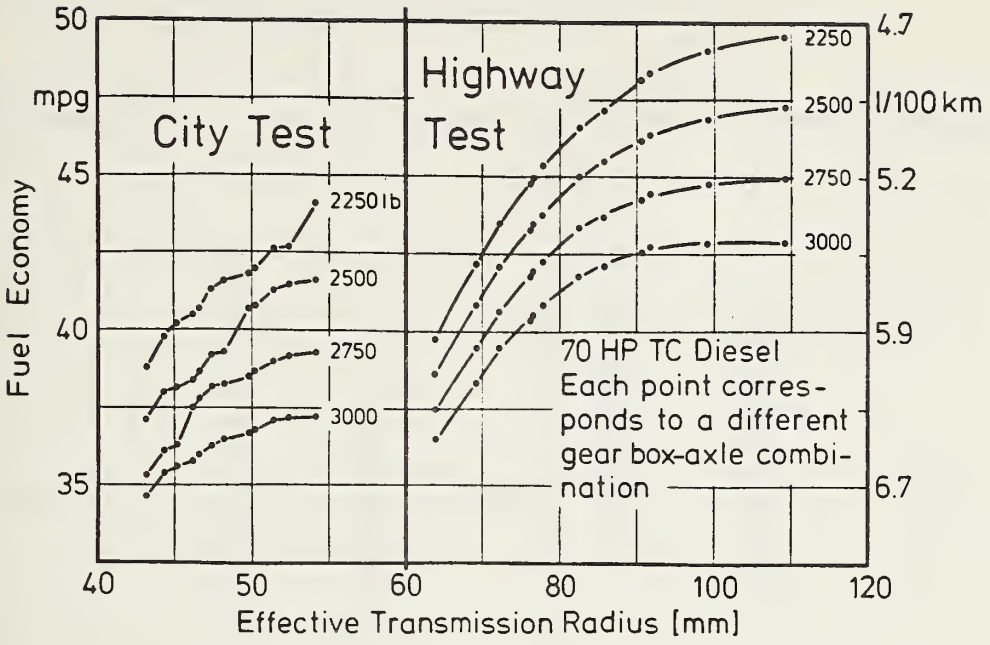

FIGURE 6.1-32: COMPUTED FUEL ECONOMY AS A FUNCTION OF THE EFFECTIVE TRANSMISSION RADIUS FOR VARIOUS VEHICLE WEIGHTS.
Note: The fuel consumption rises with the number of engine revolutions per vehicle mile

Figure 6.1-32 does not provide any information on vehicle performance. The interrelationships between fuel economy and acceleration performance must be reviewed at the same time (Appendix, Table 5). The effects on fuel economy and acceleration performance of rear axle ratio, number of gears, and transmission design combined with a 4-cylinder naturally-aspirated and turbocharged engine in a vehicle of 2,250-lb. inertia weight are shown in Figures 6.1-33 through 6.1-38.

This permits a trade-off between fuel economy and acceleration performance for different drivetrain matching. However, these trade-offs become complete only when gradeability, emissions (exhaust gas and noise) and the additional investments are taken into account (e.g. for five-speed transmissions).

The appendix contains additional data for other engines and inertia weights.

Figure 6.1-39 shows the relation of the possible fuel economy improvements caused by improved aerodynamics and lower rolling resistance of the vehicle versus vehicle inertia weight. This graph shows the computed fuel economy data for an engine/vehicle system in the 2,250-lb. inertia-weight class equipped with a 50 HP NA diesel engine for various drag coefficients times aerodynamic area and rolling resistances. The drag coefficient $C_D \cdot F = 0.77\ m^2$ equals that of the VW Rabbit. A decrease of the drag coefficient times aerodynamic area from $0.77\ m^2$ to $0.5\ m^2$ improves fuel economy by 8%.

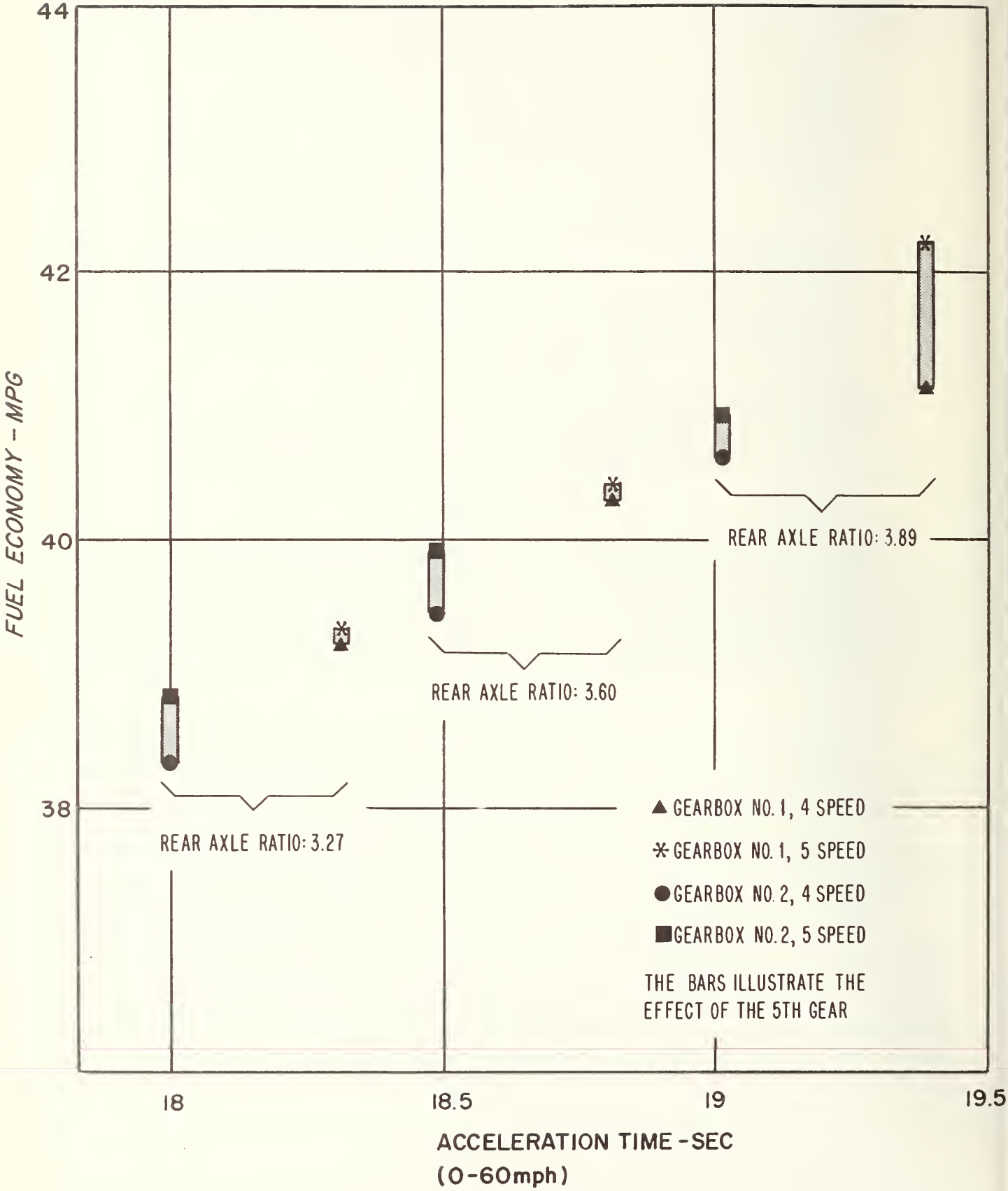

FIGURE 6.1-33: COMPUTED FUEL ECONOMY (CITY CYCLE) AND ACCELERATION PERFORMANCE FOR DIFFERENT REAR AXLE AND GEARBOX COMBINATIONS
Engine: Diesel, 4-cylinder, NA, 50 HP
Vehicle: VW Rabbit, Inertia-weight 2250 lb.
Road Load; EPA nominal

Engine: Diesel, 4-cylinder, NA, 50 HP
Vehicle: VW Rabbit, Inertia-weight 2250 lb.
Road Load: EPA nominal

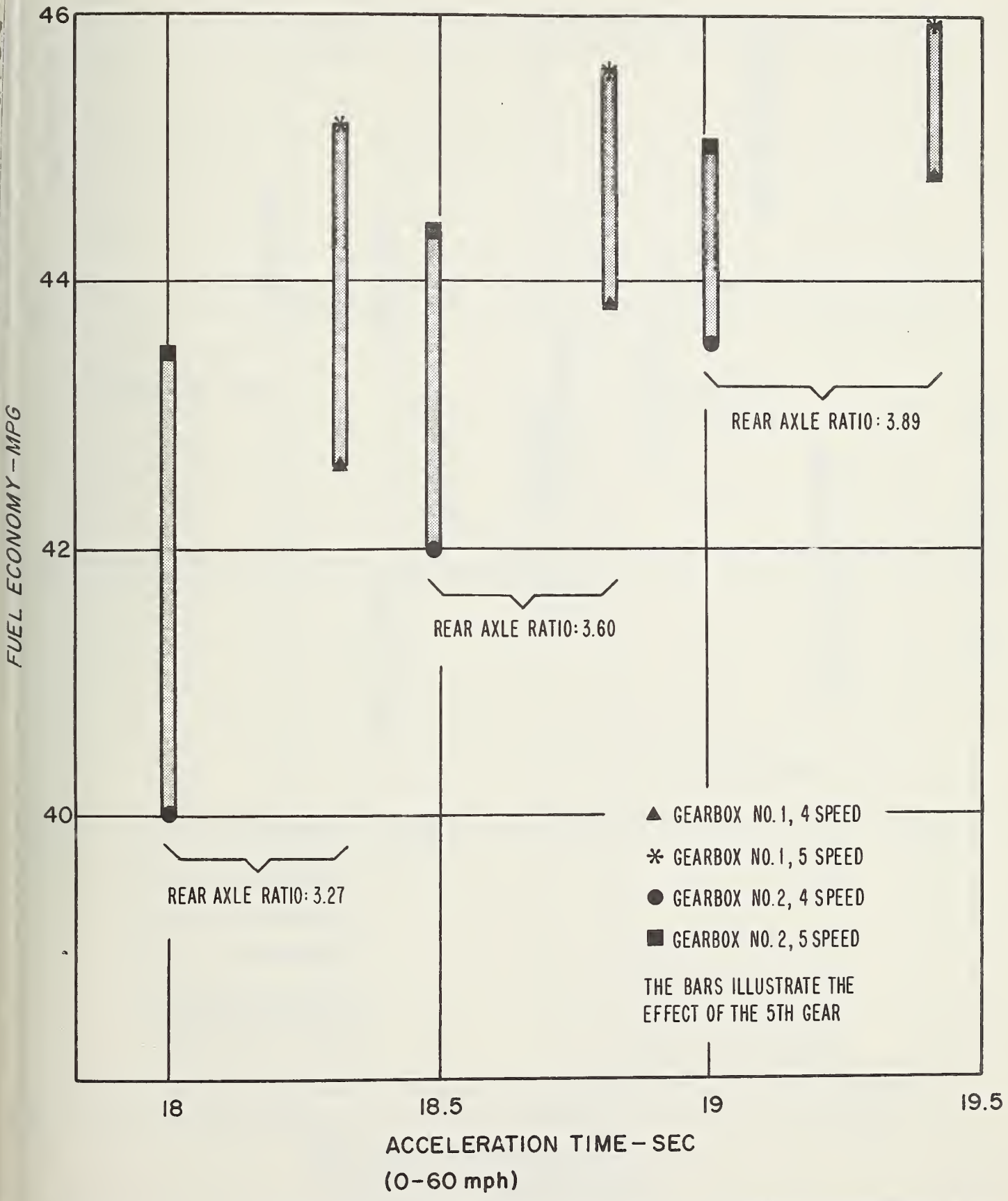

FIGURE 6.1-34: COMPUTED FUEL ECONOMY (HDC-CYCLE) AND ACCELERATION PERFORMANCE FOR DIFFERENT REAR AXLE AND GEARBOX COMBINATIONS

Vehicle: VW Rabbit, Inertia-weight 2250 lb.
Road Load: EPA nominal

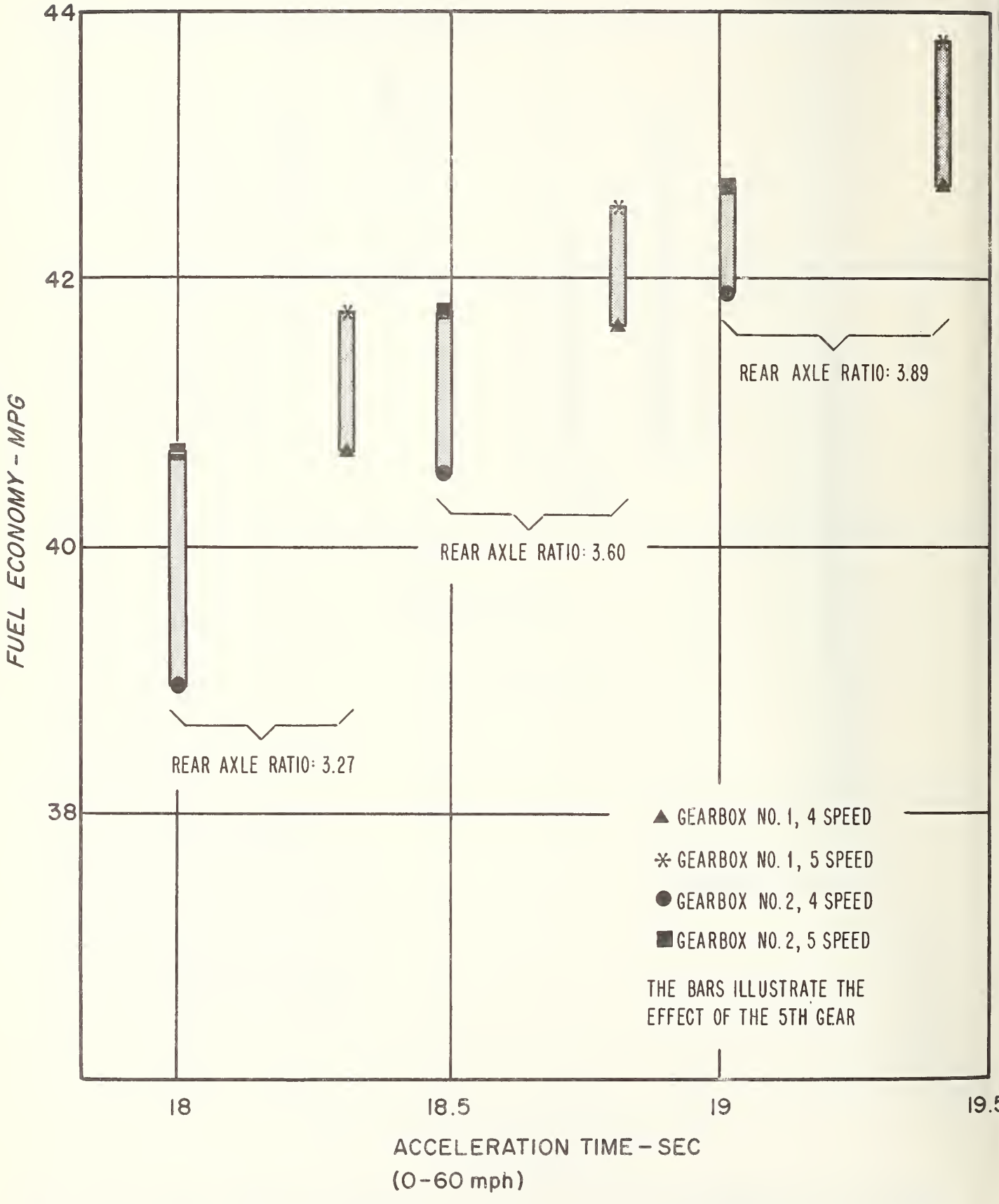

FIGURE 6.1-35: COMPUTED FUEL ECONOMY (COMPOSITE) AND ACCELERATION PERFORMANCE FOR DIFFERENT REAR AXLE AND GEARBOX COMBINATIONS

Engine: Diesel, 4-cylinder, turbocharged, 70 HP
Vehicle: VW Rabbit, Inertia-weight 2250 lb.
Road Load: EPA nominal

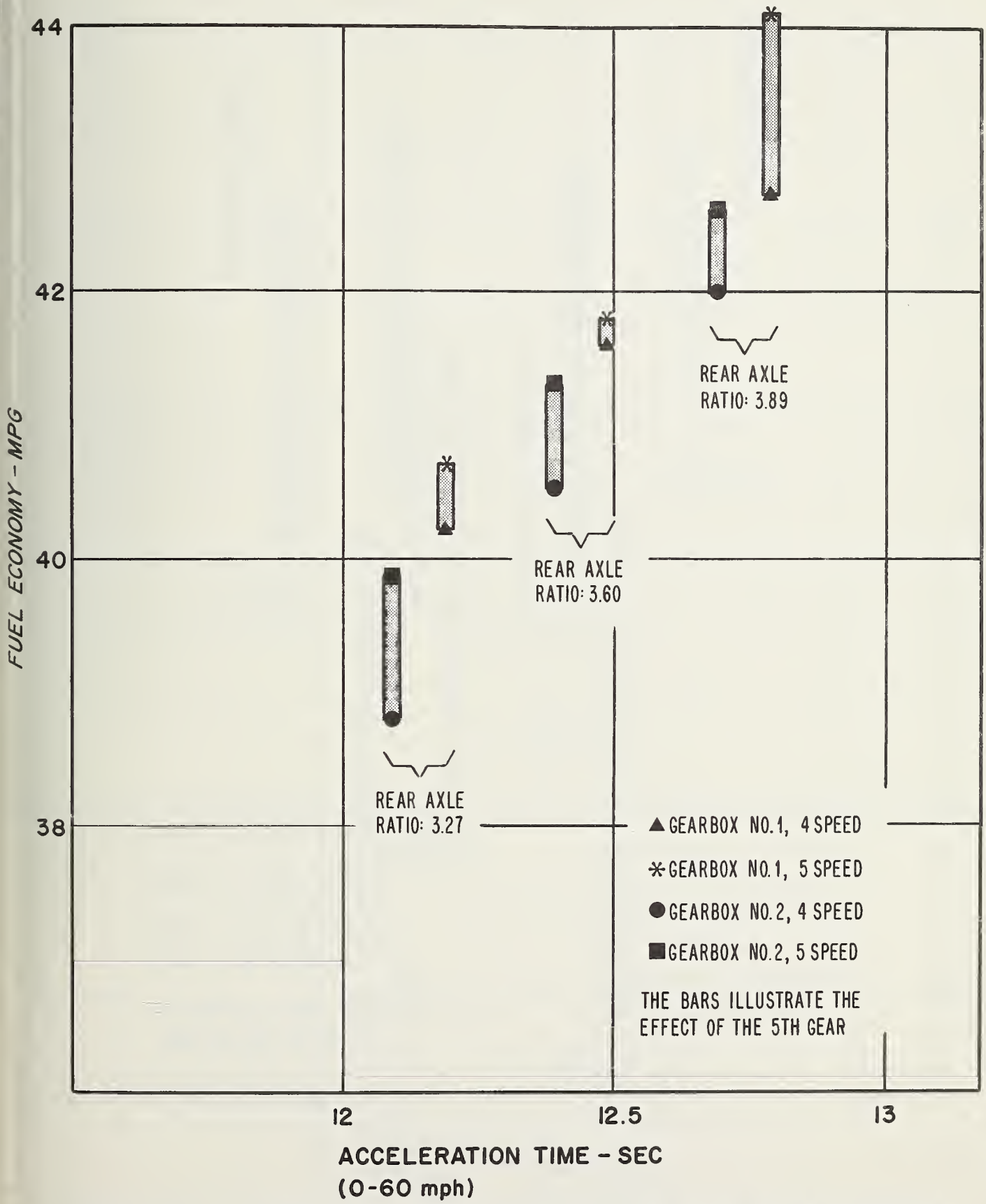

FIGURE 6.1-36: COMPUTED FUEL ECONOMY (CITY CYCLE) AND ACCELERATION PERFORMANCE FOR DIFFERENT REAR AXLE AND GEARBOX COMBINATIONS

Engine: Diesel, 4-cylinder, turbocharged, 70 HP
Vehicle: VW Rabbit, Inertia-weight 2250 lb.
Road Load: EPA nominal

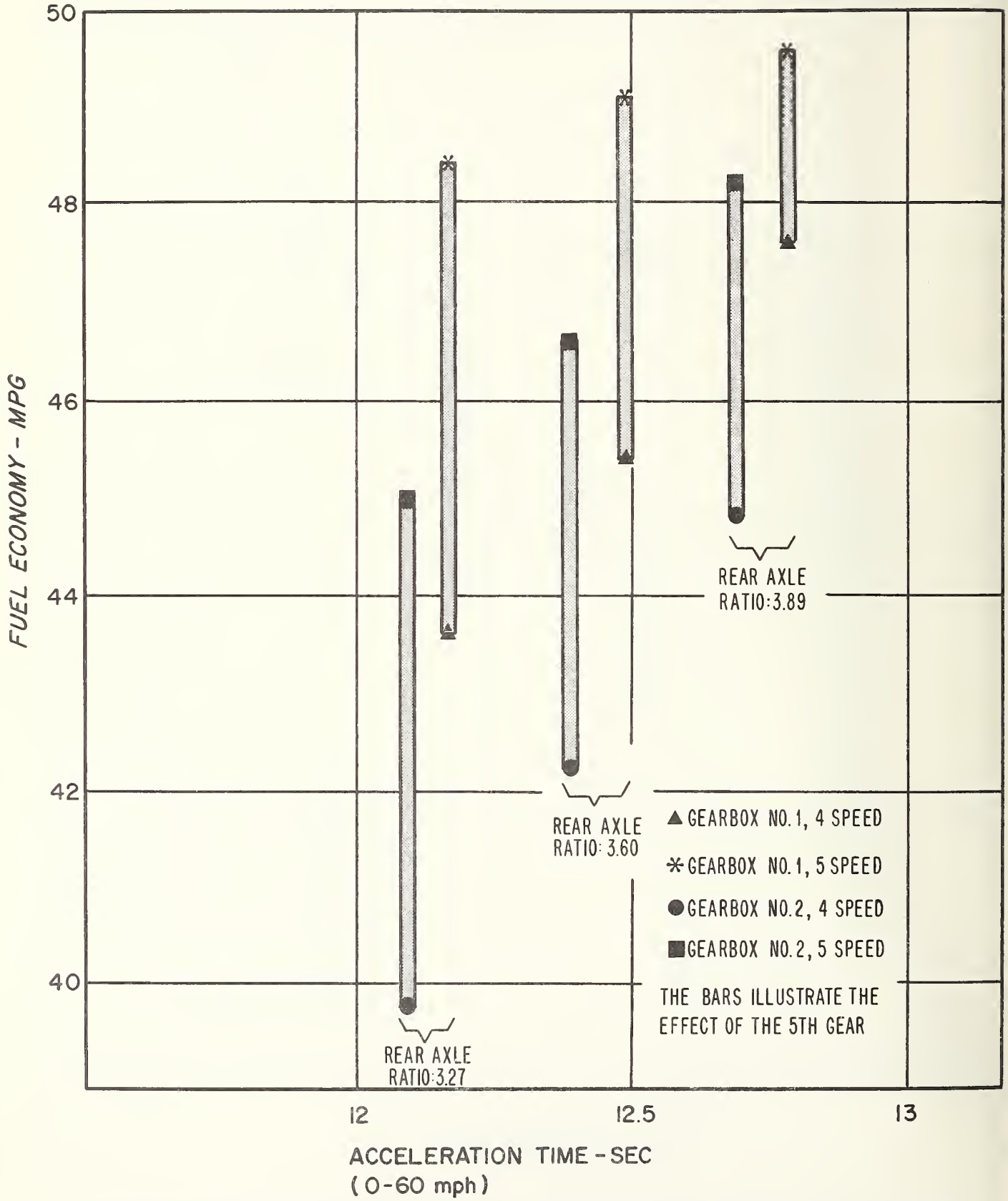

FIGURE 6.1-37: COMPUTED FUEL ECONOMY (HDC-CYCLE) AND ACCELERATION PERFORMANCE FOR DIFFERENT REAR AXLE AND GEARBOX COMBINATIONS

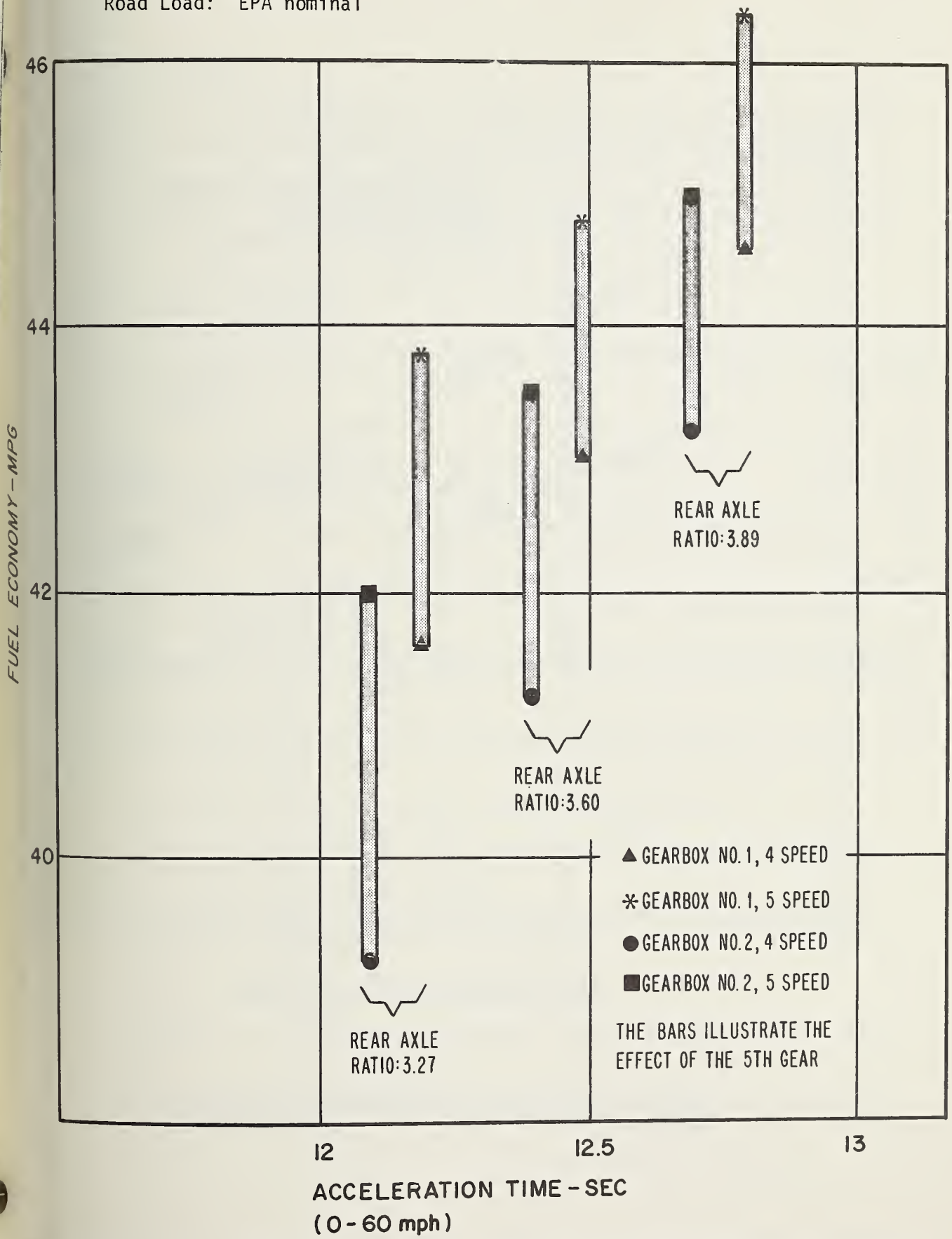

FIGURE 6.1-38: COMPUTED FUEL ECONOMY (COMPOSITE) AND ACCELERATION PERFORMANCE FOR DIFFERENT REAR AXLE AND GEARBOX COMBINATIONS

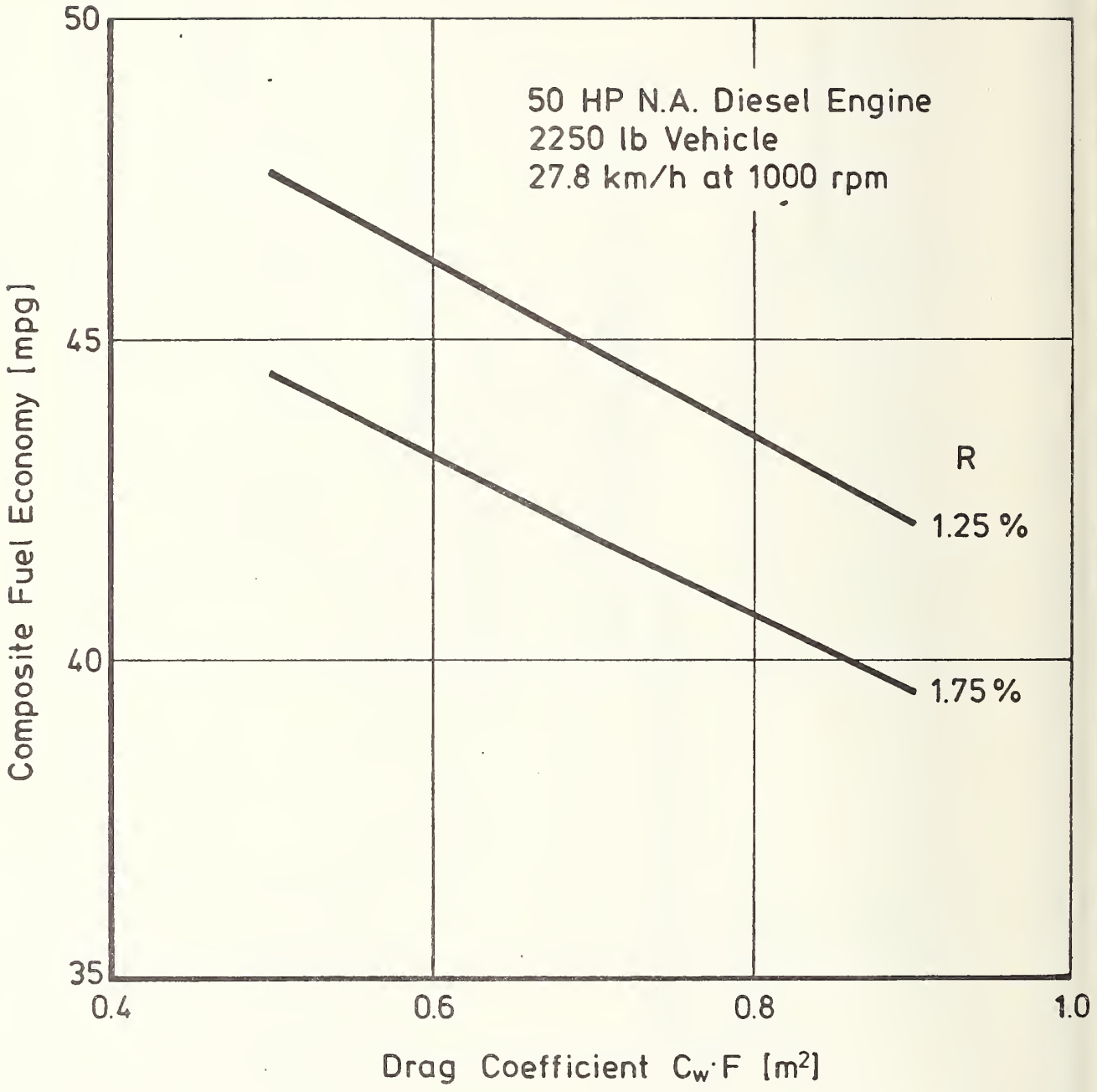

FIGURE 6.1-39: COMPUTED FUEL ECONOMY AS A FUNCTION OF DRAG AND THE ROLLING RESISTANCE

6.2 EMISSIONS

Exhaust and noise emission data was generated for several engine/vehicle systems. The investigated exhaust emissions were divided into two groups:

(1) Regulated exhaust emissions consisting of hydrocarbons (HC) expressed in terms of grams of CH_2, carbon monoxide (CO), and nitrogen oxides (NOx) expressed in terms of grams of NO_2.

(2) Unregulated exhaust emissions including
- smoke visibility
- particulates
- odorants, such as aromatic and oxygenated hydrocarbons
- sulfates,
- ammonia
- aldehydes.

The emission data was generated on engine and vehicle level. Following are the objectives of the tests on engine level:

- determination of engine operating conditions and their effects on emissions

- preparation of steady-state engine emission maps for the full range of engine speed and torque

- projections of chassis dynamometer test results for several drivetrains and vehicle inertia weights

- determination of statistically relevant operating ranges in the U.S. 1975 and HDC tests

- determination of typical dynamic engine characteristics

- support of the analytical effort of the engine/vehicle system design.

Tests on vehicle level were performed

- to generate regulated exhaust emission data

- to provide unregulated exhaust emission data

- to establish a correlation between test results on engine and vehicle level.

Noise emission data was generated by road tests.

6.2.1 Methodology for HC/CO/NOx Emission Testing

The methodology and test procedure described in the Federal Register, Vol. 41, No. 177, September, 1976, was used for the chassis dynamometer tests.

The methodology that was used on engine level tests may be classified by two groups:

(1) Projection from steady-state engine maps, and

(2) Dynamic tests on engine dynamometers.

These engine-level test methods are described in Section 6.1.1. The essential difference between the constant volume sampling (CVS) technique and these methods is the numeric integration of the product obtained by multiplying the exhaust volume flow by the respective volume concentrations instead of the dilution of the exhaust volume flow to a constant total flow.

The exhaust volume flow is determined indirectly. The intake air flow is determined indirectly. The intake air flow is determined first by measurement in the dynamic tests, or from the air-to-fuel ratio λ and the fuel-flow rate in the steady-state measurements. The exhaust volume is then computed from the intake air flow and the air-to-exhaust volume ratio as a function of the exhaust gas composition.

6.2.2 HC/CO/NOx Emission Results

The HC/CO/NOx emission results are presented in eight different formats:

(1) steady-state engine maps of specific emissions for each engine tested;

(2) steady-state engine maps of the concentration by volume in the exhaust gas;

(3) comparisons of full-load emissions of all engines tested, data extracted from the steady-state engine maps;

(4) comparisons of road-load emissions of all engine/vehicle systems tested or projected with the data extracted from the steady-state engine maps;

(5) projections of emission test results from steady-state engine maps;

(6) results of engine dynamometer tests;

(7) dynamic engine maps of emission rates including the main speed/torque zones;

(8) results of chassis dynamometer tests in accordance with the U.S. Federal Test Procedure (Federal Register, Vol. 41, No. 177, September, 1976).

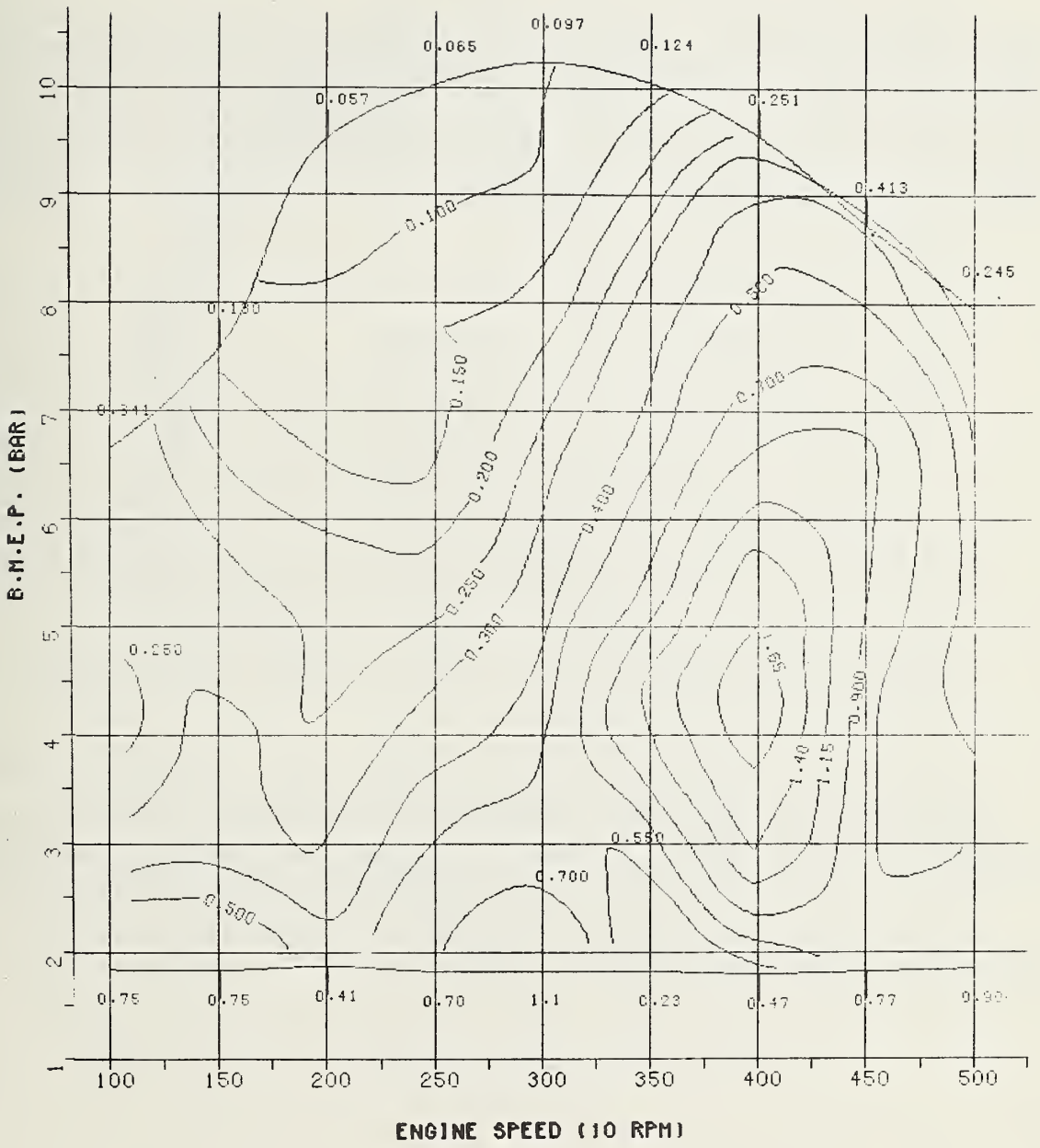

FIGURE 6.2-1: HC EMISSION (g/kWh)
70 HP TURBOCHARGED RESEARCH DIESEL ENGINE

Figures 6.2-1 through 6.2-3 are maps of the steady-state HC, CO, and NOx emissions from the 70 HP turbocharged research diesel engine. The complete set of steady-state HC/CO/NOx emission maps for the size engines that were tested on two different fuels are included in the Appendix.

Cross sections through those steady-state emission maps are used for engine characterization. Relevant cross sections are the full-load and road-load curves. Figure 6.2-4 shows the HC/CO/NOx emissions at full-load operation from four engines during engine dynamometer tests. The engines with exhaust gas recirculation are not included because there should be no EGR at full-load operation. The projected engines (6-cylinder turbocharged, and V-8) have the same specificemissions as their base engines. Figure 6.2-4 includes the following engines:

- 50 HP naturally-aspirated, 90 CID, 4 cylinders
- 70 HP turbocharged, 90 CID, 4 cylinders
- 68 HP naturally-aspirated, 130 CID, 5 cylinders
- 80 HP naturally-aspirated, 146 CID, 6 cylinders
- 50 HP naturally-aspirated EGR equal to the 50 HP naturally-aspirated
- 70 HP turbocharged EGR equal to the 70 HP turbocharged
- 100 HP naturally-aspirated, 180 CID, 8 cylinders equal to the 50 HP naturally-aspirated
- 100 HP turbocharged, 146 CID, 6 cylinders equal to the 70 HP turbocharged

The HC emission from the 5-cylinder prototype engine is markedly higher than that from the other engines, especially at 3,500 rpm because of the early stage of development (injection and combustion optimization has not been completed).

The HC emission from the 70 HP turbocharged diesel engine over the entire engine-speed range is lower than .4 g/kWh.

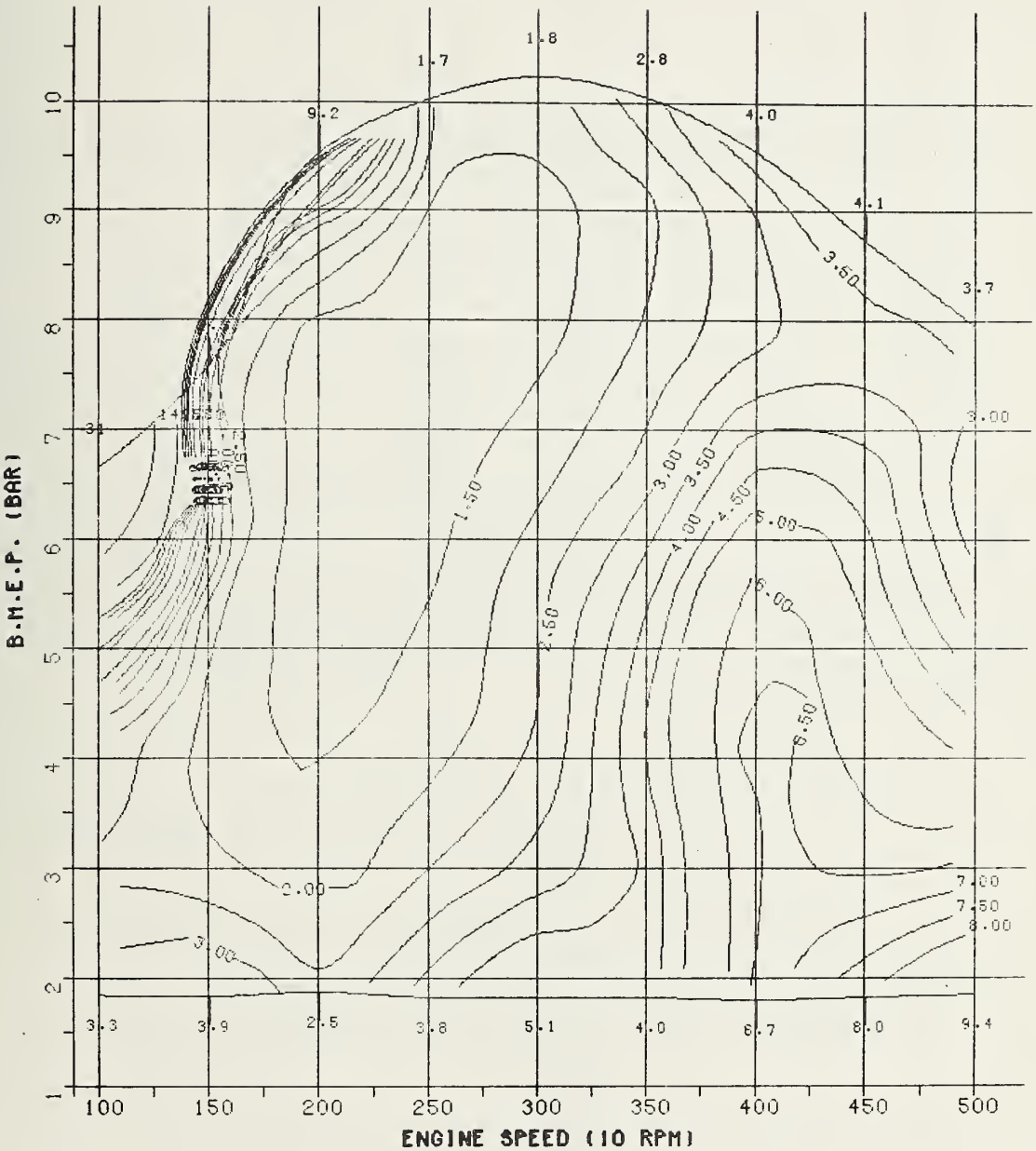

FIGURE 6.2-2: CO EMISSION (g/kWh)
70 HP TURBOCHARGED RESEARCH DIESEL ENGINE

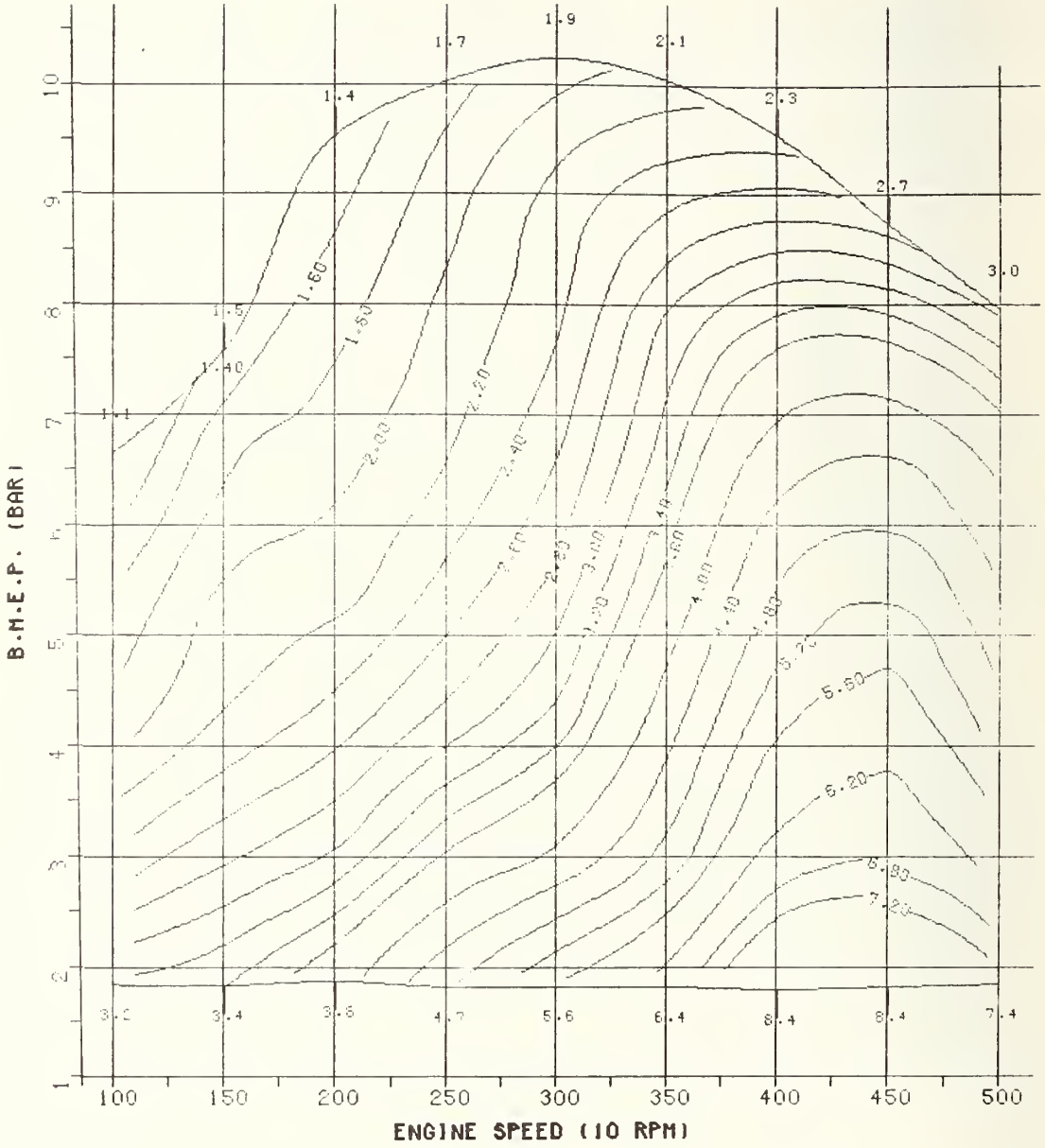

FIGURE 6.2-3: NOx EMISSION (g/kWh)
70 HP TURBOCHARGED RESEARCH DIESEL ENGINE

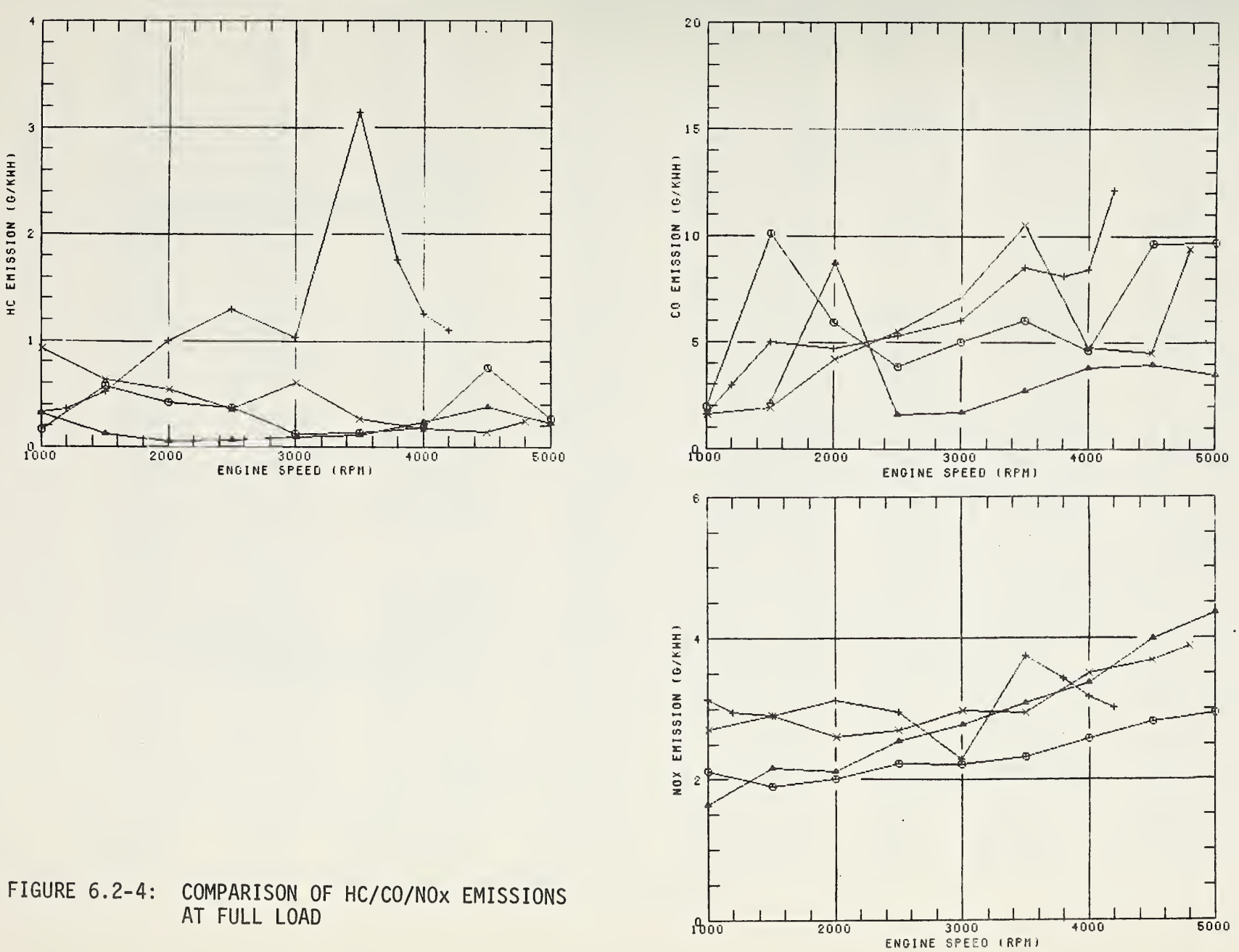

FIGURE 6.2-4: COMPARISON OF HC/CO/NOx EMISSIONS AT FULL LOAD

The CO emissions from all engines scatter around 5 g/kWh during full-load operation. The overall range of emissions produced by the four investigated engines extends from 2 through 10 g/kWh. The scatter band of the NOx emissions is comparatively narrow. The increase from 2.5 to 3.5 g/kWh during the increase in engine speed from 1,000 to 5,000 rpm is related to the higher engine temperatures at high engine speeds.

Figure 6.2-5 is a comparison of HC/CO/NOx steady-state emissions at road loads between two vehicles. One vehicle is in the 2,250-lb. and the other in the 3,000-lb. inertia-weight class. Four engines were investigated for each vehicle. Section 6.1 includes further details of the methodology that was used in the process.

Except for the 5-cylinder prototype engine, HC emissions at road loads stay below 0.5 g/mile in the vehicle velocity range from 25 to 80 mph. The HC emissions from the 5-cylinder engine range from .05 to 0.5 g/mile because of its development stage.

The CO emissions keep below 2 g/mile except for the prototype 5-cylinder engine. The HC and CO emissions from the 50 HP naturally-aspirated engine with modulated exhaust gas recirculation exceed those from the other investigated engines. The steep rise of CO emissions from the 50 HP NA engine with EGR might be attributed to some error during top-speed full-load testing. It may also have been caused by some error in the problematic tuning of EGR devices.

Exhaust gas recirculation apparently affects the NOx emissions in the vehicle velocity range up to 60 mph. The NOx emissions drop below 0.5 g/mile from those engines that have EGR. The NOx emissions increase in proportion to vehicle velocity because of the effects of higher engine temperatures at higher engine speeds.

Projections of regulated-emission test results were computed with the aid of steady-state engine maps. These projections were performed in order to determine the sensitivities of emissions to engine technology and performance and to vehicle technology and drivetrains. The absolute values should be interpreted very carefully. Table 6.2-1 includes a comparison between the projected and actual emission data produced by chassis and engine dynamometer tests.

Figure 6.2-6 shows the HC/CO/NOx emissions produced by chassis dynamometer tests in accordance with the U.S. Federal Test Procedure. Table in the Appendix includes an itemized list of test results for 15 engine/vehicle systems. These results are summarized in Table 6.2-1.

Figure 6.2-6 shows that engine/vehicle systems without EGR comply with the emission level goals of .41/3.4/2.0 g/mile of HC/CO/NOx. Additional development work is required for the 5-cylinder prototype engine in order to keep its emission levels within the required safety margin for production engines.

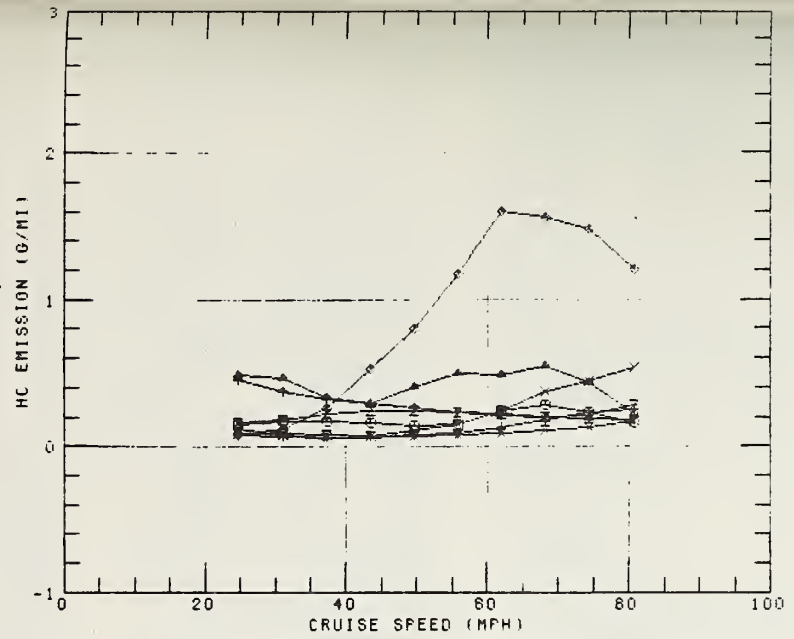

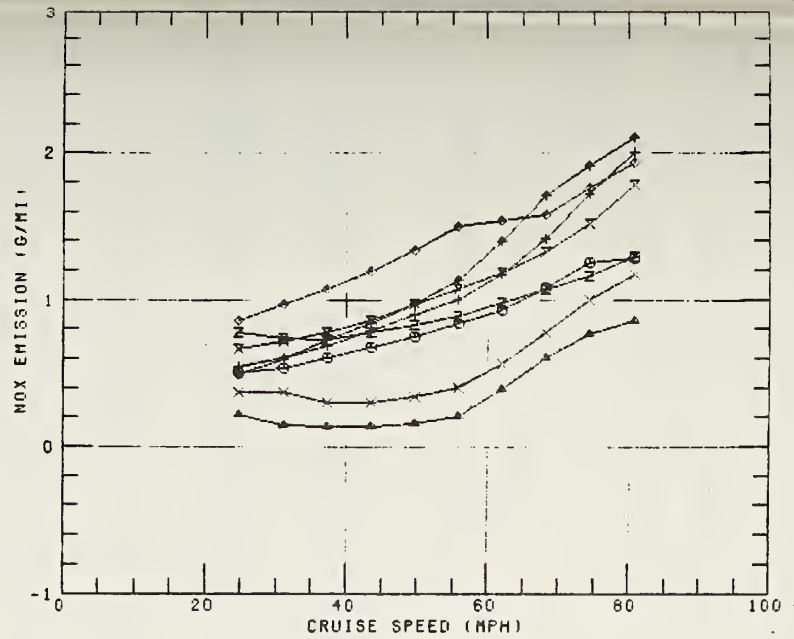

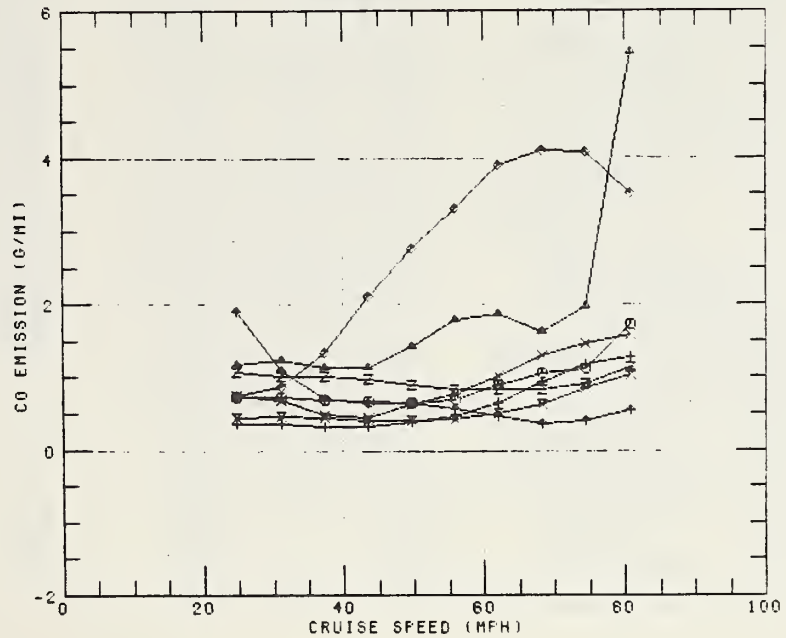

ROAD LOAD CURVES

2250 LB VEHICLE	3000 LB VEHICLE
× 70 HP TC E.G.R	Z 8 CYLINDER 180 CID N.A.
+ 70 HP TC DIESEL	X 6 CYLINDER 146 CID TC
▲ 50 HP N.A. E.G.R.	↑ 6 CYLINDER 146 CID N.A.
⊙ 50 HP N.A. DIESEL	◇ 6 CYLINDER 130 CID N.A.

FIGURE 6.2-5: COMPARISON OF HC/CO/NOx EMISSIONS AT ROAD LOAD

Inertia Weight lb	HC g/mile			CO g/mile			NOx g/mile			Engine Type
	C	E	S	C	E	S	C	E	S	
1,750	.14	.30	.30	.82	1.20	1.39	1.12	.62	.90	50 HP N.A.
	.45	.29	.37	2.79	1.73	2.09	.40	.43	.27	50 HP N.A.E.G.R.
2,000	.16	.32	.29	1.18	1.31	1.40	1.28	.71	.92	50 HP N.A.
	.41	.38	.37	2.15	2.06	2.07	.48	.49	.29	50 HP N.A. E.G.R.
2,250	.16	.39	.29	1.00	1.36	1.42	1.21	.77	.94	50 HP N.A.
	.39	.33	.36	2.48	1.96	2.05	.49	.50	.31	50 HP N.A. E.G.R.
	.15	.24	.16	.86	.80	.91	.93	.81	1.07	70 HP TC
	.29	.30	.15	3.35	1.41	1.51	.44	.32	.57	70 HP TC E.G.R.
	.21		.12	.85		.93	.83		.96	70 HP TC H_2O
	.41	.50		1.64	2.31		1.53	1.29		68 HP N.A. 5 Cylinder
2,500		.32	.29		1.42	1.45		.71	.97	50 HP N.A.
		.36	.36		2.16	2.05		.57	.34	50 HP N.A. E.G.R.
		.24	.16		.89	.96		.82	1.08	70 HP TC
		.11	.17		.99	1.54		.36	.58	70 HP TC E.G.R.
2,750	.19	.18	.16	.82	.92	1.01	1.00	.89	1.11	70 HP TC
	.16	.08	.16	.93	.60	1.53	.64	.61	.60	70 HP TC E.G.R.
	.19			.84			.86			70 HP TC H_2O
	.41	.49		1.64	2.52		1.53	1.33		68 HP N.A. 5 Cylinder
3,000	.14	.18	.16	.85	.93	1.07	1.00	.93	1.14	70 HP TC
	.14	.09	.16	.94	.66	1.52	.63	.62	.62	70 HP TC E.G.R.
	.28		.11	.98		1.11	.73		.99	70 HP TC H_2O
	.35	.43	.66	1.82	2.42	2.89	1.80	1.33	1.60	68 HP N.A. 5 Cylinder

TABLE 6.2-1: OVERVIEW OF HC/CO/NOx EMISSIONS (U.S. 1975 TEST CYCLE) FOR VARIOUS ENGINE/VEHICLE SYSTEMS
The tests were performed with the road-load power-absorption values specified in the Federal Test Procedure. The table includes projections from steady-state engine maps (S), actual engine dynamometer test results (E), and chassis dynamometer test results (C).

An increase EGR rate further reduces the NOx emissions and raises the HC/CO emissions. Figure 6.2-6 shows that an NOx emission of 0.5 g/mile can be reached in vehicles of 1,750 to 2,250-lb. inertia-weight. This, however, raises the HC emissions above the tolerance limit.

An analysis was performed of the effects of engine technology and performance on HC/CO/NOx emissions. This analysis covered the following aspects:

- Fuel ignition timing

- Water injection and EGR (these techniques were used to reach a 1 g/mile NOx level)

- Turbocharging (no significant effects on emissions were observed in naturally-aspirated and turbocharged engines of the same performance).

Engine dynamometer measurements were performed on simulated vehicles in order to determine the effects of vehicle technology on emissions. The following aspects were investigated:

- Vehicle inertia weight: Effects were observed on CO and NOx while there were hardly any effects on the NOx emissions.

- Rolling resistance R: An increase in the rolling resistance R from 1.25% to 1.75% produces a 3% increase in NOx emissions.

- Air drag coefficient C_wF (drag x frontal area): An increase of C_wF from 0.5 m^2 to 0.77 m^2 produces a 3% increase in NOx emissions.

The emission pattern is significantly affected by drivetrain matching. Drivetrain modifications will shift the operating ranges of the engine map along the hyperbolic curves of constant engine power. The contour lines of constant specific NOx emissions are perpendicular to the hyperbolas of constant engine power (see Figure 6.2-3). This shows that a shift of the operating range to lower speeds and higher torques is expected to result in a reduction of NOx emissions.

Figure 6.2-7 is a dynamic engine map produced by an engine dynamometer simulation of the U.S. 1975 Test Cycle. Contour lines of constant NOx emission rates are plotted instead of those of specific emissions in order to cover the negative torque range, too. Only those contour lines are plotted that reflect the actual speed/torque ranges covered during the test. The shaded areas are the ranges where approximately 50% of the total emissions was produced during the test. The dotted areas represent 10% of the NOx emissions. The slope of the contour lines is steeper than that of the constant-power hyperbolas. This shows that a shift of the shaded areas toward lower speeds at higher torques is expected to lead to a reduction of NOx emissions.

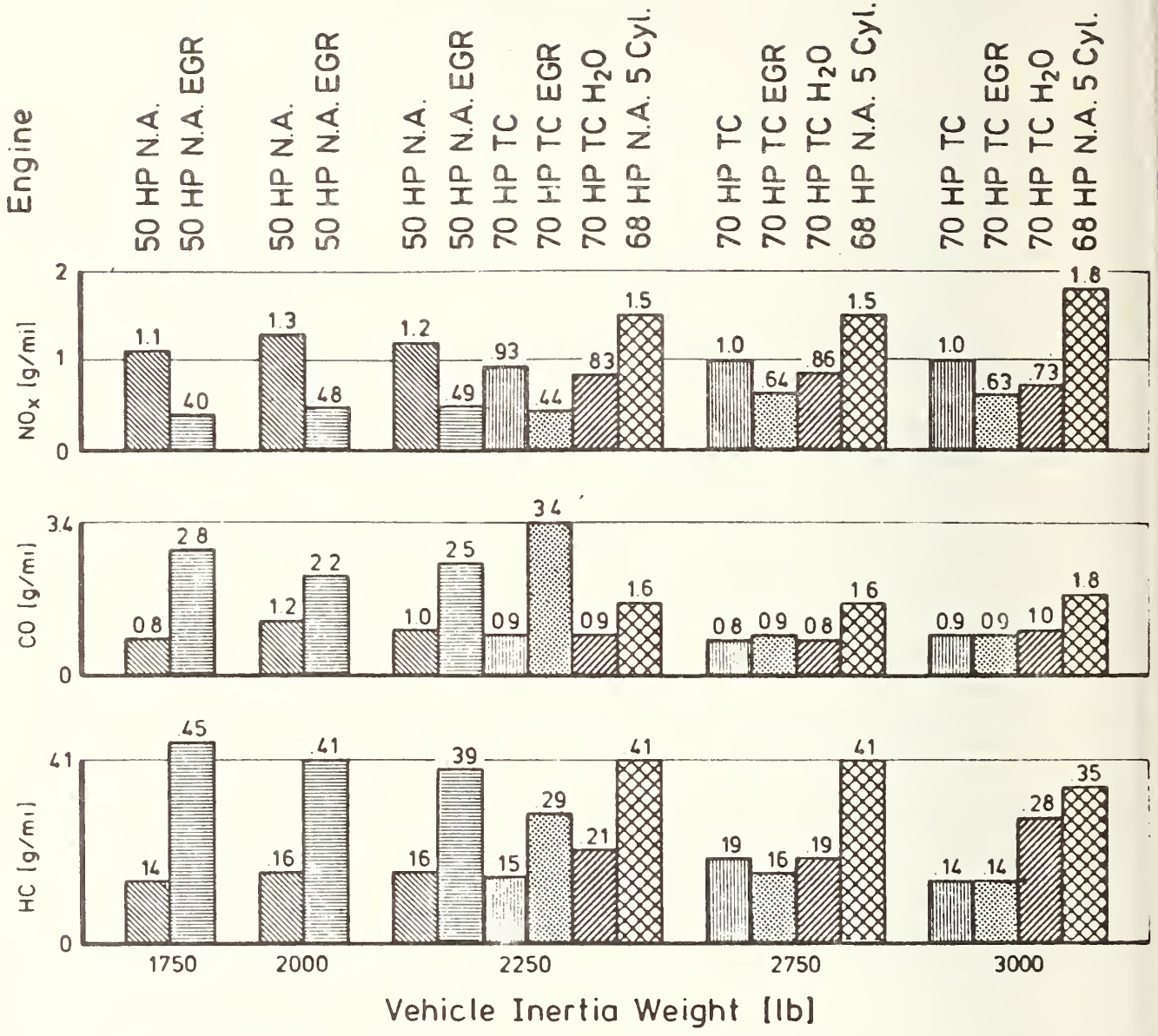

FIGURE 6.2-6: REGULATED EXHAUST EMISSIONS ACCORDING TO THE U.S. FEDERAL TEST PROCEDURE.
Deterioration factors and variances due to manufacturing have not been taken into account.

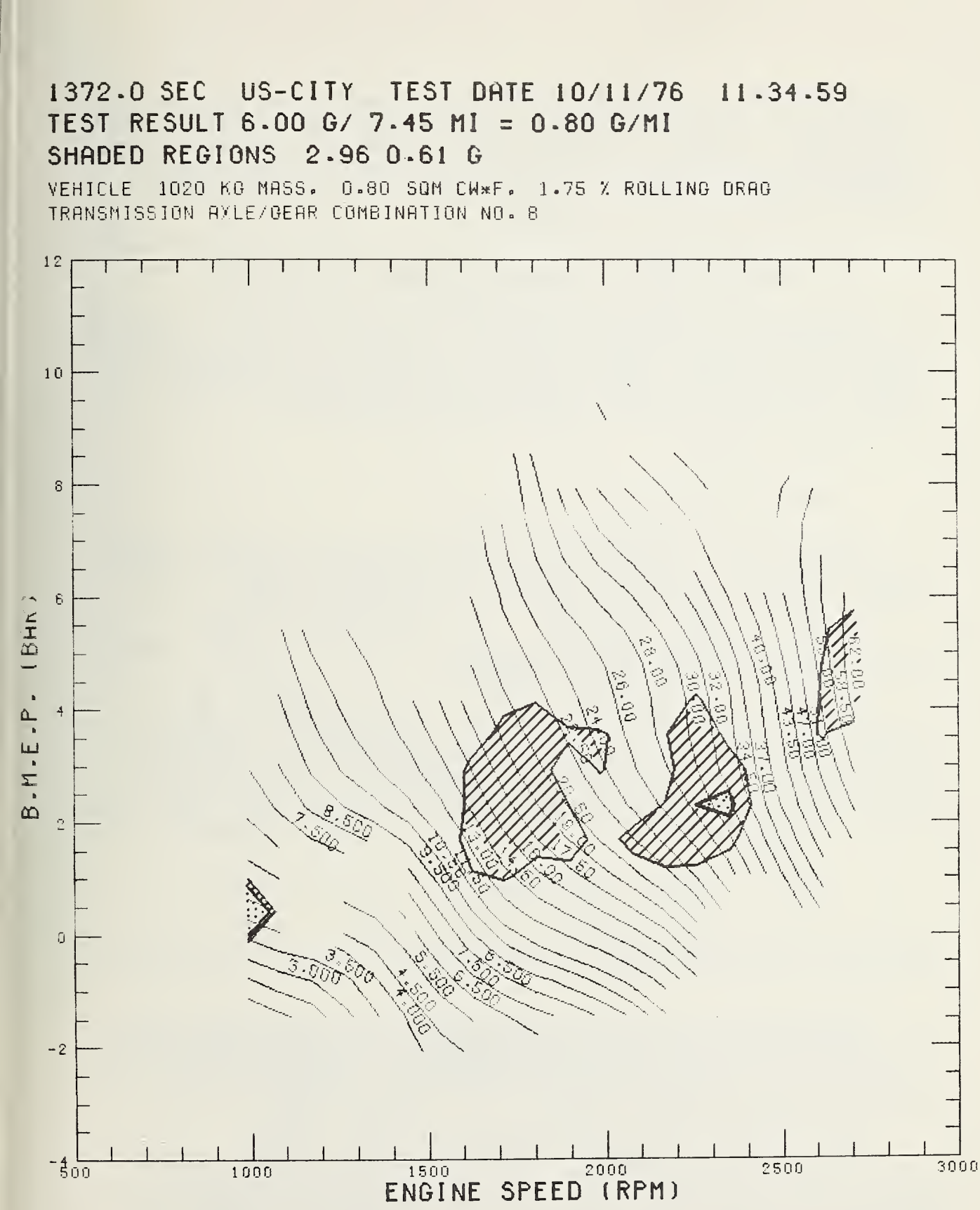

FIGURE 6.2-7: 70 HP TC, 90 CID
NOx EMISSION (G/H)

Projections of regulated emissions from steady-state engine maps were established for various drivetrains and vehicle inertia-weights (see Table 5, Appendix). Figure 6.2-8 shows the computed NOx emissions as a function of the effective transmission radius (see Section 6.1). Accordingly, drivetrain variations lead to a broader range of NOx emissions than do the effects of vehicle inertia weight.

6.2.3 Emission Levels of .41/3.4/1.0 g/mile of HC/CO/NOx

Compliance with the emission levels of .41/3.4/1.0 g/mile of HC/CO/NOx can be ensured only with modified present naturally-aspirated and turbocharged diesel engines. Modifications like that must be implemented with a particular view to production tolerances and deterioration factors. We considered two possible modifications (see Section 4.3):

- Water injection

- Modulated exhaust gas recirculation.

Tables 10 and 11 in the Appendix show the results of tests of water injection into the air intake pipe of a 70-HP TC diesel engine. This process resulted in HC/CO/NOx emissions of .25/0.8/0.8 g/mile

Engine and vehicle level tests indicated that more promising results appear to be produced by the EGR approach.

The Appendix includes the steady-state engine maps of the 50-HP naturally-aspirated and the 70 HP TC diesel engines, both of which were equipped with a modulated exhaust gas recirculation system. Figure 6.2-9 shows the rate of recirculated exhaust gas for the naturally-aspirated engine. The data for the TC engine is shown in Figure 6.2-10. Both graphs show the effective EGR contour lines which are defined as follows:

$$\text{Effective EGR} = \frac{\text{EGR}}{\lambda}$$

The effective EGR equals that of gasoline engines because of the dilution of the exhaust gas by excess air.

Figure 6.2-9 shows that the effective EGR ranges from roughly 2% at full-load operation to 20% at 4,000 rpm and 2 bar. The effective EGR is approximately 10% in the speed/torque ranges that are largely used in city and highway tests. Figure 6.2-5 shows the effects of EGR on exhaust gas emissions during road-load operation.

Table 6 in the Appendix shows emission projections on the basis of steady-state engine emission maps. This data includes the effects of water injection and EGR. In addition to the preparation of steady-state engine maps, dynamic tests were performed on an engine dynamometer (see Tables 7 and 8 in the Appendix).

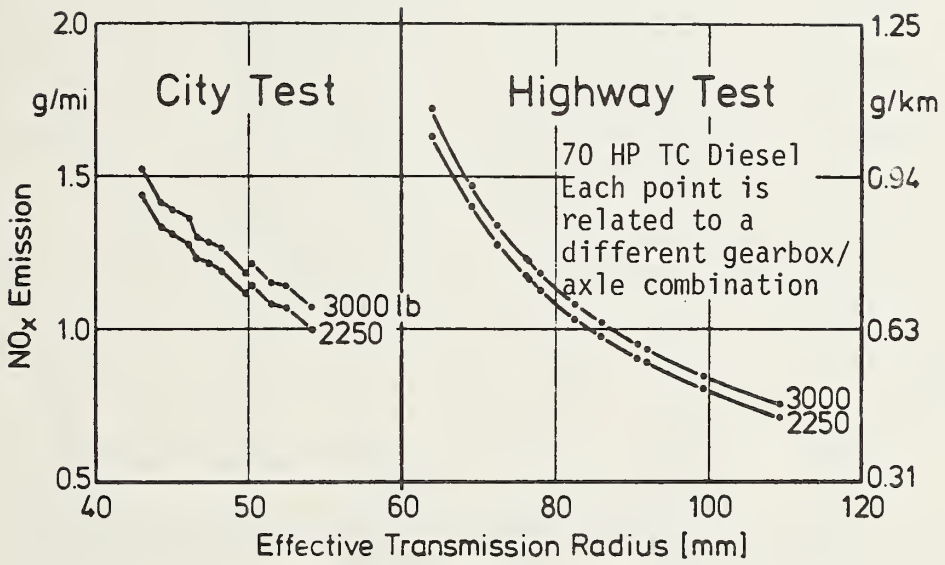

FIGURE 6.2-8: COMPUTED NOx EMISSIONS AS A FUNCTION OF THE EFFECTIVE TRANSMISSION RADIUS FOR TWO VEHICLE WEIGHTS
The graph uses steady-state data of a 70 HP turbocharged diesel engine.
Note: The effects of the transmission is greater than that of the vehicle weight.

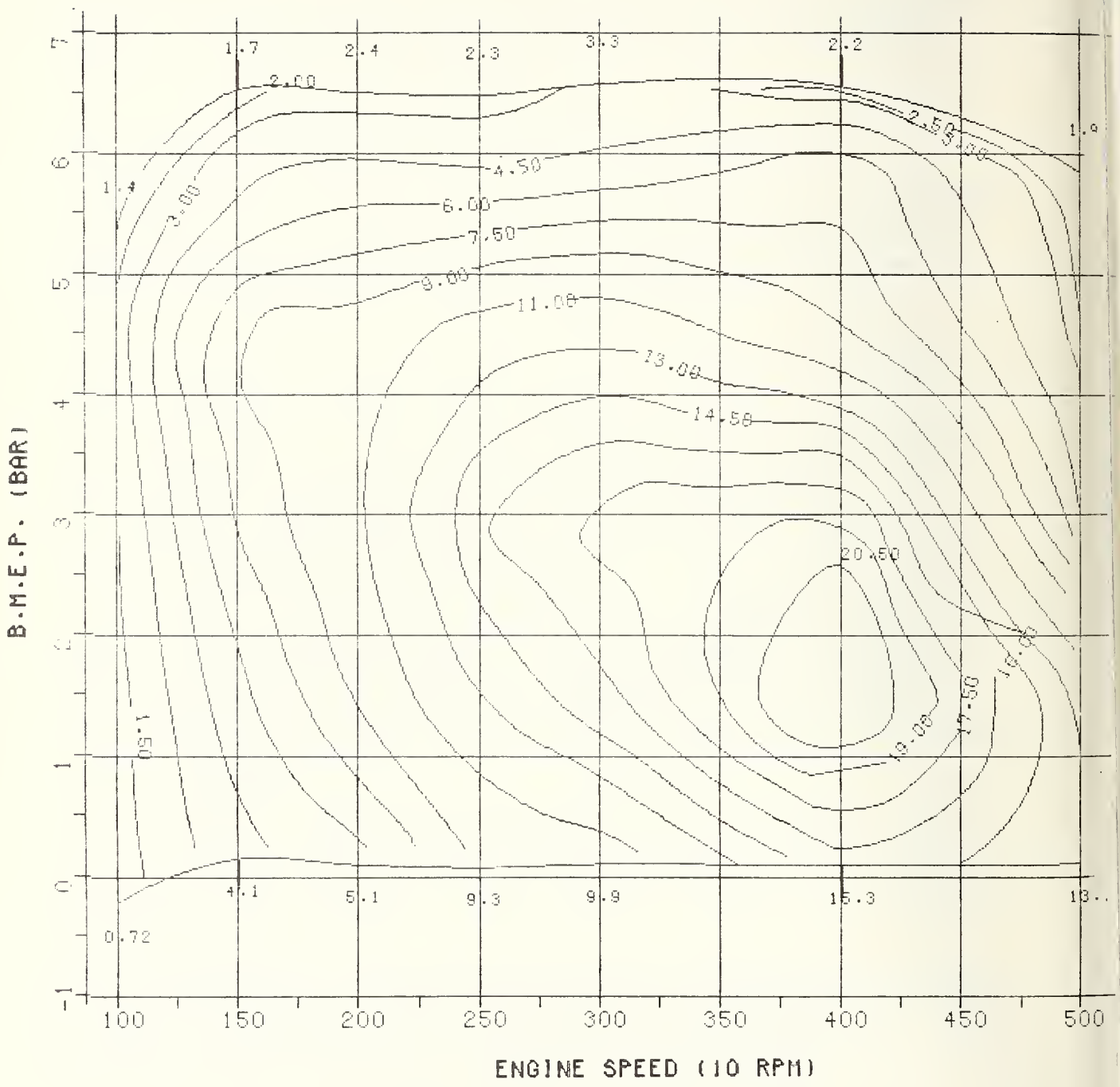

FIGURE 6.2-9: EFFECTIVE EGR (%)
50 HP NA DIESEL ENGINE WITH MODULATED EGR

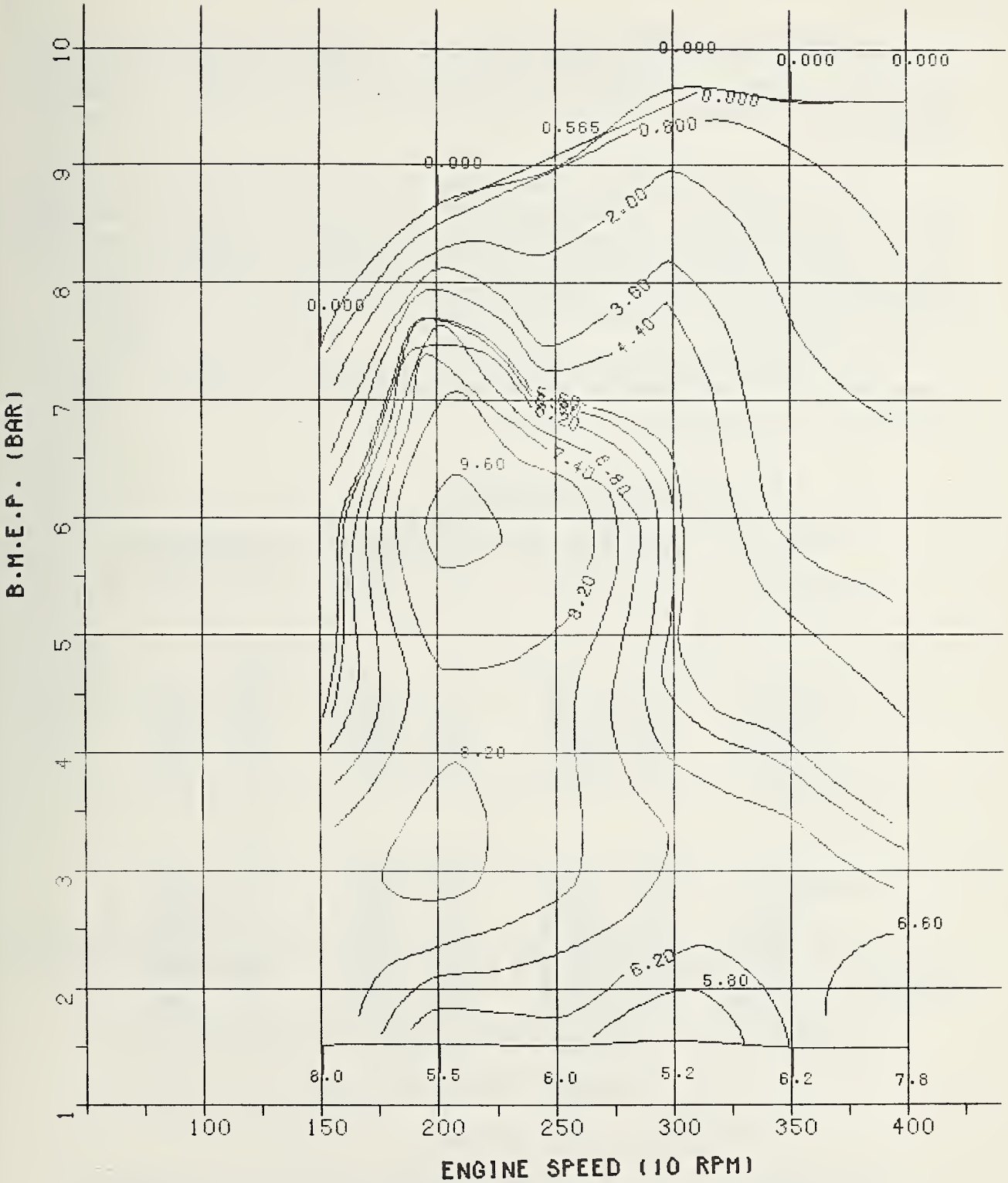

FIGURE 6.2-10: EFFECTIVE EGR (%)
70 HP TC DIESEL ENGINE WITH MODULATED EGR

The chassis dynamometer tests were run in compliance with the U.S. 1975 Test Procedure. The results are shown in Figure 6.2-11 for the 50 HP NA diesel engine and in Figure 6.2-12 for the 70 HP TC engine. The data in both figures includes the results from engine level tests for the sake of comparison.

The CO and NOx emissions from the 50 HP NA engine meet the 0.41/3.4/1.0 g/mile requirements for CO and NOx within a satisfactory marging, while the HC emission is too high. The 70 HP TC diesel engine produces better results. The difference between the emission levels from the two engines may be attributable to the problem posed by EGR distribution, which might have room for improvement in the naturally-aspirated engine.

Even though NOx emissions can be cut to less than 1 g/mile by EGR, there still are other problems to be solved before a technological breakthrough can be expected.

6.2.4 Unregulated Exhaust Emissions

The following unregulated exhaust emissions were investigated:

- Smoke
- Particulates
- Odor
- Sulfates
- Ammonia
- Aldehydes
- Noise.

The NOx emission levels affect four of these seven unregulated emission components. A reduction of the NOx level from 2 to 1 g/mile would entail the following consequences:

- a 25% increase of smoke visibility and particulate emission;
- a 0.2 TIA units increase of odorants (error of 0.25 units)
- a 4 dB (A) decrease of noise emission.

The following seven sections refer to the individual unregulated emission components.

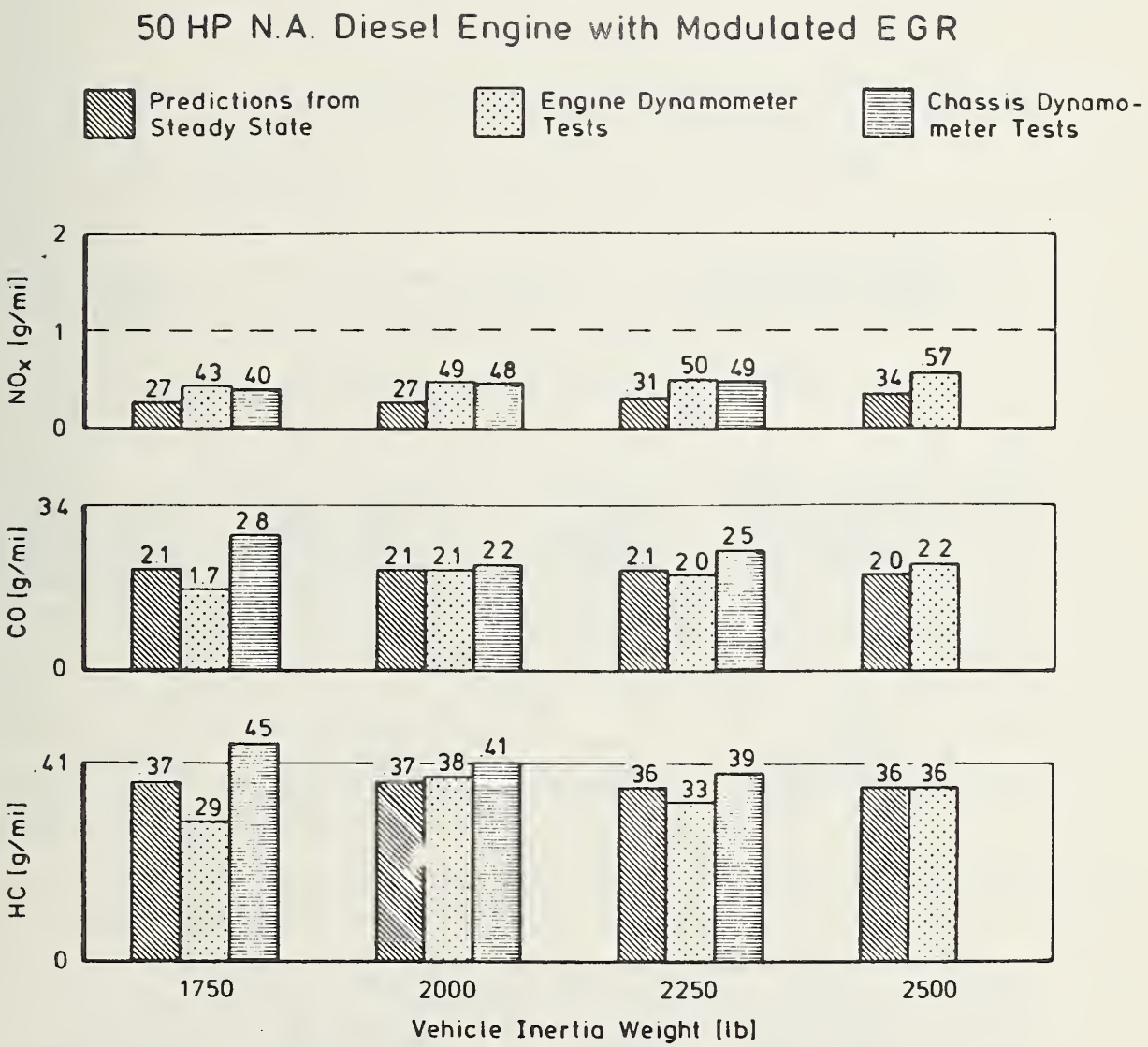

FIGURE 6.2-11: HC/CO/NOx EMISSIONS FROM A 50 HP NA DIESEL ENGINE
Engine with modulated EGR measured by three different methods.

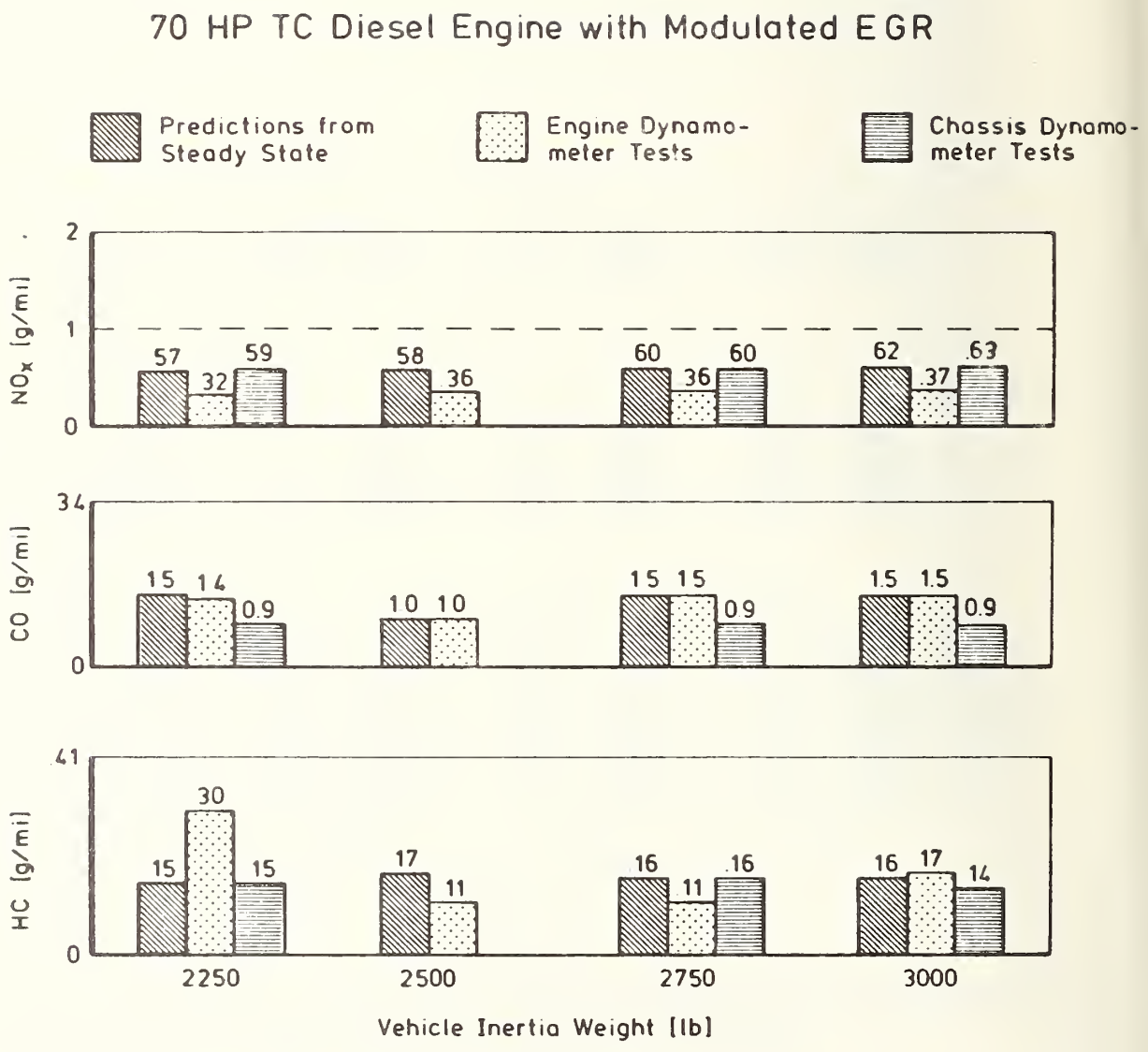

FIGURE 6.2-12: HC/CO/NOx EMISSIONS FROM A 70 HP TC DIESEL ENGINE WITH MODULATED EGR MEASURED BY THREE DIFFERENT METHODS

6.2.4.1 Smoke

The objectives of smoke measurements are as follows:

- Determination of smoke emission at full-load operation

- Preparation of steady-state smoke engine map

- Determination of smoke emission during dynamic engine operation

All measurements were taken during engine dynamometer tests except for high-altitude tests, which were run in the Alps. The latter tests will be dealt with further below.

Methodology

Two different methods are used in the determination of smoke emissions:

(1) Stained filter-paper method (Bosch Numbers)

(2) White-light absorption method (Hartridge Smoke Units, Bosch Opacimeter)

The smoke visibility Bosch Number is given by the stain intensity which results from the filtering of an exhaust gas sample. The Bosch Opacimeter ERAW 68A passes on-third of a liter of exhaust gas through an area of 7.5 cm^2 of white filter paper. During this process, the particulate content of a .445-m long exhaust gas column is precipitated on the surface of the filter paper. A photo cell is then employed to measure the reflectance of white light from the stained area of the paper. Calibration points: Bosch Number 0 for the uncontaminated surface; Bosch Number 5 for a 50% decrease in reflectance of the contaminated surface.

The Bosch method is characterized primarily by its ease of application and by its reliable results.

Bosch Number 3 is the smoke visibility limit for the exhaust gas from a vehicle under normal traffic conditions.

We used two different instruments to measure white-light absorption: The Opacimeter (we gratefully acknowledge the cooperation of Dr. Adolf of the German Bosch company who made available a prototype for test purposes), and a Hartridge Smoke Meter MK 3.

The Opacimeter is used to measure the white-light absorption coefficient K which is defined by the transmission intensity I (d) after a light path d:

$$I(d) = I(o) \exp(-K \cdot d)$$

An uninterrupted flow of exhaust gas is passed between a white-light source and a photo cell. The photo cell acts as a sensor and continuously supplies smoke data.

The Hartridge Smoke Meter works on the same basis. The difference between the Smoke Meter and the Opacimeter is the number of ports that limit the exhaust gas golumn, and the signal scale. Hartridge Smoke Units express the percentage of light absorbed in a 0.394-m light path:

$$HSU = 100\ (1 - I(d)/I(o)) \qquad \text{where } d = .394 \text{ m}$$

It was found that the correlations between the results of the different measuring methods (Figure 6.2-13) are in agreement with those published by others. The mean deviation of 0.5 Bosch Numbers or roughly 10 HSU exceeds the measuring errors.

Figure 6.2-14 shows similar correlations between Opacimeter readings and Bosch Numbers. There was agreement between previously published correlations and present measurements with errors exceeding expectations. No satisfactory explanation has been found for these errors other than the different engine operation points at which measurements were performed.

Soot is known to precipitate on the walls of the pipe through which it is passed. During extended engine operation soot precipitates continuously on the pipe walls from where it is released intermittently. Therefore, smoke visibility is higher at the intake of a pipe than at its exhaust end. This fact applies to the connecting pipes of the Opacimeter and the Hartridge Smoke Meter. Particulate precipitation was minimized when the entire exhaust gas flow was passed through the Opacimeter. Figure 6.2-15 shows the Bosch Numbers obtained from samples in the muffler (Smoke 1) and at the measuring point (light path) in the Opacimeter (Smoke 2). There is better correlation than in the previous graphs, and Smoke-2 values are 10% lower than the Smoke-1 values. Similar measurements with the Hartridge Smoke Meter show a loss of 25% by particulate deposits in the connecting pipes.

Even though the stained filter-paper method is limited to steady-state engine operation, most of the smoke measurements were performed in accordance with this approach because it is a reliable and simple method. The light absorption methods were used in some selected engine dynamometer dynamic tests. The considerable increase of exhaust back pressure in engines with EGR does not permit application of the light-absorption method. Back-pressure variations significantly affected the EGR modulations in this project.

Results

Smoke visibility of steady-state-operated engines was measured with the Bosch Smoke Tester ERAW 68A. Smoke visibility engine maps for seven different engines are presented in the Appendix. Figure 6.2-16 is the map for the 50 HP naturally-aspirated diesel production engine. The graph shows an increase in smoke in direct proportion to the increase in engine load. This is caused by the drop in excess air available for combustion. More power output is delivered at the expense of higher smoke visibility.

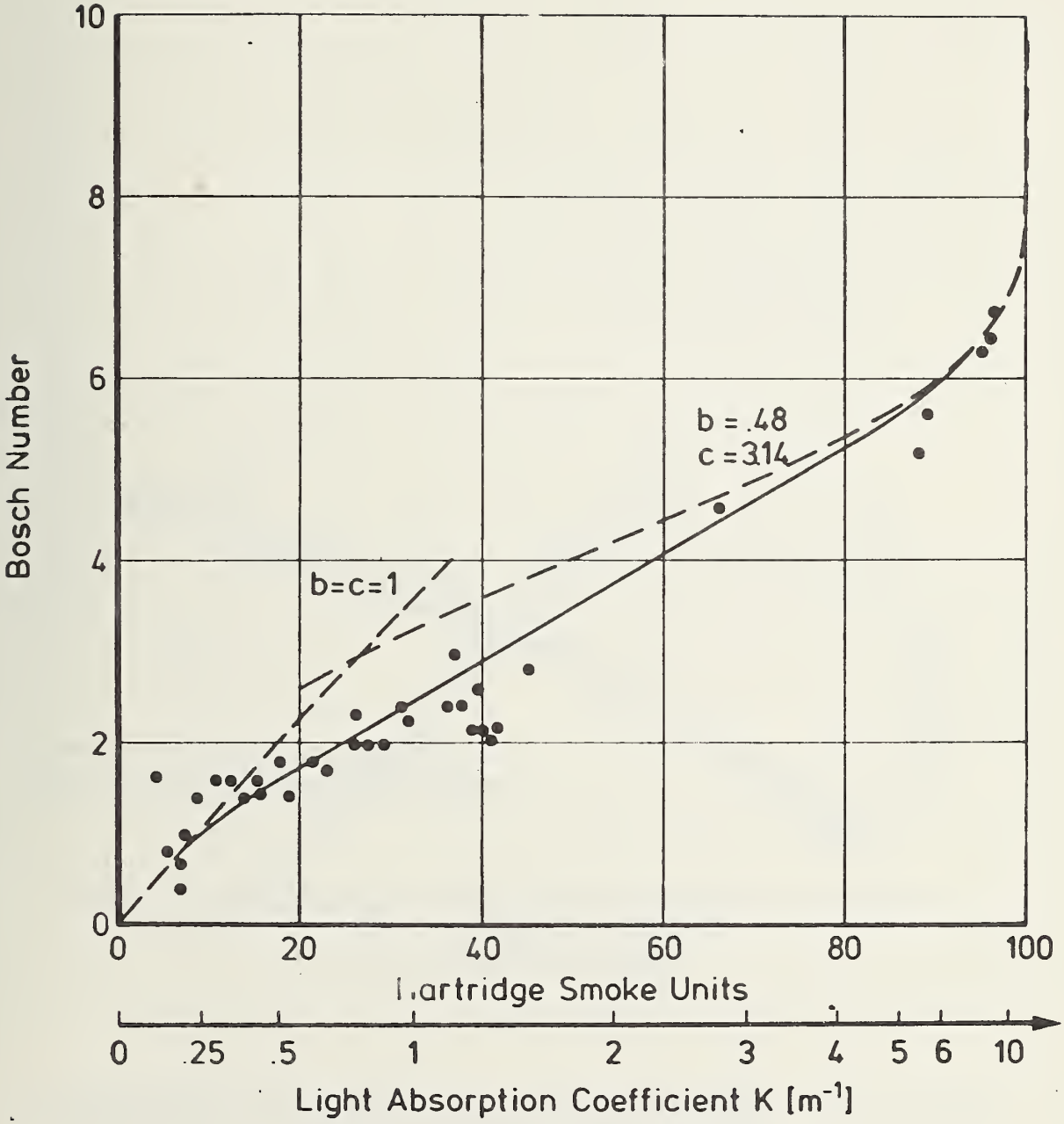

FIGURE 6.2-13: SMOKE VISIBILITY.
Correlation between Hartridge Smoke Units (0.394 m light path). Bosch Number (stain intensity produced by 1/3-liter on a 7.5 cm^2 spot of white filter paper.

Dashed line is from A. D. Wood, SAE Paper 75 1119, with the parameters b and c.
The solid line is arbitrarily drawn through the data.

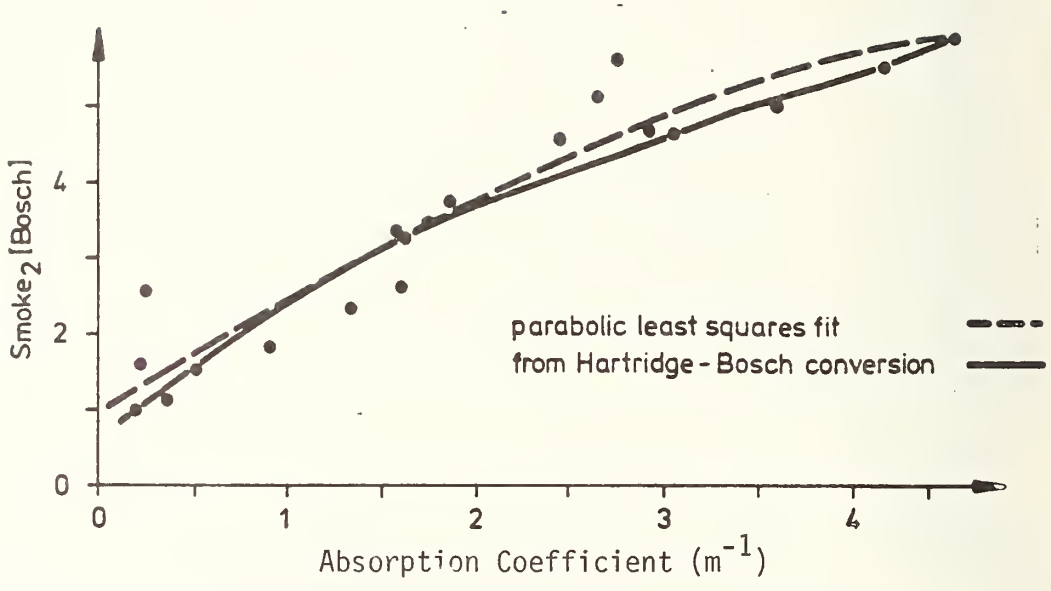

FIGURE 6.2-14: CORRELATION BETWEEN THE STAINED FILTER METHOD (SMOKE 2) AND ATTENUATION OF LIGHT TRANSMISSION (OPACIMETER).

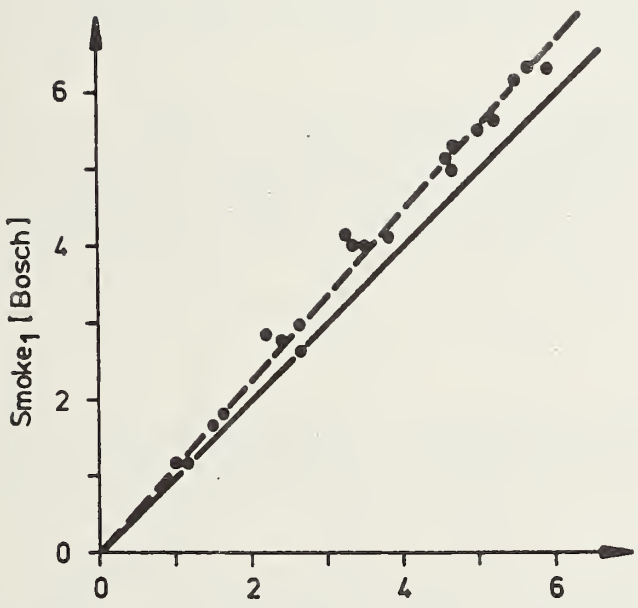

FIGURE 6.2-15: PRECIPITATION OF SMOKE

Smoke-1: Sampled at the silencer
Smoke-2: Sampled at the Opacimeter: 10% loss

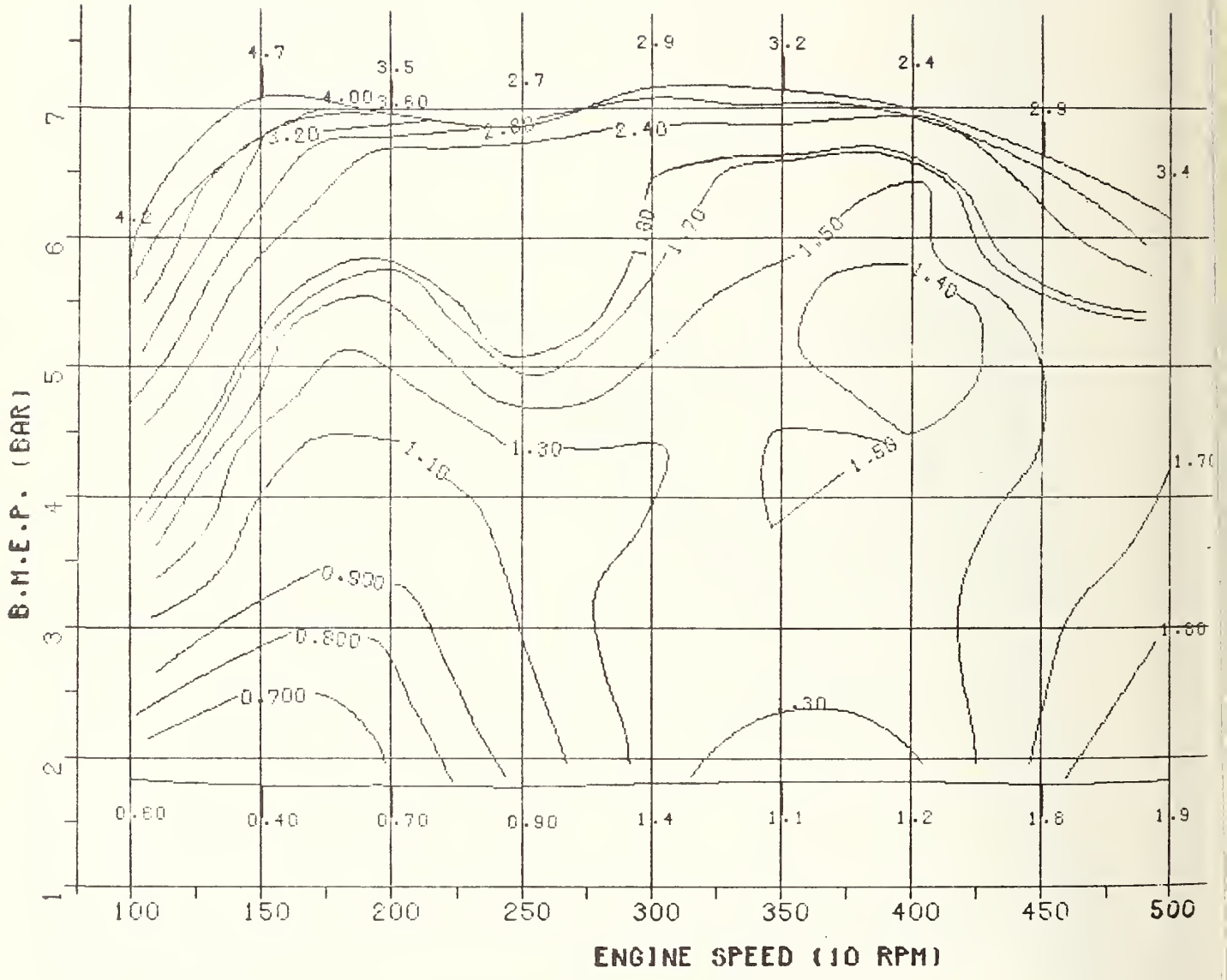

FIGURE 6.2-16: SMOKE (BOSCH NUMBER) - 50 HP NA 90-CID PRODUCTION DIESEL ENGINE

Figure 6.2-17 is a comparison of smoke visibility of four basic diesel engines and eight engine/vehicle systems. The engines with EGR are not included in the full-load smoke visibility tests because there should be no exhaust gas recirculation at full-load operation. Therefore, full-load smoke is expected to be the same for engines with and without EGR.

The 70 HP TC diesel prototype engine has a higher smoke level at full-load operation and low engine speeds. This indicates that the injection pump needs further tuning for low engine speeds. This pump is characterized by the fact that the full-load injection rate is controlled by a boost-actuated lever, the movement of which is limited by a stop. Therefore, the boost device must match the course of the full-load curve and the correction at turbocharger kick-in. It was mentioned earlier that the 5-cylinder engine injection pump had not been fully tuned at the time of the program.

The 6-cylinder 146-CID naturally-aspirated engine produces the least road-load smoke. This engine is a hand-tuned prototype and thus is indicative of the potential smoke limitation that, however, cannot yet be mass-production units.

The smoke data of the 8-cylinder 180-CID naturally-aspirated engine are projected values. They are based on the assumption that the 8-cylinder engine maps are identical with those of the 4-cylinder 90-CID naturally-aspirated production diesel engine. The resulting smoke values are lower because of the higher power-to-inertia-weight ratio.

The graph in Figure 6.2-17 includes the increase of smoke caused by EGR.

EGR modulation device tuning for satisfactory smoke levels will be possible for normal traffic conditions. Smoke emission control problems are posed by rapid transient operation conditions. The solution to these problems will require additional engineering efforts.

Figure 6.2-18 illustrates the smoke sensitivity of one engine/vehicle system to seven different fuel grades. These seven grades cover a markedly broader range than generally wil occur under real-life conditions. Five of these fuel grades are located within an acceptable scatter band, while the highest-density fuel produces much higher smoke values. Lowest smoke visibility was obtained with the lowest-density fuel grade.

The curves in Figure 6.2-19 show the effects of fuel injection timing on smoke at full-load. Tests were run on the 50 HP NA production diesel and the 70 HP TC research diesel engine. Both of these units increased their smoke emission when fuel injection was advanced. It is obvious that injection timing affects the trade-off between fuel economy and smoke and NOx emissions (see also Section 4.2.5).

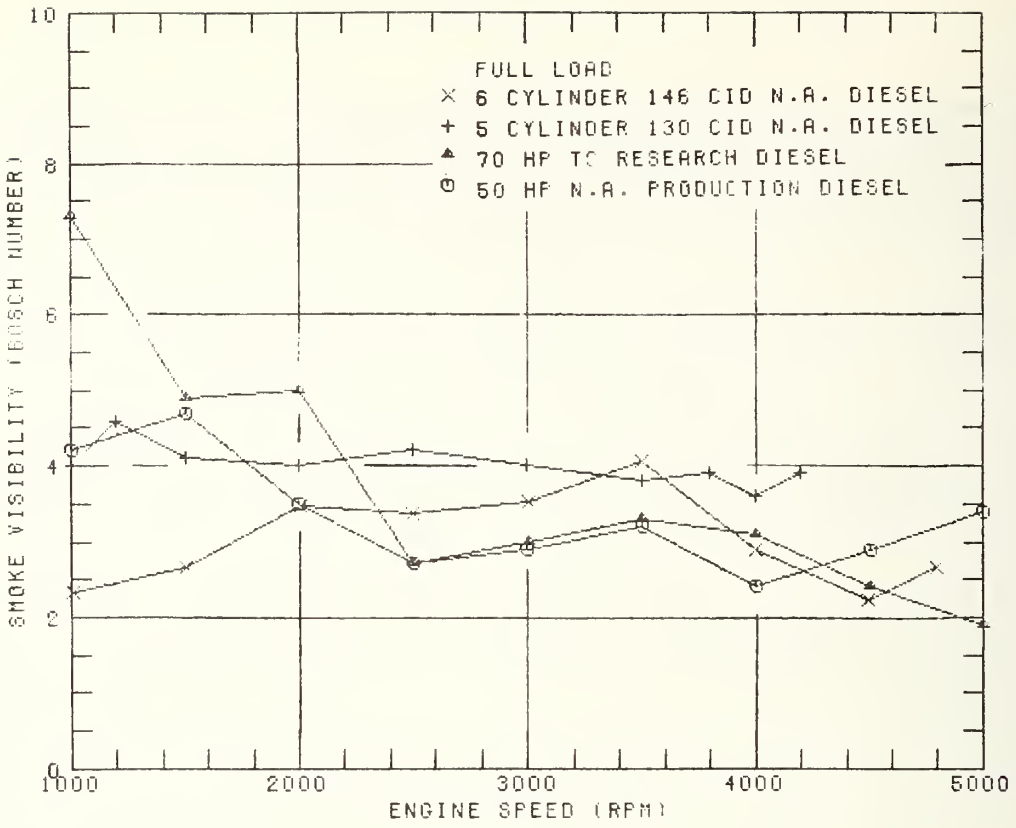

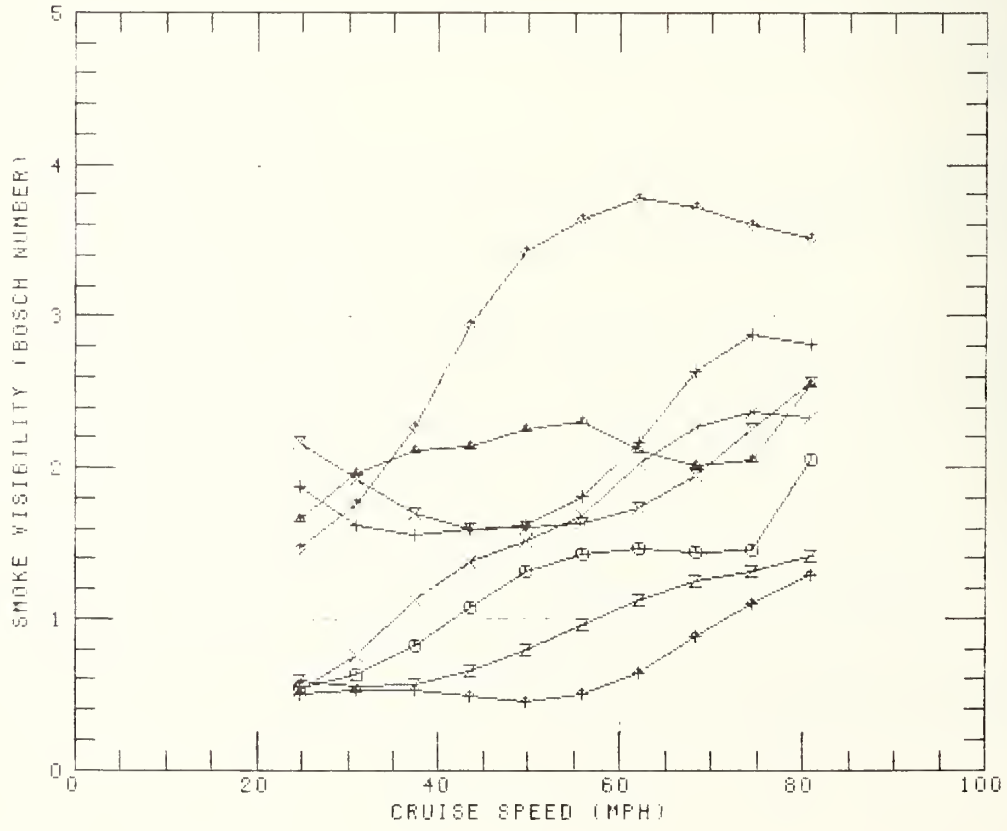

FIGURE 6.2-17: COMPARISON OF SMOKE OF VARIOUS ENGINE/VEHICLE SYSTEMS AT FULL-LOAD AND AT CONSTANT-SPEED CRUISE (TRANSMISSION IN HIGH GEAR)

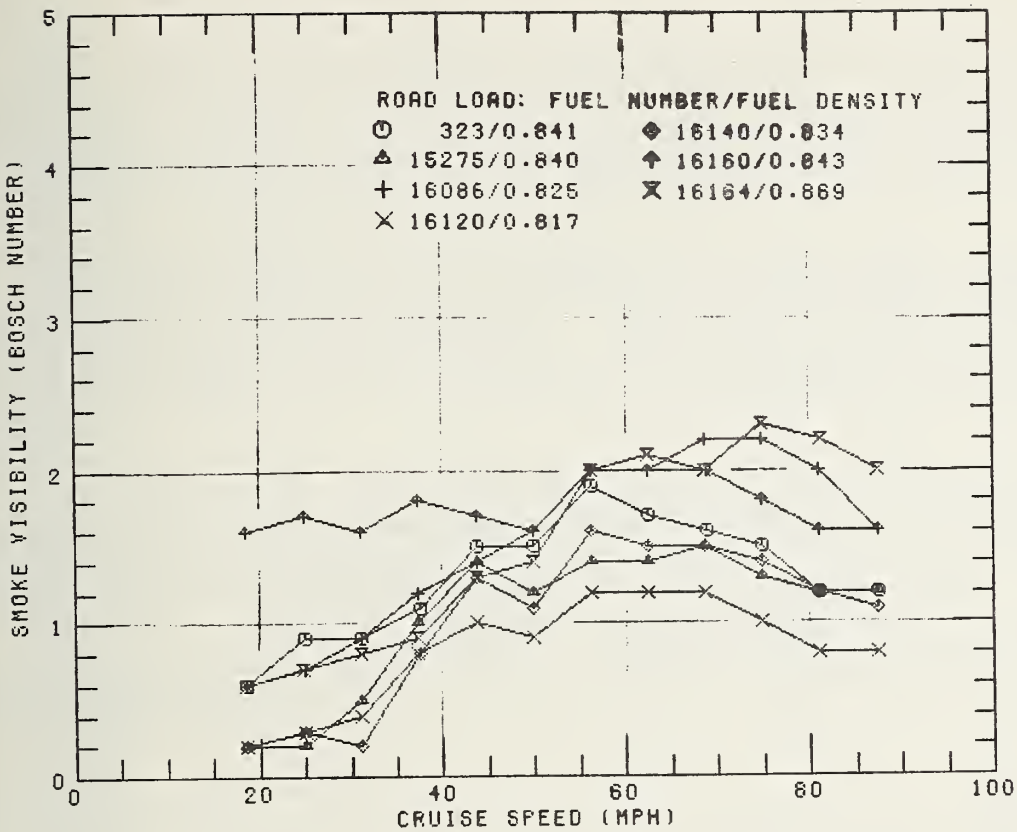

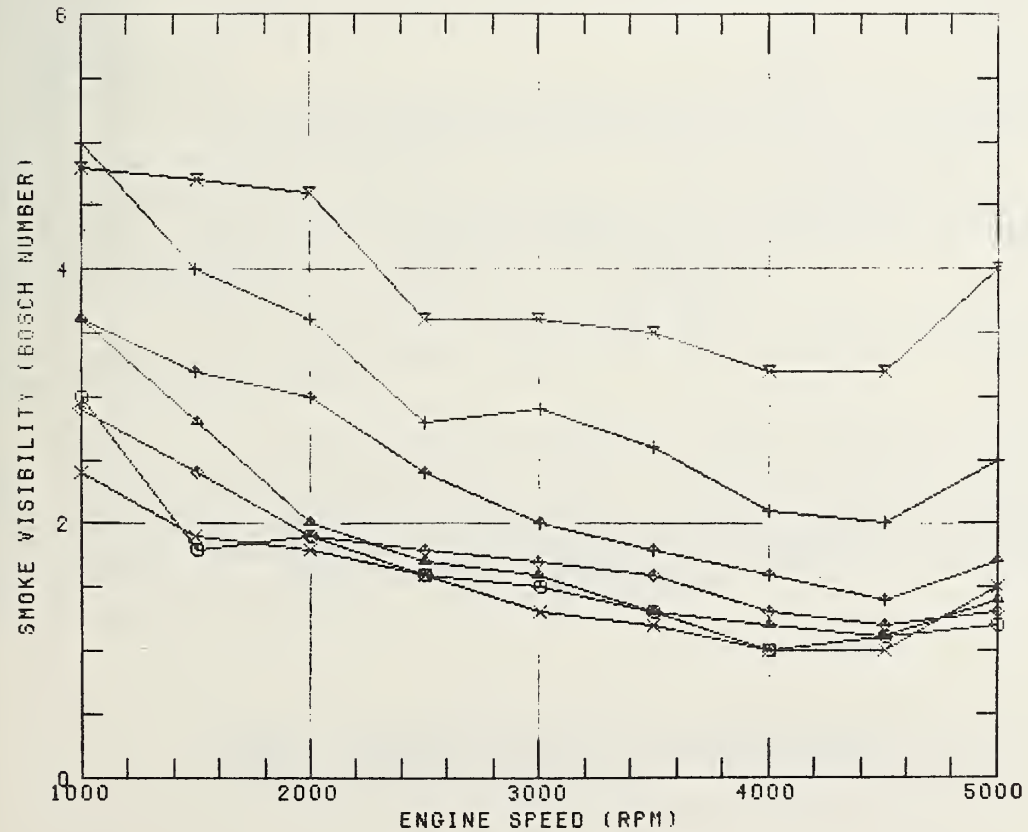

FIGURE 6.2-18: SMOKE SENSITIVITY ON DIESEL FUEL COMPOSITION

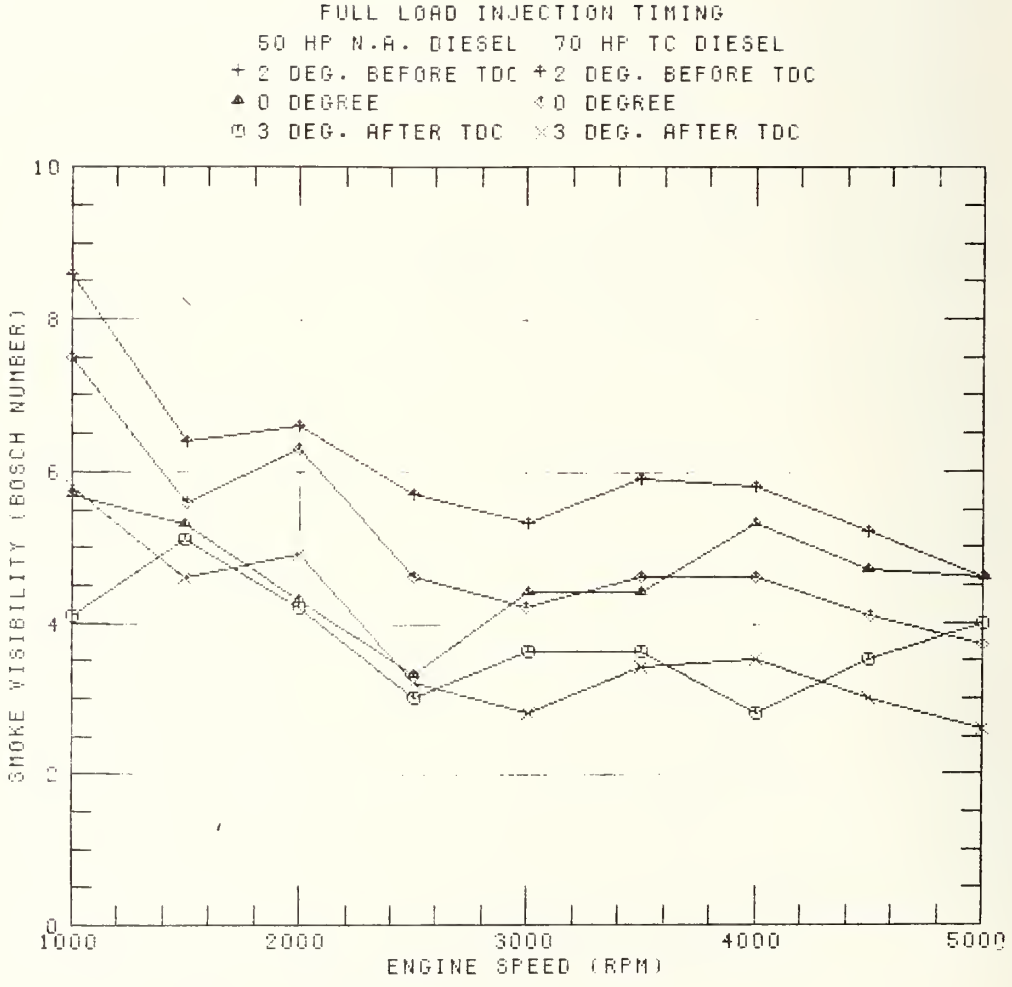

FIGURE 6.2-19: SMOKE SENSITIVITY TO FUEL INJECTION TIMING

Smoke visibility during dynamic engine operation is the same as during steady-state operation if engine speed, torque, and temperature are the same in both modes of operation due to the fast response of the injection pump. The combustion process, however, is affected by the engine temperature, i.e. smoke emission increases while the cylinder walls are cold.

Continuous records of light absorption were prepared with the Opacimeter and the Hartridge Smoke Meter during selected city and highway driving cycle simulations on the engine dynamometer. Table 6.2-2 shows the resulting average Bosch Numbers for various idle, acceleration, and cruise models. Cold and warm engine start-up temperatures are included for the sake of comparison.

It is obvious that engine temperatures during the first idle and drive-away modes affect smoke. The time interval 3 in Table 6.2-2 in the preceding table reflects fast acceleration with some seconds of full-throttle acceleration. The high-speed cruise interval 4 compared with the highway-cruise interval 6.

Table 6.2-2 shows the low level of smoke emitted by the production diesel engine in a VW Rabbit.

6.2.4.2 Particulates

This section deals with the methodology of particulate emission measurements and its results.

Methodology

The engine/vehicle systems were subjected to the U.S. City Driving Cycle (cold start) and the Sulfate Emission Driving Cycle (warm start).

A given fraction of the exhaust gas is passed through a filter. The increase in weight of the dried filter element is a measure of the amount of particulate emission.

Figure 6.2-20 is a schemati of the particulate sampling device with the aid of a dilution channel.

The mixture of exhaust gas and dilution air is moved at a constant flow rate. The average dilution ratio is 1:20. The representative sample of particulates is extracted isokinetically. All particulates including soot and sulfates retained by a fluoropore filter of a diameter of 7 cm with a pore size of 1 μm. The loaded filter element is dried at room temperature in a desiccator chamber.

Inertia Weight lb.	Time Interval 1	2	3	4	5	6	Engine Start-Up Temperature
1,750	0.8	1.4	2.3	2.1	1.7	2.2	warm
2,000	0.4	1.4	2.6	2.2	1.7	2.1	warm
	2.9	3.2	3.0	2.3			cold
2,250	0.3	1.5	2.9	2.0	1.6	1.8	warm
	2.1	3.2	2.8	1.8			cold
2,500	0.9	1.8	3.5	2.1	1.5	1.5	warm
	1.0	2.9	3.1	1.8			cold

List of Selected Time Intervals

No.	Time (s)	Mode of Operation	Driving Cycle
1	0 - 20	first idle	city
2	20 - 33	first acceleration	city
3	187 - 204	fifth acceleration	city
4	204 - 300	high-speed cruise	city
5	2 - 97	first acceleration	highway
6	97 - 740	high-speed cruise	highway

TABLE 6.2-2: SMOKE VISIBILITY DURING SELECTED TIME INTERVALS IN THE CITY AND HIGHWAY DRIVING CYCLES.
The data for the 50 HP NA production diesel engine was obtained with the aid of the light-absorption method and converted to Bosch Numbers.

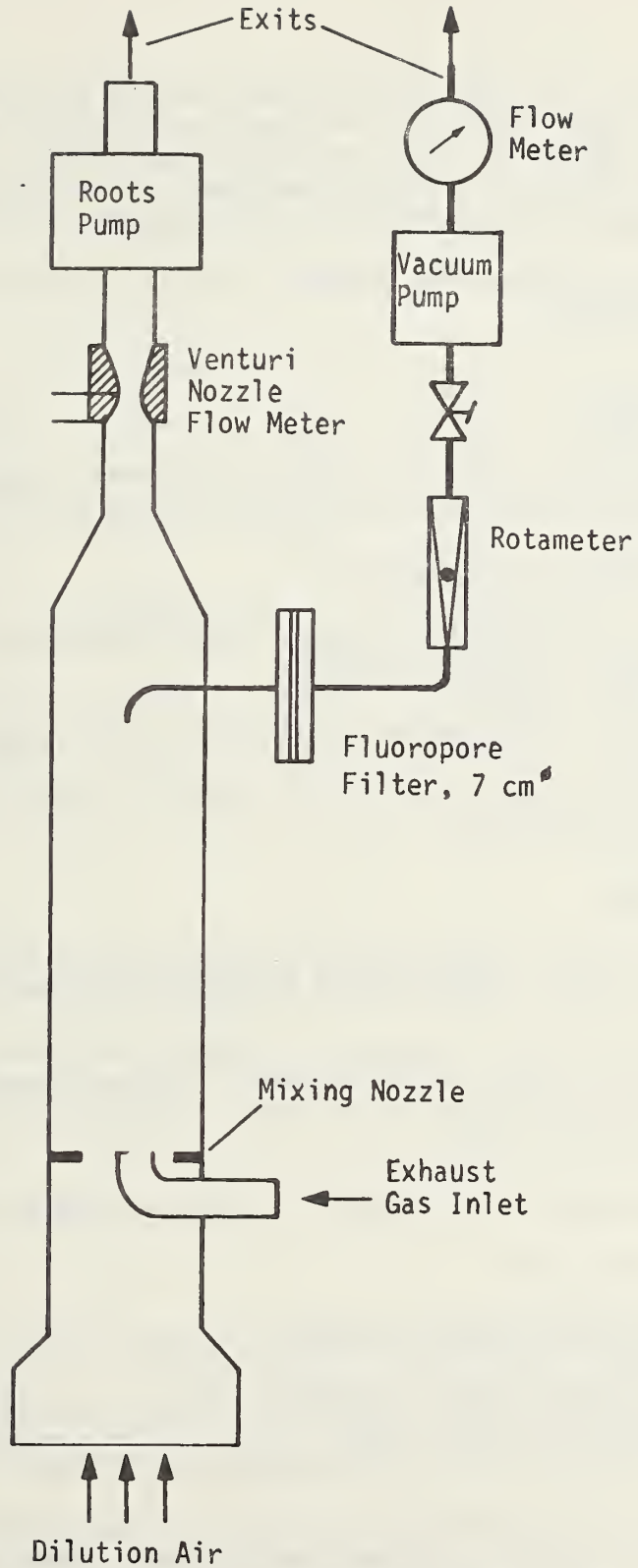

FIGURE 6.2-20: SCHEMATIC OF THE ISOKINETIC PARTICULATE SAMPLING WITH THE AID OF A DILUTION CHANNEL

Results

Table 6.2-3 is a summary of the particulate emission test results which are plotted in Figure 6.2-21. The lowest particulate emission level was produced by the 70 HP TC diesel engines without EGR. A reduction of the NOx emission level from 2 to 1 g/mile increased the particulate emission level by 25% with a properly modulated EGR (see the results of the 50 HP NA EGR engine).

The Sulfur Emission Test Schedule reveals a general trend toward lower particulate emissions.

6.2.4.3 Odor

The measurement of diesel exhaust odor poses a complex problem because of the significance of both the basic character and the intensity of the odor.

Two approaches are preferred:

- A panel of trained odor experts (sniff panel) rates the strength of several odor character notes;

- A chemical determination of odorants in the exhaust gas.

Figure 6.2-22 shows the state-of-the-art of sniff-panel odorant concentration correlations.

Methodology

Most of the odor emission data was obtained by chemical determination of odorants. The odorant samples were analyzed by Arthur D. Little, Inc.

The sampling process provides for roughly 50 liters of exhaust gas to be passed through a trap in five minutes. The trap contains 1 g chromosorb 102. The thus obtained samples are then forwarded to Arthur D. Little, Inc., for analysis within a week.

The engines were run through four different chassis dynamometer tests:

- Idle, warm engine

- 30 mph constant speed, top gear

- 55 mph constant speed, top gear

- 505 s of Federal City Driving Cycle, cold start.

A sample of 10 liters/min was drawn from the exhaust stream. The collected sample contains a larger fraction from low-speed modes and a smaller fraction from high speed modes because the total exhaust gas stream is not constant during the City Driving Cycle. The average speed during the first 505 s of the City Cycle is 25.5 mph.

Volume	Rabbit	Rabbit	Rabbit	Rabbit	Rabbit	Audi 100
	2,250	2,250	2,250	2,250	2,250	3,000
Engine	50 HP	50 HP	70 HP	70 HP	70 HP	5-cylinder
	NA	NA EGR	TC	TC EGR*	TC	NA
City	.35(3)	.45(2)	.25(1)	1.48(18)	.29(2)	.48(1)
SET	.34(2)	.41(10)	.23(1)	1.48(26)	.28(1)	.39(3)

*EGR Level exceedingly high in these values

TABLE 6.2-3: PARTICULATES EMISSION FROM VARIOUS ENGINE/VEHICLE SYSTEMS IN THE U.S. CITY AND SULFATES EMISSION DRIVING CYCLES. The figures in brackets indicate the statistical error in the last digits. All figures given in g/mile.

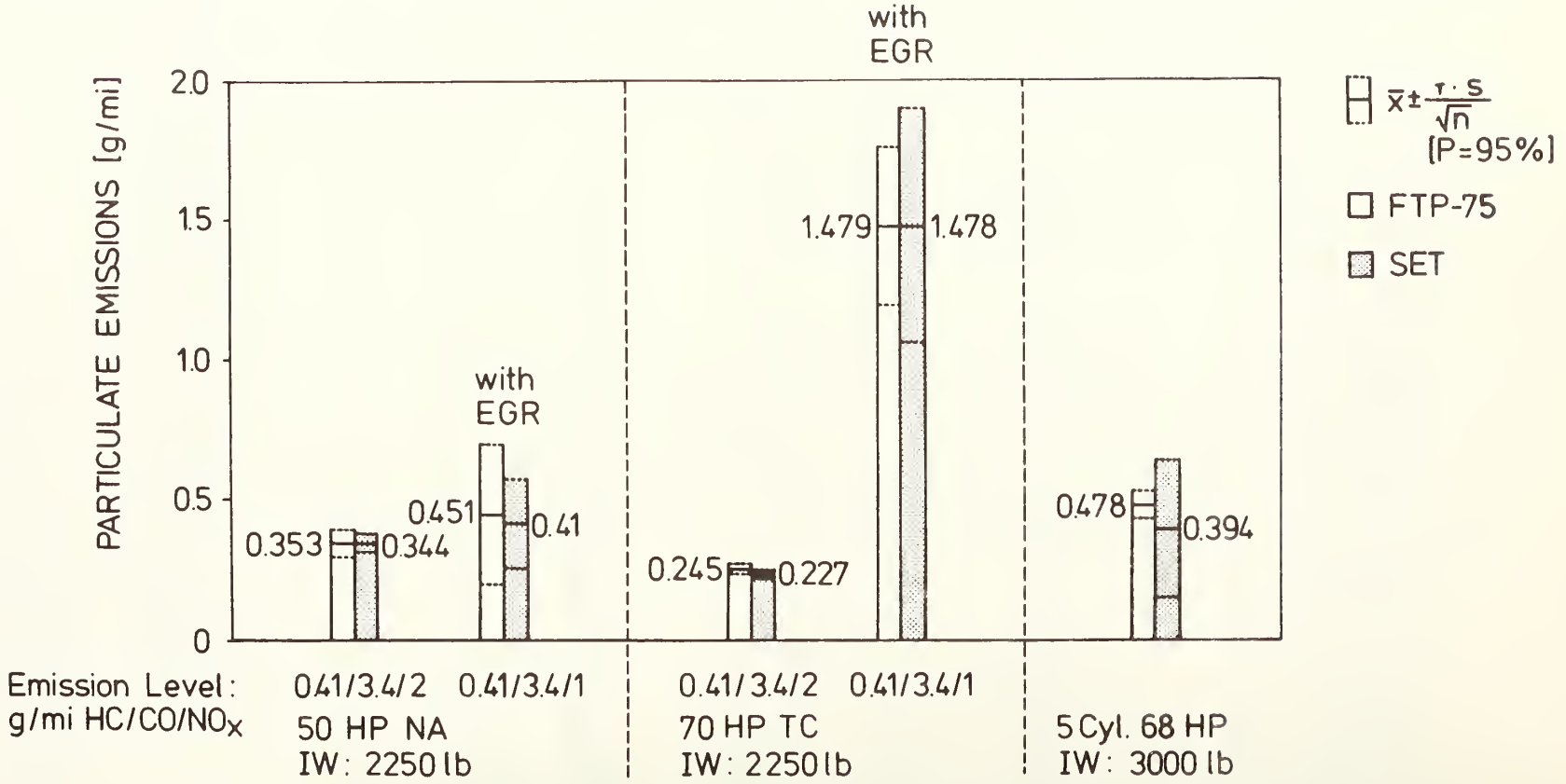

FIGURE 6.2-21: PARTICULATE EMISSIONS

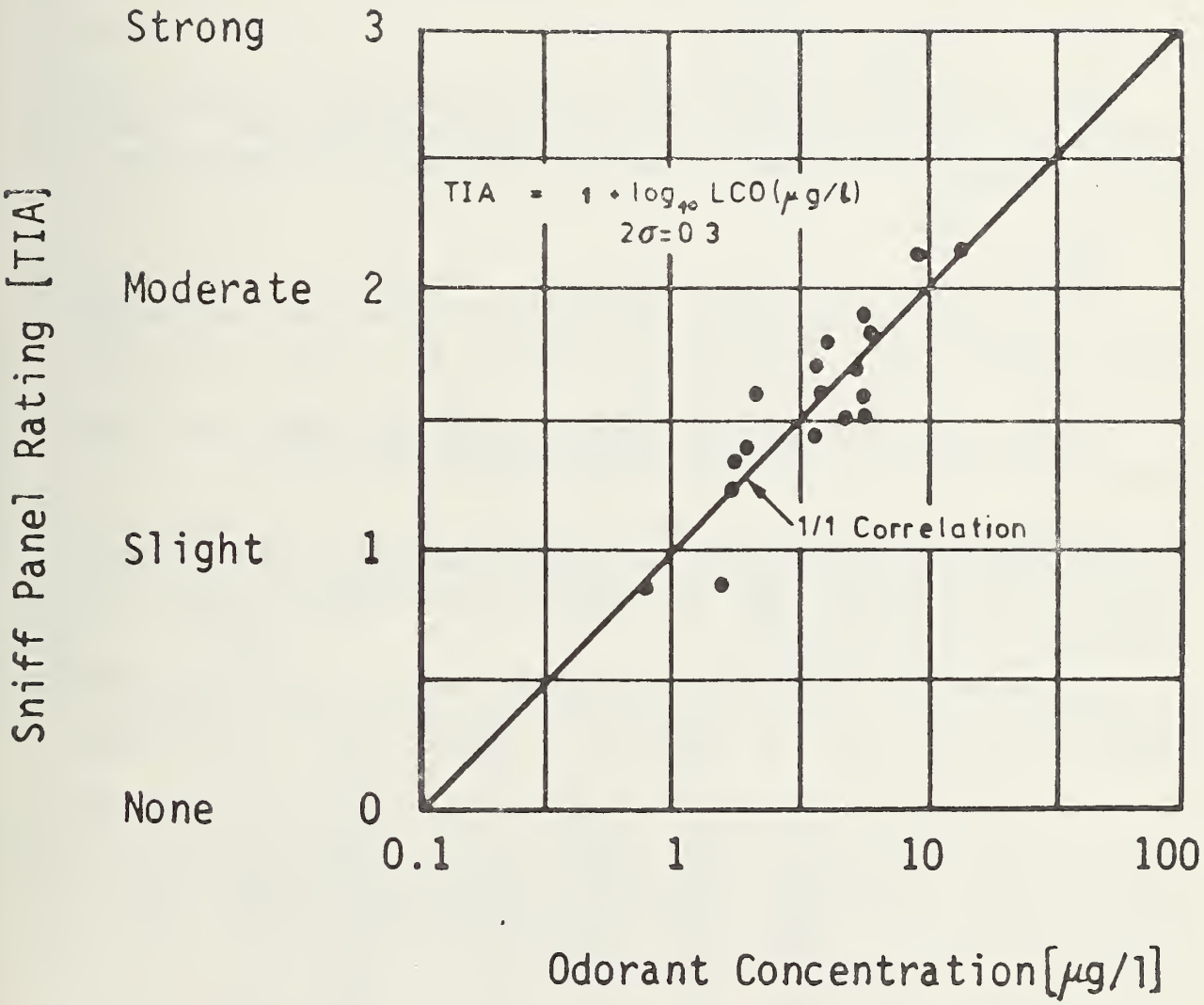

FIGURE 6.2-22: CORRELATION BETWEEN SNIFF PANEL RATING AND ODORANT CONCENTRATION.

The total odor intensity or Total Intensity of Aroma (TIA) is defined by two dominant odor character groups, i.e. smoky-burnt and oily-kerosene, each of which contributes almost equal parts to the composite odor. Both groups may be separated from the non-odorant fractions in the exhaust by liquid column chromatography. The smoky-burnt odor stems from partly oxygenated species (LCO - Liquid Column Oxygenates), and the oily-kerosene odor from aromatic species (LCA - Liquid Column Aromatics). The total aroma intensity is computed from the oxygenates concentration in the exhaust gas with the aid of the following equation:

$$TIA = 1 + \log_{10} LCO\ (\mu g/.1)$$

Some odor emission evaluations were obtained by a sniff panel. These tests were performed by Ricardo. The test comprises sniff panel scores and chemical analyses of odorants for one engine/vehicle system operated at various conditions.

Results

A total of 58 samples from 5 engine/vehicle systems were analyzed by Arthur D. Little, Inc. Table 6.2-4 is a summary of the test results which are itemized in Table 13 of the Appendix.

The City Cycle test results revealed significant effects of the fuel grade on the TIA for the 70 HP TC diesel engine.

The use of the same fuel grade in naturally-aspirated and turbocharged diesel engines did not produce any difference, except for the 5-cylinder naturally-aspirated diesel engine. This may be attributable to the comparatively high level of HC emissions.

The application of EGR for NOx reduction leads to a significant increase of odorant emissions. Proper EGR modulation may improve this condition. Odorant emissions during idle depend on the composition of the fuel grade.

Table 6.2-5 shows the results of the tests performed by Ricardo where a 50 HP NA diesel engine was tested at two different injection timings in a VW Rabbit. The results of all tests showed that the regulated emissions and the odor values were significantly larger at advanced fuel injection. The injection timing of 2^{o} before TDC obviously raises the emissions beyond the permissible level for this particular engine.

There is some correlation between sniff panel scores and TIA figures. The Reciardo values for the 3^{o} after TDC injection timing agree with the ADL values within the expected tolerance of $\pm$ 0.25 TIA units. Fuel economy and regulated emissions also agree with our data (see Table 11 in the Appendix, Engine/Vehicle System No. 7).

While there seems to be the expected correlation between HC and odorant emission, closer study cannot confirm this correlation. The TIA of 1.9 for an inertia-weight of 2,500 lb., -2^{o}, and 2,750 lb., 3^{o} in Table 6.2-5 corresponds with HC values of 0.76 and 0.24 g/mile, respectively.

	Idle	30 mph	55 mph	city
50 HP N.A. Fuel II	1.8	1.9	2.4	1.9
50 HP N.A. E.G.R.	1.6	2.1	2.8	2.5
70 HP TC Fuel II	1.7	1.6	1.9	1.9
70 HP TC VW fuel	1.5	1.6	1.7	1.5
70 HP TC E.G.R.	1.3	1.5	2.2	1.9
5 Cyl. N.A.	2.1	2.0	2.0	2.0

TABLE 6.2-4: SUMMARY OF ODORANT EMISSION (A.D.L.)
TOTAL INTENSITY OF AROMA (TIA) VALUES

Inertia Weight lb	Inject. Timing ^{o}a TDC	Operat. Mode	LCA µg/l	LCO µg/l	TIA	Sniff Panel Scores	Fuel City mpg	HC g/mi	CO g/mi	NO_x g/mi
2,000	3	City	16	1.2	1.3			.14	.55	.96
	-2	City	164	7.7	1.9					
2,250	3	Idle	0	4.0	1.6	2.5				
	-2	Idle	93	5.6	1.8	1.8				
	3	30 mph	66	6.4	1.8	1.8				
	-2	30 mph	203	9.0	2.0	2.2				
	3	55 mph	258	11.4	2.1	2.5				
	-2	55 mph	435	12.6	2.1	3.3				
	3	City	34	3.1	1.5	2.6	35.2	.25	1.06	1.57
	-2	City	269	9.5	2.0	3.2	35.5	1.23	4.71	2.94
2,500	3	City	102	6.6	1.8	2.3	35.0	.30	1.20	1.33
	-2	City	240	7.8	1.9	2.4	34.6	.76	3.18	3.54
2,750	3	City	108	7.8	1.9	1.9	36.0	.24	1.03	1.37
	-2	City	281	12.4	2.1	2.6	37.7	.87	3.12	3.06

TABLE 6.2-5: ODORANT EMISSIONS FROM A 50 HP NA DIESEL ENGINE.
Test Results, Ricardo Consulting Engineers.

6.2.4.4 Sulfate Emissions

The sulfur content of a diesel-fuel grade depends on the source of crude oil and on the refining process. Diesel fuel grades usually have a sulfur content of between 0.1 and 0.5% per weight.

Methodology

The engine/vehicle systems were operated on chassis dynamometers. The U.S. Federal City Driving Cycle (cold engine start) and the Sulfate Emission Driving Cycle (warm engine start) were used for the tests.

A well-defined fraction of the exhaust gas was filtered through a Fluoropore Filter. The content of the sulfates in the collected solids on the filter was washed out with a 60% Propanol-2 solvent.

The design of the dilution channel is the same as the one for the measurement of particulate emissions (see Figure 6.2-20).

A schematic of the set-up of the sulfate analyzing system is shown in Figure 6.2-23. This is a liquid chromatographic system. The liquid solvent (60% Isopropanol, 40% water) is pumped at high pressure through a cation exchanger and the barium chloroanilate column. The background absorption at a wave length of 310 mm is recorded with the ultraviolet detector. The sample to be analyzed may be routed to the analyzing system through the 6-way valve. The increase of ultraviolet absorption is a measure of the amount of sulfates.

The apparatus is calibrated with samples of known concentrations of ammoniasulfates.

Results

The results of sulfate emission measurements are summarized in Figure 6.2-24. The tests were conducted on a fuel grade with a sulfur content of 0.115% per weight.

No significant differences were observed in the conversion of sulfur to sulfates for both regulated emission levels or the three engine/vehicle systems under investigation.

The actual values differ by less than 10% when a fuel economy of 40 mpg is assumed.

The conversion to sulfates is easily computed for a sulfur content of 0.225% per weight.

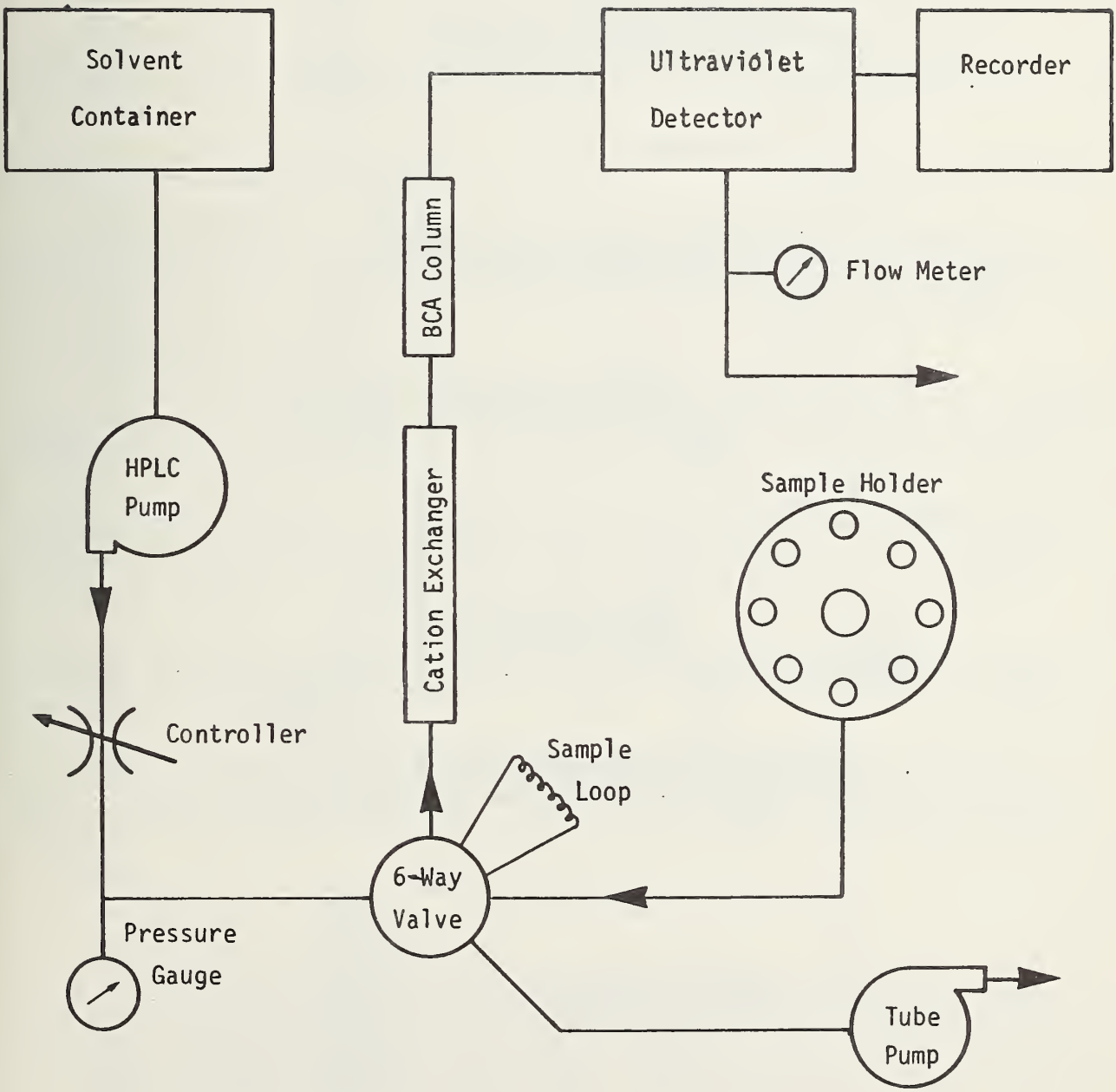

FIGURE 6.2-23: SCHEMATIC OF THE SULFATE ANALYZING SYSTEM
HPLC: High-pressure liquid chromatography
BCA: Barium Chlor Anilate

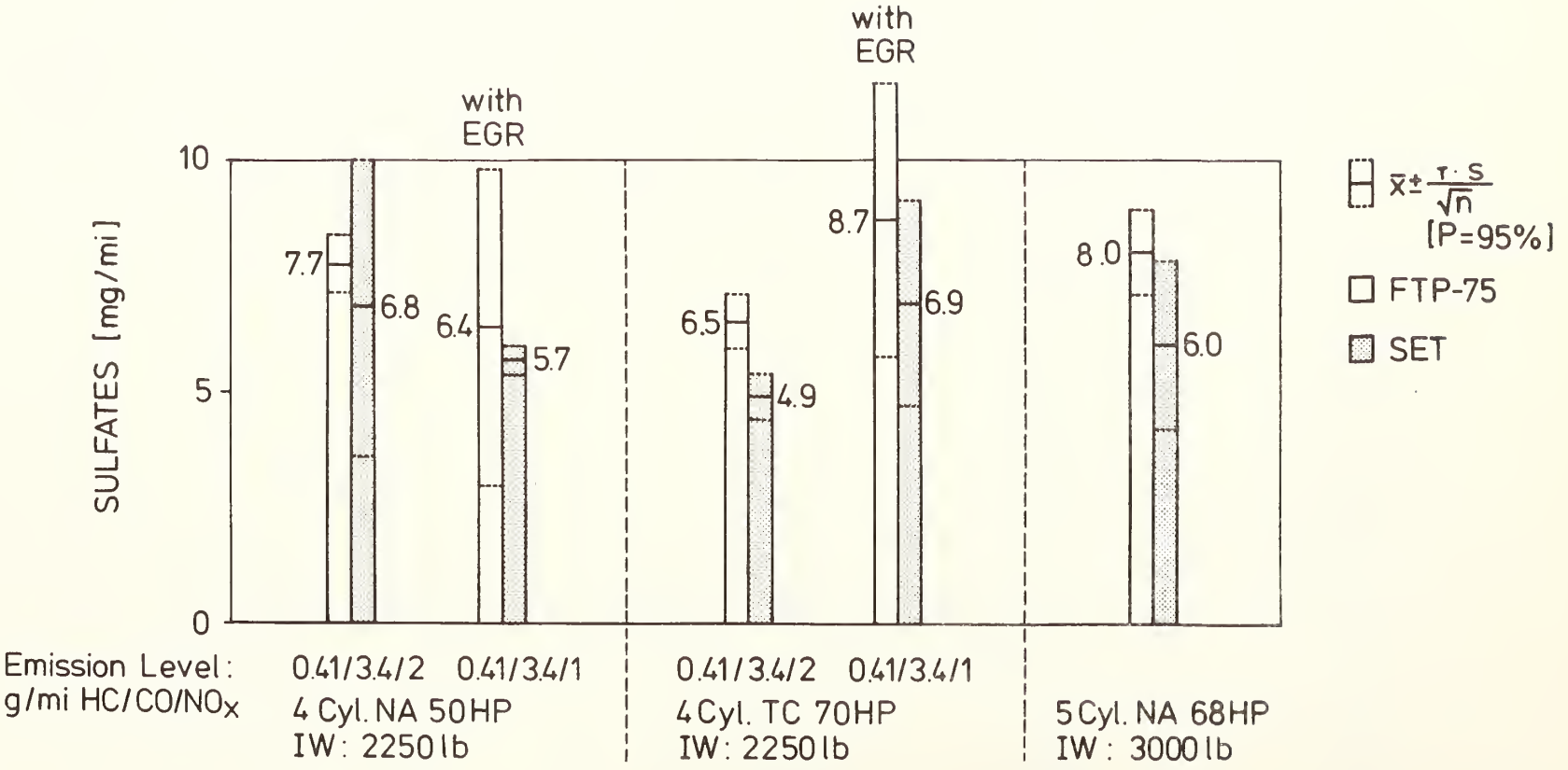

FIGURE 6.2-24: SULFATE EMISSIONS
Diesel Fuel Grade with 0.225 wt% S

Fuel Consumption: 40 mpg = 80 g/mile

Total sulfur emission: $0.225 \cdot 10^{-2} \cdot 80$ g/mile = 180 mg/mile

Molecular mass ratio: $SO_4/S = 3$

Average sulfate emission: 7.5 ± 1 mg/mile City Cycle

Average sulfate conversion: $\frac{7.5}{3 \times 180} = (1.4 \pm 0.2)\%$

The variation of sulfur content in the fuel is far larger than the variation of the conversion of the engine.

6.2.3.5 Ammonia Emission

Diesel engines are assumed to emit very little ammonia because they are not equipped with any catalyst. This assumption was confirmed by the tests described below.

Methodology

The chassis dynamometer tests of the engine/vehicle systems were performed in accordance with the U.S. Federal City Driving Cycle (cold start) and the Sulfate Emission Driving Cycle (warm-engine start).

A defined fraction of the exhaust gas is passed through washing flasks. The schematic in Figure 6.2-20 shows the dilution channel. The Fluoropore filter is replaced by washing flasks, each of which contains 1/4 liter of .01 sulfuric acid. The intake pipes were heated.

The absorbent solution is passed into a distilling apparatus. After the addition of a caustic soda solution, the ammonia is removed as water vapor and caught in a receptacle.

The distillation product is put into a 50-ml graduated flask, and 4 ml Nessler agent (Mek, Darmstadt) is added. Photometry is performed at a wavelength of 450 mm after a 20-minute soaking period (Perking Elmer Spectrometer 124).

Results

The results of the ammonia emission measurements are summarized in Table 6.2-6. The City Driving Cycle tests produced 50% higher ammonia emissions than the Sulfate Emission Test Cycle. The exhaust gas recirculation did not produce any significant effects on ammonia emissions. The ammonia emissions from the turbocharged engine are 25% lower. This difference, though, is of the same magnitude as the measurement uncertainties.

	50 HP NA	50 HP NA EGR	70 HP TC	70 HP TC EGR
City	3.9 (10)	3.2 (1.3)	2.8 (6)	2.6 (5)
SET	1.4 (8)	2.9 (9)	1.8 (3)	2.0 (6)

TABLE 6.2-6: AMMONIA EMISSION FROM 50 HP NA and 70 HP TC DIESEL ENGINES IN A 2,250-LB. VEHICLE.
The tests were performed in accordance with the Federal City Driving Cycle (cold engine start) and Sulfate Emission Driving Cycle (warm engine start). Ammonia values given in mg/mile.

Figure in parentheses are standard errors in the last digits.

6.2.4.6 Aldehydes Emissions

Aldehydes emissions are formed by quenching the chain of chemical reactions, converting oxygen and fuel to water and carbon dioxide. Formaldehyde (HCHO, molecular mass = 30) accounts for approximately 90% of all aldehydes produced during the combustion. Aldehydes are noticeable at concentrations as low as a few parts per million.

Methodology

The engine/vehicle systems were operated on chassis dynamometers. The tests were run in accordance with the U.S. Federal City Driving Cycle (cold engine start) and the Sulfur Emission Test Driving Cycle (warm engine start).

A defined fraction of the exhaust gas is conducted through washing flasks. The schematic configuration of the dilution channel is shown in Figure 6.2-20. The washing flasks replace the Fluoropore Filter.

The MBTH (3-Methyl - 2-Benzo Thiazolone Hydrazone Hydrochloride Techniques for Determining Aldehydes by the BMTH Method - CRC Report No. 415, June 1968) Method was used to analyze the water-soluble aliphatic aldehydes. The amount of aldehydes is calibrated by known quantities of formaldehyde (HCHO).

The washing flasks were filled with 25 ml MBTH solvent each. An iron chloride ($FeCl_3$) solution was added after the aldehydes had been trapped in the solvent. After a soaking period of 40 minutes the flask was filled with acetone. The absorption of light at 670 mm wavelength was measured with a Perkin Elmer Spectrometer 124.

Results

The results of aldehyde emission tests are summarized in Figure 6.2-25. The aldehyde emission is larger by a factor of 1.5 to 1.7 during the City Driving Cycle than during the sulfate emission driving cycle. No significant influence of the exhaust gas re irculation on the aldehydes emission was observed. The emission from the turbocharged diesel engine is small by 20% than that of the naturally-aspirated engines. This difference, though, is of the same magnitude as the measurement uncertainties.

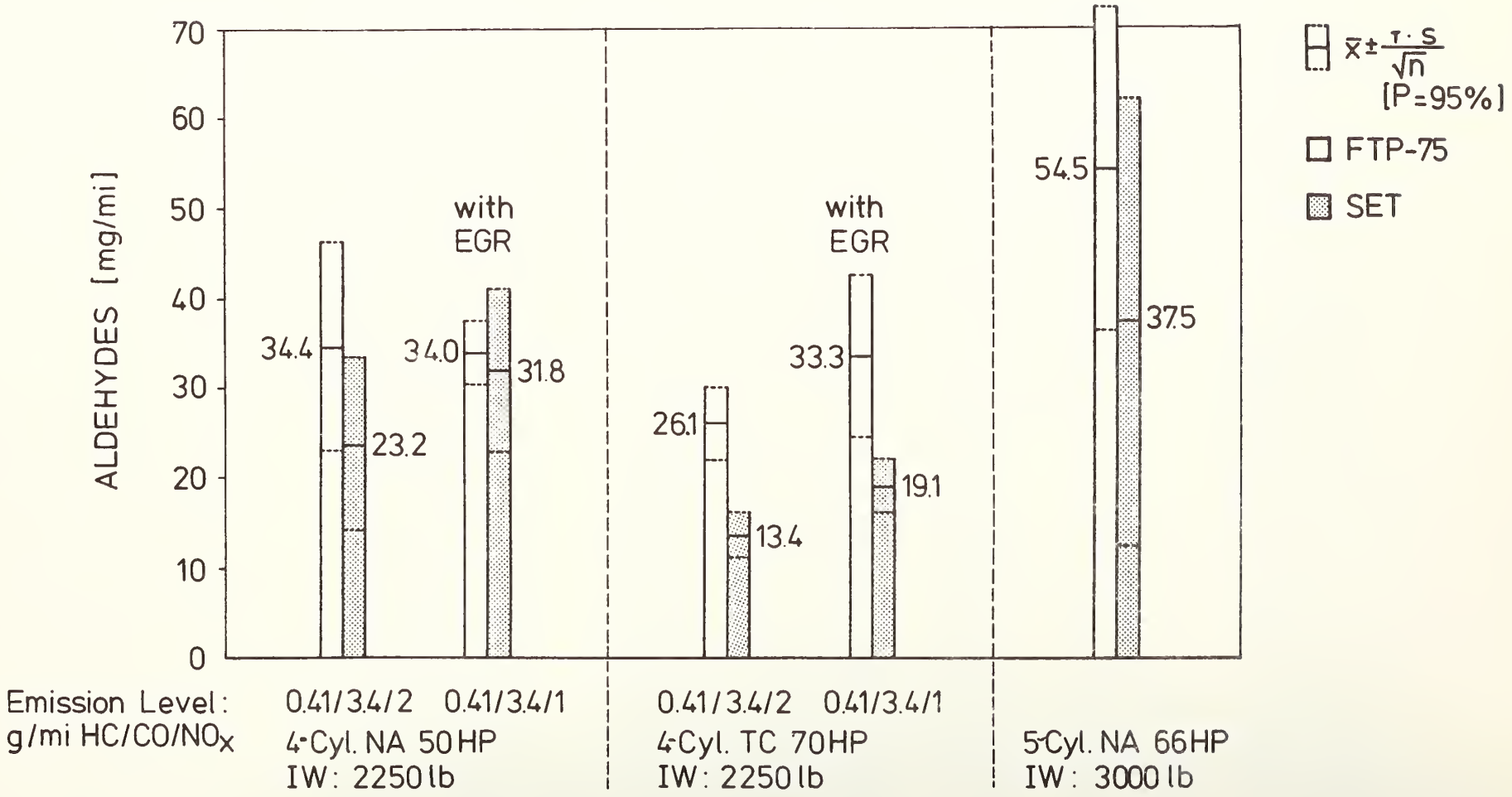

FIGURE 6.2-25: ALDEHYDE EMISSIONS

6.2.4.7 Noise

A series of tests was performed to determine the interior and exterior noise levels in dB(A) during idle, constant 30 mph speed, and full-load acceleration from 30 mph. The measurements were taken on the VW proving ground.

Acceleration Drive-By

Figure 6.2-26 shows the set-up for the noise measurement. The microphone is located at a 50-ft. distance. The vehicle approach speed is 30 mph when it reaches a line 25 ft. before a line through the microphone perpendicular to the vehicle path. From this line to a line 125 ft. beyond the zero point full-load acceleration is performed in the second transmission gear. The noise level is recorded as a function of the vehicle position. Five measurements on each side of the vehicle are recorded on one data sheet (see Figure 6.2-27). A detailed description of these noise records is given below.

The interior noise at the position of the driver's ear is measured at the zero point of the vehicle path. The average of 10 readings is marked by a dot in the noise records.

Constant-Speed Drive-By

The noise from constant-speed drive-by is measured with the same set-up as for the accelerated drive-by. The vehicle passes at a constant speed of 30 mph with the transmission in top gear. The interior noise is measured again at the position of the driver's ear.

Idle

The idle noise is measured on a modified reflecting surface in an open test range.

The engine is operated at a warm steady-state temperature at the idling speed recommended by the manufacturer. The exterior noise is measured 0.5 m away from the center of the radiator grill. The interior noise is measured as above.

Results

The main noise results are summarized in Figure 6.2-28 and Table 6.2-7 for 3 engine/vehicle systems complying with the emission level of .41/3.4/1 g/mile HC/CO/NOx:

- 50 HP, 90 CID, NA Production Diesel Engine/(Rabbit, 2250 lb.)

- 70 HP, 90 CID, TC Research Diesel Engine/(Rabbit, 2250 lb.)

- 68 HP, 130 CID, NA 5-Cylinder Diesel Engine/(Audi 100, 3000 lb.)

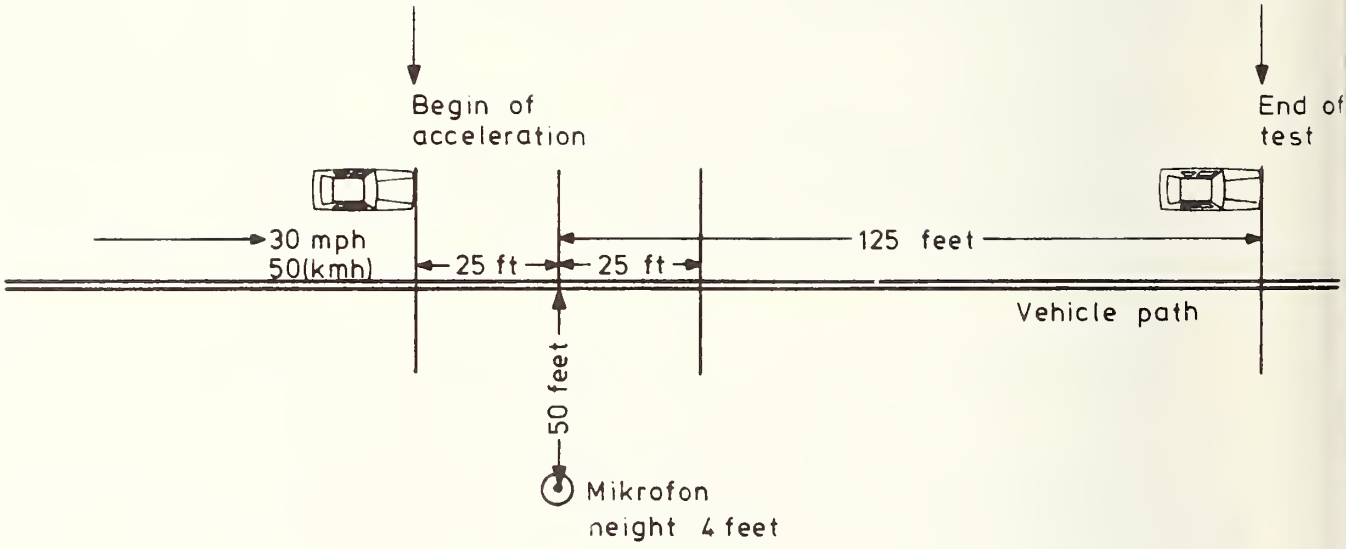

FIGURE 6.2-26: ACCELERATION DRIVE-BY
SAE J 986a requires the above set-up

GOLF D NO. 3 WITH 50 HP PRODUCTION DIESEL

Idle Noise 79 dB(A) exterior
55 dB(A) interior

FIGURE 6.2-27: NOISE EMISSION

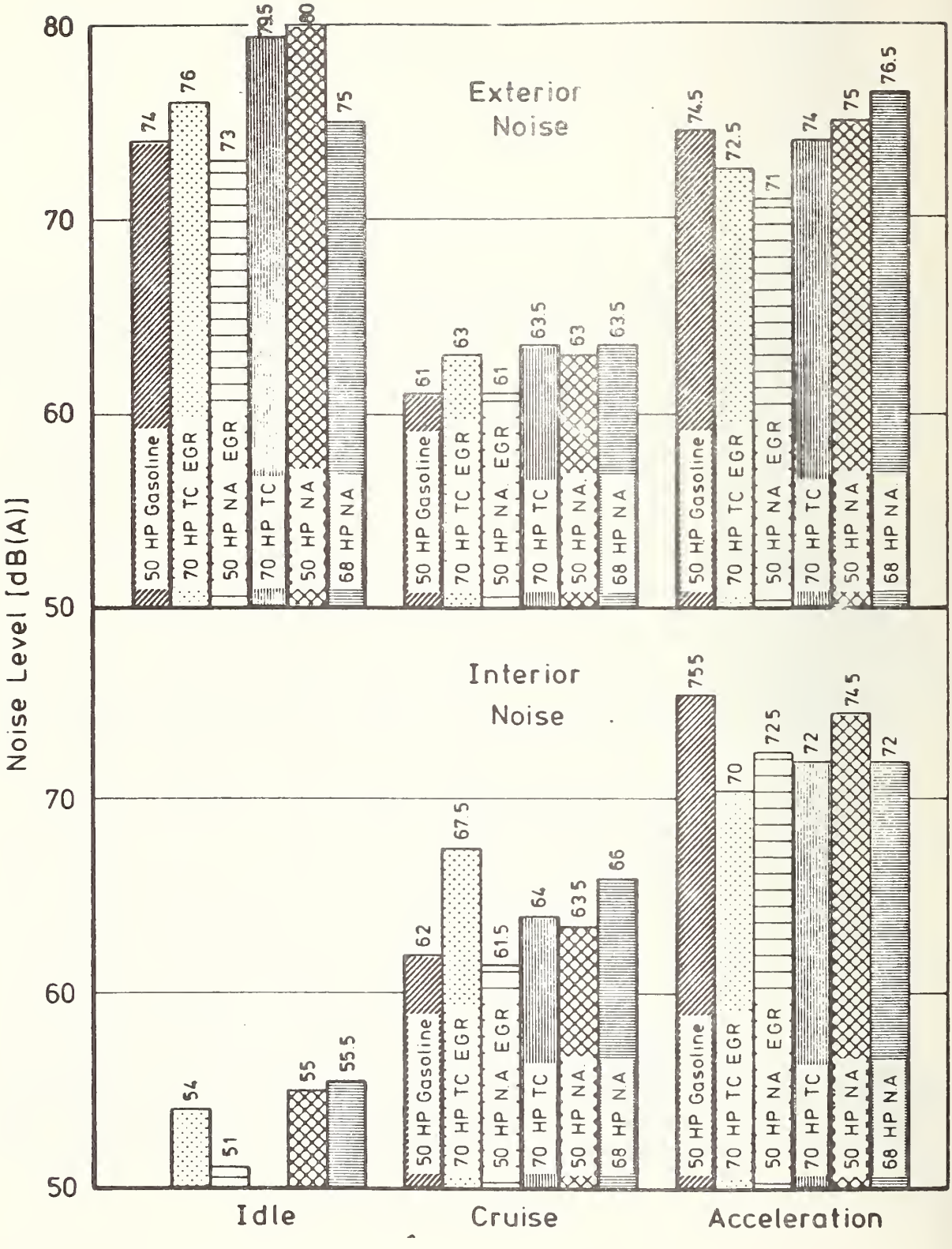

FIGURE 6.2-28: NOISE EMISSION FROM VARIOUS ENGINE/VEHICLE SYSTEMS
Exterior noise at 50-ft. distance, 30 mph cruise or full-load acceleration from 30 mph; idle noise at 0.5 m from the vehicle front. The noise tolerance is ± 1 db(A)

Engine/Vehicle System	Exterior Noise (dB(A))			Interior Noise (dB(A))		
	Idle	Const. Speed	Acceler. Drive-By	Idle	Const. Speed	Acceler. Drive-By
50 HP NA Rabbit Diesel	80	63	75	55	63.5	74.5
50 HP EGR Rabbit Diesel	73	61	71	51	61.5	72.5
50 HP Rabbit Gasoline	74	61	74.5		62	75.5
70 HP TC Rabbit	79.5	63.5	74		64	72
70 HP TC Rabbit		67*	69.5		69*	69
70 HP EGR Rabbit	76	63	72.5	54	67.5	70.5
70 HP H_2O Rabbit	81	62	73.5		62.5	72.5
5-Cylinder Audi 100	75	63.5	76.5	55.5	66	72

*Second gear instead of high-gear cruising

TABLE 6.2-7: SUMMARY OF NOISE EMISSION RESULTS
The figures given in the table may vary by $\pm$ 1 dB(A)

Two engine/vehicle systems with modulated EGR comply with the stringent emission level of 0.41/3.4/1 g/mile HC/CO/NOx:

- 50 HP, 90 CID, NA EGR Diesel Engine/(Rabbit 2250 lb.)

- 70 HP, 90 CID, TC EGR Diesel Engine/(Rabbit 2250 lb.)

One 50 HP gasoline engine (Rabbit) is included for comparison.

The lowest exterior noise emission was obtained with the 50 HP EGR engine installed in a Rabbit. This engine/vehicle system emits even less noise than the comparable gasoline engine/vehicle system. The same result applies to the interior noise level. This is a confirmation of the well-known noise reducing property of EGR.

The noise emission from the 70 HP EGR engine/vehicle system is unexpectedly large. The reason was unsatisfactory installation of the EGR modulation device in the engine compartment - the device contacts the vehicle frame. This engine/vehicle system has the potential to achieve the same noise level as that of the 50 HP EGR system.

The engine/vehicle systems with naturally-aspirated engines produced higher noise levels because of the lower gear ratio of the TC engines. The noise level during full-load acceleration does not differ significantly from that of comparable gasoline engines.

An itemized list of the noise measurements from 22 engine/vehicle systems is included in the Appendix, Table 12. The table also shows the pertinent noise levels.

Variations of about 1 dB(A) are usually observed between left- and right-side noise emission. One of the several reasons is the asymmetric exhaust pipe.

The width of the scatter band is approximately 1 dB(A). Some distinctive peaks are scattered on the records. These peaks are due to the gunfire noise from a nearby army shooting range.

Some tests were performed on wet surfaces (see Appendix, Table 12 and the itemized noise records). An increase of 6 dB(A) (63 to 69 dB(A) of the cruise noise is observed for wet surfaces.

Diesel Idle Noise

The idle noise of diesel engines is highest when the engine is cold. At least two reasons are responsible for the increased noise:

- The characteristic cold diesel knock due to ignition retardation - The fuel ignites after the major portion of the complete charge has been injected. The fuel in a warm cylinder ignites just at the beginning of the injection and allows for a controlled combustion process.

- The necessary injection advance for cold cylinder in order to compensate for the late ignition.

Figure 6.2-29 shows that the idle-noise level decreases in direct proportion to the running time of the engine. The diesel engine noise decreases by approximately 6 dB(A) during the first four minutes. The advanced fuel injection by the cold-start device increases the idle noise by 2 dB(A). This effect adds to the noisier combustion at low cylinder temperatures.

The gasoline engine behaves differently. There is a minimum idle noise at intermediate temperatures. This minimum depends on the time when the choke is shut off. A difference of about 1 dB(A) between cold and warm idling will be found for well-tuned chokes.

Figure 6.2-30 shows the varying characteristics of the acoustic pressure at idle for a diesel and gasoline engine with the same valve drives and swept volumes.

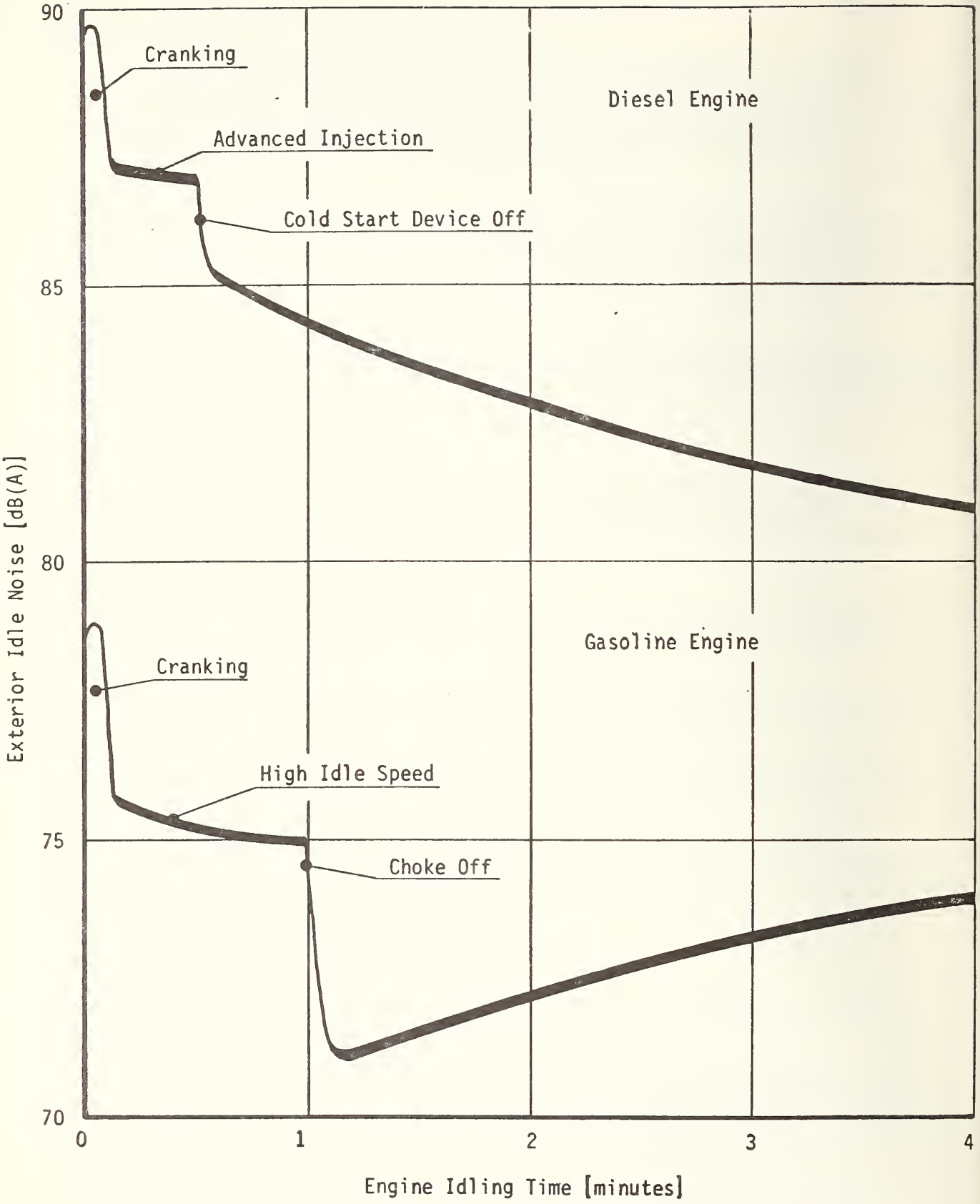

FIGURE 6.2-29: SCHEMATIC PROGRESS OF NOISE EMISSION AFTER A COLD-ENGINE START

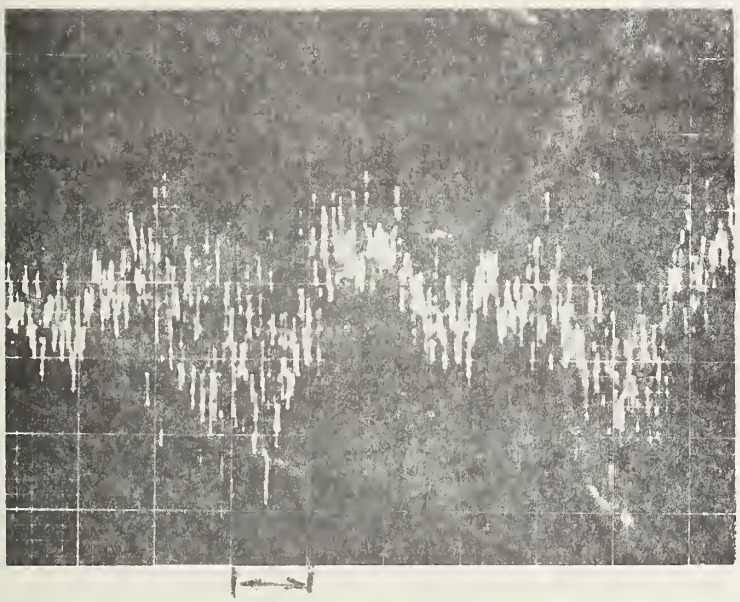

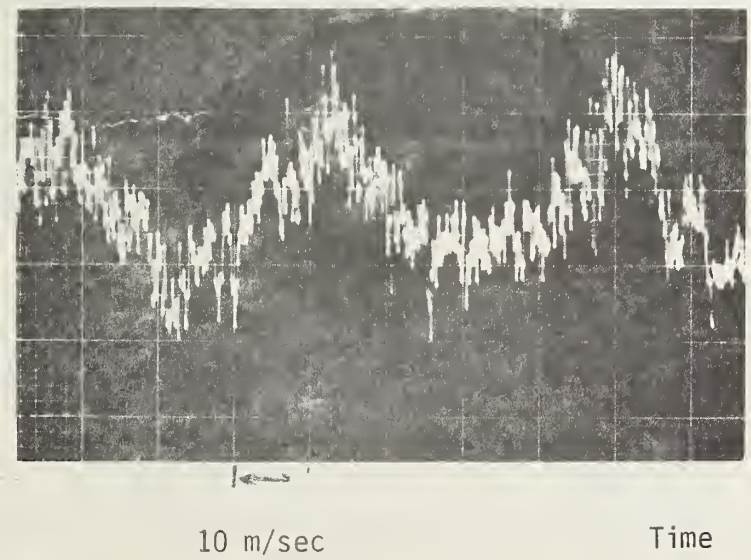

FIGURE 6.2-30: ACOUSTIC PRESSURE MEASURED AT CLOSE RANGE (50 CM) AT IDLING SPEED.
Diesel and Gasoline engine of equal swept volume

6.3 CONSUMER ATTRIBUTES

This section deals with factors and trade-offs that affect marketability.

6.3.1 Fuels and Lubricants

The 50-HP, 90-CID naturally aspirated production diesel engine was used to determine the effects of fuel, lubricant, and filter requirements on engine performance, fuel economy, and emissions. The resulting information may be considered representative of the entire engine family.

The determination of the diesel fuel characteristics and their effects on fuel economy, emissions, cold-start behavior, ignition process and engine performance was arrived at in cooperation with some oil companies, i.e. British Petroleum, Shell, and Esso. The lubricant and filter requirement studies were performed during the preparation of the diesel Rabbit production ( ). The investigations showed that the swirl-chamber requirements are similar to those of the conventional gasoline engine.

6.3.1.1 Fuel Characteristics

The diesel fuel characteristics are affected by the source of crude oil and the fuel refining method. Fuel properties such as specific gravity, cetane number, aromatics content, and volatility are included. This interrelationship poses problems in regard to the isolation of the effects of the individual parameters on various engine performance characteristics such as ignition behavior, fuel economy, cold-start behavior, and clean combustion.

The properties of diesel fuels largely are determined by the molecular structure of the fuel components, i.e. n- and i-paraffines, n- and i-olefines, naphthenes (cyclo-paraffines) as well as aromatics and their derivatives.

The characteristics of the hydrocarbons in diesel fuel generally are as follows ( ):

Straight-Chain (n) Paraffines

High cetane numbers, unfavorable cold-start behavior, low calorific value per unit volume, low density, low smoke emission tendency.

Branched-Chain (i) Paraffines

Low cetane numbers, good cold-start behavior, low calorific value per unit volume, low density, low smoke emission tendency.

Naphthenes (cyclo-) Paraffines

Medium cetane numbers, good cold-start behavior, medium calorific value per unit volume, medium density, smoke emission tendency similar to that of olefines.

Aromatics

Low cetane numbers, acceptable cold-start behavior, high calorific value per unit volume, high density, high smoke emission tendency.

It should be noted that higher molecular weights of the above substances detrimentally affect their cold-start behavior, increase their densities, and raise the boiling point.

Figure 6.3-1 shows typical relationships between cetane numbers, calorific values, and viscosity versus specific gravity. Heavier fuel blends with high relative densities have a high viscosity, low cetane numbers and a lower heat content.

Table 6.3-1 is a summary of the major characteristics of 27 different winter-grade fuels. This information was compiled by Deutsche BP AG. The three rows at the bottom are the averages and maximum and minium limits of the respective columns.

Fuel density affects the full-load injection rate because the fuel injection pump generates constant-volume injection rates. The injection pump was tuned to a average fuel density of .83 kg/liter. Low-viscosity winter fuels cause significant decreases in performance which may exceed 14% since their low viscosity raises the pump plunger leakage rate.

While diesel fuels of higher volatility may reduce smoke emissions, they may also lower the power output because of their lower specific gravity.

Higher fuel cetane numbers lower the white and blue smoke emissions after engine start-up. The same effect is produced by lowering the mid-boiling point which also affects fuel volatility.

Table 6.3-2 lists the characteristics of eight grades of diesel fuel with different components and characteristics. The components were varied markedly beyond those in commonly used diesel fuels in order to facilitate the recognition of possible fuel behavioral tendencies.

The fuel sulfur content directly affects the engine sulfate emissions because of the comparatively constant sulfur-to-sulfate conversion rate. The sulfur content of typical U.S. diesel fuels in shown in Table 6.3-3.

The engine cold-start behavior at low ambient temperatures is determined by the cold-filter plugging point, i.e. the temperature at which paraffine precipitation occurs. Table 6.3-2 shows the marked difference between the plugging points of winter and summer grade diesel fuels (grades 323 and 15275).

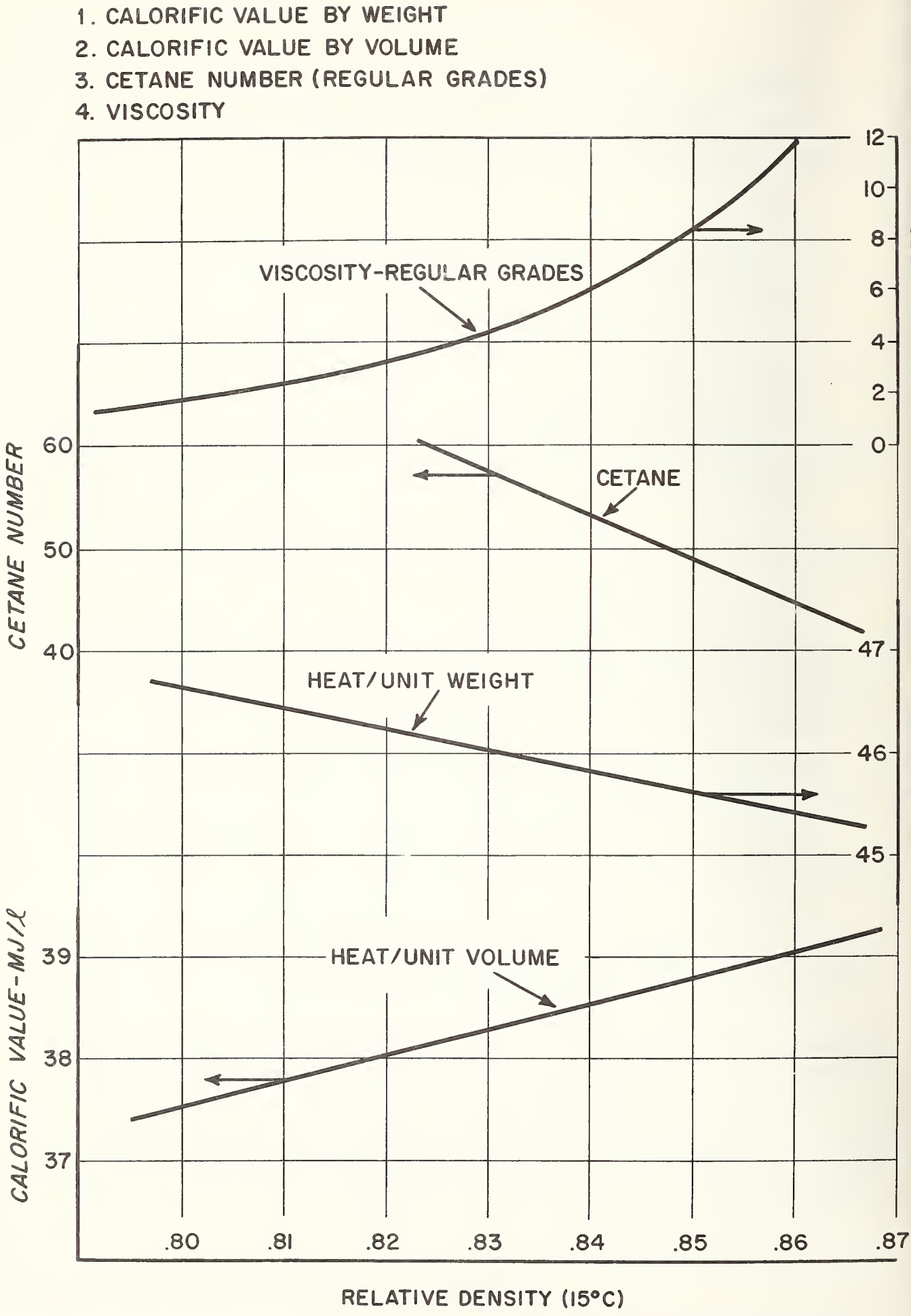

FIGURE 6.3-1: THE EFFECTS OF FUEL BLEND RELATIVE DENSITY ON MAJOR DIESEL FUEL PROPERTIES

DENSITY AT 15°C Kg/ℓ	DISTILLATION FRACTION 250°C % VOL	DISTILLATION FRACTION 350°C % VOL	BOILING END °C	FLASH POINT °C	VISCOSITY 20°C cSt	SULFUR %Wt	CLOUD POINT °C	CFPP °C	CETANE NUMBER	CETANE INDEX
0.827	54	97	353	69	3.38	0.17	- 8	-19	54.5	51.5
0.841	41	100	336	82	3.94	0.45	-16	-17	52.5	49.5
0.833	40	97	352	58	4.19	0.47	- 7	-20	54.0	55
0.834	39	100	329	60	3.92	0.36	-15	-16	55.0	53.5
0.836	39	100	328	63	3.92	0.33	-14	-15	54.5	53
0.828	47	100	344	73	3.59	0.18	-12	-17	54.0	54
0.829	44	100	343	48.5	3.73	0.35	-10	-23	55.5	54
0.825	55	100	348	68	3.48	0.27	- 9	-19	55.0	52.5
0.822	59	100	339	62	3.03	0.42	-16	-16	52.0	52
0.819	63	94	366	59	3.00	0.26	- 8	-16	51.0	50.5
0.819	62	97	354	62.5	2.85	0.43	-10	-20	53.5	50
0.824	44	100	333	62.5	3.71	0.34	-12	-14	57.0	56.5
0.828	50	98	350	61.5	3.53	0.37	-10	-19	54.5	53
0.827	52	95	360	63	3.41	0.32	- 6	-19	54.5	53
0.830	31	100	334	72	4.22	0.21	-17	-17	59.0	56
0.823	57	97	355	65	3.23	0.35	- 8	-22	54.5	52
0.827	56	98	351	65	3.26	0.39	- 8	-20	53.0	51
0.823	57	98	353	61	3.27	0.23	- 7	- 20	55.5	53
0.831	43	94	358	44	3.99	0.38	- 8	- 16	55.0	54.5
0.823	58	100	307	70	3.07	0.27	-28	- 30	54.5	53.5
0.829	49	97	354	57	3.62	0.16	- 7	-19	55.0	53.5
0.835	44	100	344	55	3.82	0.30	-10	-17	53.5	52
0.840	38	100	345	72	4.15	0.31	- 9	-14	52.0	52
0.819	53	97	354	52	3.26	0.43	-10	-18	57.0	55.5
0.833	39	97	351	68	4.16	0.47	- 8	-20	55.5	53.5
0.823	47	100	343	62.5	3.49	0.39	-11	-17	56.0	56.5
0.826	53	98	350	41	3.45	0.22	-10	-18	53.5	53
0.828	49	98	346	62	3.58	0.33	-11	-18	54.5	53
0.819	31	94	307	41	2.85	0.16	- 6	-14	51.0	49.5
0.841	63	100	366	82	4.22	0.47	-28	-30	59.0	56.5

SOURCE: DEUTSCHE BP AG

TABLE 6.3-1: SURVEY OF WINTER-GRADE DIESEL FUELS PRODUCED BY GERMAN REFINERIES AND SAMPLED DURING FEB., 1977. The three bottom lines show the average, minimum, and maximum values of the respective columns.

The ignition behavior of a diesel engine also is affected by the diesel fuel cetane number according to ASTM D 969-66. The cetane numbers of the fuels shown in Tables 6.3-1 and 6.3-2 range from 46 to 59. Cetane numbers in this range do not lead to any detrimental effects on engine ignition behavior.

The following engine characteristics are affected by diesel fuel properties:

- Performance at constant fuel volume rate
- Specific fuel consumption
- $HC/CO/NO_x$ emissions
- Unregulated emissions
- Odor
- Smoke visibility
- Noise
- Startability for winter and summer grade fuels

Table 6.3-4 and Figure 6.3-2 show the effects of diesel fuel densities on power output, specific fuel consumption, and smoke visibility. A 5% increase in diesel fuel density raises the power output by 3% and significantly intensifies smoke visibility.

The variation of diesel fuel viscosities in the range from 2.35 through 6.49 cSt does not lead to any noticeable effects (see Table 6.3-4).

LAB NO.	323	15275	16086	16095	16120	16140	16160	16164
DENSITY 15° C, kg/ℓ	.841	.840	.825	.847	.817	.834	.843	.869
VISCOSITY 20° C, cSt		4.51	3.30	4.49	2.75	4.06	5.21	6.54
AROMATICS AMS, % wt.		25.5	18.9	20.0	17.0	21.0	23.0	28.4
AROMATICS FIA, % vol.		33.5	21.0	24.5	19.0	29.5	3.8	44.5
OLEFINES AMS, % wt.		3.6	1.8	1.5	1.4	1.9	4.1	11.0
OLEFINES FIA, % vol.		0.5	0.5	0.5	-	-	-	1.5
CETANE NO. ASTMD 976-66	45.7	53.5	54.5	49.5	53.5	52.5	53.5	47.0
FLASH POINT °C	77	61.5	74	91	70	71	70	74
CLOUD POINT °C	-26	4	-10	-15	-14	-1	5	2
COLD FILTER PLUG-GING POINT CFPP °C	-27	-2	-12	-16	-14	-9	0	0
CARBON RESIDUES % vol.	1	2.5	1.5	1.5	1.5	1.5	2.0	2.0
SULFUR % wt.	.10	.82	.34	.10	.25	.42	.96	1.68
COLOR ASTM	.5	< 1.5	< 0.5	< 0.5	< 0.5	.5	< 2.5	6.0
INITIAL BOILING °C	196	168	180	206	178	181	168	177
50% vol. BOILING °C	255	274	247	264	227	261	277	299
FINAL BOILING °C	310	390	354	319	345	369	>400	380

SOURCE: DEUTSCHE ESSO AG AND DEUTSCHE SHELL AG

TABLE 6.3-2: CHARACTERISTICS OF TEST DIESEL FUELS

U.S. No. 2 diesel samples: Lab No. 323 and 16095

Region	Samples	Minimum	Average	Maximum
ASTM Grade 1d				
Eastern	27	0.01	0.084	0.26
Southern	13	0.01	0.044	0.114
Central	27	0.008	0.083	0.24
Rocky Mtn.	12	0.008	0.089	0.15
Western	15	0.004	0.104	0.26
ASTM Grade 2d				
Eastern	52	0.01	0.212	0.52
Southern	30	0.011	0.235	1.07
Central	63	0.011	0.250	0.52
Rocky Mtn.	31	0.055	0.299	0.511
Western	29	0.014	0.287	0.50

(Source: Shell)

TABLE 6.3-3: SULFUR CONTENT (WEIGHT %) U.S. DIESEL FUEL

DIESEL FUEL GRADE				ENGINE					
				3,000 rpm			4,500 rpm		
DENSITY AT 15°C kg/ℓ	VISCOSITY AT 20° C cSt	BOILING END °C	CETANE NO.	POWER kW	SPECIFIC FUEL CONSUMPTION g/kWh	SMOKE BOSCH	POWER kW	SPECIFIC FUEL CONSUMPTION g/kWh	SMOKE BOSCH
.813	2.35	297	50	22.6	331	2.6	30.5	366	3.5
.818	2.81	365	54.5				30.5	366	3.4
.820	2.65	328	51				31.1	365	3.7
.822	2.75	327	51				30.7	377	3.9
.823	2.91	331	51	23.1	335	2.7	30.7	374	3.8
.831	4.06	369	54				31.5	373	4.2
.835	4.02	326	55.5				30.7	375	4.0
.838	4.09	374	54				31.5	362	4.3
.839	3.98	366	52				31.1	365	4.0
.841	3.95	350	52	23.3	344	4.6			
.843	3.74	348	49.5	23.1	347	4.5	31.1	381	4.4
.850	6.49	358	58				31.3	373	4.3
.855	3.70	329	45	23.3	360	5.6	31.5	383	5.5

SOURCE: DEUTSCHE BP AG

TABLE 6.3-4: THE EFFECTS OF VARIOUS DIESEL FUELS ON POWER OUTPUT, FUEL CONSUMPTION, AND SMOKE VISIBILITY (50 HP 90 CID NATURALLY-ASPIRATED PRODUCTION DIESEL ENGINE

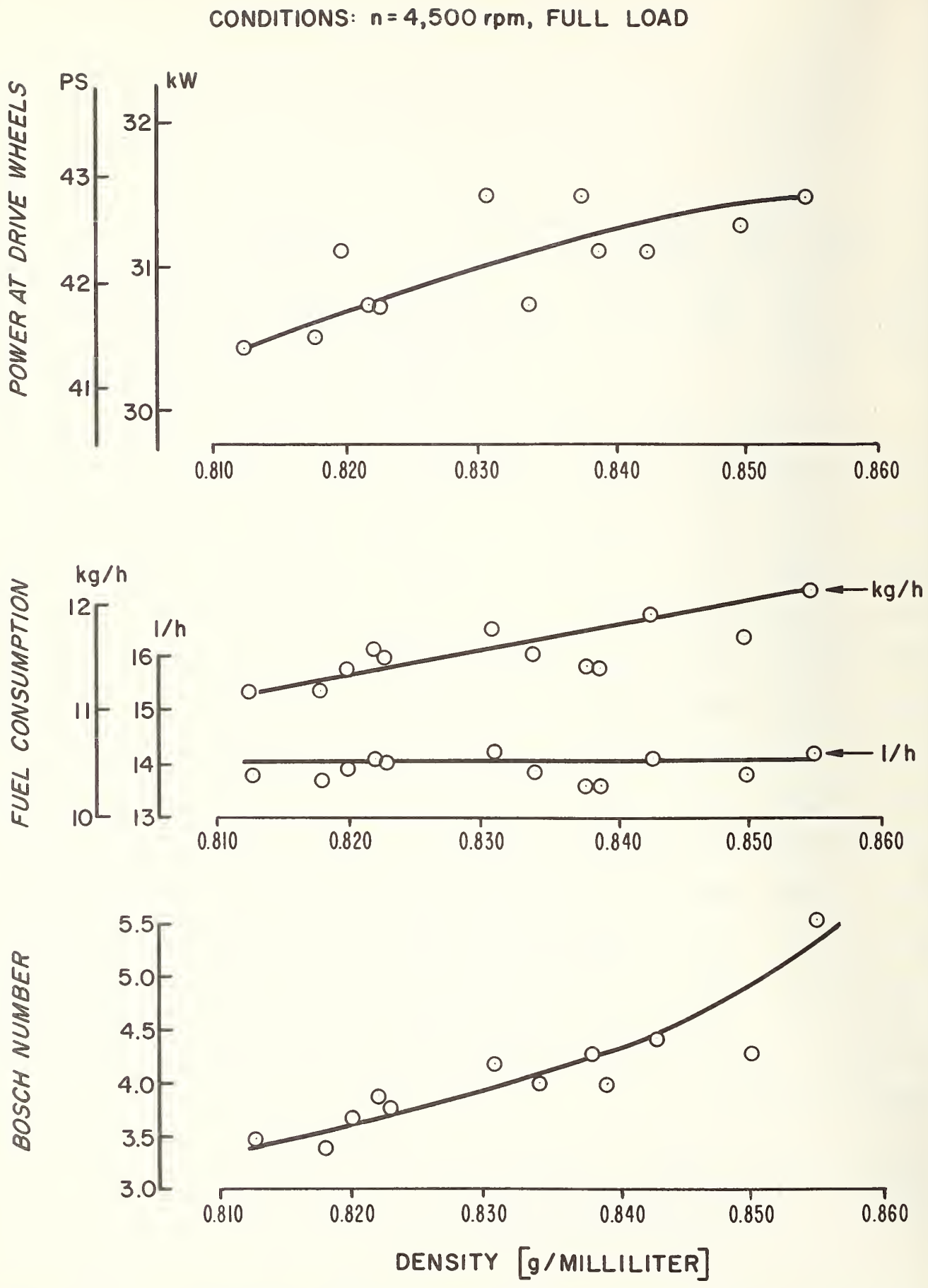

FIGURE 6.3-2: THE EFFECTS OF DIESEL-FUEL DENSITY ON ENGINE BEHAVIOR

Highest-density diesel fuels produce maximum full power output. Lowest-density fuels generate lowest full power output. Medium-density fuels do not follow this pattern of correlation between power output and fuel density.

Figure 6.3-4 shows the effects of the cetane number on engine performance. Figure 6.3-5 shows the fuel economy scatter band width of roughly ±2% of the diesel test fuels at a vehicle velocity of 50 mph.

Figures 6.3-6 through 6.3-8 present the effects of diesel fuel grades on smoke visibility, hydrocarbon and carbon oxide emissions. It is apparent that smoke visibility moves within a ± .5 Bosch number range. The HC/CO emissions vary by a factor of 5. Figure 6.3-9 shows that fuel grade variations do not have a marked effect on NO_x emissions.

Deutsche Esso AG performed an investigation of the effects of engine service life an fuel economy and regulated emissions. During this investigation, the 50-HP, 90-CID diesel production engine was run at full speed under full load for 100 hours on each of seven different grades of diesel fuel. The results of these tests are summarized in Table 6.3-5 and show that engine service life does not affect power output and NO_x emissions. The typical U.S. No. 2 diesel fuel grade (Lab. No. 16095) does not lead to any deterioration of smoke and HC emissions. Unorthodox fuel blends (e.g. Lab. No. 16164) which are not available commercially, though, form deposits in the nozzle regions and thus detrimentally affect HC emissions and smoke.

The Deutsche BP AG studied the effects of various diesel fuel grades on engine startability and noise emissions at low temperatures, and performed chassis dynamometer tests with a commercial diesel fuel grade (CP $-7^{o}C$, CFPP $-16^{o}C$), fuel blends containing 10 and 30% gasoline, and a special winter fuel grade in an engine/vehicle system consisting of a 50-HP diesel engine in a 2,250-lb car. The test cycle included engine start-up and fast acceleration to a constant vehicle velocity of roughly 70 mph. The test results are shown in Fig. 6.3-10 and indicate that fuel filter plugging may cause engine stalling within the first ten minutes of the test run.

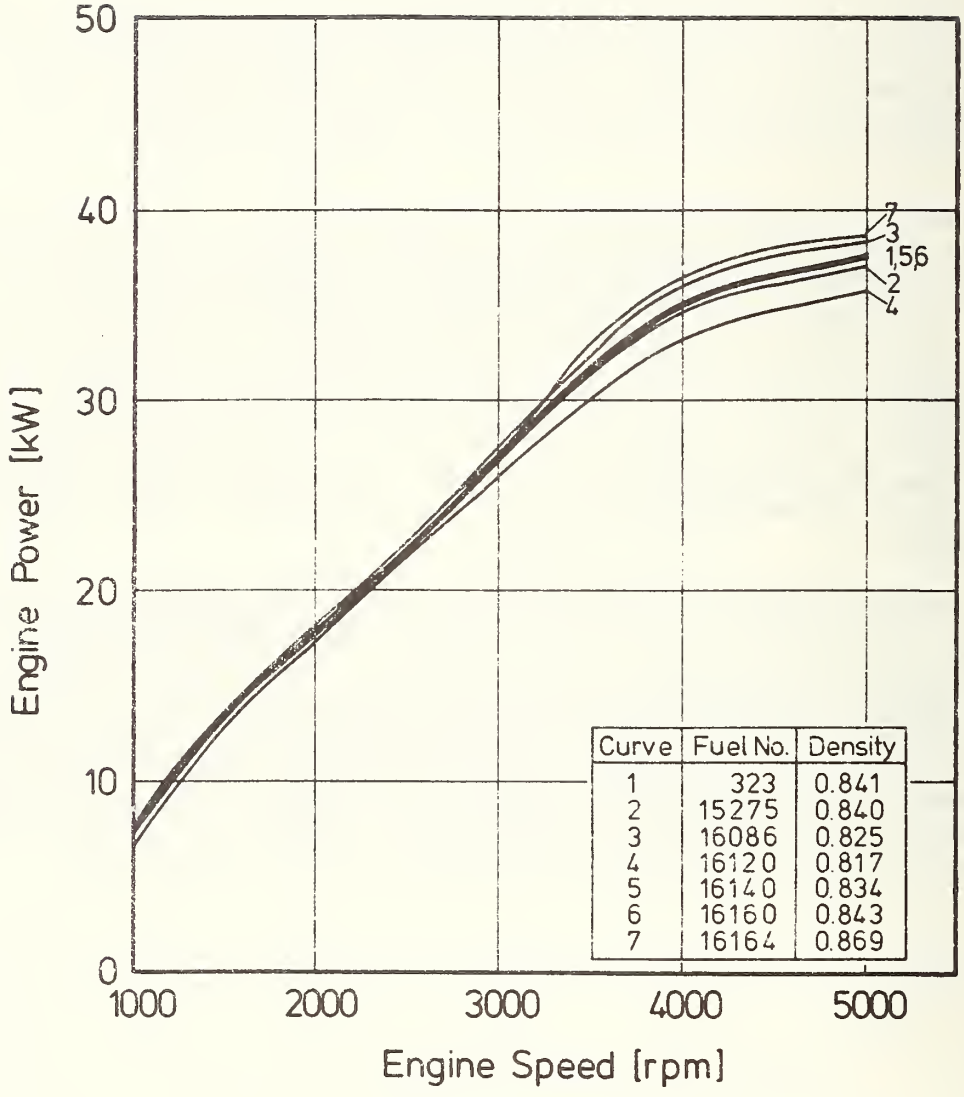

FIGURE 6.3-3: INFLUENCE OF THE FUEL ON THE FULL LOAD ENGINE POWER
50 HP NA PRODUCTION DIESEL ENGINE

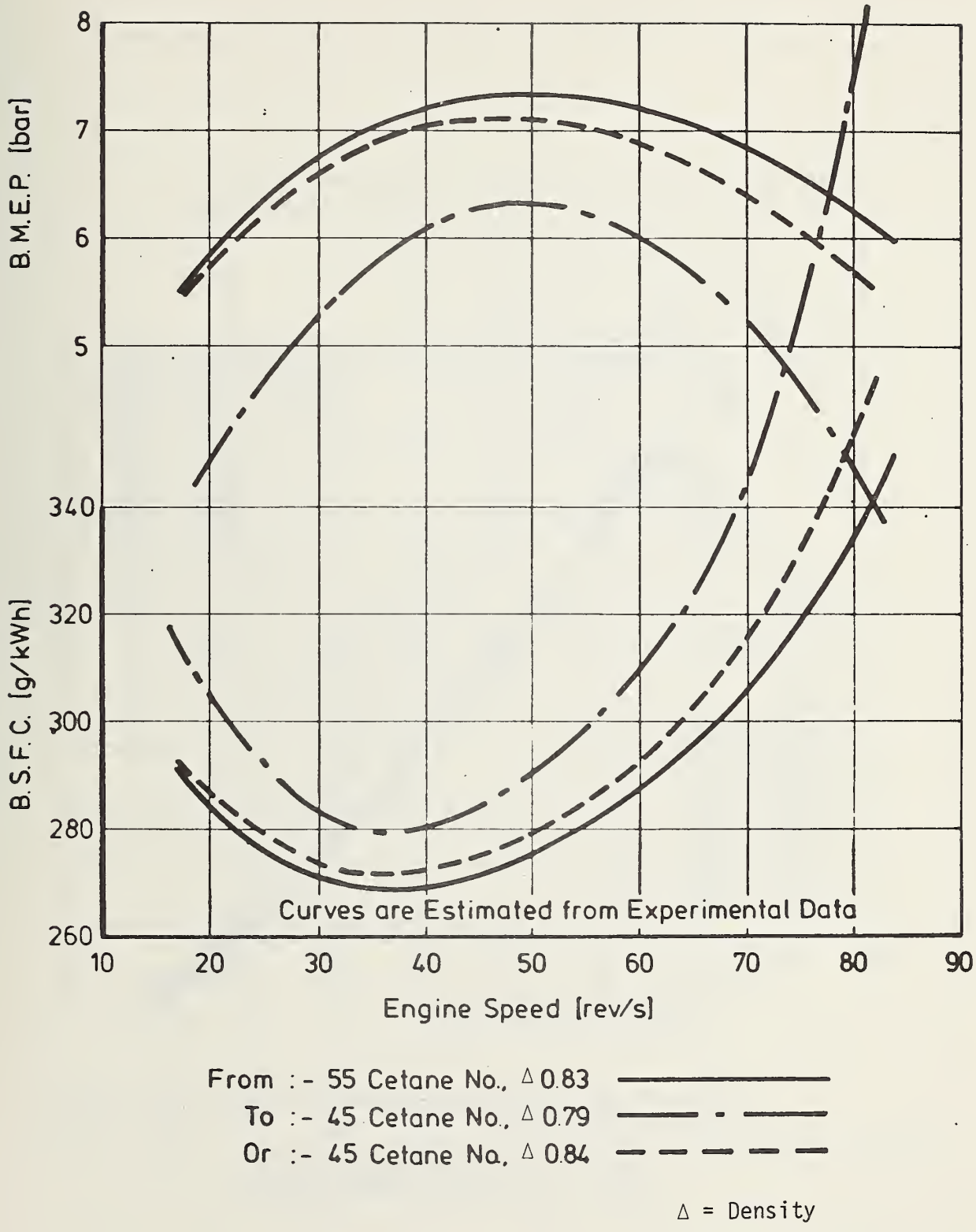

FIGURE 6.3-4: THE INFLUENCE OF CETAIN NUMBER ON PERFORMANCE, WITHOUT RE-OPTIMIZATION

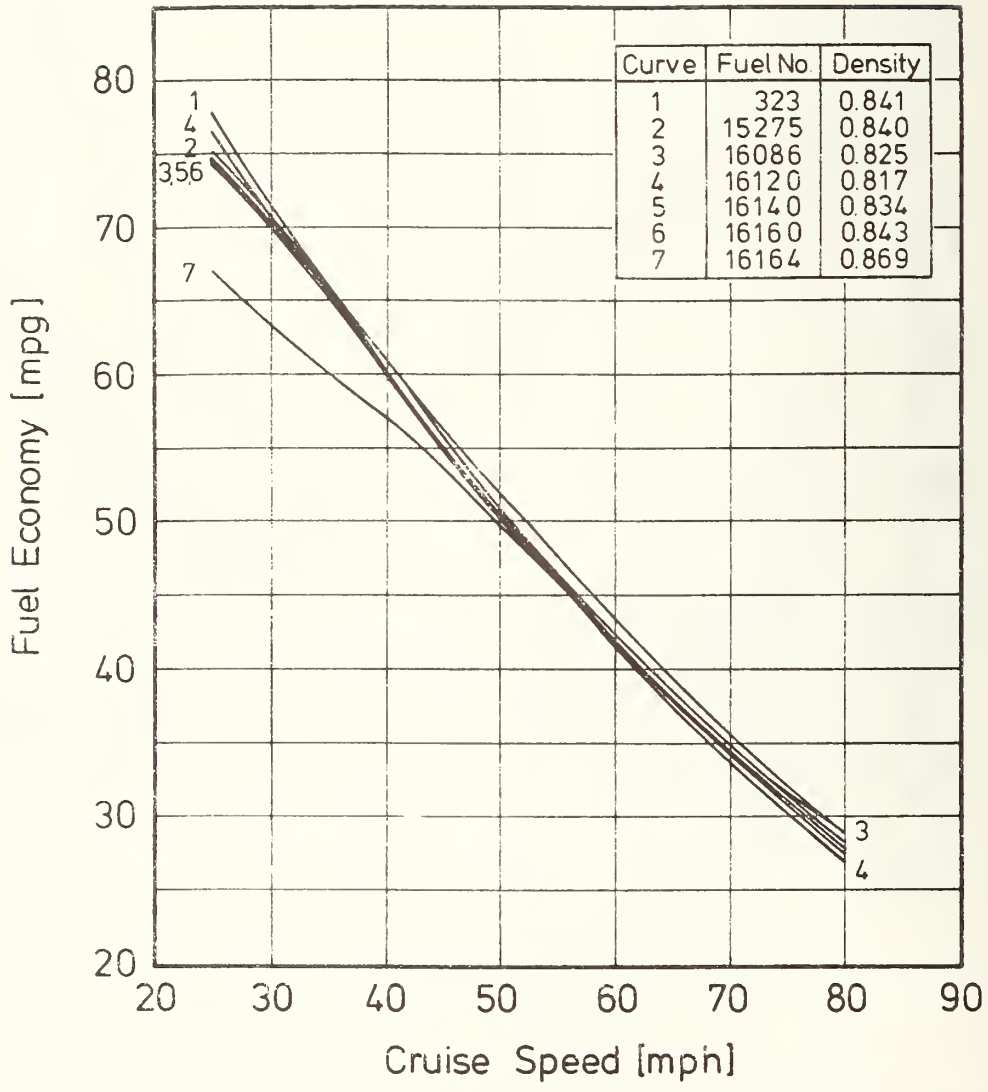

FIGURE 6.3-5: INFLUENCE OF THE FUEL ON THE ROAD LOAD FUEL ECONOMY 50 HP NA PRODUCTION DIESEL ENGINE

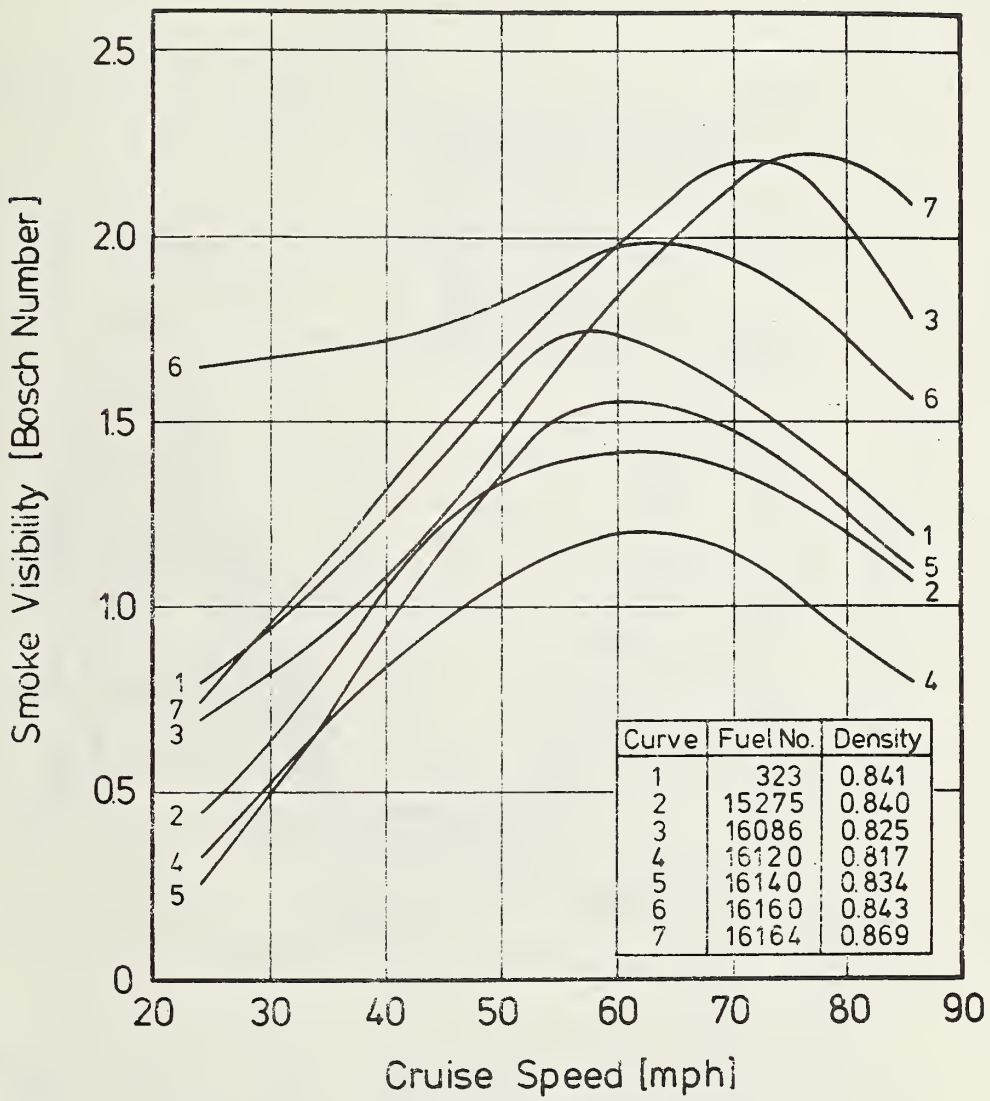

FIGURE 6.3-6: INFLUENCE OF THE FUEL ON THE ROAD LOAD SMOKE VISIBILITY 50 HP NA PRODUCTION DIESEL ENGINE

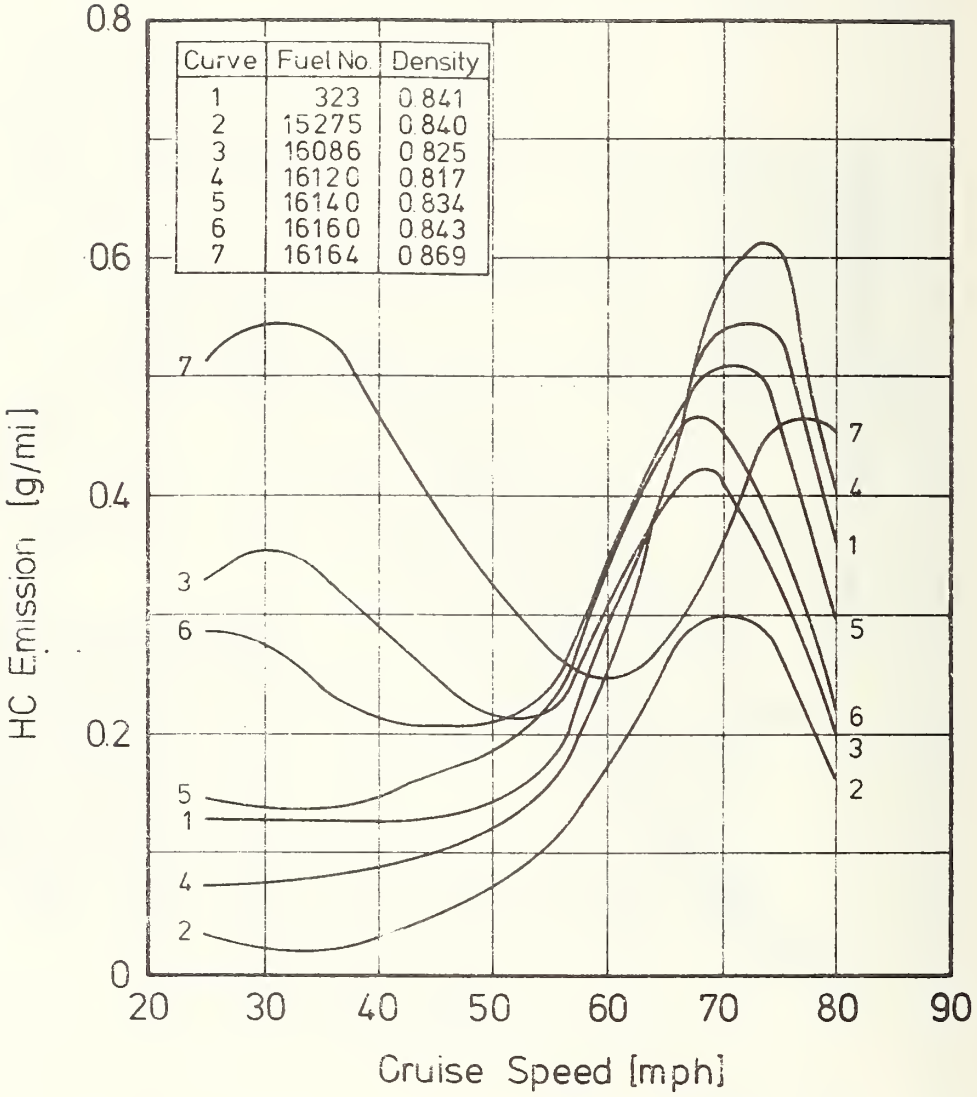

FIGURE 6.3-7: INFLUENCE OF THE FUEL ON THE ROAD LOAD HC EMISSION 50 HP NA PRODUCTION DIESEL ENGINE

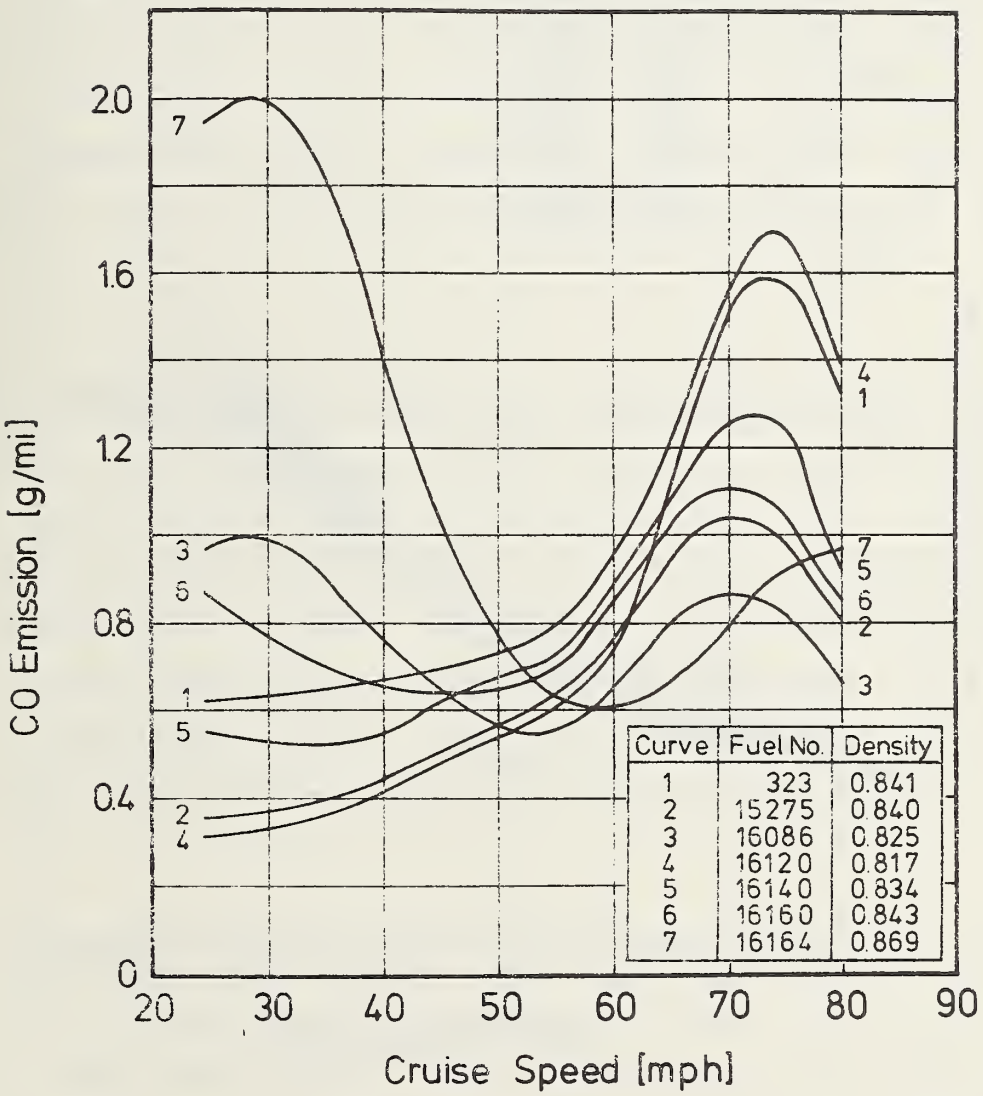

FIGURE 6.3-8: INFLUENCE OF THE FUEL ON THE ROAD LOAD CO EMISSION
50 HP NA PRODUCTION DIESEL ENGINE

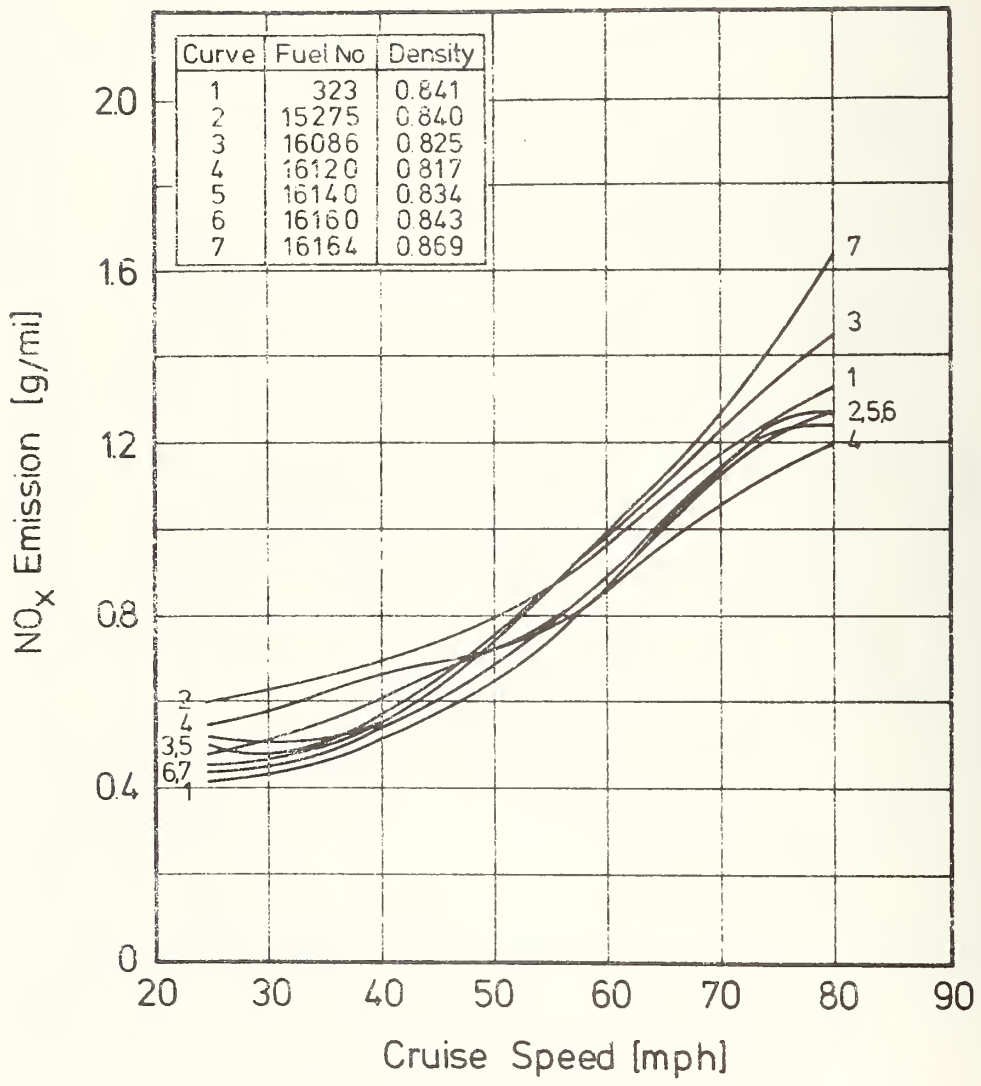

FIGURE 6.3-9: INFLUENCE OF THE FUEL ON THE ROAD LOAD NOx EMISSION 50 HP NA PRODUCTION DIESEL ENGINE

FUEL GRADE NO. 15275, DENSITY 0.840 kg/ℓ; OIL CONSUMPTION 14 g/h

TIME ELAPSED h	ATMOSPHERIC CONDITIONS °C	TORR	POWER OUTPUT kW	FUEL g/kWh	λ	EXHAUST SMOKE BOSCH	HC g/kWh	CO g/kWh	NO_x g/kWh	BLOW BY ℓ/min
0	21	755	36.8	305	1.35	1.8	.12	1.93	3.08	25
25	20	758	36.8	319	1.38	2.4	.53	4.84	3.98	25
50	22	760	36.8	305	1.36	2.2	.20	2.80	3.26	24
75	21	765	36.8	320	1.34	1.5	.18	3.33	3.07	24
100	21	746	36.8	312	1.29	2.8	.49	4.55	3.30	25

FUEL GRADE NO. 16086, DENSITY 0.825 kg/ℓ; OIL CONSUMPTION 18.4 g/h

0	19	746	36.8	293	1.41	2.6	–	4.71	3.73	24
25	19	748	33.8	300	1.51	2.9	1.29	6.73	4.42	23
50	20	753	36.1	328	1.33	2.4	1.90	8.53	3.62	18
75	18	755	36.8	315	1.39	3.0	1.78	7.58	4.03	24
100	20	756	36.8	318	1.33	3.0	1.84	9.38	3.73	22

FUEL GRADE NO. 16095, DENSITY 0.847 kg/ℓ; OIL CONSUMPTION 15.1 g/h

0	19	761	36.8	318	1.39	3.2	.67	4.48	4.21	26
25	20	762	33.8	304	1.40	2.7	.78	5.45	4.05	23
50	17	755	36.1	312	1.36	2.8	.94	5.12	3.66	23
75	27	756	36.8	316	1.28	2.8	.73	5.98	3.94	23
100	27	758	36.8	316	1.28	3.0	.90	5.98	4.20	24

TABLE 6.3-5: THE EFFECTS OF VARIOUS FUEL GRADES ON FUEL CONSUMPTION AND EXHAUST EMISSION OF A 50 HP, 90 CID NA DIESEL PRODUCTION ENGINE DURING 100-H, FULL-SPEED AND FULL-LOAD OPERATION AT 5,000 RPM

TABLE 6.3-5 (Cont.)

FUEL GRADE NO. 16120, DENSITY 0.817 kg/ℓ; OIL CONSUMPTION 13.6 g/h

TIME ELAPSED h	ATMOSPHERIC CONDITIONS °C	TORR	POWER OUTPUT kW	FUEL g/kWh	λ	EXHAUST SMOKE BOSCH	HC g/kWh	CO g/kWh	NO_x g/kWh	BLOW BY ℓ/min
0	29	755	36.8	298	1.36	2.4	.37	3.32	4.48	23
25	29	752	36.8	294	1.34	2.5	.95	5.81	4.09	24
50	28	749	35.7	320	1.27	2.4	1.05	6.99	4.11	23
75	26	753	36.8	318	1.29	3.0	.98	7.02	4.13	23
100	28	757	35.3	322	1.26	3.5	.90	9.75	4.24	25

FUEL GRADE NO. 16140, DENSITY 0.834 kg/ℓ; OIL CONSUMPTION 14.0 g/h

0	20	770	36.8	332	1.37	2.5	.19	2.94	3.67	28
25	22	756	36.8	324	1.33	3.0	.70	4.92	3.43	26
50	22	758	36.8	330	1.29	3.1	1.29	8.00	3.34	25
75	19	763	36.8	319	1.33	2.8	1.45	8.50	3.40	25
100	19	762	36.8	322	1.34	2.7	1.21	5.76	3.66	24

FUEL GRADE NO. 16160, DENSITY 0.843 kg/ℓ; OIL CONSUMPTION 13.1 g/h

0	28	753	36.4	352	1.27	2.5	.12	2.74	4.21	23
25	28	753	36.4	352	1.27	2.2	.39	4.75	4.10	23
50	28	758	36.0	374	1.26	2.0	.52	5.02	4.44	23
75	28	771	36.4	339	1.26	2.3	.48	4.87	4.01	23
100	28	759	36.0	319	1.23	3.9	.13	12.6	3.97	23

TABLE 6.3-5 (Cont.)

FUEL GRADE NO. 16164, DENSITY 0.869 kg/ℓ; OIL CONSUMPTION 18.9 g/h

TIME ELAPSED h	ATMOSPHERIC CONDITIONS °C	TORR	POWER OUTPUT kW	FUEL g/kWh	λ	EXHAUST SMOKE BOSCH	HC g/kWh	CO g/kWh	NO_x g/kWh	BLOW BY ℓ/min
0	29	765	36.8	338	1.36	2.4	.22	2.90	5.03	25
25	28	761	36.8	328	1.33	2.8	.27	3.02	4.48	25
50	28	750	36.0	338	1.22	2.4	.19	4.13	4.00	25
75	27	736	35.7	380	1.14	5.0	.18	8.65	3.70	25
100	26	729	34.9	364	1.11	4.3	.23	14.5	3.63	25

Source: Deutsche Esso A.G., January 1977
Engine oil: Essolube HDX Plus 30
Oil changes every 50 h
Oil filter changes every 100 h

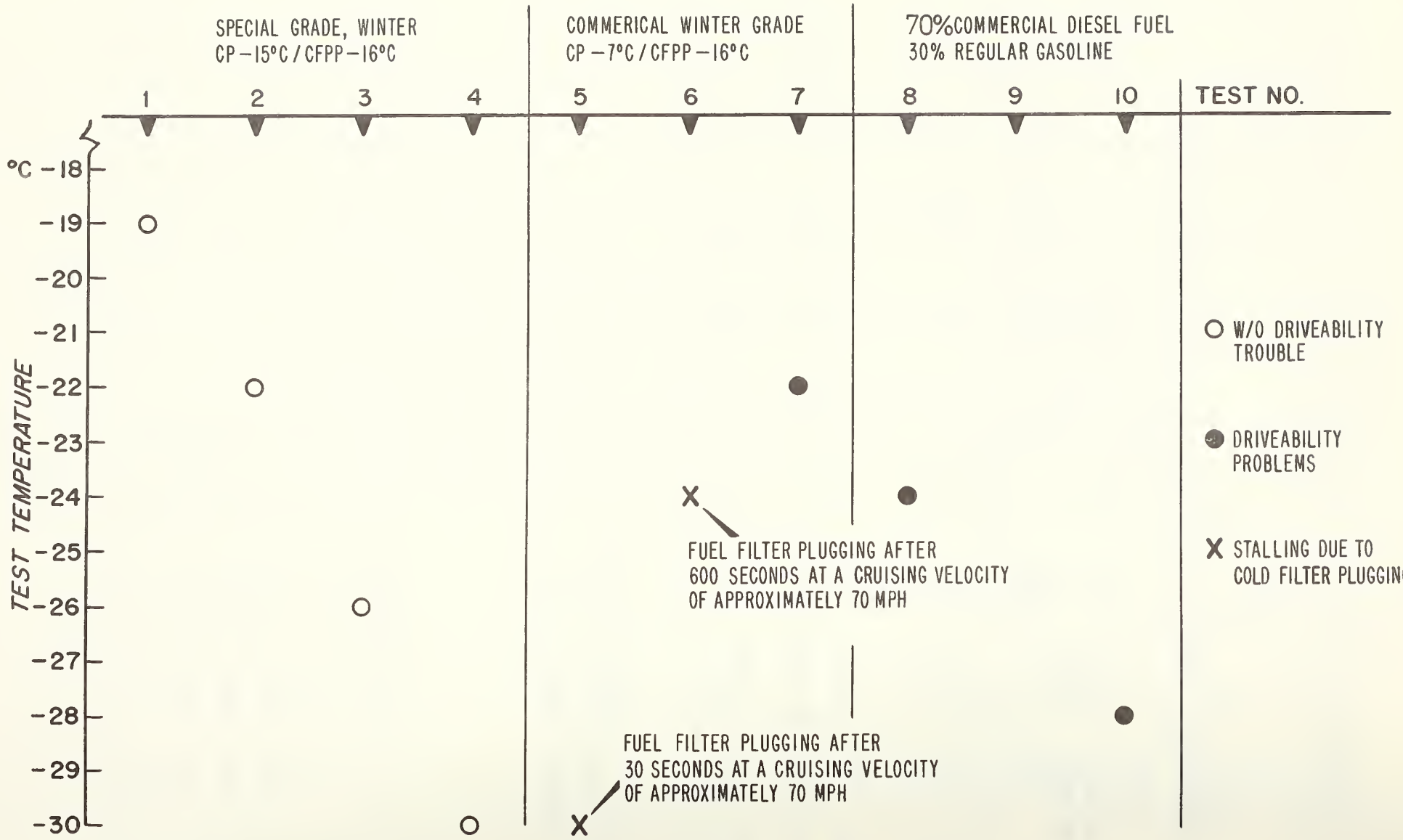

FIGURE 6.3-10: WINTER DRIVEABILITY WITH VARIOUS DIESEL FUELS

Proper diesel winter grades or diesel/gasoline or kerosene blends permit low-temperature operation. Care should be taken to use only the actually required quantity of solvents as shown in Table 6.3-6.

Ambient Temperature in °C	Mixture in % vol.			
	Summer diesel fuel	Regular gasoline or kerosene, also blend of both mixed in fuel tank	Winter diesel fuel	Regular gasoline or kerosene, also blend of both mixed in fuel tank
± 0 to - 10	80	20	100	-
- 10 to - 15	70	30	100	-
- 15 to - 20	50	50*	90	10
- 20 to - 25	-	-	70	30
below - 25	-	-	50	50*

* Kerosene only

TABLE 6.3-6: FUEL BLEND COMPONENTS

Proper fuel blends permit engine start-up without any additional aids (jumper battery, chemical starting aids, or engine oils of very low viscosity) down to -30°C (-22° F).

Figure 6.3-11 shows noise emissions at engine idle. Measurements were taken at intervals of 50 s and 5 min after engine start-up. The graph also includes noise emission measurements of the warm engine. Noise level increases were measured at decreasing ambient temperatures. A 9-dB noise level difference was observed between cold start idle at -10°C ambient

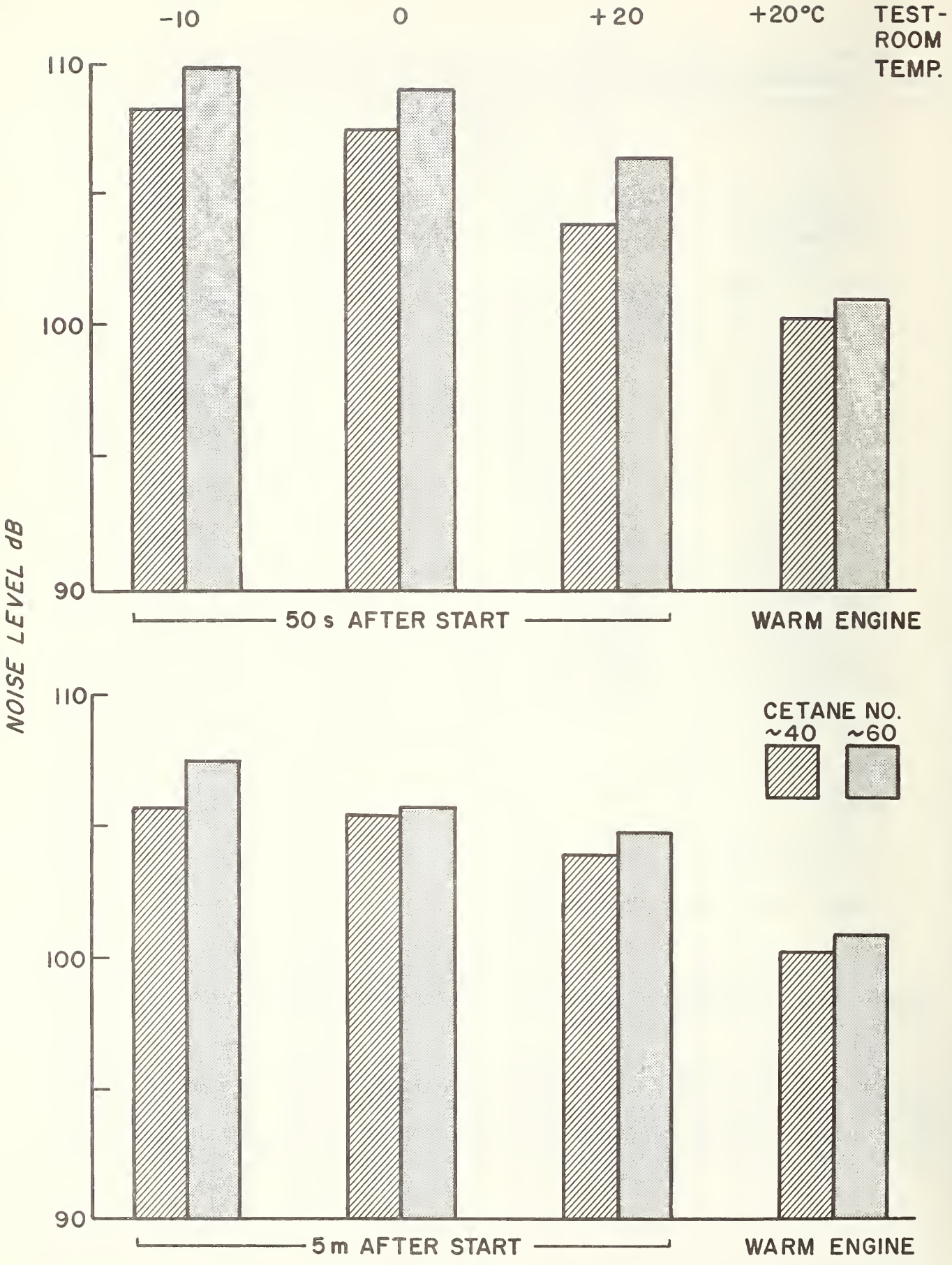

FIGURE 6.3-11: THE EFFECTS OF DIESEL FUEL IGNITION CHARACTERISTICS ON IDLE NOISE

temperature and warm idle. The idle noise level is also affected by the fuel-grade composition (e.g. 2 dB in the case of the two grades shown in Fig. 6.3-11).

6.3.1.2 Lubricants

The engine oil specifications for the VW diesel engines were prepared to ensure compliance with the various production and service requirements outlined below.

Break-In Oil

The same type of break-in oil was to be used for the diesel and spark-plug engines because both of them are assembled on the same transfer line.

The presently used lubricants generally comply with the U.S. Military Specification MIL-L-2104 b.

The break-in oil and the filter element are changed after 1,000 km.

Normal Engine Oil

Volkswagenwerk's specifications require compliance with the following demands:

- Oil change intervals at 7,500 km (three liters)
- Oil filter change intervals at 15,000 km
- Normal-quality commercial engine oil that is compatible with the VW diesel and spark-ignition engines

Volkswagen diesel engine oil viscosity specifications are the same as those for the VW spark-ignition engines. Engine oil specifications are prepared with a particular view to combustion process, piston design, required engine-oil performance and viscosity as well as oil and filter change intervals.

The break-in and the normal engine oil for the Volkswagen diesel engine family must be properly blended so that there is no formation of particulate deposits on the piston ring grooves.

The combustion process releases gases and particulates from the diesel fuel to the cold cylinder walls where they are quenched and absorbed by the engine-oil film. The volume of these emanations largely is determined by the combustion process. The direct injection process, for instance, leaves a minimum of cold surface areas in the combustion chamber and thus almost eliminates any condensation of combustion gases and particulate precipitation. Separate-chamber engines, on the other hand, have comparatively larger cold surface areas where particulate precipitation is likely to occur and thus may cause higher engine-oil contamination. Therefore, engine oil specifications for pre-chamber and swirl-chamber engines call for a higher degree of lubricant detergent capacity.

Volkswagenwerk performed extensive testing in order to establish the proper oil change intervals for the VW diesel engine family. The tests were run on three kinds of lubricants which had the same oil base but different additive, depending on their API classification:

Lubricant Data

I	SAE	30	API-CC	MIL-L-2104 b
II	SAE	30	API-SE/CC	MIL-L-46152
III	SAE	30	API-SE/CD	MIL-L-2104 C

The test cycles provided for 10-h variable-load operation followed by an oil and filter element change, and 50-h full-load operation at an oil pan temperature of 120°C.

The test results indicated an optimum oil-change interval of 7,500 km for the oil grade API-CC. These findings were confirmed by the results of a 3,000-vehicle fleet test (see Fig. 6.3-12) on the three kinds of engine-oil grade referred to above.

One of the most significant results of the fleet test was the extremely low engine oil contamination which amounted to between 1.5 and 2% per 7,500 km at the most. This minimal contamination markedly reduces any adverse cold-start behavioral characteristics.

The engine oil mean viscosity of an SAE 20w-50 lubricant was determined from 68 samples in accordance with the applicable API-SE/CC procedures. It amounted to 17.2% at a temperature of 210°C. The TBN reserve was found to be satisfactory in the fleet test. Interior wear remained below 80 ppm.

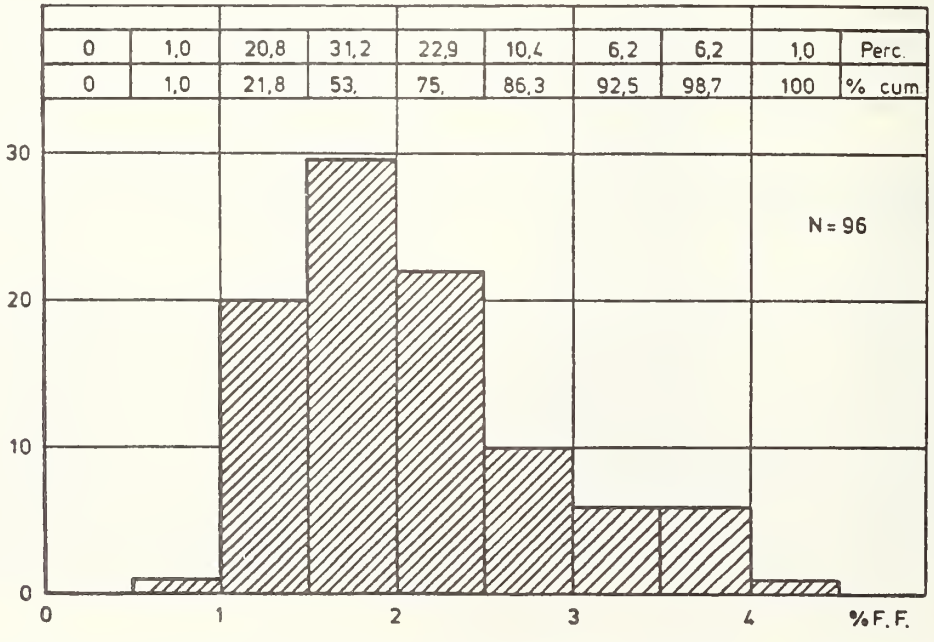

FIGURE 6.3-12: OIL POLLUTION IN VEHICLES OPERATED UNDER "ROAD CONDITIONS" Percent by Weight: Content of foreign matter according to oil change interval.

Figures 6.3-13 and 6.3-14 show the final engine oil specifications. They differ from those of most European diesel engine manufacturers.

The test results show that satisfactory cold-start behavior is provided by a multigrade lubricant based on an SAE W 15 engine oil under European and U.S. climatic conditions.

The diesel engine performance with this engine oil places it in the lower 1 H Caterpillar range (upper ring groove temperature 240°C, oil-pan temperature 130°C, at full-load operation). Therefore, shop procedures for diesel and spark ignition engines can be largely standardized, i.e.:

- The same lubricant is used for the VW diesel and spark ignition engines (API-SE/CC, MIL-L46 152, commercial grades SAE 15 W-40, 15 W-50, and 20 W-50).

- The low degree of engine oil contamination permits oil change intervals of 7,500 km and filter element change intervals of 15,000 km. The same intervals apply to VW spark ignition engines.

- The comparatively low increase in engine oil viscosity due to particulate precipitation results in favorable cold-start behavior.

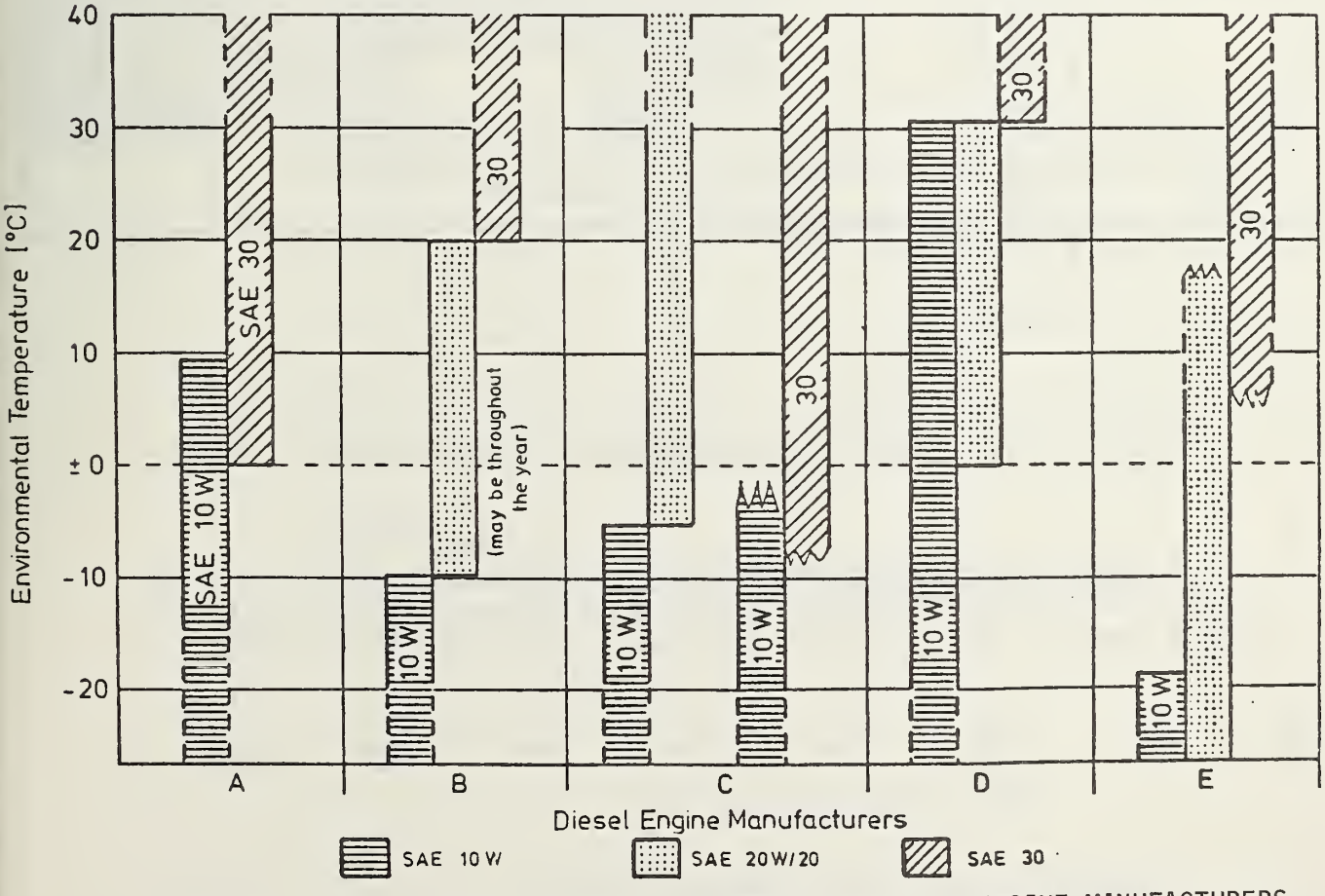

FIGURE 6.3-13: VISCOSITY SPECIFICATIONS FOR DIESEL ENGINE MANUFACTURERS IN GERMANY FOR HIGH SPEED DIESEL ENGINES

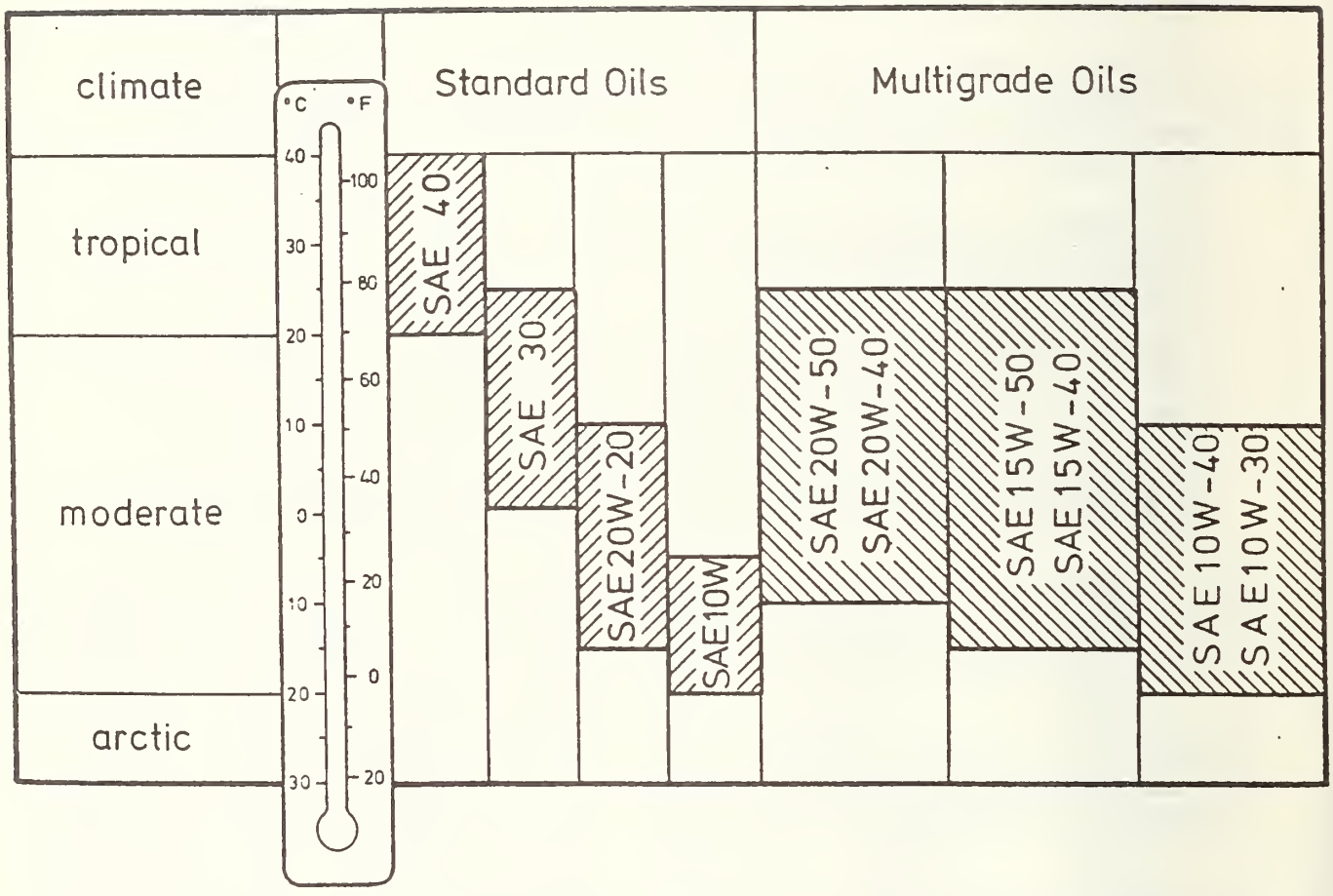

FIGURE 6.3-14: VISCOSITIES RECOMMENDED FOR THE VW DIESEL ENGINE

The effect of sump temperature on internal friction levels is shown in Figure 6.3-15. This shows a 5% reduction in internal friction levels at maximum speed by increasing the sump temperature from 60^{o} to 110^{o}C.

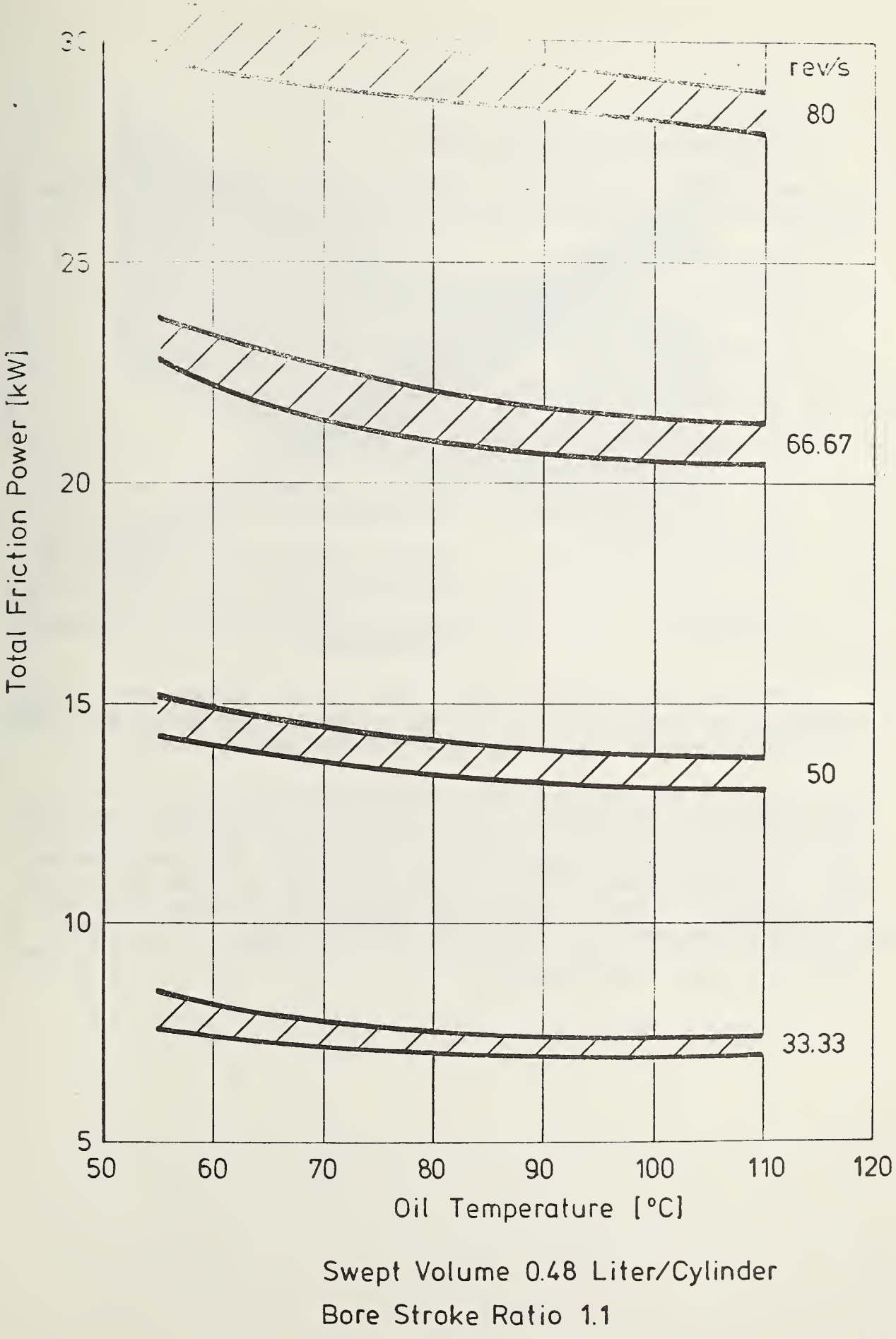

FIGURE 6.3-15: EFFECT OF OIL TEMPERATURE ON MOTORING FRICTION OF FIVE SIMILAR COMET V_B FOUR-CYLINDER ENGINES

6.3.2 Performance and Driveability

The following factors are the basis for the evaluation of the driveability of the various engine/vehicle systems:

- Acceleration capability
- Passing maneuver time
- Gradeability
- Top speed

The following definitions apply:

- Acceleration capability	Minimum time required for vehicle acceleration from 0 to 60 mph
- Passing maneuver time	Minimum time required for vehicle acceleration from 30 to 70 mph
- Gradeability	Maximum grade the vehicle can climb at constant velocity in first gear.

Performance sensitivity to engine power, vehicle weight, and different drivetrains was computed with the aid of the steady-state engine maps. Real-life vehicle hardware test results agreed with the computed data.

Table 5 in the Appendix shows the computed results for acceleration, passing maneuver, gradeability, and top speed for 12 different drivetrains in the various engine/vehicle systems. Figure 6.3-16 shows the acceleration times for the 70-HP turbocharged engine in vehicles in the inertia-weight class from 2,250 through 3,000 lbs. The graph also shows the fuel economy data that were achieved with the various transmission configurations and illustrates the significant effects of the transmission on fuel economy. It is obvious that fuel economy data comparisons may be made only for the same performance and driveability levels.

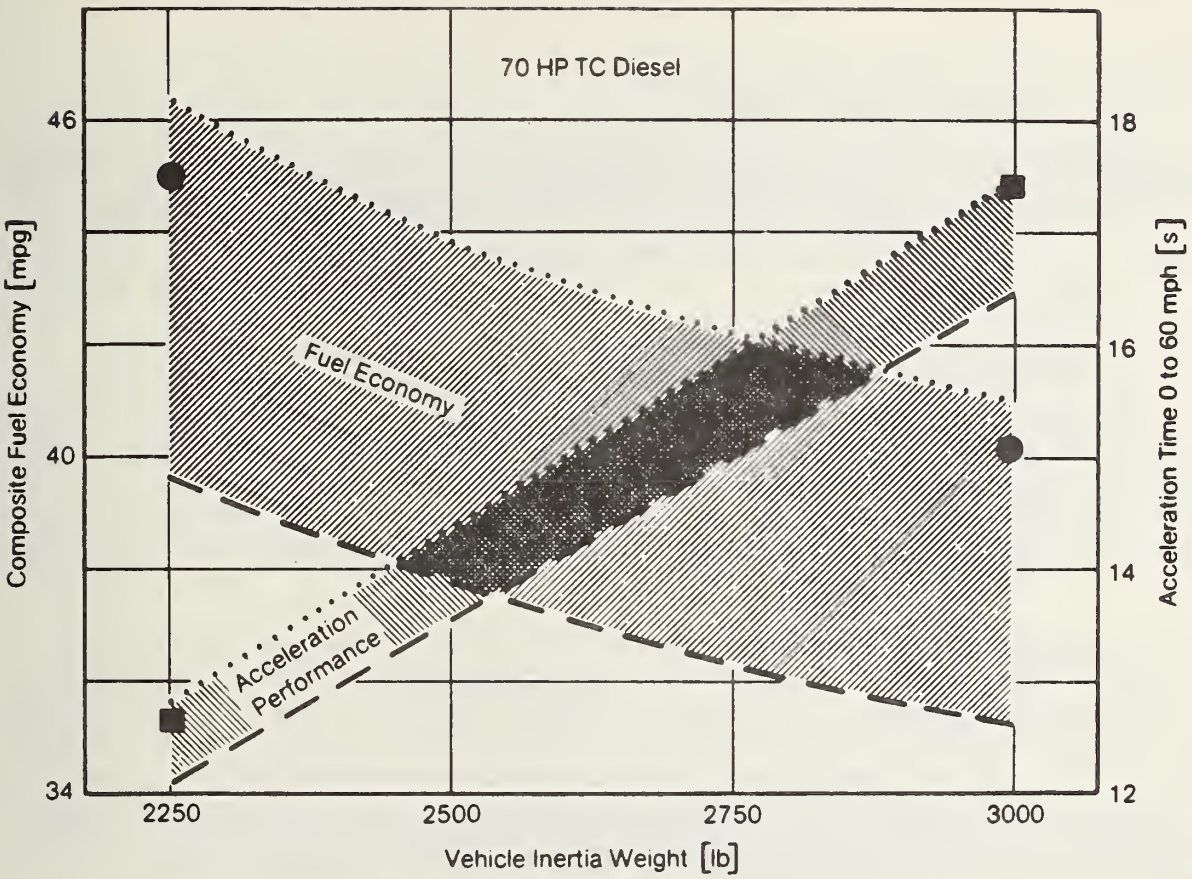

FIGURE 6.3-16: FUEL ECONOMY AND ACCELERATION PERFORMANCE AS A FUNCTION OF DRIVETRAIN RATIO AND WEIGHT.

70-HP Turbocharged Research Diesel w. Manual Transmission.
— — Limit for max. performance, top speed 75 mph, n/v = 66 rpm/mph
···· Limit for opt. fuel economy, acceptable performance, n/v = 38 rpm/mph
● Fuel economy for recommended n/v = 50 rpm/mph
■ Acceleration performance for recommended n/v = 50 rpm/mph

The figures may vary by ± 2 mpg and ± .5 sec.

6.3.3 High-Altitude Testing

The following engine and vehicle behavioral characteristics are affected by decreasing air density and increasing altitudes above sea level:

- Power output
- Startability
- Engine cooling — Decrease
- NO_x emission
- Air resistance
- CO emission
- Smoke visibility — Increase

Table 6.3-9 shows the atmospheric pressures for given altitudes. It should be noted that the pressure variations caused by meteorological conditions are comparatively minor.

Altitude		Pressure	Density	Relative Density
m	ft	Torr	g/l	
0	0	760	1.226	1.00
1,000	3,281	674	1.112	.91
2,000	6,562	596	1.007	.82
3,000	9,843	523	.910	.74
4,000	13,133	462	.819	.67
5,000	16,404	405	.736	.60

TABLE 6.3-9: VARIATION OF ATMOSPHERIC PRESSURE AND AIR DENSITY IN PROPORTION TO ALTITUDE ABOVE SEA LEVEL.

The reduced air density at high altitudes decreases the power output of a diesel engine for a given smoke level in comparison to operation at sea level. Even if the fuel injection rate remains unchanged from sea level conditions, the diesel engine power output will decrease while the smoke level will increase. The effects of altitude reduce the maximum power output by roughly 9% per 1,000 meters. Power at maximum torque speed is reduced by approximately 13% per 1,000 meters. The maximum power drop in a swirl-chamber diesel engine is in the neighborhood of 5% per 1,000 meters with a noticeable increase in smoke level.

Diesel engine performance is less severely affected by high altitudes than carbureted gasoline engine performance because of the fairly large amount of excess air available for diesel engines during partial-load operation. Carburetors in gasoline engines shift the air-to-fuel ratio to the rich side. The roughly 20% loss in power output in diesel engines at an altitude of 2,100 meters is markedly lower than the 33% power loss of the gasoline engine.

Diesel engine power and torque output during full-load operation decrease in direct proportion to the decrease of atmospheric density at higher altitudes when the engines are operated at a constant smoke level. Engine operation at constant smoke level requires an atmospheric-pressure-correcting device. Diesel engines without a correcting device are operated at constant fuel injection rates. Diesel engine operation at misfire conditions and very high smoke levels results in a significant increase in HC and particulate emissions.

The power loss does not affect vehicle maximum velocity because of the reduction of drag which decreases in direct proportion to the decrease in air density. It will, however, affect gradeability. The vehicle maximum velocity is proportional to the cubic root of the engine maximum power output. The 0-t-60 mph acceleration time T_{60}, passing-maneuver time T_{37} (30 to 70 mph) and maximum gradeability are in direct proportion to the engine power output. Table 6.3-10 shows the performance data computed from the full-load power curves in Fig. 6.3-16, and the assumed gear-axle combination No. 3 (see Appendix).

Vehicle Inertia Weight	Top Speed	Accelerat. 0 → 60 mph	Accelerat. 30 → 70 mph	Grade-ability	Code
lb	mph	s	s	%	
1,750	86	14.9	18.4	41	1
	85	17.6	21.5	38	2
	82	19.3	24.9	35	3
2,000	85	17.1	21.6	40	1
	84	20.3	25.5	33	2
	81	22.4	29.8	30	3
2,250	84	19.6	25.2	34	1
	83	23.2	29.8	28	2
	80	25.6	35.3	26	3
2,500	83	22.0	29.1	30	1
	82	26.3	34.6	25	2
	80	29.0	41.5	23	3

Code: 4 - Sea Level; 2 - 2,000 m, const. fuel level;
3 - 2,000 m, const. smoke level.

TABLE 6.3-10: PERFORMANCE DATA FOR THE OPERATION OF AN ENGINE/VEHICLE SYSTEM AT SEA LEVEL AND AT 2,000 m ABOVE SEA LEVEL.

Table 6.3-11 shows the results of fuel-economy and regulated emission tests in the European Alps at an altitude of 1,628 m (see Figures 6.3-17 and 6.3-18). The results of the warm test were produced by substituting the cold-phase bag data with the data of the last phase.

Fuel economy data did not vary significantly except for a 10% drop in fuel economy in EGR-equipped engines. This illustrates the lower amount of excess air in engines with EGR. The engine thus operates closer to the smoke limit as indicated by the Bosch number.

The exhaust gas emissions show the following typical variations:

- HC emissions keep constant up to an altitude of 1,600 m
- CO emissions rise by 50%
- NO_X emissions drop by 25%.

VW Rabbit, 50 HP, 90 CID, N.A.						
Inertia Weight lb	Road Load HP	Fuel City mpg	HC g/m	CO g/m	NO_x g/m	Remarks
2,250	7.3	38.8	.26	1.26	.96	cold
		40.2	.25	1.19	.95	warm
		37.3	.29	1.33	.99	cold
		38.4	.27	1.33	.98	warm
		37.1	.25	.90	1.15	sea level, cold
VW Rabbit, 50 HP, 90 CID, N.A., EGR						
		38.5	.38	3.29	.31	cold
		40.3	.35	3.24	.48	warm
		43.4	.36	1.56	.48	sea level, cold

VW Rabbit, 70 HP, 90 CID, TC						
2,250	7.3	41.1 42.3 43.7	.18 .16 .14	.97 .86 .71	.78 .79 .96	cold warm sea level, cold
Audi 100, 68 HP, 130 CID, N.A.						
3,000	10.4	27.9 28.8 28.1 28.6 27.6	.48 .44 .49 .47 .35	2.02 1.98 2.28 2.35 1.82	1.24 1.24 1.20 1.20 1.80	cold warm cold warm sea level, cold

TABLE 6.3-11: FUEL ECONOMY AND REGULATED EMISSION TEST RESULTS MEASURED AT 1,628 m ABOVE SEA LEVEL.

The sea-level data is included for comparison.

Constant fuel injection rate operation increases smoke visibility in direct proportion to the increase in altitude. The increase of smoke visibility is determined by the initial injection pump setting.

Smoke measurements were performed on the driveability-test diesel vehicles at two altitudes:

- Low altitude of 750 m (Zell am See, Austria)
- High altitude of 2,300 m (Großglockner Mountain Road, Austria)

The maximum smoke number of all vehicles was set at a Bosch number of 2.5 in the low altitude tests at 3/4 load. The vehicles were not equipped with altitude correcting devices. The gradient of the test track portion of the Großglockner Mountain Road was selected in order to provide for full load operation in 2nd gear. Table 6.3-12 shows the results of the smoke measurements at three given engine speeds.

	1,500 rpm	3,000 rpm	Top Speed
Rabbit, 4 Cyl., N.A.	5.1	5.0	5.2
Rabbit, 4 Cyl., TC Prototype	5.3	3.4	3.6
Rabbit, 4 Cyl., N.A. Prototype EGR	6.5	8.0	8.8
Audi 5000, 5 Cyl., N.A. Prototype	7.0	6.3	5.4
Opel Rekord D	6.9	6.2	8.7
Peugeot 504 D	9.3	7.7	8.5

TABLE 6.3-12: FULL-LOAD BOSCH NUMBERS FOR VARIOUS DIESEL-ENGINE VEHICLES AT AN ALTITUDE OF 2,300 m.

The figures in this table illustrate the steep increase in the smoke number of all vehicles as the altitude rises. The smoke numbers at an engine speed of 3,000 rpm are somewhat lower depending on the curve of the air-fuel ratio. The modulated EGR causes a marked decrease of the air-fuel ratio at engine speeds of 1,500 and 3,000 rpm and thus produces a steep increase of the Bosch number. Engine misfire was observed. The turbocharger significantly improves the air-fuel ratio at higher engine speeds and thus lowers the smoke numbers, except for the 1,500-rpm operating point where the charge pressure is insufficient. The turbocharger thus operates as an altitude correcting system. The injection pumps of the prototype vehicles were not yet optimized in the lower engine speed range. The combustion processes of the two non-VW vehicles were tuned closer to the smoke limit.

Figure 6.3-19 shows the effects of different cetane numbers on misfire tendencies at different altitudes.

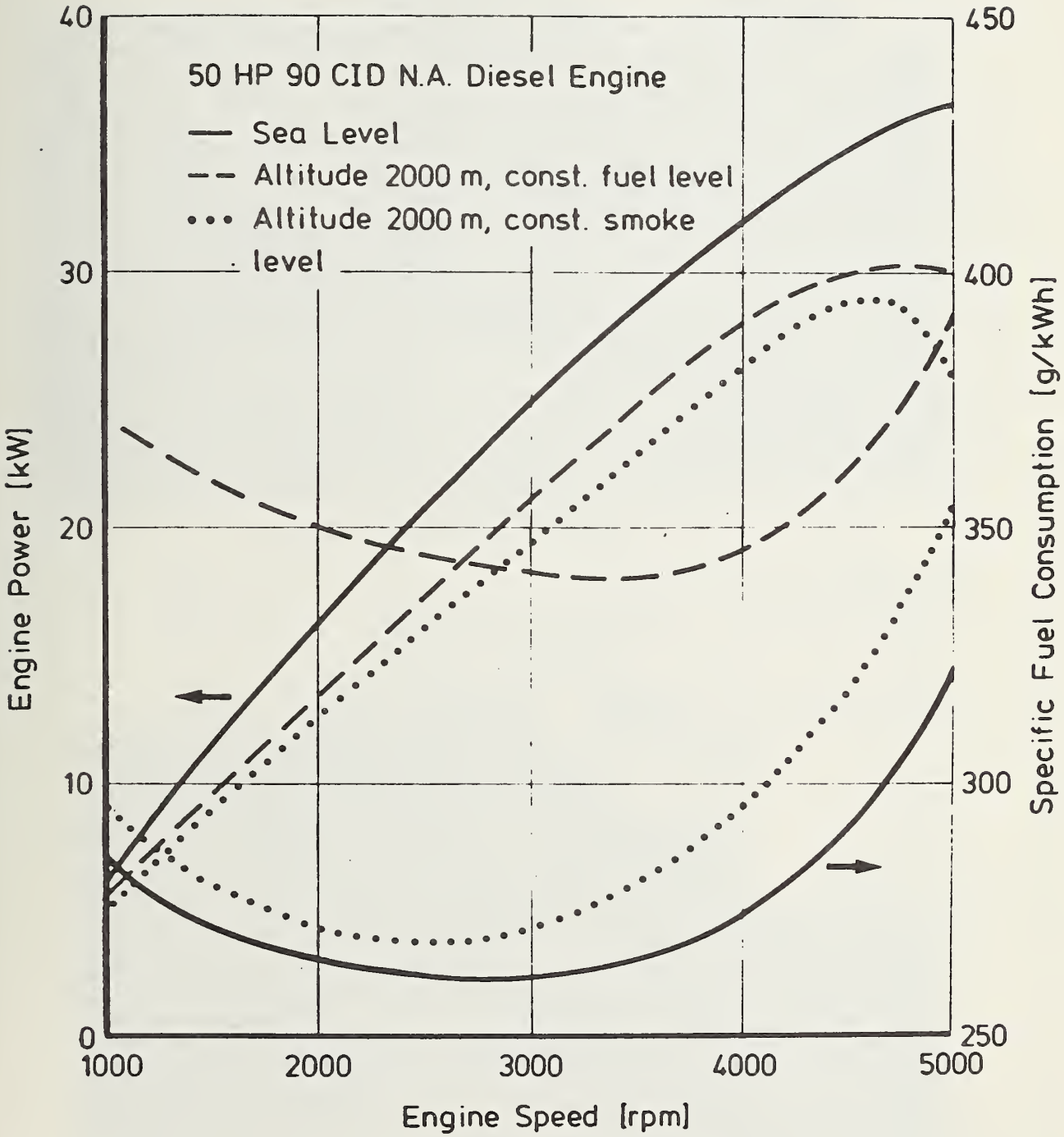

FIGURE 6.3-16: FULL-LOAD POWER AND SPECIFIC FUEL CONSUMPTION OF A 50 HP NATURALLY-ASPIRATED DIESEL ENGINE AT SEA LEVEL AND AT AN ALTITUDE OF 2000 M.

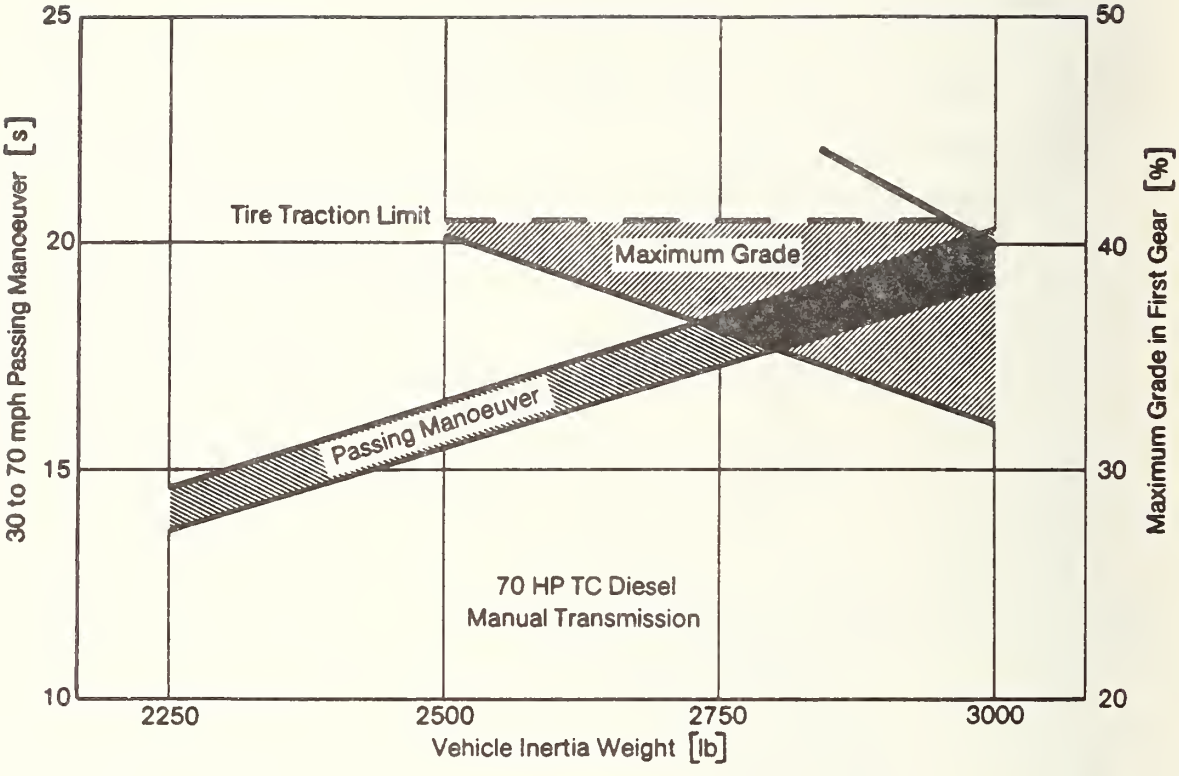

Figure 6.3-17: TIME RANGE FOR A 30 TO 70 MPH PASSING MANEUVER AND MAXIMUM GRADE AS A FUNCTION OF DRIVETRAIN RATIO AND WEIGHT.

70-HP turbocharged diesel engine; manual transmission; front-wheel drive.

FIGURE 6.3-17: GROSSGLOCKNER HOCHALPENSTRASSE (MOUNTAIN ROAD)

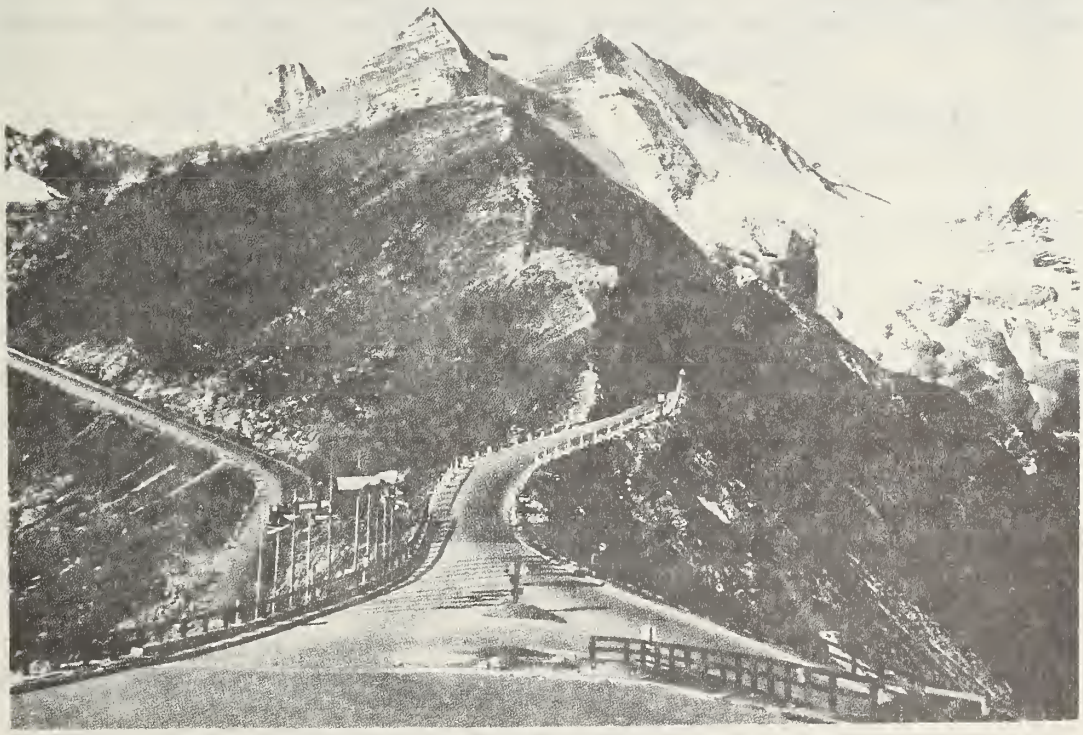

FIGURE 6.3-18: TEST TRACK FUSCHER TÖRL

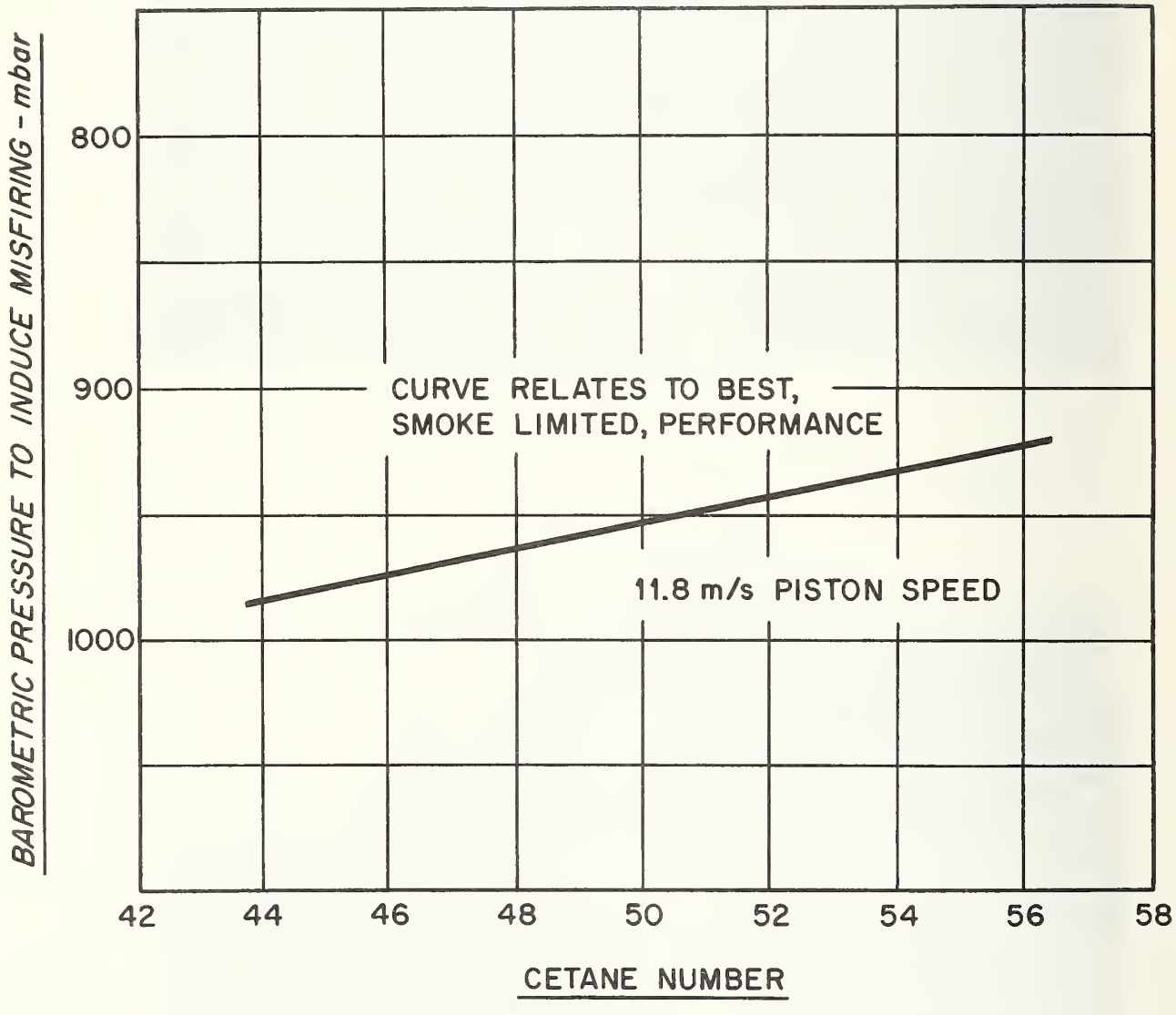

FIGURE 6.3-19: THE EFFECTS OF CETANE NUMBERS ON MISFIRE TENDENCIES AT LOW BAROMETRIC PRESSURES

6.3.4 Durability and Maintenance

Analyses were performed of the results of extensive durability and other Volkswagen tests that had been run prior to this Contract (300 vehicles equipped with the 50-HP, 4-cylinder N.A. diesel engine in '77 VW Rabbits and Dashers). The results of the analyses show that diesel engines are more durable than spark-ignition engines. Volkswagen had also run dynamometer endurance tests at full-load engine operation for 83% of the total test time. The results of these tests showed that the service life of the 4-cylinder N.A. diesel engine could be double that of a comparable spark-ignition engine.

An analysis was made of the EPA durability test results from the above fleet in order to determine the exhaust gas emission behavior as a function of service life. Fuel economy and emissions of the naturally-aspirated diesel engines were found to be comparatively stable over 50,000 miles.

With these findings in mind, commercially available U.S. diesel fuels are not expected to cause engine trouble. Tests were performed in cooperation with oil companies on seven different diesel fuel grades that differed in cetane numbers (47 - 53.5), aromatics content (17 - 28.4 % wt), CFPP (0° to -23°C), and end point FBP (319 to > 400°C). It was found that satisfactory cold-start behavior can be ensured with a multigrade lubricant based on SAE W 15 oil. The same lubricant can be used in diesel and spark-ignition engines. Because of the low degree of engine-oil contamination, 7,500-km oil change and 15,000-km filter change intervals were established. The same intervals are specified for VW spark ignition engines.

Analyses of oil viscosity changes as a function of mileage show only minor changes because of little soot formation.

The maintenance requirements for VW diesel engines differ from those for other diesel engines. They are less demanding because of the small volume of soot deposited in the lubricant.

The toothed-belt drive design in the VW diesel engines further facilitates economical maintenance because the belt is not elastic and does not require any lubrication.

Some design modifications may be required for mass-produced turbo-charged diesel engines in regard to pistons, piston pins, cooling system and lubricants, because of the higher operating temperatures and peak pressures.

6.3.5 Initial Cost

The diesel engine is more expensive than a gasoline engine of comparable output, even if the higher weight of the diesel unit can be kept down by light-weight construction. The higher cost is caused by the lower power output per liter of displacement of the diesel engine and by the more complex engineering efforts (e.g. to the injection system). The price difference is reduced substantially, though, when the additional exhaust gas treatment systems are taken into consideration that are required by gasoline engines, e.g. catalysts and sophisticated air/fuel mixture formation devices. The extra price for the Rabbit diesel compared with the gasoline-engine Rabbit is only $300. It should be borne in mind, though, that the gasoline-engine powered Rabbit has a higher power output.

The diesel Rabbit engine does not have the following components of the gasoline-powered Rabbit engine:

- Air/fuel mixture device
- Ignition and spark plugs
- Exhaust gas treatment systems, such as catalysts and secondary-air pump, and exhaust-gas recirculation

The following components must be added for the diesel engine:

- Diesel fuel injection pump with injection nozzles
- Preheating system
- Vacuum pump (possible0
- Stronger starter

The following components may require modifications for diesel operation:

- Cylinder head (to be modified for swirl-chamber inserts)
- Crankcase
- Crankshaft and pistons
- Belt drive
- Complex intake system design
  (The intake system of a gasoline engine with fuel injection is similarly complex.)

The diesel engine requires a stronger battery and, in some instances, a modified engine suspension and noise damping.

The linear rise of the acceleration time along with the vehicle inertia weight shows that rolling resistance and drag are negligible for acceleration from low vehicle velocities.

Figure 6.3-17 shows the passing maneuver time and gradeability for vehicles in the inertia weight class from 2,250 to 3,000 lbs with turbocharged engine. Gradeability is limited by tire traction which may amount to between 41 and 45%, depending on the type of drive (front or rear wheel drive).

Driveability cannot be determined by objective measurements. Subjective driver judgement of the following characteristics was taken into account:

- Startability (number of successful cold starts vs. total number of starts)
- Idle quality (smoothness of engine running)
- Noise
- Surge (short, abrupt power fluctuations at any speed or load)
- Hesitation (temporary lack of engine response to accelerator actuation)
- Pick-up performance
- Acceleration jolt

Each vehicle was tested by a panel of expert drivers who awarded merit points to each of the above-mentioned characteristics. Scores ranged from 0 to 10 merit points. A minimum of five points was required for customer acceptance. The test schedule included a cold-start,full-load pick-up, cruise, and deceleration. The same driving cycle is used to determine the warm driveability characteristics.

The driveability tests were performed in the Alps at an altitude of 2,200 m (7,200 ft) at a temperature of approximately $0^{o}C$.

The subjective driveability profile is formed by the average of the merit points plotted in the order of operating modes. The subjective driveability profiles lend themselves for comparisons between various engine/vehicle systems. The results are shown in Table 6.3-7.

Figure 6.3-18 is a comparison of driveability profiles of a diesel and gasoline engine of the same output. The cold start behavior of the diesel engine is more acceptable, except for its idle noise. No difference was found in the warm-up and warm-running phases.

Figure 6.3-19 is a comparison between the driveability profiles of a turbocharged 70-HP diesel engine and a 78-HP gasoline engine which meets the U.S. emission standards of '77. The startability of this diesel

has room for improvement. The noise level of the gasoline engine was found to be lower. In other areas, the diesel engine driveability profile was found to be equal to that of the reference gasoline engine. The results of the comparisons are in favor of the diesel engine because of its better idling quality.

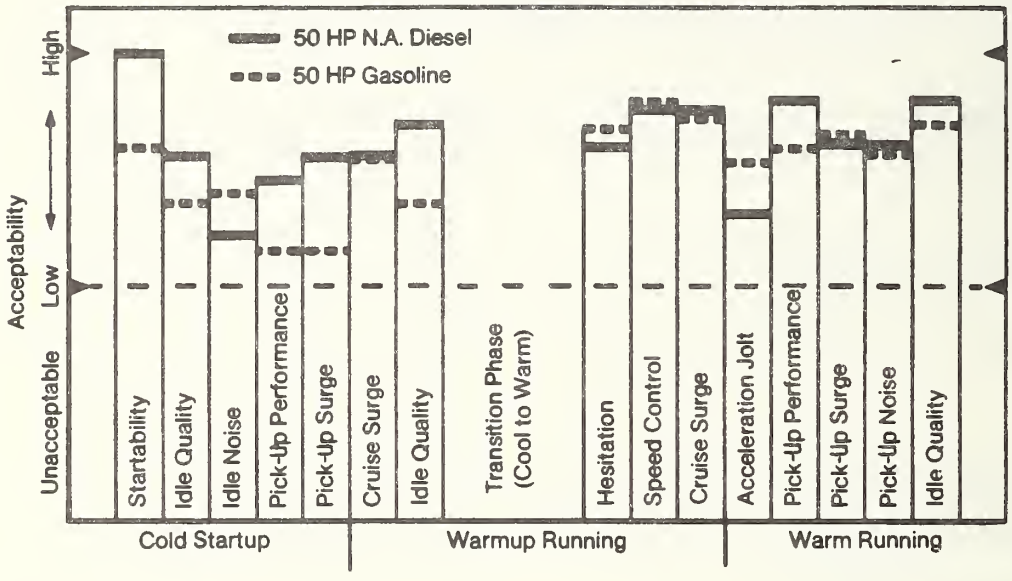

FIGURE 6.3-18: SUBJECTIVE DRIVEABILITY PROFILE
50-HP diesel and 50-HP gasoline Rabbit with carburetor, not sold in the U.S.

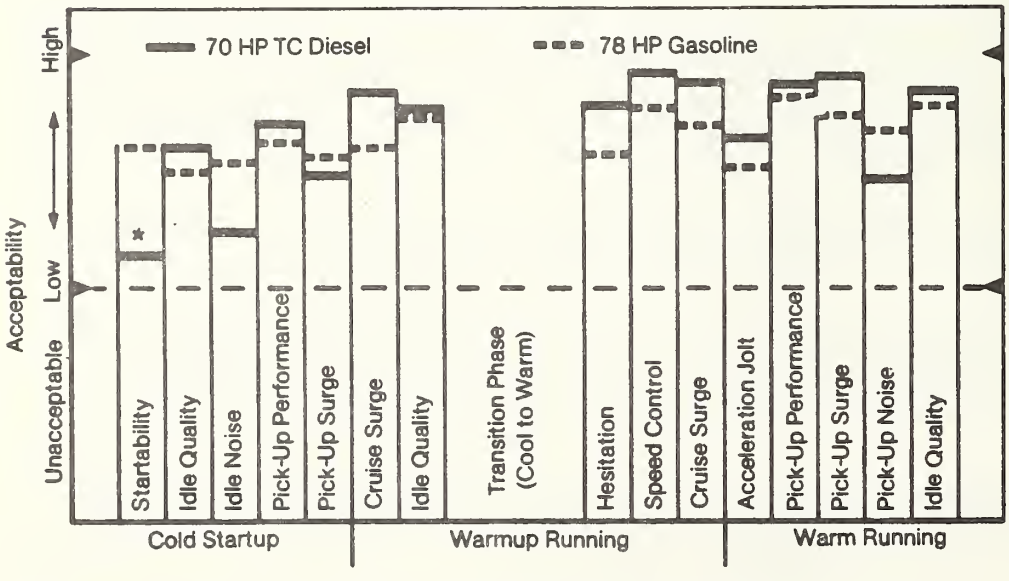

Rabbit

FIGURE 6.3-19: SUBJECTIVE DRIVEABILITY PROFILE
*TC diesel, May, '77
70-HP turbocharged diesel and 78-HP gasoline Rabbit.

Figure 6.3-20 shows the deterioration of a driveability profile by EGR which is applied in order to meet stringent emission standards. While startability may be improved, severe problems continue to be posed by surge and pick-up performance.

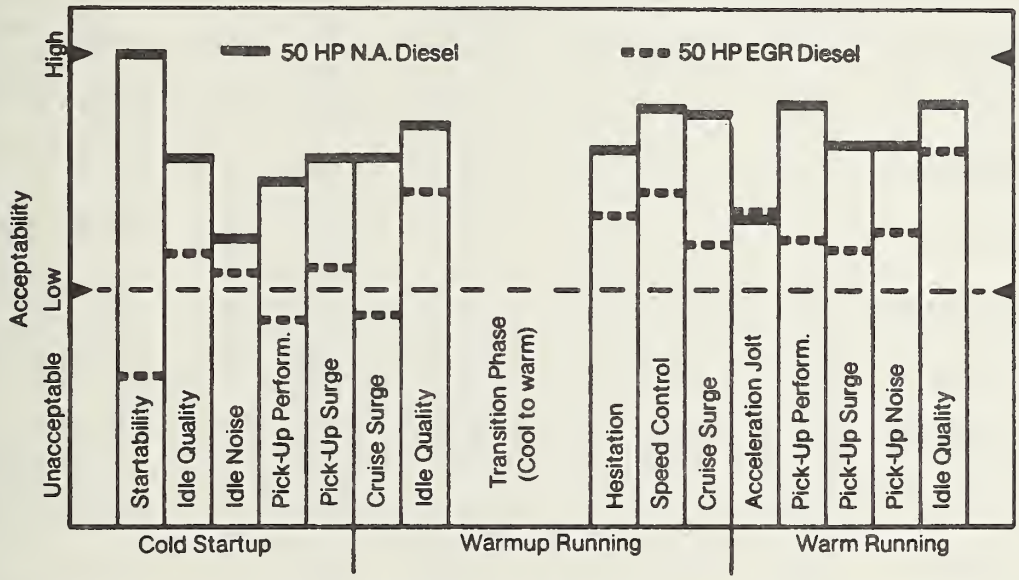

FIGURE 6.3-20: SUBJECTIVE DRIVEABILITY PROFILE
Comparison of a Rabbit with 50-HP diesel production engine and a Rabbit with the same engine, equipped with a research EGR device.

A second approach was used in addition to the mere subjective assessment. Engine speed, torque and oil temperature with accelerator travel and vehicle velocity data was recorded and compared with the driveability test results. A highly skilled and experienced test driver evaluated the recorded speed torque patterns of the same vehicles on the same test track. The results are shown in Table 6.3-8. These results essentially agree with the data in Table 6.3-7. Some behavioral characteristics are assessed differently, e.g. hesitation of the 50-HP N.A. engine with EGR.

	50-HP N.A.	50-HP EGR	50-HP Gasol.	68-HP 5-Cyl.	70-HP TC	78-HP Gasol.	Opel	Peugeout
Startability	10.0	3.2	8.0	3.0	5.7	8.0	4.4	10.0
Idle Quality	7.8	5.8	6.8	4.9	8.0	7.5	6.6	6.6
Idle Noise	6.1	5.4	7.0	5.9	6.2	7.7	6.3	5.6
Pick-up Perf.	7.3	4.4	5.8	6.7	8.5	8.1	6.8	6.7
Pick-up Surge	7.8	5.5	5.8	6.3	7.4	7.8	8.7	7.8
Cruise Surge	7.8	4.5	7.8	7.8	9.2	8.0	8.6	8.1
Idle Quality	8.5	7.1	6.8	8.4	8.9	8.7	8.5	8.8
Hesitation	8.0	6.6	8.4	7.8	8.9	7.9	8.4	7.1
Speed Control	8.9	7.1	9.0	8.2	9.6	8.9	8.9	7.4
Cruise Surge	8.8	6.0	8.7	8.9	9.4	8.5	8.6	8.1
Accel. Jolt	6.6	6.7	7.7	5.3	8.2	7.6	6.2	6.4
Pick-up Perf.	9.0	6.1	8.0	9.1	9.4	9.1	8.1	7.2
Pick-up Surge	8.1	5.9	8.3	7.6	9.5	8.7	8.9	7.5
Pick-up Noise	8.1	6.3	7.9	7.1	7.3	8.4	7.2	7.4
Idle Quality	9.0	8.0	8.5	8.7	9.2	8.9	9.2	9.2

TABLE 6.3-7: SUBJECTIVE DRIVEABILITY PROFILES. AVERAGE OF MERIT POINTS AWARDED BY A PANEL OF NINE TRAINED DRIVERS.

	50-HP N.A. Diesel	50-HP EGR Diesel	50-HP Gasoline	68-HP 5-Cyl. Diesel	70-HP TC Diesel	78-HP Gasoline
Startability	10	10	10	3	10	9
Idle Quality	10	3	8	3	8	7
Pick-up Perf.	7	4	3	7	9	8
Pick-up Surge	4	4	3	7	7	8
Cruise Surge	8	3	9	8	8	8
Idle Quality	10	10	9	8	10	9
Hesitation	10	1	7	10	8	8
Speed Control	10	6	10	10	10	10
Cruise Surge	8	5	10	10	10	8
Accel. Jolt	8	4	6	4	8	8
Pick-up Perf.	10	8	10	10	10	10
Pick-up Surge	8	8	8	7	9	8
Idle Quality	10	10	9	9	10	9

TABKE 6.3-8: DRIVEABILITY MERIT POINTS FROM RECORDS OF ENGINE SPEED AND TORQUE, AND VEHICLE VELOCITY.

7. EVALUATION OF THE RELATIVE MERITS OF INSTALLING DIESEL ENGINES IN FRONT-, MID-, AND REAR-ENGINE CONFIGURATIONS WITH A SPECIAL VIEW TO THREE SAFETY LEVELS

A large number of different parameters must be assessed to determine the advantages and disadvantages of various engine/vehicle configurations. These parameters define the vehicle body, drive train, occupant comfort, noise, handling, accident avoidance, crashworthiness, etc. The funds and time available for this program, though, did not permit a comprehensive evaluation of this magnitude.

Therefore, efforts were restricted to the investigation of some essential parameters, such as vehicle length, wheelbase, vehicle weight, axle-load distribution, location of center of gravity, and luggage space. In compliance with the overall contractual stipulations, the installation study was performed for engines in the rated power output range from 50 to 100 HP for vehicles in the inertia-weight class from 2,250 through 3,000 lbs. and for the safety levels of 30, 40, and 45 mph against a frontal fixed barrier. All presently valid FVMSS were to be complied with.

7.1 APPROACH

Methods of computer-aided design presented themselves as suitable for application in this study. However, there are no computer programs at this time that can cover the entire complexity of the problems posed by the combination of various engine/vehicle configurations and safety levels. Therefore, we decided to prepare preliminary draft designs for the various concepts. On the basis of these designs, assessments were made of the advantages and disadvantages of the individual concepts.

7.1.1 Baseline Definition

The objective of our efforts was to determine the relative merits of the individual configurations. Therefore, a common baseline was to be defined first to provide for comparability of the results.

The vehicles selected for the study had to have similar characteristics in regard to

- Powerplant/drivetrain concept

- Design configuration

- Energy management concepts.

The baseline vehicles selected were three vehicle types which met the above criteria. All of them had self-supporting bodies, front-wheel drive, and similar energy management concepts:

- VW Rabbit (2,250 lbs. IW, Figure 7.1-1)

- VW Dasher (2,500 lbs. IW, Figure 7.1-2)

- Audi 100 (3,000 lbs IW, Figure 7.1-3)

7.1.2 Roominess Fixed and Variable

Two approaches were used to determine the effects of the various engine/vehicle configurations and safety levels. The one approach provided for constant interior dimensions of the baseline vehicles and the determination of the effects of the various engine/vehicle configurations and safety levels on the exterior dimensions. The other approach provided for constant exterior vehicle dimensions and the determination of the effects on the interior dimensions. Vehicle weight, axle-load distribution, wheelbase, location of center of gravity, luggage space, etc., were determined at the same time.

7.1.3 Engine/Drivetrain/Vehicle Configuration

Investigations were conducted on six engine/drivetrain/vehicle configurations (see Figure 7.1-4):

- Front engine, longitudinal, front-wheel drive (Conceptual Design I)

- Front engine, transverse, front-wheel drive (Conceptual Design II)

- Front engine, longitudinal, rear-wheel drive (Conceptual Design III)

- Mid-engine, transverse, rear-wheel drive (Conceptual Design IV)

- Rear engine, transverse, rear-wheel drive (Conceptual Design V)

- Rear engine, longitudinal, rear-wheel drive (Conceptual Design VI)

The analysis was based on the following five production, pre-production and research diesel engines:

- 4-cylinder, in-line, NA, 50 HP

- 4-cylinder, in-line, TC, 70 HP

- 5-cylinder, in-line, NA, 68 HP

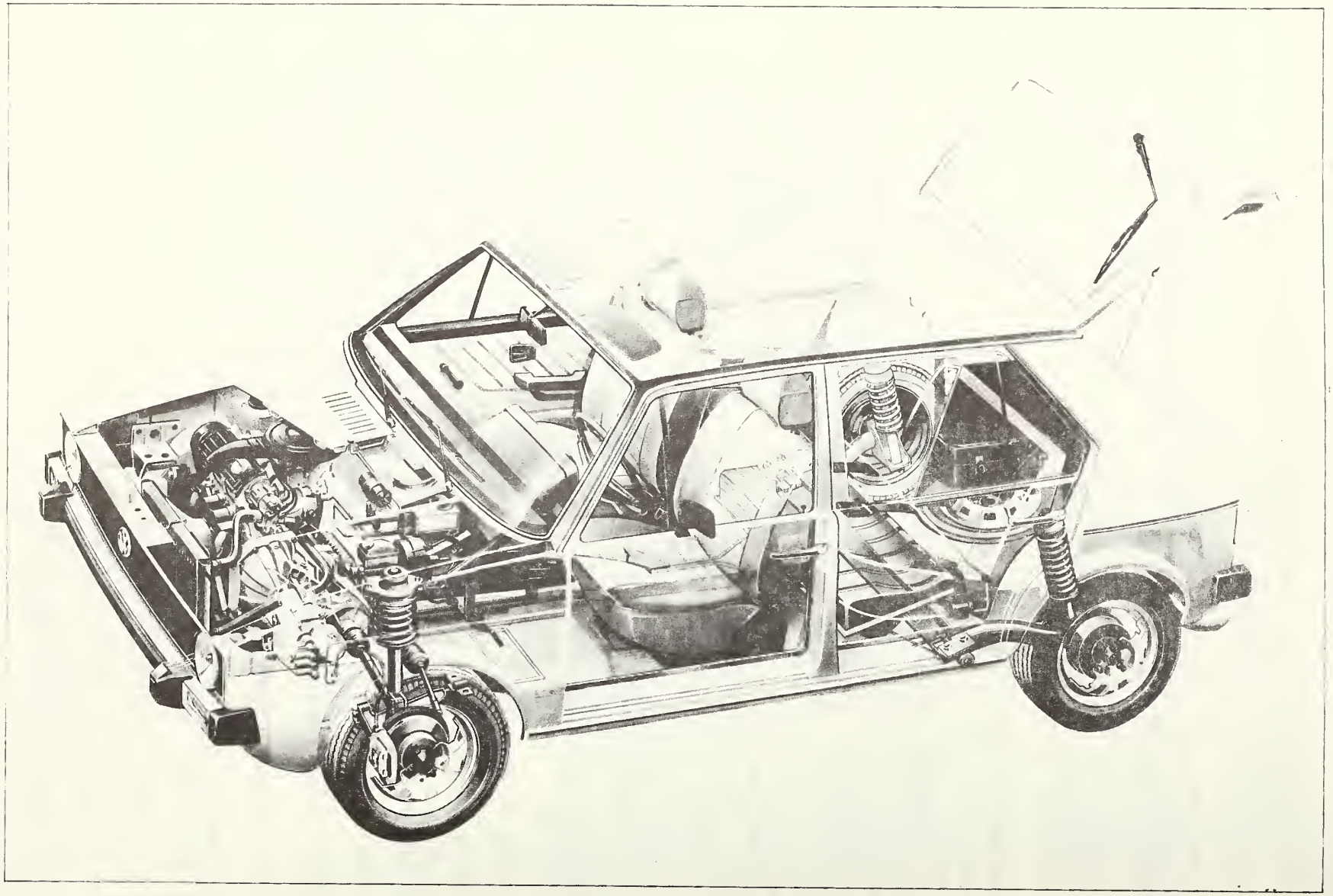

FIGURE 7.1-1: VW GOLF (RABBIT)

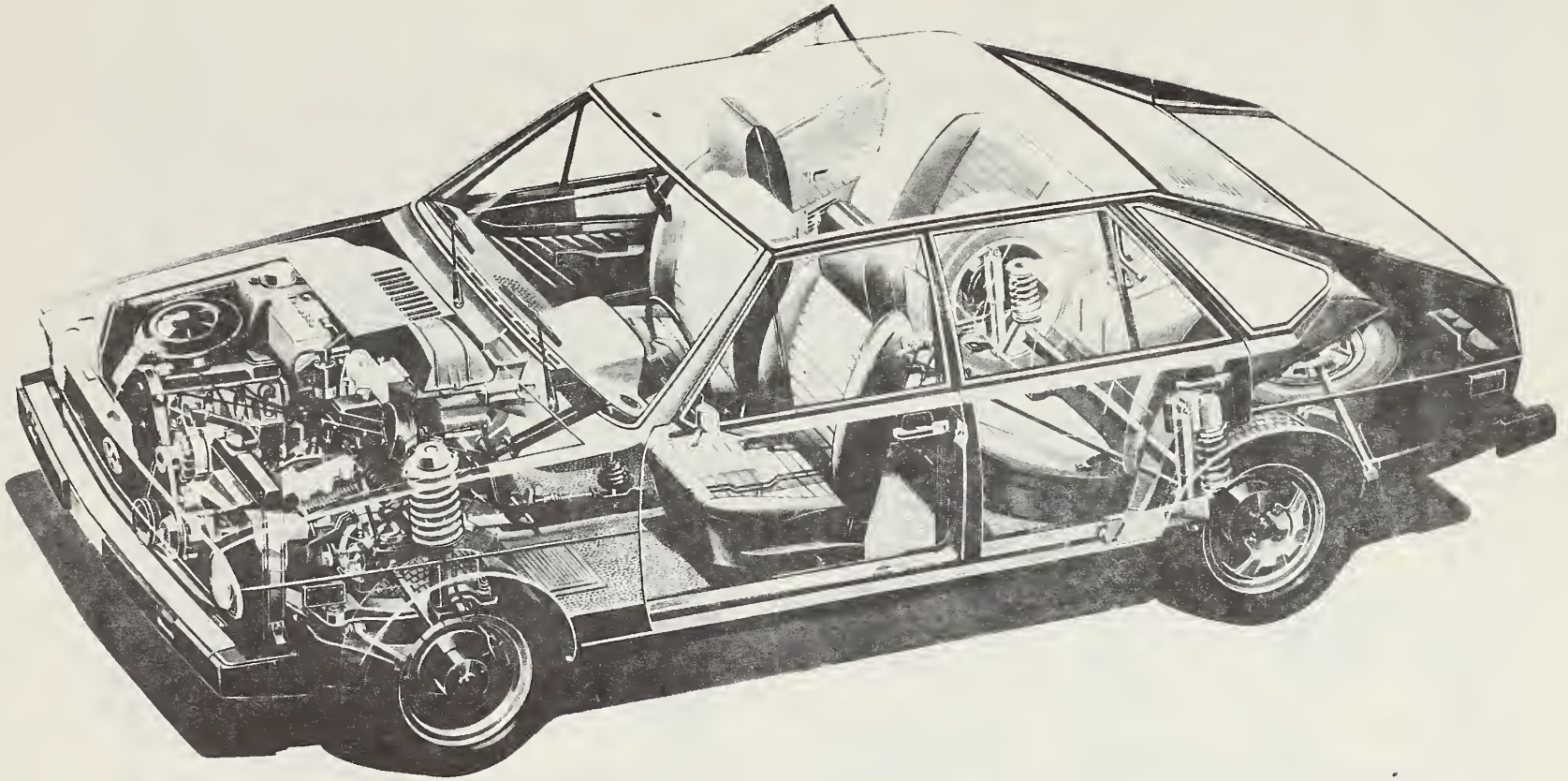

FIGURE 7.1-2: VW DASHER

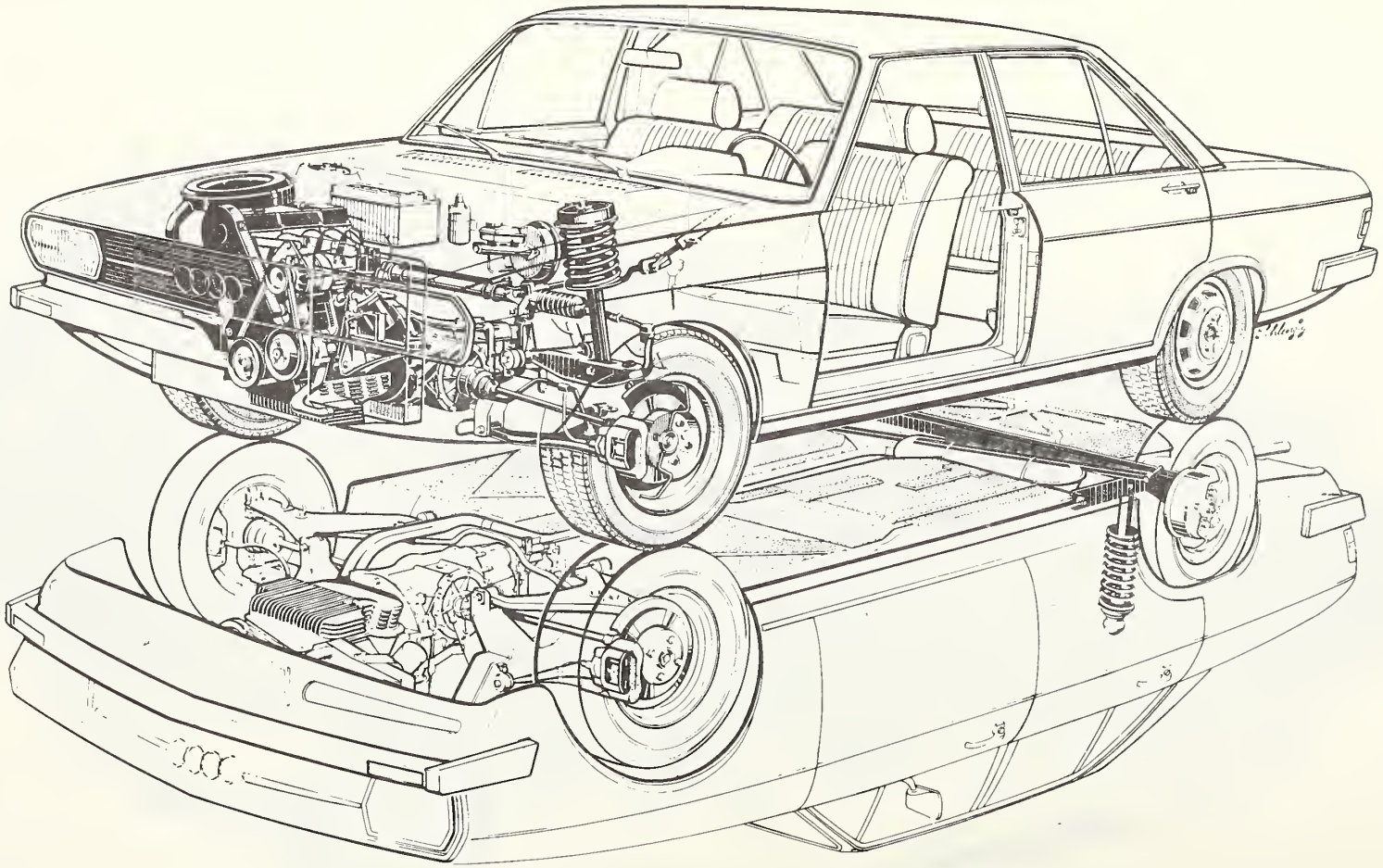

FIGURE 7.1-3: AUDI 100

- 6-cylinder, in-line, NA, 75 HP

- 8-cylinder, V, NA, 100 HP

Only useful engine/vehicle configurations for each of the three vehicle types were investigated for a power-to-weight ratio in the range of .022 through .031 HP/lb. These configurations are shown in Figure 7.1-4.

7.1.4 Safety Considerations

The effects were to be investigated for frontal-impact specifications of 30, 40, and 45 mph impact velocities against a frontal-fixed barrier. Consideration was to be given to compliance with the criteria established in FMVSS 208. The safety effects essentially are reflected in changes to the longitudinal dimensions and to the vehicle weight. An essential factor is the crash distance required for the individual safety levels (see Figure 7.1-4). This distance is the result of a proper match between vehicle restraint system and vehicle deformation characteristics.

Crash tests have shown that in the first approximation a rectangular deformation characteristic may be assumed for the frontal structure and a mean deceleration of 25 g (Figure 7.1-5) for the vehicles in this study.

The performance of the restraint systems (Table 7.1-1) for various impact velocities and a mean deceleration level of 25 g were confirmed with the aid of sled tests. All restraint systems met the FMVSS 208 survival criteria. The space available for occupant forward displacement was not exceeded in the three vehicles.

The restraint system characteristics shown in Table 7.1-1 were used to determine the crash length required for a mean vehicle deceleration of 25 g and a rectangular deceleration curve (Figure 7.1-6). When we assume that the firewall is not to penetrate into the vehicle interior during a crash, the required crash length together with the hard engine dimensions easily permits the computation of the required front-structure length of the vehicle (Figure 7.1-4).

7.1.5 Determination of Vehicle Weight Change

To determine the vehicle weight change as a function of the various engine/drivetrain/vehicle configurations and safety levels we used a weight analysis that had been prepared for a VW 1500 (Figure 7.1-7). Table 7.1-2 shows the vehicle weight per inch for the VW 1500, VW Rabbit, VW Dasher, and the Audi 100. The weight per inch does not include the engine weight nor the weight of the electrical cables. The weight table required some adjustments for the Audi 100 because this car is not in the weight class of the VW 1500. A curb weight comparison was used to add the additional weight of the Audi 100 to the individual data in the table. Curb weight and axle load distribution were determined with the aid of summation of forces and moments.

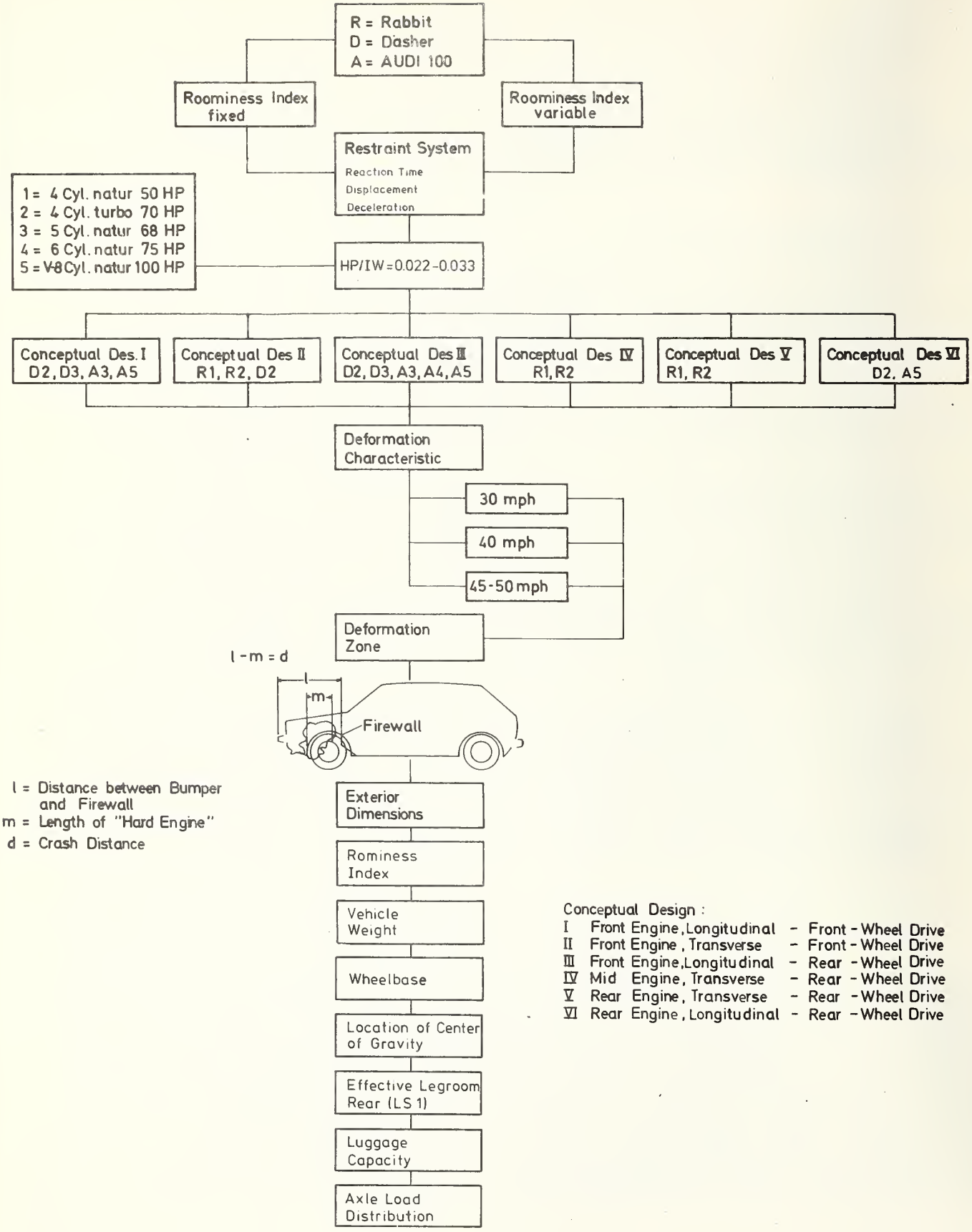

FIGURE 7.1-4: CONCEPTUAL DESIGNS STUDIED

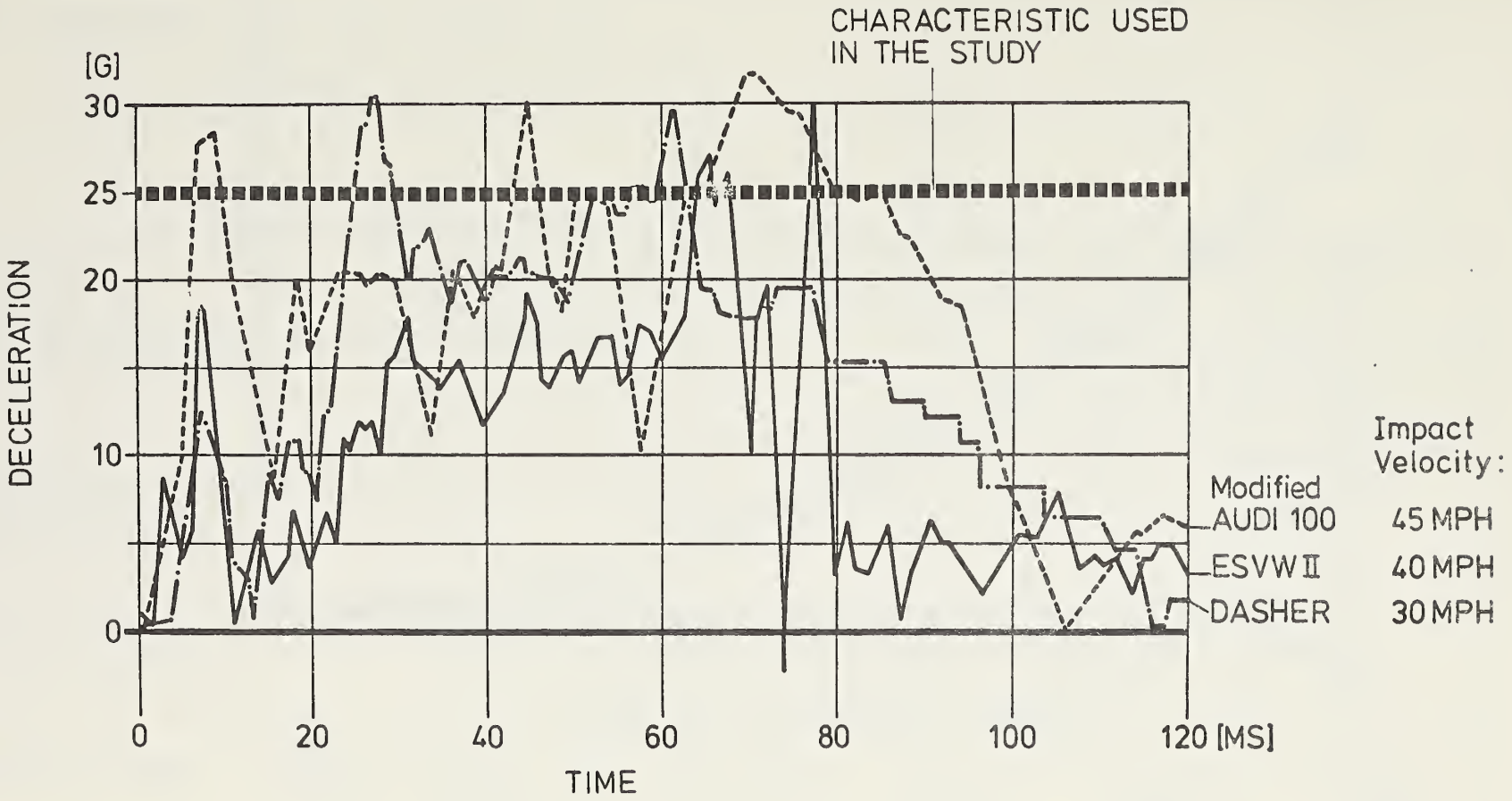

FIGURE 7.1-5: TYPICAL VEHICLE DECELERATION CHARACTERISTICS

Restraint System	Impact Velocity MPH	Average Sled Deceleration G	Forward Displacement			Head Deceleration G	HIC	Chest Deceleration G	SI	Pelvis Deceleration G
			Head cm	Chest cm	Pelvis cm					
Two-Point Shoulder Belt and Knee Bar	30	22.7	47	26	18.3	50	386	41	146	51
Two-Point Shoulder Belt and Knee Bar, Force Limiter and Preloader	40	27.1	63	34	18	61	684	41	424	43
Two-Point Shoulder Belt and Knee Bar, Force Limiter and Preloader	50	26.5	65	38	33	55	815	41	403	45

TABLE 7.1-1: RESTRAINT SYSTEM CHARACTERISTICS

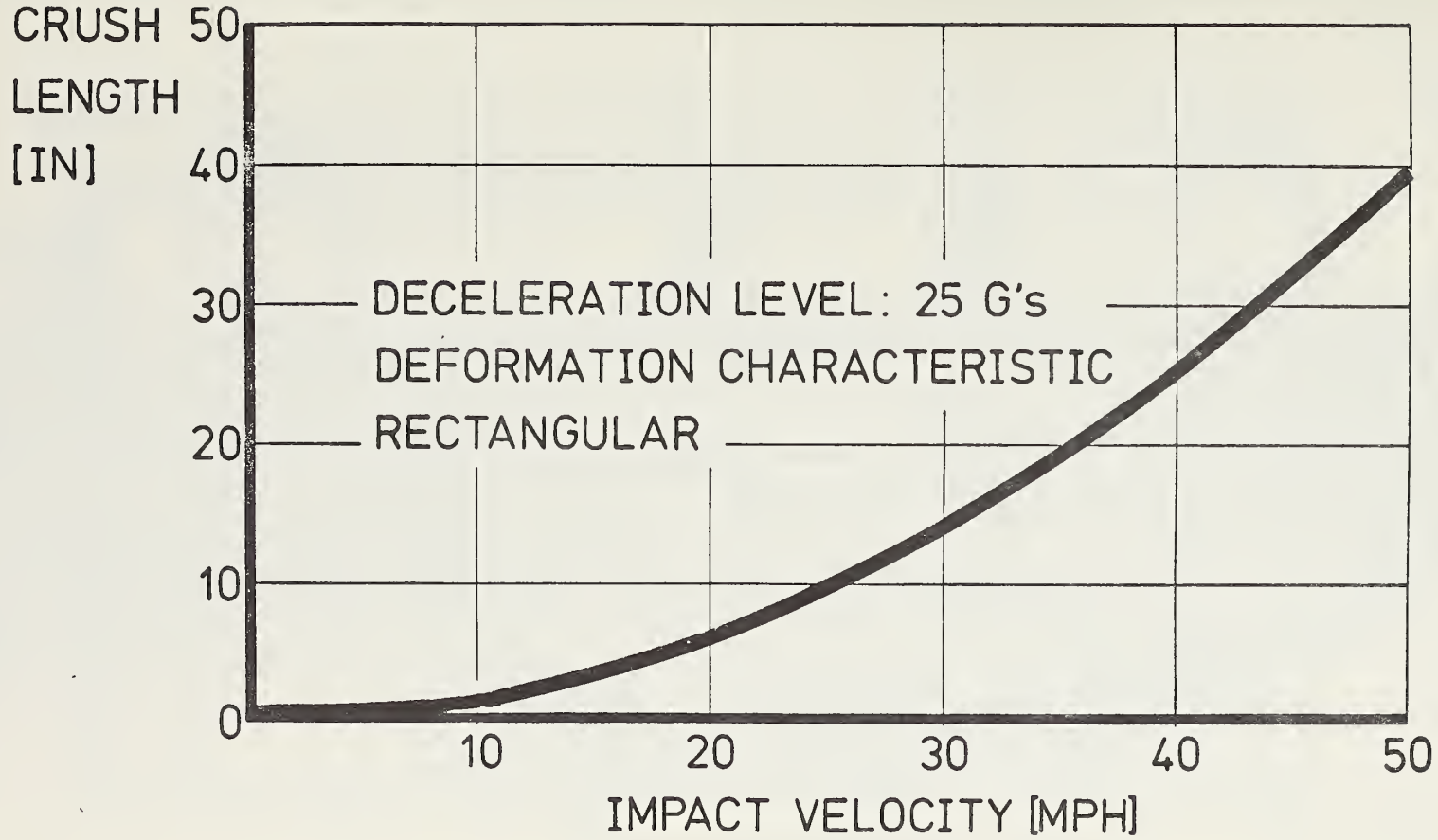

FIGURE 7.1-6: CRUSH LENGTH VERSUS IMPACT VELOCITY

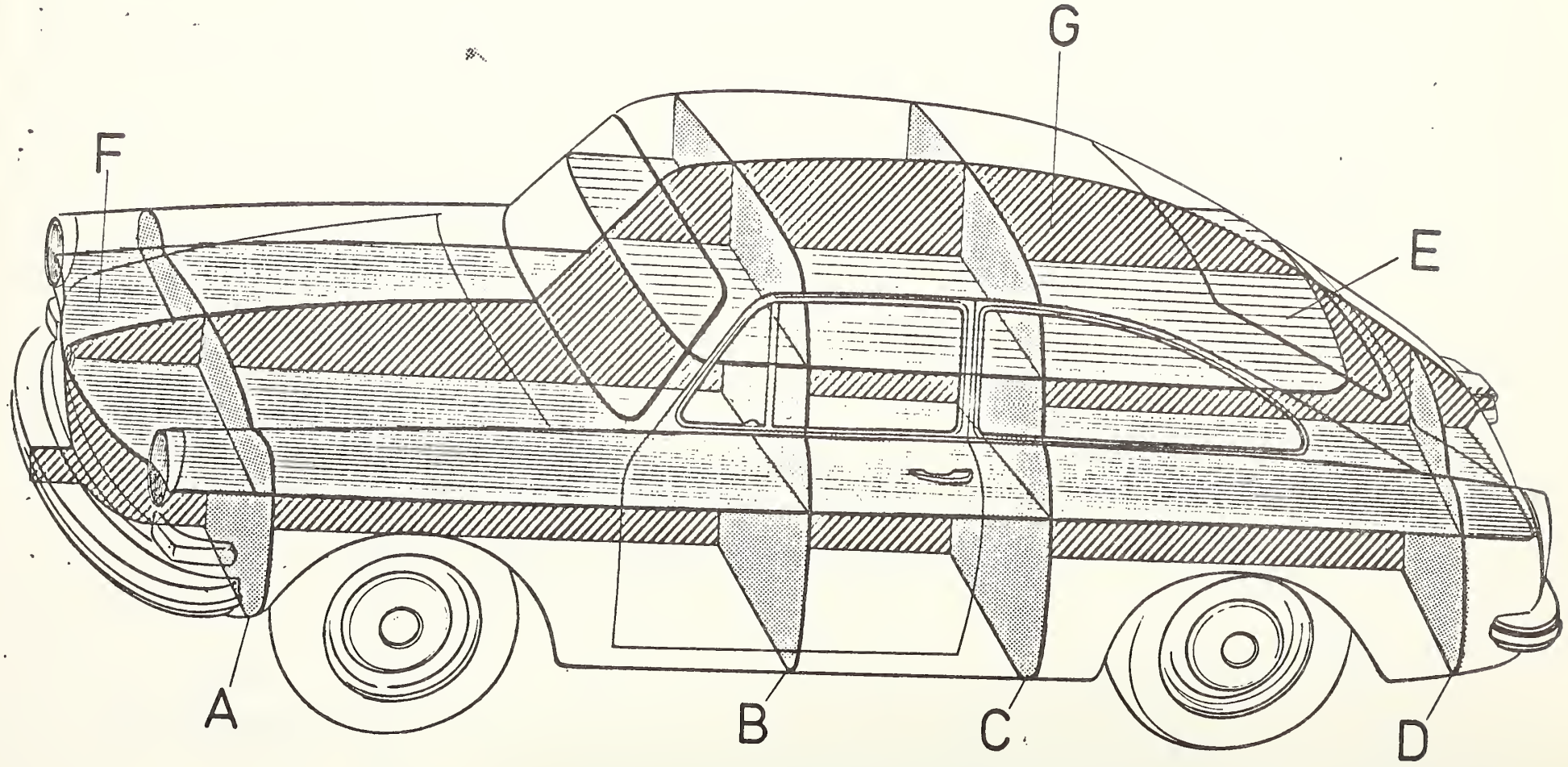

FIGURE 7.1-7: TYPICAL VEHICLE CROSS SECTIONS FOR WEIGHT ANALYSIS (VW 1500)

SECTION	LB/INCH VW 1500	LB/INCH VW Rabbit	LB/INCH VW Dasher	LB/INCH AUDI 100
A	1.96	IDENTICAL TO VW 1500 (Assumed)	IDENTICAL TO VW 1500 (Assumed)	2.35
B	3.69			4.42
C	4.08			4.92
D	2.68			3.24
E	4.76			5.71
F	8.95			10.74
G	8.28			7.16

TABLE 7.1-2: WEIGHT PER INCH OF TYPICAL VEHICLE SECTIONS

7.2 TYPICAL CONCEPTUAL DESIGN

Within the framework of this study fifteen project drafts were prepared where the interior dimensions of the reference vehicles were kept constant, and three project drafts together with another 12 partial project drafts were prepared that provided for variable interior dimensions of the reference vehicles. Figures 7.2-1 through 7.2-3 show typical conceptual designs for the VW Rabbit, VW Dasher and Audi 100. All other design concepts are shown in the Appendix.

7.3 EFFECTS OF ENGINE SIZE AND ENGINE/DRIVETRAIN/VEHICLE CONFIGURATION ON VEHICLE WEIGHT

Figure 7.3-1 shows the increases and decreases in weight for the individual concepts and vehicles. The safety level of 30 mph and the interior dimensions were kept constant (Roominess Index fixed). The mid-engine configuration of the VW Rabbit, however, reduces the seating capacity to two. However, the length of the greenhouse was not changed (see Figure 7.3-2). Therefore, this design concept was assigned to the Roominess Index Fixed category. Figure 7.3-1 shows that the engine/vehicle configuration Front-Engine Longitudinal, Rear-Wheel Drive, which is common in the U.S., basically leads to higher vehicle weights than the compact designs with front-wheel drive.

Figure 7.3-1 also shows the superiority of the front-wheel drive in regard to the lower weight of engines with high specific output. This becomes particularly apparent when a comparison is made between the 5-cylinder NA diesel and the 4-cylinder diesel TC in the VW Dasher (Figures 7.3-3 and 7.3-4). Both of these engines produce roughly the same output.

7.4 EFFECTS OF DIESEL ENGINE/VEHICLE CONFIGURATION AND SAFETY LEVEL ON THE TYPICAL VEHICLE VARIABLES EVALUATED (FIXED ROOMINESS INDEX OF REFERENCE VEHICLE)

The vehicle design is affected substantially by the various Safety Levels (I - III) in addition to the diesel engine/vehicle configuration. This section presents these effects on a number of significant vehicle variables, such as vehicle length, weight, axle-load distribution, wheelbase, location of center of gravity, and luggage capacity. The term Roominess Index Fixed means that the base model roominess index is kept for all configurations and safety levels, and that changes become apparent in the exterior dimensions only.

The roominess index is computed by adding up seven major interior dimensions. These dimensions are defined in the MVMA as follows:

- H 30 H-point to heel point front

- H 61 effective head room front

- H 63 effective head room rear

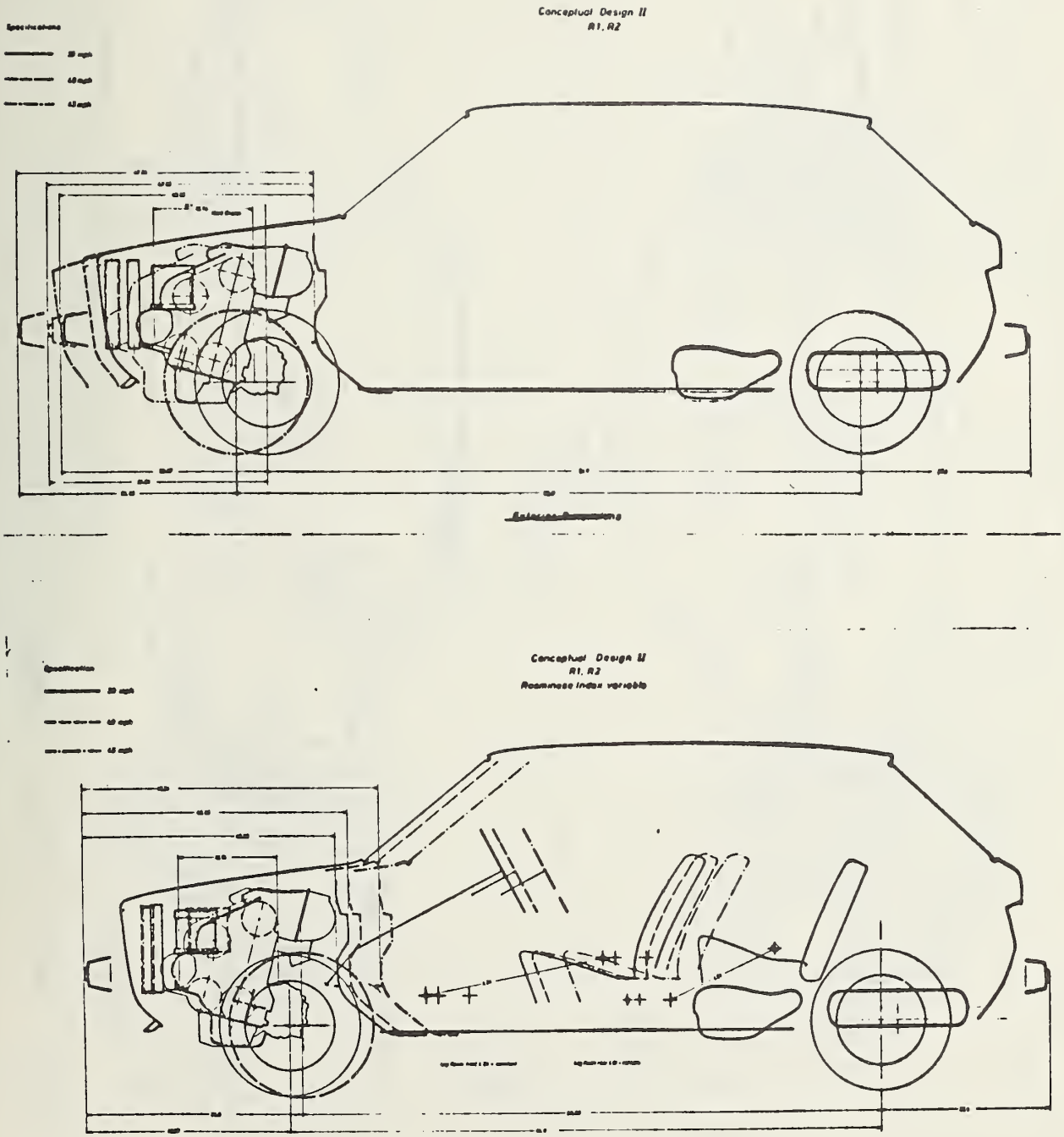

FIGURE 7.2-1: TYPICAL CONCEPTUAL DESIGNS (VW RABBIT)

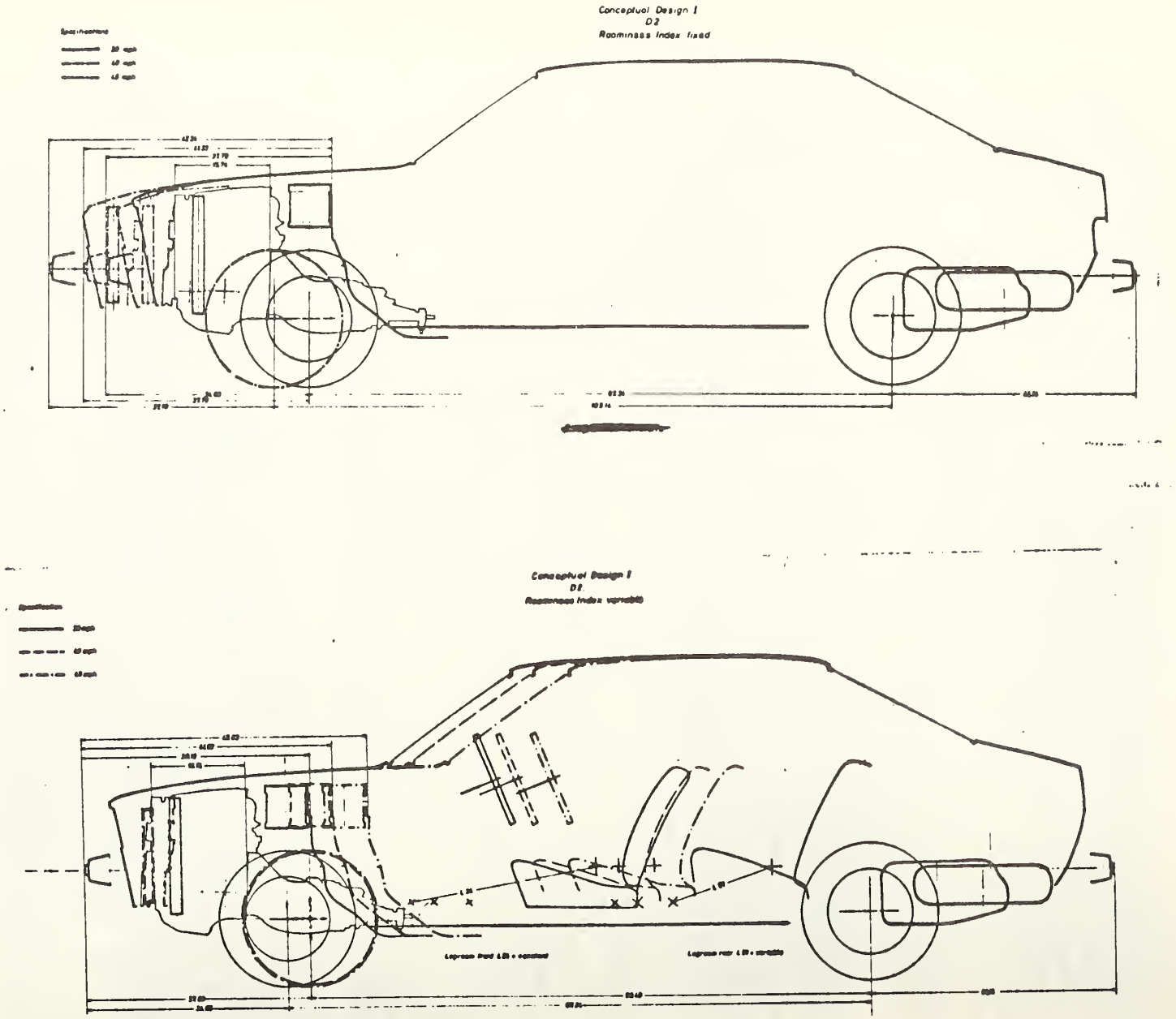

FIGURE 7.2-2: TYPICAL CONCEPTUAL DESIGN (VW DASHER)

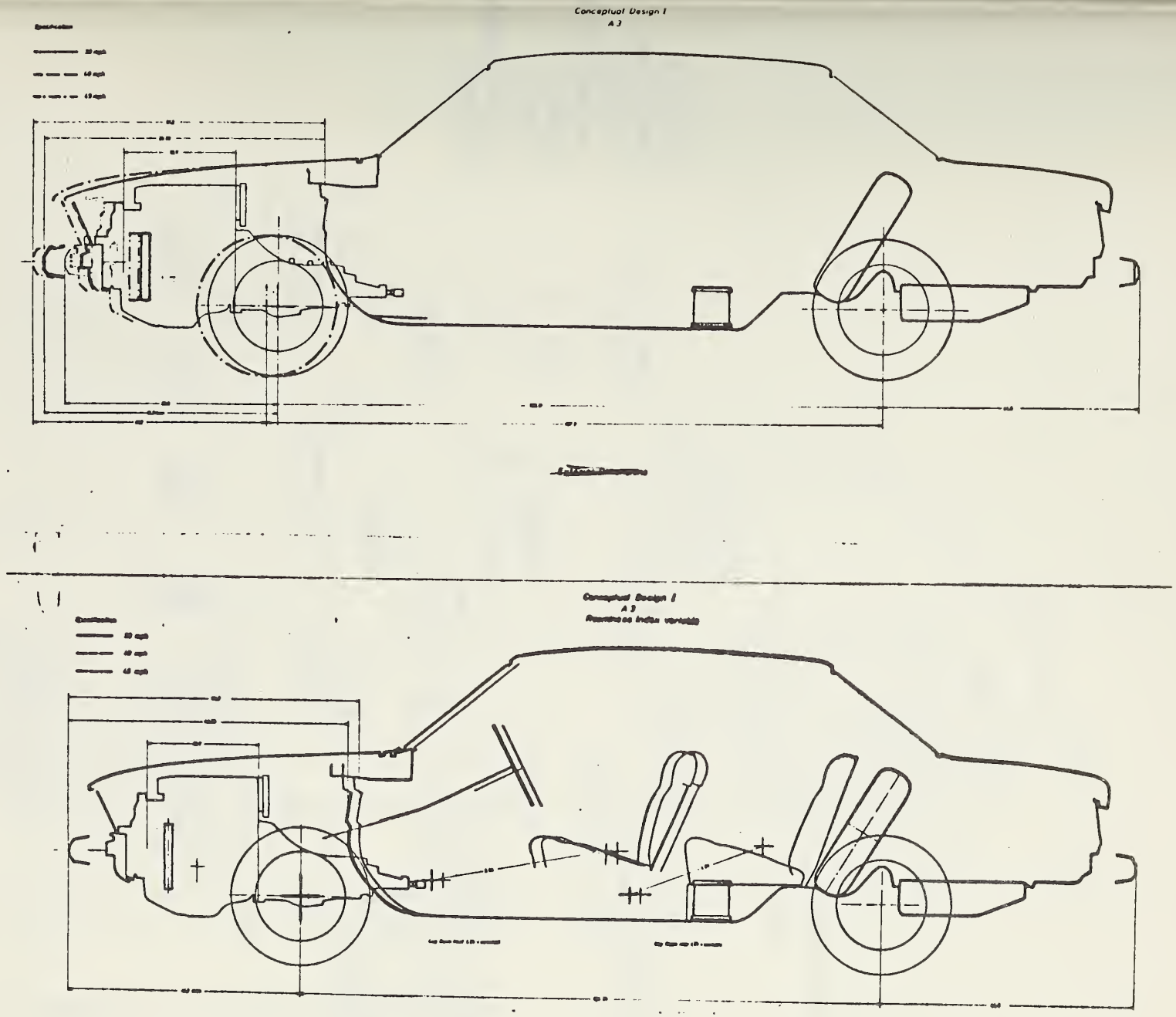

FIGURE 7.2-3: TYPICAL CONCEPTUAL DESIGN (AUDI 100)

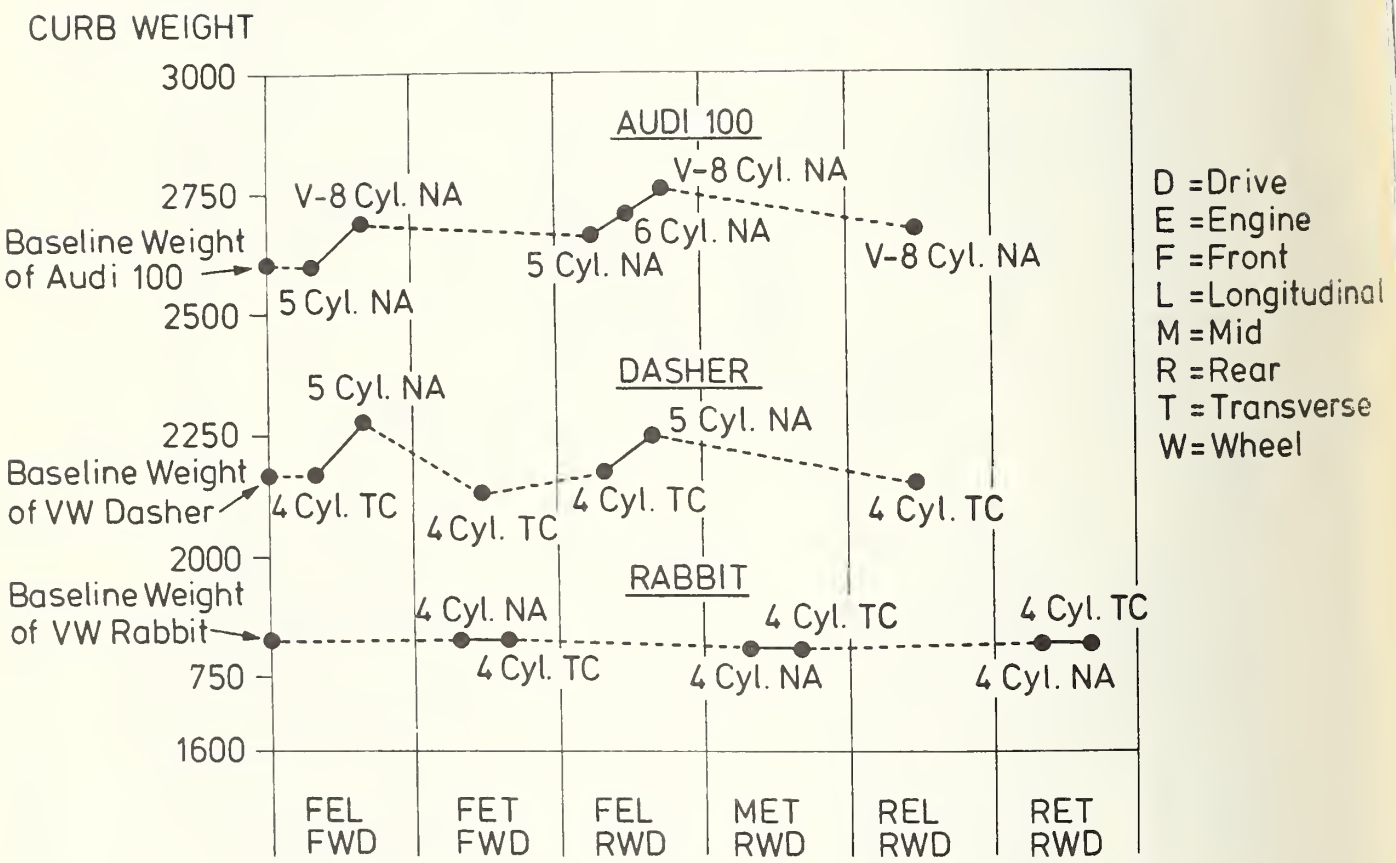

FIGURE 7.3-1: COMPARISON OF CURB WEIGHT OF THE CONCEPTUAL DESIGN AT CONSTANT SAFETY LEVEL (30 MPH)

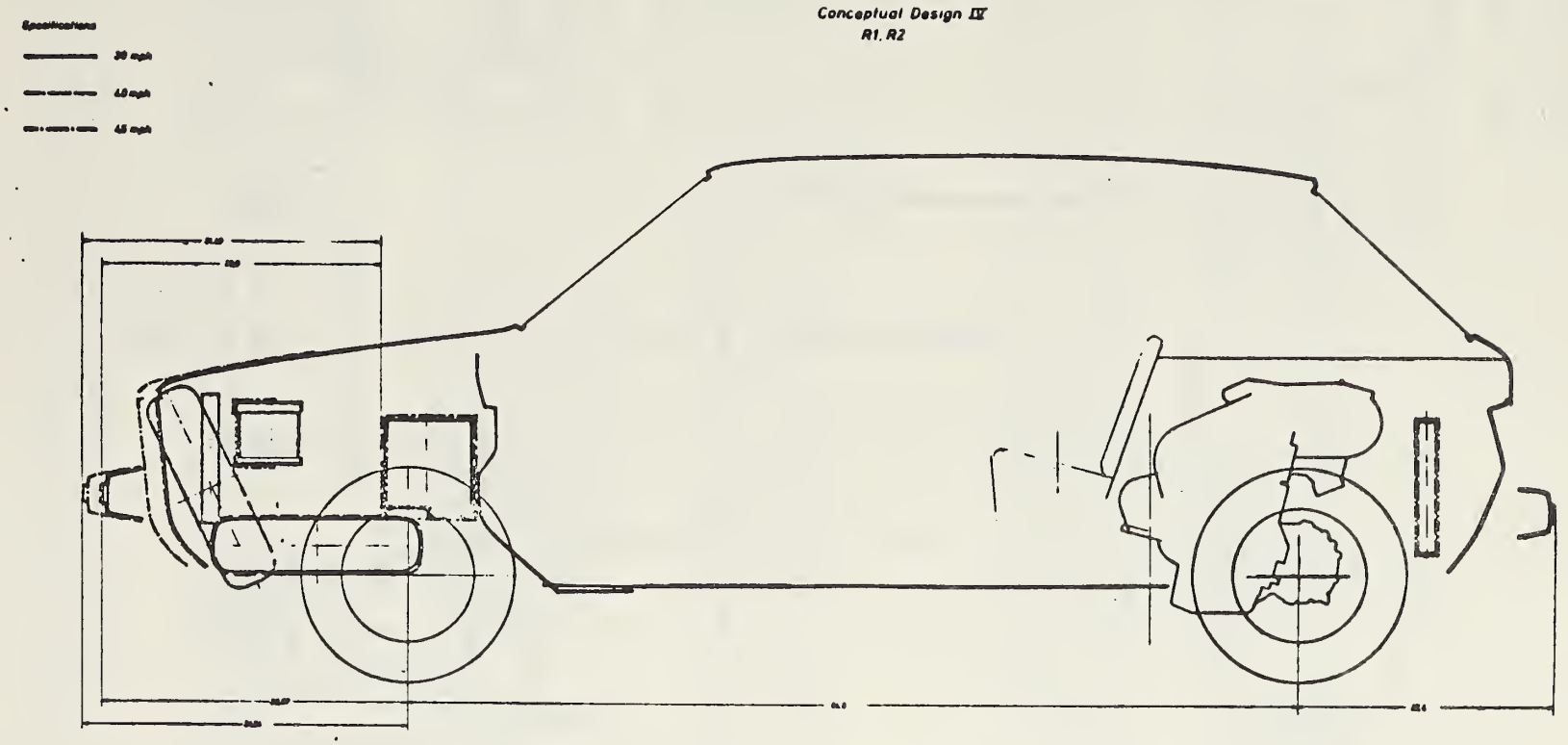

FIGURE 7.3-2: VW RABBIT WITH MID-ENGINE CONFIGURATION

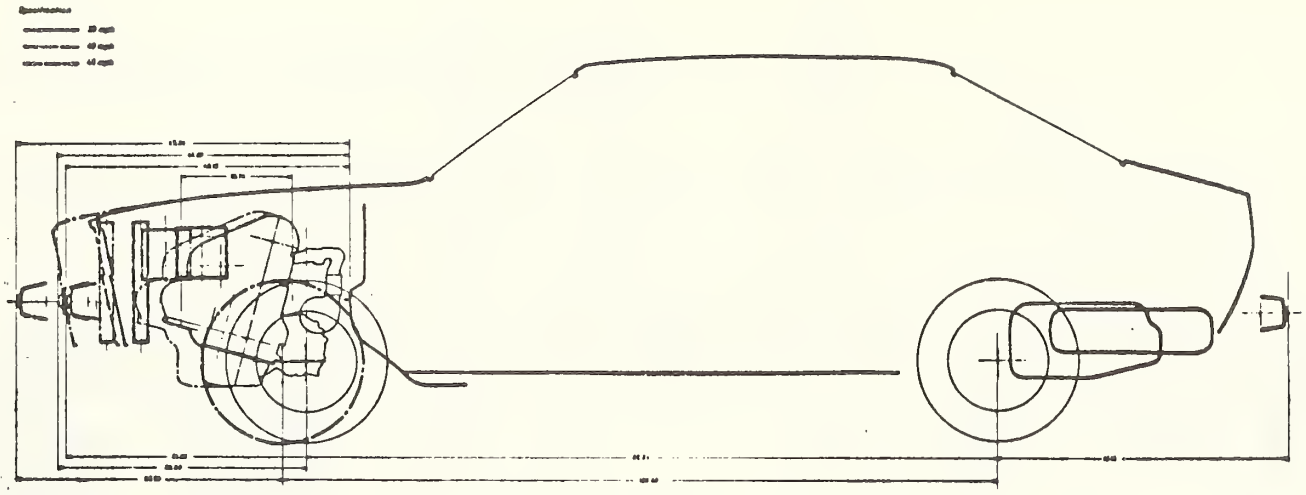

FIGURE 7.3-3: VW DAHSER WITH 4-CYLINDER TC DIESEL ENGINE

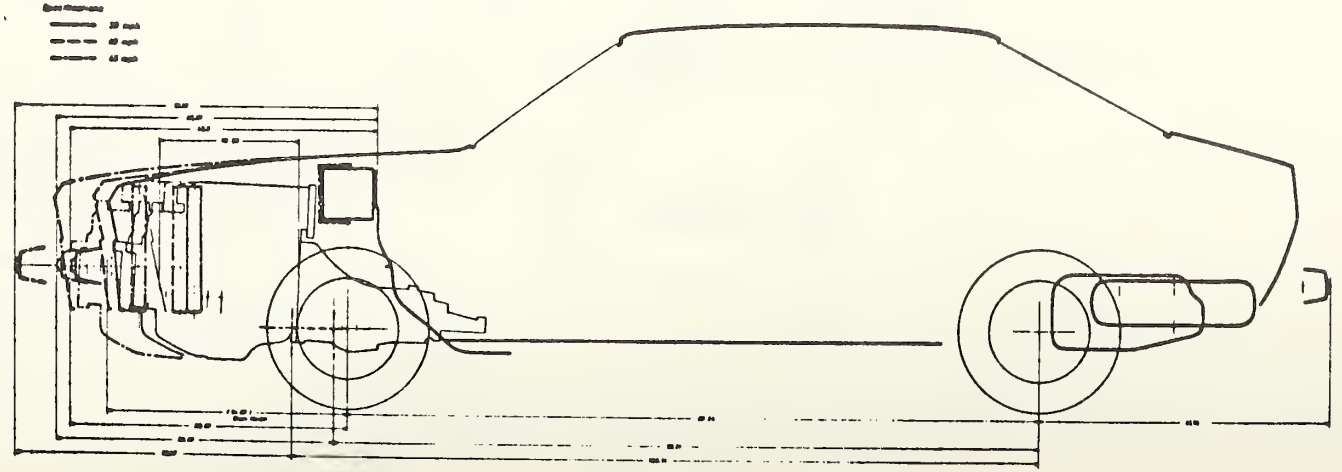

FIGURE 7.3-4: VW DASHER WITH 5-CYLINDER NA DIESEL ENGINE

- L 34 maximum effective legroom accelerator

- L 51 maximum effective legroom

- W 3 shoulder room front

- W 4 shoulder room rear.

7.4.1 Effects on Vehicle Length

When the effects of the engine/vehicle configuration are investigated without taking any advanced safety requirements into consideration, it becomes apparent that there is no need for a change in the exterior dimensions of the VW Rabbit for the various configurations (Figure 7.4-1). A longitudinally mounted five-cylinder diesel combined with front-wheel drive requires longitudinal extension in the VW Dasher and in the Audi 100 (see Figures 7.4-2 and 7.4-3).

Compliance with the safety requirements entails much more pronounced effects. This applies especially in those cases where the engine/vehicle concept provides for a front engine with front-wheel drive, and where the engine is unusually long. Mid-engine and rear-engine concepts are much more favorable because they leave the entire front portion of the vehicle as an energy-absorbing zone.

7.4.2 Effects on Vehicle Weight

The vehicle weight is reduced by compact design concepts such as front engine with front-wheel drive and mid- or rear engine with rear-wheel drive. This applies also in the case of more stringent safety requirements (see Figures 7.4-4 and 7.4-5). The combination of front engine and rear-wheel drive with low or high safety requirements does not lead to any major change in vehicle weight (see Figure 7.4-6).

The lower structural front-axle requirements and the thus lower weight of the component element accounts for the lower vehicle weight of the VW Rabbit even at higher impact velocities with the ensuing longitudinal extension of the vehicle in the case of mid- and rear-engine concepts with rear-wheel drive. Another way to save weight is the substitution of a longitudinally mounted engine by a transverse engine (see Figures 7.4-2 and 7.4-5).

7.4.3 Effects on Front/Rear Weight Distribution

The design concept of a vehicle should try to avoid changes in vehicle driveability under a variety of load conditions, i.e. there should be no change in the axle-load distribution during severe changes in the load condition (from curb weight to full payload) to the extent that the vehicle behavior changes from understeering to oversteering.

The axle load distribution is shown in Figures 7.4-7 through 7.4-9. It is obvious that the mid-engine/rear-wheel-drive and the front-engine/rear-wheel-drive configurations offer favorable solutions to this problem. However,

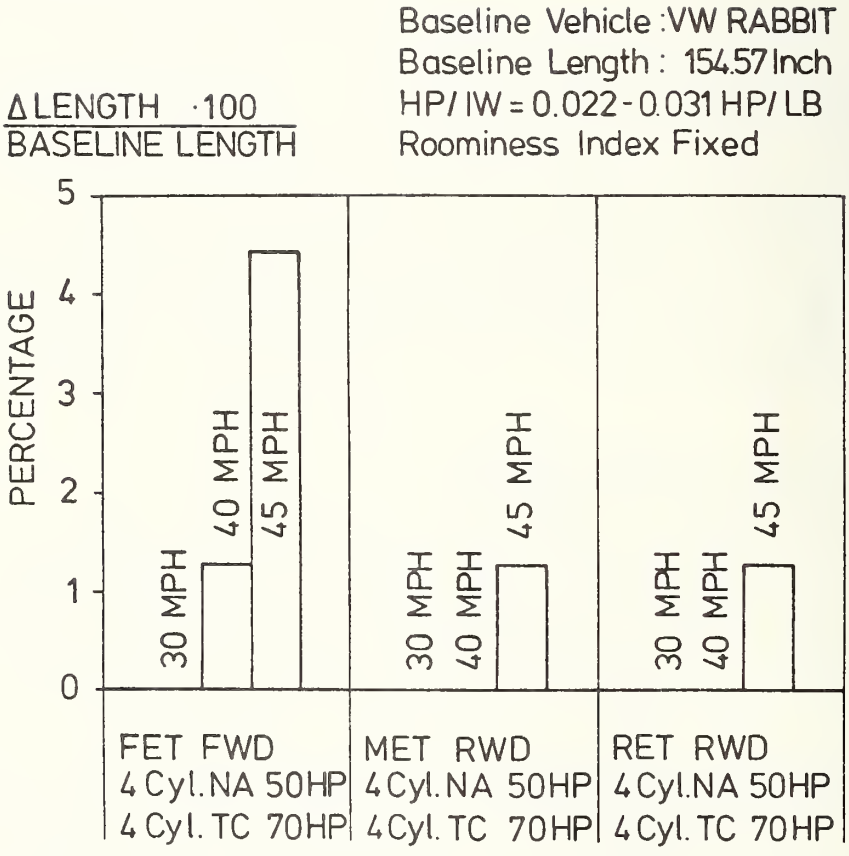

FIGURE 7.4-1: EFFECT OF DIESEL ENGINE/VEHICLE CONFIGURATION AND SAFETY LEVEL ON VEHICLE LENGTH

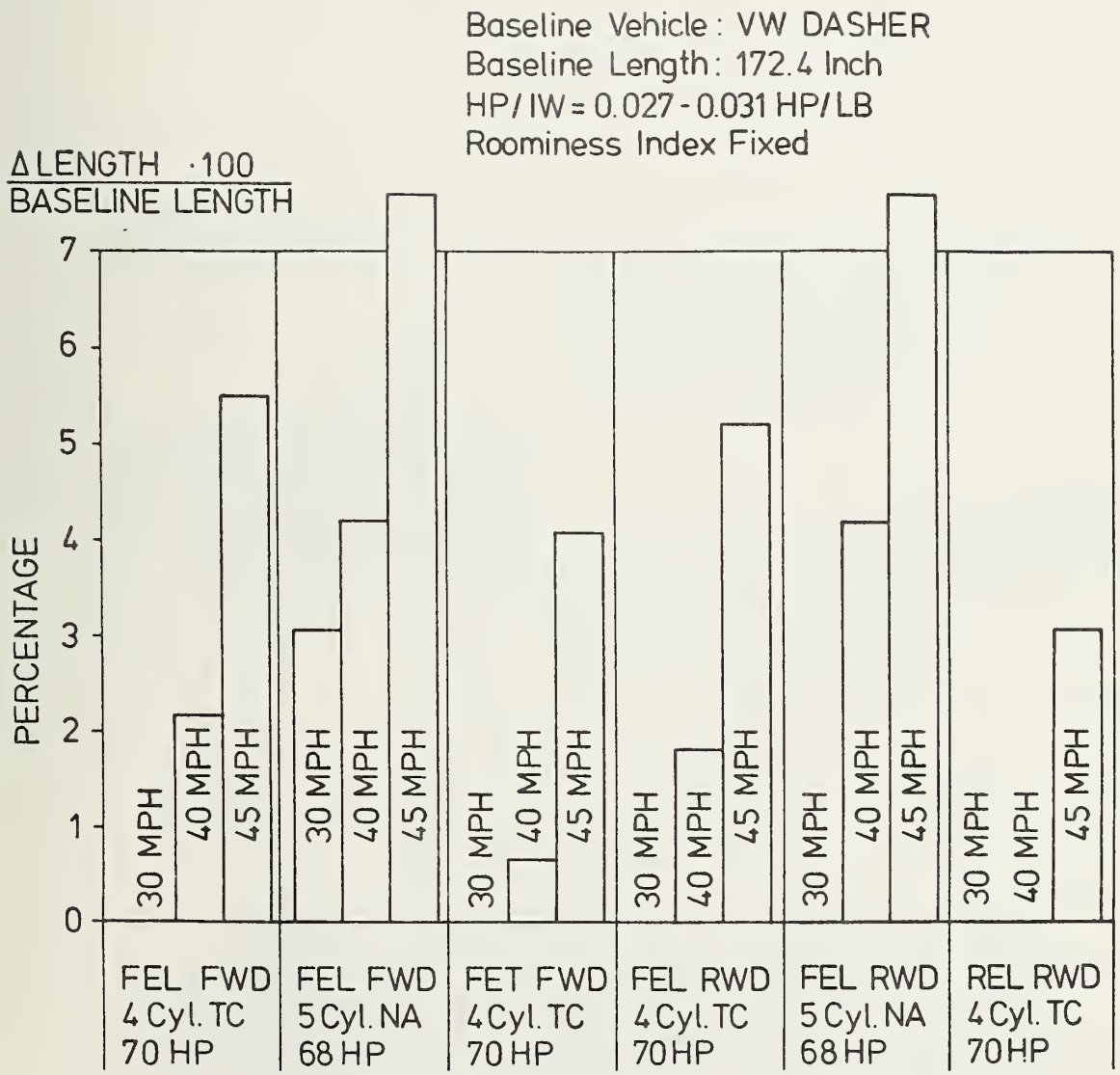

FIGURE 7.4-2: EFFECT OF DIESEL ENGINE/VEHICLE CONFIGURATION AND SAFETY LEVEL ON VEHICLE LENGTH

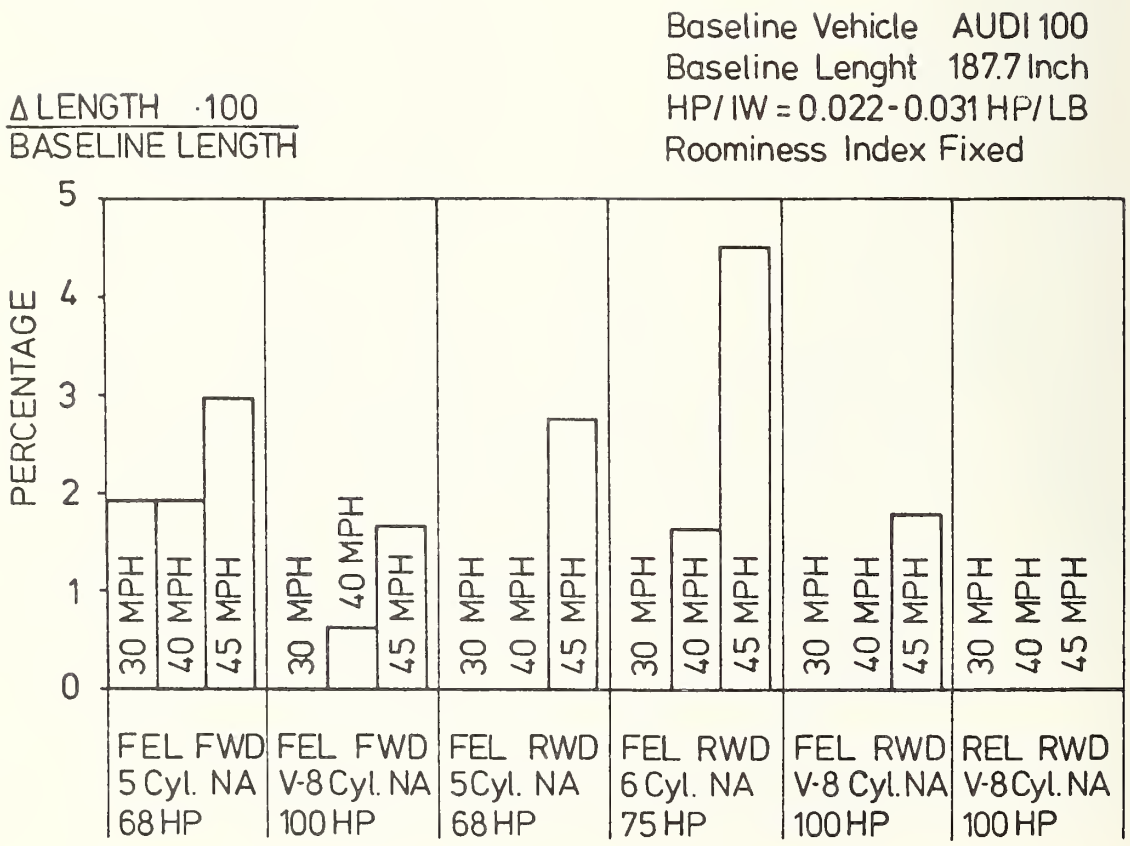

FIGURE 7.4-3: EFFECT OF DIESEL ENGINE/VEHICLE CONFIGURATION AND SAFETY LEVEL ON VEHICLE LENGTH

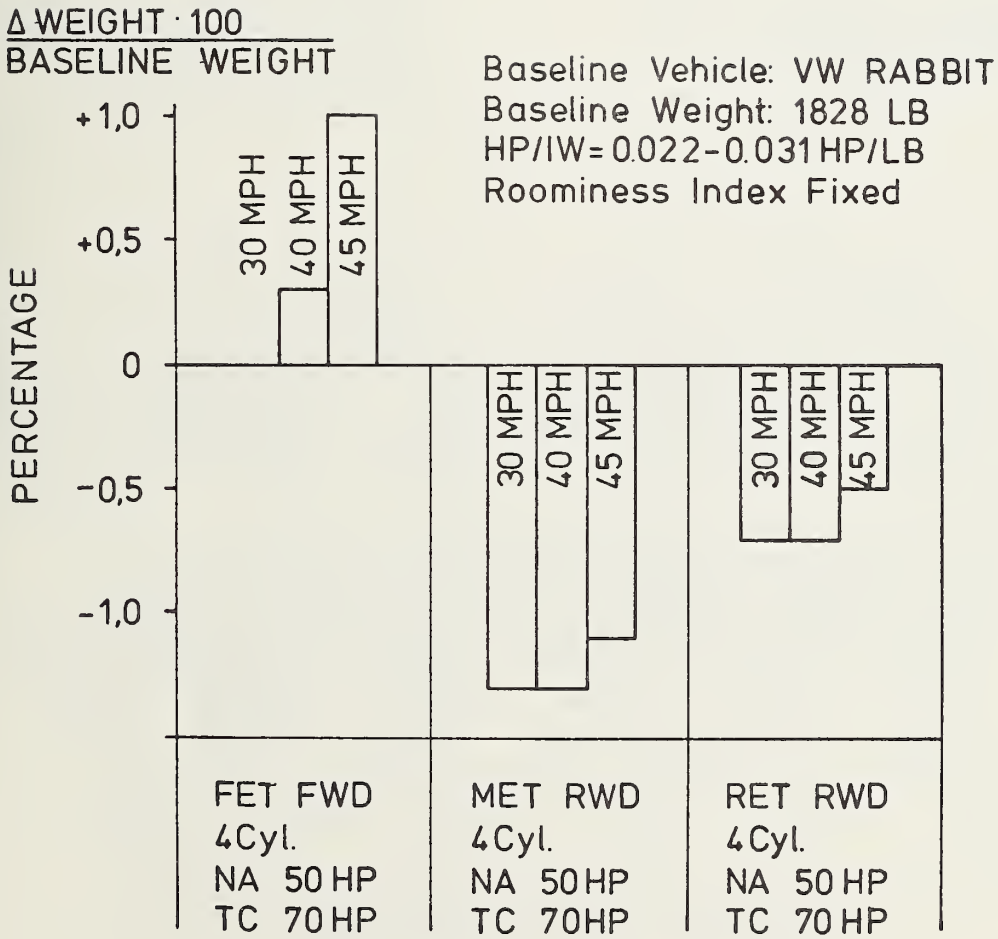

FIGURE 7.4-4: EFFECT OF DIESEL ENGINE/VEHICLE CONFIGURATION AND SAFETY LEVEL ON VEHICLE WEIGHT

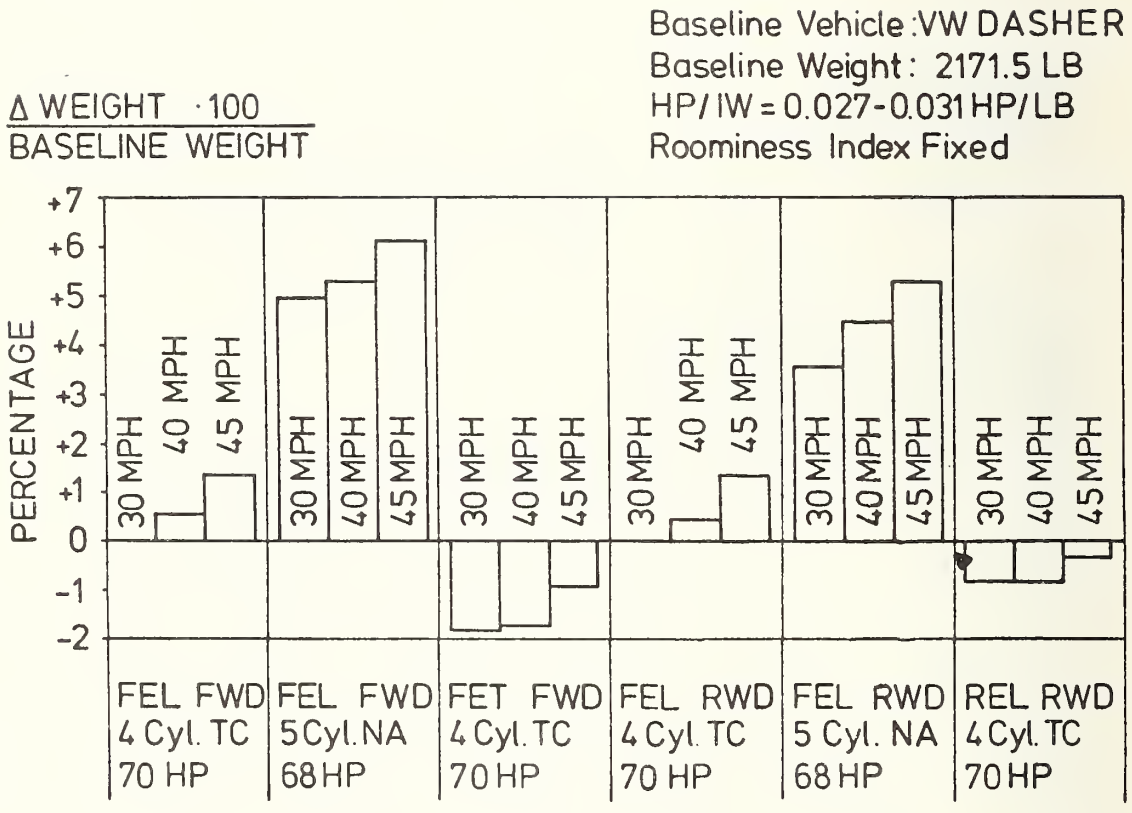

FIGURE 7.4-5: EFFECT OF DIESEL ENGINE/VEHICLE CONFIGURATION AND SAFETY LEVEL ON VEHICLE WEIGHT

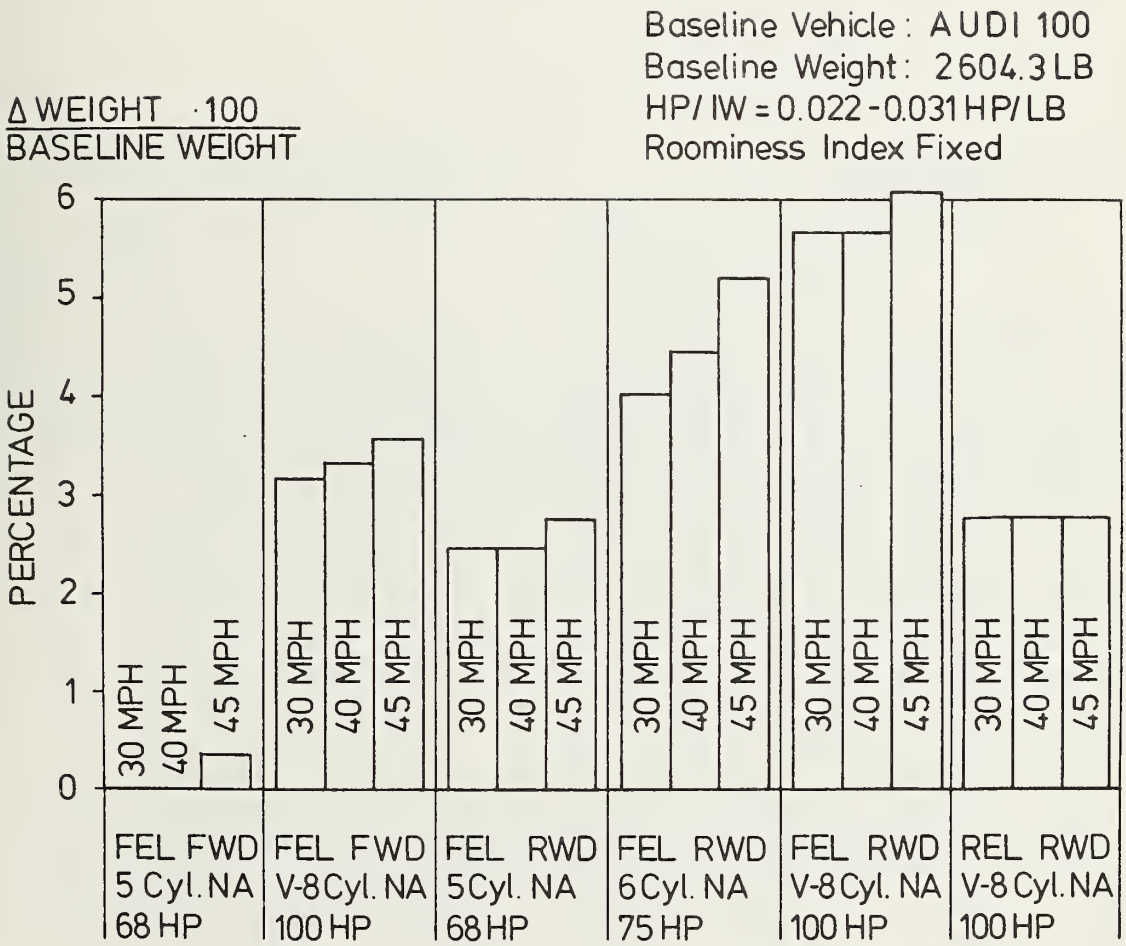

FIGURE 7.4-6: EFFECT OF DIESEL ENGINE/VEHICLE CONFIGURATION AND SAFETY LEVEL ON VEHICLE WEIGHT

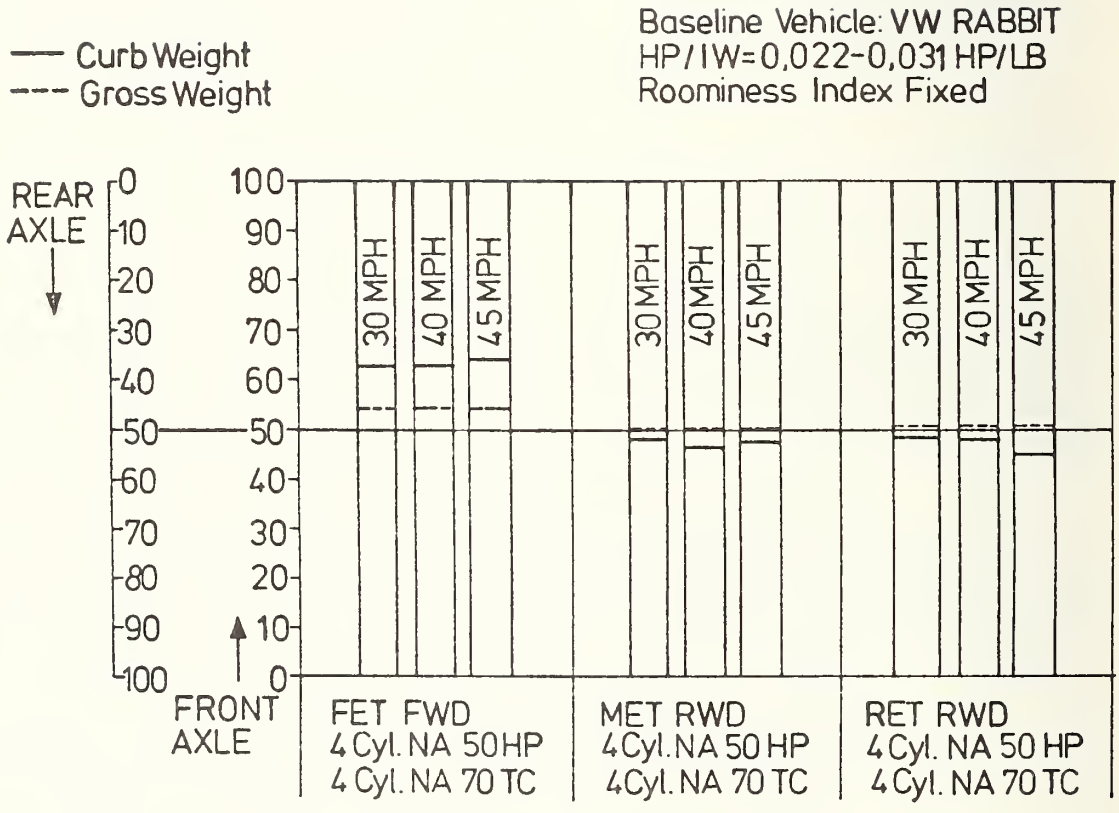

FIGURE 7.4-7: EFFECT OF DIESEL ENGINE/VEHICLE CONFIGURATION AND SAFETY LEVEL ON FRONT/REAR WEIGHT DISTRIBUTION

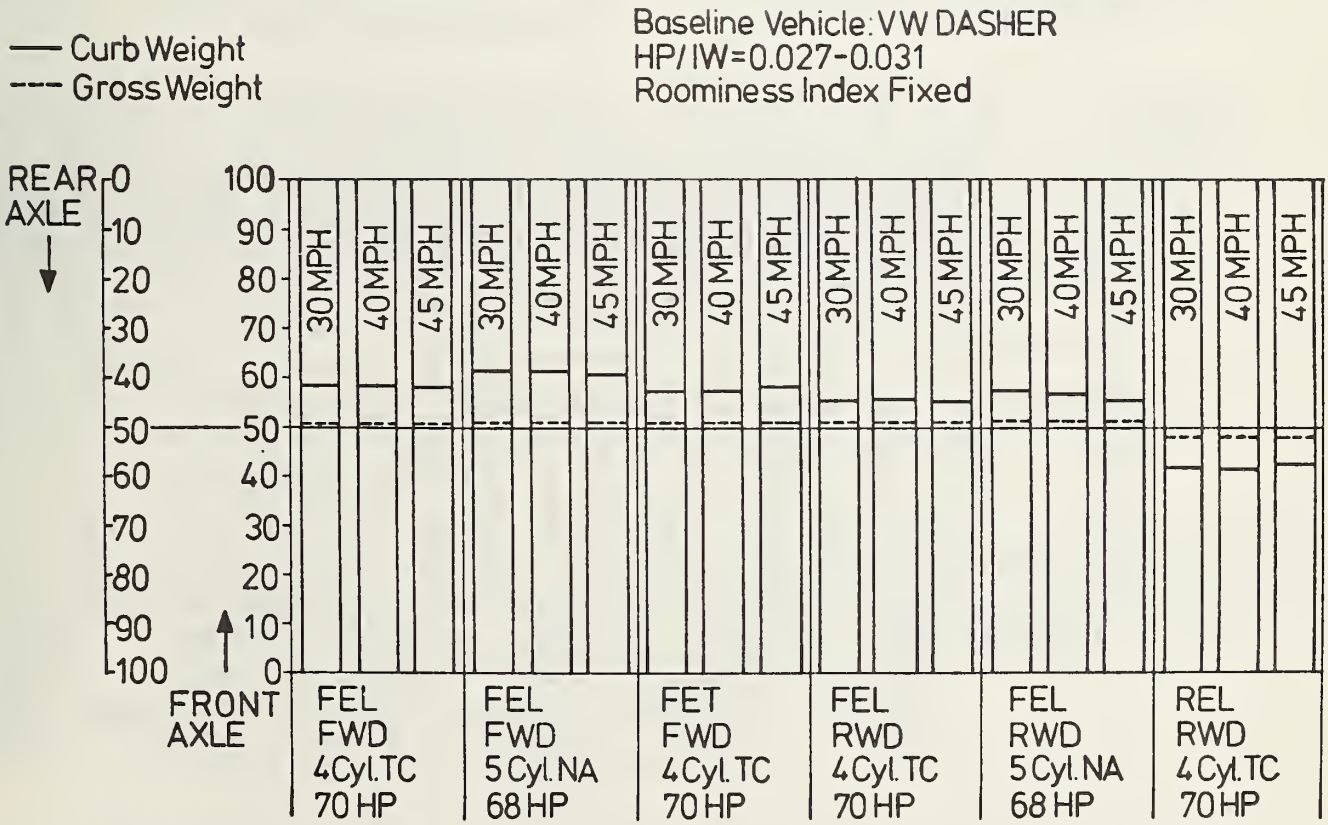

FIGURE 7.4-8: EFFECT OF DIESEL ENGINE/VEHICLE CONFIGURATION AND SAFETY LEVEL ON FRONT/REAR WEIGHT DISTRIBUTION

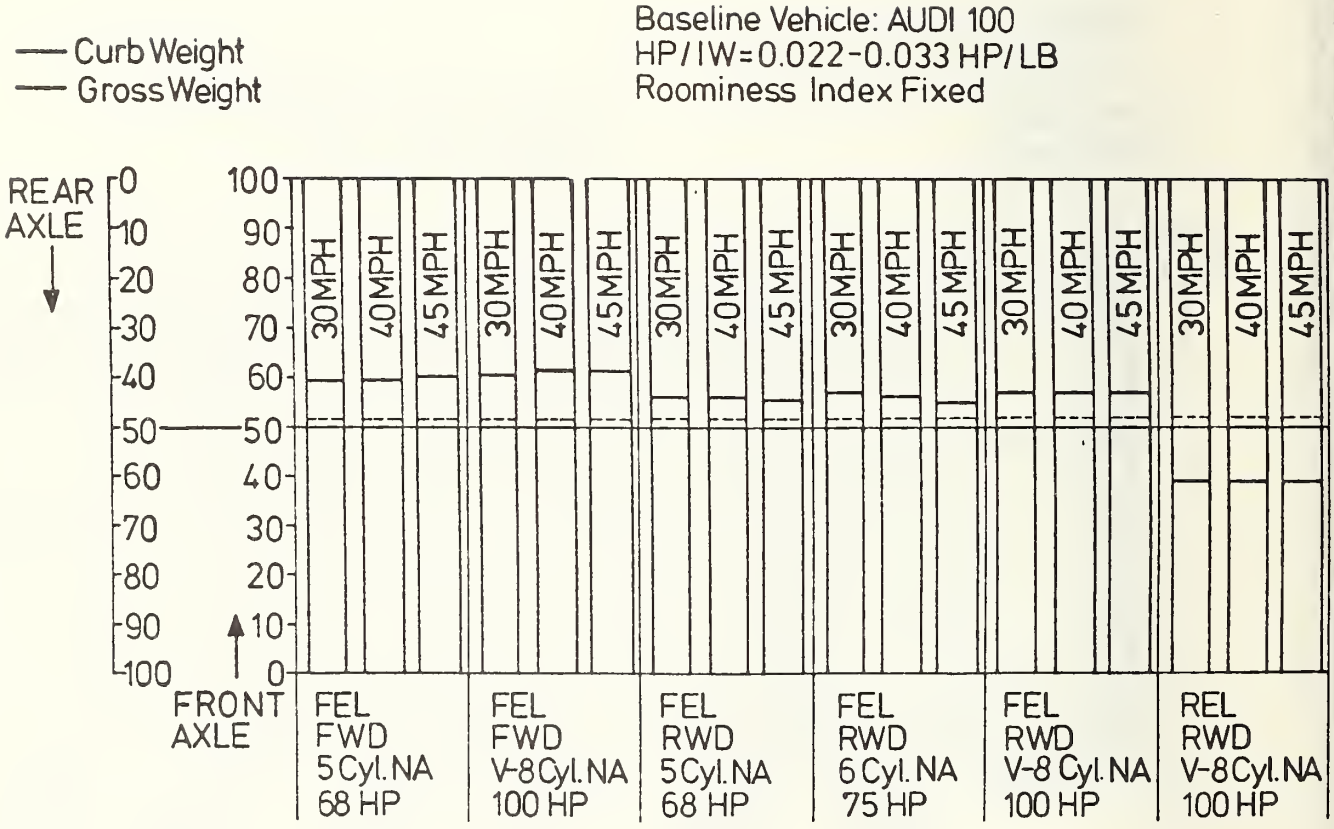

FIGURE 7.4-9: EFFECT OF DIESEL ENGINE/VEHICLE CONFIGURATION AND SAFETY LEVEL ON FRONT/REAR WEIGHT DISTRIBUTION

all various concepts we investigated are in a permissible range. An essential requirement for all preliminary designs was the best possible axle-load distribution.

7.4.4 Effects on Wheelbase

Changes to the wheelbase primarily occurred in those cases where especially long in-line front-mounted engines were installed, and where stringent safety requirements were to be satisfied. The results are shown in Figures 7.4-10 through 7.4-12.

7.4.5 Effects on the Location of the Center of Gravity

Mid-engine and rear-engine concepts tend to shift the center of gravity towards the rear of the vehicle (Figures 7.4-13 through 7.4-15).

7.4.6 Effects on Luggage Capacity

Table 7.4-1 shows the luggage capacity trends for the individual engine/vehicle configurations and safety levels. The framework of this study only permits an overall evaluation of the vehicle luggage capacity because the nature of the investigations does not allow precise capacity measurements. It may be seen from Table 7.4-1 that luggage capacity is reduced with mid-engine and rear-engine/rear-wheel concepts.

7.5 EFFECTS OF DIESEL ENGINE/VEHICLE CONFIGURATIONS AND SAFETY LEVEL ON TYPICAL VEHICLE VARIABLES EVALUATED (VARIABLE ROOMINESS INDEX OF REFERENCE VEHICLE)

The term Roominess Index Variable means that the exterior vehicle dimensions are kept constant. The effects are investigated of engine/vehicle configuration and safety requirements on the vehicle interior dimensions, leg room rear (L 51), weight, axle-load distribution, wheelbase and luggage capacity. This is illustrated in Figures 7.2-2 through 7.2-4.

7.5.1 Effects on Interior Dimensions

The mid-engine concept detrimentally affects vehicle interior space utilization when the effects of safety measures are disregarded (see Figure 7.5-1). A reduction of interior space must also be anticipated when extremely long in-line engines are used in the front-engine configuration of the Audi 100 (engine forward of front axle). This is shown in Figure 7.5-3. Figures 7.5-1 through 7.5-3 show further effects of the engine/vehicle configuration and safety level on the roominess index.

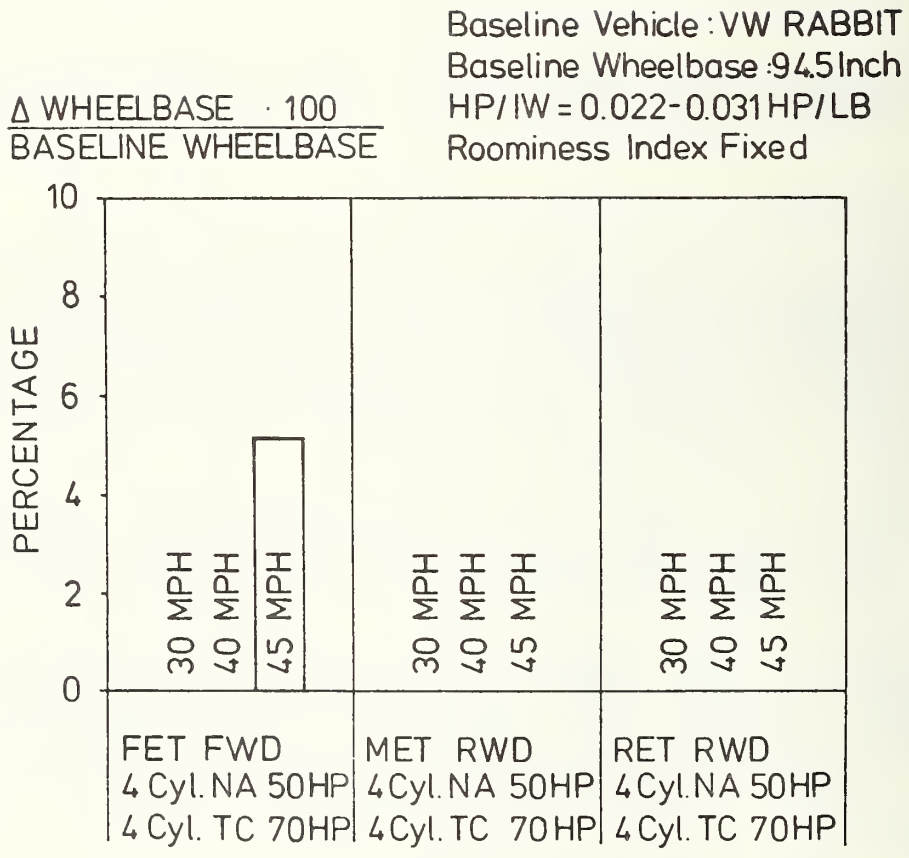

FIGURE 7.4-10: EFFECT OF DIESEL ENGINE/VEHICLE CONFIGURATION AND SAFETY LEVEL ON WHEELBASE

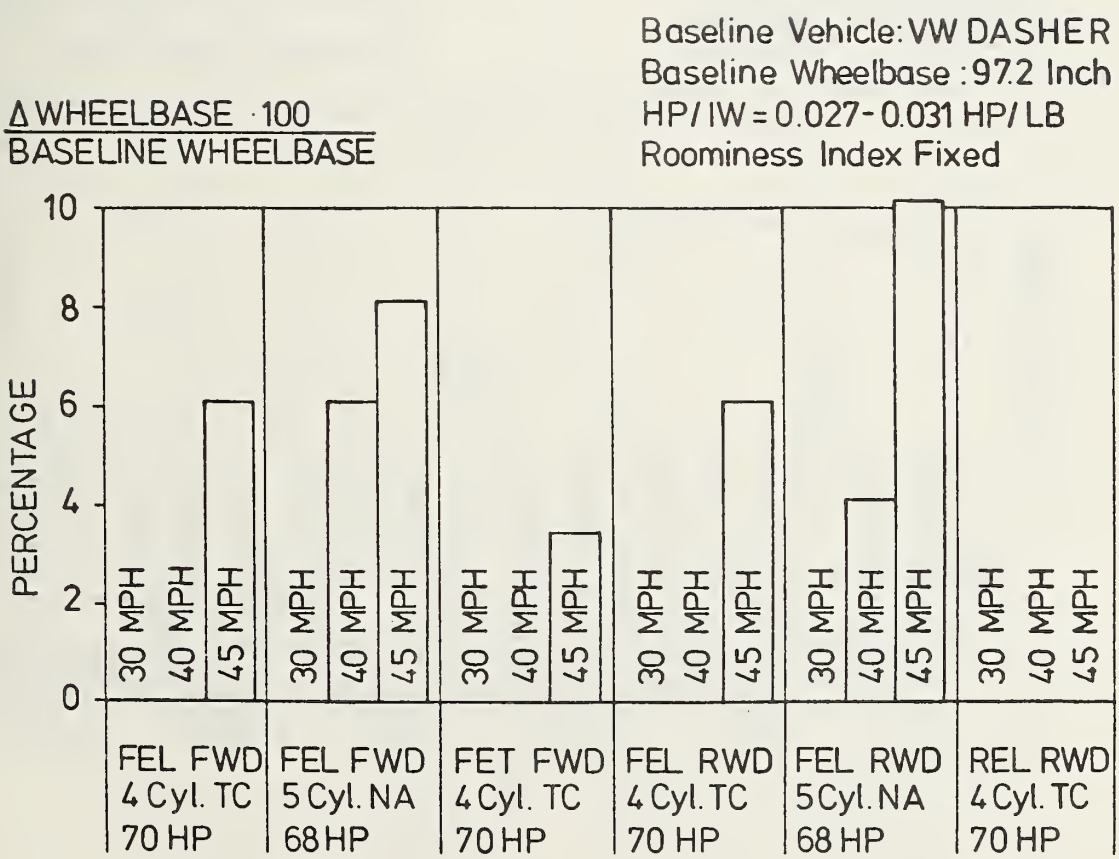

FIGURE 7.4-11: EFFECT OF DIESEL ENGINE/VEHICLE CONFIGURATION AND SAFETY LEVEL ON WHEELBASE

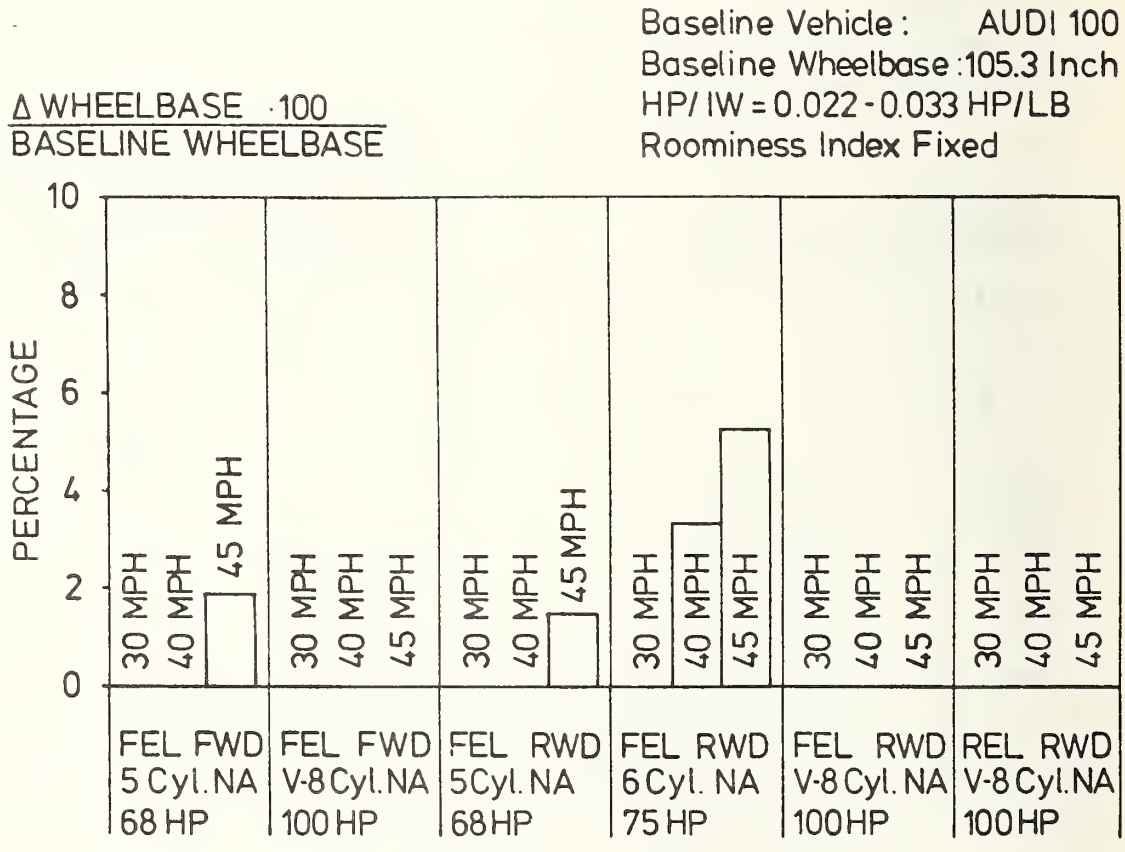

FIGURE 7.4-12: EFFECT OF DIESEL ENGINE/VEHICLE CONFIGURATION AND SAFETY LEVEL ON WHEELBASE

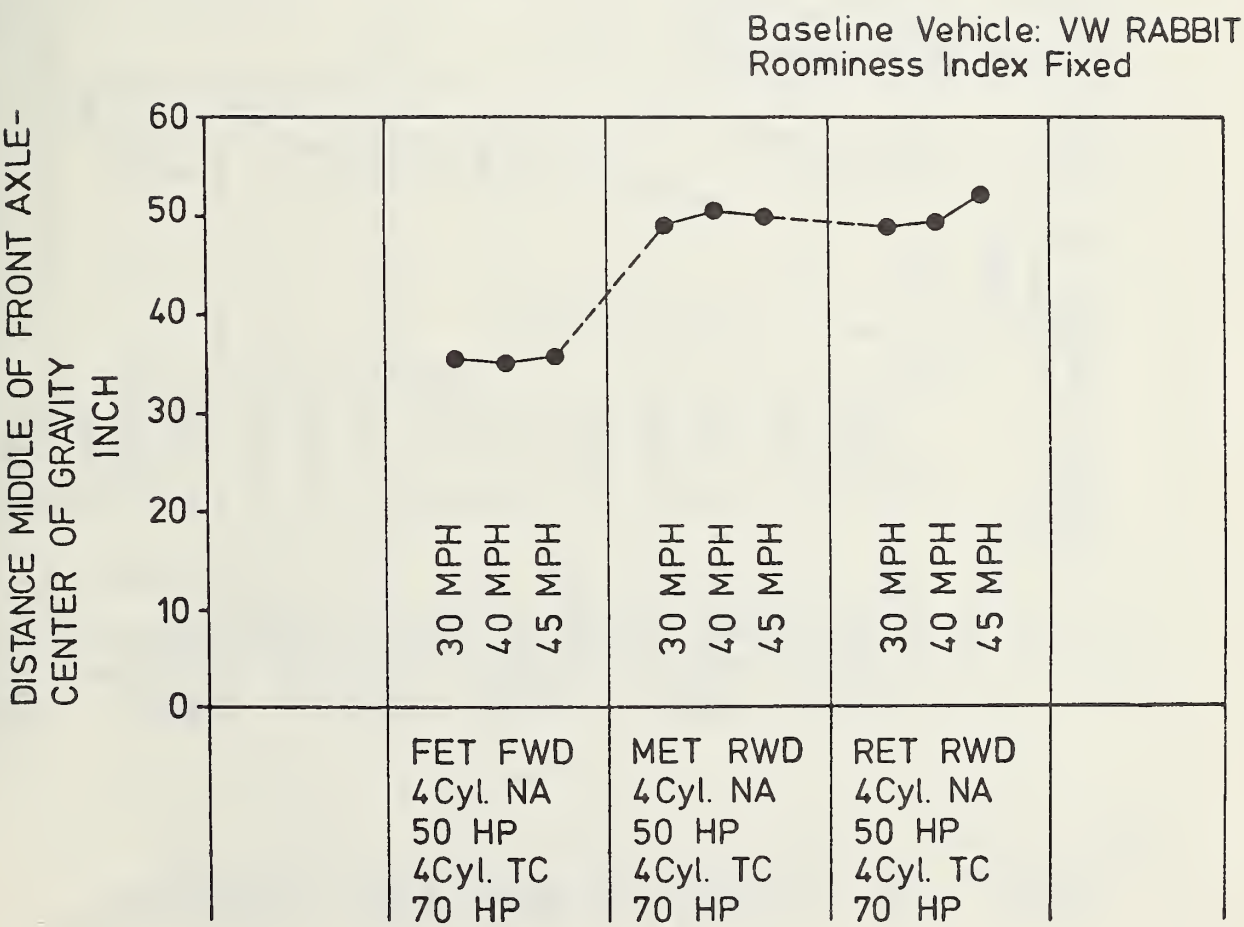

FIGURE 7.4-13: EFFECT OF DIESEL ENGINE/VEHICLE CONFIGURATION AND SAFETY LEVEL ON LOCATION OF CENTER OF GRAVITY

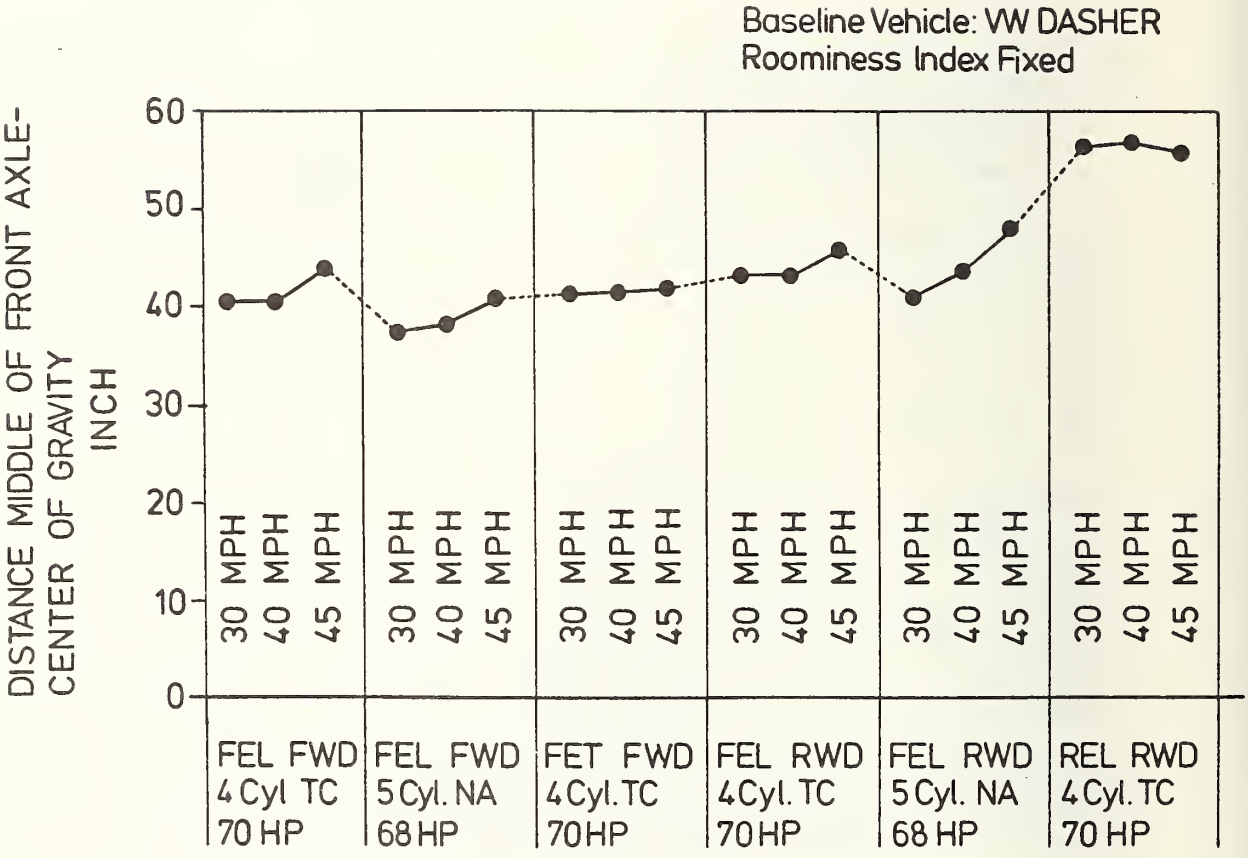

FIGURE 7.4-14: EFFECT OF DIESEL ENGINE/VEHICLE CONFIGURATION AND SAFETY LEVEL ON LOCATION OF CENTER OF GRAVITY

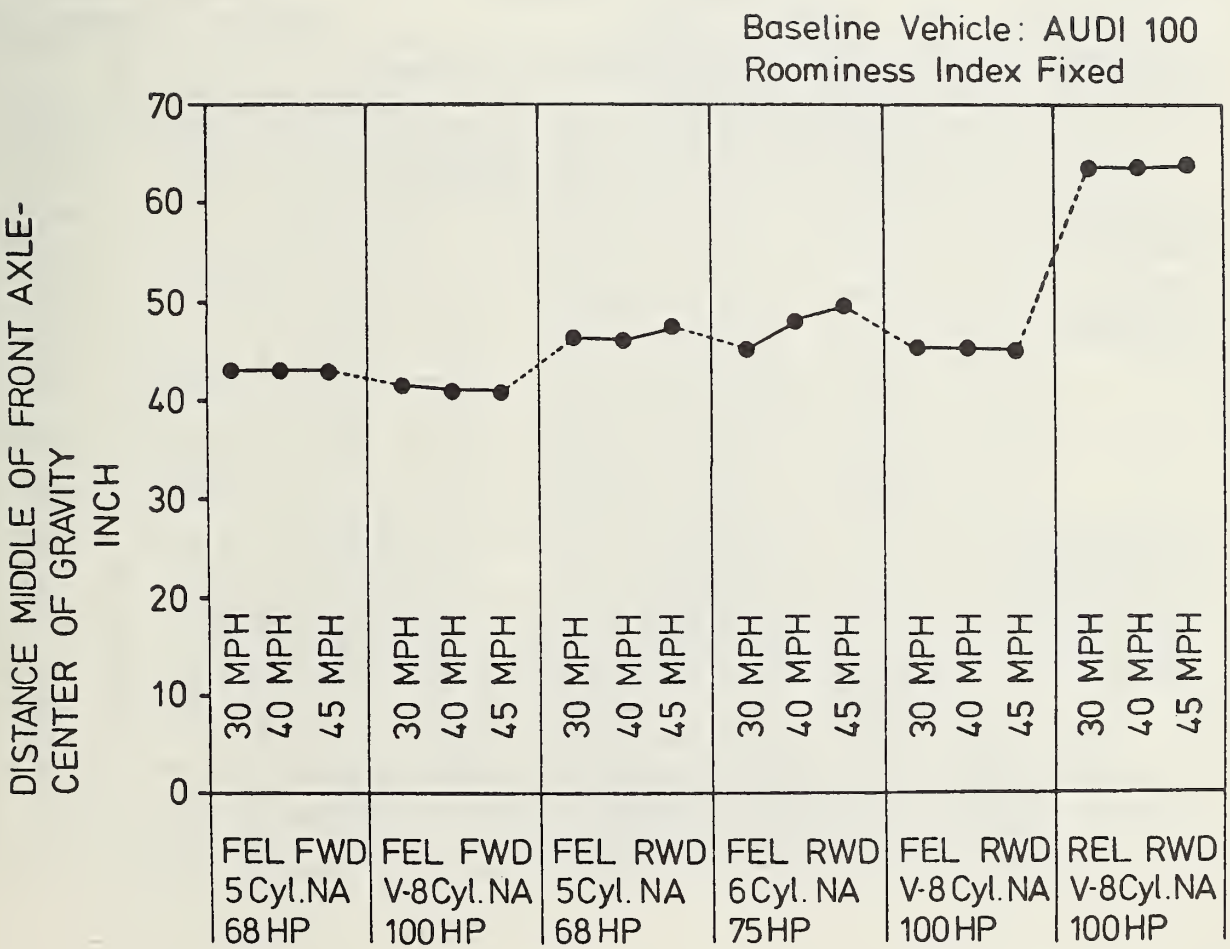

FIGURE 7.4-15: EFFECT OF DIESEL ENGINE/VEHICLE CONFIGURATION AND SAFETY LEVEL ON LOCATION OF CENTER OF GRAVITY

Vehicle Type	Conceptual Design	Safety Level		
		30 MPH	40 MPH	45 MPH
RABBIT	FET FWD 4 Cyl. NA 50 HP, TC 70 HP	0	0	0
12.4 Cu-ft Baseline	MET RWD 4 Cyl. NA 50 HP, TC 70 HP	–	–	–
	RET RWD 4 Cyl. NA 50 HP, TC 70 HP	–	–	–
DASHER	FEL FWD 4 Cyl. TC 70 HP	0	0	0
17.7 Cu-ft Baseline	FEL FWD 5 Cyl. NA 68 HP	0	0	0
	FET FWD 4 Cyl. TC 70 HP	0	0	0
	FEL RWD 4 Cyl. TC 70 HP	0	0	0
	FEL RWD 5 Cyl. NA 68 HP	0	0	0
	REL RWD 4 Cyl. TC 70 HP	–	–	–
AUDI 100	FEL FWD 5 Cyl. NA 68 HP	0	0	0
21.3 Cu-ft Baseline	FEL FWD V-8 Cyl. NA 100 HP	0	0	0
	FEL RWD 5 Cyl. NA 68 HP	0	0	0
	FEL RWD 6 Cyl. NA 75 HP	0	0	0
	FEL RWD V-8 Cyl. NA 100 HP	0	0	0
	REL RWD V-8 Cyl. NA 100 HP	–	–	–

TABLE 7.4-1: LUGGAGE CAPACITY (ROOMINESS INDEX FIXED)
- Decreased luggage capacity
0 No change in luggage capacity

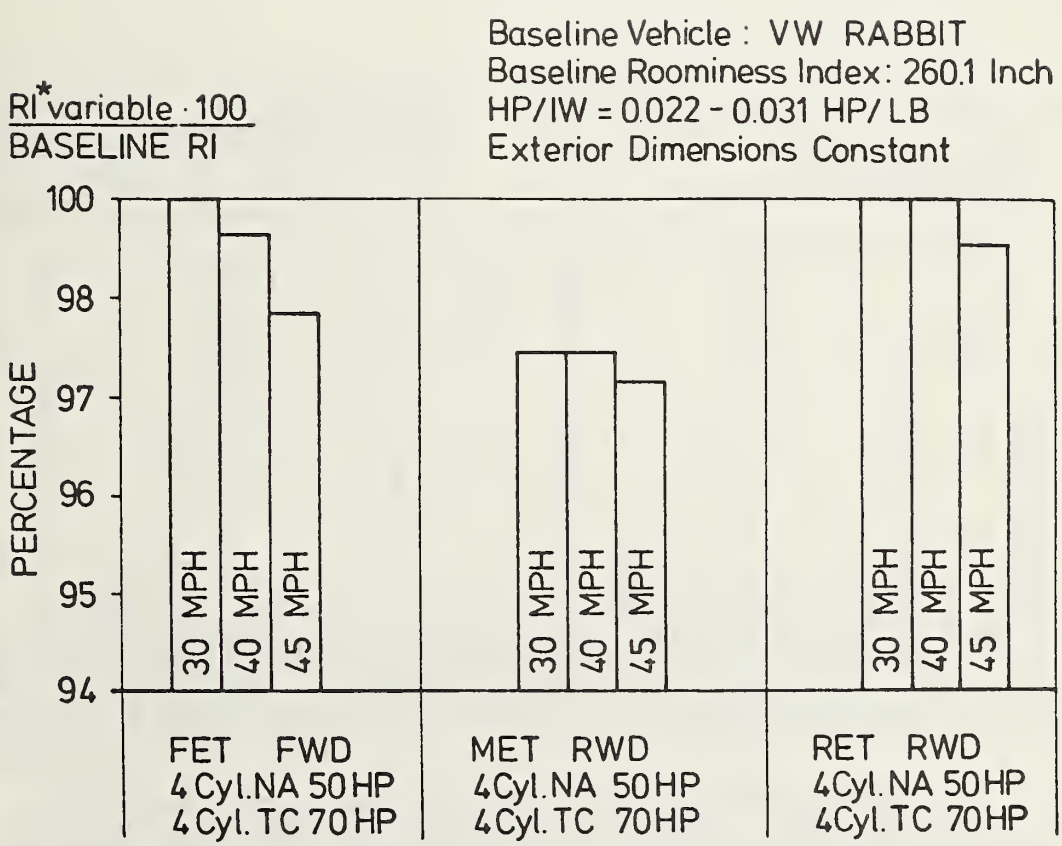

FIGURE 7.5-1: EFFECT OF DIESEL ENGINE/VEHICLE CONFIGURATION AND SAFETY LEVEL ON VEHICLE ROOMINESS

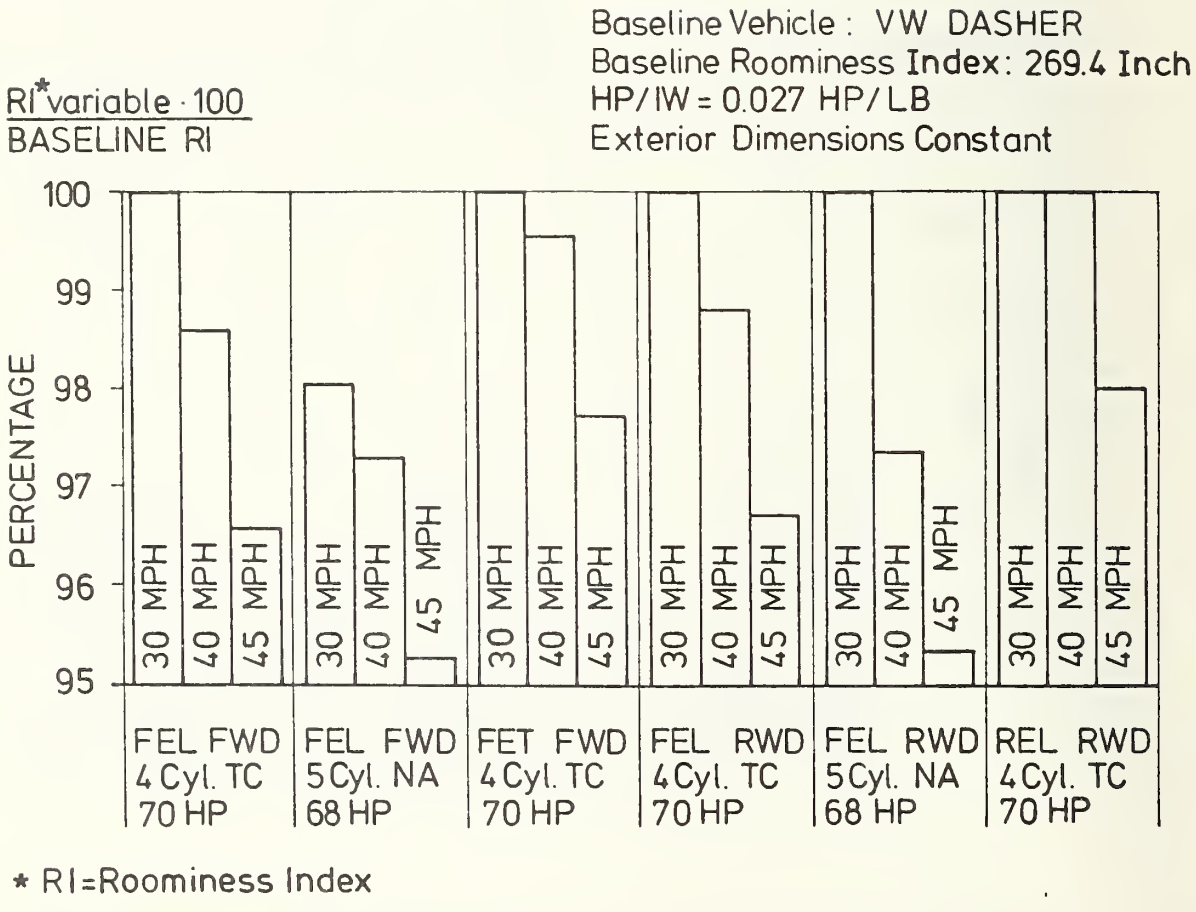

FIGURE 7.5-2: EFFECT OF DIESEL ENGINE/VEHICLE CONFIGURATION AND SAFETY LEVEL ON VEHICLE ROOMINESS

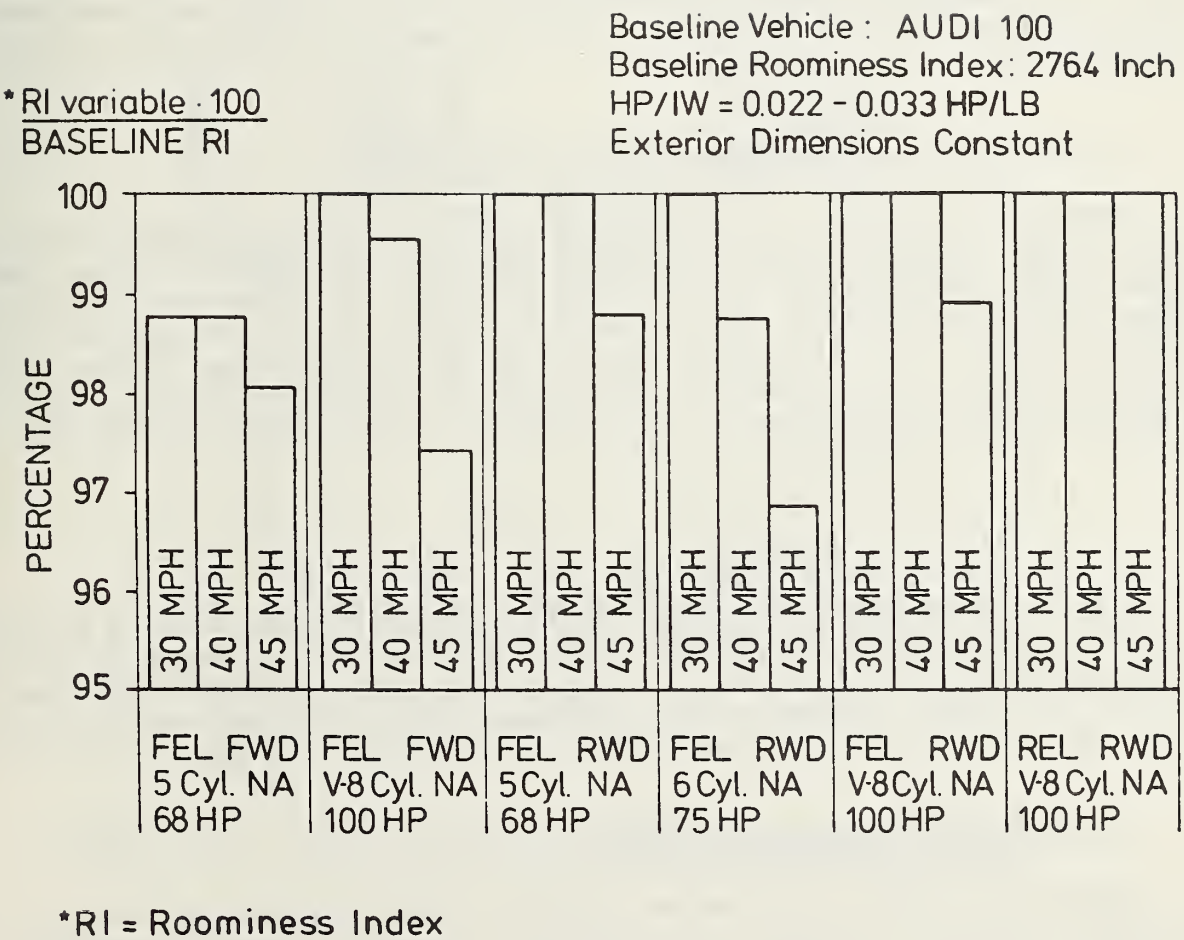

FIGURE 7.5-3: EFFECT OF DIESEL ENGINE/VEHICLE CONFIGURATION AND SAFETY LEVEL ON VEHICLE ROOMINESS

7.5.2 Effects on Effective Leg Room Rear (L 51)

Figures 7.5-4 through 7.5-6 show the effects of engine/vehicle configurations and safety levels on the effective leg room rear (L 51). The most adverse effects are produced by the mid-engine configuration and the front-wheel driven 5-cylinder Audi 100.

7.5.3 Effects on Vehicle Weight

Figures 7.5-7 through 7.5-9 show the weight changes as a result of the various engine/vehicle configurations and safety levels. An increase in the safety level leads to a reduction of weight in all concepts except for the Audi 100 with rear engine (REL, RWD, V-8, NA, 100 HP). There is an easy explanation for this decrease in weight: While the extension of the energy-absorbing zone in the front structure of the vehicle for compliance with higher safety levels lead to an increase in weight of the front portion of the vehicle, the shortening of the greenhouse saves comparatively more weight at the same time because the specific weight of the occupant cell is higher than that of the vehicle front portion.

7.5.4 Effects on Front/Rear Weight Distribution

A comparison between the axle-load distribution of the conceptual designs with constant interior dimensions and constant exterior dimensions shows that higher safety levels lead to a broad scatter band of axle-load distributions between vehicle curb weight and full payload, especially in the case of constant exterior dimensions in mid-engine and rear-engine concepts (see Figures 7.5-10 through 7.5-12). It follows that this condition causes more severe changes in vehicle driveability compared with the conceptual designs that provide for constant interior dimensions.

7.5.5 Effects on Wheelbase

The installation of a 5-cylinder engine in the front-wheel drive design concept of the VW Dasher and the Audi 100 requires a shorter wheelbase already at the 30 mph frontal-fixed-barrier impact velocity (see Figures 7.5-14 and 7.5-15). All other concepts require wheelbase changes starting at the safety levels of 40 or 45 mph only (see Figures 7.5-13 through 7.5-15).

7.6.6 Effects on Luggage Capacity

The design concepts for constant exterior dimensions lead to similar conditions as do the concepts that provide for constant interior dimensions (see Table 7.5-1).

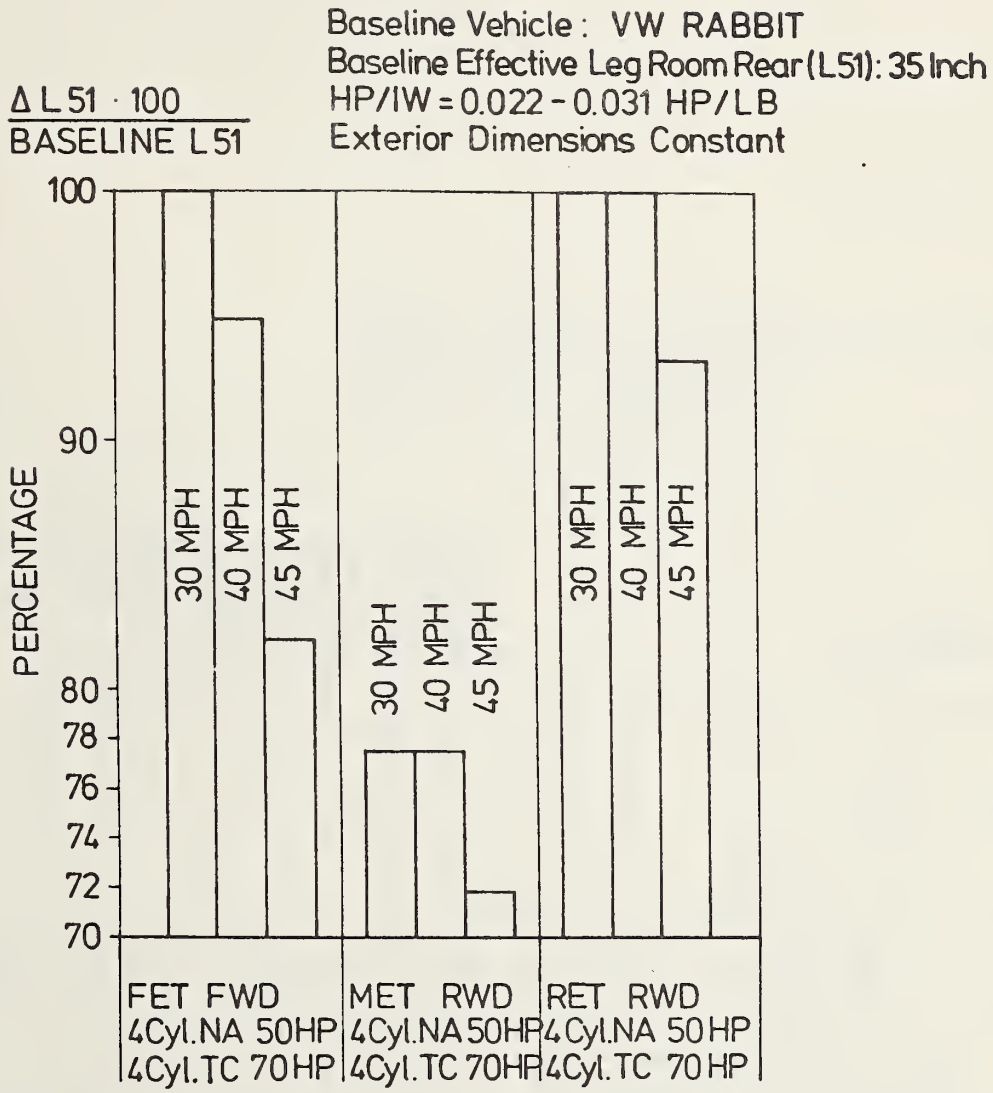

FIGURE 7.5-4: EFFECT OF DIESEL ENGINE/VEHICLE CONFIGURATION AND SAFETY LEVEL ON EFFECTIVE LEG ROOM REAR (L51)

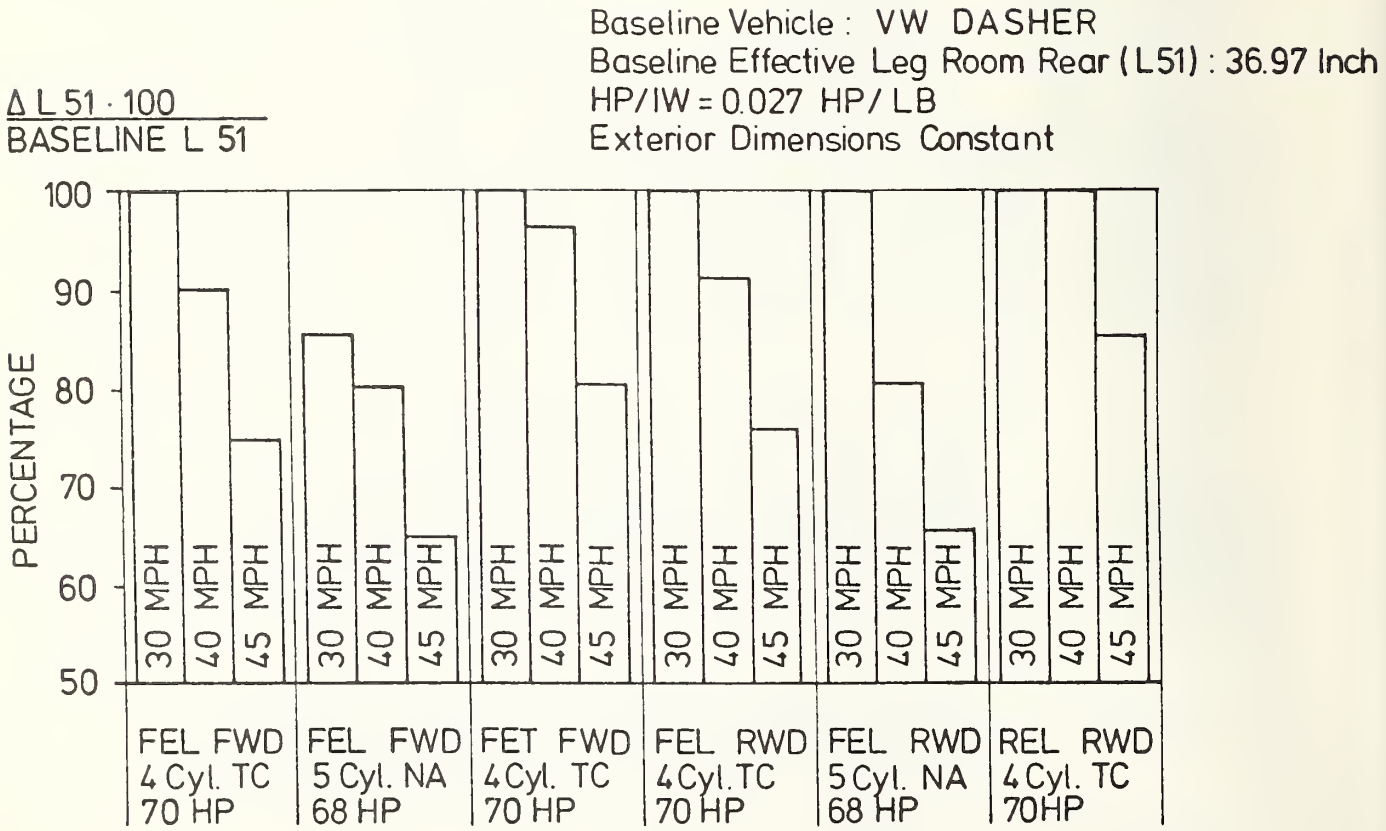

FIGURE 7.5-5: EFFECT OF DIESEL ENGINE/VEHICLE CONFIGURATION AND SAFETY LEVEL ON EFFECTIVE LEG ROOM REAR (L 51)

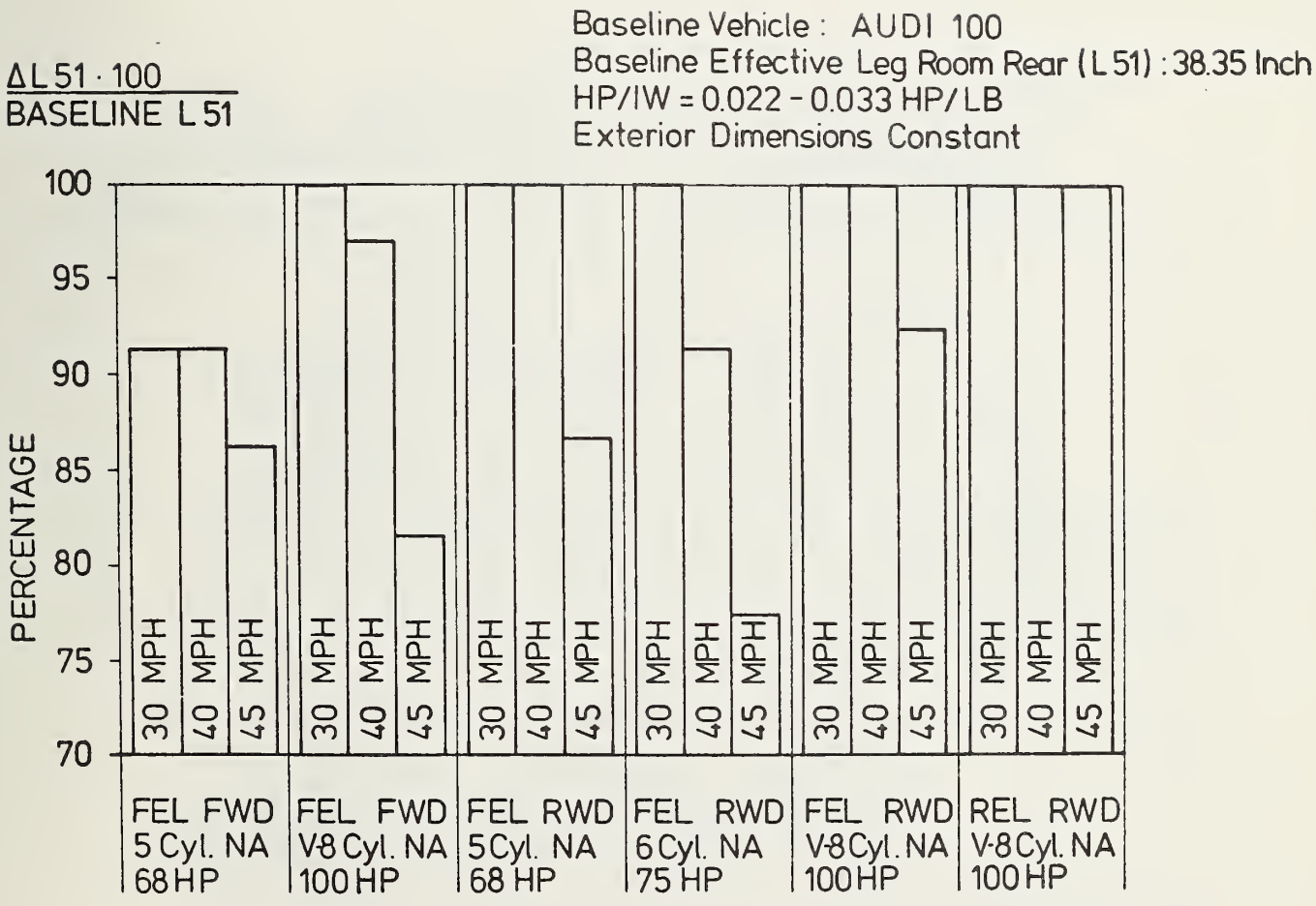

FIGURE 7.5-6: EFFECT OF DIESEL ENGINE/VEHICLE CONFIGURATION ON EFFECTIVE LEG ROOM REAR (L 51)

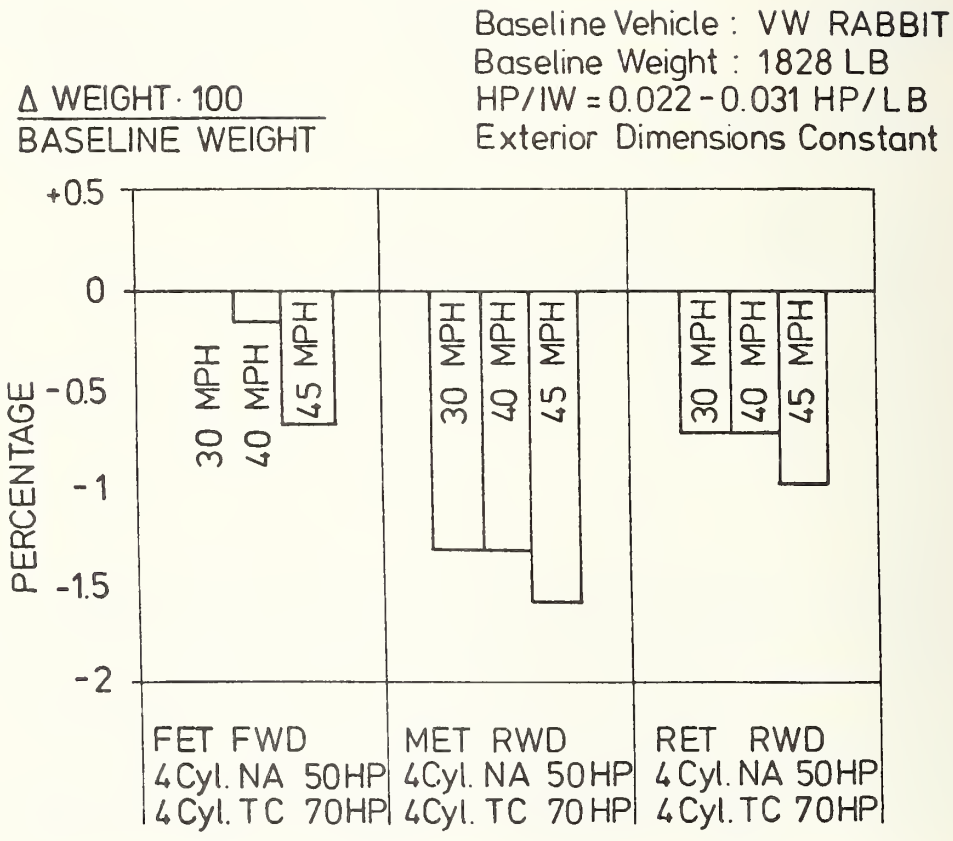

FIGURE 7.5-7: EFFECT OF DIESEL ENGINE/VEHICLE CONFIGURATION AND SAFETY LEVEL ON VEHICLE WEIGHT

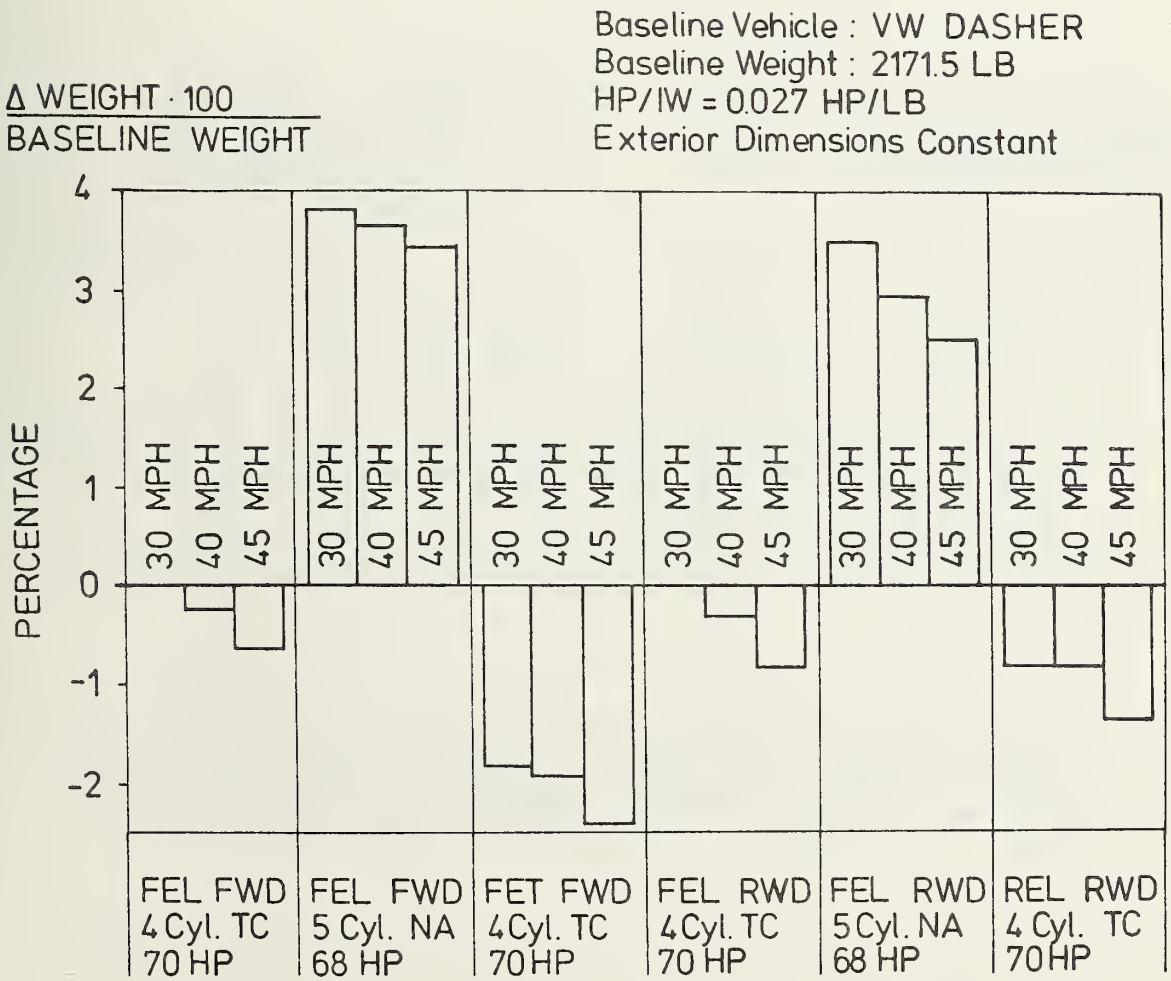

FIGURE 7.5-8: EFFECT OF DIESEL ENGINE/VEHICLE CONFIGURATION AND SAFETY LEVEL ON VEHICLE WEIGHT

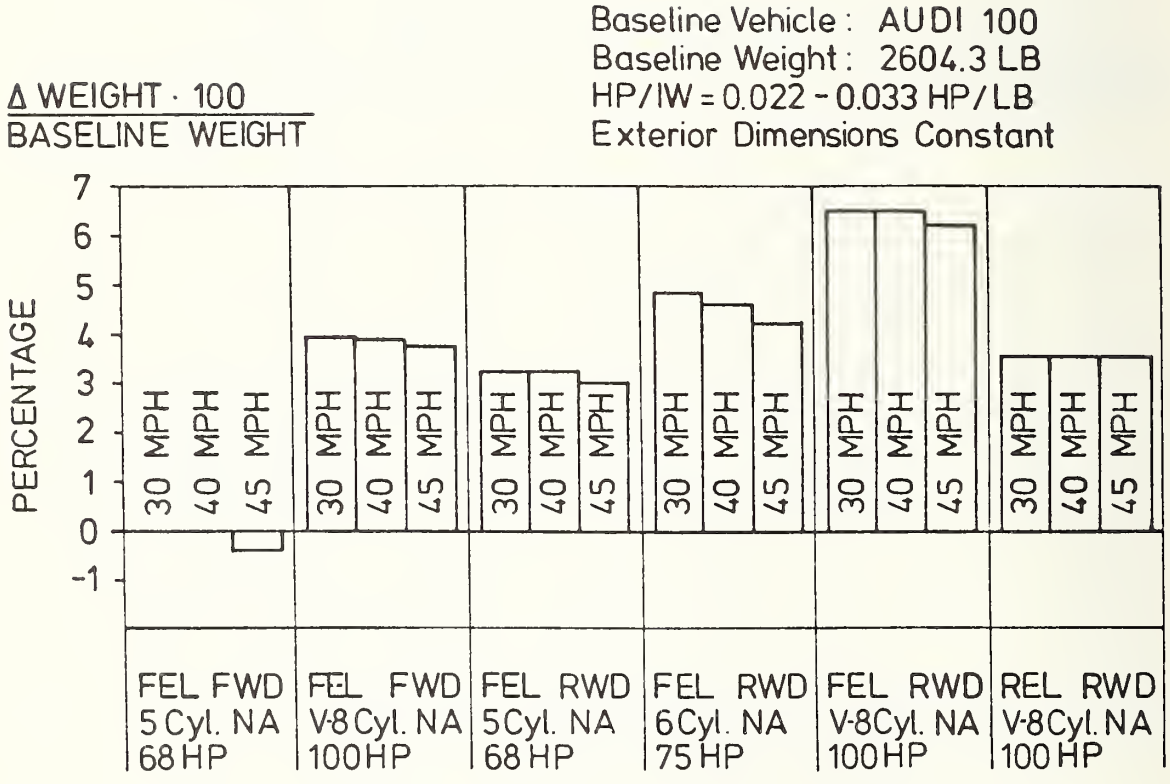

FIGURE 7.5-9: EFFECT OF DIESEL ENGINE/VEHICLE CONFIGURATION AND SAFETY LEVEL ON VEHICLE WEIGHT

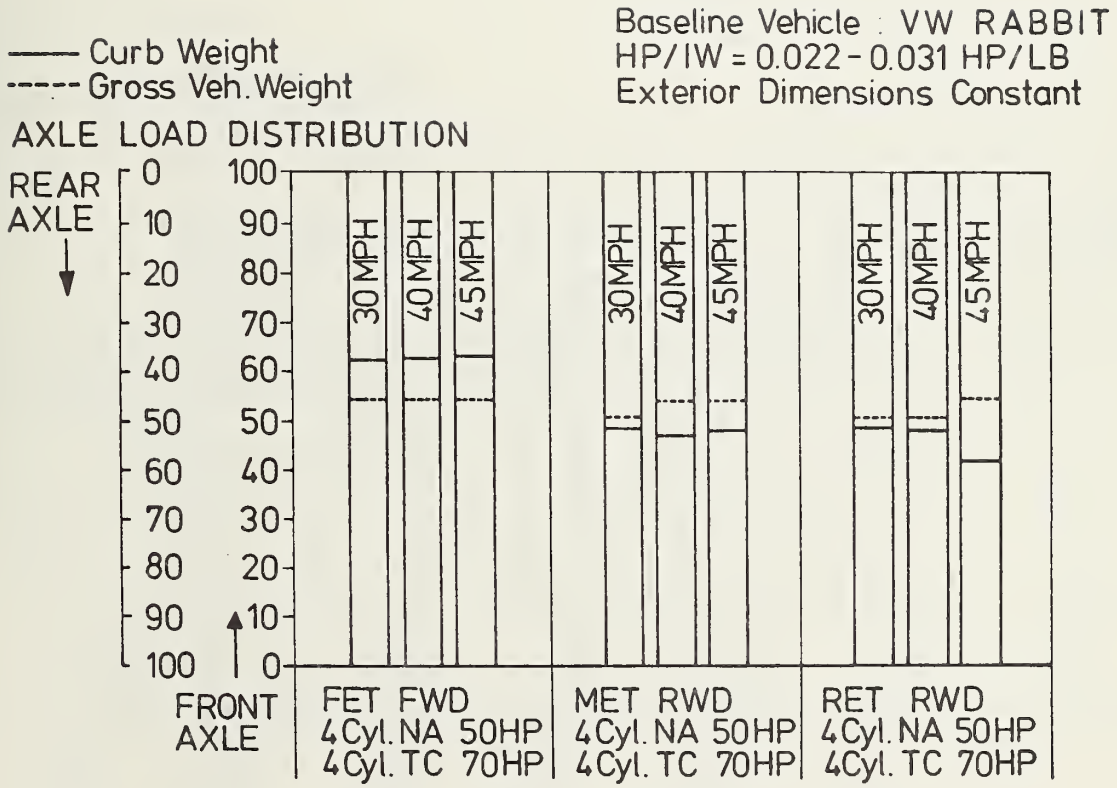

FIGURE 7.5-10: EFFECT OF DIESEL ENGINE/VEHICLE CONFIGURATION AND SAFETY LEVEL ON FRONT/REAR WEIGHT DISTRIBUTION

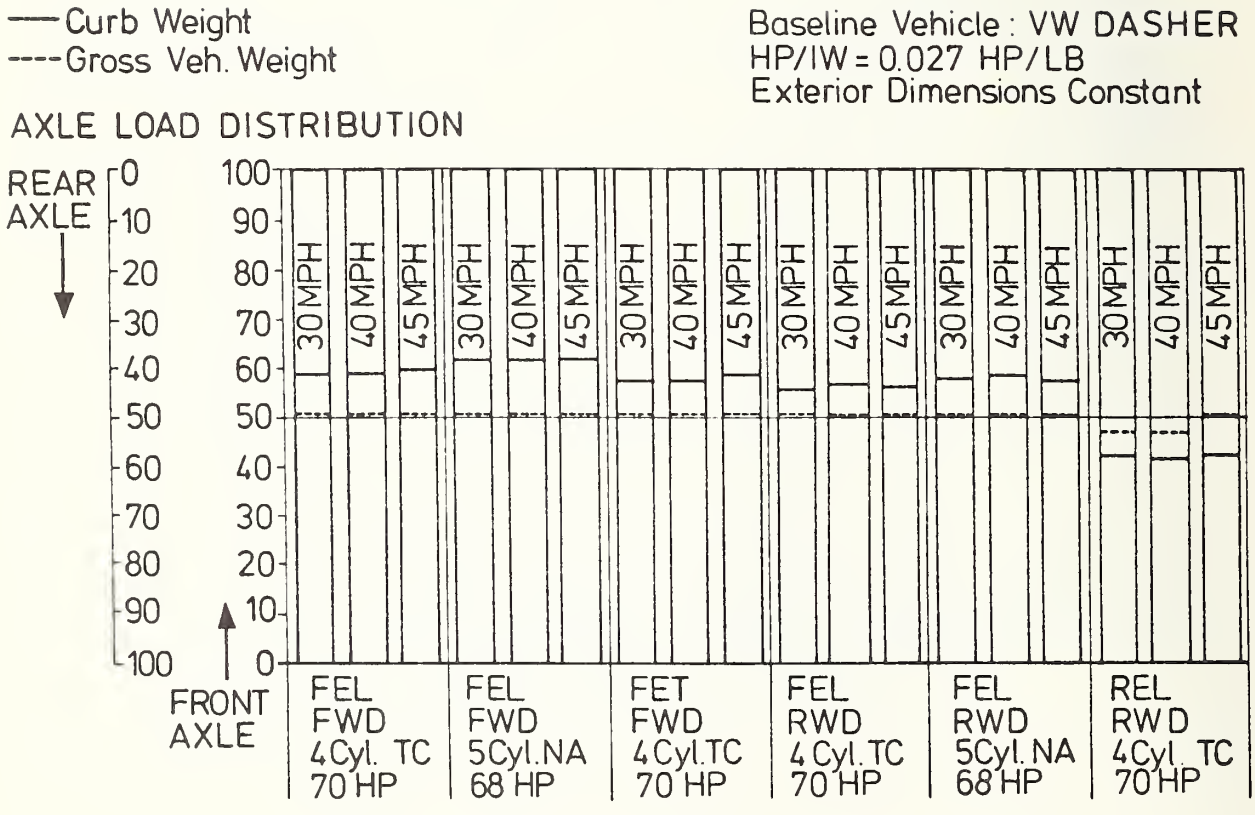

FIGURE 7.5-11: EFFECT OF DIESEL ENGINE/VEHICLE CONFIGURATION AND SAFETY LEVEL ON FRONT/REAR WEIGHT DISTRIBUTION

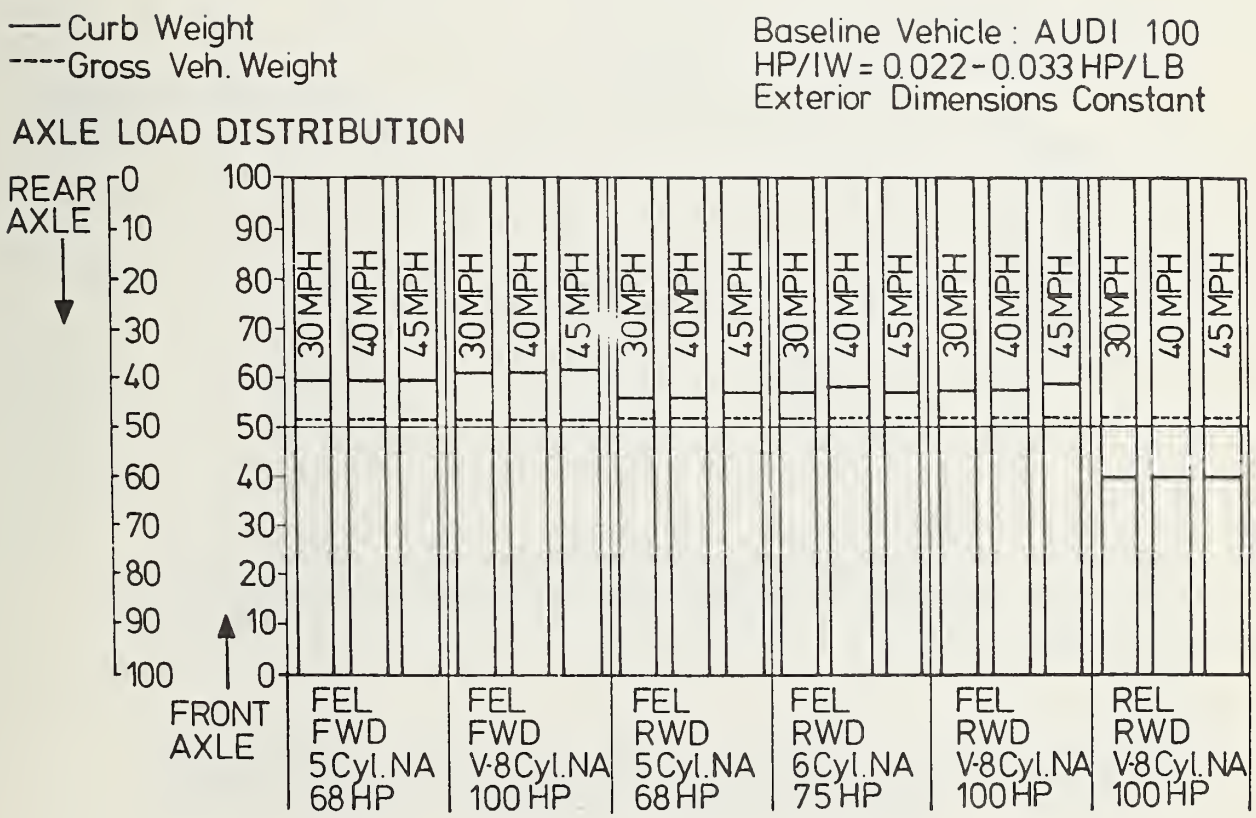

FIGURE 7.5-12: EFFECT OF DIESEL ENGINE/VEHICLE CONFIGURATION AND SAFETY LEVEL ON FRONT/REAR WEIGHT DISTRIBUTION

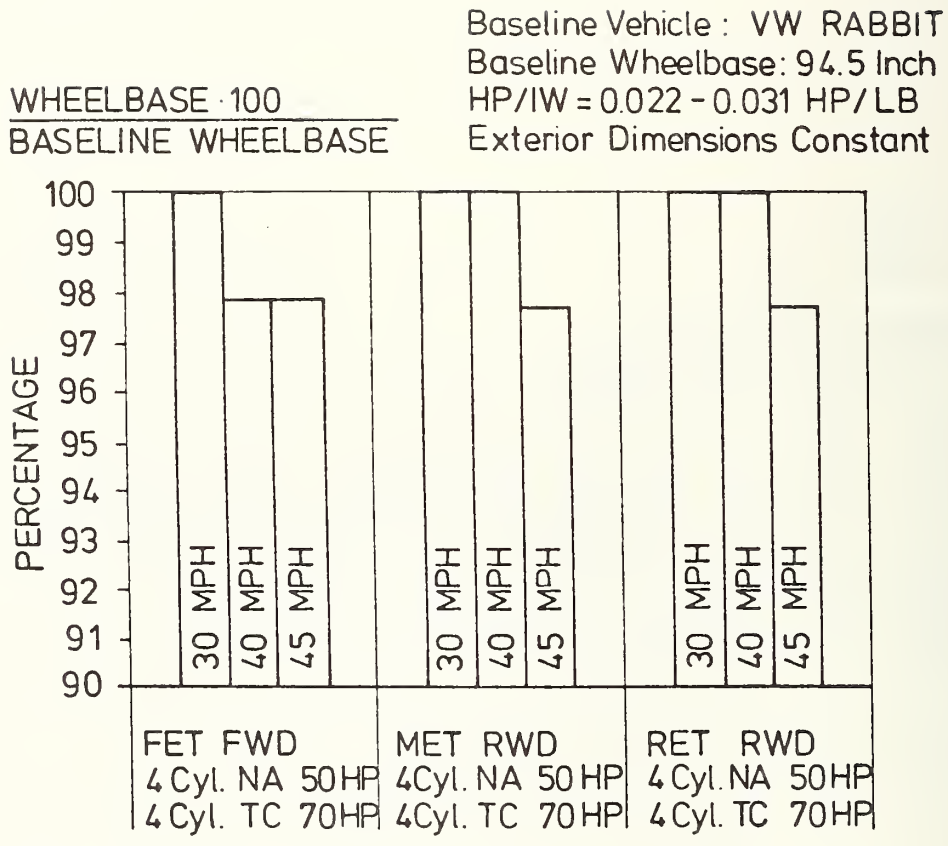

FIGURE 7.5-13: EFFECT OF DIESEL ENGINE/VEHICLE CONFIGURATION AND SAFETY LEVEL ON WHEELBASE

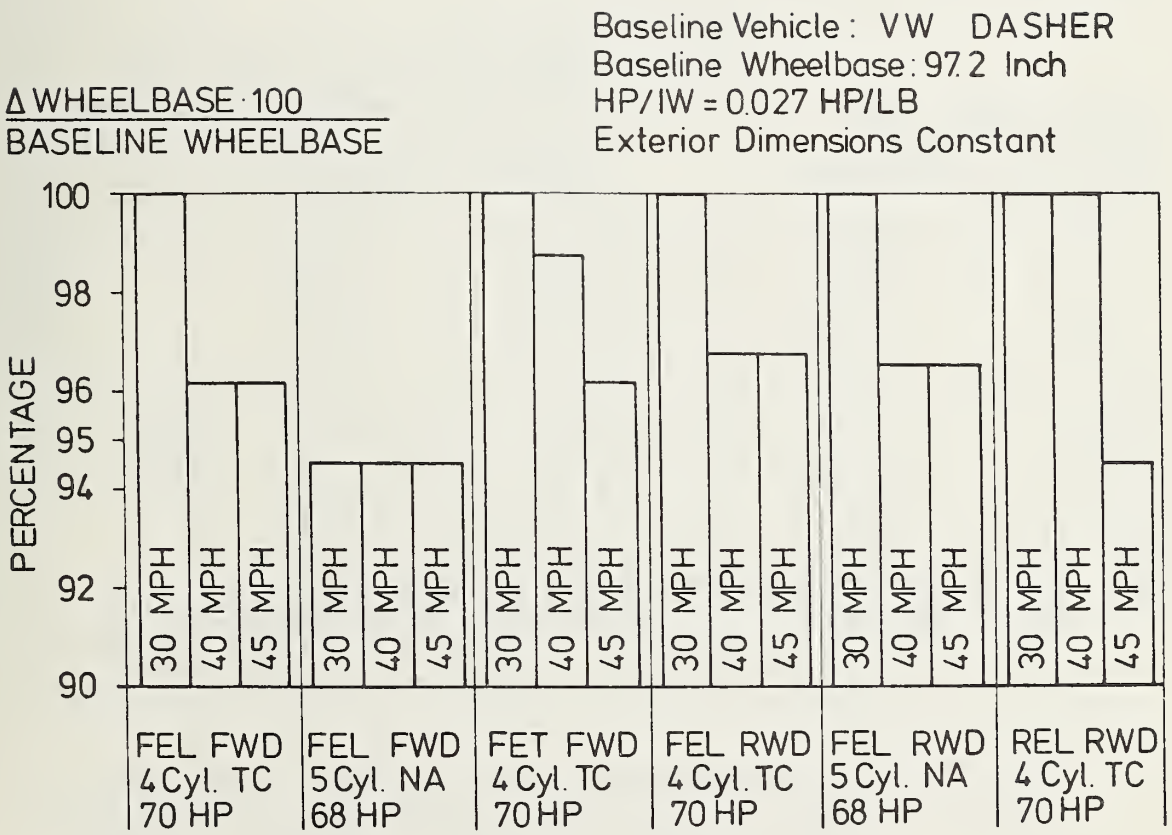

FIGURE 7.5-14: EFFECT OF DIESEL ENGINE/VEHICLE CONFIGURATION AND SAFETY LEVEL ON WHEELBASE

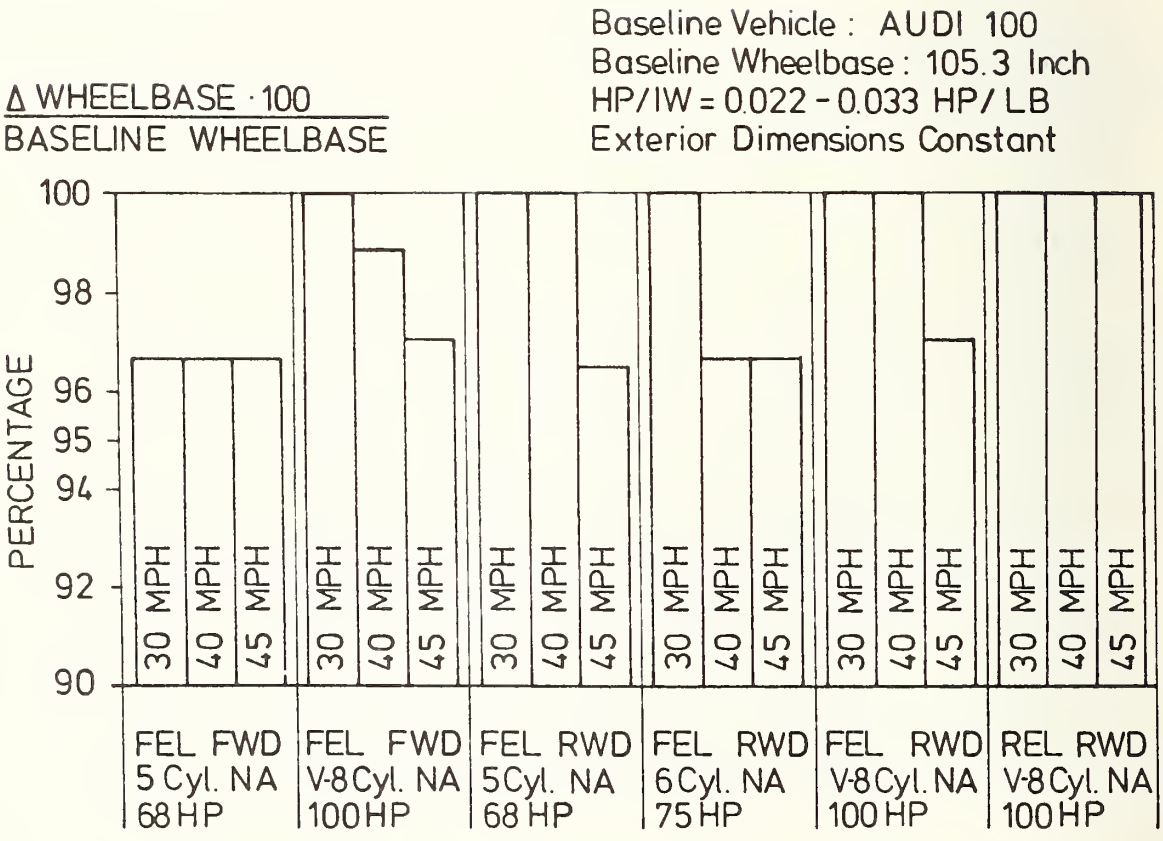

FIGURE 7.5-15: EFFECT OF DIESEL ENGINE/VEHICLE CONFIGURATION AND SAFETY LEVEL ON WHEELBASE

Vehicle Type	Conceptual Design	Safety Level		
		30 MPH	40 MPH	45 MPH
VW RABBIT	FET FWD 4 Cyl. NA 50 HP, TC 70 HP	0	0	0
12.4 Cu-ft Baseline	MET RWD 4 Cyl. NA 50 HP, TC 70 HP	–	–	–
	RET RWD 4 Cyl. NA 50 HP, TC 70 HP	–	–	–
DASHER	FEL FWD 4 Cyl. TC 70 HP	0	0	0
17.7 Cu-ft Baseline	FEL FWD 5 Cyl. NA 68 HP	0	0	0
	FET FWD 4 Cyl. TC 70 HP	0	0	0
	FEL RWD 4 Cyl. TC 70 HP	0	0	0
	FEL RWD 5 Cyl. NA 68 HP	0	0	0
	REL RWD 4 Cyl. TC 70 HP	–	–	–
AUDI 100	FEL FWD 5 Cyl. NA 68 HP	0	0	0
21.3 Cu-ft Baseline	FEL FWD V-8 Cyl. NA 100 HP	0	0	0
	FEL RWD 5 Cyl. NA 68 HP	0	0	0
	FEL RWD 6 Cyl. NA 75 HP	0	0	0
	FEL RWD V-8 Cyl. NA 100 HP	0	0	0
	REL RWD V-8 Cyl. NA 100 HP	–	–	–

TABLE 7.5-1: LUGGAGE CAPACITY (EXTERIOR DIMENSIONS CONSTANT)
- Decreased luggage capacity
0 No luggage capacity change

8.0 APPLICATIONS

Two vehicles were supplied to the Department of Transportation - Transportation Systems Center in order to demonstrate the compatibility of lightweight diesel engines with advanced vehicle concepts, and to verify the test results obtained by Volkswagen.

8.1 VW Rabbit with a turbocharged diesel engine

This vehicle is a production Rabbit made for the U.S. and equipped with a turbocharged diesel engine (see Figures 8.1-1 and 8.1-2).

8.1.1 General Specifications

Body Type	2-door hatchback
Curb weight	2,061 lb
Inertia weight	2,250 lb
Overall length	155.3 in.
Overall width	62.1 in.
Overall height	55.5 in.
Wheelbase	94.5 in.
Seating capacity	4

8.1.2 Engine and Drivetrain Specifications

Engine	4-cylinder turbocharged diesel
Bore/stroke	3.012/3.149 in.
Displacement	90 cu. in.
Compression ratio	23
Transmission	4-speed manual
Gear ratio	3.45, 1.54, 1.32, .97
Axle ratio	3.48

This vehicle was subjected to preliminary testing by the U.S. Environmental Protection Agency.

8.1.2 VW Test Results

Because of the advanced VW automotive technology, the road-load setting is lower than the rated value given in the Federal Register.

Fuel Economy	Urban	42.0 mpg
	Highway	56.0 mpg
	Composite	47.3 mpg
Emissions	HC	.22 g/mile
	CO	.98 g/mile
	NO_x	.93 g/mile

Acceleration time from 0 to 60 mph 15 sec.

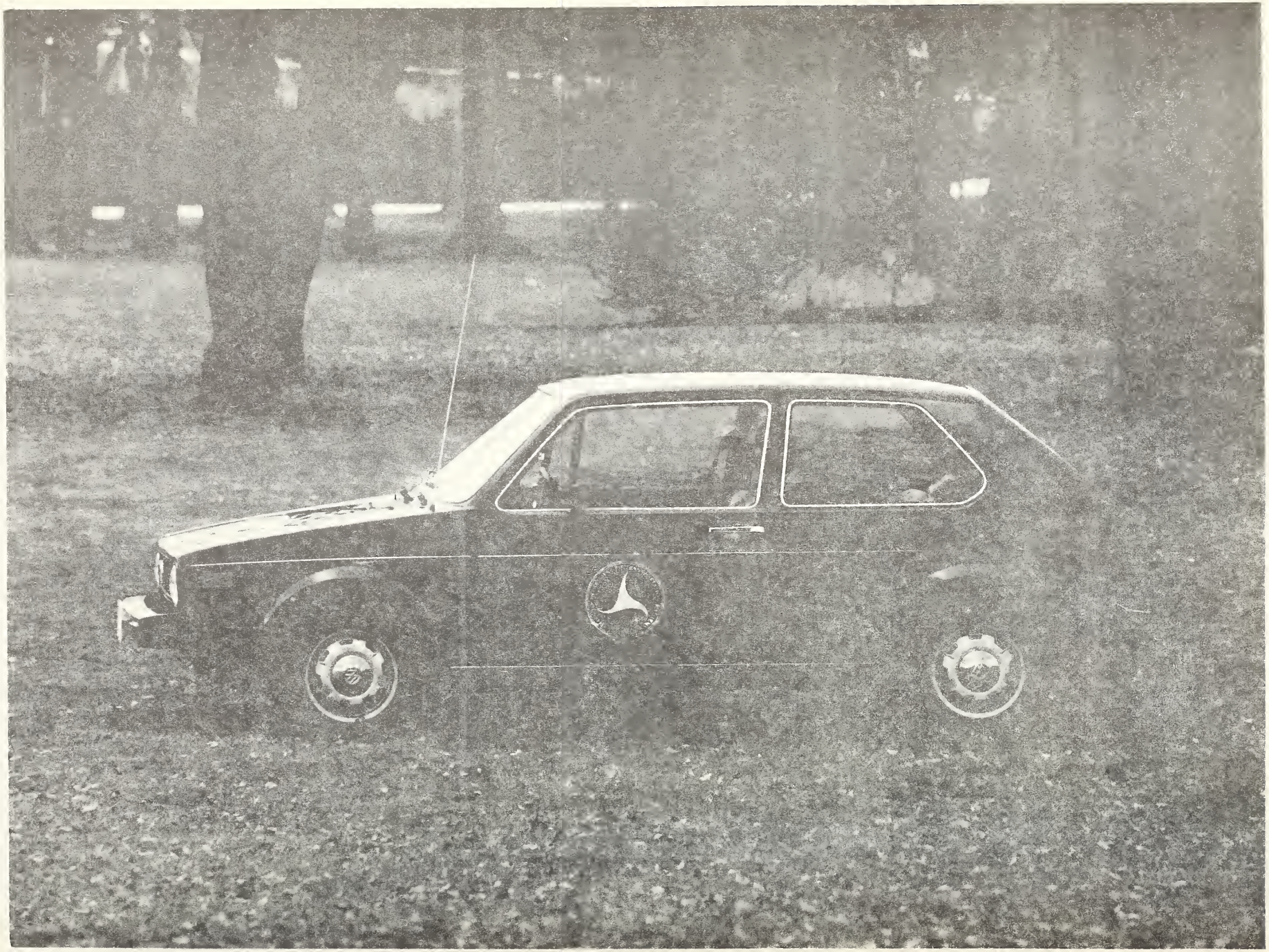

FIGURE 8.1-1: PRODUCTION RABBIT EQUIPPED WITH A TURBOCHARGED DIESEL ENGINE

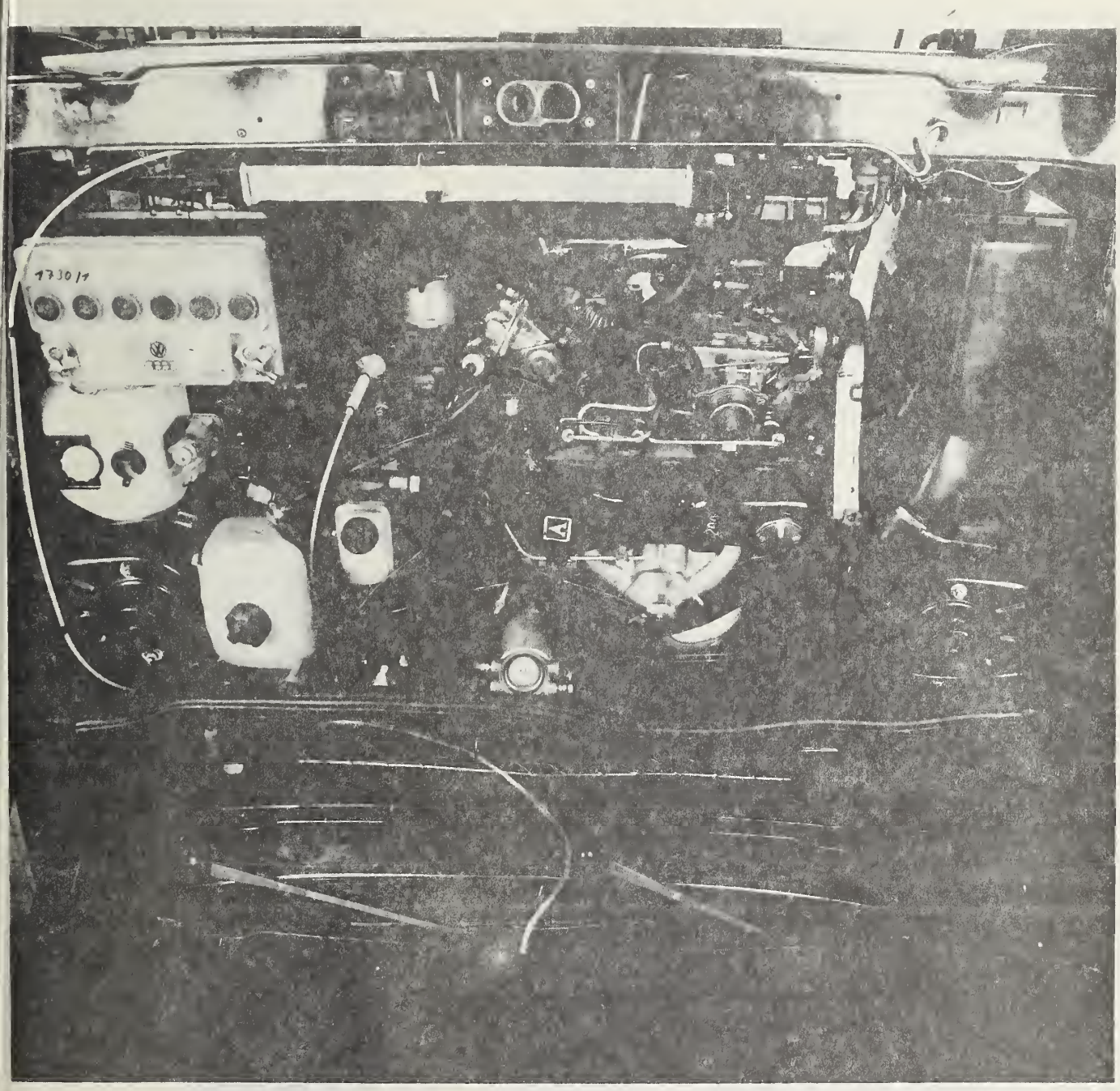

FIGURE 8.1-2: ENGINE COMPARTMENT OF THE PRODUCTION RABBIT WITH TURBOCHARGED DIESEL ENGINE

8.2 INTEGRATED RESEARCH VEHICLE

In order to demonstrate the compatibility of light-weight diesel power plants characterized by low emission levels and very good fuel economy wtih vehicles of advanced safety features and high performance, an Integrated Research Vehicle (IRVW Integrated Research Volkswagen. See Figures 8.2-1 and 8.2-2)was designed and built on the basis of the so-called ESVW II (Experimental Safety VW II).

8.2.1 General Specifications

Body type	2-door, hatchback
Overall length	155.3 in.
Overall width	63.4 in.
Overall height	53.9 in.
Wheelbase	94.5 in.
Curb weight	2,070 lb
Seating capacity	4

8.2.2 Engine and Drivetrain Specifications

Engine	4-cylinder turbocharged diesel
Bore/stroke	3.012/3.149 in.
Displacement	90 cu. in.
Compression ratio	23
Transmission	5-speed manual
Gear ratios	3.45, 1.94, 1.29, .75
Axle ratio	3.7

8.2.3 Safety Features

The vehicle body has a special frame structure (see Fig. 8.2-3) which contributes to controlled crash behavior during frontal impacts at velocities of up to 40 mph. The front seats of the vehicle are equipped with a passive two-point belt-kneebar restraint system with automatic retractor, belt preloader and force limiter (Fig. 8.2-4).

FIGURE 8.2-1: THE IRVW (INTEGRATED RESEARCH VOLKSWAGEN

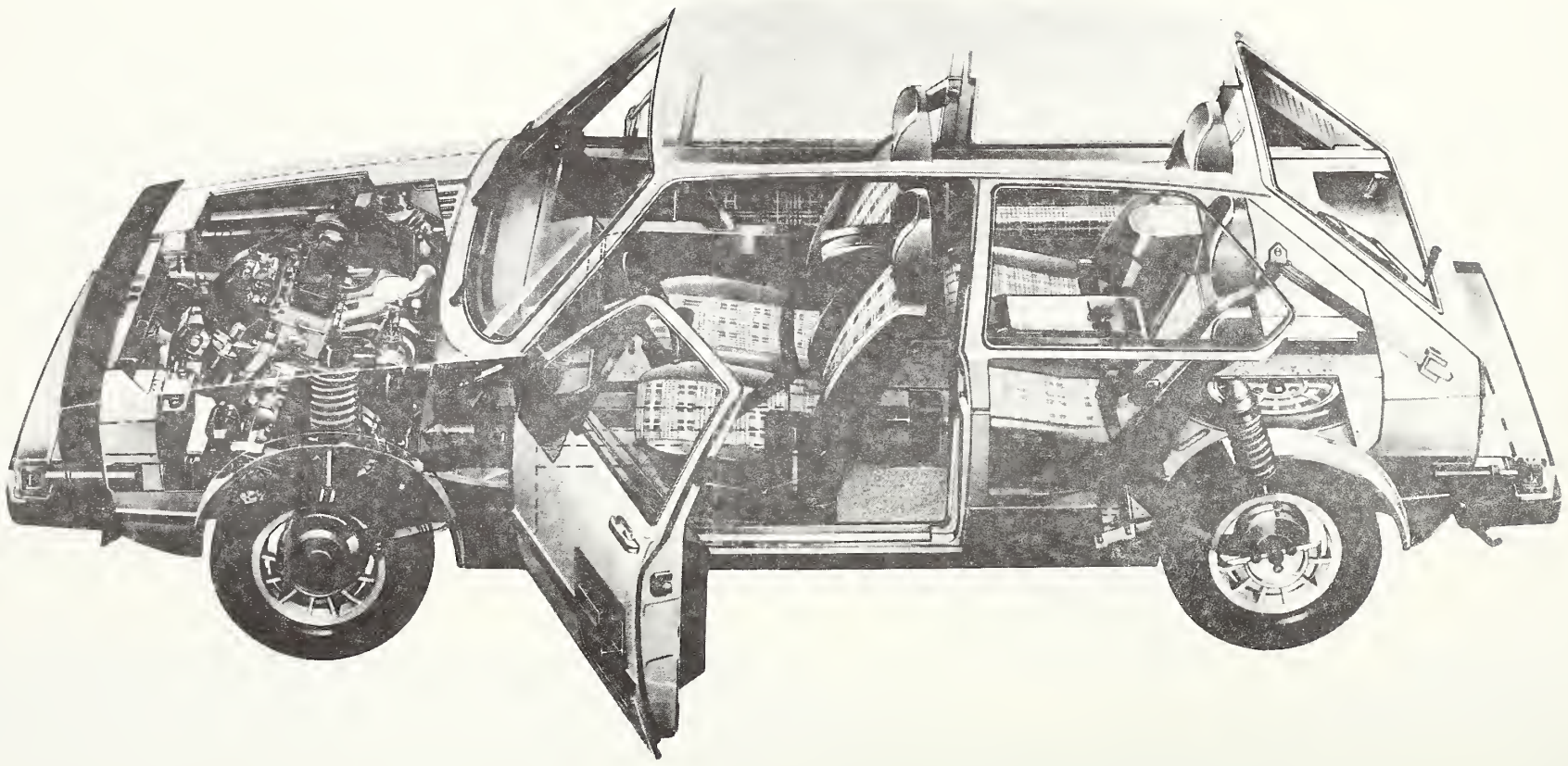

FIGURE 8.2-2: CUTAWAY VIEW OF THE IRVW (INTEGRATED RESEARCH VOLKSWAGEN

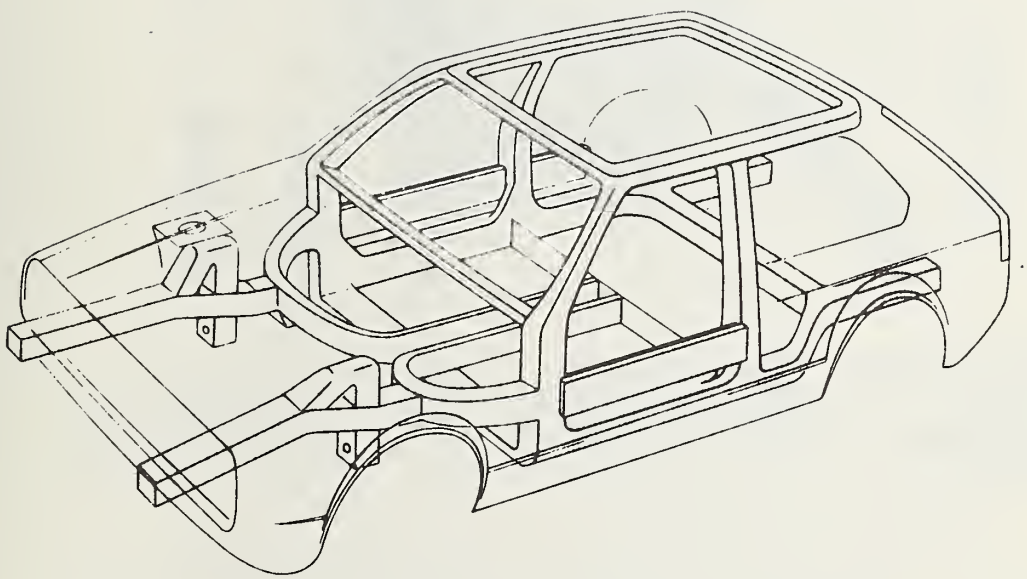

FIGURE 8.2-3: IRVW FRAME SYSTEM

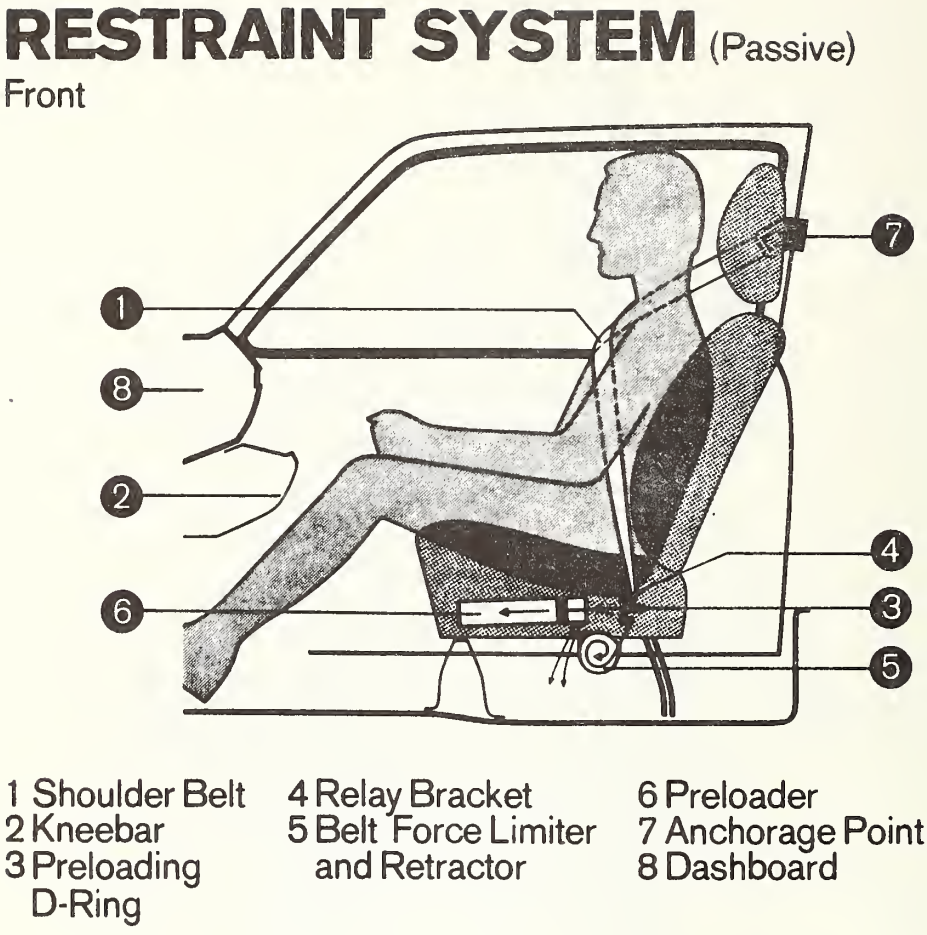

FIGURE 8.2-4: RESTRAINT SYSTEM (PASSIVE), FRONT

The rear seat passenger belt system (Fig. 8.2-5) is a three-point belt system with automatic retractor, preloading device and force-limiter. It is an active system and permits one-hand operation.

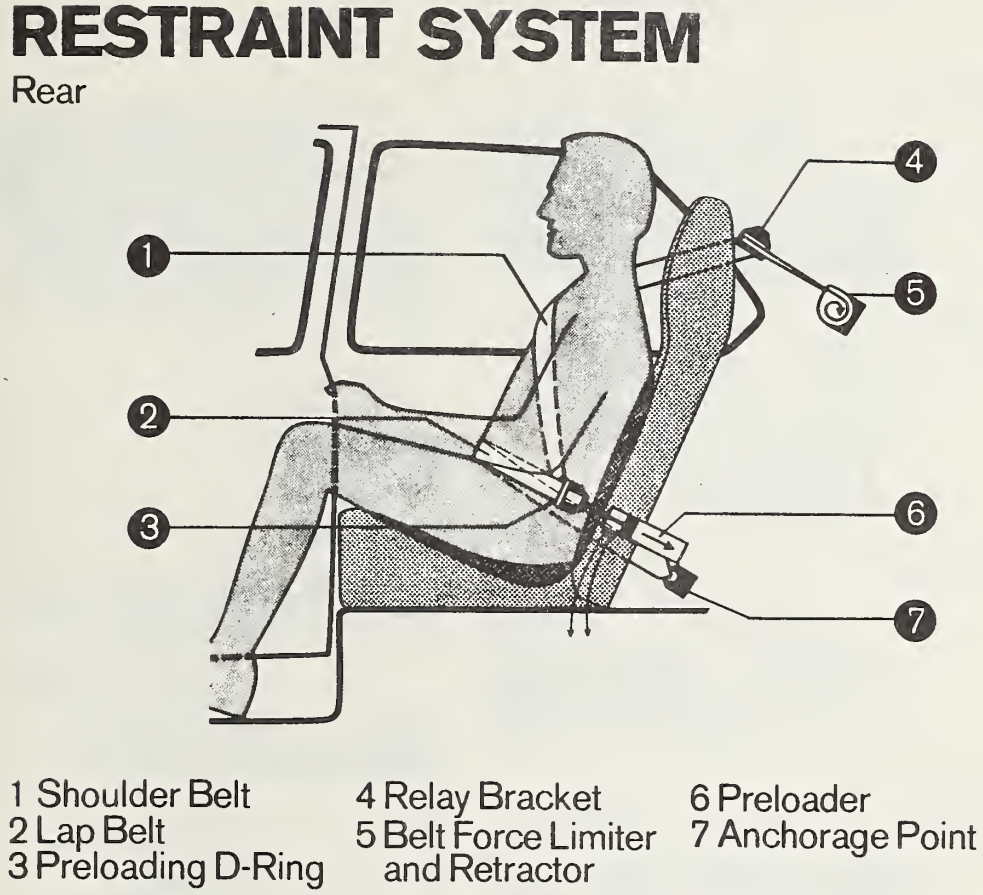

FIGURE 8.2-5: RESTRAINT SYSTEM, REAR

A frontal collision crash test was performed between the ESVW II (1,100 kp) and a heavy vehicle (1,800 kp) was performed in order to provide compatibility data. The closing velocity was 100 km/h (60 mph).

The ESVW II and the heavy vehicle did not suffer any major deformation of their occupant compartments.

The crash test results are shown in Table 8.2-1 and indicate that they remained well below the specified limits (Figure 8.2-6).

CRASH TESTS

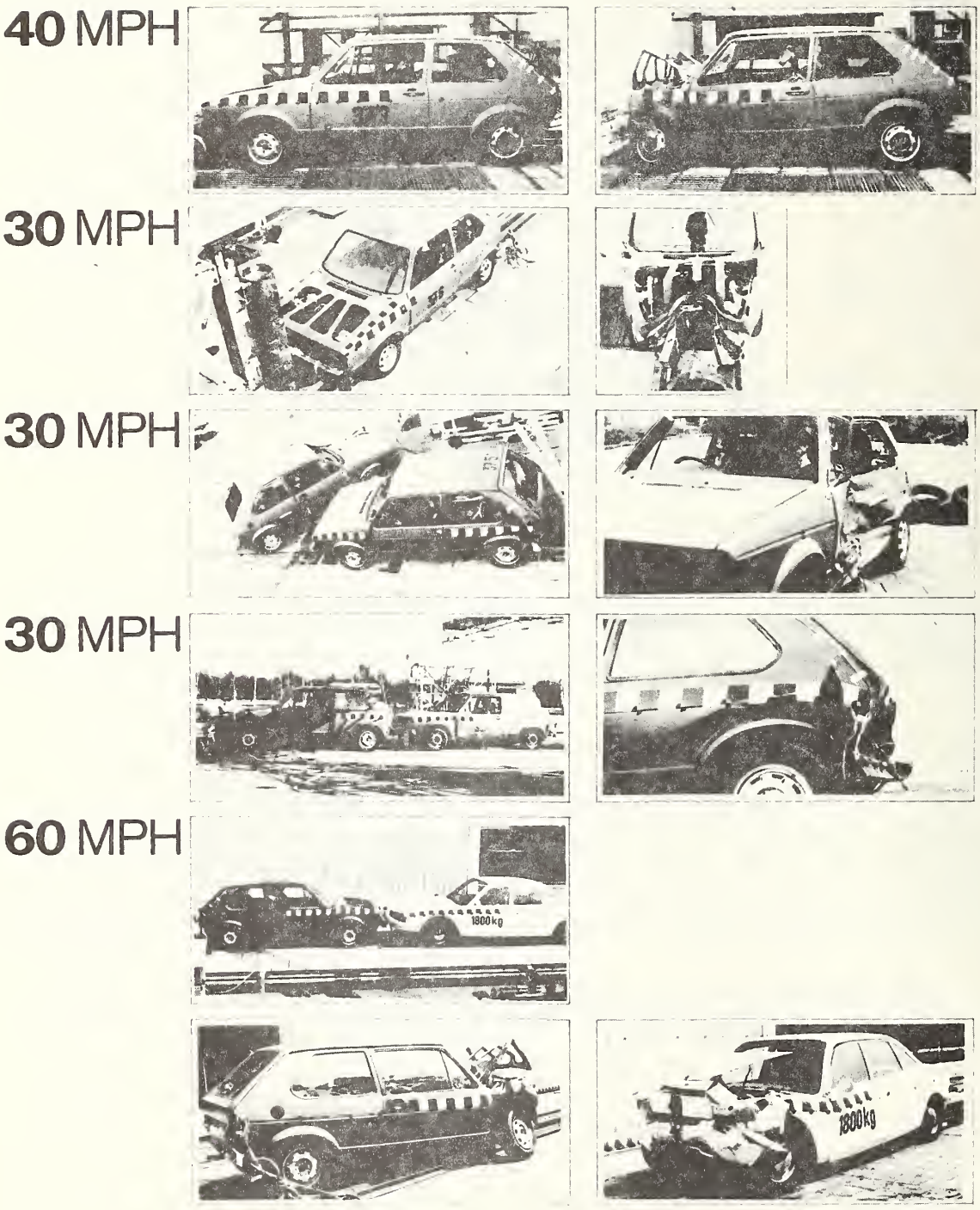

FIGURE 8.2-6: CRASH TESTS ON THE ESVW II

CRASH TEST RESULTS

	HIC Head			SI Chest			FEMUR LOAD			
Tolerance Level	1000			1000			771 KP			
							Driver		Front Passenger	
	Driver	Front Passenger	Rear (left) Passenger	Driver	Front Passenger	Rear (left) Passenger	Left	Right	Left	Right
40 MPH Frontal Fixed Barrier Impact	600	600	440	380	370	210	525	680	740	550
30 MPH Frontal Fixed Pole Impact	200	200	290	200	200	140	540	285	280	460
30 MPH Car-to-Car Side Collision	20	20	90*	20	20	50*	-**	275	-**	175
30 MPH Car-to-Car Rear End Collision	40	180	50	25	25	50	80	40	100	100
60 MPH Closing Speed at a Frontal Collision with a Heavy Vehicle	400	400	600	180	270	220	510	600	480	490

*Rear passenger on right side, impact at right side
**Not measured

TABLE 8.2-1: CRASH TEST RESULTS, ESVW II

8.2.4 Fuel Economy and Emission Testing, IRVW

The following emission and fuel economy data was measured by the Volkswagen Mobile Emission Laboratory:

		TEST 1	TEST 2	TEST 3	
FTP	HC	.284	.261	.271	g/mile
	CO	.64	1.24	.56	g/mile
	NO_x	.691	.713	.663	g/mile
	CO_2	187	188.7	187	g/mile
	MPG	53.9	53.4	54.1	
HDC	HC	.02	.02	.02	g/mile
	CO	.271	.24	.25	g/mile
	NOx	.627	.631	.633	g/mile
	MPG	69.9	70.8	69.5	

The following shift points were used:

1 - 2 at 11 mph

2 - 3 at 21 mph

3 - 4 at 32 mph

4 - 5 at 42 mph.

During the FTP, now downshifts were performed. Downshifts during the HDC were performed to 4th gear at 269 seconds. The fuel used during the tests at the Volkswagen Mobile Laboratory was Diesel No.2. The tires were 155 SR 13 (original equipment).

Noise level measurements in accordance with SAE J 986a showed 71 dB.

The combination of five-speed transmission and turbocharger in the IRVW improves its mileage, reduces engine noise and emissions, and raises engine performance.

Figure 8.2-7 shows typical fuel economy data at steady-state operation.

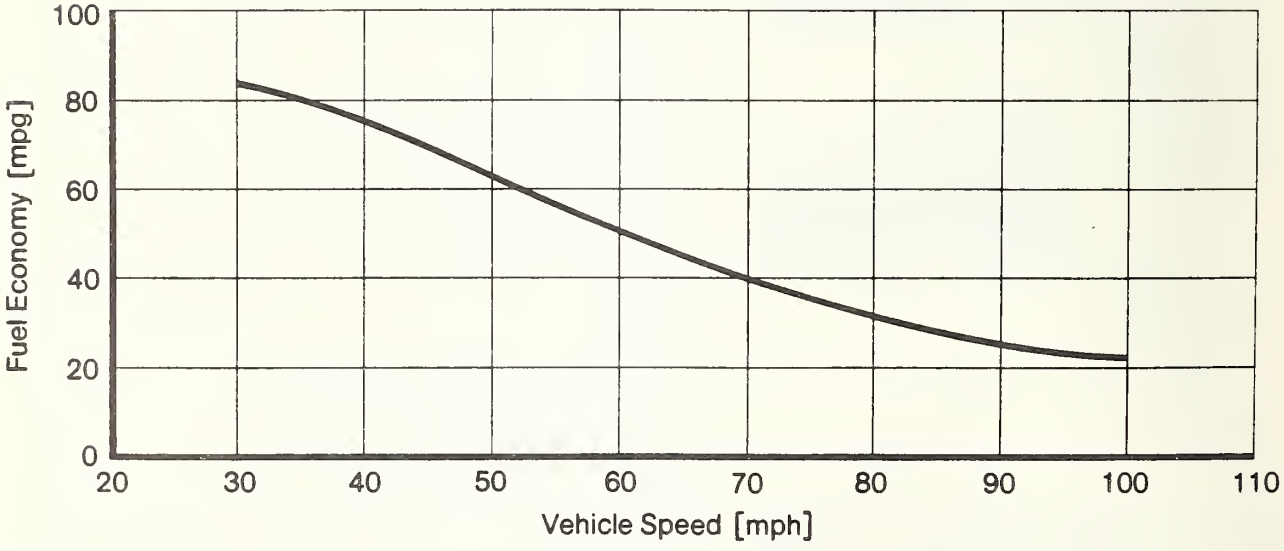

FIGURE 8.2-7: FUEL ECONOMY AT STEADY-STATE OPERATION, IRVW

The acceleration performance of the vehicle is shown in Figure 8.2-8.

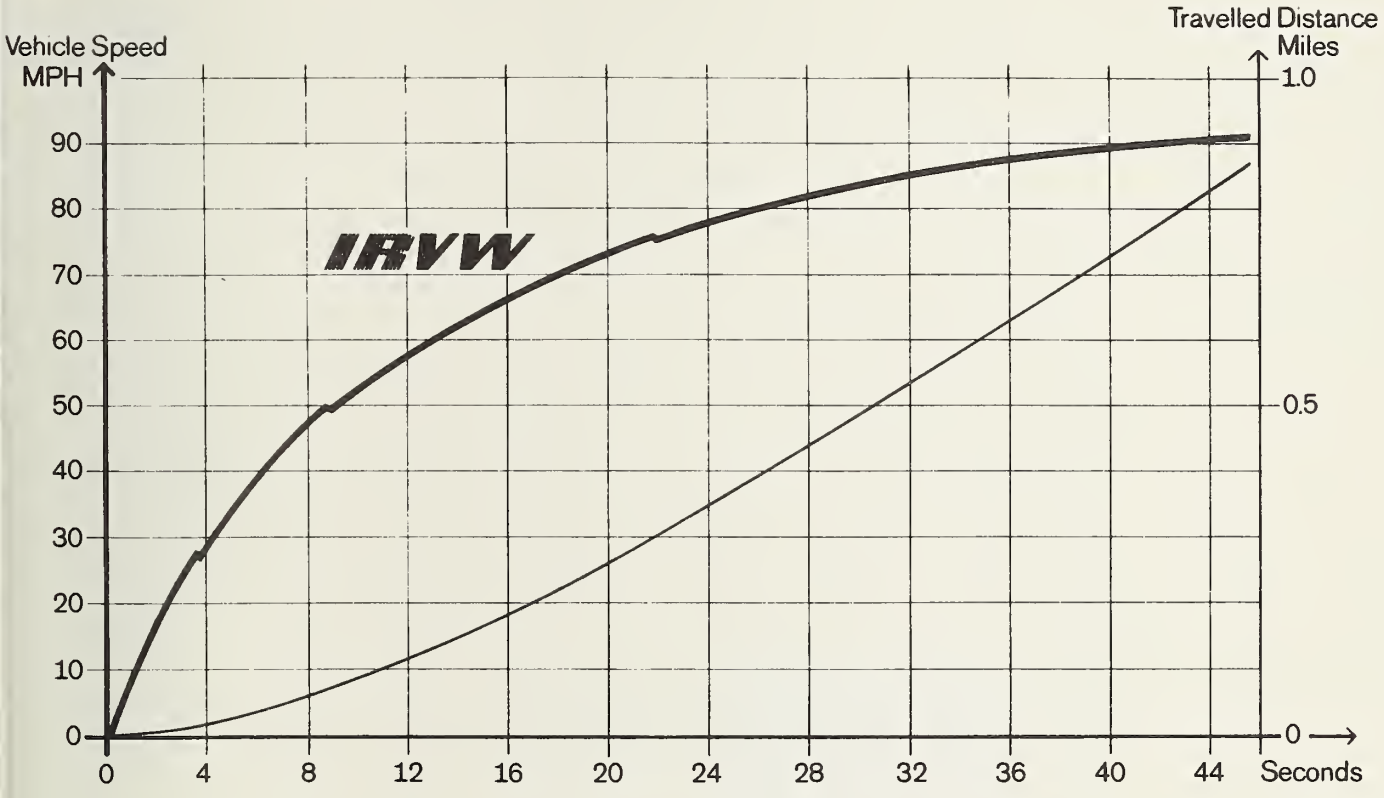

FIGURE 8.2-8: ACCELERATION PERFORMANCE OF THE IRVW.

U.S. DEPARTMENT OF TRANSPORTATION
RESEARCH AND SPECIAL PROGRAMS ADMINISTRATION
TRANSPORTATION SYSTEMS CENTER
KENDALL SQUARE, CAMBRIDGE, MA. 02142